CHRONIC OXIDATIVE STRESS AND INFLAMMATION-RELATED DISEASES – THE PROTECTIVE POTENTIAL OF MEDICINAL PLANTS AND NATURAL PRODUCTS

EDITED BY: Annalisa Chiavaroli, Enkelejda Goci and Lucia Recinella
PUBLISHED IN: Frontiers in Pharmacology

frontiers Research Topics

frontiers

ISSN 1664-8714
ISBN 978-2-83250-363-8
DOI 10.3389/978-2-83250-363-8

About Frontiers

Frontiers is more than just an open-access publisher of scholarly articles: it is a pioneering approach to the world of academia, radically improving the way scholarly research is managed. The grand vision of Frontiers is a world where all people have an equal opportunity to seek, share and generate knowledge. Frontiers provides immediate and permanent online open access to all its publications, but this alone is not enough to realize our grand goals.

Frontiers Journal Series

The Frontiers Journal Series is a multi-tier and interdisciplinary set of open-access, online journals, promising a paradigm shift from the current review, selection and dissemination processes in academic publishing. All Frontiers journals are driven by researchers for researchers; therefore, they constitute a service to the scholarly community. At the same time, the Frontiers Journal Series operates on a revolutionary invention, the tiered publishing system, initially addressing specific communities of scholars, and gradually climbing up to broader public understanding, thus serving the interests of the lay society, too.

Dedication to Quality

Each Frontiers article is a landmark of the highest quality, thanks to genuinely collaborative interactions between authors and review editors, who include some of the world's best academicians. Research must be certified by peers before entering a stream of knowledge that may eventually reach the public - and shape society; therefore, Frontiers only applies the most rigorous and unbiased reviews.
Frontiers revolutionizes research publishing by freely delivering the most outstanding research, evaluated with no bias from both the academic and social point of view. By applying the most advanced information technologies, Frontiers is catapulting scholarly publishing into a new generation.

What are Frontiers Research Topics?

Frontiers Research Topics are very popular trademarks of the Frontiers Journals Series: they are collections of at least ten articles, all centered on a particular subject. With their unique mix of varied contributions from Original Research to Review Articles, Frontiers Research Topics unify the most influential researchers, the latest key findings and historical advances in a hot research area! Find out more on how to host your own Frontiers Research Topic or contribute to one as an author by contacting the Frontiers Editorial Office: frontiersin.org/about/contact

CHRONIC OXIDATIVE STRESS AND INFLAMMATION-RELATED DISEASES – THE PROTECTIVE POTENTIAL OF MEDICINAL PLANTS AND NATURAL PRODUCTS

Topic Editors:
Annalisa Chiavaroli, University of Studies G. d'Annunzio Chieti and Pescara, Italy
Enkelejda Goci, Aldent University, Albania
Lucia Recinella, University of Studies G. d'Annunzio Chieti and Pescara, Italy

Citation: Chiavaroli, A., Goci, E., Recinella, L., eds. (2022). Chronic Oxidative Stress and Inflammation-Related Diseases – The Protective Potential of Medicinal Plants and Natural Products. Lausanne: Frontiers Media SA.
doi: 10.3389/978-2-83250-363-8

Table of Contents

frontiers in Pharmacology

ORIGINAL RESEARCH
published: 24 August 2021
doi: 10.3389/fphar.2021.723922

Salidroside Ameliorated Intermittent Hypoxia-Aggravated Endothelial Barrier Disruption and Atherosclerosis *via* the cAMP/PKA/RhoA Signaling Pathway

Linyi Li[1,2,3], *Yunyun Yang*[1,2,3], *Huina Zhang*[1,2,3], *Yunhui Du*[1,2,3], *Xiaolu Jiao*[1,2,3], *Huahui Yu*[1,2,3], *Yu Wang*[1,2,3], *Qianwen Lv*[1,2,3], *Fan Li*[1,2,3], *Qiuju Sun*[1,2,3] *and Yanwen Qin*[1,2,3]*

[1]*The Key Laboratory of Upper Airway Dysfunction-Related Cardiovascular Diseases, Beijing Anzhen Hospital, Beijing Institute of Heart, Lung and Blood Vessel Diseases, Capital Medical University, Beijing, China,* [2]*The Key Laboratory of Remodeling-Related Cardiovascular Diseases, Beijing Anzhen Hospital, Ministry of Education, Capital Medical University, Beijing, China,* [3]*Beijing Institute of Heart, Lung and Blood Vessel Disease, Beijing, China*

OPEN ACCESS

Edited by:
Annalisa Chiavaroli, University of Studies G. d'Annunzio Chieti and Pescara, Italy

Reviewed by:
Maria Luisa Del Moral, University of Jaén, Spain
Ina Yosifova Aneva, Bulgarian Academy of Sciences, Bulgaria

***Correspondence:**
Yanwen Qin
qinyanwen@vip.126.com

Specialty section:
This article was submitted to Ethnopharmacology, a section of the journal Frontiers in Pharmacology

Received: *11 June 2021*
Accepted: *11 August 2021*
Published: *24 August 2021*

Citation:
Li L, Yang Y, Zhang H, Du Y, Jiao X, Yu H, Wang Y, Lv Q, Li F, Sun Q and Qin Y (2021) Salidroside Ameliorated Intermittent Hypoxia-Aggravated Endothelial Barrier Disruption and Atherosclerosis via the cAMP/PKA/RhoA Signaling Pathway. Front. Pharmacol. 12:723922. doi: 10.3389/fphar.2021.723922

Background: Endothelial barrier dysfunction plays a key role in atherosclerosis progression. The primary pathology of obstructive sleep apnea-hypopnea syndrome is chronic intermittent hypoxia (IH), which induces reactive oxygen species (ROS) overproduction, endothelial barrier injury, and atherosclerosis. Salidroside, a typical pharmacological constituent of Rhodiola genus, has documented antioxidative, and cardiovascular protective effects. However, whether salidroside can improve IH-aggravated endothelial barrier dysfunction and atherosclerosis has not been elucidated.

Methods and results: In normal chow diet-fed ApoE$^{-/-}$ mice, salidroside (100 mg/kg/d, p. o.) significantly ameliorated the formation of atherosclerotic lesions and barrier injury aggravated by 7-weeks IH (21%–5%–21%, 120 s/cycle). In human umbilical vein endothelial cells (HUVECs), exposure to IH (21%–5%–21%, 40 min/cycle, 72 cycles) decreased transendothelial electrical resistance and protein expression of vascular endothelial cadherin (VE-cadherin) and zonula occludens 1. In addition, IH promoted ROS production and activated ras homolog gene family member A (RhoA)/Rho-associated protein kinase (ROCK) pathway. All of these effects of IH were reversed by salidroside. Similar to salidroside, ROCK-selective inhibitors Y26732, and Fasudil protected HUVECs from IH-induced ROS overproduction and endothelial barrier disruption. Furthermore, salidroside increased intracellular cAMP levels, while the PKA-selective inhibitor H-89 attenuated the effects of salidroside on IH-induced RhoA/ROCK suppression, ROS scavenging, and barrier protection.

Conclusion: Our findings demonstrate that salidroside effectively ameliorated IH-aggravated endothelial barrier injury and atherosclerosis, largely through the cAMP/PKA/RhoA signaling pathway.

Keywords: atherosclerosis, obstructive sleep apnea-hypopnea syndrome, intermittent hypoxia, salidroside, endothelial barrier

INTRODUCTION

Atherosclerotic cardio- or cerebrovascular diseases are common causes of morbidity and mortality worldwide (Gibbons et al., 2021). Atherosclerosis is the pathological basis of peripheral arterial disease, coronary heart disease, and stroke. In addition to traditional risk factors such as hereditary susceptibility, aging, hypertension, obesity, diabetes, and smoking, obstructive sleep apnea-hypopnea syndrome (OSA) that affect up to 100 million people worldwide has emerged as a new significant and independent risk factor for atherosclerosis (Ali et al., 2014; Souza et al., 2021). OSA is characterized by repetitive episodes of hypopnea or apnea due to upper airway collapse during sleep (Lévy et al., 2015). OSA prevalence in patients with coronary heart disease ranges from 30 to 58% (Bradley and Floras, 2009). OSA causes endothelial dysfunction (Hoyos et al., 2015; Khalyfa et al., 2016), unstable plaque characteristics (Trzepizur et al., 2014; Konishi et al., 2019), and atherosclerosis (Wattanakit et al., 2008; Ma et al., 2016; Zhou et al., 2017). Recently, one of the largest studies in this area to date (n = 2009) found that OSA is independently associated with increased carotid intima-media thickness in a dose-responsive manner (Souza et al., 2021), reinforcing the role of OSA as a potential nontraditional risk factor for atherosclerosis.

Chronic intermittent hypoxia (CIH), a main feature of OSA, is characterized by repeated circulating hypoxemia and reoxidation (Lévy et al., 2015). CIH induces atherosclerosis in murine models and plays a critical role in OSA-associated cardiovascular morbidities (Drager et al., 2013; Gautier-Veyret et al., 2013; Gileles-Hillel et al., 2014). Endothelial barriers are crucial for maintaining vascular homeostasis. In atherosclerosis, endothelial barrier function is impaired, which triggers the formation of atherosclerotic plaques (Sun et al., 2011; Döring et al., 2017; Pi et al., 2018). CIH has been shown to increase vascular permeability and endothelial barrier dysfunction (Makarenko et al., 2014). However, whether CIH destroys vascular endothelial barriers to promote atherosclerosis remains unknown.

CIH can reportedly increase reactive oxygen species (ROS) generation, which subsequently cause vascular endothelial cadherin (VE-cadherin) cleavage, endothelial barrier injury, and dysfunction (Makarenko et al., 2014; Harki et al., 2021). Ras homolog gene family member A (RhoA) and its downstream Rho-associated protein kinase (ROCK) play crucial roles in both oxidative stress and endothelial barrier function (Shimokawa and Satoh, 2015; Komarova et al., 2017; Dee et al., 2019; Cong and Kong, 2020). cAMP/protein kinase A (PKA) signaling is a potent protective pathway to stabilize the endothelial barrier in response to oxidative stress, and an essential negative regulator of RhoA/ROCK (Qiao et al., 2003; Cong and Kong, 2020).

Salidroside is a typical pharmacological constituent found in medicinal plants under the Rhodiola genus. In addition to their anti-fatigue and anti-hypoxia roles in traditional medicine, Rhodiola extract, and salidroside also displayed medicinal properties as anti-cardiovascular diseases agents, which was mainly attributed to their antioxidant effects (Li et al., 2017; Zhao et al., 2021). *Rhodiola crenulata* exerts protective effects on hypoxia/high glucose-induced endothelial dysfunction and CIH-induced cardiac apoptosis (Lai et al., 2015; Chang et al., 2018; Huang et al., 2020). *Rhodiola rosea* extract attenuated pulmonary hypertension in chronic hypoxic rats (Kosanovic et al., 2013) and inhibited atherosclerosis formation in high fat diet-fed rabbits (Shen et al., 2008). Salidroside exhibited activity similar to that of Rhodiola extract. Salidroside improved CIH-mediated myocardial cell apoptosis (Zhong et al., 2010; Lai et al., 2014), chronic persistent hypoxia-induced pulmonary hypertension (Chen et al., 2016) and high fat diet-related atherosclerosis (Xing et al., 2015; Bai et al., 2020; Song et al., 2021) in animal models. Moreover, salidroside suppresses oxidative stress-induced HUVECs cell injury (Zhao et al., 2013; Zhu et al., 2016). Our previous study also demonstrated that salidroside could improve homocysteine-induced endothelium-dependent relaxation dysfunction by reducing oxidative stress (Leung et al., 2013). However, the effect of salidroside on endothelial barrier and CIH-aggravated atherosclerosis has not been reported. Wang et al. found that salidroside attenuated inflammatory responses by inhibiting the RhoA/ROCK pathway in vascular smooth muscle cells (Wang et al., 2021). Guan et al. reported that salidroside attenuated hydrogen peroxide-induced cell damage by elevating cAMP levels (Guan et al., 2011). Therefore, in the present study, we hypothesized that salidroside protects the integrity of endothelial barriers and alleviates CIH-aggravated atherosclerosis through effects on cAMP/PKA/RhoA signaling.

MATERIALS AND METHODS

Reagents

The following drugs were used: salidroside (98% purity; Sigma-Aldrich, St. Louis, MO, United States), H-89 dihydrochloride hydrate (PKA-specific inhibitor; Sigma-Aldrich), Y-27632 dihydrochloride (ROCK-specific inhibitor; Tocris Bioscience, Bristol, United Kingdom), and Fasudil hydrochloride (ROCK-specific inhibitor, Tocris Bioscience). All drugs were freshly dissolved in medium at the beginning of each experiment. The following primary antibodies were purchased from the cited commercial sources: zonula occludens 1 (ZO-1, Invitrogen, Carlsbad, CA, United States), VE-cadherin (Santa Cruz Biotechnology, Santa Cruz, CA, United States), CD31 (Invitrogen), ROCK (Abcam, Cambridge, United Kingdom), RhoA (Invitrogen and Abcam), and GAPDH (Abcam). FITC-conjugated anti-rabbit and anti-mouse secondary antibodies were purchased from Abcam.

Experiments in ApoE$^{-/-}$ Mice

All animal handling complied with the standard animal welfare regulations of Capital Medical University (Beijing, China). The Animal Subjects Committee of Capital Medical University approved the animal study protocol. Animals were randomly assigned to the experimental groups. Ten-week-old male ApoE$^{-/-}$ mice were purchased from HFK Bioscience (Beijing, China). All animals were fed a normal chow diet and maintained in a controlled environment with 12-h light/dark cycles,

temperature of 22 ± 2°C, and humidity of 50 ± 2%. To deliver CIH, mice were housed in an OxyCycler A84 System (BioSpherix, Redfield, NY, United States). Briefly, a gas control system regulated the room airflow (N_2 and O_2). A series of programs and flow regulators enabled manipulation of the fraction of inspired O_2 from 21 to 5.0% over a 90-s period, followed by rapid reoxygenation to normal air levels via a burst of 100% O_2 in the succeeding 30-s period. Hypoxic events occurred at a rate of one event per 120 s throughout the 12-h light period. During the 12-h dark period, CIH animals were maintained in a normoxic environment. Non-CIH mice were exposed to normoxia at all times. Mice were randomly assigned to one of three groups ($n = 8$ in each group): 1) control, mice not subjected to CIH, N.S., p. o.; 2) CIH, mice subjected to CIH, N.S., p. o.; and 3) CIH plus salidroside (CIH + Sali), mice subjected to CIH and salidroside (100 mg/kg/d), p. o. After 7 weeks, all mice were anesthetized with pentobarbital sodium and arterial blood were collected by cardiac puncture from the left ventricle. Then mice were perfused with ice-cold saline solution and their ascending aortas were collected for Oil Red O staining. Plaque sizes were quantified using Image-Pro Plus software (Media Cybernetic, Tokyo, Japan). Serial cross-sections (8 μm) of the heart throughout the entire aortic valve area were cut with a cryostat (CM 1900; Leica, Wetzlar, Germany). Sections stained with VE-cadherin (1:50; Cat. No. Sc-9989, Santa Cruz), CD31 (1:50; Cat. No. PA5-16301, Invitrogen), ROCK (1:100; Cat. No. 39749, Abcam), or RhoA (1: 50; Cat. No. PA5-87403, Invitrogen) were digitally scanned (Pannoramic DESK, P-MIDI, P250; 3DHISTECH, Budapest, Hungary) to obtain images for analysis by a previously described method (Yang et al., 2020). The methods for oral glucose tolerance test, insulin tolerance test, and biochemical analysis are included in the **Supplementary Material**.

Cell Culture and Treatment

All experiments using human umbilical vein endothelial cells (HUVECs) were approved by the Medical Ethics Committee of Beijing Anzhen Hospital (Approval No. 2017005) and conducted in accordance with guidelines of the Declaration of Helsinki. Written informed consent was obtained from all participating donors. Human umbilical cord veins were donated by the Maternal and Child Care Service Centre in Beijing, China. HUVECs were isolated, purified, and identified as described previously (Qin et al., 2012). Cells were cultured in VascuLife Basal Medium (Lifeline Cell Technology, Frederick, MD) supplemented with 2% fetal bovine serum, 5 ng/ml recombinant human epidermal growth factor, 10 mM L-glutamine, 1 mg/ml hydrocortisone hemisuccinate, 0.75 U/mL heparin sulfate, 0.2% EnGS (Lifeline Cell Technology), 10^4 U/mL penicillin, and 10^4 U/mL streptomycin (HyClone, Logan, UT) in humidified incubator with 95% air (v/v) and 5% CO_2 (v/v) at 37°C. HUVECs were used from passages 2–5.

The intermittent hypoxia (IH) protocol consisted of alternating cycles of 20-min hypoxia (1% O_2 and 5% CO_2) and 20-min reoxygenation (21% O_2 and 5% CO_2), using a BioSpherix OxyCycler C42 system (BioSpherix, Redfield, NY, United States). The total duration of one cycle was 40 min. Cultured HUVECs were pretreated with the indicated concentration of drugs for 2 h and then exposed to the indicated number of cycles of IH.

Measurement of Transendothelial Electrical Resistance

HUVECs were seeded in the top chambers of 24-well Transwell plates (8.0-μm pore size; Cat. No. 35-3097; Becton-Dickinson, Franklin Lakes, NJ, United States) at a density of 1×10^4 cells/well. Volumes of culture media in the top and lower chambers were 300 and 700 μL, respectively. TEER was measured using a Millicell-ERS (MERS00002; Millipore, Burlington, MA, United States), as previously described (Li et al., 2015). Values for blank wells and cell wells represented the blank resistance (R blank) and sample resistance (R Sample), respectively. The following calculation was performed: TEER = (R Sample)–(R blank). The effect of IH on TEER was determined in HUVECs after 9, 18, 36, 72, and 108 cycles of IH exposure. The effect of drugs on permeability was determined in HUVECs pretreated with salidroside (10 μM or 100 μM), H-89 (10 μM), Y27632 (10 μM), or Fasudil (10 μM) for 2 h before exposure to either normoxia or 72 cycles of IH.

Measurement of HUVEC Permeability to FITC-Dextran

HUVECs were seeded in the top chambers of 24-well Transwell plates (0.4-μm pore size polyester membrane inserts; Corning, Corning, NY, United States) at a density of 1×10^4 cells/well. Volumes of culture media in the top and lower chambers were 200 and 700 μL, respectively. Permeability was measured by adding 1 mg/ml FITC-dextran (70 kDa; Sigma-Aldrich) immediately after IH exposure. Following a 20-min incubation with FITC-dextran, 100 μL of medium was aspirated from each of the lower chambers into wells of black 96-well microplates (Nunc, Roskilde, Denmark). The fluorescence value of each well was determined by an EnSpire 2300 Multimode Plate Reader (PerkinElmer, Waltham, MA, United States) at a 490-nm excitation wavelength and 525-nm emission wavelength. The effect of IH on permeability of HUVECs to FITC-dextran was determined after 9, 18, 36, 72, and 108 cycles of IH exposure. The effect of salidroside on permeability was determined in HUVECs pretreated with salidroside (10 μM or 100 μM) for 2 h before exposure to either normoxia or 72 cycles of IH.

Assay of ROS Production

Intracellular ROS was detected by fluorescence microscopy and quantitated by a plate reader using 2′,7′-dichlorofluorescein diacetate (DCFH-DA, Sigma-Aldrich) as the probe, as previously described (Naha et al., 2010). HUVECs were cultured in black 96-well microplates (Nunc) at a density of 4×10^5 cells/mL in 100 μL of medium. After exposure to drugs under normoxia or IH, microplates were washed with 100 μL/well of phosphate-buffered saline (PBS) and then 100 μL of 10 μM DCFH-DA was added to each well. After incubating the microplates at 37°C for 20 min and washing three times with PBS, an EnSpire 2300 plate reader was used to quantify the

fluorescence of each well at a 490-nm excitation wavelength and 525-nm emission wavelength. Fluorescence images were obtained with a Ni-U Nikon Upright Microscope equipped with a DS-Ri2 color charge-coupled device (Nikon, Tokyo, Japan). The effect of each drug on ROS production was determined in HUVECs pretreated with salidroside (10 μM or 100 μM), Tiron (10 μM), H-89 (10 μM), Y27632 (10 μM), or Fasudil (10 μM) for 2 h before exposure to either normoxia or 72 cycles of IH.

GST Pull-Down Assay to Evaluate RhoA Activity

After experimental treatments, HUVECs were lysed and cell lysates were collected. The supernatant was centrifuged at 4°C at 700 g for 10 min. The resulting protein was quantified by bicinchoninic acid method, and GST-RBD fusion was added to the total protein samples of each group. After incubation at 4°C for 1 h, protein samples were centrifuged at 1900 g for 3 min. The precipitated protein was GST-bound. Expression of RhoA protein in total and GST-bound samples was detected by western blot using a rabbit monoclonal RhoA antibody (1:1,000; Cat. No. ab187027, Abcam). RhoA protein in the total protein sample was expressed as total RhoA, while RhoA protein in the GST-bound protein sample was expressed as GTP-RhoA. The ratio of GTP-RhoA expression to total RhoA expression reflected the activity level of RhoA in HUVECs.

Measurement of Intracellular cAMP

HUVECs were cultured by seeding 100 μL of cell suspension with a density of 1×10^5 cells/mL in wells of 24-well plates. After exposure to drugs under normoxia or IH, intracellular cAMP was extracted with hydrochloric acid (HCl, 0.1 M). cAMP concentrations were assessed with a cAMP Assay Kit (Cat. No. ab65355, Abcam) according to the manufacturer's protocol. The effect of drugs on intracellular cAMP was determined in HUVECs pretreated with salidroside (10 μM or 100 μM) for 2 h before exposure to either normoxia or 72 cycles of IH.

Immunostaining for HUVECs

HUVECs were exposed to either normoxia or 72 cycles of IH, and then fixed with methanol for 30 min at −40°C. After blocking with 3% bovine serum albumin for 30 min, cells were incubated overnight with primary antibodies against VE-cadherin (1:100; Cat. No. 36-1900, Invitrogen) and ZO-1 (1:100; Cat. No. 33-9100, Invitrogen). The following day, cells were washed three times with PBS and incubated with FITC-conjugated anti-mouse and TRITC-conjugated anti-rabbit secondary antibodies (1:200) for 1 h at room temperature. Images of immunofluorescence staining were acquired with a Leica TCS SP2 confocal laser-scanning microscope.

Western Blot Analysis

To extract protein from HUVECs, a protein extraction kit containing protease inhibitors and a protein phosphatase inhibitor cocktail was used (Thermo Fisher Scientific). Equal amounts of protein (30 μg/lane) were separated by 10% sodium dodecyl sulfate polyacrylamide gel electrophoresis. Blots were probed overnight at 4°C with primary antibodies (1:1,000), washed with Tris-buffered saline containing Tween 20, and incubated with secondary antibodies (1:10,000; ZSGB-BIO, Beijing, China) for 1 h at room temperature. Finally, blots were washed, incubated with SuperSignal™ WestFemto Maximum Sensitivity Substrate (Thermo Fisher Scientific), and analyzed using a ChemiDoc™ Touch Imaging System (Bio-Rad, Hercules, CA, United States).

Statistical Analysis

Data were analyzed using Prism 5.0 software (GraphPad Software, San Diego, CA) and are presented as mean ± standard deviation (SD). In all cases, the results of at least three independent experiments were used. Statistical comparisons between two groups were performed using Student's *t*-test. Multiple comparison tests used one-way analysis of variance with Bonferroni's procedure. Values of $p < 0.05$ were considered statistically significant.

RESULTS

Salidroside Alleviated Atherosclerotic Lesion Formation in CIH-Exposed ApoE$^{-/-}$ Mice

Analysis of Oil Red O staining revealed a significant increasein lipid accumulation ($p < 0.01$) in aortic sinus tissue of CIH mice compared with control mice, as well as a significant decrease ($p < 0.05$) in CIH + Sali mice compared with CIH mice (**Figures 1A,B**). Salidroside did not alter fasting blood glucose, oral glucose tolerance, fasting blood triglyceride, fasting total blood cholesterol, or insulin sensitivity levels in CIH-exposed ApoE$^{-/-}$ mice (**Supplementary Figures S1A–E**). To determine the effect of salidroside on endothelial barriers in CIH-exposed ApoE$^{-/-}$ mice, immunohistochemistry, and immunofluorescence double staining was conducted to measure expression levels of VE-cadherin, CD31, and ROCK in aortic plaques. As shown in **Figures 1A,C–E**, a significant decrease in VE-cadherin ($p < 0.001$) and significant increase of ROCK ($p < 0.01$) were observed in the CIH group compared with the control group. Meanwhile, salidroside significantly increased VE-cadherin ($p < 0.001$) and significantly attenuated ROCK expression ($p < 0.01$).

Salidroside Ameliorated IH-Induced Endothelial Barrier Dysfunction in HUVECs

Endothelial barrier function was assayed by measuring TEER and permeability to FITC-dextran in HUVECs immediately after IH exposure. Compared with the normoxia group, IH exposure significantly decreased TEER ($p < 0.001$) and increased permeability to FITC-dextran ($p < 0.001$) of HUVECs in a time-dependent manner, reaching a plateau with 72 cycles of IH (**Figures 2A,B**). Therefore, the following studies were performed on HUVECs exposed to 72 cycles of IH. Pretreatment of HUVECs with salidroside (10 μM or100 μM) dose-dependently and significantly increased TEER ($p < 0.01$) and decreased permeability to FITC-dextran ($p < 0.01$) compared with the IH group (**Figures 2C,D**).

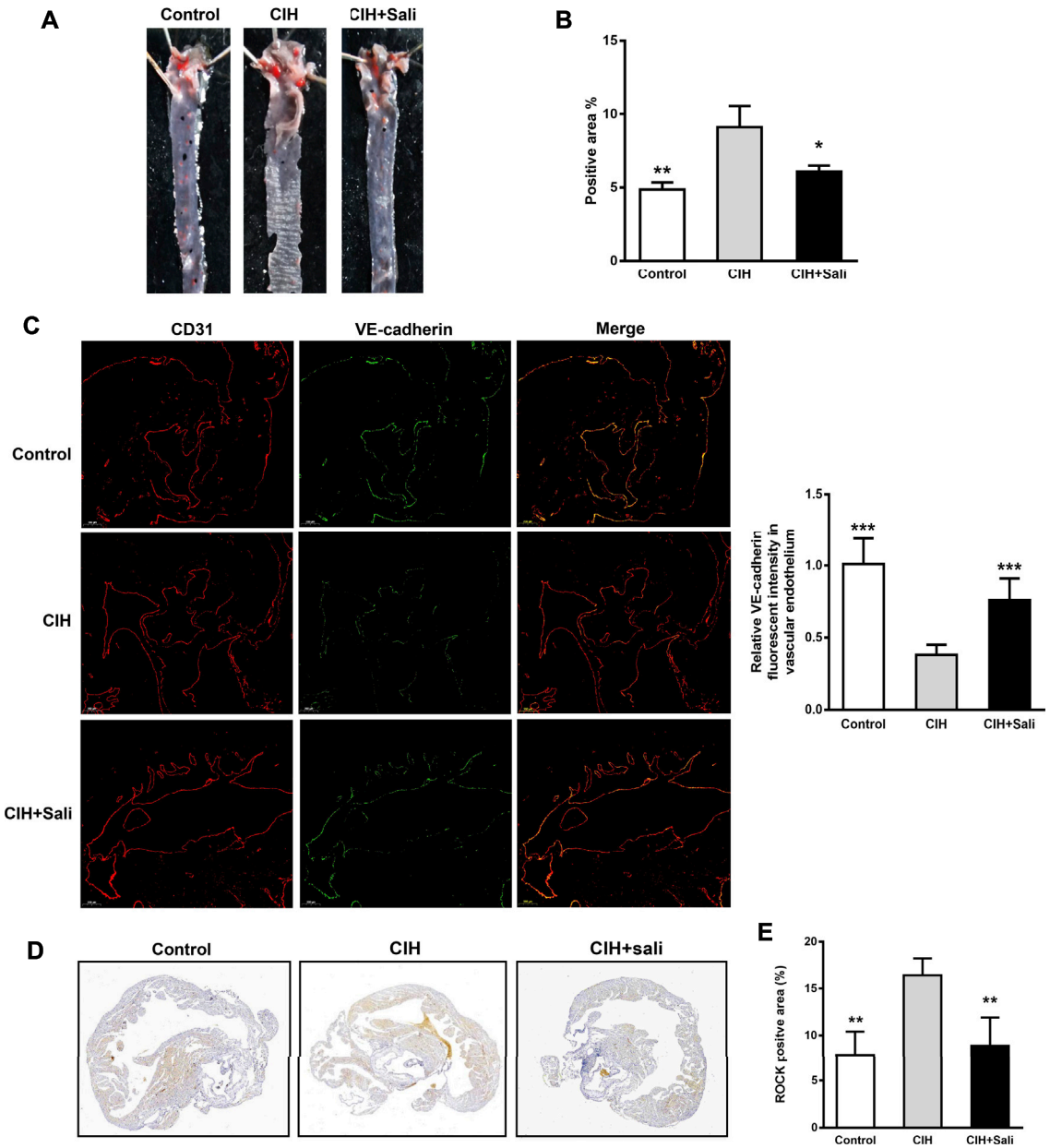

FIGURE 1 | Salidroside attenuated CIH-aggravated atherosclerosis in ApoE$^{-/-}$ mice. Male ApoE$^{-/-}$ mice were randomly divided into normoxia (control), CIH, and CIH + Sali groups. After experimental intervention for 7 weeks, mice were sacrificed under anesthesia **(A)** Representative images of aortic Oil Red O staining **(B)** Quantitative summary of atherosclerotic lesions in aortas (n = 4) **(C)** Immunofluorescence staining of VE-cadherin and CD31 and relative fluorescent intensity of VE-cadherin in the endothelium of aortic roots (5 × magnification, n = 3 sections per tissue, at least three analysis sites per slide) **(D)** Plaques of aortic roots were stained with ROCK (2 × magnification) **(E)** Quantitative summary of ROCK expression in aortic root plaques (n = 4). CIH, chronic intermittent hypoxia; Sali, salidroside; VE-cadherin, vascular endothelial cadherin; ROCK, Rho-associated protein kinase. All data are presented as mean ± SD. *p < 0.05, **p < 0.01, and ***p < 0.001 compared with CIH group.

Salidroside Ameliorated the Suppressive Effect of IH on VE-Cadherin and ZO-1 Expression in HUVECs

As shown in **Figures 3A,B**, IH-exposed HUVECs displayed obvious disruptions of VE-cadherin and ZO-1 by immunofluorescence staining that were dose-dependently ameliorated by salidroside pretreatment. Similarly, western blot assay results showed that IH exposure significantly reduced protein expression levels of VE-cadherin (p < 0.001) and ZO-1 (p < 0.001), but this effect was largely reversed by salidroside pretreatment (p < 0.001, **Figures 3C–E**).

Salidroside Attenuated IH-Induced ROS Overproduction in HUVECs

ROS play a major role in IH-related endothelial dysfunction. To determine whether salidroside attenuated IH-induced

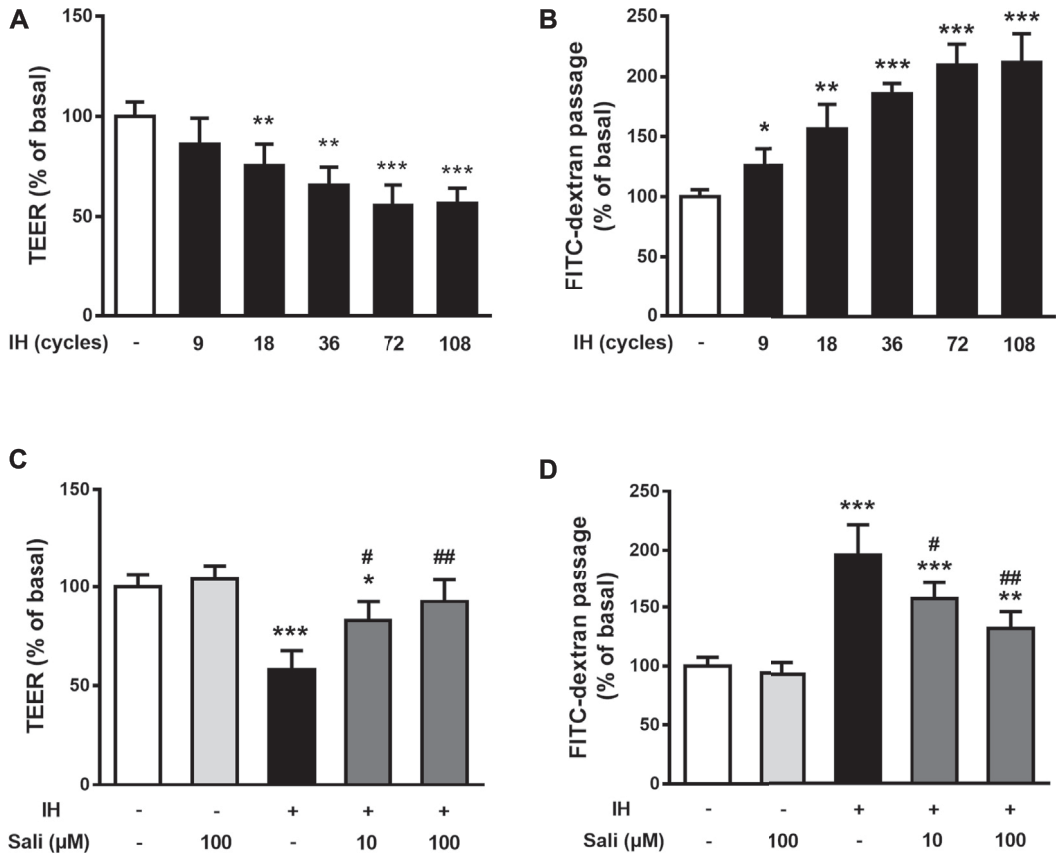

FIGURE 2 | Salidroside ameliorated IH-induced endothelial barrier dysfunction in HUVECs. The effects of IH on TEER **(A)** and permeability to FITC-dextran **(B)** were determined in HUVECs after 9, 18, 36, 72, 108 cycles of IH exposure. Effects of Sali on TEER **(C)** and permeability to FITC-dextran **(D)** were determined in HUVECs pretreated with Sali (10 μM or 100 μM) for 2 h before exposure to either normoxia or 72 cycles of IH. IH, intermittent hypoxia [one cycle includes reducing O_2 for a 20-min hypoxia period (5% O_2 and 5% CO_2) followed by 20-min reoxygenation (21% O_2 and 5% CO_2)]; Sali, salidroside; TEER, transendothelial electrical resistance. All data are presented as mean ± SD. #$p < 0.05$ and ##$p < 0.01$ compared with IH group; *$p < 0.05$, **$p < 0.01$, and ***$p < 0.001$ compared with normoxia group.

oxidative stress in HUVECs, intracellular ROS production was measured by a fluorescent method. Immunostaining revealed elevated ROS production in the IH group, which was decreased in groups treated with salidroside (10 and 100 μM) or the ROS scavenger Tiron (**Figure 4A**). Quantification of fluorescence assay results further showed that exposure to 72 cycles of IH significantly increased ROS production ($p < 0.001$) in HUVECs, while salidroside could dose-dependently and significantly suppress ROS production ($p < 0.001$) in IH-exposed HUVECs (**Figure 4B**).

Salidroside Elevated Intracellular cAMP in IH-Exposed HUVECs

Endothelial cAMP is one of the most potent endothelial barrier stabilizers. As shown in **Figure 5A**, IH exposure did not affect cellular cAMP levels in HUVECs. However, salidroside significantly increased cAMP levels up to 2.4-fold compared with the IH group ($p < 0.001$).

Salidroside Suppressed IH-Induced Elevation of RhoA Activity and ROCK Protein Expression in HUVECs Through the PKA Pathway

We next examined the effect of salidroside on RhoA activity and ROCK protein expression in HUVECs. Exposure of HUVECs to 72 cycles of IH significantly upregulated RhoA activity ($p < 0.001$) and ROCK ($p < 0.001$) expression. Pretreatment of HUVECs with salidroside significantly reduced IH-induced increases in RhoA activity ($p < 0.001$) and ROCK expression ($p < 0.01$). The PKA-specific inhibitor H-89 significantly attenuated the effect of salidroside on reducing RhoA/ROCK signaling ($p < 0.001$, **Figures 5B–D**).

Salidroside Ameliorated IH-Induced ROS Overproduction and Endothelial Barrier Dysfunction in HUVECs *via* cAMP/PKA/RhoA Signaling

The ROCK-selective inhibitors Y27632 and Fasudil were employed to further explore the mechanism of salidroside. IH

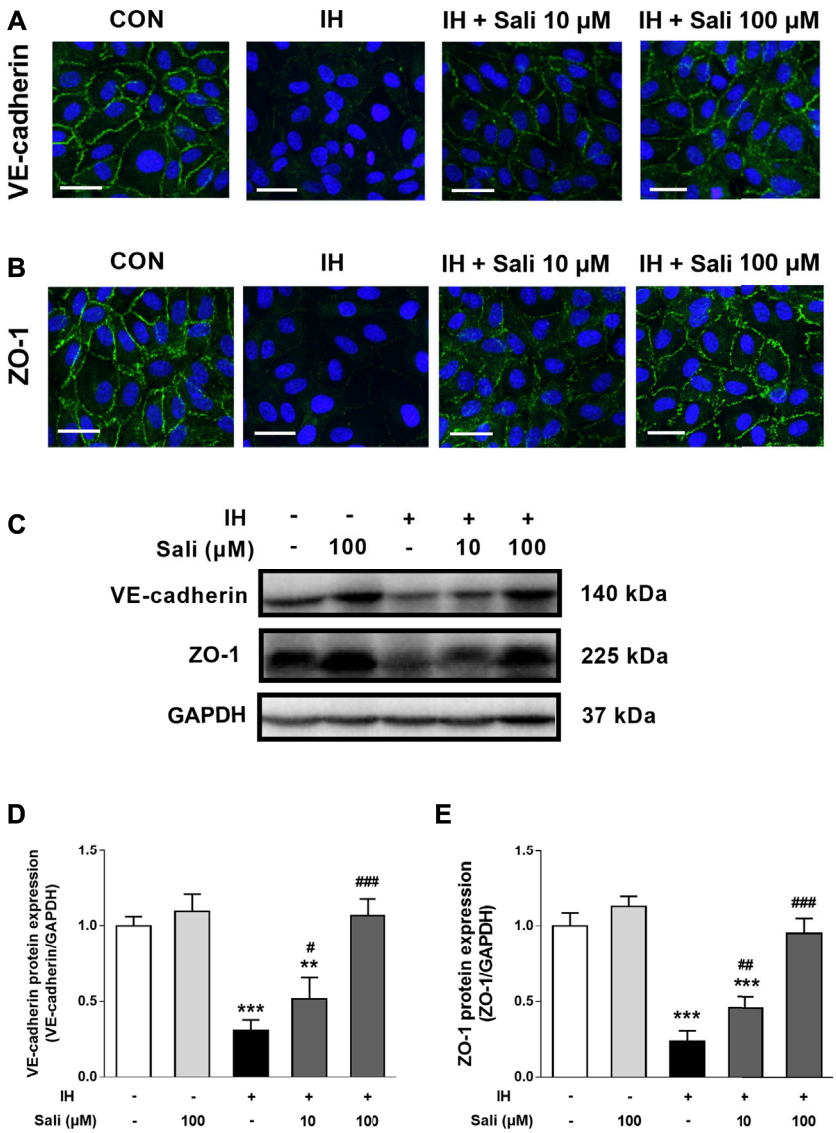

FIGURE 3 | Salidroside ameliorated the suppressive effect of IH on VE-cadherin and ZO-1 expression in HUVECs. HUVECs were pretreated with Sali (10 μM or 100 μM) for 2 h before exposure to 72 cycles of IH **(A)** Immunofluorographs of VE-cadherin (20 × magnification; Bar = 50 μm) and **(B)** ZO-1 (20 × magnification; Bar = 50 μm) **(C)** VE-cadherin and ZO-1 protein levels were measured by western blot analysis **(D–E)** Relative protein levels of VE-cadherin and ZO-1 were quantified by densitometry analysis. IH, intermittent hypoxia; Sali, salidroside; VE-cadherin, vascular endothelial cadherin; ZO-1, zonula occludens 1. All data are presented as mean ± SD. #$p < 0.05$, ##$p < 0.01$, and ###$p < 0.001$ compared with IH group; **$p < 0.01$ and ***$p < 0.001$ compared with normoxia group.

exposure increased ROS production and induced barrier dysfunction in HUVECs, the effects of which were significantly attenuated by salidroside ($p < 0.01$). Similar to salidroside, pretreatment of HUVECs with Y27632 or Fasudil markedly ameliorated IH-induced ROS generation ($p < 0.001$) and barrier disruption ($p < 0.01$ or $p < 0.001$). Moreover, the inhibitory effects of salidroside on IH-induced ROS accumulation ($p < 0.001$) and endothelial barrier disruption ($p < 0.001$) were significantly attenuated by H-89 (**Figures 6A,B**). Taken together, these results suggest that salidroside ameliorated IH-induced ROS production and barrier dysfunction in HUVECs *via* the cAMP/PKA/RhoA signaling pathway.

DISCUSSION

The observations of this study can be summarized as follows. Firstly, salidroside ameliorated CIH-induced atherosclerosis progression and barrier injury in normal chow diet-fed $ApoE^{-/-}$ mice. Secondly, salidroside inhibited the deleterious effect of IH on barrier function of HUVECs through effects on cAMP/PKA/RhoA signaling. Furthermore, similar to salidroside, the ROCK inhibitors Y27632 and Fasudil protected HUVECs from IH-induced ROS overproduction and endothelial barrier disruption. This research demonstrates for the first time that salidroside has a protective effect on endothelial

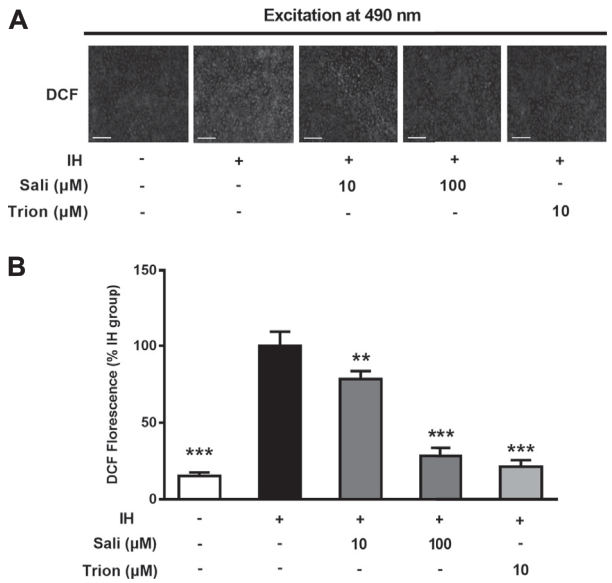

FIGURE 4 | Salidroside attenuated IH-induced ROS overproduction in HUVECs. Intracellular ROS levels were determined in HUVECs pretreated with Sali (10 μM or 100 μM) or Tiron (10 μM) for 2 h before exposure to either normoxia or 72 cycles of IH. DCFH-DA was used as a fluorescent probe for ROS. Tiron was used as a positive control **(A)** Fluorographs of intracellular ROS were acquired with a fluorescence microscope (5 × magnification; Bar = 500 μm) **(B)** Fluorescence quantification results of intracellular ROS. IH, intermittent hypoxia; Sali, salidroside; DCFH-DA, 2′,7′-dichlorofluorescein diacetate; ROS, reactive oxygen species. All data are presented as mean ± SD. $^{*}p < 0.05$ and $^{***}p < 0.001$ compared with IH group.

barrier function *via* cAMP/PKA/RhoA signaling. These results also suggest that RhoA/ROCK signaling plays important roles in IH-induced oxidative stress and disruption of endothelial integrity, representing a novel mechanism by which sleep breathing disorders exacerbate atherosclerosis.

Clinical and basic studies have demonstrated a causal relationship between CIH and atherosclerosis. Continuous positive airway pressure (CPAP) treatment, which is mainly used to correct CIH in OSA patients, can reduce intima-media thickness and femoral artery wave velocity to improve the early signs of atherosclerosis (Drager et al., 2007; Chen et al., 2017). In addition, CIH promoted atherosclerotic plaque formation in both normal and high cholesterol diet-fed ApoE$^{-/-}$ mice (Drager et al., 2013; Gautier-Veyret et al., 2013; Gileles-Hillel et al., 2014) However, CPAP cannot improve the incidence or mortality rate of cardiovascular diseases in OSA patients, and compliance with CPAP treatment was shown to be very low in actual practice (McEvoy et al., 2016; Peker et al., 2016). Therefore, potential drugs for OSA-related atherosclerotic cardiovascular diseases remain to be further investigated. Salidroside can improve atherosclerosis in high fat diet-fed ApoE$^{-/-}$ mice (Bai et al., 2020; Song et al., 2021). However, the effect of salidroside on CIH-related atherosclerosis has not been reported. Consistent with previous studies, our results indicate that CIH can significantly promote the progression of atherosclerosis in normal chow diet-fed ApoE$^{-/-}$ mice. However, we are the first to report that salidroside can significantly reduce CIH-aggravated plaque progression.

Endothelial barrier dysfunction is the key factor in triggering and aggravating the formation of atherosclerosis. Previous studies showed that endothelial cells in the intima of human atherosclerotic plaques are wider and the endothelial barrier is destroyed, leading to infiltration of various inflammatory cells and the formation of lipid-rich foam cells, a key pathological change of atherosclerosis (Pi et al., 2018). The fundamental basis for barrier function is predominantly maintained by adherens junctions and tight junctions (Komarova et al., 2017). The adherent junction protein VE-cadherin and tight junction protein ZO-1 are important factors to maintain and regulate endothelial barrier function. CIH can reportedly increase vascular permeability and impair endothelial barrier function by VE-cadherin cleavage (Makarenko et al., 2014; Harki et al., 2021). Consistent with previous studies, exposure of HUVECs to IH decreased TEER, increased permeability to FITC-dextran, and suppressed expression of junction proteins VE-cadherin and ZO-1. *In vivo*, CIH significantly reduced VE-cadherin expression in the aortas of ApoE$^{-/-}$ mice. We found that salidroside significantly improved IH-induced endothelial barrier injury in both ApoE$^{-/-}$ mice and HUVECs, suggesting that salidroside may alleviate CIH-aggravated atherosclerosis by improving endothelial barrier damage, and endothelial barrier dysfunction may be a mechanism by which IH aggravates atherosclerosis.

Oxidative stress caused by ROS overproduction is a common mechanism of endothelial barrier dysfunction in both OSA and atherosclerotic diseases (Lévy et al., 2015). The RhoA/ROCK pathway plays a crucial role in ROS augmentation and endothelial barrier function (Shimokawa and Satoh, 2015; Komarova et al., 2017; Dee et al., 2019; Cong and Kong, 2020). Accumulating evidence indicates that Rho-kinase inhibitors have beneficial effects for the treatment of cardiovascular diseases (Dai et al., 2018; Lei et al., 2020). Exposure to IH activated RhoA/Rho-kinase in the aorta and mesenteric arteries of animal models, which is required for IH-induced arterial remodeling, and hypertension (de Frutos et al., 2010; Lu et al., 2017; Li et al., 2018). However, it remains unknown whether the RhoA/ROCK pathway is involved in IH-induced endothelial barrier dysfunction and, if so, what mechanisms are involved. In the present study, we observed that IH increased ROCK expression in the aortas of ApoE$^{-/-}$ mice, as well as ROS generation, RhoA activity, and ROCK expression in HUVECs. Furthermore, the ROCK-selective inhibitors Y27632 and Fasudil attenuated IH-induced ROS overproduction and endothelial barrier disruption. These results suggest that the RhoA/ROCK pathway is essential for IH-induced ROS augmentation and endothelial barrier dysfunction. Because ROS also activates the RhoA/ROCK pathway in endothelial cells (Lu et al., 2017; Li et al., 2018), IH-induced ROS overproduction likely activates RhoA/ROCK pathway, thus creating a vicious cycle for ROS augmentation and endothelial barrier breakdown. Salidroside treatment reversed the increase of ROCK expression in aortas of chronic IH-exposed ApoE$^{-/-}$ mice. Moreover, similar to the ROCK-selective inhibitors Y26732 and Fasudil, salidroside reduced RhoA/ROCK activation and protected HUVECs from ROS overproduction and endothelial

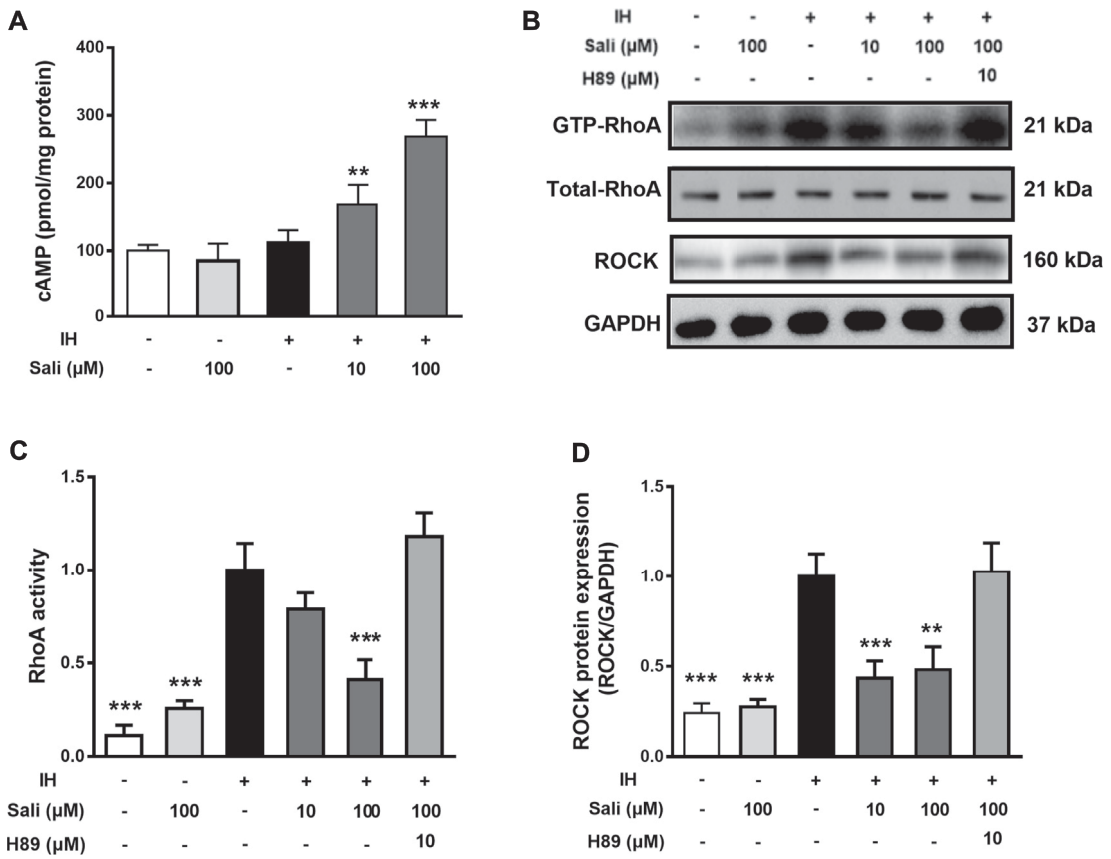

FIGURE 5 | Salidroside suppressed IH-induced elevation of RhoA activity and ROCK protein expression in HUVECs through the cAMP/PKA pathway. HUVECs were pretreated with Sali (10 μM or 100 μM) or the PKA inhibitor H-89 for 2 h before exposure to 72 cycles of IH **(A)** Intracellular cAMP levels, as well as **(B)** RhoA activity and ROCK protein levels were measured **(C–D)** Relative levels of RhoA activity and ROCK protein expression were quantified by densitometry analysis. IH, intermittent hypoxia; Sali, salidroside; RhoA, ras homolog gene family member A; ROCK, Rho-associated protein kinase. All data are presented as mean ± SD. $^{*}p < 0.05$ and $^{***}p < 0.001$ compared with IH group.

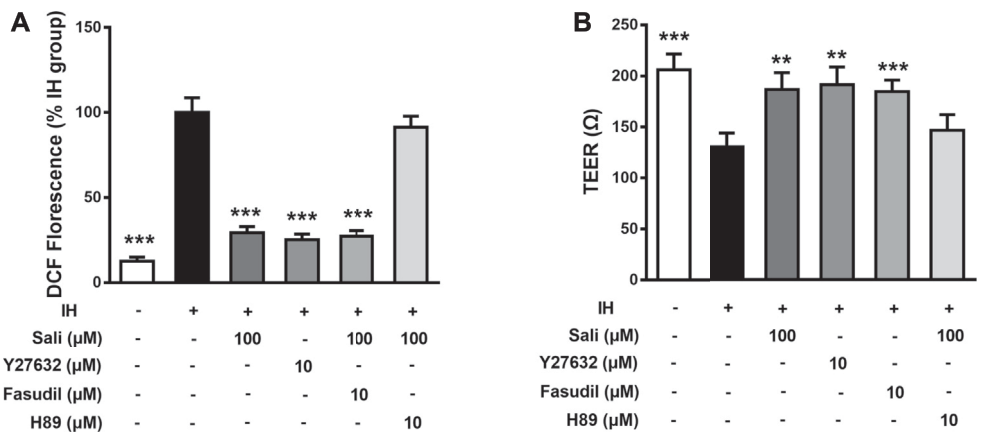

FIGURE 6 | Salidroside ameliorated IH-induced ROS overproduction and barrier dysfunction in HUVECs *via* the cAMP/PKA/RhoA signaling pathway. Effects of drugs on ROS generation **(A)** and TEER **(B)** were determined in HUVECs pretreated with Sali (100 μM), H-89 (10 μM), Y27632 (10 μM), or Fasudil (10 μM) for 2 h before exposure to either normoxia or 72 cycles of IH. IH, intermittent hypoxia; Sali, salidroside; ROS, reactive oxygen species; TEER, transendothelial electrical resistance. All data are presented as mean ± SD of three experiments. $^{***}p < 0.001$ compared with IH group.

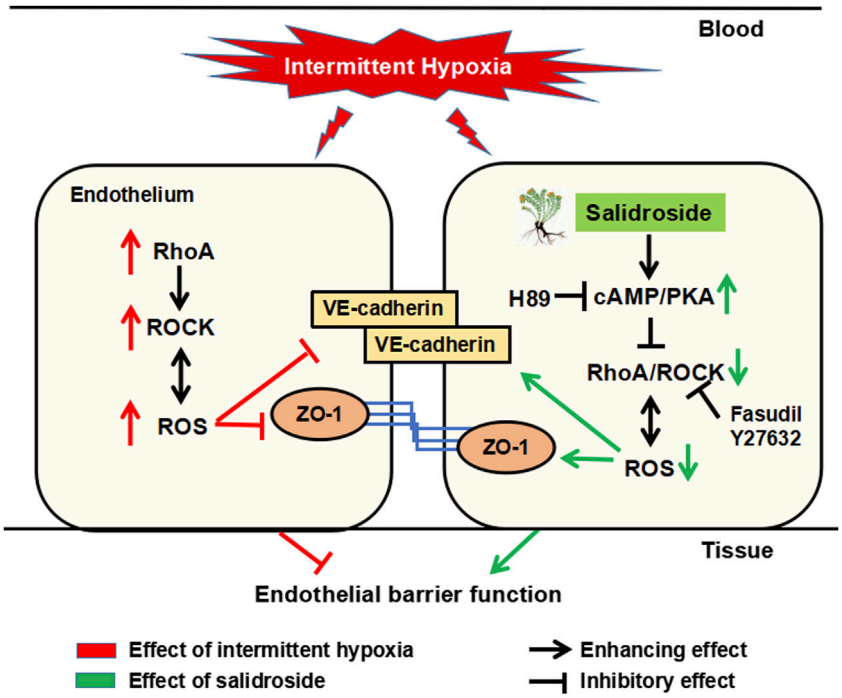

FIGURE 7 | Schematic diagram of the potential mechanism by which salidroside protects against IH-induced ROS overproduction and barrier disruption in the endothelium. Salidroside increased intracellular cAMP levels, which subsequently activated PKA in HUVECs. Activated cAMP/PKA suppressed IH-induced elevation of RhoA and ROCK, and thereafter inhibited ROS generation. In turn, reduced ROS production inhibited RhoA/ROCK expression, breaking the vicious cycle of ROS augmentation induced by IH in the endothelium. IH, intermittent hypoxia; ROS, reactive oxygen species; RhoA, ras homolog gene family member A; ROCK, Rho-associated protein kinase; PKA, protein kinase A.

barrier disruption induced by IH. These results suggest that the molecular mechanism by which salidroside improved IH-mediated endothelial barrier dysfunction and atherosclerosis was be related to the RhoA/ROCK signaling pathway.

An increase in endothelial cAMP is one of the most potent triggers to stabilize the endothelial barrier against almost any barrier-compromising stimulus (Schlegel and Waschke, 2014; Radeva and Waschke, 2018). Furthermore, cAMP/PKA is an essential negative regulator of RhoA/ROCK (Qiao et al., 2003; Cong and Kong, 2020). Our results suggest that salidroside significantly increased the cAMP level of IH-exposed HUVEC cells (2.4-fold), whereas the PKA-specific inhibitor H-89 attenuated the RhoA/ROCK inhibition, ROS clearance, and barrier protection effects of salidroside. These findings indicate that cAMP/PKA activation acts upstream of RhoA/ROCK inhibition to elicit the endothelial barrier-protective effect of salidroside.

Salidroside did not affect the glucolipid metabolism or insulin sensitivity of CIH-exposed ApoE$^{-/-}$ mice. Therefore, the beneficial effects of salidroside were not secondary to the improvement of glucolipid metabolism or insulin resistance. Moreover, the present results indicate that salidroside has only a moderate regulatory effect under pathophysiological conditions. Under normal conditions, barrier-forming junction proteins undergo dynamic regulation of assembly and disassembly. During these processes, proper Rho activity is very important to maintain the endothelial barrier in a healthy state (Terry et al., 2010). The application of salidroside did not inhibit RhoA activity below a physiological level, but instead maintained RhoA activity at a medium activation level in IH-treated HUVECs, which could provide reliable evidence for the safety of salidroside. However, it remains far from clinical application. The study provides a reference for future clinical research.

In summary, salidroside exerted significant barrier-protective and anti-atherosclerosis effects against IH *via* the cAMP/PKA/RhoA signaling pathway (**Figure 7**). We propose that this evidence supports potential therapeutic actions of salidroside in applications for OSA-associated vascular system protection.

DATA AVAILABILITY STATEMENT

The original contributions presented in the study are included in the article/**Supplementary Material**, further inquiries can be directed to the corresponding author.

ETHICS STATEMENT

The studies involving human participants were reviewed and approved by the Medical Ethics Committee of Beijing Anzhen Hospital (Approval No. 2017005). The patients/participants provided their written informed consent to participate in this

study. The animal study was reviewed and approved by The Animal Subjects Committee of Capital Medical University approved the animal study protocol.

AUTHOR CONTRIBUTIONS

LL designed and performed research, and wrote the paper; YY, HZ, YD, XJ, HY, YW, QL, FL, and QS performed research and analyzed data; YQ designed research.

FUNDING

This study was supported by the Beijing Talents Fund (No. 2016000021469G193), Natural Science Foundation of China (Grant Nos. 81970224 and 81670331), Beijing Natural Science Foundation (Grant No. 7192030), and the Beijing Billion Talent Project (No. 2017-A-10).

ACKNOWLEDGMENTS

We thank Liwen Bianji, Edanz Group China (www.liwenbianji.cn/ac), for editing the English text of a draft of this manuscript.

SUPPLEMENTARY MATERIAL

The Supplementary Material for this article can be found online at: https://www.frontiersin.org/articles/10.3389/fphar.2021.723922/full#supplementary-material

REFERENCES

Ali, S. S., Oni, E. T., Warraich, H. J., Blaha, M. J., Blumenthal, R. S., Karim, A., et al. (2014). Systematic Review on Noninvasive Assessment of Subclinical Cardiovascular Disease in Obstructive Sleep Apnea: New Kid on the Block!. *Sleep Med. Rev.* 18, 379–391. doi:10.1016/j.smrv.2014.01.004

Bai, X., Jia, X., Lu, Y., Zhu, L., Zhao, Y., Cheng, W., et al. (2020). Salidroside-mediated Autophagic Targeting of Active Src and Caveolin-1 Suppresses Low-Density Lipoprotein Transcytosis across Endothelial Cells. *Oxid Med. Cel Longev* 2020, 9595036. doi:10.1155/2020/9595036

Bradley, T. D., and Floras, J. S. (2009). Obstructive Sleep Apnoea and its Cardiovascular Consequences. *Lancet* 373, 82–93. doi:10.1016/S0140-6736(08)61622-0

Chang, P. K., Yen, I. C., Tsai, W. C., Chang, T. C., and Lee, S. Y. (2018). Protective Effects of Rhodiola Crenulata Extract on Hypoxia-Induced Endothelial Damage via Regulation of AMPK and ERK Pathways. *Int. J. Mol. Sci.* 19. doi:10.3390/ijms19082286

Chen, L. D., Lin, L., Lin, X. J., Ou, Y. W., Wu, Z., Ye, Y. M., et al. (2017). Effect of Continuous Positive Airway Pressure on Carotid Intima-media Thickness in Patients with Obstructive Sleep Apnea: A Meta-Analysis. *PLoS ONE* 12, e0184293. doi:10.1371/journal.pone.0184293

Chen, M., Cai, H., Yu, C., Wu, P., Fu, Y., Xu, X., et al. (2016). Salidroside Exerts Protective Effects against Chronic Hypoxia-Induced Pulmonary Arterial Hypertension via AMPKα1-dependent Pathways. *Am. J. Transl Res.* 8, 12–27.

Cong, X., and Kong, W. (2020). Endothelial Tight Junctions and Their Regulatory Signaling Pathways in Vascular Homeostasis and Disease. *Cell. Signal.* 66, 109485. doi:10.1016/j.cellsig.2019.109485

Dai, Y., Luo, W., and Chang, J. (2018). Rho Kinase Signaling and Cardiac Physiology. *Curr. Opin. Physiol.* 1, 14–20. doi:10.1016/j.cophys.2017.07.005

de Frutos, S., Caldwell, E., Nitta, C. H., Kanagy, N. L., Wang, J., Wang, W., et al. (2010). NFATc3 Contributes to Intermittent Hypoxia-Induced Arterial Remodeling in Mice. *Am. J. Physiol. Heart Circ. Physiol.* 299, H356–H363. doi:10.1152/ajpheart.00341.2010

Dee, R. A., Mangum, K. D., Bai, X., Mack, C. P., and Taylor, J. M. (2019). Druggable Targets in the Rho Pathway and Their Promise for Therapeutic Control of Blood Pressure. *Pharmacol. Ther.* 193, 121–134. doi:10.1016/j.pharmthera.2018.09.001

Döring, Y., Noels, H., van der Vorst, E. P. C., Neideck, C., Egea, V., Drechsler, M., et al. (2017). Vascular CXCR4 Limits Atherosclerosis by Maintaining Arterial Integrity: Evidence from Mouse and Human Studies. *Circulation* 136, 388–403. doi:10.1161/CIRCULATIONAHA.117.027646

Drager, L. F., Bortolotto, L. A., Figueiredo, A. C., Krieger, E. M., and Lorenzi, G. F. (2007). Effects of Continuous Positive Airway Pressure on Early Signs of Atherosclerosis in Obstructive Sleep Apnea. *Am. J. Respir. Crit. Care Med.* 176, 706–712. doi:10.1164/rccm.200703-500OC

Drager, L. F., Yao, Q., Hernandez, K. L., Shin, M. K., Bevans-Fonti, S., Gay, J., et al. (2013). Chronic Intermittent Hypoxia Induces Atherosclerosis via Activation of Adipose Angiopoietin-like 4. *Am. J. Respir. Crit. Care Med.* 188, 240–248. doi:10.1164/rccm.201209-1688OC

Gautier-Veyret, E., Arnaud, C., Bäck, M., Pépin, J. L., Petri, M. H., Baguet, J. P., et al. (2013). Intermittent Hypoxia-Activated Cyclooxygenase Pathway: Role in Atherosclerosis. *Eur. Respir. J.* 42, 404–413. doi:10.1183/09031936.00096512

Gibbons, G. H., Seidman, C. E., and Topol, E. J. (2021). Conquering Atherosclerotic Cardiovascular Disease - 50 Years of Progress. *N. Engl. J. Med.* 384, 785–788. doi:10.1056/NEJMp2033115

Gileles-Hillel, A., Almendros, I., Khalyfa, A., Zhang, S. X., Wang, Y., and Gozal, D. (2014). Early Intermittent Hypoxia Induces Proatherogenic Changes in Aortic wall Macrophages in a Murine Model of Obstructive Sleep Apnea. *Am. J. Respir. Crit. Care Med.* 190, 958–961. doi:10.1164/rccm.201406-1149LE

Guan, S., Wang, W., Lu, J., Qian, W., Huang, G., Deng, X., et al. (2011). Salidroside Attenuates Hydrogen Peroxide-Induced Cell Damage through a cAMP-dependent Pathway. *Molecules* 16, 3371–3379. doi:10.3390/molecules16043371

Harki, O., Tamisier, R., Pépin, J.-L., Bailly, S., Mahmani, A., Gonthier, B., et al. (2021). VE-cadherin Cleavage in Sleep Apnoea: New Insights into Intermittent Hypoxia-Related Endothelial Permeability. *Eur. Respir. J.*, 2004518. doi:10.1183/13993003.04518-2020

Hoyos, C. M., Melehan, K. L., Liu, P. Y., Grunstein, R. R., and Phillips, C. L. (2015). Does Obstructive Sleep Apnea Cause Endothelial Dysfunction? A Critical Review of the Literature. *Sleep Med. Rev.* 20, 15–26. doi:10.1016/j.smrv.2014.06.003

Huang, L. Y., Yen, I. C., Tsai, W. C., and Lee, S. Y. (2020). Rhodiola Crenulata Suppresses High Glucose-Induced Matrix Metalloproteinase Expression and Inflammatory Responses by Inhibiting ROS-Related HMGB1-TLR4 Signaling in Endothelial Cells. *Am. J. Chin. Med.* 48, 91–105. doi:10.1142/S0192415X20500056

Khalyfa, A., Kheirandish-Gozal, L., Khalyfa, A. A., Philby, M. F., Alonso-Álvarez, M. L., Mohammadi, M., et al. (2016). Circulating Plasma Extracellular Microvesicle microRNA Cargo and Endothelial Dysfunction in Children with Obstructive Sleep Apnea. *Am. J. Respir. Crit. Care Med.* 194, 1116–1126. doi:10.1164/rccm.201602-0323OC

Komarova, Y. A., Kruse, K., Mehta, D., and Malik, A. B. (2017). Protein Interactions at Endothelial Junctions and Signaling Mechanisms Regulating Endothelial Permeability. *Circ. Res.* 120, 179–206. doi:10.1161/CIRCRESAHA.116.306534

Konishi, T., Kashiwagi, Y., Funayama, N., Yamamoto, T., Murakami, H., Hotta, D., et al. (2019). Obstructive Sleep Apnea Is Associated with Increased Coronary Plaque Instability: an Optical Frequency Domain Imaging Study. *Heart Vessels* 34, 1266–1279. doi:10.1007/s00380-019-01363-8

Kosanovic, D., Tian, X., Pak, O., Lai, Y. J., Hsieh, Y. L., Seimetz, M., et al. (2013). Rhodiola: an Ordinary Plant or a Promising Future Therapy for Pulmonary Hypertension? a Brief Review. *Pulm. Circ.* 3, 499–506. doi:10.1086/674303

Lai, M. C., Lin, J. G., Pai, P. Y., Lai, M. H., Lin, Y. M., Yeh, Y. L., et al. (2015). Effects of Rhodiola Crenulata on Mice Hearts under Severe Sleep Apnea. *BMC Complement. Altern. Med.* 15, 198. doi:10.1186/s12906-015-0698-0

Lai, M. C., Lin, J. G., Pai, P. Y., Lai, M. H., Lin, Y. M., Yeh, Y. L., et al. (2014). Protective Effect of Salidroside on Cardiac Apoptosis in Mice with Chronic

Intermittent Hypoxia. *Int. J. Cardiol.* 174, 565–573. doi:10.1016/j.ijcard.2014.04.132

Lei, S., Peng, F., Li, M. L., Duan, W. B., Peng, C. Q., and Wu, S. J. (2020). LncRNA-SMILR Modulates RhoA/ROCK Signaling by Targeting miR-141 to Regulate Vascular Remodeling in Pulmonary Arterial Hypertension. *Am. J. Physiol. Heart Circ. Physiol.* 319, H377–377H391. doi:10.1152/ajpheart.00717.2019

Leung, S. B., Zhang, H., Lau, C. W., Huang, Y., and Lin, Z. (2013). Salidroside Improves Homocysteine-Induced Endothelial Dysfunction by Reducing Oxidative Stress. *Evid. Based Complement. Alternat Med.* 2013, 679635. doi:10.1155/2013/679635

Lévy, P., Kohler, M., McNicholas, W. T., Barbé, F., McEvoy, R. D., Somers, V. K., et al. (2015). Obstructive Sleep Apnoea Syndrome. *Nat. Rev. Dis. Primers* 1, 15015. doi:10.1038/nrdp.2015.15

Li, J. R., Zhao, Y. S., Chang, Y., Yang, S. C., Guo, Y. J., and Ji, E. S. (2018). Fasudil Improves Endothelial Dysfunction in Rats Exposed to Chronic Intermittent Hypoxia through RhoA/ROCK/NFATc3 Pathway. *PLoS ONE* 13, e0195604. doi:10.1371/journal.pone.0195604

Li, L., Hu, J., He, T., Zhang, Q., Yang, X., Lan, X., et al. (2015). P38/MAPK Contributes to Endothelial Barrier Dysfunction via MAP4 Phosphorylation-dependent Microtubule Disassembly in Inflammation-Induced Acute Lung Injury. *Sci. Rep.* 5, 8895. doi:10.1038/srep08895

Li, Y., Wu, J., Shi, R., Li, N., Xu, Z., and Sun, M. (2017). Antioxidative Effects of Rhodiola Genus: Phytochemistry and Pharmacological Mechanisms against the Diseases. *Curr. Top. Med. Chem.* 17, 1692–1708. doi:10.2174/1568026617666161116141334

Lu, W., Kang, J., Hu, K., Tang, S., Zhou, X., Xu, L., et al. (2017). The Role of the Nox4-Derived ROS-Mediated RhoA/Rho Kinase Pathway in Rat Hypertension Induced by Chronic Intermittent Hypoxia. *Sleep Breath* 21, 667–677. doi:10.1007/s11325-016-1449-2

Ma, L., Zhang, J., and Liu, Y. (2016). Roles and Mechanisms of Obstructive Sleep Apnea-Hypopnea Syndrome and Chronic Intermittent Hypoxia in Atherosclerosis: Evidence and Prospective. *Oxid Med. Cel Longev* 2016, 8215082. doi:10.1155/2016/8215082

Makarenko, V. V., Usatyuk, P. V., Yuan, G., Lee, M. M., Nanduri, J., Natarajan, V., et al. (2014). Intermittent Hypoxia-Induced Endothelial Barrier Dysfunction Requires ROS-dependent MAP Kinase Activation. *Am. J. Physiol. Cel Physiol* 306, C745–C752. doi:10.1152/ajpcell.00313.2013

McEvoy, R. D., Antic, N. A., Heeley, E., Luo, Y., Ou, Q., Zhang, X., et al. (2016). CPAP for Prevention of Cardiovascular Events in Obstructive Sleep Apnea. *N. Engl. J. Med.* 375, 919–931. doi:10.1056/NEJMoa1606599

Naha, P. C., Davoren, M., Lyng, F. M., and Byrne, H. J. (2010). Reactive Oxygen Species (ROS) Induced Cytokine Production and Cytotoxicity of PAMAM Dendrimers in J774A.1 Cells. *Toxicol. Appl. Pharmacol.* 246, 91–99. doi:10.1016/j.taap.2010.04.014

Peker, Y., Glantz, H., Eulenburg, C., Wegscheider, K., Herlitz, J., and Thunström, E. (2016). Effect of Positive Airway Pressure on Cardiovascular Outcomes in Coronary Artery Disease Patients with Nonsleepy Obstructive Sleep Apnea. The RICCADSA Randomized Controlled Trial. *Am. J. Respir. Crit. Care Med.* 194, 613–620. doi:10.1164/rccm.201601-0088OC

Pi, X., Xie, L., and Patterson, C. (2018). Emerging Roles of Vascular Endothelium in Metabolic Homeostasis. *Circ. Res.* 123, 477–494. doi:10.1161/CIRCRESAHA.118.313237

Qiao, J., Huang, F., and Lum, H. (2003). PKA Inhibits RhoA Activation: a protection Mechanism against Endothelial Barrier Dysfunction. *Am. J. Physiol. Lung Cel Mol. Physiol.* 284, L972–L980. doi:10.1152/ajplung.00429.2002

Qin, W., Lu, W., Li, H., Yuan, X., Li, B., Zhang, Q., et al. (2012). Melatonin Inhibits IL1β-induced MMP9 Expression and Activity in Human Umbilical Vein Endothelial Cells by Suppressing NF-Kb Activation. *J. Endocrinol.* 214, 145–153. doi:10.1530/JOE-12-0147

Radeva, M. Y., and Waschke, J. (2018). Mind the gap: Mechanisms Regulating the Endothelial Barrier. *Acta Physiol. (Oxf)* 222. doi:10.1111/apha.12860

Schlegel, N., and Waschke, J. (2014). cAMP with Other Signaling Cues Converges on Rac1 to Stabilize the Endothelial Barrier- a Signaling Pathway Compromised in Inflammation. *Cell Tissue Res* 355, 587–596. doi:10.1007/s00441-013-1755-y

Shen, W., Fan, W. H., and Shi, H. M. (2008). Effects of Rhodiola on Expression of Vascular Endothelial Cell Growth Factor and Angiogenesis in Aortic Atherosclerotic Plaque of Rabbits. *Zhongguo Zhong Xi Yi Jie He Za Zhi* 28, 1022–1025.

Shimokawa, H., and Satoh, K. (2015). Light and Dark of Reactive Oxygen Species for Vascular Function: 2014 ASVB (Asian Society of Vascular Biology). *J. Cardiovasc. Pharmacol.* 65, 412–418. doi:10.1097/FJC.0000000000000159

Song, T., Wang, P., Li, C., Jia, L., Liang, Q., Cao, Y., et al. (2021). Salidroside Simultaneously Reduces De Novo Lipogenesis and Cholesterol Biosynthesis to Attenuate Atherosclerosis in Mice. *Biomed. Pharmacother.* 134, 111137. doi:10.1016/j.biopha.2020.111137

Souza, S. P., Santos, R. B., Santos, I. S., Parise, B. K., Giatti, S., Aielo, A. N., et al. (2021). Obstructive Sleep Apnea, Sleep Duration, and Associated Mediators with Carotid Intima-media Thickness: the ELSA-Brasil Study. *Arterioscler. Thromb. Vasc. Biol.* 41, 1549–1557. doi:10.1161/ATVBAHA.120.315644

Sun, C., Wu, M. H., and Yuan, S. Y. (2011). Nonmuscle Myosin Light-Chain Kinase Deficiency Attenuates Atherosclerosis in Apolipoprotein E-Deficient Mice via Reduced Endothelial Barrier Dysfunction and Monocyte Migration. *Circulation* 124, 48–57. doi:10.1161/CIRCULATIONAHA.110.988915

Terry, S., Nie, M., Matter, K., and Balda, M. S. (2010). Rho Signaling and Tight junction Functions. *Physiology (Bethesda)* 25, 16–26. doi:10.1152/physiol.00034.2009

Trzepizur, W., Martinez, M. C., Priou, P., Andriantsitohaina, R., and Gagnadoux, F. (2014). Microparticles and Vascular Dysfunction in Obstructive Sleep Apnoea. *Eur. Respir. J.* 44, 207–216. doi:10.1183/09031936.00197413

Wang, C., Nan, X., Pei, S., Zhao, Y., Wang, X., Ma, S., et al. (2021). Salidroside and Isorhamnetin Attenuate Urotensin II-induced I-nflammatory R-esponse In V-ivo and In V-itro: Involvement in R-egulating the RhoA/ROCK II P-athway. *Oncol. Lett.* 21, 292. doi:10.3892/ol.2021.12553

Wattanakit, K., Boland, L., Punjabi, N. M., and Shahar, E. (2008). Relation of Sleep-Disordered Breathing to Carotid Plaque and Intima-media Thickness. *Atherosclerosis* 197, 125–131. doi:10.1016/j.atherosclerosis.2007.02.029

Xing, S. S., Yang, X. Y., Zheng, T., Li, W. J., Wu, D., Chi, J. Y., et al. (2015). Salidroside Improves Endothelial Function and Alleviates Atherosclerosis by Activating a Mitochondria-Related AMPK/PI3K/Akt/eNOS Pathway. *Vascul. Pharmacol.* 72, 141–152. doi:10.1016/j.vph.2015.07.004

Yang, Y. Y., Li, L. Y., Jiao, X. L., Jia, L. X., Zhang, X. P., Wang, Y. L., et al. (2020). Intermittent Hypoxia Alleviates β-Aminopropionitrile Monofumarate Induced Thoracic Aortic Dissection in C57BL/6 Mice. *Eur. J. Vasc. Endovasc Surg.* 59, 1000–1010. doi:10.1016/j.ejvs.2019.10.014

Zhao, C. C., Wu, X. Y., Yi, H., Chen, R., and Fan, G. (2021). The Therapeutic Effects and Mechanisms of Salidroside on Cardiovascular and Metabolic Diseases: an Updated Review. *Chem. Biodivers.* 18, e2100033. doi:10.1002/cbdv.202100033

Zhao, X., Jin, L., Shen, N., Xu, B., Zhang, W., Zhu, H., et al. (2013). Salidroside Inhibits Endogenous Hydrogen Peroxide Induced Cytotoxicity of Endothelial Cells. *Biol. Pharm. Bull.* 36, 1773–1778. doi:10.1248/bpb.b13-00406

Zhong, H., Xin, H., Wu, L. X., and Zhu, Y. Z. (2010). Salidroside Attenuates Apoptosis in Ischemic Cardiomyocytes: a Mechanism through a Mitochondria-dependent Pathway. *J. Pharmacol. Sci.* 114, 399–408. doi:10.1254/jphs.10078fp

Zhou, M., Guo, B., Wang, Y., Yan, D., Lin, C., and Shi, Z. (2017). The Association between Obstructive Sleep Apnea and Carotid Intima-media Thickness: a Systematic Review and Meta-Analysis. *Angiology* 68, 575–583. doi:10.1177/0003319716665985

Zhu, Y., Zhang, Y. J., Liu, W. W., Shi, A. W., and Gu, N. (2016). Salidroside Suppresses HUVECs Cell Injury Induced by Oxidative Stress through Activating the Nrf2 Signaling Pathway. *Molecules* 21. doi:10.3390/molecules21081033

Conflict of Interest: The authors declare that the research was conducted in the absence of any commercial or financial relationships that could be construed as a potential conflict of interest.

Publisher's Note: All claims expressed in this article are solely those of the authors and do not necessarily represent those of their affiliated organizations, or those of the publisher, the editors and the reviewers. Any product that may be evaluated in this article, or claim that may be made by its manufacturer, is not guaranteed or endorsed by the publisher.

frontiers in Pharmacology

ORIGINAL RESEARCH
published: 07 September 2021
doi: 10.3389/fphar.2021.703965

Xiaoyaosan Exerts Antidepressant Effect by Downregulating RAGE Expression in Cingulate Gyrus of Depressive-Like Mice

Weixin Yan[1,2†], Zhaoyang Dong[3†], Di Zhao[1], Jun Li[1], Ting Zeng[1], Chan Mo[1], Lei Gao[1,4] and Zhiping Lv[1*]*

[1]School of Traditional Chinese Medicine, Southern Medical University, Guangzhou, China, [2]The First Affiliated Hospital of Guangzhou University of Chinese Medicine, Guangzhou, China, [3]School of Nursing, Guangzhou University of Chinese Medicine, Guangzhou, China, [4]Zhujiang Hospital, Southern Medical University, Guangzhou, China

OPEN ACCESS

Edited by:
Enkelejda Goci,
Aldent University, Albania

Reviewed by:
Nasra Ayuob,
Mansoura University, Egypt
Esther Del Olmo,
University of Salamanca, Spain
Wei Lu,
Qingdao University, China

***Correspondence:**
Lei Gao
raygaolei@smu.edu.cn
Zhiping Lv
lzp48241@126.com

[†]These authors have contributed equally to this work

Specialty section:
This article was submitted to Ethnopharmacology, a section of the journal Frontiers in Pharmacology

Received: 01 May 2021
Accepted: 22 July 2021
Published: 07 September 2021

Citation:
Yan W, Dong Z, Zhao D, Li J, Zeng T, Mo C, Gao L and Lv Z (2021) Xiaoyaosan Exerts Antidepressant Effect by Downregulating RAGE Expression in Cingulate Gyrus of Depressive-Like Mice. Front. Pharmacol. 12:703965. doi: 10.3389/fphar.2021.703965

Xiaoyaosan (XYS), as a classic Chinese medicine compound, has been proven to have antidepressant effect in many studies, but its mechanism has not been clarified. In our previous studies, we found that chronic stress can induce depressive-like behavior and lead to emotion-related cingulate gyrus (Cg) dysfunction, as well as the decrease of neurotrophic factors and the increase of inflammatory-related proteins. Therefore, we speculated that XYS may play an antidepressant role by regulating the inflammation-related receptor of advanced glycation protein end product (RAGE) to affect the functional connectivity (FC) signal of the Cg and improve the depressive-like behavior. In order to verify this hypothesis, we analyzed the FC and RAGE expression in the Cg of depressive-like mice induced by chronic unpredictable mild stress (CUMS) and verified it with RAGE knockout mice. At the same time, we detected the effect of XYS on the depressive-like behavior, expression of RAGE, and the FC of the Cg of mice. The results showed that the FC of the Cg of depressive-like mice induced by CUMS was weakened, and the expression of RAGE was upregulated. The antidepressant effect of XYS is similar to that of fluoxetine hydrochloride, which can significantly reduce the depressive-like behavior of mice and inhibit the expression of the RAGE protein and mRNA in the Cg, and increase the FC of the Cg in mice. In conclusion, XYS may play an antidepressant role by downregulating the expression of RAGE in the Cg of depressive-like mice induced by CUMS, thereby affecting the functional signal and improving the depressive-like behavior.

Keywords: chronic stress, xiaoyaosan, functional connectivity, cingulate gyrus, receptor of advanced glycation protein end product

Abbreviations: ALFFs, amplitude of low-frequency fluctuations; BDNF, brain-derived neurotrophic factor; Cg, cingulate gyrus; CUMS, chronic unpredictable mild stress; DAMPs, damage-associated molecular patterns; FC, functional connectivity; FH, fluoxetine hydrochloride; FST, force swimming test; HPLC-MS/MS, high-performance liquid chromatography–mass spectrometry; IF, immunofluorescence; MDD, major depressive disorder; RAGE, related receptor of advanced glycation protein end product; rs-fMRI, resting-state functional magnetic resonance imaging; Rt-qPCR, real-time quantitative PCR; SPT, sucrose preference test; TST, tail suspension test; XYS, Xiaoyaosan.

INTRODUCTION

Major depressive disorder (MDD), as a complex mental disease, seriously affects people's physical and mental health, and significantly increases the risk of suicide. At present, chronic stress–induced neuroinflammation plays an important role in the progress of MDD (Beurel et al., 2020). It may be a key regulator of disease, increasing the susceptibility to depression (Beurel et al., 2020).

Studies have found that in MDD patients, there is a strong relationship between symptoms of depression and inflammatory factors. The levels of IL-1β, IL-6, TNF-α, and CRP in peripheral blood of MDD patients were significantly increased (Haapakoski et al., 2015; Liu et al., 2017; Felger et al., 2020), and the levels of inflammatory factors in cerebrospinal fluid were abnormal (Haapakoski et al., 2015). At the same time, the expression of inflammatory factors in different tissues of depression animal model also increased (Pan et al., 2014; Zhang et al., 2015; Xie et al., 2020). Moreover, depression is closely related to inflammation damage-associated molecular patterns (DAMPs) (Franklin et al., 2018; Xie et al., 2021). Studies have shown that inflammasome produced by the activation of "aseptic inflammation" interacts with DAMPs to activate the receptor of advanced glycation end products (RAGE) and stimulate inflammatory cascade reaction (Bolos et al., 2018; Franklin et al., 2018; Franklin et al., 2018; Xie et al., 2021). Although chronic inflammation plays a role in the pathophysiology of depression, the mechanism of inflammation activation in emotional disorders and its effect on the brain functional connectivity (FC) are still unclear. In order to clarify its pathogenesis, we can combine it with noninvasive neuroimaging resting-state functional magnetic resonance imaging (rs-fMRI) to further explore the relationship between brain-related inflammatory signals and changes in the brain FC.

It is well known that the cingulate gyrus (Cg) cortex plays a regulatory role in the pathogenesis of depression (Ebert and Ebmeier, 1996; Rolls, 2019). As the so-called emotional cortex, it is an important transit station in the emotional transmission loop (Ebert and Ebmeier, 1996; Philippi et al., 2015; Riva-Posse et al., 2019). In the study of suicide in young patients with MDD, it is found that the changes of the FC in the anterior Cg may be related to its neural mechanism (Qiu et al., 2020). In addition, there are abnormal cerebral blood flow and metabolism in the posterior Cg of patients with MDD, which suggests that depression may have a low function on the posterior Cg (Videbech, 2000). In our previous rs-fMRI studies (Huang et al., 2018), it was found that depressive-like mice were induced by chronic unpredictable mild stress (CUMS), accompanied by abnormal changes of amplitude of low-frequency fluctuations (ALFFs) of the Cg. FC can evaluate the activity of brain regions by measuring the correlation of functional signal connectivity between different brain regions. It may be an important indicator for the evaluation of the brain function in depression (Mulders et al., 2015; Han et al., 2019). Unfortunately, there are a few studies that used FC of rs-fMRI to explore the antidepressant effect of drugs, including traditional Chinese drugs and prescriptions.

In traditional Chinese medicine, depression is caused by exogenous pathogenic factors and endogenous physical disorders. Xiaoyaosan (XYS) was first recorded in the Taiping Huimin Heji Jufang in the Song Dynasty of China (960–1127 AD), which was widely used as a traditional Chinese medicine prescription in the treatment of various diseases by generations of doctors (Ding et al., 2014; Zhu et al., 2019; Chen et al., 2020; Lee et al., 2021; Zhu et al., 2021). It is more effective for mental disorders, especially MDD. Previous studies have found that XYS can significantly improve the depressive-like behavior of rats induced by CUMS (Zhu et al., 2014), reverse the tryptophan kynurenine metabolic pathway (Zhu et al., 2014; Wang et al., 2018), and can protect the inflammatory injury of hippocampal neurons caused by LPS (Shi et al., 2019). Many research works have focused on exploring the molecular mechanism of antidepressant with traditional Chinese medicine prescriptions, but there is little research evidence about the combination of brain-functional imaging and molecular targets for depression. In this study, we established a CUMS depression model in mice, combined with $RAGE^{-/-}$ mice, to explore the mechanism of neuroinflammation and brain functional connection, and further supplement the imaging evidence of the antidepressant mechanism of XYS.

MATERIALS AND METHODS

Ethics Statement and Animals

All experiments were approved and implemented in strict accordance with the requirements of the Institutional Animal Care Unit Committee in Administration Office of Laboratory Animals of Nanfang Hospital (NFYY-2014-53) and the National Institutes of Health guide for the care and use of laboratory animals (NIH Publications No. 8023, revised 1978).

Eight-week-old male C57BL/6J (wild-type) mice were purchased from Guangzhou Qingle Life Science Co., Ltd. (China), and male RAGE knockout mice (C57BL/6J background) aged 6–8 weeks were obtained from Professor Qiaobing Huang, School of Basic Medicine, Southern Medical University. All animals were group-housed and maintained in standard conditions, light/dark cycle for 12 h, suitable temperature, and humidity, with free access to food and water. In the experiment of pathogenesis of depression (see **Figures 1–4**), all mice were randomly divided into the Control group and the CUMS group, the $Control^{RAGE-/-}$ group and the $CUMS^{RAGE-/-}$ group, and the n = 8/group. Among them, the CUMS group and the $CUMS^{RAGE-/-}$ group were given CUMS program for 28 days (Yang et al., 2018). After behavioral experiment, rs-fMRI of anesthetized mice in each group was scanned. In the experiment of the pharmacodynamic mechanism (see **Figures 5, 6**), mice were randomly divided into the vehicle group, the CUMS group, the XYS treatment group, the fluoxetine hydrochloride (FH) treatment group, and the n = 8/group. The CUMS group, the XYS group, and the FH group mice were established with a 28-day CUMS program. Simultaneously, the intragastric dose of XYS and FH was calculated according to the equivalent dose formula of human

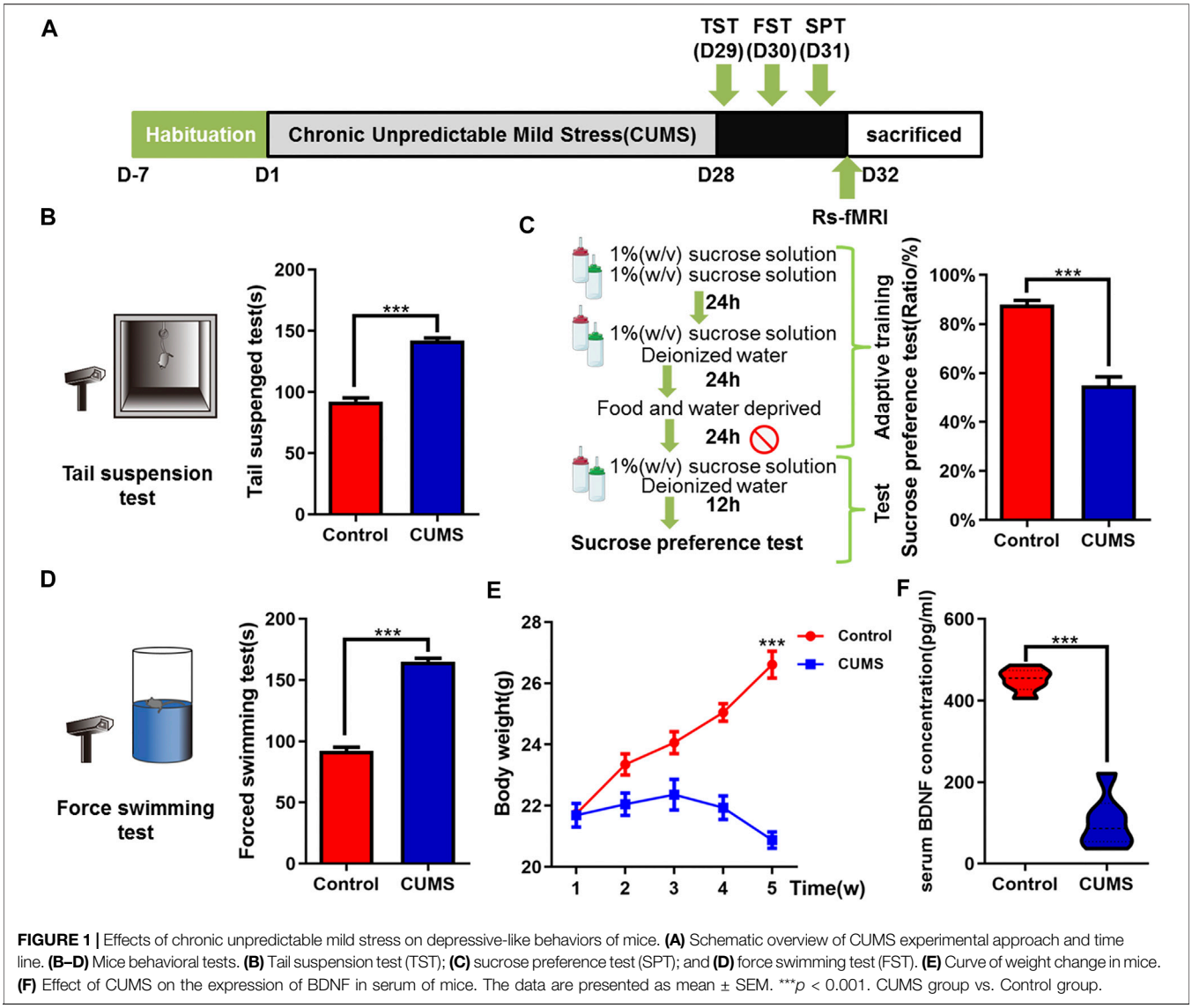

FIGURE 1 | Effects of chronic unpredictable mild stress on depressive-like behaviors of mice. **(A)** Schematic overview of CUMS experimental approach and time line. **(B–D)** Mice behavioral tests. **(B)** Tail suspension test (TST); **(C)** sucrose preference test (SPT); and **(D)** force swimming test (FST). **(E)** Curve of weight change in mice. **(F)** Effect of CUMS on the expression of BDNF in serum of mice. The data are presented as mean ± SEM. ***$p < 0.001$. CUMS group vs. Control group.

and animal. The vehicle group and the CUMS group were given normal saline by gavage, once a day. The XYS group and the FH group were given with Xiaoyaosan (0.25 g/kg/d) and FH (2.6 mg/kg/d) by gavage, respectively, once a day for 28 consecutive days (Yan et al., 2018). The mice were euthanized by intraperitoneal injection of an overdosed pentobarbital sodium solution. Blood samples were collected from the heart, centrifuged for 3,000 rpm for 10 min at room for serum, and the brain was obtained by heart perfusion with iced PBS. All brain tissues were immediately packed according to the brain atlas and frozen in liquid nitrogen. All the samples were stored at −80°C until further detection.

Preparation of Drugs

XYS is composed of Poria [Poria cocos (Schw.) Wolf], Radix *Angelica sinensis* [*Angelica sinensis* (Oliv.) Diels], Rhizoma *Zingiberis recens* (*Zingiber officinale* Rosc.), Rhizoma *Atractylodis* Macrocephalae (*Atractylodes macrocephala* Koidz.), Radix Bupleuri (*Bupleurum chinense* DC.), Radix Paeoniae *alba* (*Paeonia lactiflora* Pall.), *Herba* Menthae (*Mentha haplocalyx* Briq.), and Radix Glycyrrhizae (*Glycyrrhiza uralensis* Fisch.). The raw herbs were purchased from Nanfang Hospital of Southern Medical University. A total of 185 g of nine herbs were mixed, and aqueous extracts of XYS were extracted by boiling for 1 h by 10 volumes of distilled water (v/m) at the molecular biology laboratory of Traditional Chinese Medicine of Southern Medical University. The supernatant was collected and concentrated to obtain the final concentration of 1.9 g/ml for use and detection. The quality of XYS was identified by high-performance liquid chromatography–mass spectrometry (HPLC-MS/MS) (see the *Supplementary Materials* for details (Zhu et al., 2014)). Fluoxetine hydrochloride (Lilly Suzhou Pharmaceutical Co., Ltd., No. j20080016) was purchased from Nanfang Hospital and dissolved in deionized water to 0.2 mg/ml and stored at −80°C.

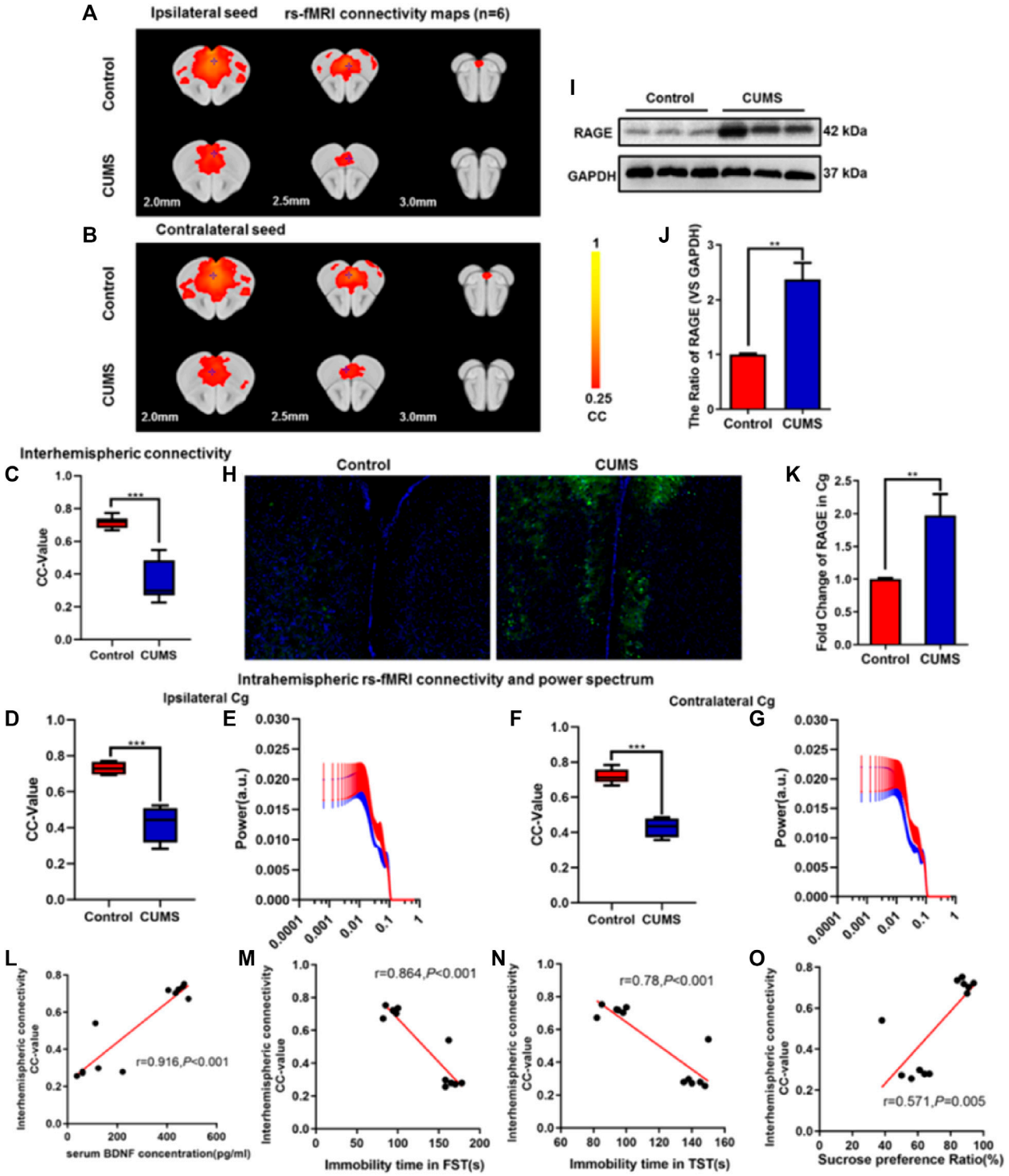

FIGURE 2 | Effect of chronic stress on functional connectivity (FC) of cingulate gyrus (Cg) in depressive-like mice. **(A–B)** Rs-fMRI connectivity maps of Cg in two groups of mice: ipsilateral seed **(A)** and contralateral seed **(B)**. **(C)** Quantification of interhemispheric rs-fMRI connectivity. **(D–G)** Quantification of intrahemispheric rs-fMRI connectivity **(D, F)** and the respective power spectrum **(E, G)** of ipsilateral and contralateral Cg in 4 groups of mice. **(H)** Immunofluorescence expression of RAGE in the Cg of mice. **(I–J)** Western blot and semi-quantitative results of RAGE in the Cg of mice. **(K)** The mRNA fold change of RAGE in Cg of mice was detected by qPCR. **(L–O)** Relationship between interhemispheric connectivity CC-value and BDNF **(L)** expression in serum and depressive-like behavior [FST **(M)**, TST **(N)**, and SPT **(O)**] in mice. The data are presented as mean ± SEM. Two sample T-test. Rs-fMRI maps generated by correlation analysis of band-pass filtered (0.005–0.1 Hz) BOLD signals using a seed defined in the ipsilateral and contralateral side. Seed location is indicated by a blue crosshair. Quantification of the interhemispheric rs-fMRI connectivity (n = 6). $^{**}p < 0.01$, $^{***}p < 0.001$. CUMS group vs. Control group.

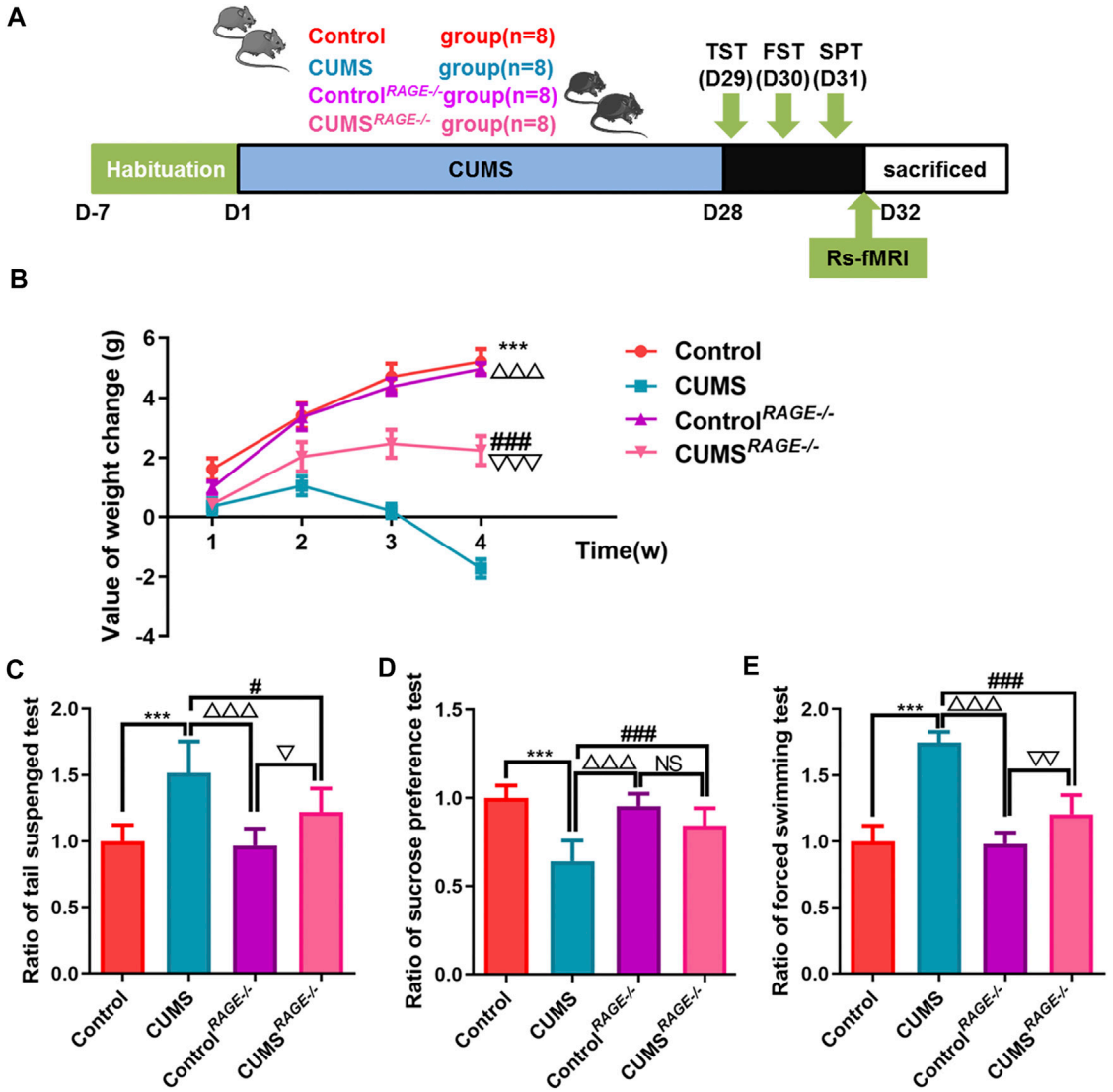

FIGURE 3 | Effect of RAGE gene knockout on the behavior of depressive-like mice induced by chronic stress. **(A)** Schematic overview of experimental approach and time line. **(B)** The value of body weight changes in mice. **(C–E)** Mice behavioral tests. **(C)** Tail suspension test (TST); **(D)** sucrose preference test (SPT); and **(E)** force swimming test (FST). One-way ANOVA followed by Bonferroni's *post hoc* test; $^{***}p < 0.001$, CUMS group vs. Control group; $^{\#}p < 0.05$ and $^{\#\#\#}p < 0.001$, CUMS group vs. CUMS$^{RAGE-/-}$ group; $^{\triangle\triangle\triangle}p < 0.001$, CUMS group vs. Control$^{RAGE-/-}$ group; error bars indicate mean ± SEM.

Chronic Unpredictable Mild Stress Procedures

The CUMS protocol was performed according to the modification method of Willner and Xueliang shang (Willner, 2005; Shang et al., 2017; Yang et al., 2018). Animals were subjected to various unpredictable stresses once per day over a period of 28 days. The procedures applied included cage shaking (one time/s, 5 min), cage tilting 45° (8 h), cold swimming (13 ± 1°C, 5 min), food and water deprivation (24 h), tail pinching (60 s, 1 cm from the end of the tail), moist bedding (8 h), warm swimming (37 ± 2°C, 5 min), overnight illumination (12 h), tail pinching (90 s), no stress, reversing day and night (24 h), and tail pinching (120 s). One of these stresses was given in a random order, daily. Control mice were left undisturbed except for necessary procedures such as routine cage cleaning. A variety of unpredictable stresses were applied daily throughout the CUMS period.

Mice Behavioral Tests

Tail Suspension Test

The tail suspension test (Castagne et al., 2011) which was specifically designed to evaluate depression in mice was performed. Briefly, the session was recorded by a video camera, and the total immobile time was scored. Small movements confined to only the front limbs, and momentum-induced oscillations and pendulums that followed previous mobility bouts were not regarded as mobility. We recorded for

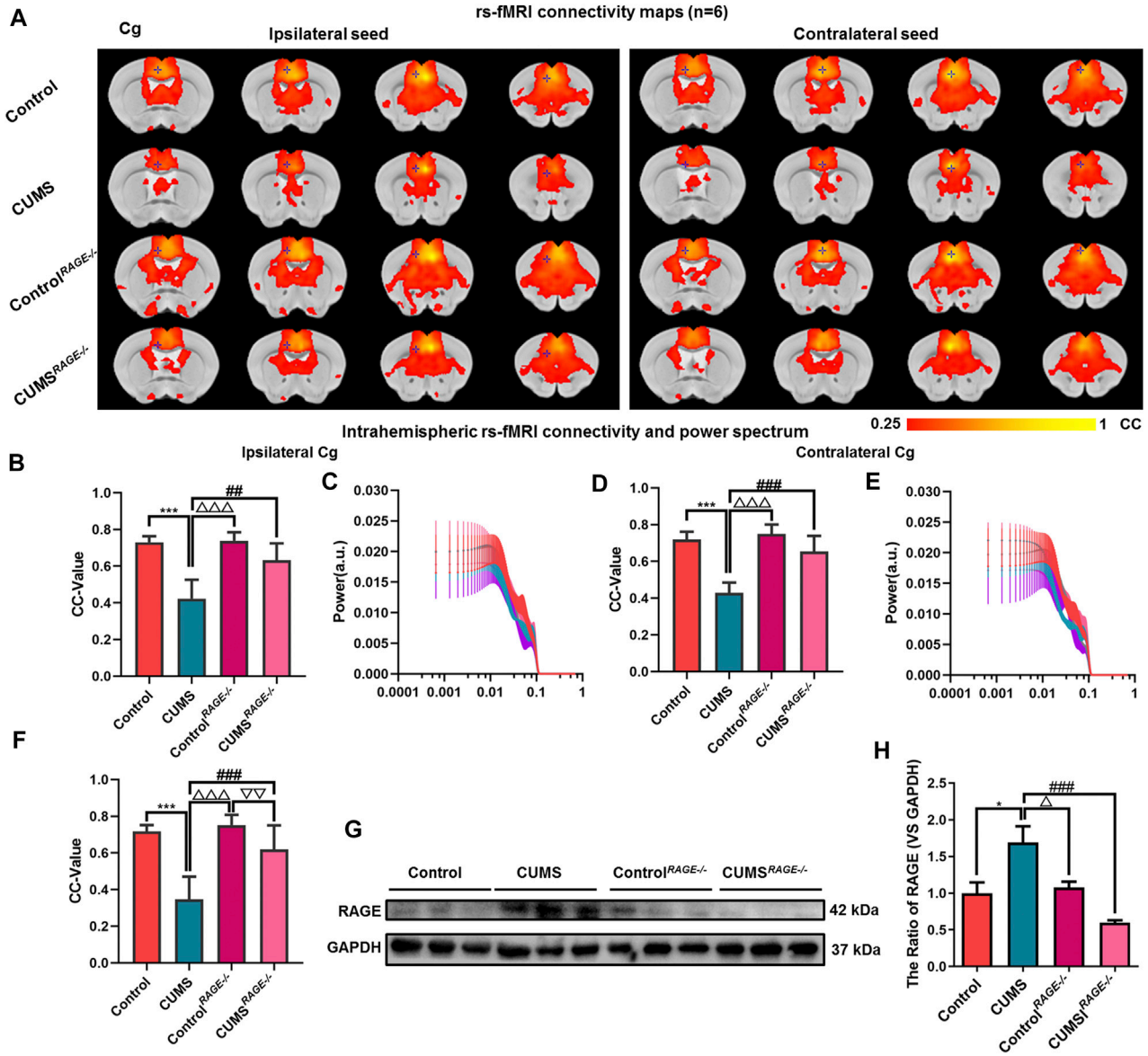

FIGURE 4 | Effect of RAGE knockout on brain functional connectivity in depressive-like mice induced by chronic stress. **(A, F)** Rs-fMRI connectivity maps of the Cg in four groups of mice **(A)**, corresponding quantification of interhemispheric connectivity **(F)**. **(B–E)** Quantification of intrahemispheric rs-fMRI connectivity **(B, D)** and the respective power spectrum **(C, E)** of ipsilateral and contralateral Cg in four groups of mice. **(G–H)** Western blot and semi-quantitative results of RAGE in the Cg of mice. The data are presented as mean ± SEM. One-way ANOVA followed by Bonferroni's *post hoc* test; $^{*}p < 0.05$ and $^{***}p < 0.001$, CUMS group vs. Control group; $^{\#\#}p < 0.01$, $^{\#\#\#}p < 0.001$, CUMS group vs. CUMS$^{RAGE-/-}$ group; $^{\triangle}p < 0.05$, $^{\triangle\triangle\triangle}p < 0.001$, CUMS group vs. Control$^{RAGE-/-}$ group; $^{\triangledown\triangledown}p < 0.01$, CUMS$^{RAGE-/-}$ group vs. Control$^{RAGE-/-}$ group.

6 min, and the last 4 min session of the immobility time of the tail suspension experiment was evaluated. Immobility was defined as floating with only small movements necessary to keep the head above water.

Force Swimming Test

A force swimming test (Castagne et al., 2011) which has been widely used to probe depressive-like behaviors in rodents was performed. Briefly, mice were placed in a plastic cylinder (height: 50 cm, diameter: 10 cm) containing 38 cm of water at 25 ± 1°C and videotaped for 6 min, and the last 4 min session was scored by an observer blind to the treatment conditions.

Sucrose Preference Test

Sucrose preference is a test index to determine whether pleasure is absent in reward stimulation. SPT includes two parts (Liu et al., 2018): an adaptive training part and a test part. During the training, the mice were put into two bottles of 1% (w/v) sucrose solution in each cage for the first 24 h, and then one bottle was changed into deionized water for 24 h. After the adaptation, the mice were fasted

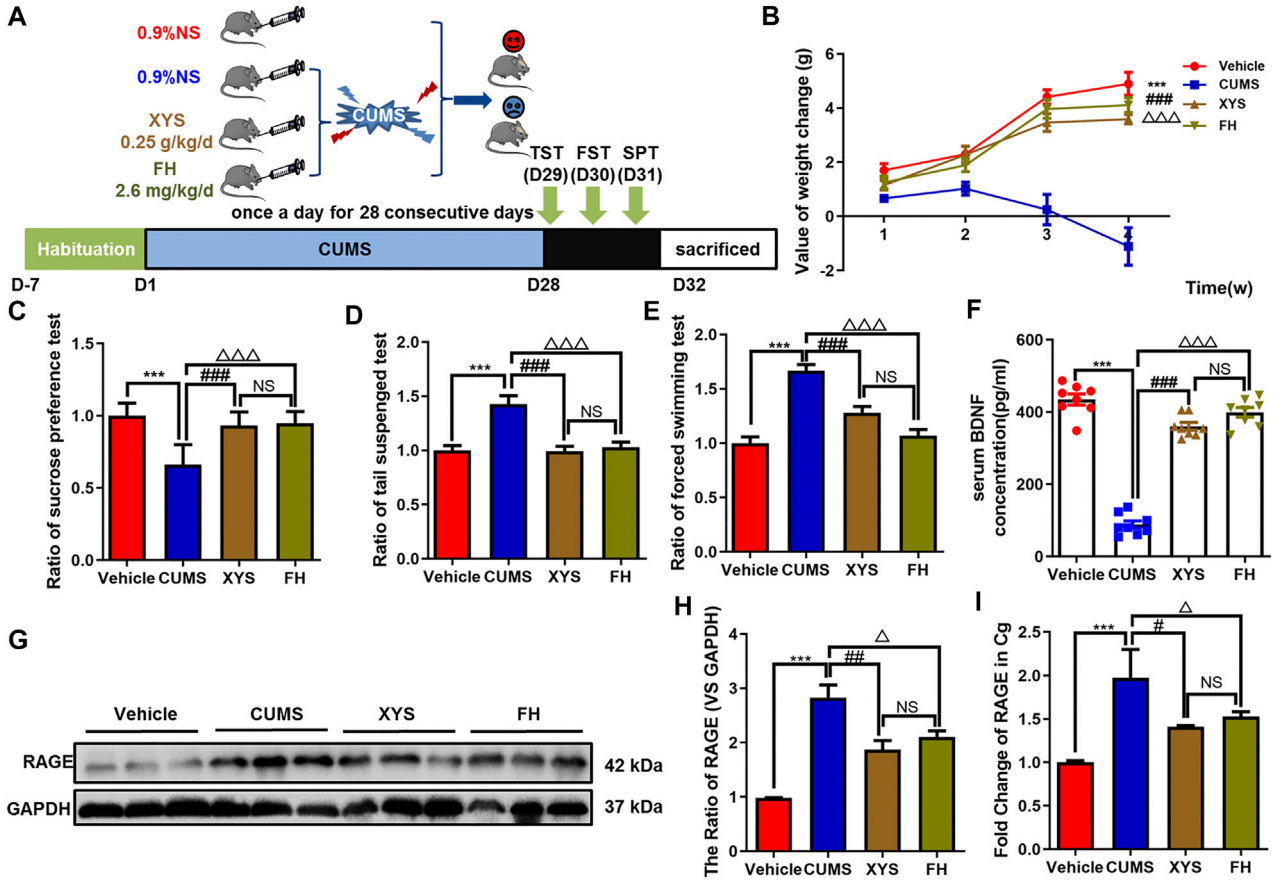

FIGURE 5 | Effect of Xiaoyaosan on behavior and the expression of RAGE in depressive-like mice. **(A)** Schematic overview of experimental approach and time line. **(B)** The value of body weight changes in mice. **(C–E)** Mice behavioral tests. **(C)** Sucrose preference test (SPT); **(D)** tail suspension test (TST); and **(E)** force swimming test (FST). **(F)** The expression of BDNF in serum of mice. **(G–H)** Western blot and semi-quantitative results of RAGE in Cg of mice. **(I)** The mRNA fold change of RAGE in Cg of mice was detected by qPCR. One-way ANOVA followed by Bonferroni's *post hoc* test; $^{***}p < 0.001$, CUMS group vs. Control group; $^{\#}p < 0.05$, $^{\#\#}p < 0.01$ and $^{\#\#\#}p < 0.001$, CUMS group vs. XYS group; $^{\triangle}p < 0.05$, $^{\triangle\triangle\triangle}p < 0.001$, CUMS group vs. FH group; error bars indicate mean ± SEM.

for 24 h, and then tested for 12 h. In the test, one is 1% (w/v) sucrose solution, and the other is deionized water; fasting occurred, and 12 h later, we weigh two bottles, record the data, and calculate the sucrose solution preference index.

Rs-fMRI Data Acquisition

After the behavioral tests of mice, 7.0T small animal MRI scanner (Bruker Biospin GmbH, Germany) was used for brain scanning. The mice were anesthetized with gas isoflurane (0–0.3% isoflurane, 0.2 mg/kg i.p of pancuronium bromide, and 0.04 mg/kg/hr S.C of dexmedetomidine). Mice were fixed on the animal bed to reduce head movement and equipped with surface coil and body coil, which can meet the imaging needs. The heart rate and respiratory frequency of the mice were monitored by a physiological monitor, and the normal body temperature of the mice was maintained by a hot water circulation system. The operation and processing system: paravision 6.0. EPI sequence parameters: protocol = ax-T1w, matrix size = 192 × 128, resolution = 0.14 × 0.14 × 1.0 mm, slice gap = 0.05 mm, slice thickness = 1.40 mm, TE = 9.01 ms, TR = 603.94 ms, averages = 32, scantime = 5 min 10 s, repetitions = 1, and volume = 1. SPM 12 software was used for image preprocessing; the following were performed: 1) DICOM data were converted to the NIFTI format for analysis, 2) data quality was checked, 3) time layer was corrected, 4) head movement correction was performed by six parameters, 5) spatial standardization was performed, 6) gauss smoothing was done, 7) nonlinear drift was performed to avoid the error of equipment, 8) the low frequency filter is 0.01–0.08 Hz, and 9) the functional connection value (CC value) and power spectrum were further analyzed and calculated by MATLAB software. The threshold range of voxel level is 0.25–1.

Enzyme-Linked Immunosorbent Assay

Serum samples of mice were collected. A mouse BDNF (CSB-E04505m, CUSABIO) Quantikine ELISA Kit was used, according to the manufacturer's instructions. Absorbance at 450 nm was determined using a spectrophotometry analyzer (Thermo Fisher Scientifc, Finland).

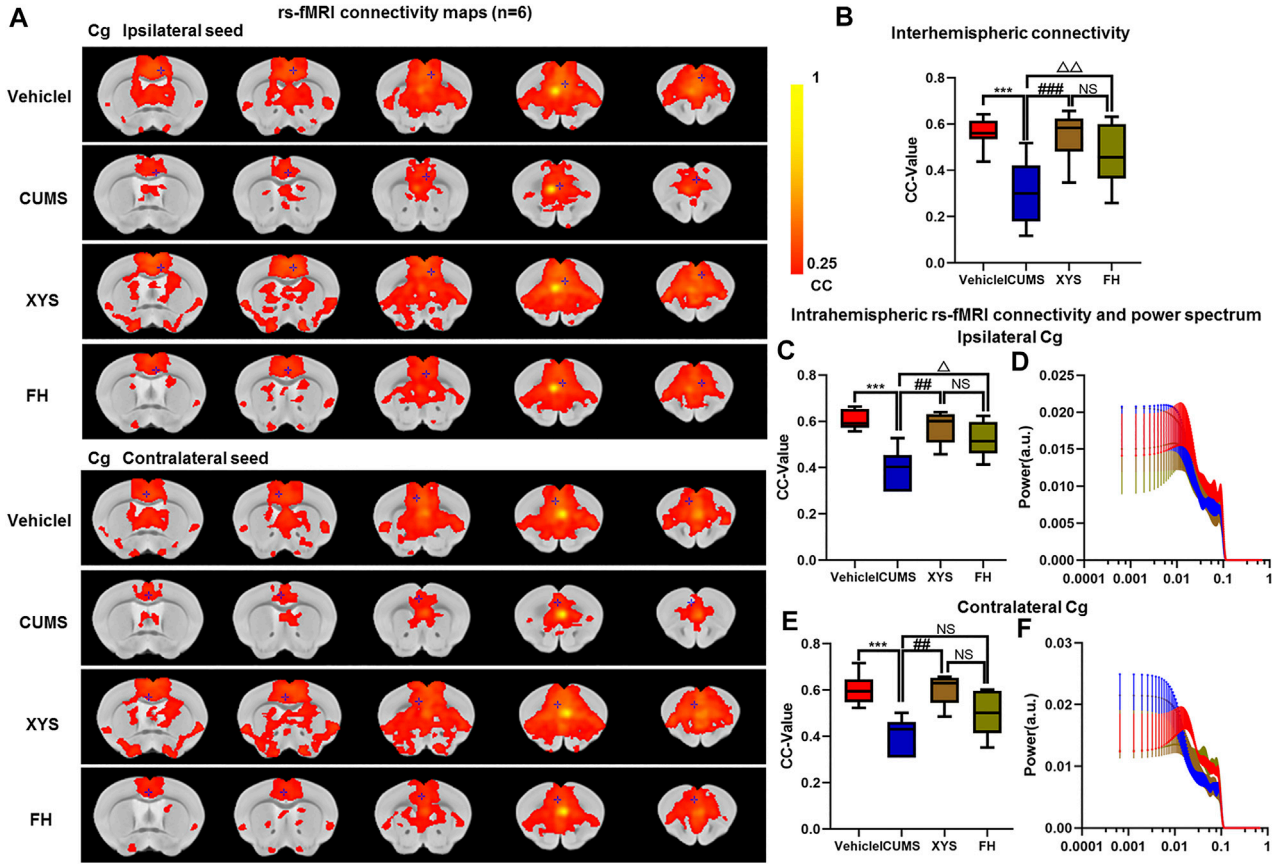

FIGURE 6 | Effect of Xiaoyaosan on brain functional connectivity in depressive-like mice induced by chronic stress. **(A, B)** Rs-fMRI connectivity maps of Cg in four groups of mice **(A)**, corresponding quantification of interhemispheric connectivity **(B)**. **(B–E)** Quantification of intrahemispheric rs-fMRI connectivity **(C, E)** and the respective power spectrum **(D, F)** of ipsilateral and contralateral Cg in four groups of mice. The data are presented as mean ± SEM. One-way ANOVA followed by Bonferroni's *post hoc* test; ***$p < 0.001$, CUMS group vs. Vehicle group; ##$p < 0.01$ and ###$p < 0.001$, CUMS group vs. XYS group; $^{\triangle}p < 0.05$, $^{\triangle\triangle}p < 0.01$, CUMS group vs. FH group; error bars indicate mean ± SEM.

Western Blot Analysis

The protein was extracted from tissues in the precooled RIPA lysate containing 1% phosphatase inhibitor and a protease inhibitor and isolated from 11% SDS-PAGE gel, and the membrane was blocked with 5% fetal bovine serum albumin in 1xTBST at RT for 2 h, then incubated overnight at 4°C with primary antibodies against GAPDH (1:2,000, CST, 5174s) and RAGE (1:1,000, abcam, ab37647). The secondary antibody was incubated (1:2000, CST, 7,074). The bands were detected by the chemiluminescence detection system (Bio-Rad Laboratories, Hercules, CA, United States) and quantified by ImageJ software.

Real-Time Quantitative PCR

Total RNA was extracted from Cg and purified according to the standard procedure (Gao et al., 2016). Total purified RNA was reverse-transcribed into cDNA by a Reverse Transcription Kit (k1622, Thermo Scientific, United States). The primer for RAGE was designed at https://www.ncbi.nlm.nih.gov/tools/primer-blast/ (forward primer: TGACCCTGACCTGTGCCATC; reverse primer: CCTCATCCTCATGCCCTACCTC). RT-qPCR was performed on the ABI 7500 real-time fluorescent quantitative PCR instrument (United States) using SYBR Green (420A, Takara, Japan). Cycle threshold values of genes of interest were normalized to gene GAPDH (forward primer: CCCAGCTTAGGTTCATCA GGT; reverse primer: TACGGCCAAATCCGTTCACA).

Immunofluorescence Staining

First, tissues were fixed with 4% paraformaldehyde at 4°C for 24 h and sliced into 30-μm-thick coronal sections. Second, the sections were blocked in 5% normal goat serum for 1 h at RT and then incubated in the primary antibody (1:800, ab37647, Abcam) at 4°C overnight. After washing with PBS at least three times, sections were incubated with the secondary antibody: dilution of Alexa 633-conjugated goat anti-rabbit antibody (1:500, Invitrogen) or Alexa 488-conjugated anti-rabbit antibody (1:250, Invitrogen) for 1 h at room temperature. Afterward, it was extensively washed by PBS and the cell nucleus was labeled by DAPI, and the free-floating sections with the positive staining by IF was captured and analyzed by a laser scanning confocal microscope (C2+, Nikon, Japan) (Gao et al., 2018).

Statistical Analysis

Data were analyzed by used GraphPad Prism 8.0.2 software, SPM 12, and REST software. All quantitative data are shown as mean ± SEM of three independent experiments at least. Two-group comparisons were assessed with Student's t-test. Multigroup comparisons were analyzed with one-way ANOVA, followed by the Bonferroni *post hoc* test on dependent experimental designs. p-value < 0.05 was considered as significant.

RESULTS

Chronic unpredictable Mild Stress–Induced Depressive-Ike Behavior in Mice

To explore the therapeutic efficacy of XYS on depression *in vivo*, we first established the CUMS-induced mouse depression model. As expected, continuous CUMS exposure (**Figure 1A**) led to macroscopically distinct depressive-like behavior in mice. Compared with the control group, the CUMS group mice had significantly reduced sucrose consumption (p < 0.001, **Figure 1C**) and longer immobility time of TST and FST (both *Ps* < 0.001, **Figures 1B,D**). The appetite and weight of CUMS mice decreased significantly (p < 0.001, **Figure 1E**). An ELISA kit was used to detect the level of BDNF in the peripheral serum of mice. Compared with the control group, the expression of BDNF in the serum of the CUMS group was significantly downregulated (p < 0.001, **Figure 1F**).

Chronic stress Decreased Functional Connectivity and Increased RAGE Expression in the Cg of Mice

In order to further verify the effect of CUMS on the FC of the Cg in depressive-like mice, rs-fMRI was used, and the Cg was used as a seed point to further analyze the changes of its interhemispheric or intrahemispheric FC. As shown in **Figures 2A,B**, compared with the control group, the intensity of the FC and the area of connection of the Cg were decreased in the CUMS group (**Figures 2A,B**). The FC between interhemispheres of Cg was decreased (p < 0.001, **Figure 2C**), and ipsilateral and contralateral intrahemispheres of the Cg was decreased (both *Ps* < 0.001, **Figures 2D,F**). However, there was no significant difference in the power spectrum of the intralateral hemisphere (p = 0.815, p = 0.963, **Figures 2E,G**). Meanwhile, immunofluorescence showed that the expression of RAGE was increased in CUMS mice (**Figure 2H**), and Western blot experiment also got the same result trend (p = 0.004, **Figures 2I,J**). qPCR results showed that the expression of RAGE mRNA in the Cg of CUMS mice was upregulated (p = 0.007, **Figure 2K**). There were positive correlations between interhemispheric connectivity CC-value of Cg and BDNF (L) expression in serum and SPT(O) in mice (r = 0.916, p < 0.001; r = 0.571, p = 0.005, **Figures 2L,O**). In addition, we found a negative correlation among interhemispheric connectivity CC-value of Cg, FST (M), and TST (N) in mice (r = 0.864, r = 0.78, *Ps* < 0.001, **Figures 2M,N**).

RAGE Gene Knockout can Improve the Depressive-Like Behavior Induced by Chronic Stress in Mice

In order to further confirm that reducing RAGE expression can reduce the occurrence of the depressive-like behavior, $RAGE^{-/-}$ mice were employed for our experiment and rs-fMRI data were collected (**Figure 3A**). Compared with the CUMS group, the value of body weight changes increased in $CUMS^{RAGE-/-}$ mice (p < 0.001, **Figure 3B**), improved depressive-like behavior, increased the ratio of sucrose consumption (p < 0.001, **Figure 3D**), and shortened the ratio of immobility time of TST and FST (p = 0.01; p < 0.001, **Figures 3C,E**, respectively). Compared with the Control group, there was no significant difference in the value of body weight changes, and the ratio of sucrose consumption and immobility time of TST and FST in the $Control^{RAGE-/-}$ group (p = 0.894, p = 0.983, p = 0.751, p = 0.989, **Figures 3B–E**).

RAGE Gene Knockout can Resist the Damage of Functional Connectivity of the Cg in Mice Induced by Chronic Stress

There was no significant difference in the power spectrum of bilateral hemispheres of the Cg of four groups (p = 0.970, p = 0.994, **Figures 4C,E**). Then, compared with the Control group, there were no significant differences in the expression of RAGE and FC of the Cg in $Control^{RAGE-/-}$ mice (p = 0.996, p = 0.827, p = 0.791, p = 0.978, **Figures 4A,B,D,F–H**,). At the same time, It was also found that rs-fMRI connectivity and area between interhemispheres of the Cg in $CUMS^{RAGE-/-}$ mice were increased compared with CUMS mice (p < 0.001, **Figures 4A,F**). The FC of the ipsilateral and contralateral intrahemispheres of the Cg increased and the expression of RAGE of the Cg decreased in $CUMS^{RAGE-/-}$ mice (p = 0.011, p < 0.001, p < 0.001, **Figures 4A,B,D,F–H**).

XYS Alleviated the Depressive-Like Behavior of Mice Induced by CUMS and Downregulated the Expression of RAGE in the Cg of Mice

In this study, we observed that compared with CUMS mice, the ratio of weight change and sucrose preference of the XYS group mice increased significantly (both *Ps* < 0.001, **Figures 5B,C**), which were similar to that of FH mice (both *Ps* < 0.001, **Figures 5B,C**). The ratio resting time of FST and TST in the XYS group mice or the FH group mice were significantly shorter than that in CUMS mice (both *Ps* < 0.001, **Figures 5D,E**). Moreover, we detected the level of BDNF in serum and found that XYS and FH could significantly improve the expression of BDNF in serum of chronic stress mice (both *Ps* < 0.001, **Figure 5F**). These results suggest that XYS can significantly reduce the depressive-like behavior induced by chronic stress in mice. Meanwhile, the results showed that compared with CUMS mice, the expression of RAGE in the Cg of XYS and FH mice was significantly decreased (p = 0.004, p = 0.028, **Figures 5G,H**), and the expression of RAGE mRNA was also decreased (p =

0.012, $p = 0.042$, **Figure 5I**). There was no significant difference in body weight, behavior, BDNF expression in serum, RAGE expression, and the RAGE mRNA level in the Cg between the XYS group and the FH group ($p = 0.431$, $p = 0.992$, $p = 0.962$, $p = 0.063$, $p = 0.159$, $p = 0.695$, $p = 0.811$, **Figures 5B–I**).

XYS Significantly Increased the Functional Connectivity of Cingulate Cortex in Chronic Stress–Induced Depressive-Like Mice

Our experimental findings revealed that there was no significant difference in the power spectrum of bilateral hemispheres of the Cg of four groups ($p = 0.976$, $p = 0.973$, **Figures 6D,F**). It was also found that rs-fMRI connectivity and area between interhemispheres of the Cg in XYS and FH mice were increased compared with CUMS mice ($p < 0.001$, $p = 0.01$, **Figures 6A,B**). The FC of the ipsilateral and contralateral intrahemisphere of the Cg increased in XYS and FH mice ($p = 0.002$, $p = 0.026$; $p = 0.002$, $p = 0.224$, **Figures 6A,C,E**). Then, compared with the FH mice, there were no significant differences in the FC of the Cg in XYS mice ($p = 0.294$, $p = 0.587$, $p = 0.143$, **Figures 6A–C,E**). Collectively, above results suggest that XYS can increase the FC of the Cg of depressive-like mice, which were attributed to enhancing the blood oxygen signal of the Cg and reducing the activation of inflammation.

DISCUSSION

Due to long-term exposure stress, high incidence rate, and severe economic burdens, depression has attracted global attention in recent years (Beurel et al., 2020). Chronic stress can lead to low-grade inflammatory reaction, cell-mediated immune activation, and so on, and then lead to abnormal nerve conduction and brain functional network disorder, which are closely related to the occurrence of depression (Franklin et al., 2018; Xie et al., 2020; Xie et al., 2021). At present, although many studies focus on the molecular imaging mechanism and drug treatment of depression, there are still no specific targeted drugs and compound preparations for depression. In the present work, we have elaborated the mechanism of inflammation and brain functional connection of depression, as well as the protective effect of XYS. It was found that XYS could improve the depressive-like behavior and brain FC in mice, and its protective effect could be ascribed at least partly due to reducing the accumulation of RAGE in the Cg and weakening the activation of RAGE-mediated inflammatory signal, thus enhancing the protective effect on brain FC.

The regulating effect of XYS and related prescriptions on emotion has been confirmed in many studies (Zhang et al., 2012; Jing et al., 2015; Liu et al., 2015). We used high-performance liquid chromatography (HPLC) to identify the components of XYS, which contains complex compounds that may be responsible for its antidepressant effect (Zhu et al., 2014). Through the establishment of the CUMS mice depression model and the verification of three different behavior tests of depression, it was found that XYS could improve the weight of mice and reduce the occurrence of the depressive-like behavior in CUMS mice. Sucrose preference is a test index to determine whether pleasure is absent (Liu et al., 2018). The immobility time of FST and TST were used to evaluate behavioral despair (Castagne et al., 2011). As expected, XYS can increase the preference of sucrose water, reduce the immobility time of FST and TST, and improve the depressive-like/despair mood of mice, which is consistent with previous reports (Ding et al., 2017). Brain-derived neurotrophic factor (BDNF) in peripheral blood is closely related to the depressive-like behavior, which can be used to indirectly reflect the lack of neurotrophic substances in the brain of mice, so as to infer the secretion and synthesis of BDNF. We found that the serum BDNF level was positively correlated with interhemispheric connectivity of the Cg in mice. At the same time, XYS can improve the level of BDNF in peripheral blood caused by CUMS, and further verify the effectiveness of XYS on emotion regulation, which is consistent with previous studies (Zhu et al., 2014; Ding et al., 2017).

In the study of the brain function in depression, FC can reflect the relationship between specific brain regions and the whole brain (He et al., 2020). The Cg, as the so-called emotional cortex, is an important link in the emotional transmission loop, which regulates the signal transduction of emotional neural activity (Ebert and Ebmeier, 1996; Philippi et al., 2015; Riva-Posse et al., 2019). In MDD patients, the function of anterior and posterior Cg was low and blood flow metabolism was abnormal (Videbech, 2000; Qiu et al., 2020). Modified Xiaoyaosan reversed the ReHo value in some abnormal brain areas of CUMS mice (Bi et al., 2019) and corrected the BOLD signal function and the hippocampal nerve function (Gao et al., 2018). Interestingly, using the Cg as the seed point analysis, we found that both interhemisphereric and intrahemispheric FC decreased in chronic stress–induced depressive-like mice, which was consistent with the results of clinical MDD reports (Yang et al., 2016; Qiu et al., 2020). At the same time, it was found that interhemispheric connectivity of the Cg was negatively correlated with TST and FST, and positively correlated with SPT in mice. However, intragastric administration of XYS for 4 weeks dramatically ameliorated the reduction of the FC of the Cg. Importantly, our results indicated that XYS can act on the Cg to alleviate the damage of FC caused by chronic stress, but its mechanism needs to be further explored.

As we all know, long-term chronic stress exposure is still considered to be a key pathogenic factor in the development of depression (Maes, 1999; Miller et al., 2009; Wohleb et al., 2016). It mediates the activation of aseptic chronic inflammation-DAMPs, acts on the "transit station" RAGE, connects the further transmission of inflammatory signals, and affects behavioral changes (Deane et al., 2003; Zhang et al., 2015; Franklin et al., 2018; Xie et al., 2021). Published literatures have indicated that RAGE may drive the neuro-inflammatory response of patients with depression to chronic stress (Franklin et al., 2018; Yang et al., 2020). In our study, IF staining showed that the expression level of RAGE increased in the Cg of CUMS mice, which was further confirmed by Western blot and qPCR experiments. As mentioned above, RAGE acts as an inflammatory mediator receptor and plays a crucial role in regulating the brain function and

inflammatory activation. In the current study, we used *RAGE* knockout mice to further confirm that the deletion of RAGE can significantly improve the depressive-like behavior and weight change of mice induced by CUMS, and the FC of the bilateral Cg is significantly increased, which is reflected in the resistance of *RAGE* knockout mice to the susceptibility of depression, and indicates that the knockout or inhibition of RAGE expression plays a key role in the treatment of MDD. It is reported that XYS can inhibit immune inflammatory activation and reduce the levels of colon proinflammatory cytokine to improve depressive-like behavior by regulating the TLR4/NLRP3 inflammasome signaling pathway (Zhu et al., 2021). XYS also can reduce the blood-brain barrier injury induced by chronic stress through glucocorticoid receptor (Yu et al., 2020). However, whether the efficacy of XYS against inflammatory response is involved in change of FC of brain regions against depression has not been addressed until now. Importantly, our results indicated that XYS was able to significantly reduce the expression level of RAGE in the Cg of CUMS depressive-like mice. In addition, oral administration of XYS significantly elevated the inter- and intrahemispheric FC of the Cg in depressive-like mice, which is similar to the results of $RAGE^{-/-}$ mice, further confirming that XYS can downregulate the expression of RAGE in the Cg and reduce the loss of the FC, thus improving the depressive-like behavior of mice. These data suggest that XYS may exert its antidepressant effects *via* reducing the accumulation of RAGE in the Cg and weakening the activation of RAGE-mediated inflammatory signals, thereby increasing the protection of brain FC.

CONCLUSION

This work suggests that XYS may act as an antagonist of RAGE, increasing the FC of the Cg and alleviating the depressive-like behavior. The protective mechanism of XYS may at least partly be ascribed to the decrease of RAGE accumulation in Cg as well as the attenuated RAGE-mediated inflammatory signal activation, thereby increasing the protection of brain FC. All these results provide strong preclinical evidence for XYS as a promising compound drug for the prevention and treatment of depression.

DATA AVAILABILITY STATEMENT

The original contributions presented in the study are included in the article/**Supplementary Material**; further inquiries can be directed to the corresponding authors.

ETHICS STATEMENT

The animal study was reviewed and approved by the Institutional Animal Care Unit Committee in Administration Office of Laboratory Animals of Nanfang Hospital (NFYY-2014-53).

AUTHOR CONTRIBUTIONS

WY conducted experiments for image acquisition and sampling. WY and TZ analyzed the image data and completed the relevant sample detection. CM, JL, and DZ analyzed the experimental data. LG and ZL supervised the work. All authors contributed to experimental design and results interpretation. WY, ZD, and DZ drafted and revised the manuscript. All data were generated in-house, and no paper mill was used. All authors read and approved the final manuscript.

FUNDING

This study was supported by the National Natural Science Foundation of China (grant numbers 81873170, 82004091, 81873271, and 81230085) and Administration of Traditional Chinese Medicine of Guangdong Province (No. 20201089).

SUPPLEMENTARY MATERIAL

The Supplementary Material for this article can be found online at: https://www.frontiersin.org/articles/10.3389/fphar.2021.703965/full#supplementary-material

REFERENCES

Beurel, E., Toups, M., and Nemeroff, C. B. (2020). The Bidirectional Relationship of Depression and Inflammation: Double Trouble. *Neuron* 107 (2), 234–256. doi:10.1016/j.neuron.2020.06.002

Bi, Y., Huang, P., Dong, Z., Gao, T., Huang, S., Gao, L., et al. (2019). Modified Xiaoyaosan Reverses Aberrant Brain Regional Homogeneity to Exert Antidepressive Effects in Mice. *Neuropathology* 39 (2), 85–96. doi:10.1111/neup.12540

Bolós, M., Perea, J. R., Terreros-Roncal, J., Pallas-Bazarra, N., Jurado-Arjona, J., Ávila, J., et al. (2018). Absence of Microglial CX3CR1 Impairs the Synaptic Integration of Adult-Born Hippocampal Granule Neurons. *Brain Behav. Immun.* 68, 76–89. doi:10.1016/j.bbi.2017.10.002

Castagné, V., Moser, P., Roux, S., and Porsolt, R. D. (2011). Rodent Models of Depression: Forced Swim and Tail Suspension Behavioral Despair Tests in Rats and Mice. *Curr. Protoc. Neurosci.* Chapter 8, Unit 8.10A. doi:10.1002/0471142301.ns0810as55

Chen, C., Yin, Q., Tian, J., Gao, X., Qin, X., Du, G., et al. (2020). Studies on the Potential Link between Antidepressant Effect of Xiaoyao San and its Pharmacological Activity of Hepatoprotection Based on Multi-Platform Metabolomics. *J. Ethnopharmacology* 249, 112432. doi:10.1016/j.jep.2019.112432

Deane, R., Du Yan, S., Submamaryan, R. K., Larue, B., Jovanovic, S., Hogg, E., et al. (2003). RAGE Mediates Amyloid-β Peptide Transport across the Blood-Brain Barrier and Accumulation in Brain. *Nat. Med.* 9 (7), 907–913. doi:10.1038/nm890

Ding, X.-F., Liu, Y., Yan, Z.-Y., Li, X.-J., Ma, Q.-Y., Jin, Z.-Y., et al. (2017). Involvement of Normalized Glial Fibrillary Acidic Protein Expression in the Hippocampi in Antidepressant-like Effects of Xiaoyaosan on Chronically Stressed Mice. *Evidence-Based Complement. Altern. Med.* 2017, 1–13. doi:10.1155/2017/19605842017

Ding, X.-F., Zhao, X.-H., Tao, Y., Zhong, W.-C., Fan, Q., Diao, J.-X., et al. (2014). Xiao Yao San Improves Depressive-like Behaviors in Rats with Chronic Immobilization Stress through Modulation of Locus Coeruleus-Norepinephrine System. *Evidence-Based Complement. Altern. Med.* 2014, 1–10. doi:10.1155/2014/605914

Ebert, D., and Ebmeier, K. P. (1996). The Role of the Cingulate Gyrus in Depression: from Functional Anatomy to Neurochemistry. *Biol. Psychiatry* 39 (12), 1044–1050. doi:10.1016/0006-3223(95)00320-7

Felger, J. C., Haroon, E., Patel, T. A., Goldsmith, D. R., Wommack, E. C., Woolwine, B. J., et al. (2020). What Does Plasma CRP Tell Us about Peripheral and central Inflammation in Depression? *Mol. Psychiatry* 25 (6), 1301–1311. doi:10.1038/s41380-018-0096-3

Franklin, T. C., Wohleb, E. S., Zhang, Y., Fogaça, M., Hare, B., and Duman, R. S. (2018). Persistent Increase in Microglial RAGE Contributes to Chronic Stress-Induced Priming of Depressive-like Behavior. *Biol. Psychiatry* 83 (1), 50–60. doi:10.1016/j.biopsych.2017.06.034

Franklin, T. C., Xu, C., and Duman, R. S. (2018). Depression and Sterile Inflammation: Essential Role of Danger Associated Molecular Patterns. *Brain Behav. Immun.* 72, 2–13. doi:10.1016/j.bbi.2017.10.025

Gao, L., Chen, X., Peng, T., Yang, D., Wang, Q., Lv, Z., et al. (2016). Caveolin-1 Protects against Hepatic Ischemia/reperfusion Injury through Ameliorating Peroxynitrite-Mediated Cell Death. *Free Radic. Biol. Med.* 95, 209–215. doi:10.1016/j.freeradbiomed.2016.03.023

Gao, L., Huang, P., Dong, Z., Gao, T., Huang, S., Zhou, C., et al. (2018). Modified Xiaoyaosan (MXYS) Exerts Anti-depressive Effects by Rectifying the Brain Blood Oxygen Level-dependent fMRI Signals and Improving Hippocampal Neurogenesis in Mice. *Front. Pharmacol.* 9, 1098. doi:10.3389/fphar.2018.01098

Haapakoski, R., Mathieu, J., Ebmeier, K. P., Alenius, H., and Kivimäki, M. (2015). Cumulative Meta-Analysis of Interleukins 6 and 1β, Tumour Necrosis Factor α and C-Reactive Protein in Patients with Major Depressive Disorder. *Brain Behav. Immun.* 49, 206–215. doi:10.1016/j.bbi.2015.06.001

Han, K.-M., De Berardis, D., Fornaro, M., and Kim, Y.-K. (2019). Differentiating between Bipolar and Unipolar Depression in Functional and Structural MRI Studies. *Prog. Neuro-Psychopharmacology Biol. Psychiatry* 91, 20–27. doi:10.1016/j.pnpbp.2018.03.022

He, Z., Lu, F., Sheng, W., Han, S., Pang, Y., Chen, Y., et al. (2020). Abnormal Functional Connectivity as Neural Biological Substrate of Trait and State Characteristics in Major Depressive Disorder. *Prog. Neuro-Psychopharmacology Biol. Psychiatry* 102, 109949. doi:10.1016/j.pnpbp.2020.109949

Huang, P., Gao, T., Dong, Z., Zhou, C., Lai, Y., Pan, T., et al. (2018). Neural Circuitry Among Connecting the hippocampus, Prefrontal Cortex and Basolateral Amygdala in a Mouse Depression Model: Associations Correlations between BDNF Levels and BOLD - fMRI Signals. *Brain Res. Bull.* 142, 107–115. doi:10.1016/j.brainresbull.2018.06.019

Jing, L.-L., Zhu, X.-X., Lv, Z.-P., and Sun, X.-G. (2015). Effect of Xiaoyaosan on Major Depressive Disorder. *Chin. Med.* 10, 18. doi:10.1186/s13020-015-0050-0

Lee, J., Sung, W.-S., Kim, E.-J., and Kim, Y. W. (2021). Xiaoyao-san, a Traditional Chinese Herbal Formula, for the Treatment of Irritable Bowel Syndrome. *Medicine (Baltimore)* 100 (10), e24019. doi:10.1097/MD.0000000000024019

Liu, C.-C., Wu, Y.-F., Feng, G.-M., Gao, X.-X., Zhou, Y.-Z., Hou, W.-J., et al. (2015). Plasma-metabolite-biomarkers for the Therapeutic Response in Depressed Patients by the Traditional Chinese Medicine Formula Xiaoyaosan: A 1H NMR-Based Metabolomics Approach. *J. Affective Disord.* 185, 156–163. doi:10.1016/j.jad.2015.05.005

Liu, C. S., Adibfar, A., Herrmann, N., Gallagher, D., and Lanctôt, K. L. (2016). Evidence for Inflammation-Associated Depression. *Curr. Top. Behav. Neurosci.* 31, 3–30. doi:10.1007/7854_2016_2

Liu, M.-Y., Yin, C.-Y., Zhu, L.-J., Zhu, X.-H., Xu, C., Luo, C.-X., et al. (2018). Sucrose Preference Test for Measurement of Stress-Induced Anhedonia in Mice. *Nat. Protoc.* 13 (7), 1686–1698. doi:10.1038/s41596-018-0011-z

Maes, M. (1999). Major Depression and Activation of the Inflammatory Response System. *Adv. Exp. Med. Biol.* 461, 25–46. doi:10.1007/978-0-585-37970-8_2

Miller, A. H., Maletic, V., and Raison, C. L. (2009). Inflammation and its Discontents: the Role of Cytokines in the Pathophysiology of Major Depression. *Biol. Psychiatry* 65 (9), 732–741. doi:10.1016/j.biopsych.2008.11.029

Mulders, P. C., van Eijndhoven, P. F., Schene, A. H., Beckmann, C. F., and Tendolkar, I. (2015). Resting-state Functional Connectivity in Major Depressive Disorder: A Review. *Neurosci. Biobehavioral Rev.* 56, 330–344. doi:10.1016/j.neubiorev.2015.07.014

Pan, Y., Chen, X.-Y., Zhang, Q.-Y., and Kong, L.-D. (2014). Microglial NLRP3 Inflammasome Activation Mediates IL-1β-related Inflammation in Prefrontal Cortex of Depressive Rats. *Brain Behav. Immun.* 41, 90–100. doi:10.1016/j.bbi.2014.04.007

Philippi, C. L., Motzkin, J. C., Pujara, M. S., and Koenigs, M. (2015). Subclinical Depression Severity Is Associated with Distinct Patterns of Functional Connectivity for Subregions of Anterior Cingulate Cortex. *J. Psychiatr. Res.* 71, 103–111. doi:10.1016/j.jpsychires.2015.10.005

Qiu, H., Cao, B., Cao, J., Li, X., Chen, J., Wang, W., et al. (2020). Resting-state Functional Connectivity of the Anterior Cingulate Cortex in Young Adults Depressed Patients with and without Suicidal Behavior. *Behav. Brain Res.* 384, 112544. doi:10.1016/j.bbr.2020.112544

Riva-Posse, P., Holtzheimer, P. E., and Mayberg, H. S. (2019). Cingulate-mediated Depressive Symptoms in Neurologic Disease and Therapeutics. *Handb Clin. Neurol.* 166, 371–379. doi:10.1016/B978-0-444-64196-0.00021-2

Rolls, E. T. (2019). The Cingulate Cortex and Limbic Systems for Emotion, Action, and Memory. *Brain Struct. Funct.* 224 (9), 3001–3018. doi:10.1007/s00429-019-01945-2

Shi, B. Y., Rao, Z. L., Luo, J., Liu, X. B., Fang, Y., Cao, H. J., et al. (2019). [Protective Effect and Mechanism of Xiaoyao San on Lipopolysaccharide-Induced Hippocampal Neurons Injury]. *Zhongguo Zhong Yao Za Zhi* 44 (4), 781–786. doi:10.19540/j.cnki.cjcmm.20181101.003

Shang, X., Shang, Y., Fu, J., and Zhang, T. (2017). Nicotine Significantly Improves Chronic Stress-Induced Impairments of Cognition and Synaptic Plasticity in Mice. *Mol. Neurobiol.* 54(6), 4644–4658. doi:10.1007/s12035-016-0012-2

Videbech, P. (2000). PET Measurements of Brain Glucose Metabolism and Blood Flow in Major Depressive Disorder: a Critical Review. *Acta Psychiatr. Scand.* 101 (1), 11–20. doi:10.1034/j.1600-0447.2000.101001011.x

Wang, J., Li, X., He, S., Hu, L., Guo, J., Huang, X., et al. (2018). Regulation of the Kynurenine Metabolism Pathway by Xiaoyao San and the Underlying Effect in the hippocampus of the Depressed Rat. *J. Ethnopharmacology* 214, 13–21. doi:10.1016/j.jep.2017.11.037

Willner, P. (2005). Chronic Mild Stress (CMS) Revisited: Consistency and Behavioural-Neurobiological Concordance in the Effects of CMS. *Neuropsychobiology* 52(2), 90–110. doi:10.1159/000087097

Wohleb, E. S., Franklin, T., Iwata, M., and Duman, R. S. (2016). Integrating Neuroimmune Systems in the Neurobiology of Depression. *Nat. Rev. Neurosci.* 17 (8), 497–511. doi:10.1038/nrn.2016.69

Xie, J., Bi, B., Qin, Y., Dong, W., Zhong, J., Li, M., et al. (2021). Inhibition of Phosphodiesterase-4 Suppresses HMGB1/RAGE Signaling Pathway and NLRP3 Inflammasome Activation in Mice Exposed to Chronic Unpredictable Mild Stress. *Brain Behav. Immun.* 92, 67–77. doi:10.1016/j.bbi.2020.11.029

Xie, L., Gu, Z., Liu, H., Jia, B., Wang, Y., Cao, M., et al. (2020). The Anti-depressive Effects of Hesperidin and the Relative Mechanisms Based on the NLRP3 Inflammatory Signaling Pathway. *Front. Pharmacol.* 11, 1251. doi:10.3389/fphar.2020.01251

Yan, Z., Jiao, H., Ding, X., Ma, Q., Li, X., Pan, Q., et al. (2018). Xiaoyaosan Improves Depressive-like Behaviors in Mice through Regulating Apelin-APJ System in Hypothalamus. *Molecules* 23 (5), 1073. doi:10.3390/molecules23051073

Yang, B. K., Qin, J., Nie, Y., and Chen, J. C. (2018). Sustained Antidepressant Action of the N-methyl-D-aspartate R-eceptor A-ntagonist MK-801 in a C-hronic U-npredictable M-ild S-tress M-odel. *Exp. Ther. Med.* 16 (6), 5376–5383. doi:10.3892/etm.2018.6876

Yang, F., Wang, H., Chen, H., Ran, D., Tang, Q., Weng, P., et al. (2020). RAGE Signaling Pathway in hippocampus Dentate Gyrus Involved in GLT-1 Decrease Induced by Chronic Unpredictable Stress in Rats. *Brain Res. Bull.* 163, 49–56. doi:10.1016/j.brainresbull.2020.06.020

Yang, R., Gao, C., Wu, X., Yang, J., Li, S., and Cheng, H. (2016). Decreased Functional Connectivity to Posterior Cingulate Cortex in Major Depressive Disorder. *Psychiatry Res. Neuroimaging* 255, 15–23. doi:10.1016/j.pscychresns.2016.07.010

Yu, S., Fu, L., Lu, J., Wang, Z., and Fu, W. (2020). Xiao-Yao-San Reduces Blood-Brain Barrier Injury Induced by Chronic Stress *In Vitro* and Vivo via Glucocorticoid Receptor-Mediated Upregulation of Occludin. *J. Ethnopharmacology* 246, 112165. doi:10.1016/j.jep.2019.112165

Zhang, Y., Han, M., Liu, Z., Wang, J., He, Q., and Liu, J. (2012). Chinese Herbal Formula Xiao Yao San for Treatment of Depression: a Systematic Review of Randomized Controlled Trials. *Evidence-Based Complement. Altern. Med.* 2012, 1–13. doi:10.1155/2012/931636

Zhang, Y., Liu, L., Liu, Y.-Z., Shen, X.-L., Wu, T.-Y., Zhang, T., et al. (2015). NLRP3 Inflammasome Mediates Chronic Mild Stress-Induced Depression in Mice via Neuroinflammation. *Int. J. Neuropsychopharmacol.* 18 (8), pyv006. doi:10.1093/ijnp/pyv006

Zhu, H.-Z., Liang, Y.-D., Hao, W.-Z., Ma, Q.-Y., Li, X.-J., Li, Y.-M., et al. (2021). Xiaoyaosan Exerts Therapeutic Effects on the Colon of Chronic Restraint Stress Model Rats via the Regulation of Immunoinflammatory Activation Induced by the TLR4/NLRP3 Inflammasome Signaling Pathway. *Evidence-Based Complement. Altern. Med.* 2021, 1–18. doi:10.1155/2021/6673538

Zhu, H.-Z., Liang, Y.-D., Ma, Q.-Y., Hao, W.-Z., Li, X.-J., Wu, M.-S., et al. (2019). Xiaoyaosan Improves Depressive-like Behavior in Rats with Chronic Immobilization Stress through Modulation of the Gut Microbiota. *Biomed. Pharmacother.* 112, 108621. doi:10.1016/j.biopha.2019.108621

Zhu, X., Xia, O., Han, W., Shao, M., Jing, L., Fan, Q., et al. (2014). Xiao Yao San Improves Depressive-like Behavior in Rats through Modulation Ofβ-Arrestin 2-Mediated Pathways in Hippocampus. *Evidence-Based Complement. Altern. Med.* 2014, 1–13. doi:10.1155/2014/902516

Conflict of Interest: The authors declare that the research was conducted in the absence of any commercial or financial relationships that could be construed as a potential conflict of interest.

Publisher's Note: All claims expressed in this article are solely those of the authors and do not necessarily represent those of their affiliated organizations, or those of the publisher, the editors, and the reviewers. Any product that may be evaluated in this article, or claim that may be made by its manufacturer, is not guaranteed or endorsed by the publisher.

frontiers in Pharmacology

SYSTEMATIC REVIEW
published: 01 October 2021
doi: 10.3389/fphar.2021.728758

The Efficacy of Triptolide in Preventing Diabetic Kidney Diseases: A Systematic Review and Meta-Analysis

Dongning Liang[1,2], *Hanwen Mai*[1,2], *Fangyi Ruan*[1,2] *and Haiyan Fu*[1]*

[1]State Key Laboratory of Organ Failure Research, National Clinical Research Center of Kidney Disease, Guangdong Provincial Key Laboratory of Renal Failure Research, Division of Nephrology, Nanfang Hospital, Southern Medical University, Guangzhou, China, [2]The First Medical College, Southern Medical University, Guangzhou, China

Ethnopharmacological Relevance: Triptolide (TP), the primary biologically active ingredient of *Tripterygium wilfordii Hook F* (TWHF), possesses the potential to solve the shortcomings of TWHF in treating diabetic kidney disease (DKD) in the clinic.

Aim of the Study: We conducted a meta-analysis to evaluate the efficacy of TP in treating DKD and offer solid evidence for further clinical applications of TP.

Materials and Methods: Eight databases (CNKI, VIP, CBM, WanFang, PubMed, Web of Science, EMBASE, and Cochrane library) were electronically searched for eligible studies until October 17, 2020. We selected animal experimental studies using TP *versus* renin–angiotensin system inhibitors or nonfunctional liquids to treat DKD by following the inclusion and exclusion criteria. Two researchers independently extracted data from the included studies and assessed the risk of bias with the Systematic Review Centre for Laboratory Animal Experimentation Risk of Bias tool. Fixed-effects meta-analyses, subgroup analyses, and meta-regression were conducted using RevMan 5.3 software. Inplasy registration number: INPLASY2020100042.

Results: Twenty-six studies were included. Meta-analysis showed that TP significantly reduced albuminuria (14 studies; standardized mean difference SMD: –1.44 [–1.65, –1.23], I^2 = 87%), urine albumin/urine creatinine ratio (UACR) (8 studies; SMD: –5.03 [–5.74, –4.33], I^2 = 84%), total proteinuria (4 studies; SMD: –3.12 [–3.75, –2.49], I^2 = 0%), serum creatinine (18 studies; SMD: –0.30 [–0.49, –0.12], I^2 = 76%), and blood urea nitrogen (12 studies; SMD: –0.40 [–0.60, –0.20], I^2 value = 55%) in DKD animals, compared to the vehicle control. However, on comparing TP to the renin–angiotensin system (RAS) inhibitors in DKD treatment, there was no marked difference in ameliorating albuminuria (3 studies; SMD: –0.35 [–0.72, 0.02], I^2 = 41%), serum creatinine (3 studies; SMD: –0.07 [–0.62, 0.48], I^2 = 10%), and blood urea nitrogen (2 studies; SMD: –0.35 [–0.97, 0.28], I^2 = 0%). Of note, TP exhibited higher capacities in reducing UACR (2 studies; SMD: –0.66 [–1.31, –0.01], I^2 = 0%) and total proteinuria (2 studies; SMD: –1.18 [–1.86, –2049], I^2 = 0%). Meta-regression implicated that the efficacy of TP in reducing DKD albuminuria was associated with applied dosages. In addition, publication bias has not been detected on attenuating albuminuria between TP and RAS inhibitors after the diagnosis of DKD.

Systematic Review Registration: https://clinicaltrials.gov/, identifier INPLASY2020100042

OPEN ACCESS

Edited by:
Annalisa Chiavaroli,
University of Studies G.d'Annunzio Chieti and Pescara, Italy

Reviewed by:
Sofia Viana,
University of Coimbra, Portugal
Gabino Garrido,
Catholic University of the North, Chile

***Correspondence:**
Haiyan Fu
hy_fu426@126.com

Specialty section:
This article was submitted to Ethnopharmacology, a section of the journal Frontiers in Pharmacology

Received: *22 June 2021*
Accepted: *12 August 2021*
Published: *01 October 2021*

Citation:
Liang D, Mai H, Ruan F and Fu H (2021) The Efficacy of Triptolide in Preventing Diabetic Kidney Diseases: A Systematic Review and Meta-Analysis. Front. Pharmacol. 12:728758. doi: 10.3389/fphar.2021.728758

Keywords: triptolide, renin-angiotensin system inhibitor, diabetic kidney diseases, albuminuria, kidney function

INTRODUCTION

Diabetic kidney disease (DKD) is a chronic clinical condition characterized by micro- or macro-albuminuria followed by a progressive decline in kidney functions (Fu et al., 2019; Kopel et al., 2019). Over the past years, the incidence of DKD and its mortality has been largely underestimated (Rao et al., 2012). As a major driver of excess mortality in diabetes (Koye et al., 2018), DKD places growing financial burdens on diabetes management on a global scale (Slabaugh et al., 2015), especially in emerging and developing economies (Thomas et al., 2016). At present, antidiabetic medications and renin–angiotensin system (RAS) inhibitors are routinely used to prevent DKD from entering end-stage renal disease (ESRD) (Hostetter, 2001). However, this first-line therapy for DKD has been considered unsatisfying because of its potential side effects, such as diabetic ketoacidosis (Fadini et al., 2017) and reversible AKI (Onuigbo, 2011). Therefore, a systemic evaluation of the efficacy and safety of the current therapeutic strategies for DKD is urgently needed.

Tripterygium wilfordii Hook F (TWHF), a well-known Chinese herb, has been intensely developed and widely applied in treating nephritis or DKD in the clinic (Li et al., 2014; Huang et al., 2020; Xu et al., 2020; Guo Y et al., 2021). However, restricted by its adverse reactions and complex pharmacology (Hong et al., 2016; Ren et al., 2019; Huang et al., 2020), the extracts from TWHF have become a new focus in the field. The primary biologically active ingredient of TWHF, triptolide (TP), was discovered in 1972 (Kupchan et al., 1972). It is a striking target for total synthesis because of its intriguing structural features and promising biological activities (Zhang et al., 2019). TP can suppress inflammation and enhance cytoprotection by inhibiting the secretion of proinflammatory cytochemokines (Zhao et al., 2000; Zhou et al., 2003; Krakauer et al., 2005; Lu et al., 2005; Liu et al., 2006; Hoyle et al., 2010; Hou et al., 2019). Similar to TWHF, TP also induces organ or tissue damages (Xi et al., 2017), including hepatotoxicity (Li et al., 2014), nephrotoxicity (Yang et al., 2011), and reproductive toxicity (Ni et al., 2008). Along with advances in technology, TP exhibits great capacities in enhancing its efficacy, reducing side effects, and improving bioavailability through the nanostructured TP delivery system (Ren et al., 2021). Furthermore, the newly designed and synthesized water-soluble TP derivatives also demonstrated their safety and efficacy (Liu, 2011). These innovations significantly increased the application of TP in treating DKD. In this study, in contrast to RAS inhibitors and nonfunctional liquids, the primary objective is to systemically evaluate the efficacy of TP in animal models with DKD. Our analyses provide confidence for clinicians to design personalized therapeutic strategies for DKD under the current precision medicine model.

METHODS

This systematic review adhered to the preferred reporting items for systematic reviews and meta-analysis guidelines (Moher et al., 2009). The review protocol was registered in INPLASY before the beginning of the experiment (registration number: INPLASY2020100042).

Publication Searching

We followed the Systematic Review Center for Laboratory Animal Experimentation (SYRCLE) step-by-step guide (Leenaars et al., 2012) to draw up the search strategy. Animal experimental studies of "TP treats DKD" were electronically searched in China National Knowledge Infrastructure (CNKI), Chinese Science and Technology Journal Database (VIP), Chinese Biomedical Database (CBM), WanFang, PubMed, Web of Science, EMBASE, and Cochrane library published from database inception to October 17, 2020. The search strategy consists of following three search components: triptolide AND DKD/diabetic nephropathy AND animals, using the Medical Subject Heading (MeSH) terms and keywords to perform searching. A pre-published animal filter (Hooijmans et al., 2010) was applied to limit the range for animal studies. All references of eligible articles were screened carefully for additional analyses.

Inclusion and Exclusion Criteria

Included criteria: 1. Population: All animal models with DKD, regardless of species, age, or sex. 2. Intervention: The experimental groups used TP as monotherapy in any dosage. Comparison: The control groups received equal volumes of a nonfunctional liquid (normal saline) or did not receive treatment or recommended therapies according to clinical practice guidelines, including RAS inhibitors (angiotensin-converting enzyme inhibitors, ACEIs, or angiotensin AT (1)-receptor blockers, ARBs). 3. Study design: TP prepared in various forms, including extracts, granules, and injections, was eligible. 4. Outcome: The outcomes were changed in albuminuria, proteinuria excretion, and kidney function (serum creatinine, SCr, and blood urea nitrogen, BUN). 5. The literature is published either in Chinese or English.

Excluded criteria: 1. No *in vivo* studies (*in vitro* studies, clinical trials, review articles, case reports, comments, editorials, and abstracts). 2. Additional hypoglycemics were used during treatment. 3. Assessing TP combined with other herbal ingredients or complementary therapies. 4. Repeated literature. 5. Full text was not found.

Data Extraction and Quality Assessment

Studies according to the inclusion criteria were considered eligible for the analyses. Data of each included study were extracted by two authors independently and cross-checked in terms of the author, publication year, animal models (species, sex, weight, method of modeling, and the criteria for successful modeling), TP intervention (the type of intervention, dosage, and the duration of intervention), and outcomes. When results were only reported graphically, the graph data were measured using GetData, software downloaded on the website (http://getdata.com.ru/). The total quality assessment of each study was evaluated based on the Systematic Review Centre for Laboratory Animal Experimentation Risk of Bias tool (Hooijmans et al., 2014). According to its guidance, each domain of individual studies was graded as low, unclear, or high risk of bias.

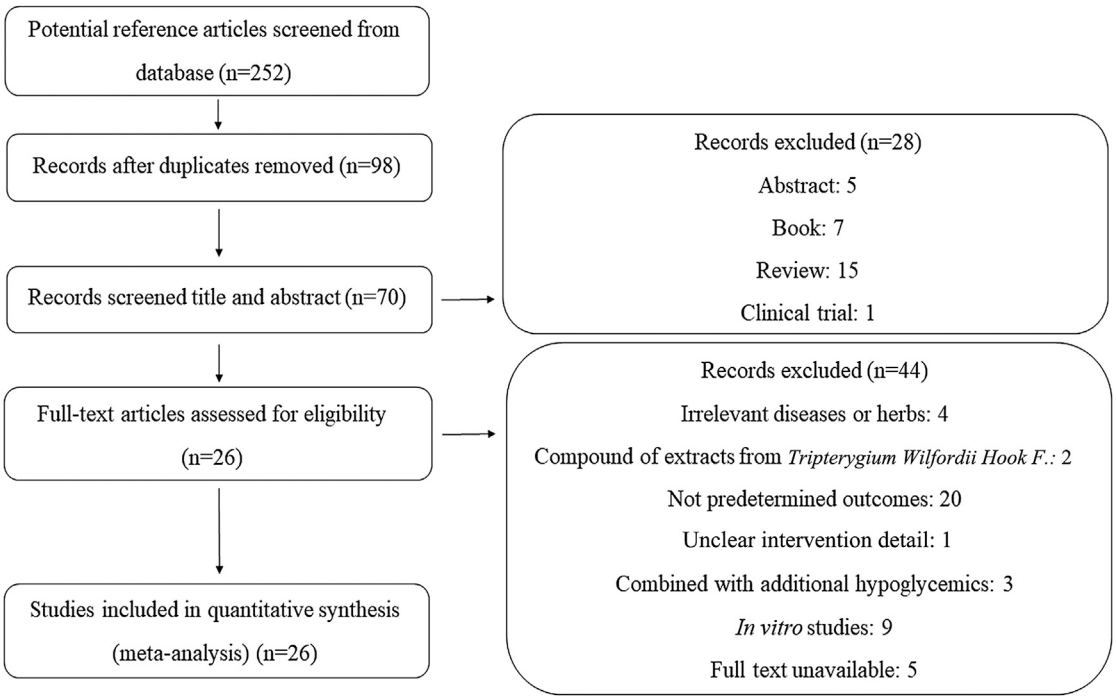

FIGURE 1 | Flow chart of the screening process.

Statistical Analysis

RevMan 5.3 software and Stata 15.1 software were used for data analysis. Studies were divided into two compilations to assess the differences between the TP and control groups and the differences between the TP and the RAS inhibitor groups. Continuous variables were expressed as standardized mean differences (SMDs) with a 95% confidence interval. A fixed effect was used in meta-analysis. Heterogeneity among the included studies was checked by using the chi-square test and I^2 test. Substantial heterogeneity was considered to exist when $I^2 > 50\%$. Subgroup analyses and meta-regression were carried out to explore the possible sources of heterogeneity. High-risk studies were removed one by one from the group of the synthesized studies, and the remaining studies were re-analyzed to estimate the robustness of the results. Publication bias was evaluated by Begg's test, Egger's test, and the visual inspection of funnel plots for asymmetry.

RESULTS

Search Results

As illustrated in **Figure 1**, we identified 252 articles throughout the database. After removing duplications and screening the articles based on the titles and abstracts, the full texts of 70 studies were assessed for eligibility. Forty-four additional studies were excluded with the reasons being unclear intervention details and no predetermined outcomes, combining other extracts from TWHF or additional hypoglycemics for treatment, unavailable full texts, presenting *in vitro* experiments, and no relevance to diseases or herbs. Therefore, 26 studies were ultimately included in the analyses.

Characteristics of the Included Studies

The details of the study characteristics are presented in **Table 1**. Twenty-six studies were published between 2008 and 2020. Five articles (Ma et al., 2013; Guo et al., 2016; Dong et al., 2017; Han et al., 2017; Li et al., 2017) were published in English, and the remaining 21 articles were published in Chinese. Four articles (Ma, 2009; Zhu, 2013; Han, 2018; Xue, 2018) were exhibited as dissertations, and the others were published in peer-reviewed journals. All research works tested the effects of TP on DKD, reporting at least one clinical parameter, including albuminuria, proteinuria, UACR, or kidney function. Among them, seven studies (Ma, 2009; Ma et al., 2009; Qao et al., 2009; Li et al., 2013; An et al., 2017; Dong et al., 2017; Ren et al., 2020) performed comparisons between TP and ACEI or ARB in treating DKD. Twenty-three studies used male Sprague–Dawley (SD) and Wistar rats, and the remaining three studies (Qao et al., 2009; Fan et al., 2018; Ren et al., 2020) used mutant or transgenic mice. The methods of modeling and the types of interventions are stated above. The duration of intervention ranged from 4 to 12 weeks. The dosage of TP varied from 0.2 ug/kg/d to 1.8 g/kg/d; 0.2 mg/kg/d was the commonly administered dose.

Risk of Bias of the Studies Included

According to SYRCLE's risk of bias tool for animal studies, two researchers (MH and RF) independently evaluated all included

TABLE 1 | Characteristics of the studies included in the review.

Included studies (author, year)	Species(Sex, n = experimental/ control group)	Weight (g)	Method of modeling	The criteria for modeling successfully	Type of intervention	Dosage (mg/kg/ d)	Intervention duration (week)	Outcomes
An et al. (2017)	SD rats (male 20/9)	225 ± 25	HFD (4w)+STZI (60 mg/kg)	1. FBG>16.7 mmol/L (72 h of STZI) 2. Symptoms such as obvious polyuria (72 h of STZI)	T: TG C: SG	0.2/0.4	4	1. 24-h urinary albumin
Dong et al. (2017)	SD rats (male 24/12)	225 ± 25	HFD (4w)+STZI (60 mg/kg)	1. FBG>16.7 mmol/L (72 h of STZI) 2. Symptoms such as obvious polyuria (72 h of STZI)	T: TG C: SG	0.2/0.4	4	1. 24-h urinary protein
Fan et al. (2018)	C57BL/6-Ins2Akita (male 24/8)	NM	/	NM	T: TG C: SG	0.025/ 0.050/ 0.100	8	1. 24-h urinary albumin 2. SCr 3. BUN
Gao et al. (2009)	BKS db/db diabetic mice (male: female = 1: 1 36/18)	NM	/	NM	T: TG C: SG	0.025/ 0.050	12	1. 24-h urinary albumin
Guo et al. (2016)	SD rats (male 45/15)	Unavailable data from the graph	HFD (4w)+STZI (30 mg/kg)	1. Rats with blood glucose levels>16.7 mmol/L	T: TG C: distilled water	6/12/24	4	1. 24- h urinary albumin 2. BUN
Han et al. (2017)	SD rats (male 10/10)	170 ± 10	HFD (6w)+STZI (30 mg/Kg/d, 3 days)	1. FBG>16.7 mmol/L (72 h of STZI) 2.24 h UMA levels>30 mg (2 weeks of DME)	T: TG C: SG	0.10	12	1. 24-h urinary albumin 2. SCr 3. BUN
Han (2018)	SD rats (male 10/10)	170 ± 10	HFD (8w)+STZI (30 mg/kg)	1. Random blood glucose levels of 2 or more times> 16.7 mmol/L (1 week of STZI) 2. Obvious increase of UMA level compared to NC group (6 weeks of DME)	T: TG C: DMSO	0.10	12	1. 24-h urinary albumin 2. SCr 3. BUN
Li et al. (2013)	SD rats (male 8/8)	200 g ± 20	HFD (8w)+STZI (30 mg/kg)	1. Blood glucose levels ≥16.7 mmol/L (1 week of STZI) 2.ISI ≤ ALN (1 week of STZI)	T: TG C: SG	0.2	8	1. UACR 2. SCr 3. BUN
Li et al. (2015)	SD rats (male 15/15)	230 g ± 20	HFD (4w)+STZI (30 mg/kg)	1. Random blood glucose levels ≥16.7 mmol/L (5 days of STZI)	T: TG C: edible vegetable oil	0.2	4	1. 24-h urinary albumin
Li et al. (2017)	SD rats (male 11/12)	NM	HFD (8w)+STZI (30 mg/kg)	1. Random blood glucose levels ≥16.7 mmol/L (72 h of STZI) 2.24 h UMA levels ≥30 mg (NM)	T: TG C: SG	0.2	12	1. 24-h urinary albumin 2. SCr 3. BUN
Liu et al. (2014)	SD rats (male 8/8)	190 ± 10	STZI (60 mg/kg)	1. Blood glucose level ≥16.7 mmol/L (72 h of STZI)	T: TG C: SG	0.2	8	1. 24-h urinary albumin 2. SCr 3. BUN
Ma et al. (2008)	Wistar rats (male 7/7)	200 ± 20	HFD (4w)+STZI (30 mg/kg)	1. Blood glucose level ≥16.7 mmol/L (1 week of STZI) 2. Blood pressure ≥ ALN (1 week of STZI) 3. Blood lipid ≥ ALN (1 week of STZI) 4. ISI ≤ ALN (1 week of STZI)	T: TG C: SG	0.2	12	1. UACR 2. SCr
Ma et al. (2009)	Wistar rats (male 12/12)	200 ± 20	HFD (8w)+ STZI (30 mg/kg)	1. Blood glucose level ≥16.7 mmol/L (1 week of STZI) 2. Blood pressure ≥ ALN (1 week of STZI) 3. Blood lipid ≥ ALN (1 week of STZI) 4.ISI ≤ ALN (1 week of STZI)	T: TG C: NaCMC	0.10	8	1. UACR
Ma et al. (2010)	Wistar rats (14/14)	200 ± 20	HFD (8w)+ STZI (30 mg/kg)	1. FBG ≥10.0 mmol/L (1 week of STZI) 2. ISI ≤ ALN (1 week of STZI)	T: TG C: NaCMC	0.2	8	1. UACR 2. SCr

(Continued on following page)

TABLE 1 | (*Continued*) Characteristics of the studies included in the review.

Included studies (author, year)	Species(Sex, n = experimental/ control group)	Weight (g)	Method of modeling	The criteria for modeling successfully	Type of intervention	Dosage (mg/kg/ d)	Intervention duration (week)	Outcomes
Ma et al. (2013)	Wistar rats (male 12/11)	200 ± 20	HFD (8w)+ STZI (30 mg/kg)	NM	T: TG C: DMSO	0.1	8	1. UACR 2. SCr 3. BUN
Ma et al. (2009)	Wistar rats (male 14/14)	200 ± 20	HFD (8w)+ STZI (30 mg/kg)	1. FBG ≥10.0 mmol/L (1 week of STZI) 2. ISI ≤ ALN (1 week of STZI)	T: TG C: DMSO	0.2	8	1. 24-h urinary albumin 2. SCr
Ren et al. (2020)	BKS-db/db mice (male 6/6)	38.25 ± 1.42	/	NM	T: TG C: SG	0.05	8	1. 24-h urinary albumin 2. Plasma Cr
Wang et al. (2013)	SD rats (male 16/16)	200 ± 20	HFD (8w)+ STZI (30 mg/kg)	1. Blood glucose levels ≥16. 7 mmol/L (1 week of STZI) 2. ISI ≤ ALN (1 week of STZI)	T: TG C: SG	0.2	8	1.UACR 2.Scr 3.BUN
Wang and Yu (2017a)	SD rats (male 10/10)	190 ± 20	STZI (65 mg/kg)	1. Blood glucose levels ≥16. 7 mmol/L (1 week of STZI) 2. Glycosuria levels ≥ +++ (three consecutive days after 1 week of STZI)	T: TG C: SG	0.2	8	1.24 h urinary protein 2.Scr
Wang and Yu (2017b)	SD rats (male 10/10)	190 ± 20	STZI (65 mg/kg)	1. Blood glucose levels ≥16. 7 mmol/L (1 week of STZI) 2. Glycosuria levels ≥ +++ (three consecutive days after 1 week of STZI)	T: TG C: SG	0.2	8	1.24 h urinary protein 2.Scr
Wang and Yu (2017c)	SD rats (male 10/10)	190 ± 20	STZI (65 mg/kg)	1. Blood glucose levels ≥16. 7 mmol/L (1 week of STZI) 2. Glycosuria levels ≥ +++ (three consecutive days after 1 week of STZI)	T: TG C: SG	0.2	8	1. 24-h urinary protein 2. SCr
Xue et al., 2012	Wistar rats (male 9/7)	200 ± 20	HFD(8w) + STZI(30mg/ Kg)	1. Blood glucose levels ≥10.0 mmol/L (1 week of STZI) 2. ISI ≥ ALN (1 week of STZI)	T:TG C:DMSO	0.2	8	1. 24 h urinary protein 2. SCr
Chen et al. (2018)	SD rats (male 15/15)	160 ± 8	HFD (8w)+ STZI (30 mg/kg)	1. Random blood glucose levels of 2 or more times> 16.7 mmol/L (1 week of STZI)	T: TG C: SG	0.2	12	1. 24-h urinary albumin 2. SCr 3. BUN
Ye and Hong (2015)	SD rats (male 44/22)	NM	STZI (60 mg/kg)	1. Blood glucose levels ≥16.7 mmol/L (72 h of STZI) 2. Glycosuria levels ≥ +++ (three consecutive days after 72 h of STZ injection)	T: TG C: SG	0.2	12	1. 24-h urinary albumin
You et al. (2015)	SD rats (male 13/13)	170 ± 10	STZI (52 mg/kg/d, 5 days)	1. Blood glucose levels ≥16.7 mmol/L (72 h of STZI) 2. Glycosuria levels ≥ +++ (72 h of STZI)	T: TG C: drinking water	NM	8	1. 24-h urinary albumin
Zhu (2013)	SD rats (male 44/22)	180 ± 20	STZI (60 mg/kg)	1. Blood glucose levels ≥16.7 mmol/L (72 h of STZI) 2. Glycosuria levels ≥ +++ (three consecutive days after 72 h of STZ injection)	T: TG C: SG	0.2/0.4	12	1. 24-h urinary albumin 2. SCr 3. BUN
NM: no mentioned	HFD: high fat diet	STZI: STZ injection	FBG: fasting blood glucose	ALN: the average levels of normal animals	TG: triptolide gavage	SG: 0.9% saline gavage	DME: diabetes model established	
Dong et al. (2017)	SD rats (male 12/12)	225 ± 25	HFD (4w)+STZ (60 mg/kg)	1. FBG>16.7 mmol/L (72 h) 2. Symptoms such as obvious polyuria (72 h of STZI)	T: TG P: benazepril hydrochloride	T:0.2/ 0.4 P:10	4	1. 24-h urinary protein

(Continued on following page)

TABLE 1 | (*Continued*) Characteristics of the studies included in the review.

Included studies (author, year)	Species(Sex, n = experimental/ control group)	Weight (g)	Method of modeling	The criteria for modeling successfully	Type of intervention	Dosage (mg/kg/ d)	Intervention duration (week)	Outcomes
An et al. (2017)	SD rats (male 10/10)	225 ± 25	HFD (4w)+STZI (60 mg/kg)	1. FBG>16.7 mmol/L (72 h of STZI) 2. Symptoms such as obvious polyuria (72 h of STZI)	T: TG P: benazepril hydrochloride	T:0.2/ 0.4 P:10	4	1. 24-h urinary albumin
Gao et al. (2009)	db/db diabetic mice (male:female = 1:1 18/18)	NM	/	NM	T: TG P: valsartan	T:0.025/ 0.050 P: 20	12	1. 24-h urinary albumin
Li et al. (2013)	SD rats (male 8/8)	200 g ± 20	HFD (8w)+STZ (30 mg/kg)	1. Blood glucose levels ≥16.7 mmol/L (1 week of STZI) 2. ISI ≤ ALN (1 week of STZI)	T: TG P: irbesartan	T:0.2 P:50	8	1. UACR 2. SCr 3. BUN
Ma et al. (2009)	Wistar rats (male 14/14)	200 ± 20	HFD (8w)+ STZ (30 mg/kg)	1. FBG ≥10.0 mmol/L (1 week of STZI) 2. ISI ≤ ALN (1 week of STZI)	T: TG P: irbesartan	T:0.2 P:50	8	1. 24-h urinary albumin 2. SCr
Ren et al. (2020)	BKS-db/db mice (male 6/6)	38.25 ± 1.42	NM	NM	T: TG P: telmisartan	T:0.050 P:5	8	1. 24-h urinary albumin 2. Plasma cr
NM: no mentioned	HFD: high-fat diet	STZI: STZ injection	FBG: fasting blood glucose	ALN: the average levels of normal animals	TG: triptolide gavage	SG: 0.9% saline gavage		

studies. The detailed results of the analyses of bias are shown in **Figures 2A,B**. No studies fulfilled all methodological criteria that were analyzed. Regarding selection bias, random sequence generation processes were not reported clearly in 76.92% of studies (n = 20). In terms of the animals' baseline characteristics, 23 studies (88.46%) did not report this information. The unclear risks of the bias found in the studies were related to allocation concealment, blinding of caregivers, and/or investigators or outcome assessors. Nine studies (34.62%) showed incomplete information regarding random housing. Three studies (11.54%) reported unclear arbitrary outcome assessment of detection bias for relevant outcome measures. Two studies (7.70%) presented a high risk for incomplete outcome data, while three (11.54%) for selective outcome reporting. Only one research (3.85%) suggests other potential sources of bias.

Effects of TP in Treating DKD

Effects on the Changes of Albuminuria, Urine Albumin/ Urine Creatinine Ratio (UACR), or Proteinuria

The change in albuminuria was measured in 14 studies (Qao et al., 2009; Zhu, 2013; Liu et al., 2014; Li et al., 2015; Ye and Hong et al., 2015; You et al., 2015; Guo et al., 2016; An et al., 2017; Han et al., 2017; Li et al., 2017; Fan et al., 2018; Han, 2018; Xue, 2018; Ren et al., 2020). The pooled estimation indicated that TP reduced albuminuria significantly (SMD: −1.44 [−1.65, −1.23], I^2 = 87%), albeit with substantial heterogeneity (**Figure 3**).

Because of the heterogeneity associated with these studies, we performed the subgroup analyses of treatment duration (p < 0.00001), the dosage of triptolide (p = 0.002), method of modeling (p = 0.0003), and species of modeling (p = 0.85). Moreover, the meta-regression results showed that there was a linear relationship between the effect and low doses of TP. The studies in which dosage was more significant than 400 μg/kg/d were considered the high-dosage subgroup, whereas others were considered the low-dosage subgroup. The sensitivity analysis found no significant changes.

Eight studies (Li et al., 2013; Ma et al., 2008; Ma, 2009; Ma et al., 2009; Ma et al., 2010; Ma et al., 2013; Wang et al., 2013; Xue et al., 2012) examined the UACR. The outcome was −5.03 mg/mg (95% CI [−5.74, −4.33]), though heterogeneity was significant (I^2 = 84%, **Figure 4**). Through sensitivity analysis, it is found that heterogeneity was significantly reduced when Wang's study (Wang et al., 2013) was eliminated (the I^2 value reduced from 84% to 0) (**Figure 5**).

As for proteinuria, the meta-analysis result of the four studies (Dong et al., 2017; Wang and Yu, 2017a; Wang and Yu, 2017b; Wang and Yu, 2017c) also suggested that it lowered the level of proteinuria. The I^2 value was less than 50% (**Figure 6**). Since the study (Dong et al., 2017) contained two groups, we divided it into Dong et al., 2017-A and -B in this meta-analysis.

Effects on Kidney Function Changes

The kidney function was reflected by measuring the concentration of serum creatinine (SCr) and blood urea nitrogen (BUN) in the included studies. The pooled result of 18 studies (Fan et al., 2018; Guo et al., 2016; Han et al., 2017; Han, 2018; Liu et al., 2014; Li et al., 2013; Li et al., 2017; Ma et al., 2008; Ma, 2009; Ma et al., 2010; Ren et al., 2020; Wang et al., 2013; Wang and Yu, 2017a, 2017b, 2017c; Xue et al., 2012; Xue, 2018; Zhu, 2013) showed that TP had a positive effect on reducing SCr levels, with an SMD (and 95% CI) of −0.30 [−0.49, −0.12](**Figure 7**). The study (Fan et al., 2018) contained three groups. We then divided it into Fan et al., 2018-A, and -B, and -C

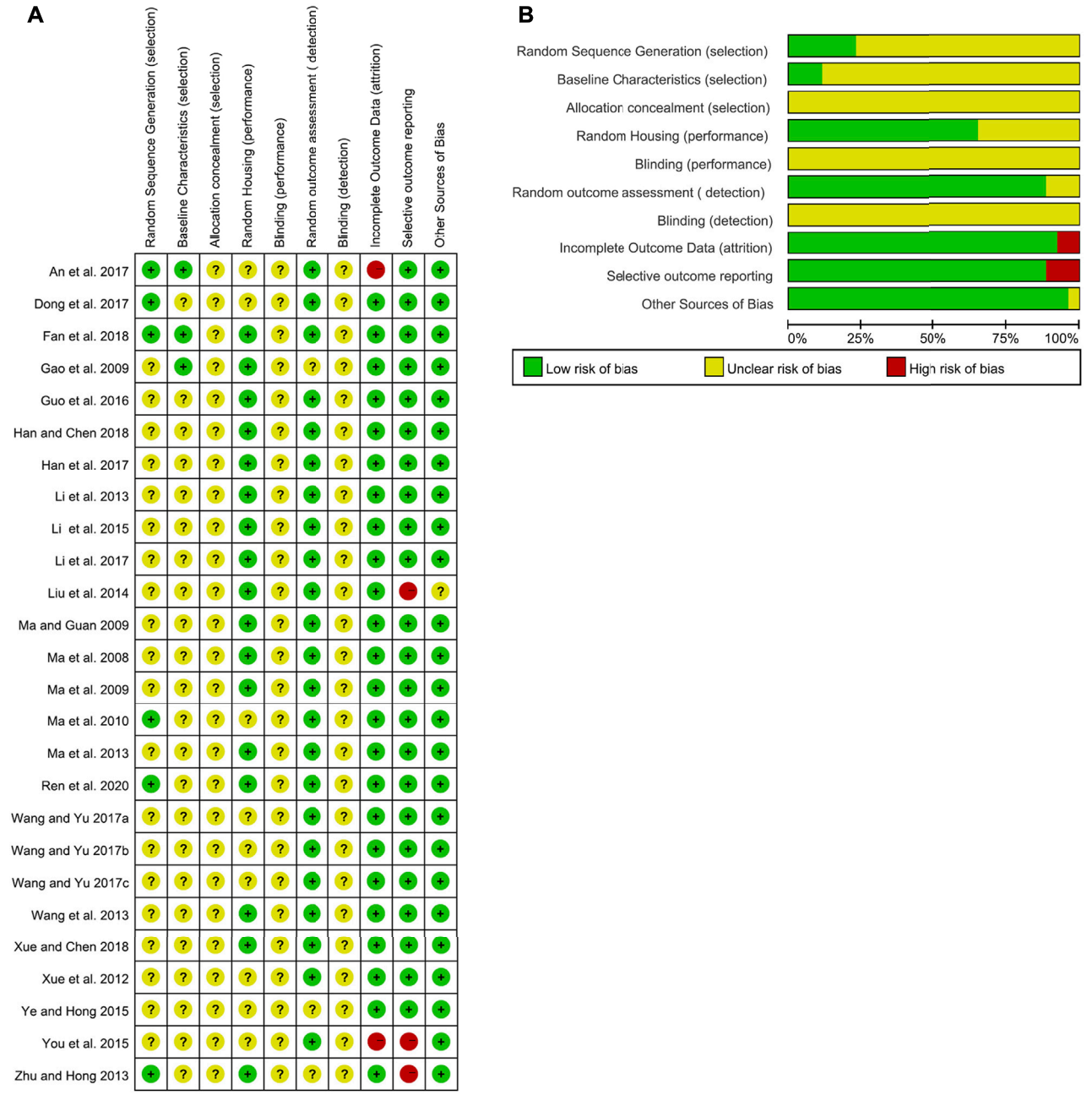

FIGURE 2 | Risk of bias of the included studies. **(A)** Summary of the risk of bias. **(B)** Summary of the risk-of-bias assessment.

in this meta-analysis. Although these results showed high heterogeneity (I^2 value= 76%), no outliers were identified by using the sensitivity analysis. Neither treatment duration nor the dosage of TP in subgroup analyses showed differences in SCr levels.

The BUN levels were examined in 12 studies (Ma, 2009; Li et al., 2013; Ma et al., 2013; Wang et al., 2013; Zhu, 2013; Liu et al., 2014; Guo et al., 2016; Han et al., 2017; Li et al., 2017; Fan et al., 2018; Han, 2018; Xue, 2018) (**Figure 8**). The meta-analysis results showed that the performance of TP was excellent in reducing BUN levels (SMD: −0.40 [−0.60, −0.20], I^2 = 55%), compared to the control group.

Comparison of TP and ACEI or ARB in Treating DKD

Effects on the Changes of Albuminuria, Urinary Albumin/Urine Creatinine Ratio (UACR), or Proteinuria

We found three studies (An et al., 2017; Qao et al., 2009; Ren et al., 2020) which analyzed albuminuria (**Figure 9A**), two

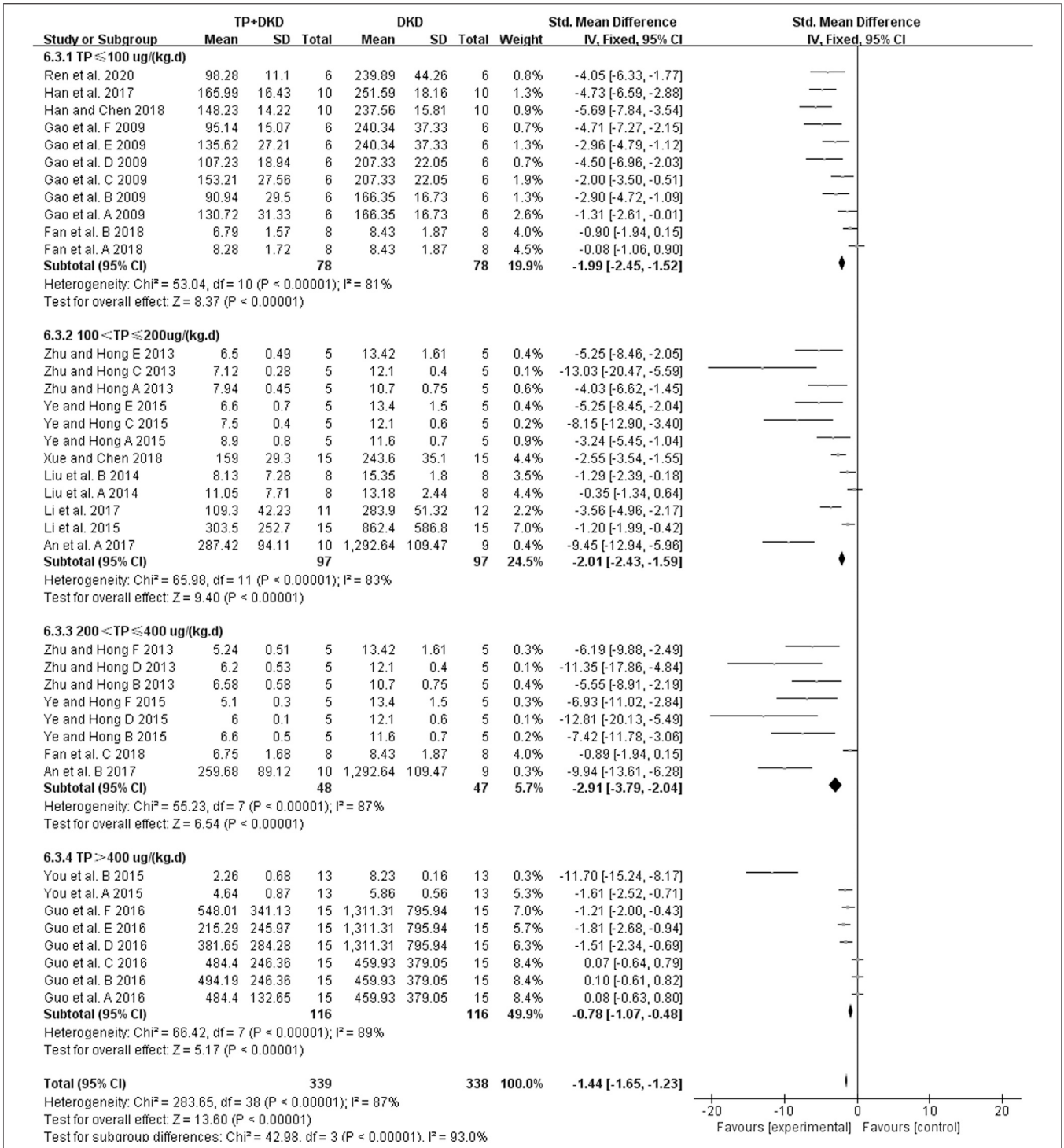

FIGURE 3 | Forest plot of albuminuria outcome.

studies (Li et al., 2013, Ma et al., 2009) which analyzed the urine albumin/urine creatinine ratio (UACR) (**Figure 9B**), and one (Dong et al., 2017) which analyzed proteinuria (**Figure 9C**).

The combined results suggested no differences in albuminuria (SMD: −0.35 [−0.72, 0.02], I^2 = 41%) between TP and ACEI or ARB. Interestingly, TP significantly reduced proteinuria (SMD: −1.18 [−1.86, −0.49], I^2 = 0%) and the UACR (SMD: −0.66

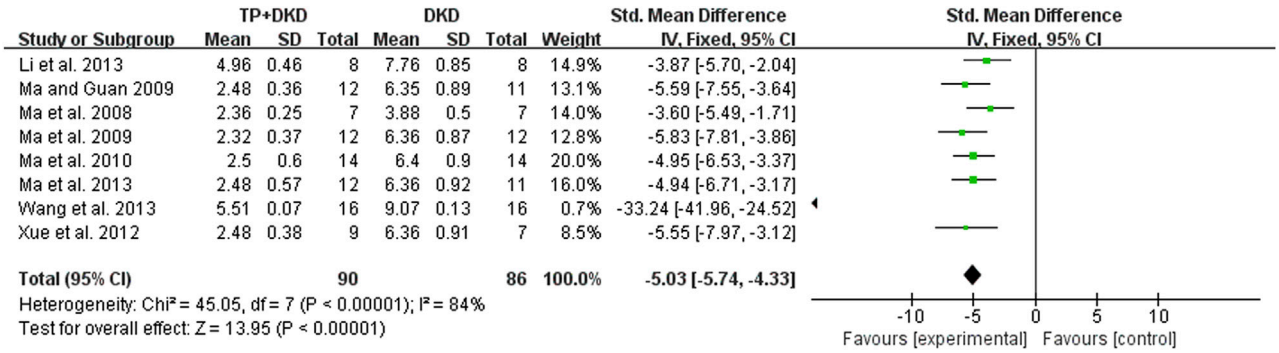

FIGURE 4 | Forest plot of UACR outcome.

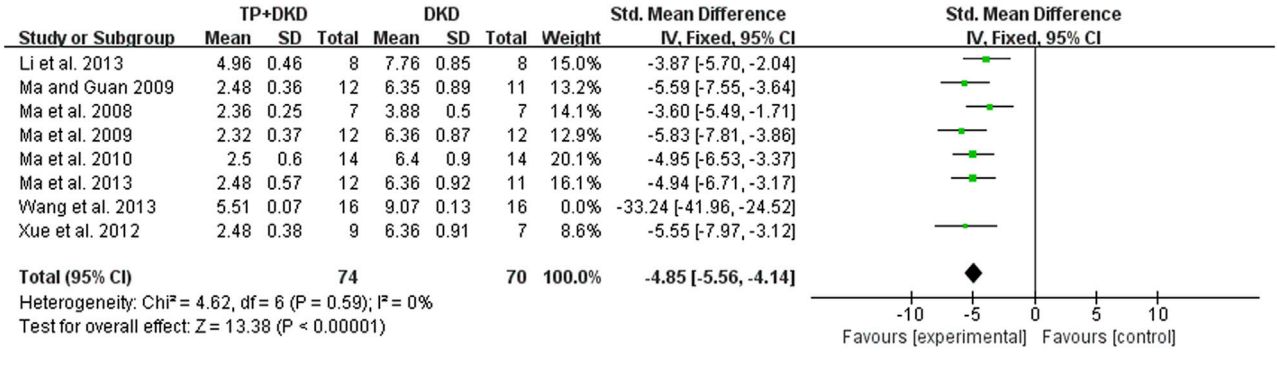

FIGURE 5 | Forest plot of UACR outcome (not included by Wang et al., 2013).

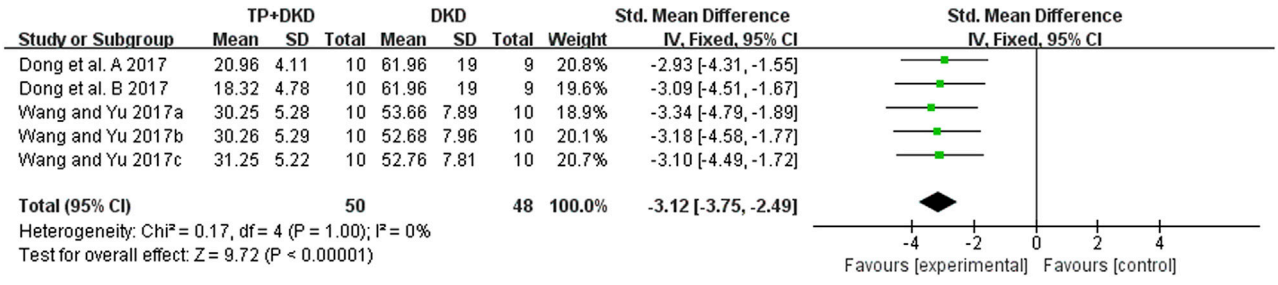

FIGURE 6 | Forest plot of UP outcome.

[−1.31, −0.01], I^2 = 0%). Due to data limitations, the reliability of this result was reduced.

Effects on Kidney Function Changes

Three studies evaluated the effects of TP on SCr, and two studies assessed BUN. The pooled results implicated that, when comparing TP and ACEI or ARB, no significant differences were shown on the changes of SCr (SMD: −0.07 [−0.62, 0.48], I^2 = 10%) (**Figure 10A**) and BUN (SMD: −0.35 [−0.97, 0.28], I^2 = 0%) (**Figure 10B**).

Publication Bias

Begg's and Egger's tests were used to analyze albuminuria changes after treating DKD with TP. The funnel plot of the tests was asymmetric, and the outcome of *p*-value was less than 0.05, both of which indicated that there was publication bias (**Figure 11A**). The potential publication bias might be due to the high percentage of positive results being published. There was no publication bias for the effects on albuminuria between TP and ACEI or ARB in treating DKD (**Figure 11B**).

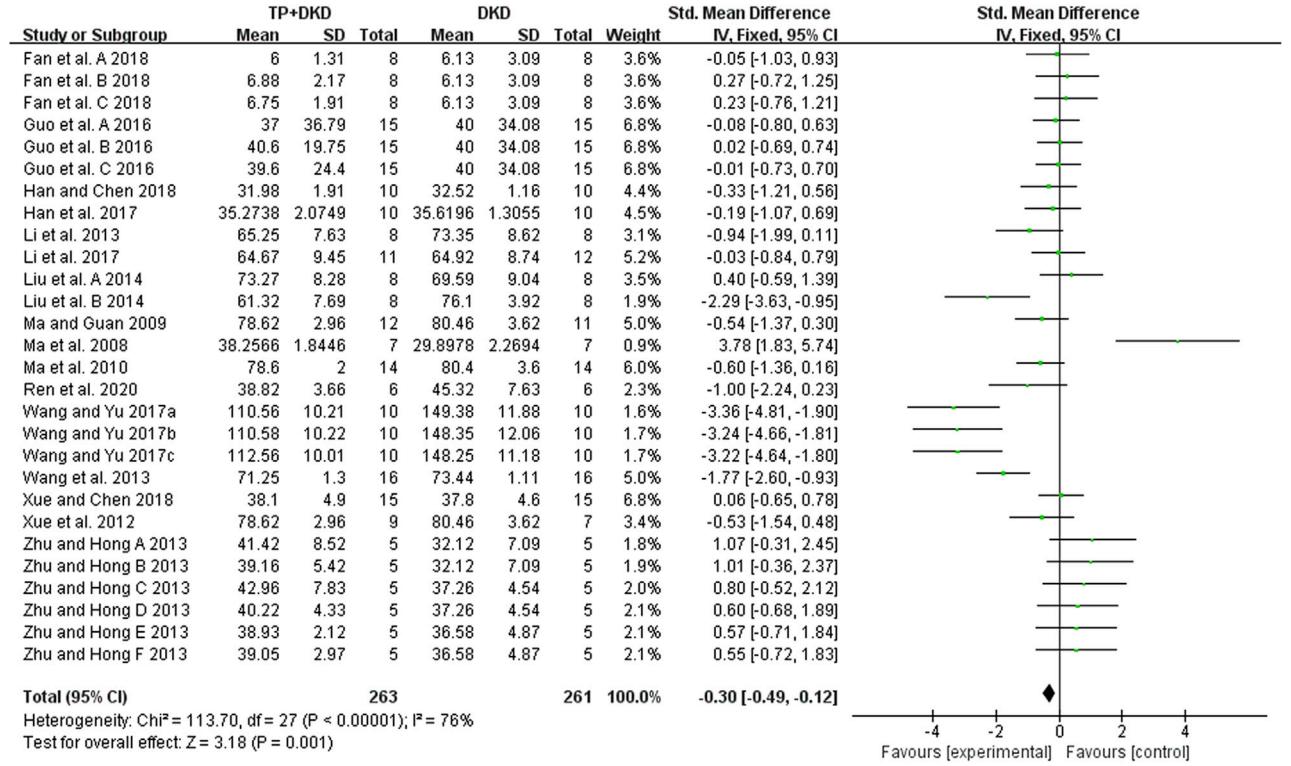

FIGURE 7 | Forest plot of SCr outcome.

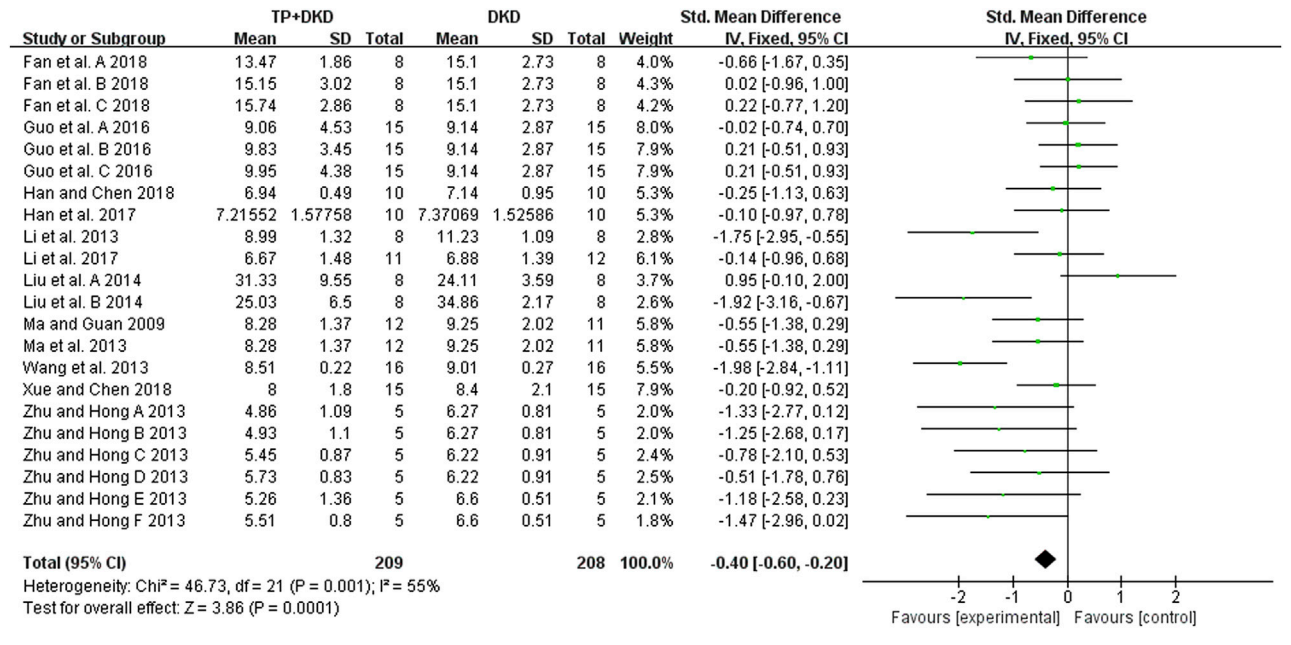

FIGURE 8 | Forest plot of BUN outcome.

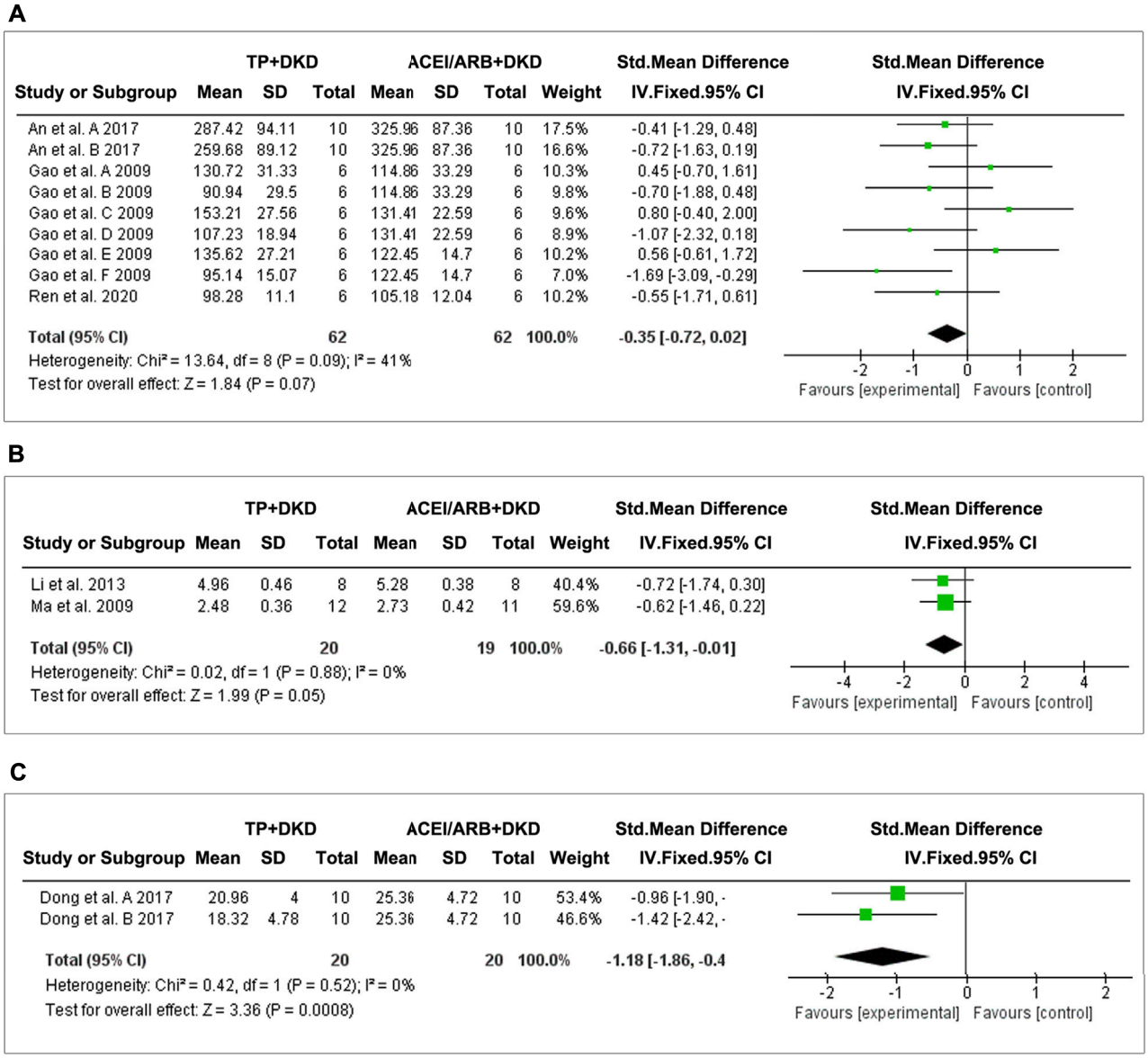

FIGURE 9 | Forest plot of **(A)** albuminuria, **(B)** UACR, and **(C)** total proteinuria outcome comparing with RAS inhibitor.

DISCUSSION

Currently, there are no effective treatments to halt DKD in the clinic which is a global health concern. The data on comparing the efficacy and safety of the current DKD therapeutic interventions remain lacking. Herein, we performed a systematic review by including 26 studies to analyze the effects of TP, an extract from a traditional Chinese herb, in treating DKD. We collected the majority of therapeutic parameters used in DKD diagnosis or clinical response evaluation, including albuminuria, proteinuria, UACR, SCr, and BUN. Serving as a characteristic indicator of the constant deterioration of DKD (de Boer et al., 2011), albuminuria and proteinuria play a key role in renal disease progression and cardiovascular events (Lin et al., 2018). It is also a sensitive biomarker for the lesions caused by DKD (Guh, 2010). As for early DKD screening (McGrath and Edi, 2019), UACR, a preferred measure of albuminuria (Sumida et al., 2020), is recommended to be detected routinely in diabetic patients who have the potential risk of renal impair (Association, 2019). In addition, to maximize the sensitivity of screening tests, SCr (Kramer, 2004) and BUN (Xie et al., 2018) are recommended as effective indicators, associating closely in renal function assessment (Zhuang et al., 2020). Under the intervention of TP, the assessment of its efficacy will be best done with the comprehensive analyzation toward the floating of the parameters above.

Our study found that TP markedly decreases proteinuria and albuminuria in DKD animal models, consistent with the previous report (Yuan et al., 2019). Since the 24-hr urinary albumin

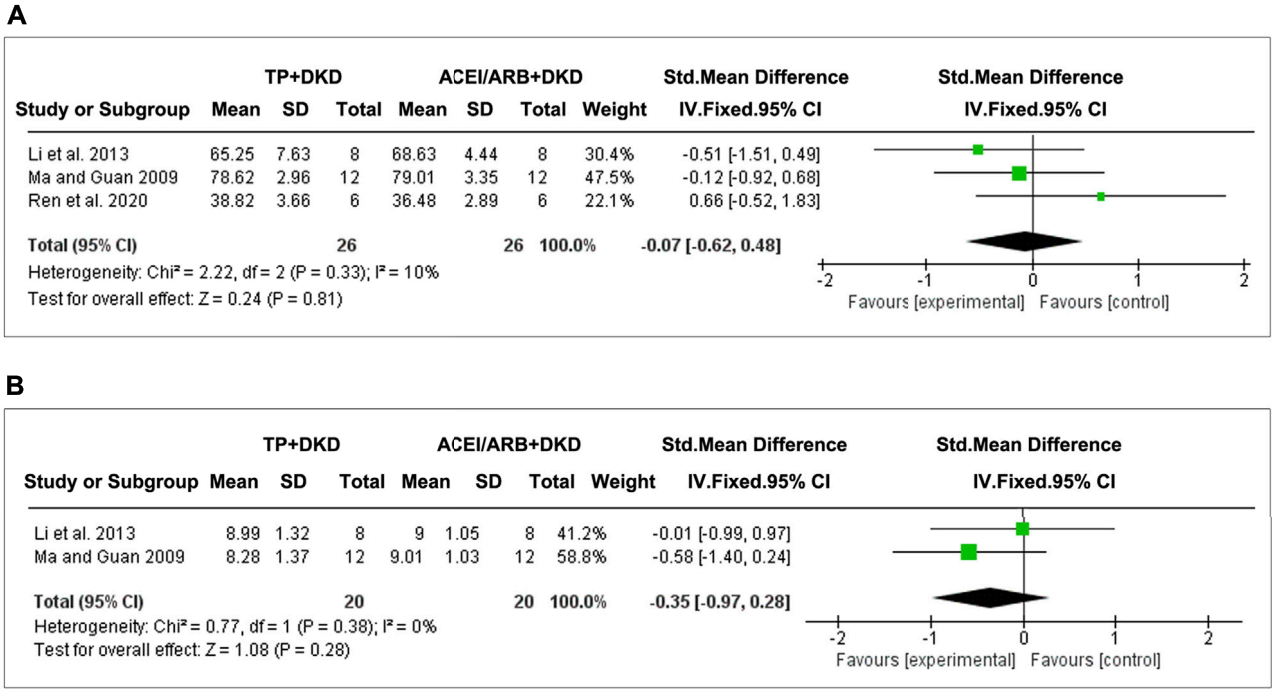

FIGURE 10 | Forest plots of **(A)** SCr and **(B)** BUN outcomes compared with RAS inhibitors.

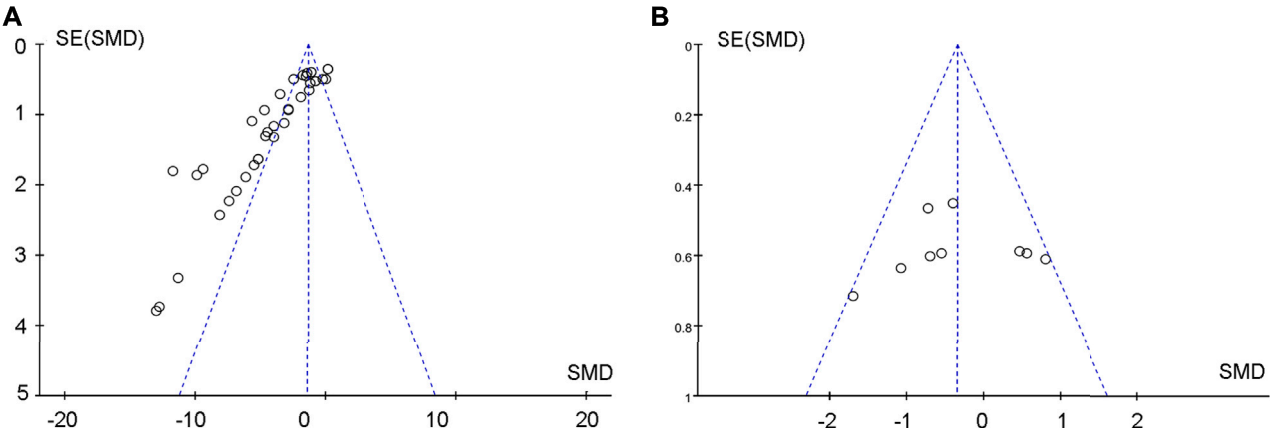

FIGURE 11 | Public bias of the effects of **(A)** TP and **(B)** TP *versus* RAS inhibitors on DKD.

showed a high heterogeneity ($\chi^2 = 283.65$, $I^2 = 87\%$, **Figure 3**), we further analyzed TP effects by setting up different subgroups according to the dosages and the duration of TP treatment. Although the heterogeneity remains high, the result did exhibit significant differences ($\chi^2 = 42.98$, $p < 0.00001$, $I^2 = 93.0\%$, **Figure 3**) among the subgroups. According to meta-regression analysis in the low-dose subgroups (TP ≤ 400 ug/kg/d), the anti-albuminuric effects were enhanced with increasing dosage. In contrast, such effects declined in the high-dose subgroups (TP > 400 ug/kg/d). Similar results were not observed in the duration subgroup during TP treatment. It might be due to the functional "working window" of TP being relatively narrow. In other words, the therapeutic dose of TP is close to its toxic dose (Li et al., 2014; Fan et al., 2018).

A key finding of our analyses is that the effects of TP on reducing albuminuria have no differences compared to RAS inhibitors in DKD models. It is well known that RAS inhibitors are the cornerstone therapy of DKD. We speculate that such equivalent effects of TP and RAS inhibitors should attribute to the following mechanisms: 1) TP protects podocytes by inactivating the Toll-like receptor/NF-κB signaling pathway in diseased glomeruli which maintains the integrity of slit-diaphragm proteins such as

nephrin and podocin (Ma et al., 2010; Wang et al., 2013; Ren et al., 2020). 2) TP ameliorates inflammation by regulating the balance of T-helper cells and repressing macrophage infiltration (Zhu, 2013; Guo et al., 2016). 3) TP alleviates oxidative stress by downregulating the renal cortex oxidative carbonyl protein and nitrotyrosine (Dong et al., 2017). 4) TP reduces glomerular mesangial cell proliferation by inactivating the PDK1/AKT/mTOR pathway (Han et al., 2017). 5) TP ameliorates glomerulosclerosis by suppressing the Notch1 pathway and regulating the content of Glut-1 and Glut-4 (You et al., 2015; Han, 2018). Of note, Li reported that a combination of TP and RAS inhibitors (irbesartan) reduced albuminuria synergistically (Li et al., 2013). The involved mechanism is unclear.

TP is the major effective monomer of the mixture, tripterygium glycosides (TGs). TG is the commercialized and commonly used extract from the TWHF herb in treating primary nephritis. In contrast to TG, TP has a similar effect on decreasing proteinuria and albuminuria induced by nephritis and DKD (Li et al., 2019). Specific to DKD intervention, the advantages of TP lies in its precision. However, a major concern regarding TP in clinical use is its multi-organ toxicity and the narrow therapeutic window (Li et al., 2014; Liu et al., 2019; Xu et al., 2019; Li et al., 2020). TP is the most important ingredient that leads to toxicity (Li et al., 2015). Primarily, triptolide is eliminated through hepatic and renal pathways. It has been revealed that the induction or inhibition of CYP3A played an important role in TP-induced hepatotoxicity (Shen et al., 2014). In addition to CYP-mediated metabolism, P-glycoprotein also played an important role in the disposition of TP and TP-induced hepatotoxicity (Xiao-Mei et al., 2013). Furthermore, members of the cytochrome P450 protein family that are involved in fatty acid (FA) metabolism, such as CYP2E1, showed the correlation between TP and its damage in kidneys. The proteomics data further suggested that FAs were involved in TP-induced toxicity (Menglin et al., 2017). Along with the advances in technology, this shortcoming of TP has been partially solved through building innovative drug delivery systems, developing water-soluble analogs, designing combinational strategies, and inventing derivatives based on structure–activity relationships (Chen et al., 2018; Liu et al., 2019). For instance, TP-encapsulated mesoscale nanoparticles (TP-MNPs) could be delivered explicitly to diseased organs to exert their therapeutic effects (Deng et al., 2019). Impressively, triptolide aminoglycoside (TPAG) is also able to protect against renal ischemia/reperfusion injury with lower toxicity to the kidney, liver, genital system, and immune system (Qi et al., 2015). A new medication developed based on TP, 14-succinate triptolide-fragment peptide (TPS-PF-$A_{299\text{-}585}$), attenuates the thickening of the glomerular basement membrane in a membranous nephropathic rodent model. *In vitro*, TPS-PF-$A_{299\text{-}585}$ presents anti-inflammatory activities equivalent to those of TP in the cultured kidney epithelial cells after incubation with lipopolysaccharides (Yuan et al., 2015). Intriguingly, a low-dose 14-succinyl triptolide-lysozyme (TPS-LZM) significantly hampered the progression of renal ischemia/reperfusion, whereas triptolide or lysozyme could not functionally work individually (Zhang et al., 2009). These renovations are promising and likely to be translated into DKD treatment in the clinical setting. In addition, a combinational prescription of TP, catalpol, and Panax notoginseng saponins markedly attenuates hepatotoxicity induced by TP (Zhou et al., 2018). It should be pointed out that it is a principle used to improve herbal effects and decrease its toxicity by regulating the formula in Chinese medicine. Therefore, the concrete drug–drug interactions need to be further explored.

A major issue in our current study is the high heterogeneity of the effect size of 24-h urinary albumin in DKD. At the subgroup layer, a remarkable difference ($\chi2$ = 16.07, p = 0.0003, I^2 = 87.6%) was present among subgroups of modeling. At present, there are no ideal experimental models that show all characteristics of DKD in humans. Different animal models or backgrounds could easily cause heterogeneity. Interestingly, no statistical difference ($\chi2$ = 0.04, p = 0.85, I^2 = 0%) was shown among the subgroups of strains (groups of genetic DN animal models and a group of Sprague–Dawley rats). Furthermore, our study has difficulties evaluating the risk of bias because the experiment information is lacking in some studies. Moreover, potential publication bias is shown (**Figure 11**). It suggests that negative outcomes are published rarely. Also, the data of certain indexes are inadequate, and the side effect profiles and adverse events are absent. With regard to this, the effects of TP might be overestimated. We should be cautious in interpreting the results.

Specific to the sensitivity analysis of UACR (**Figures 4**, **5**), Wang's study is considered as the main factor causing high heterogeneity. Based on the full text of the article, the composition and duration of high-fat diets, streptozotocin (STZ) administration, the timing of TP treatment, and weight of animals were similar to others except Ma et al., 2008. A significant difference was that SD rats were used by Li et al., 2013 and Wang et al., 2013, whereas Wistar rats were used by others. Marques *et al.* found that most metabolic effects, such as hyperleptinemia and decreased oral glucose tolerance, created by a high-fat diet revealed themselves earlier or more prominently in Wistar rats rather than SD rats, although the influence caused by the high-fat diet were generally alike in both strains (Marques et al., 2016). In comparison, the studies conducted by Li et al., 2013 and Wang et al., 2013, which utilized SD rats, have a slightly higher UACR in DKD groups than other studies. It is unclear whether the impact of STZ injection or the treatment of TP is different in those two strains. However, the remaining studies seemed to be a homogeneous group after removing the study conducted by Wang et al., 2013. Compared to others, Wang's study had a larger sample size and presented a more advanced level of UACR with a minor standard deviation in both DKD and TP groups. Accordingly, it had a larger standardized mean difference effect size and confidence interval. Consequently, we ascribed the prominent effects of the study by Wang et al., 2013 to the better administration or careful treatment in the entire experiment. In addition, the standards of successfully established DKD models were different among studies included. The factors mentioned above result in multiple metabolic conditions and kidney lesions causing

heterogeneity. Pooled effect sizes showed that TP decreased SCr and BUN slightly with lower heterogeneity.

There are some limitations in this review. First, as only two studies creating the group of TP combined with an RAS inhibitor, we did not have enough data to appraise the effects of this medication—co-administration in DKD models. In addition, the high heterogeneity of various factors resulted in subgroup analysis on dosage, and the treatment duration of triptolide failed to reduce it. Significant differences were caused by discordance in strains, methodologies, and criteria for modeling, stages of disease, dosages and durations of intervention, and even experiment management in each trial. It is hard to avoid it now, since there is no agreement on the establishment of animal models of DKD yet. Therefore, differences in dose, formula, and duration remain existent in the included studies in which DKD was totally induced by high-fat dietary intervention plus streptocizin injection. Furthermore, the potential bias and comparatively small studies resulted in overrated curative powers. Thus, the conclusion should be interpreted and generalized carefully. More preclinical trials with rigorous designing need to be performed to strengthen the evidence in the future.

CONCLUSION

Triptolide exhibits similar pharmacological effects to RAS inhibitors on reducing albuminuria and preserving renal function after the onset of DKD. Although there was data heterogeneity, this meta-analysis result provides the clinicians with potential options in designing interventional strategies for DKD patients. Meanwhile, the renovations on TP derivatives and drug-delivering systems are believed to be promising to shed light on DKD prevention in the future.

DATA AVAILABILITY STATEMENT

The original contributions presented in the study are included in the article/Supplementary Material; further inquiries can be directed to the corresponding author.

AUTHOR CONTRIBUTIONS

DL and HF conceived the project. DL, HM, and FR wrote and revised the manuscript. DL, FR, and HM constructed the mathematical model. DL, HM, and FR edited the manuscript. HF supervised the entire project.

FUNDING

This work was supported by the National Natural Science Foundation of China (Grants 81970587 and 81770737) and the Guangzhou Regenerative Medicine and Health Guangdong Laboratory (grants 2018GZR110104001 and 2018GZR0201003), and College Students' Innovative Entrepreneurial Training Plan Program (S201912121084). Fu H is the recipient of the Outstanding Youths Development Scheme of Nanfang Hospital (2015J006) and Southern Medical University (2020JQPY004).

REFERENCES

An, Z., Dong, X., Guo, Y., Zhou, J., and Qin, T. (2017). Effect of Triptolide on Urinary Albumin Excretion in Rats with Diabetic Nephropathy. *J. Nanchang Univ. Sci.* 57, 27–29. doi:10.13764/j.cnki.ncdm.2017.01.007

Association, A. D. (2019). 11. Microvascular Complications and Foot Care: Standards of Medical Care in Diabetes-2019. *Diabetes Care* 42 (Suppl. 1), S124–s138. doi:10.2337/dc19-S011

Chen, S. R., Dai, Y., Zhao, J., Lin, L., Wang, Y., and Wang, Y. (2018). A Mechanistic Overview of Triptolide and Celastrol, Natural Products from Tripterygium Wilfordii Hook F. *Front. Pharmacol.* 9, 104–113. doi:10.3389/fphar.2018.00104

de Boer, I. H., Rue, T. C., Cleary, P. A., Lachin, J. M., Molitch, M. E., Steffes, M. W., et al. (2011). Long-term Renal Outcomes of Patients with Type 1 Diabetes Mellitus and Microalbuminuria: an Analysis of the Diabetes Control and Complications Trial/Epidemiology of Diabetes Interventions and Complications Cohort. *Arch. Intern. Med.* 171, 412–420. doi:10.1001/archinternmed.2011.16

Deng, X., Zeng, T., Li, J., Huang, C., Yu, M., Wang, X., et al. (2019). Kidney-targeted Triptolide-Encapsulated Mesoscale Nanoparticles for High-Efficiency Treatment of Kidney Injury. *Biomater. Sci.* 7, 5312–5323. doi:10.1039/c9bm01290g

Dong, X. G., An, Z. M., Guo, Y., Zhou, J. L., and Qin, T. (2017). Effect of Triptolide on Expression of Oxidative Carbonyl Protein in Renal Cortex of Rats with Diabetic Nephropathy. *J. Huazhong Univ. Sci. Technolog Med. Sci.* 37, 25–29. doi:10.1007/s11596-017-1689-9

Fadini, G. P., Bonora, B. M., and Avogaro, A. (2017). SGLT2 Inhibitors and Diabetic Ketoacidosis: Data from the FDA Adverse Event Reporting System. *Diabetologia* 60, 1385–1389. doi:10.1007/s00125-017-4301-8

Fan, H., Yang, J., Wang, M., Du, J., and Fang, F. (2018). Experimental Study of Tripterygium Glycosides in Delaying the Progression of Diabetic Nephropathy. *Chin. J. Clin. Healthc.* 21, 377–382. doi:10.3969/J.issn.16726790.2018.03.024

Fu, H., Liu, S., Bastacky, S. I., Wang, X., Tian, X. J., and Zhou, D. (2019). Diabetic Kidney Diseases Revisited: A New Perspective for a new era. *Mol. Metab.* 30, 250–263. doi:10.1016/j.molmet.2019.10.005

Gao, Q., Liu, Z., Qin, W., Zheng, C., Zhang, M., Zeng, C., et al. (2009). Triptolide Ameliorates Proteinuria and Improves Renal Lesion in Diabetic Db/db Mice. *Chin. J. Nephrol. Dial. Transpl.* 18, 519–528. doi:10.3969/j.issn.1006-298X.2009.06.004

Guh, J. Y. (2010). Proteinuria versus Albuminuria in Chronic Kidney Disease. *Nephrology (Carlton)* 15 Suppl 2 (Suppl. 2), 53–56. doi:10.1111/j.1440-1797.2010.01314.x

Guo, H., Pan, C., Chang, B., Wu, X., Guo, J., Zhou, Y., et al. (2016). Triptolide Improves Diabetic Nephropathy by Regulating Th Cell Balance and Macrophage Infiltration in Rat Models of Diabetic Nephropathy. *Exp. Clin. Endocrinol. Diabetes* 124, 389–398. doi:10.1055/s-0042-106083

Guo, Y., Guo, N., Wang, J., Wang, R., and Tang, L. (2021). Retrospective Analysis of Tripterygium Wilfordii Polyglycoside Combined with Angiotensin Receptor Blockers for the Treatment of Primary Membranous Nephropathy with Subnephrotic Proteinuria. *Ren. Fail.* 43, 729–736. doi:10.1080/0886022X.2021.1918555

Han, F., Xue, M., Chang, Y., Li, X., Yang, Y., Sun, B., et al. (2017). Triptolide Suppresses Glomerular Mesangial Cell Proliferation in Diabetic Nephropathy Is Associated with Inhibition of PDK1/Akt/mTOR Pathway. *Int. J. Biol. Sci.* 13, 1266–1275. doi:10.7150/ijbs.20485

Han, F. (2018). *Study on the Mechanism of Triptolide in Improving Diabetic Nephropathy via PDK1/Akt and miR-137/Notch1 Pathway*. Dissertation. Tianjin (China). Tianjin Medicial university.

Hong, Y., Gui, Z., Cai, X., and Lan, L. (2016). Clinical Efficacy and Safety of Tripterygium Glycosides in Treatment of Stage IV Diabetic Nephropathy: A Meta-Analysis. *Open Med. (Wars)* 11, 611–617. doi:10.1515/med-2016-0099

Hooijmans, C. R., Rovers, M. M., de Vries, R. B., Leenaars, M., Ritskes-Hoitinga, M., and Langendam, M. W. (2014). SYRCLE's Risk of Bias Tool for Animal Studies. *BMC Med. Res. Methodol.* 14, 43. doi:10.1186/1471-2288-14-43

Hooijmans, C. R., Tillema, A., Leenaars, M., and Ritskes-Hoitinga, M. (2010). Enhancing Search Efficiency by Means of a Search Filter for Finding All Studies on Animal Experimentation in PubMed. *Lab. Anim.* 44, 170–175. doi:10.1258/la.2010.009117

Hostetter, T. H. (2001). Prevention of End-Stage Renal Disease Due to Type 2 Diabetes. *N. Engl. J. Med.* 345, 910–912. doi:10.1056/NEJM200109203451209

Hou, W., Liu, B., and Xu, H. (2019). Triptolide: Medicinal Chemistry, Chemical Biology and Clinical Progress. *Eur. J. Med. Chem.* 176, 378–392. doi:10.1016/j.ejmech.2019.05.032

Hoyle, G. W., Hoyle, C. I., Chen, J., Chang, W., Williams, R. W., and Rando, R. J. (2010). Identification of Triptolide, a Natural Diterpenoid Compound, as an Inhibitor of Lung Inflammation. *Am. J. Physiol. Lung Cel. Mol. Physiol.* 298, L830–L836. doi:10.1152/ajplung.00014.2010

Huang, W. J., Liu, W. J., Xiao, Y. H., Zheng, H. J., Xiao, Y., Jia, Q., et al. (2020). Tripterygium and its Extracts for Diabetic Nephropathy: Efficacy and Pharmacological Mechanisms. *Biomed. Pharmacother.* 121, 109599. doi:10.1016/j.biopha.2019.109599

Kopel, J., Pena-Hernandez, C., and Nugent, K. (2019). Evolving Spectrum of Diabetic Nephropathy. *World J. Diabetes* 10, 269–279. doi:10.4239/wjd.v10.i5.269

Koye, D. N., Magliano, D. J., Nelson, R. G., and Pavkov, M. E. (2018). The Global Epidemiology of Diabetes and Kidney Disease. *Adv. Chronic Kidney Dis.* 25, 121–132. doi:10.1053/j.ackd.2017.10.011

Krakauer, T., Chen, X., Howard, O. M., and Young, H. A. (2005). Triptolide Attenuates Endotoxin- and Staphylococcal Exotoxin-Induced T-Cell Proliferation and Production of Cytokines and Chemokines. *Immunopharmacol. Immunotoxicol.* 27, 53–66. doi:10.1081/iph-51294

Kramer, H. (2004). Screening for Kidney Disease in Adults with Diabetes Mellitus: Don't Forget Serum Creatinine. *Am. J. Kidney Dis.* 44, 921–923. doi:10.1053/j.ajkd.2004.09.00210.1016/s0272-6386(04)01277-6

Kupchan, S. M., Court, W. A., Dailey, R. G., Gilmore, C. J., and Bryan, R. F. (1972). Triptolide and Tripdiolide, Novel Antileukemic Diterpenoid Triepoxides from Tripterygium Wilfordii. *J. Am. Chem. Soc.* 94, 7194–7195. doi:10.1021/ja00775a078

Leenaars, M., Hooijmans, C. R., van Veggel, N., ter Riet, G., Leeflang, M., Hooft, L., et al. (2012). A Step-by-step Guide to Systematically Identify All Relevant Animal Studies. *Lab. Anim.* 46, 24–31. doi:10.1258/la.2011.011087

Li, J., Shen, F., Guan, C., Wang, W., Sun, X., Fu, X., et al. (2014). Activation of Nrf2 Protects against Triptolide-Induced Hepatotoxicity. *PLoS One* 9, e100685. doi:10.1371/journal.pone.0100685

Li, K., Luan, J., Sui, A., Ma, R., Zhou, L., and Wang, Y. (2013). Influence of Irbesrtan Combined with Triptolide on ANGPTL2 and VEGF in the Kidney of 2 Type Diabetes Rat Models. *Chin. J. Integr. Tradit. West.* 14, 959–962. https://kns.cnki.net/kcms/detail/detail.aspx?FileName=JXSB201311009&DbName=CJFQ2013.

Li, M., Hu, T., Tie, C., Qu, L., Zheng, H., and Zhang, J. (2017). Quantitative Proteomics and Targeted Fatty Acids Analysis Reveal the Damage of Triptolide in Liver and Kidney. *Proteomics* 17, 1700001. doi:10.1002/pmic.201700001

Li, W., Bai, X., Wu, Y., Huang, W., Tian, X., and Men, H. (2015). Protective Effect of Triptolide on Kidney of Early Diabetes Mellitus (DM)Model Rats. *J. Hebei North. Univ. Sci. Ed.* 31, 77–80. doi:10.3969/j.issn.1673-1492.2015.05.017

Li, X. J., Jiang, Z. Z., and Zhang, L. Y. (2014). Triptolide: Progress on Research in Pharmacodynamics and Toxicology. *J. Ethnopharmacol.* 155, 67–79. doi:10.1016/j.jep.2014.06.006

Li, X. X., Du, F. Y., Liu, H. X., Ji, J. B., and Xing, J. (2015). Investigation of the Active Components in Tripterygium Wilfordii Leading to its Acute Hepatotoxicty and Nephrotoxicity. *J. Ethnopharmacol.* 162, 238–243. doi:10.1016/j.jep.2015.01.004

Li, X. Y., Wang, S. S., Han, Z., Han, F., Chang, Y. P., Yang, Y., et al. (2017). Triptolide Restores Autophagy to Alleviate Diabetic Renal Fibrosis through the miR-141-3p/PTEN/Akt/mTOR Pathway. *Mol. Ther. Nucleic Acids* 9, 48–56. doi:10.1016/j.omtn.2017.08.011

Li, Y., Hu, Q., Li, C., Liang, K., Xiang, Y., Hsiao, H., et al. (2019). PTEN-induced Partial Epithelial-Mesenchymal Transition Drives Diabetic Kidney Disease. *J. Clin. Invest.* 129, 1129–1151. doi:10.1172/JCI121987

Li, Y., Chen, S., Xia, X., Peng, Y., Yang, X., and Wang, G. (2020). Analysis on Adverse Reactions Caused by Preparations Containing Tripterygium Wilfordii in Henan Province from 2004 to 2019. *Drugs Clin.* 35, 988–994. doi:10.7501/j.issn.1674-5515.2020.05.036

Lin, Y. C., Chang, Y. H., Yang, S. Y., Wu, K. D., and Chu, T. S. (2018). Update of Pathophysiology and Management of Diabetic Kidney Disease. *J. Formos. Med. Assoc.* 117, 662–675. doi:10.1016/j.jfma.2018.02.007

Liu, B., Fan, D., Shu, H., He, X., Lyu, C., and Lyu, A. (2019). Side Effect and Attenuation of Triptolide. *Chin. J. Exp. Tradit. Med. Formulae* 25, 181–190. doi:10.13422/j.cnki.syfjx.20191429

Liu, Q., Chen, T., Chen, G., Li, N., Wang, J., Ma, P., et al. (2006). Immunosuppressant Triptolide Inhibits Dendritic Cell-Mediated Chemoattraction of Neutrophils and T Cells through Inhibiting Stat3 Phosphorylation and NF-kappaB Activation. *Biochem. Biophys. Res. Commun.* 345, 1122–1130. doi:10.1016/j.bbrc.2006.05.024

Liu, Q. (2011). Triptolide and its Expanding Multiple Pharmacological Functions. *Int. Immunopharmacol.* 11, 377–383. doi:10.1016/j.intimp.2011.01.012

Liu, Q., Chen, S., Liu, F., Wang, X., Shi, Z., and Chen, H. (2014). Effects of Triptolide on Expressions of NF-Kb,NOS and VEGF in Glomeruli of Diabetes Mellitus Rats. *J. Clin. Exp. Med.* 13, 1925–1929. doi:10.3969/j.issn.1671-4695.2014.23.002

Lu, Y., Fukuda, K., Nakamura, Y., Kimura, K., Kumagai, N., and Nishida, T. (2005). Inhibitory Effect of Triptolide on Chemokine Expression Induced by Proinflammatory Cytokines in Human Corneal Fibroblasts. *Invest. Ophthalmol. Vis. Sci.* 46, 2346–2352. doi:10.1167/iovs.05-0010

Ma, R., Liu, L., Liu, X., Wang, Y., Jiang, W., and Xu, L. (2013). Triptolide Markedly Attenuates Albuminuria and Podocyte Injury in an Animal Model of Diabetic Nephropathy. *Exp. Ther. Med.* 6, 649–656. doi:10.3892/etm.2013.1226

Ma, R., Liu, L., Xu, Y., and Jiang, W. (2008). Protective Effect of Riptolide on Renal Tissures in Type 2 Diabetic Rats. *Chin. J. Hypertens.* 16, 1120–1124. doi:10.3969/j.issn.1673-7245.2008.12.01710.11569/wcjd.v16.i33.3775

Ma, R., Liu, X., Liu, L., and Li, H. (2010). Effects of Triptolide on the Podocyte Protein Expression of Nephrin and Podocin and its Mechanism in Type 2 Diabetic Rats. *Chin. J. Diabetes Mellit.* 02, 291–296. doi:10.3760/cma.j.issn.1674-5809.2010.04.013

Ma, R. (2009). *The Protective Effect of the Combination of Triptolide and Irbesartan on the Podocytes in Type 2 Diabetic Rat Model and its mechanismDissertation*. Shandong (China): Shandong University.

Ma, R., Wang, Y., Wei, Z., Lu, H., Liu, L., and Guan, G. (2009). Effect of Triptolide on Podocyte Injury and its Mechanism in the Kidney of 2 Type Diabetic Rats. *Chin. J. Immunol.* 25, 404–408. https://kns.cnki.net/kcms/detail/detail.aspx?FileName=ZMXZ200905007&DbName=CJFQ2009.

McGrath, K., and Edi, R. (2019). Diabetic Kidney Disease: Diagnosis, Treatment, and Prevention. *Am. Fam. Physician* 99, 751–759. doi:10.1002/0470021616.ch2

Moher, D., Liberati, A., Tetzlaff, J., and Altman, D. G. (2009). Preferred Reporting Items for Systematic Reviews and Meta-Analyses: the PRISMA Statement. *BMJ* 339, b2535. doi:10.1136/bmj.b2535

Ni, B., Jiang, Z., Huang, X., Xu, F., Zhang, R., Zhang, Z., et al. (2008). Male Reproductive Toxicity and Toxicokinetics of Triptolide in Rats. *Arzneimittelforschung* 58, 673–680. doi:10.1055/s-0031-1296570

Onuigbo, M. A. (2011). Can ACE Inhibitors and Angiotensin Receptor Blockers Be Detrimental in CKD Patients? *Nephron. Clin. Pract.* 118, c407–19. doi:10.1159/000324164

Qi, B., Wang, X., Zhou, Y., Han, Q., He, L., Gong, T., et al. (2015). A Renal-Targeted Triptolide Aminoglycoside (TPAG) Conjugate for Lowering Systemic Toxicities of Triptolide. *Fitoterapia* 103, 242–251. doi:10.1016/j.fitote.2015.04.008

Rao, C., Adair, T., Bain, C., and Doi, S. A. (2012). Mortality from Diabetic Renal Disease: a Hidden Epidemic. *Eur. J. Public Health* 22, 280–284. doi:10.1093/eurpub/ckq205

Ren, D., Zuo, C., and Xu, G. (2019). Clinical Efficacy and Safety of Tripterygium Wilfordii Hook in the Treatment of Diabetic Kidney Disease Stage IV: A Meta-Analysis of Randomized Controlled Trials. *Medicine (Baltimore)* 98, e14604. doi:10.1097/MD.0000000000014604

Ren, L., Zhu, M., Zhu, H., Ding, M., Fei, D., Huo, L., et al. (2020). Effect of Triptolide on Podocytes in Mice with Diabetic Nephropathy by Regulating Toll-like Receptor (TLR)/Nuclear Factor-Kb (NF-Kb) Signal Pathway. *Zhejiang*

J. Integr. Tradit. Chin. West. Med. 30, 191–195. doi:10.3969/j.issn.1005-4561.2020.03.007

Ren, Q., Li, M., Deng, Y., Lu, A., and Lu, J. (2021). Triptolide Delivery: Nanotechnology-Based Carrier Systems to Enhance Efficacy and Limit Toxicity. *Pharmacol. Res.* 165, 105377. doi:10.1016/j.phrs.2020.105377

Shen, G., Zhuang, X., Xiao, W., Kong, L., Tan, Y., and Li, H. (2014). Role of CYP3A in Regulating Hepatic Clearance and Hepatotoxicity of Triptolide in Rat Liver Microsomes and sandwich-cultured Hepatocytes. *Food Chem. Toxicol.* 71, 90–96. doi:10.1016/j.fct.2014.05.020

Slabaugh, S. L., Curtis, B. H., Clore, G., Fu, H., and Schuster, D. P. (2015). Factors Associated with Increased Healthcare Costs in Medicare Advantage Patients with Type 2 Diabetes Enrolled in a Large Representative Health Insurance Plan in the US. *J. Med. Econ.* 18, 106–112. doi:10.3111/13696998.2014.979292

Sumida, K., Nadkarni, G. N., Grams, M. E., Sang, Y., Ballew, S. H., Coresh, J., et al. (2020). Conversion of Urine Protein-Creatinine Ratio or Urine Dipstick Protein to Urine Albumin-Creatinine Ratio for Use in Chronic Kidney Disease Screening and Prognosis : An Individual Participant-Based Meta-Analysis. *Ann. Intern. Med.* 173, 426–435. doi:10.7326/m20-0529

Thomas, M. C., Cooper, M. E., and Zimmet, P. (2016). Changing Epidemiology of Type 2 Diabetes Mellitus and Associated Chronic Kidney Disease. *Nat. Rev. Nephrol.* 12, 73–81. doi:10.1038/nrneph.2015.173

Wang, D., and Yu, R. (2017c). Effects of Triptolide on Expressions of iNOS and COX-2 in Renal Tissue of Diabetic Nephropathy Rats. *Prog. Anat. Sci.* 23, 148–150. doi:10.16695/j.cnki.1006-2947.2017.02.011

Wang, D., and Yu, R. (2017a). Effects of Triptolide on Expressions of PGE2 and NF-Kb in Renal Tissue of Diabetic Nephropathy Rats. *Prog. Anat. Sci.* 23, 10–12. doi:10.16695/j.cnki.1006-2947.2017.01.003

Wang, D., and Yu, R. (2017b). Effects of Triptolide on Expressions of TNF-α and MCP-1 in Renal Tissue of Diabetic Nephropathy Rats. *Prog. Anat. Sci.* 23, 71–73. doi:10.16695/j.cnki.1006-2947.2017.01.020

Wang, Y., Li, K., Hu, M., and Luan, J. (2013). Influence of ANGPTL2 on the Podocytes in the Kidney of 2 Type Diabetes Rat Models and Effect of Triptolide. *Chin. J. Clin. Ed.* 7, 10746–10751. doi:10.3877/cma.j.issn.1674-0785.2013.23.082

Xi, C., Peng, S., Wu, Z., Zhou, Q., and Zhou, J. (2017). WITHDRAWN: Toxicity of Triptolide and the Molecular Mechanisms Involved. *Environ. Toxicol. Pharmacol.* 90, 531–541. doi:10.1016/j.biopha.2017.04.00310.1016/j.etap.2017.09.013

Xie, Y., Bowe, B., Li, T., Xian, H., Yan, Y., and Al-Aly, Z. (2018). Higher Blood Urea Nitrogen Is Associated with Increased Risk of Incident Diabetes Mellitus. *Kidney Int.* 93, 741–752. doi:10.1016/j.kint.2017.08.033

Xu, L., Zhao, B., Wang, H., Liu, L., Chen, A., Wang, H., et al. (2020). Tripterygium Wilfordii Hook F Treatment for Stage IV Diabetic Nephropathy: Protocol for a Prospective, Randomized Controlled Trial. *Biomed. Res. Int.* 2020, 9181037. doi:10.1155/2020/9181037

Xu, Y., Fan, Y. F., Zhao, Y., and Lin, N. (2019). [Overview of Reproductive Toxicity Studies on Tripterygium Wilfordii in Recent 40 years]. *Zhongguo Zhong Yao Za Zhi* 44, 3406–3414. doi:10.19540/j.cnki.cjcmm.20190524.401

Xue, M. (2018). *Effect of Triptolide on Diabetic Renal Tubular Epithelial-Mesenchymal Transition via miR-188- 5p/PTEN Pathway Master's Thesis*. Tianjin (China): Tianjin Medical University.

Xue, X., Zhai, L., Liu, X., and Ma, R. (2012). The Effect and Significance of Triptolide on the Expression of Nephrin,Podocin in Type 2 Diabetic Rat Kidneys. *J. Clin. Ration. Drug Use* 05, 9–11. doi:10.3969/j.issn.1674-3296.2012.21.005

Yang, F., Zhuo, L., Ananda, S., Sun, T., Li, S., and Liu, L. (2011). Role of Reactive Oxygen Species in Triptolide-Induced Apoptosis of Renal Tubular Cells and Renal Injury in Rats. *J. Huazhong Univ. Sci. Technolog Med. Sci.* 31, 335–341. doi:10.1007/s11596-011-0377-4

Ye, X., and Hong, Y. (2015). Effect of Triptolide on the Expression of Regulated upon Activation normal T-Cell Expressed and Secreted in Renal Tissue of Diabetic Nephropathy Rats. *Chin. J. Clin. Pharmacol.* 31, 31–33. doi:10.13699/j.cnki.1001-6821.2015.01.010

You, L., Guo, H., and Li, Y. (2015). Influence of Triptolide on the Expression of Glut-1, Glut-4 in Kidney of Diabetic Ne-Phropathy Rats. *Pract. Pharm. Clin. Remedies* 18, 390–393. doi:10.14053/j.cnki.ppcr.201504004

Yuan, K., Li, X., Lu, Q., Zhu, Q., Jiang, H., Wang, T., et al. (2019). Application and Mechanisms of Triptolide in the Treatment of Inflammatory Diseases-A Review. *Front. Pharmacol.* 10, 1469–1512. doi:10.3389/fphar.2019.01469

Yuan, Z. X., Wu, X. J., Mo, J., Wang, Y. L., Xu, C. Q., and Lim, L. Y. (2015). Renal Targeted Delivery of Triptolide by Conjugation to the Fragment Peptide of Human Serum Albumin. *Eur. J. Pharm. Biopharm.* 94, 363–371. doi:10.1016/j.ejpb.2015.06.012

Zhang, X., Xiao, Z., and Xu, H. (2019). A Review of the Total Syntheses of Triptolide. *Beilstein J. Org. Chem.* 15, 1984–1995. doi:10.3762/bjoc.15.194

Zhang, Z., Zheng, Q., Han, J., Gao, G., Liu, J., Gong, T., et al. (2009). The Targeting of 14-succinate Triptolide-Lysozyme Conjugate to Proximal Renal Tubular Epithelial Cells. *Biomaterials* 30, 1372–1381. doi:10.1016/j.biomaterials.2008.11.035

Zhao, G., Vaszar, L. T., Qiu, D., Shi, L., and Kao, P. N. (2000). Anti-inflammatory Effects of Triptolide in Human Bronchial Epithelial Cells. *Am. J. Physiol. Lung Cel. Mol. Physiol.* 279, L958–L966. doi:10.1152/ajplung.2000.279.5.L958

Zhou, H. F., Niu, D. B., Xue, B., Li, F. Q., Liu, X. Y., He, Q. H., et al. (2003). Triptolide Inhibits TNF-Alpha, IL-1 Beta and NO Production in Primary Microglial Cultures. *Neuroreport* 14, 1091–1095. doi:10.1097/01.wnr.0000073682.00308.47

Zhou, L., Zhou, C., Feng, Z., Liu, Z., Zhu, H., and Zhou, X. (2018). Triptolide-induced Hepatotoxicity Can Be Alleviated when Combined with Panax Notoginseng Saponins and Catapol. *J. Ethnopharmacol.* 214, 232–239. doi:10.1016/j.jep.2017.12.033

Zhu, J. (2013). *Effect of Triptolide on the Expression of RANTES in the Kidney of Diabetic Rats Master's Thesis*. Zhejiang (China). Zhejiang Chinese Medical University.

Zhuang, X.-M., Shen, G.-L., Xiao, W.-B., Tan, Y., Lu, C., and Li, H. (2013). Assessment of the Roles of P-Glycoprotein and Cytochrome P450 in Triptolide-Induced Liver Toxicity in sandwich-cultured Rat Hepatocyte Model. *Drug Metab. Dispos* 41, 2158–2165. doi:10.1124/dmd.113.054056

Zhuang, Z., Wang, Z. H., Huang, Y. Y., Zheng, Q., and Pan, X. D. (2020). Protective Effect and Possible Mechanisms of Ligustrazine Isolated from Ligusticum Wallichii on Nephropathy in Rats with Diabetes: A Preclinical Systematic Review and Meta-Analysis. *J. Ethnopharmacol* 252, 112568. doi:10.1016/j.jep.2020.112568

Conflict of Interest: The authors declare that the research was conducted in the absence of any commercial or financial relationships that could be construed as a potential conflict of interest.

Publisher's Note: All claims expressed in this article are solely those of the authors and do not necessarily represent those of their affiliated organizations, or those of the publisher, the editors and the reviewers. Any product that may be evaluated in this article, or claim that may be made by its manufacturer, is not guaranteed or endorsed by the publisher.

frontiers in Pharmacology

ORIGINAL RESEARCH
published: 18 October 2021
doi: 10.3389/fphar.2021.737764

Securidaca inappendiculata Polyphenol Rich Extract Counteracts Cognitive Deficits, Neuropathy, Neuroinflammation and Oxidative Stress in Diabetic Encephalopathic Rats via p38 MAPK/Nrf2/HO-1 Pathways

Xiaojun Pang[1], *Emmanuel Ayobami Makinde*[2,3], *Fredrick Nwude Eze*[4] *and Opeyemi Joshua Olatunji*[2]*

[1]Department of Neurosurgery, Affiliated Hangzhou Chest Hospital, Zhejiang University School of Medicine, Hangzhou, China, [2]Faculty of Thai Traditional Medicine, Prince of Songkla University, Hat Yai, Thailand, [3]Griffith Institute for Drug Discovery, Griffith University, Brisbane, QLD, Australia, [4]Faculty of Pharmaceutical Sciences, Prince of Songkla University, Hat Yai, Songkhla, Thailand

OPEN ACCESS

Edited by:
Lucia Recinella,
University of Studies G.d'Annunzio Chieti and Pescara, Italy

Reviewed by:
Nadia L. Caram-Salas,
National Council of Science and Technology, Mexico
Zeliha Selamoglu,
Niğde Ömer Halisdemir University, Turkey

***Correspondence:**
Opeyemi Joshua Olatunji
opeyemi.j@psu.ac.th

Specialty section:
This article was submitted to Ethnopharmacology, a section of the journal Frontiers in Pharmacology

Received: 07 July 2021
Accepted: 01 October 2021
Published: 18 October 2021

Citation:
Pang X, Makinde EA, Eze FN and Olatunji OJ (2021) Securidaca inappendiculata *Polyphenol Rich Extract Counteracts Cognitive Deficits, Neuropathy, Neuroinflammation and Oxidative Stress in Diabetic Encephalopathic Rats via p38 MAPK/Nrf2/HO-1 Pathways.* Front. Pharmacol. 12:737764. doi: 10.3389/fphar.2021.737764

Diabetic encephalopathy is one of the serious emerging complication of diabetes. *Securidaca inappendiculata* is an important medicinal plant with excellent antioxidant and anti-inflammatory properties. This study investigated the neuroprotective effects of *S. inappendiculata* polyphenol rich extract (SiPE) against diabetic encephalopathy in rats and elucidated the potential mechanisms of action. Type 2 diabetes mellitus (T2DM) was induced using high fructose solution/intraperitoneal injection of streptozotocin and the diabetic rats were treated with SiPE (50, 100 and 200 mg/kg) for 8 weeks. Learning and memory functions were assessed using the Morris water and Y maze tests, depressive behaviour was evaluated using forced swimming and open field tests, while neuropathic pain assessment was assessed using hot plate, tail immersion and formalin tests. After the experiments, acetylcholinesterase (AChE), oxidative stress biomarkers and proinflammatory cytokines, caspase-3 and nuclear factor kappa-light-chain-enhancer of activated B (NF-κB) were determined by ELISA kits. In addition, the expression levels of p38, phospho-p38 (p-p38), nuclear factor erythroid 2–related factor 2 (Nrf2) and heme oxygenase-1 (HO-1) were determined by western blot analyses. The results indicated that SiPE administration significantly lowered blood glucose level, attenuated body weight loss, thermal/chemical hyperalgesia, improved behavioural deficit in the Morris water maze, Y maze test and reduced depressive-like behaviours. Furthermore, SiPE reduced AChE, caspase-3, NF-κB, malonaldehyde malondialdehyde levels and simultaneously increased antioxidant enzymes activity in the brain tissues of diabetic rats. SiPE administration also significantly suppressed p38 MAPK pathway and upregulated the Nrf2 pathway. The findings suggested that SiPE exerted antidiabetic encephalopathy effects via modulation of oxidative stress and inflammation.

Keywords: diabetic encephalopathy, *Securidaca inappendiculata*, oxidative stress, inflammation, MAPK pathway, Nrf2 pathway

INTRODUCTION

Type 2 diabetes mellitus (T2DM) is a lifelong complex metabolic disease that affects several millions of individuals globally. T2DM is characterized by unrelenting rise in blood glucose levels (hyperglycemia) resulting from several factors including insulin resistance, unhealthy lifestyle and obesity (Baglietto-Vargas et al., 2016; Zeliha and Canan, 2018; Gao et al., 2021). The yearly increase in the number of T2DM patients as well as the mortality accrued to the disease is alarming, thus constituting a major global public health issue. T2DM has been linked to multiple devastating complications such as neuropathy, cardiovascular disease, nephropathy, retinopathy and encephalopathy (Olatunji et al., 2018). Diabetic encephalopathy (DE) is a microvascular complication that affects the central nervous system (CNS), specifically the brain. The clinical features associated with DE includes progressive cognitive dysfunction, electrophysiological, structural and neurochemical abnormalities, leading to degeneration of the CNS and dementia (Cai et al., 2011; Soares et al., 2012; Biessels and Despa, 2018; Chen et al., 2018). It has been demonstrated that prolonged chronic hyperglycemia and hyperlipidemia contributes to the pathogenesis of DE (Chen et al., 2021).

The etiology of DE is quite complex and it is yet to be fully comprehended, however several biochemical pathways and factors have been proposed as a potential link between hyperglycemia and DE, including oxidative stress, inflammation, glucotoxicity, metal accumulation and lipotoxicity. Oxidative stress is thought to be the key mechanism in the initiation and progression of DE (Soares et al., 2012; Biessels and Despa, 2018; Erukainure et al., 2019). The brain is particularly vulnerable to reactive oxygen species (ROS) and oxidative insult due to its high demand for oxygen and glucose for energy generation through oxidative metabolic processes (McCall, 2004). As such, the increase in blood glucose level experienced during diabetes increases oxidative metabolism in the brain leading to uncontrolled generation of ROS and other reactive radicals, resulting in oxidative stress and eventually brain damage (Rossetti et al., 1990). In addition, the brain is abundant in redox active metals and polyunsaturated fatty acids, which actively participate in catalysing ROS formation and substrates for lipid peroxidation, respectively. Furthermore, the low levels of endogenous antioxidant machineries in the brain makes it almost impossible to effectively eliminate the excessive ROS and oxidative stress formed due to hyperglycemia (Smit et al., 1991; Su et al., 2004). With the increase in the incidence of diabetes, developing potent agents with strong antioxidant and anti-inflammatory properties could be a breakthrough in ameliorating diabetes and DE.

Natural products, especially medicinal plants have been extensively explored due to their potential applicability and prospects in the management of diabetes and diabetic complications. The recent surge in the use of medicinal plant as antidiabetic agents has been attributed to their low toxicity as well as their perceived efficacy (Olatunji et al., 2018; Makinde et al., 2020). *Securidaca inappendiculata* Hassk (SI) is a plant native to tropical America and it is widely grown in the tropical regions of China, especially Guangdong, Guangxi, Hainan and Yunnan provinces. SI is extensively used in Chinese folk medicine for treating inflammatory related diseases particularly rheumatic arthritis (Wang et al., 2021). In addition to its anti-inflammatory effects, SI has been reported to possess other pharmacological effects including antidiabetic, antioxidant, anticancer, hepatoprotective and cytotoxic effects (Zha et al., 2015; Ji et al., 2019; Olatunji et al., 2021). The phytochemical constituents in SI have been reported to include xanthones, neolignan glycosides and triterpene saponins (Zuo et al., 2014a; Ji et al., 2019). Our previous studies indicated that SI displayed robust antidiabetic and antioxidant effects in T2DM rats (Olatunji et al., 2021), however, there are no previous studies on the ameliorative role of SI on diabetic complications, especially DE. As such, this present study investigated the neuroprotective effects of SI in high fructose and streptozotocin induced diabetic rats. Concomitantly, given the role of oxidative damage and inflammation in T2DM and DE, we evaluated the impact of the treatment on oxidative and inflammatory markers in the brain tissues of the diabetic rats.

MATERIALS AND METHODS

Chemicals and Reagents

Streptozotocin (STZ) was obtained from Alfa Aesar (Massachusetts, United States). ELISA kits for the estimation of proinflammatory cytokines (TNF-α, IL-6 and IL-1β) were procured from Abcam (Cambridge, United Kingdom), while biochemical kits for the estimation of antioxidants enzymes and malondialdehyde levels were purchased from Abbkine Scientific (Wuhan, China). All other chemicals used were of analytical grade.

Preparation of Plant Extract

The dried stem samples of *Securidaca inappendiculata* Hassk was procured from Chinese Medicinal Herbs Market, Bozhou, Anhui Province, China. The plant samples was authenticated by Associate Professor Dr Jian Zuo, Department of Traditional Chinese Medicine, Wannan Medical College, Wuhu, China. A voucher specimen was deposited at the herbarium of the college. The extraction protocol for the plant material was according to our previous report (Olatunji et al., 2021). The dried extract (SiPE) was preserved at 4°C for further use.

Animals

All the protocols used in the animal experiment were thoroughly reviewed and approved by the animal ethics

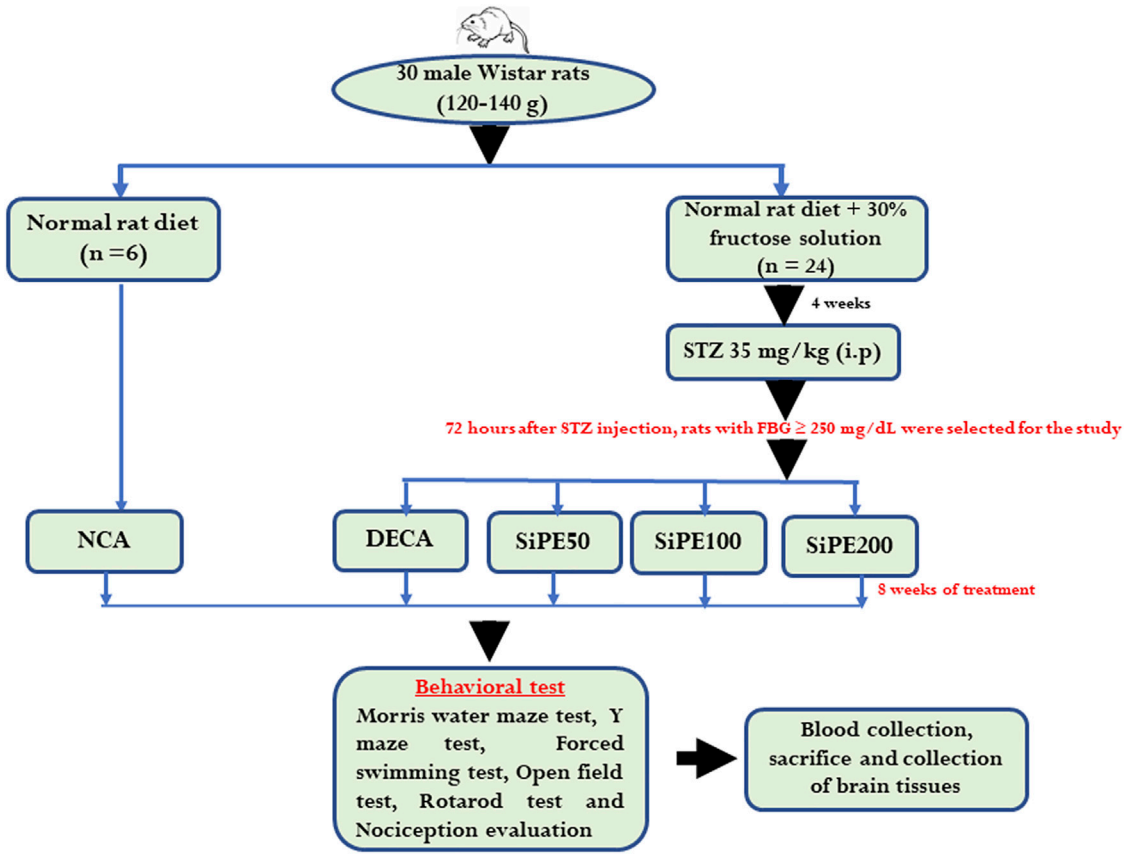

FIGURE 1 | Schematic diagram showing the experimental protocol.

committee of Prince of Songkla University (ethics approval number: 2562-04-051). Male 6 weeks old Wistar rats (160 ± 20 g) used in this study were supplied by Siam Nobura International Animal Company (Bangkok, Thailand). The rats were housed in specific pathogen-free animal house laboratory with six rats per cage and acclimatized for 1 week before the start of the experiment. During the acclimatization period, the rats were offered unlimited access to normal rat chow and water. Thereafter, the animals were divided into two groups; one group with six rats were fed with normal rat chow and water for 4 weeks (normal control animals; NCA), while the other group comprising of 24 rats were also fed with normal rat chow and 30% fructose solution for 4 weeks. Experimental diabetes was induced in 12 h fasted rats by intraperitoneal injection of STZ (35 mg/kg) dissolved in citrate buffer (pH 4.5). Diabetes was confirmed after 72 h of STZ injection by applying a drop of blood from the tail tip of the rats on glucose test strips (Accu-Check Guide, Roche). Rats with fasting blood glucose (FBG) level above 13.9 mmol/L were regarded as successful modelled diabetic rats and were further assigned into four groups:

1) DECA group (diabetic animals treated with normal saline).
2) SiPE50 group (diabetic animals treated with SiPE at 50 mg/kg).
3) SiPE100 group (diabetic animals treated with SiPE at 100 mg/kg).
4) SiPE200 group (diabetic animals treated with SiPE at 200 mg/kg).

Oral treatment with SiPE was initiated immediately after confirmation of diabetes for 56 days (8 weeks). The choice of the doses of SiPE used was based on previous reports (Zuo et al., 2014c; Olatunji et al., 2021). The fasting blood glucose level was measured once a week with an Accu Check Guide glucometer, while changes in the body weight gain of all the animals was also measured once a week with a weighting balance. After the treatment schedule, the rats were subjected to series of behavioural test to evaluate cognitive impairment, neuropathy and motor coordination (**Figure 1**).

Behavioural Studies

Morris Water Maze Test

The procedures and dimension of the circular pool used in the experiment was based on previously reported method of Chen et al. (2021). The temperature of the water was maintained at 25 ± 2°C throughout the experiment. The test was performed four times a day, with 30 min intervals between each test for five consecutive days. The animals were subjected to 4 days of acquisition trial, during this period the height of the escape

platform was arranged to be 1 cm below the water surface. For each session during the escape latency test (days 1-4), the animals were randomly placed into the pool wall from different positions (four quadrants A, B, C and D) in succession with their heads raised up and allowed to adapt to the surface of the water for 1-2 s before been gently released to swim freely to locate the submerged platform. The time taken for the rats to locate the position of the submerged escape platform was recorded within 60 s. The rats that were able to locate the escape platform within the allotted time were allowed to stay on the platform for an additional 10 s before they were returned to their respective cages. Otherwise, the rats that were unable to locate the position of the platform within the allotted 60 s were gradually guided to the position of the platform and were also allowed to remain on the platform for 10 s. On the fifth day of the experiment (exploratory experiment) the hidden platform was removed and the time spent by each rats in the target quadrant within 60 s was recorded.

Y Maze Test

The Y maze test was used to evaluate spontaneous alternation of recognition using previously described method (Olasehinde et al., 2020). The maze was made up of three similar arms (1, 2, 3) with dimensions of 35 cm long, 30 cm high and 15 cm wide, stationed at equal angles. The rats were introduced into the maze from the end of one arm and allowed to freely navigate through the maze for 5 min. Spontaneous alternation was evaluated by the pattern of complete entry into each arm (the rat's hind paws goes entirely into the arm). The frequency of alternation into the arms was recorded based on successive entries into the three arms on overlapping triplet sets (123, 231, 312 . . .).

Forced Swimming Test

The forced swimming test was accessed based on previously reported method (Mu et al., 2020; Tsafack et al., 2021). The swimming apparatus consisted of a transparent cylinder shaped container (30 cm × 45 cm) filled with water at 25°C to a depth of 25 cm. In the pre-test training session, the rats were individually placed in the cylinder and forced to swim for 15 min. After 24 h, the animals were subjected to a 5 min session of the forced swimming. The total immobility and swimming time was recorded. Immobility time was defined as the period the rats stopped swimming, struggling and remained afloat motionlessly or only the movements necessary to keep their head above the water surface.

Open Field Test

The open field test (OFT) was performed using previously described method of Santiago et al. (2010). The rats were placed in the middle of an open rectangular field with floors divided into six rectangular units. The number of crossings with all four paws and rearing with the front paws was recorded for 5 min.

Rotarod Performance Test

The rotarod test was used for evaluating balance and motor coordination according to previous study (Shoaib et al., 2019; Saraswat et al., 2020). The rotarod apparatus consisted of a panel of rod rotating at a maximum speed of 15 rpm. The animals were allowed three sessions of training for three consecutive days. During the training session, the animals were placed on a rotating rod accelerating from 0–15 rpm and the ability of the rats to remain on the rotating rod was recorded. The animals that remained on the rotating rod by the end of the cut of time limit were given a maximum score of 600 s.

Nociception Evaluation

Pain perception and pain thresholds in the treated rats was evaluated using the hot plate, tail immersion and formalin test. The tail immersion test was carried out using a water bath maintained at 52°C. The tails of the rats were submerged in a hot water bath set at 52.5 ± 0.5°C until the rats displays the first response of either tail flicking, withdrawal or struggle. A cut off time of 12 s was set. Shortening of the tail withdrawal time is indicative of hyperalgesia (Kishore et al., 2017). The hot plate test was performed on a hot plate set at 52 ± 0.5°C. The animals were placed on the hotplate apparatus and the latency of the first sign of either paw licking, shaking or jumping was perceived as an index of pain threshold. A cut-off time of 60 s was set to avoid tissue damage.

The formalin test was evaluated by injecting 50 µL of 2.5% formalin under the plantar dorsal surface of the right hind paw of each of the rats. The rats were placed inside a transparent open glass container. The scoring of the nociceptive behaviours started immediately after formalin injection and continued for 30 min. The early phase of the pain-related behaviours (including severe licking, biting, lifting) were recorded for the first 5 min after formalin administration, followed by a brief quiescent period and then a late phase of sustained tonic pain period (15-30 min).

Organ Collection

After the behavioural test, the rats were fasted overnight and euthanized with an intraperitoneal injection of thiopental sodium (150 mg/kg). The brain tissues of the animals were rapidly excised, washed with normal saline to remove residual blood, weighed and a small portion of the brain was preserved in 10% buffered formalin for histopathological analysis, while the remaining part was homogenised in phosphate buffer, centrifuged at 3,500 rpm for 15 min at 4°C. The supernatant obtained was thereafter preserved at −80°C for further biochemical analysis.

Hematoxylin and Eosin Staining

The formalin preserved brain tissues were dehydrated in graded series of alcohol, embedded in paraffin and cut into thickness of 5 µm. The section was further stained with hematoxylin and eosin and slides were visualized under light microscope.

Determination of Acetylcholinesterase Activity in the Brain

The AchE activity in the brain tissue homogenates was determined as previously described by Ellman's method (Ellman et al., 1961).

Determination of Oxidative Stress Biomarkers in the Brain

The concentration of glutathione peroxidase (GPx), glutathione (GSH), superoxide dismutase (SOD), catalase

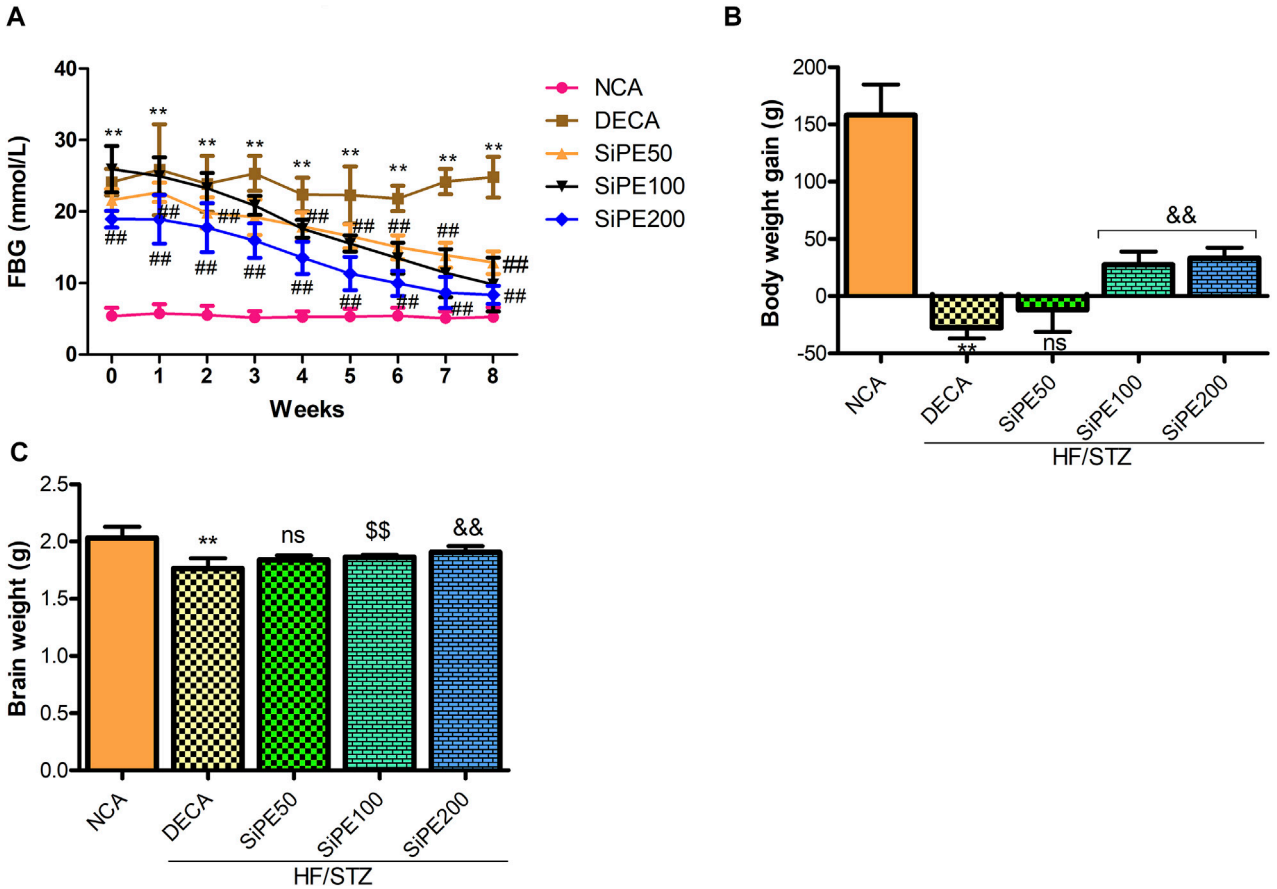

FIGURE 2 | Effect of SiPE treatment on biochemical features in HF/STZ-induced diabetic encephalopathic rats. SiPE treatment at dose of 50, 100 or 200 mg/kg significantly reduced **(A)** fasting blood glucose levels. SiPE treatment at dose of 100 or 200 mg/kg significantly **(B)** improved body weight gain and **(C)** brain weight compared to DECA group. Data are presented as mean ± SD ($n = 6$) and one-way ANOVA test was applied. $^{**}p < 0.001$ indicates statistical significance compared to NCA group. $\#\#p < 0.001$, $\&\&p < 0.01$ and $\$\$p < 0.05$ indicate statistical significance compared to DECA group. ns: not significant compared to DECA group.

(CAT) and lipid peroxidation product malonaldehyde (MDA) in the brain tissues homogenate were detected using biochemical assay kits from Abbkine Scientific Biotechnology (Wuhan, China) following the manufacturers protocol.

Determination of Proinflammatory Biomarkers in the Brain

The levels of proinflammatory cytokines including tumor necrosis factor alpha (TNF-α), interleukin 6 (IL-6) and interleukin one beta (IL-1β) were determined using ELISA kits from Abcam (Cambridge, United Kingdom) following the procedures of the manufacturer.

Western Blot Analysis

Protein expression were determined using western blot analysis. The brain tissues were homogenised in ice-cold RIPA buffer and the protein content was determined using a BCA protein assay kit (Beyotime Biotechnology, Shanghai, China). Equal amount of proteins were electrophoresed on 10% sodium dodecyl sulfatepolyacrylamide gel electrophoresis (SDS-PAGE) and subsequently transferred to nitrocellulose membranes. The membranes were blocked with 5% non-fat milk for 1 h. Thereafter, the membranes were incubated overnight with primary antibodies: p-p38, p38, Nrf2 and HO-1 (Abcam, Cambridge, United Kingdom). at 4°C overnight. After washing with tris-buffered saline, the membranes were further incubated with horseradish-peroxidase conjugated secondary antibodies for 2 h at room temperature. Finally enhanced chemiluminescence reagent (ECL) was used to visualize the bands and bands were analyzed densitometrically using Image J.

Statistical Analysis

Data were analysed using GraphPad Prism 5 (GraphPad, San Diego, CA, United States) and the results were reported as mean ± SD. Statistical significance was determined using one-way ANOVA together with Newman-Keuls multiple comparison test. Statistical significance was set at $p < 0.05$.

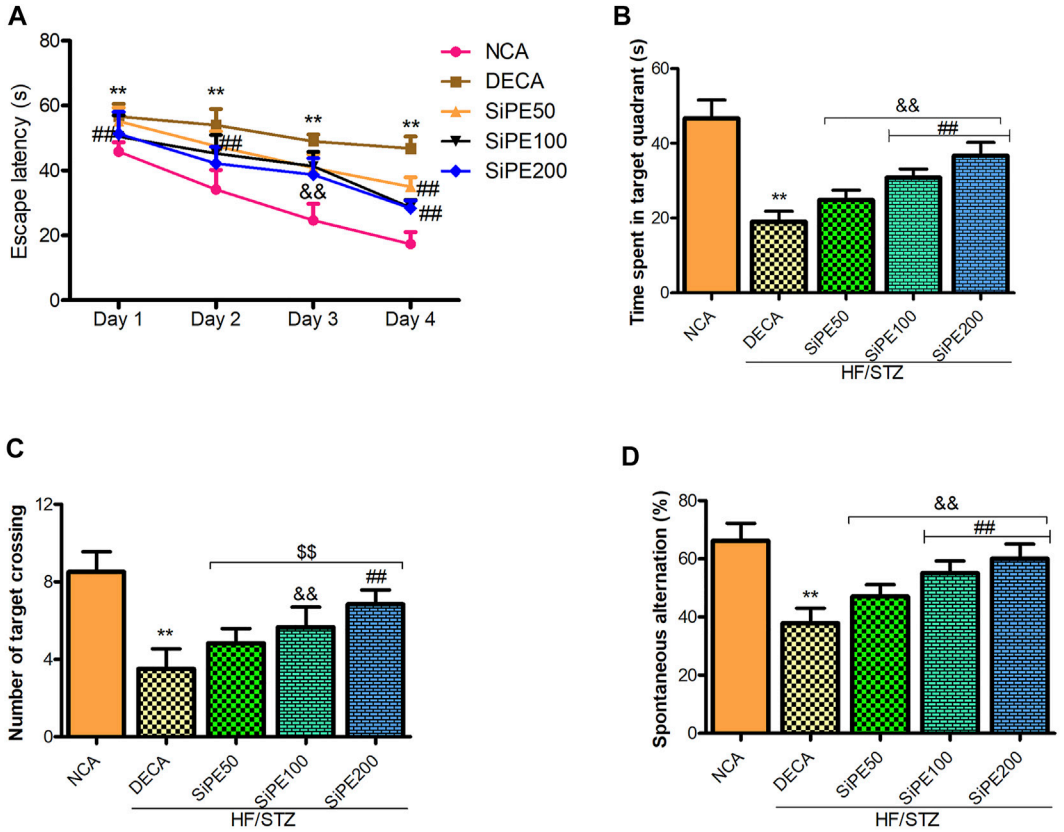

FIGURE 3 | Effect of SiPE treatment on behavioural parameters in HF/STZ-induced diabetic encephalopathic rats. SiPE treatment at dose of 50, 100 or 200 mg/kg significantly improved **(A)** escape latency, **(B)** time spent in the target quadrant, **(C)** number of target crossing and **(D)** spontaneous alternation compared to DECA group. Data are presented as mean ± SD (n = 6) and one-way ANOVA test was applied. **p < 0.001 indicates statistical significance compared to NCA group. ##p < 0.001, &&p < 0.01 and $$$p$ < 0.05 indicate statistical significance compared to DECA group.

RESULTS

Effects of SiPE on FBG, Body Weight Gain and Brain Weight

As shown in **Figure 2A**, the rats administered with STZ had FBG levels >13.9 mmol/L which were significantly higher (p < 0.01) than the corresponding FBG level of rats in the NCA group. Whereas, significant and dose dependent decrease was observed in the final FBG levels of rats that received SiPE (50, 100 and 200 mg/kg) after 8 weeks of supplementation when compared to the untreated DECA group (**Figure 2A**). Furthermore, as indicated in **Figure 2B**, the rats in the DECA group showed significant weight loss compared with the NCA group (p < 0.01). After 8 weeks of treatment with SiPE, there were significantly improvement in the weight of rats compared with the DECA group. Furthermore, the diabetic rats treated with SiPE showed increased brain weight when compared to DECA control group (**Figure 2C**).

SiPE Improved Learning and Memory Abilities of Diabetes Mellitus Rats

Next, we performed Morris water maze and Y maze test to evaluate the effect of SiPE on memory and learning impairments in T2DM rats. As indicated in **Figure 3A**, the rats in the DECA group spent significantly longer time to locate the hidden platform during the 4 days trial period compared to the NCA group (**Figure 3A**). Whereas, the escape latency time of the SiPE treated groups were significantly shorter compared to the DECA group (**Figure 3A**). In the space exploration test, it was observed that the DECA rats spent significantly shorter time in the target quadrant when compared to the NCA rats. Supplementation with SiPE significantly and dose dependently increased the time spent in the target quadrant when compared to the DECA group (**Figure 3B**). Additionally, the number of target crossing of rats in the DECA group was significantly reduced compared to the NCA group, whereas, the diabetic rats treated with SiPE showed increased number of target quadrant crossing when compared to the DECA group (**Figure 3C**).

In the Y maze test, there was a significant decrease in the percentage of spontaneous alternations in the DECA group compared to the NCA group (**Figure 3D**). On the contrary, the reduction in percentage of spontaneous alternations observed in the DECA group was obviously reversed in the SiPE treated groups (50, 100 and 200 mg/kg) (p < 0.01; **Figure 3D**).

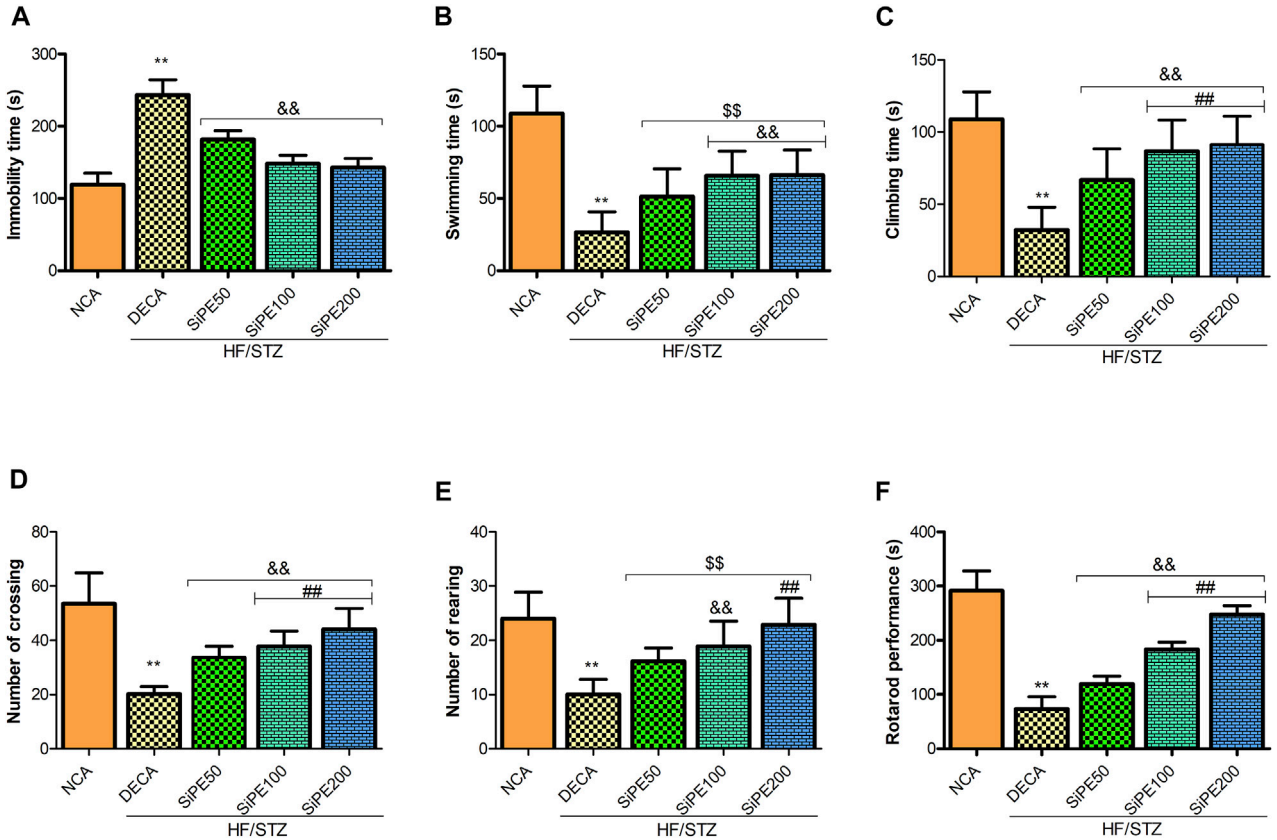

FIGURE 4 | Effect of SiPE treatment on depressive-like behaviours and motor coordination in HF/STZ-induced diabetic encephalopathic rats. SiPE treatment at dose of 50, 100 or 200 mg/kg significantly ameliorated **(A)** immobility time, **(B)** swimming time, **(C)** climbing time, **(D)** number of crossing, **(E)** number of rearing and **(F)** rotarod performance compared to DECA group. Data are presented as mean ± SD (n = 5–6) and one-way ANOVA test was applied. $^{**}p < 0.001$ indicates statistical significance compared to NCA group. $\#\#p < 0.001$, $\&\&p < 0.01$ and $\$\$p < 0.05$ indicate statistical significance compared to DECA group.

Effect of SiPE on Immobility Time in Forced Swimming Test and Open Field Test

Figures 4A–C shows the effect of SiPE on immobility time, swimming and climbing time in the FST. The DECA rats showed significantly increased immobile time, with a corresponding decrease in the time spent swimming and climbing when compared to the NCA rats. In contrast, the diabetic rats that received SiPE showed significantly reduced immobility time as well as increased swimming and climbing time in comparison to the rats in the DECA group (**Figures 4A–C**). Additionally, the number of crossing and rearing of the DECA group was significantly decreased when compared to the NCA and SiPE treated rats (**Figures 4D,E**).

Effect of SiPE on Motor Coordination

As shown in **Figure 4F**, the DECA rats showed significant reduction in endurance and motor coordination as indicated by the reduced time spent on the rotating rod when compared to the time spent by the NCA rats. In contrast, treatment with SiPE significantly and dose dependently increased the time spent on the rotarod compared to the DECA rats (**Figure 4F**).

Effects of SiPE on Pain Scores

As shown in **Figure 5**, compared with the NCA group, the pain perception of the DECA group was significantly increased as indicated by marked reduction in the tail and paw withdrawal latencies in the tail immersion and hot plate test, respectively (**Figures 5A,B**). In addition, the nociceptive reaction of the untreated DECA group in the formalin test was significantly increased as indicated by high incidence of pain response (paw licking, biting and biting) in both the early and late phases (**Figures 5C,D**). Whereas, administration of SiPE significantly reduced both thermal and chemical induced hyperalgesia as portrayed by the increased level of pain perception in the treated rats (**Figures 5A–D**).

Effects of SiPE on Oxidative Stress Biomarkers in the Brain of Diabetes Mellitus Rats

As shown in **Figure 6A**, the level of lipid peroxidation (MDA) in the brain tissues of the DECA group was significantly higher than the NCA group, whereas MDA level was significantly lowered in SiPE treated groups compared with the DECA group. The activities of GPx, GSH, CAT and SOD in the brain of DECA rats were also observed to

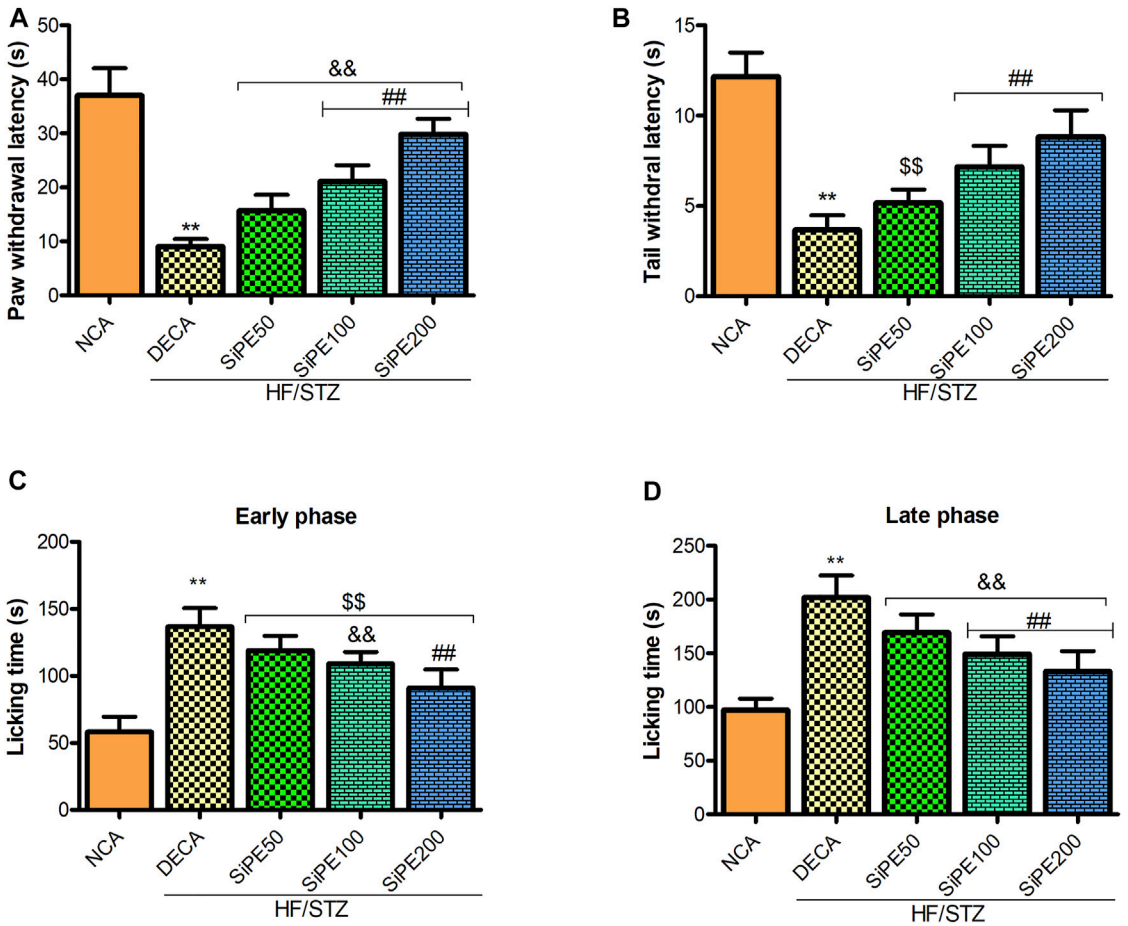

FIGURE 5 | Effect of SiPE treatment on thermal and chemical hyperalgesia in HF/STZ-induced diabetic encephalopathic rats. SiPE treatment at dose of 50, 100 or 200 mg/kg significantly ameliorated **(A)** paw withdrawal latency, **(B)** tail withdrawal latency, **(C)** paw licking time (early phase) and **(D)** paw licking time (late phase) compared to DECA group. Data are presented as mean ± SD ($n = 6$) and one-way ANOVA test was applied. $^{**}p < 0.001$ indicates statistical significance compared to NCA group. $\#\#p < 0.001$, $\&\&p < 0.01$ and $\$\$p < 0.05$ indicate statistical significance compared to DECA group.

be notably reduced in comparison to the NCA rats (**Figures 6B–E**). On the contrary, the activities of the aforementioned antioxidant enzymes in the SiPE treated groups were significantly upregulated when juxtaposed with the DECA group (**Figures 6A–E**).

Effects of SiPE on Proinflammatory Cytokines in the Brain of Diabetes Mellitus Rats

We investigated the effect of SiPE on proinflammatory cytokines in the brain tissues of the treated rats. **Figures 7A–C** indicated that the DECA group showed increased concentration of TNF-α, IL-6 and IL-1β compared to the NCA group, while the increased levels of proinflammatory cytokines were significantly reduced by SiPE treatment (**Figures 7A–C**). Additionally, NF-κB levels was significantly increased in the brain tissues of the DECA rats compared with the NCA group, while the levels was dose dependently and significantly reduced after treatment with SiPE (**Figure 7D**).

Effects of SiPE on AChE and Caspase-3

In the current study, the levels of AChE and caspase-3 in the brain of the untreated DECA group was significantly heightened by approximately 3 and 4 folds respectively when compared with the NCA group. Nevertheless, the administration of SiPE attenuated AChE and caspase-3 levels compared to the DECA group (**Figures 8A,B**).

Effects of SiPE on Histopathological Analysis Using Hematoxylin and Eeosin Staining

The results from the representative H&E staining of the brain tissues of the treated is shown in **Figure 9**. The DECA control representative image displayed obvious pathological alterations including glial proliferation and neuron apoptosis (**Figure 9B**). However, changes in brain architecture were abrogated in the rats treated with SiPE compared to the DECA rats (Figure 89C-E).

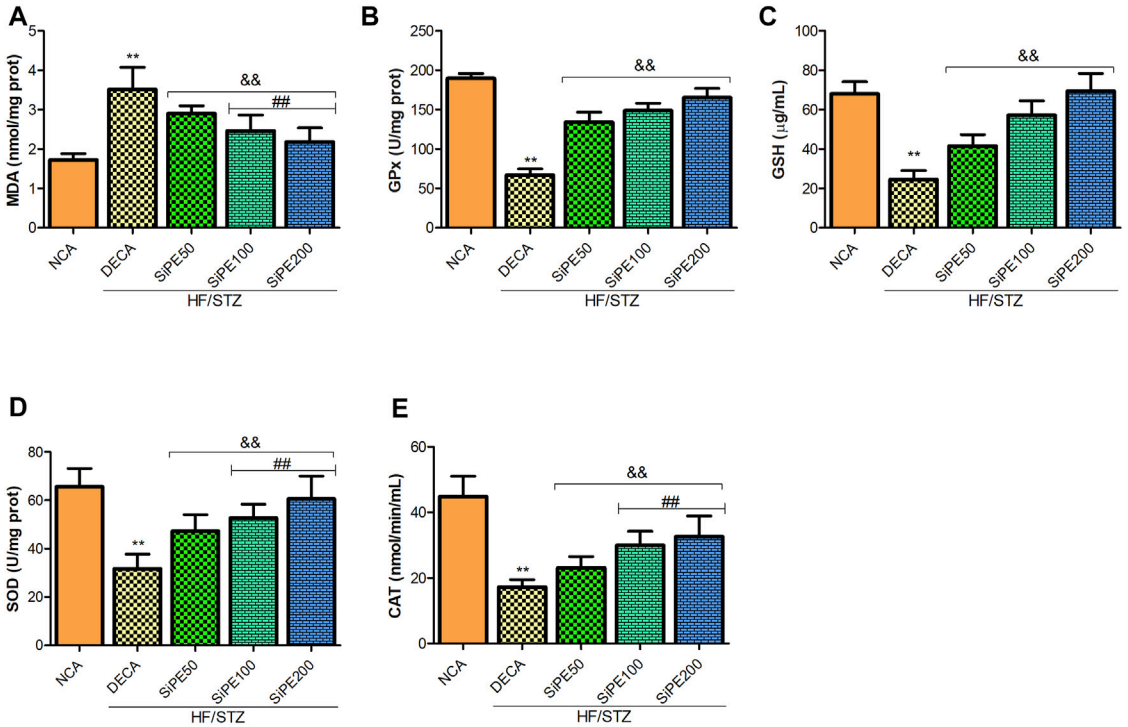

FIGURE 6 | Effect of SiPE treatment on oxidative stress/antioxidant biomarkers in HF/STZ-induced diabetic encephalopathic rats. SiPE treatment at doses of 50, 100 or 200 mg/kg caused significant decrease in **(A)** brain malondialdehyde (MDA) levels compared to DECA group. SiPE treatment reversed HF/STZ induced reduction in **(B)** brain glutathione peroxidase (GPx), **(C)** reduced glutathione (GSH), **(D)** superoxide dismutase (SOD) and **(E)** catalase (CAT). Data are presented as mean ± SD (n = 6) and one-way ANOVA test was applied. $^{**}p < 0.001$ indicates statistical significance compared to NCA group. $\#\#p < 0.001$, $\&\&p < 0.01$ and $\$\$p < 0.05$ indicate statistical significance compared to DECA group.

Effects of SiPE on MAPK-p38 Signaling Pathway

The effects of SiPE on the expression of MAPK signaling (p38 and p-p38) are shown in **Figure 10**. The results indicated that p-p38 expression was significantly increased in the DECA groups, while treatment with SiPE suppressed the phosphorylation of p38 in the treated rats (**Figure 10**). These results suggested that SiPE suppressed the activation of p38 MAPK pathway in the brain tissues of diabetic rats.

Effect of SiPE on Nrf2 Signaling Pathway

The effects of SiPE on Nrf2 signaling pathway in the treated rats are shown in **Figure 10**. The DECA group showed reduced expression of nuclear Nrf2 and HO-1 compared to the normal control group. While SiPE treated groups exhibited increased expression of Nrf2 and HO-1 compared to the DECA group.

DISCUSSION

DE is a complex complication arising from uncontrolled hyperglycemia and the complex nature of DE has encouraged and increased the use of alternative avenues for treating the disease. Increasing number of studies have shown that medicinal plants have shown effectiveness in regulating biochemical, neurological and behavioural alterations in diabetic models due to their multi-constituents and multitarget nature (Kim et al., 2016). This study investigated the neuroprotective effects of SiPE in diabetic rats. The results indicated that after 8 weeks of treatment, SiPE significantly improved hyperglycemia induced memory and cognitive dysfunction, hyperalgesia as well and attenuated inflammatory and oxidative stress responses in the brain tissues of the treated diabetic rats.

Increasing evidences have suggested that diabetic patients are more prone to developing Alzheimer's disease, vascular dementia, cognitive deficits and brain atrophy (Jayaraman and Pike, 2014; Ye et al., 2018). Hyperglycemia plays a crucial role in neuronal damage through the instigation of oxidative stress sensitive pathways leading to neuronal apoptosis and damage. In addition, diabetic alterations has been largely reported to influence learning and memory function (Thakur et al., 2016; Chandrasekaran et al., 2020; Shin et al., 2021). As such, maintaining normal glycaemic control is paramount in the treatment of diabetes so as to prevent any diabetic associated complication including DE. The results from our study indicated that high fructose/STZ induced diabetes was associated with significantly high levels of FBG and reduced body weight gain which was consistent with results from other previous studies (Makinde et al., 2020; Gao et al., 2021).

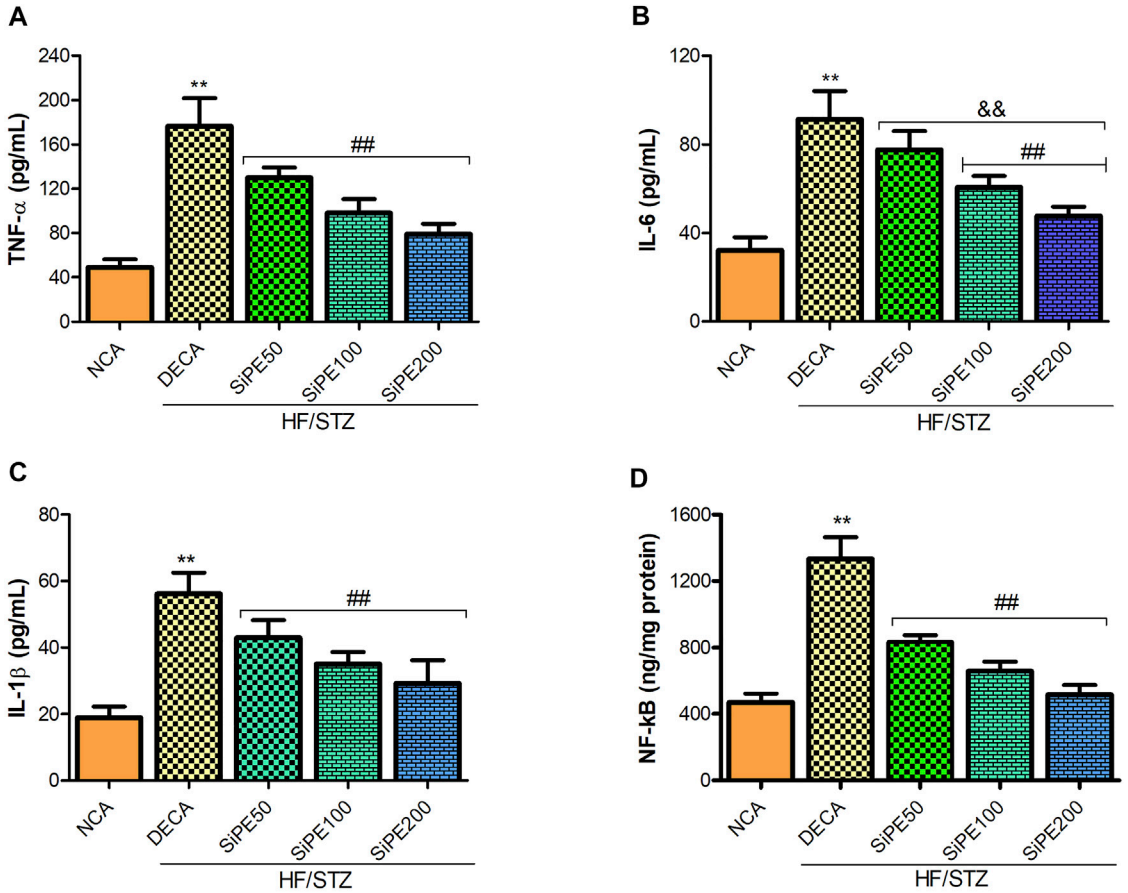

FIGURE 7 | Effect of SiPE treatment on inflammatory mediators in HF/STZ-induced diabetic encephalopathic rats. SiPE treatment at doses of 50, 100 or 200 mg/kg caused significant decrease in **(A)** brain tumor necrosis factor alpha (TNF-α), **(B)** interleukin 6 (IL-6), **(C)** interleukin one beta (IL-1β) and **(D)** nuclear factor kappa-light-chain-enhancer of activated B (NF-κB) compared to DECA group. Data are presented as mean ± SD ($n = 5–6$) and one-way ANOVA test was applied. $^{**}p < 0.001$ indicates statistical significance compared to NCA group. $\#\#p < 0.001$, $\&\&p < 0.01$ and $\$\$p < 0.05$ indicate statistical significance compared to DECA group.

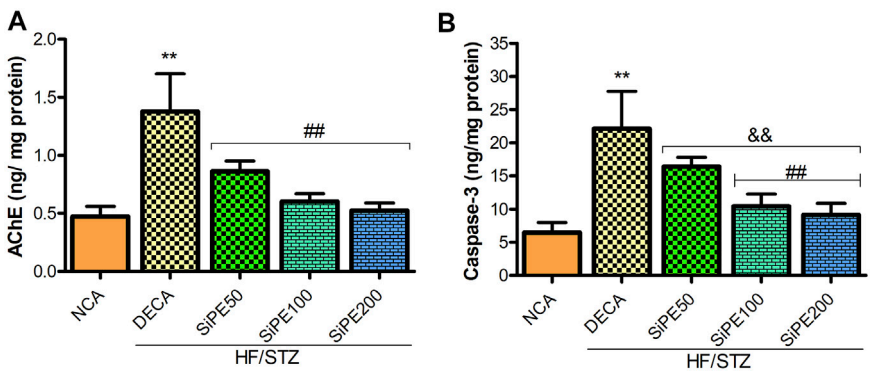

FIGURE 8 | Effect of SiPE treatment on biochemical parameters in HF/STZ-induced diabetic encephalopathic rats. SiPE treatment at doses of 50, 100 or 200 mg/kg caused significant reduction in **(A)** acetylcholinesterase (AChE) and **(B)** caspase-3 levels compared to DECA group. Data are presented as mean ± SD ($n = 6$) and one-way ANOVA test was applied. $^{**}p < 0.001$ indicates statistical significance compared to NCA group. $\#\#p < 0.001$, $\&\&p < 0.01$ and $\$\$p < 0.05$ indicate statistical significance compared to DECA group.

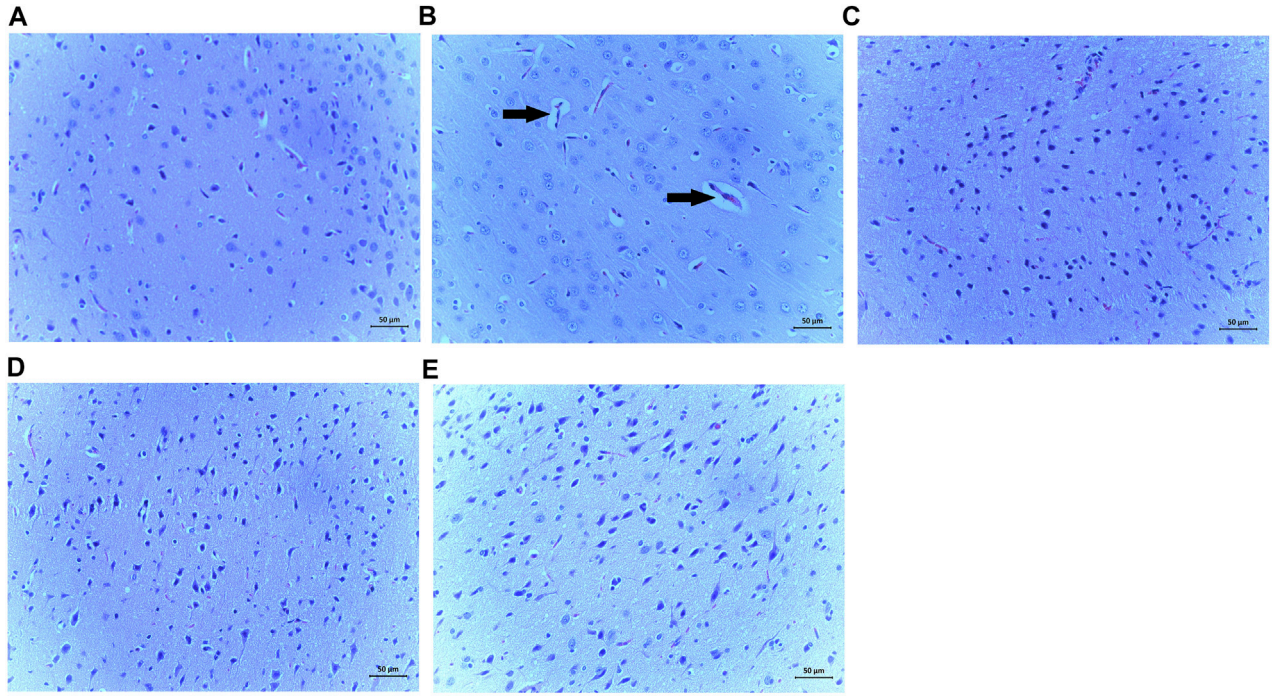

FIGURE 9 | Effect of SiPE treatment on histopathological features in HF/STZ-induced diabetic encephalopathic rats. Representative images of H&E staining of brain tissues showing **(A)** NCA group, **(B)** DECA group, **(C)** SiPE50 group, **(D)** SiPE100 group and **(E)** SiPE200 group. (magnification ×200, scale bar = 50 μm).

There are accumulating clinical and experimental evidences that suggests that diabetes can lead to impaired cognitive function. In this current study, diabetes induced significant memory and learning impairments in the MWMT and Y-maze test, which is in accordance with previous reports (Gocmez et al., 2019; Chen et al., 2021). The occurrence of neuropathy is a common phenomenon in diabetic patients and it significantly affects neuroplasticity and cognitive retention (Tian et al., 2016; Gocmez et al., 2019). The findings from this study indicated that diabetes induced learning, memory and locomotive activity impairments were attenuated after treatment with SiPE. The rats treated with SiPE had significantly shorter escape latency as well as improved percentage alternation, suggesting improvement in spatial learning and memory.

Depression is one of the comorbidity associated with diabetes mellitus. In fact diabetes and depression have been shown to display a bifacial etiology, as patients suffering from depression have a higher risk of developing T2DM due to the activation of several pathways that can initiate insulin resistance (Champaneri et al., 2010; Deischinger et al., 2020). In addition, previous studies have illustrated that anxiety and depression are characteristic features associated with diabetic neuropathy (Mbiantcha et al., 2019; Tsafack et al., 2021). FST and OFT are the most commonly used behavioural studies for evaluating antidepressant activity of pharmacological agents (Dulawa et al., 2004; Cryan et al., 2005). A behavioural depressive state is indicated by increase in immobility time displayed by experimental animals in the OFT and FST tests (Shalam et al., 2007). In line with previous studies, we observed that diabetic rats exhibited depressive like behaviour as indicated by increased immobility time in the FST, as well as reduced locomotive activity in the OFT test when compared to the normoglycemic rats (de Morais et al., 2014, de Morais et al., 2016; Tsafack et al., 2021). SiPE administration significantly reduced the immobility time and increased the swimming time as well as the exploratory behaviour in the FST and OFT, respectively.

In this study, we observed that AChE activity in the brain of diabetic rats were significantly increased. Several studies have reported a striking and direct relationship between increased brain cholinesterase activity and impaired cognitive function in diabetes (Schmatz et al., 2009; Zarrinkalam et al., 2018; Agunloye and Oboh, 2021). The marked increase in the activity of brain AChE in the diabetic rats corroborates the results of the MWM and Y-maze test. Interestingly, treatment with SiPE significantly ameliorated AChE activity in the brain of diabetic rats. These results were consistent with previous studies on diabetes induced cognitive dysfunction (Mushtaq et al., 2014).

Diabetes has also been reported to significantly affect pain response (Kishore et al., 2018; Abo-Salem et al., 2020). Hyperalgesia, a condition that is exemplified by extreme sensitivity to painful stimuli is one of the most often encountered complication of diabetes, and it arises due to damages to peripheral nerves (Lee-Kubli et al., 2014; Hasanein et al., 2020). Motor and sensory nerve conduction dysfunction, numbness and chronic pain are characteristics features that have been well documented to correlate with chronic hyperglycemia (Edwards et al., 2008). Previous studies have also reported

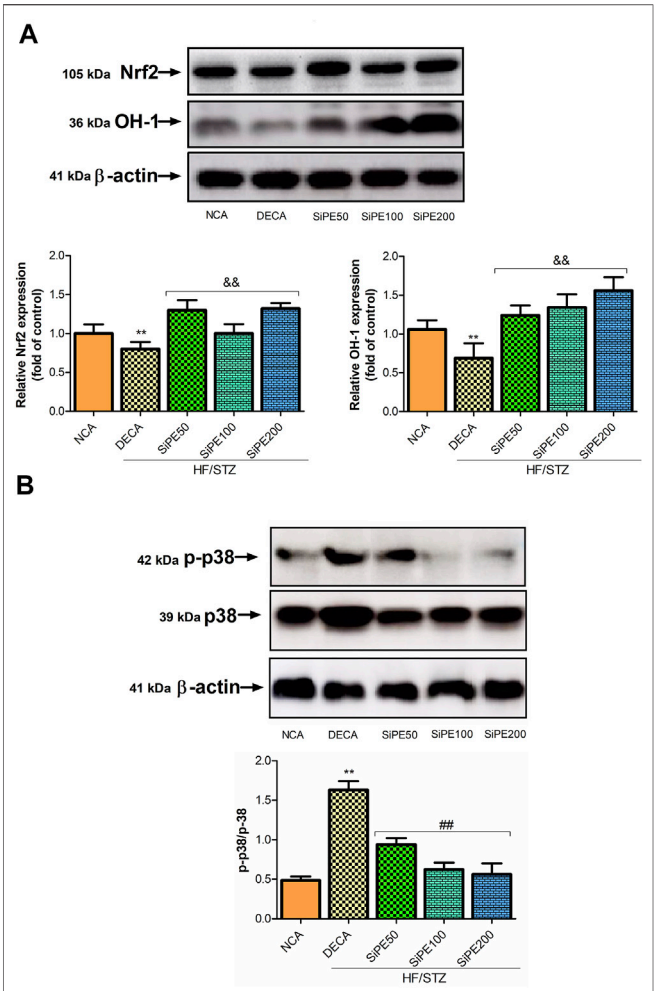

FIGURE 10 | Protein expressions of p-38, p-p38, Nrf2 and HO-1 in the brain tissues from NCA, DECA and SiPE treated groups. Data are presented as mean ± SD (n = 6) and one-way ANOVA test was applied. $^{**}p < 0.001$ indicates statistical significance compared to NCA group. $\#\#p < 0.001$, $\&\&p < 0.01$ and $\$\$p < 0.05$ indicate statistical significance compared to DECA group.

increased pain sensation in diabetic animal models (Kishore et al., 2017; Abo-Salem et al., 2020). In this study, marked decrease in nociceptive threshold in the hotplate and tail immersion test were observed in the diabetic rats, suggesting that the diabetic rats displayed increased hyperalgesia. Treatment with SiPE dose dependently and significantly ameliorated thermal hyperalgesia in the treated rats. Additionally, the increased occurrence of formalin elicited flinching responses in diabetic rats is indicative of abnormal responses to nociceptive stimuli, which has been extensively reported in previous studies (Kaur et al., 2017; Hasanein et al., 2020). In the present study the injection of formalin lead to a biphasic nocifensive flinching, licking or biting behaviour that was amplified in the diabetic animals. The administration of SiPE (50, 100 and 200 mg/kg) lowered the occurrence of chemical hyperalgesia during phases 1 (neurogenic phase) and 2 (inflammatory phase) of the formalin test.

Oxidative stress is a major player in the mechanism associated with diabetic cognitive decline and multiple studies have demonstrated that the pathophysiology and progression of DE is extensively mediated by free radical-induced oxidative stress (Jing et al., 2013; Gocmez et al., 2019; Chen et al., 2021). Excessive increase in oxidative stress coupled with impaired antioxidant defence attributed to uncontrolled hyperglycemia encourages the generation of ROS, which subsequently inactivates nitric oxide bioavailability in diabetes induced endothelial dysfunction, leading to impaired cerebral perfusion, neuronal damage, brain injury and diabetic induced neurodegeneration (Ceriello, 2003; Gocmez et al., 2019). In this study, the activities of SOD, GPx and CAT in the brain tissues of diabetic rats were significantly lowered, while lipid peroxidation (MDA) level was increased. These alterations in the brain oxidative stress and antioxidant defence capacity may be attributed to hyperglycemia induced over generation of ROS, which might have overshadowed the brain antioxidant homeostasis. These results were in consonance with other previous studies revealing loss or reduced brain antioxidant enzymes activity in DE models (Erukainure et al., 2019; Zhang et al., 2020). Treatment with SiPE reversed the decline in antioxidant enzymes activity, while concomitantly reducing lipid peroxidation (MDA) levels in the brain of the treated rats.

On the other hand, prolonged hyperglycemia instigated oxidative stress has also been shown to be a primary facilitator of inflammatory reactions, which aggravates the progression of cognitive decline and brain injury in diabetes. Proinflammatory cytokines including TNF-α, IL-6 and IL-1β are notable cytokines that rapidly responds to oxidative damages and they have been extensively implicated in central and peripheral inflammatory reactions in diabetes (Ola et al., 2014; Wang et al., 2020; Xianchu et al., 2021). Enhanced proinflammatory cytokines concentration directly affects synaptic activity and neurotransmission of neurons, resulting in cognitive dysfunction. In the current study, TNF-α, IL-6 and IL-1β levels were significantly increased in the brain tissues of diabetic rats, while treatment with SiPE exhibited potent anti-inflammatory prowess by significantly abating the level of these cytokines in the treated rats. These results agree with previous studies on the anti-inflammatory potentials of SiPE, especially its effects on cytokine levels in models of inflammation (Zuo et al., 2020).

Oxidative stress can activate a number of apoptotic and inflammatory pathways including caspases and NF-κB pathways, which further complicates DE. NF-κB is a vital transcriptional factor that regulates immunity and it is also extensively involved in the activation of several inflammatory cytokines including TNF-α, IL-6 and IL-1β. Emerging evidences has implicated NF-κB in the pathologies of multiple diseases including diabetes and diabetic complications (Syed et al., 2020; Chen et al., 2021). Consistent with the studies by Chen et al. (2021) and Liu et al. (2020), our study found that diabetes induced significant increase in NF-κB levels in the brain tissues of diabetic rats. Supplementation with SiPE attenuated NF-κB levels, indicating that SiPE displayed strong anti-inflammatory capacity. Furthermore, our study also observed increase in caspase 3 levels in the brain tissues of diabetic rats.

Numerous literatures have established the pivotal pathological roles of oxidative stress and proinflammatory cytokines in apoptosis. Notably ROS generation and the resulting oxidative stress in the mitochondrial can lead to mitochondria dysfunction through the release of several apoptosis factors including cytochrome C and caspase 3 into the cytosol, which ultimately leads to apoptotic cell death (Kannan and Jain, 2000; Wang et al., 2020). Increased levels or over activation of apoptosis players including caspase-3 have been implicated in the pathophysiology of many chronic disorders including Alzheimer, Parkinson and diabetes (Kannan and Jain, 2000). Consistent with previous observation, our result indicated that SiPE supplementation decreased the levels of caspase-3 in the brain of diabetic rats (Tian et al., 2016).

Nrf2 is a transcriptional factor that is very sensitive to redox changes and it is responsible for promoting the expression of antioxidant genes in response to oxidative insult (Ma and Long, 2016; Xu et al., 2021). Under normal biological conditions, Nrf2 binds to Keap1, which restrict its ability to bind to antioxidant related element (ARE). However, in the event of oxidative stress, Nrf2 is released from Keap1, degraded and binds to ARE, thus activating Nrf2-target genes such as NQO1 and HO-1 (Ma and Long, 2016; Wen et al., 2019). In addition, HO-1 has been demonstrated to play a very important role in inflammation due to its suppressive ability on proinflammatory mediators (Ma and Long, 2016; Saha et al., 2020). In this present study, diabetes down regulated the expression of Nrf2/HO-1 which was in accordance with the results from previous study (Ma and Long, 2016; Xu et al., 2021). SiPE ameliorated these alterations by up-regulating Nrf2/HO-1 expressions in the brain tissues of the treated rats.

The mitogen-activated protein kinase (MAPK) pathway has been linked to a number of pathogenic responses including inflammation and oxidative stress. Supporting evidences have shown that MAPK signaling pathways are critically involved in the pathogenesis of several diabetic complications (Lu et al., 2020). Specifically, MAPK p38 pathway has been reported to be activated in diabetes (Ma et al., 2015; Zhao et al., 2021). The results from this study demonstrated that SiPE attenuated diabetes associated activation of p38 MAPK and increase in p-p38 phosphorylation.

Meanwhile, several evidences have demonstrated that plant polyphenols exhibited protective effects against several diseases including diabetes, inflammation, obesity, liver injury and neurodegenerative diseases (Daglia et al., 2014; Tang et al., 2014; Olatunji et al., 2017; Silva and Pogačnik, 2020). The considerable quantity of polyphenols in *S. inappendiculata* provides significant antioxidant and anti-inflammatory effects (Ji et al., 2021; Olatunji et al., 2021). Our previous study on the phytochemical analysis of SiPE extract using UHPLC-ESI-QTOF-MS affirmed the phenolic-richness of the plant, mainly glycosylated polyphenolic derivates, including natsudaidain 3-(4-O-3-hydroxy-3-methylglutaroylglucoside), pectolinarin, centaurein, mirificin, eriodictyol, acanthoside D, neocuscutoside C, oenanthoside A, methylpicraquassioside A, furocoumarinic acid glucoside, hydroxycinnamic acid glycoside, embelin, 5-O-methylembelin, irisxanthone and euxanthone. In addition, the extracts of SiPE have been reported to contain xanthones such as 1,3,7-trihydroxyl-xanthone, 1,3,7-trihydroxyl-2-methoxyl-xanthone, 1,7-dihydroxyl-3,4-dimethoxyl-xanthone, 1,7-dihydroxyl-xanthone, 2-hydroxyl-1,7-dimethoxyl-xanthone, and 7-hydroxyl-1,2-dimethoxyl-xanthone. These compounds have been reported to have varied therapeutic potentials, including robust antioxidant, antidiabetic, anti-inflammatory and analgesic activities (Zuo et al., 2014b; Zuo et al., 2014c; Olatunji et al., 2021). On the basis of our results, we propose that the polyphenol-rich component of SiPE may have been responsible for the potential antidiabetic encephalopathic activity observed in this study.

CONCLUSION

Overall, this study illustrated that SiPE reduced blood glucose levels, attenuated learning and memory dysfunction and reduced neuronal damage in diabetic rats. The findings further suggested that the ameliorative impact of SiPE on diabetic encephalopathy may be attributed to its ability to reduce oxidative stress and pro-inflammatory cytokines, as well as modulate MAPK p38 signaling pathway and the promotion of Nrf2 signaling pathway.

DATA AVAILABILITY STATEMENT

The original contributions presented in the study are included in the article/Supplementary Material, further inquiries can be directed to the corresponding author.

ETHICS STATEMENT

The animal study was reviewed and approved by All procedures were approved by the Ethics Committee of Prince of Songkla University, Thailand.

AUTHOR CONTRIBUTIONS

OO conceived and designed the experiment. XP, OO and EM performed the experiment and analysed the data. OO wrote the manuscript. FE assisted in the *in vivo* experiment. All the authors approved the final version of the manuscript.

FUNDING

The research was supported by University Income Funds of the Prince of Songkla University, Thailand for the year 2020 (TTM6302008S).

REFERENCES

Abo-Salem, O. M., Ali, T. M., Harisa, G. I., Mehanna, O. M., Younos, I. H., and Almalki, W. H. (2020). Beneficial Effects of (-)-Epigallocatechin-3-O-Gallate on Diabetic Peripheral Neuropathy in the Rat Model. *J. Biochem. Mol. Toxicol.* 34, e22508. doi:10.1002/jbt.22508

Agunloye, O. M., and Oboh, G. (2021). Effect of Diet Supplemented with *P. Ostreatus* and *L. Subnudus* on Memory index and Key Enzymes Linked with Alzheimer's Disease in Streptozotocin-Induced Diabetes Rats. *J. Food Biochem.* 45, e13355. doi:10.1111/jfbc.13355

Baglietto-Vargas, D., Shi, J., Yaeger, D. M., Ager, R., and LaFerla, F. M. (2016). Diabetes and Alzheimer's Disease Crosstalk. *Neurosci. Biobehav. Rev.* 64, 272–287. doi:10.1016/j.neubiorev.2016.03.005

Biessels, G. J., and Despa, F. (2018). Cognitive Decline and Dementia in Diabetes Mellitus: Mechanisms and Clinical Implications. *Nat. Rev. Endocrinol.* 14 (10), 591–604. doi:10.1038/s41574-018-0048-7

Cai, X. J., Xu, H. Q., and Lu, Y. (2011). C-peptide and Diabetic Encephalopathy. *Chin. Med. Sci. J.* 26, 119–125. doi:10.1016/s1001-9294(11)60031-x

Ceriello, A. (2003). New Insights on Oxidative Stress and Diabetic Complications May lead to a "causal" Antioxidant Therapy. *Diabetes Care* 26, 1589–1596. doi:10.2337/diacare.26.5.1589

Champaneri, S., Wand, G. S., Malhotra, S. S., Casagrande, S. S., and Golden, S. H. (2010). Biological Basis of Depression in Adults with Diabetes. *Curr. Diab. Rep.* 10, 396–405. doi:10.1007/s11892-010-0148-9

Chandrasekaran, K., Choi, J., Arvas, M. I., Salimian, M., Singh, S., Xu, S., et al. (2020). Nicotinamide Mononucleotide Administration Prevents Experimental Diabetes-Induced Cognitive Impairment and Loss of Hippocampal Neurons. *Int. J. Mol. Sci.* 21, 3756. doi:10.3390/ijms21113756

Chen, R., Shi, J., Yin, Q., Li, X., Sheng, Y., Han, J., et al. (2018). Morphological and Pathological Characteristics of Brain in Diabetic Encephalopathy. *J. Alzheimers Dis.* 65, 15–28. doi:10.3233/JAD-180314

Chen, X., Famurewa, A. C., Tang, J., Olatunde, O. O., and Olatunji, O. J. (2021). Hyperoside Attenuates Neuroinflammation, Cognitive Impairment and Oxidative Stress via Suppressing TNF-A/nf-κB/caspase-3 Signaling in Type 2 Diabetes Rats. *Nutr. Neurosci.*, 1–11. doi:10.1080/1028415X.2021.1901047

Cryan, J. F., Mombereau, C., and Vassout, A. (2005). The Tail Suspension Test as a Model for Assessing Antidepressant Activity: Review of Pharmacological and Genetic Studies in Mice. *Neurosci. Biobehav. Rev.* 29, 571–625. doi:10.1016/j.neubiorev.2005.03.009

Daglia, M., Di Lorenzo, A., Nabavi, S. F., Talas, Z. S., and Nabavi, S. M. (2014). Polyphenols: Well beyond the Antioxidant Capacity: Gallic Acid and Related Compounds as Neuroprotective Agents: You Are what You Eat!. *Curr. Pharm. Biotechnol.* 15, 362–372. doi:10.2174/1389201015041408251207 37

de Morais, H., de Souza, C. P., da Silva, L. M., Ferreira, D. M., Baggio, C. H., Vanvossen, A. C., et al. (2016). Anandamide Reverses Depressive-like Behavior, Neurochemical Abnormalities and Oxidative-Stress Parameters in Streptozotocin-Diabetic Rats: Role of CB1 Receptors. *Eur. Neuropsychopharmacol.* 26, 1590–1600. doi:10.1016/j.euroneuro.2016.08.007

de Morais, H., de Souza, C. P., da Silva, L. M., Ferreira, D. M., Werner, M. F., Andreatini, R., et al. (2014). Increased Oxidative Stress in Prefrontal Cortex and hippocampus Is Related to Depressive-like Behavior in Streptozotocin-Diabetic Rats. *Behav. Brain Res.* 258, 52–64. doi:10.1016/j.bbr.2013.10.011

Deischinger, C., Dervic, E., Leutner, M., Kosi-Trebotic, L., Klimek, P., Kautzky, A., et al. (2020). Diabetes Mellitus Is Associated with a Higher Risk for Major Depressive Disorder in Women Than in Men. *BMJ Open Diabetes Res. Care* 8, e001430. doi:10.1136/bmjdrc-2020-001430

Dulawa, S. C., Holick, K. A., Gundersen, B., and Hen, R. (2004). Effects of Chronic Fluoxetine in Animal Models of Anxiety and Depression. *Neuropsychopharmacology* 29, 1321–1330. doi:10.1038/sj.npp.1300433

Edwards, J. L., Vincent, A. M., Cheng, H. T., and Feldman, E. L. (2008). Diabetic Neuropathy: Mechanisms to Management. *Pharmacol. Ther.* 120, 1–34. doi:10.1016/j.pharmthera.2008.05.005

Ellman, G. L., Courtney, K. D., Andres, V., Jr, and Feather-Stone, R. M. (1961). A New and Rapid Colorimetric Determination of Acetylcholinesterase Activity. *Biochem. Pharmacol.* 7, 88–95. doi:10.1016/0006-2952(61)90145-9

Erukainure, O. L., Ijomone, O. M., Sanni, O., Aschner, M., and Islam, M. S. (2019). Type 2 Diabetes Induced Oxidative Brain Injury Involves Altered Cerebellar Neuronal Integrity and Elemental Distribution, and Exacerbated Nrf2 Expression: Therapeutic Potential of Raffia palm (*Raphia Hookeri*) Wine. *Metab. Brain Dis.* 34, 1385–1399. doi:10.1007/s11011-019-00444-x

Gao, L., Zhang, W., Yang, L., Fan, H., and Olatunji, O. J. (2021). Stink Bean (*Parkia Speciosa*) Empty Pod: a Potent Natural Antidiabetic Agent for the Prevention of Pancreatic and Hepatorenal Dysfunction in High Fat Diet/streptozotocin-Induced Type 2 Diabetes in Rats. *Arch. Physiol. Biochem.*, 1–7. doi:10.1080/13813455.2021.1876733

Gocmez, S. S., Şahin, T. D., Yazir, Y., Duruksu, G., Eraldemir, F. C., Polat, S., et al. (2019). Resveratrol Prevents Cognitive Deficits by Attenuating Oxidative Damage and Inflammation in Rat Model of Streptozotocin Diabetes Induced Vascular Dementia. *Physiol. Behav.* 201, 198–207. doi:10.1016/j.physbeh.2018.12.012

Hasanein, P., Emamjomeh, A., Chenarani, N., and Bohlooli, M. (2020). Beneficial Effects of Rutin in Diabetes-Induced Deficits in Acquisition Learning, Retention Memory and Pain Perception in Rats. *Nutr. Neurosci.* 23, 563–574. doi:10.1080/1028415X.2018.1533269

Jayaraman, A., and Pike, C. J. (2014). Alzheimer's Disease and Type 2 Diabetes: Multiple Mechanisms Contribute to Interactions. *Curr. Diab. Rep.* 14, 476. doi:10.1007/s11892-014-0476-2

Ji, C., Dai, S., Liu, H., Dong, J., Liu, C., and Zuo, J. (2021). Polyphenols from *Securidaca Inappendiculata* Alleviated Acute Lung Injury in Rats by Inhibiting Oxidative Stress Sensitive Pathways. *Chin. Herb. Med.* 13 (3), 381–388. doi:10.1016/j.chmed.2020.09.007

Ji, J., Wang, Q., Wang, M., Chen, J., and Li, X. (2019). New Lignan Glycosides from the Stems of *Securidaca Inappendiculata* Hassk. *Phytochemistry Lett.* 31, 58–62. doi:10.1016/j.phytol.2019.03.011

Jing, Y. H., Chen, K. H., Kuo, P. C., Pao, C. C., and Chen, J. K. (2013). Neurodegeneration in Streptozotocin-Induced Diabetic Rats Is Attenuated by Treatment with Resveratrol. *Neuroendocrinology* 98, 116–127. doi:10.1159/000350435

Kannan, K., and Jain, S. K. (2000). Oxidative Stress and Apoptosis. *Pathophysiology* 7, 153–163. doi:10.1016/s0928-4680(00)00053-5

Kaur, N., Kishore, L., and Singh, R. (2017). Therapeutic Effect of Linum usitatissimum L. In STZ-Nicotinamide Induced Diabetic Nephropathy via Inhibition of AGE's and Oxidative Stress. *J. Food Sci. Technol.* 54, 408–421. doi:10.1007/s13197-016-2477-4

Kim, J. M., Park, S. K., Guo, T. J., Kang, J. Y., Ha, J. S., Lee, du. S., et al. (2016). Anti-amnesic Effect of *Dendropanax Morbifera* via JNK Signaling Pathway on Cognitive Dysfunction in High-Fat Diet-Induced Diabetic Mice. *Behav. Brain Res.* 312, 39–54. doi:10.1016/j.bbr.2016.06.013

Kishore, L., Kaur, N., and Singh, R. (2018). Effect of Kaempferol Isolated from Seeds of *Eruca Sativa* on Changes of Pain Sensitivity in Streptozotocin-Induced Diabetic Neuropathy. *Inflammopharmacology* 26, 993–1003. doi:10.1007/s10787-017-0416-2

Kishore, L., Kaur, N., and Singh, R. (2017). Bacosine Isolated from Aerial Parts of *Bacopa Monnieri* Improves the Neuronal Dysfunction in Streptozotocin-Induced Diabetic Neuropathy. *J. Funct. Foods* 34, 237–247. doi:10.1016/j.jff.2017.04.044

Lee-Kubli, C. A., Mixcoatl-Zecuatl, T., Jolivalt, C. G., and Calcutt, N. A. (2014). Animal Models of Diabetes-Induced Neuropathic Pain. *Curr. Top. Behav. Neurosci.* 20, 147–170. doi:10.1007/7854_2014_280

Liu, S., Zheng, M., Li, Y., He, L., and Chen, T. (2020). The Protective Effect of Geniposide on Diabetic Cognitive Impairment through BTK/TLR4/NF-κB Pathway. *Psychopharmacology (Berl)* 237, 465–477. doi:10.1007/s00213-019-05379-w

Lu, C. H., Ou, H. C., Day, C. H., Chen, H. I., Pai, P. Y., Lee, C. Y., et al. (2020). Deep Sea Minerals Ameliorate Diabetic-Induced Inflammation via Inhibition of TNFα Signaling Pathways. *Environ. Toxicol.* 35, 468–477. doi:10.1002/tox.22882

Ma, C., and Long, H. (2016). Protective Effect of Betulin on Cognitive Decline in Streptozotocin (STZ)-induced Diabetic Rats. *Neurotoxicology* 57, 104–111. doi:10.1016/j.neuro.2016.09.009

Ma, P., Mao, X. Y., Li, X. L., Ma, Y., Qiao, Y. D., Liu, Z. Q., et al. (2015). Baicalin Alleviates Diabetes-associated C-ognitive D-eficits via M-odulation of M-itogen-A-ctivated P-rotein K-inase S-ignaling, B-rain-derived N-eurotrophic F-actor and A-poptosis. *Mol. Med. Rep.* 12, 6377–6383. doi:10.3892/mmr.2015.4219

Makinde, E. A., Radenahmad, N., Adekoya, A. E., and Olatunji, O. J. (2020). *Tiliacora Triandra* Extract Possesses Antidiabetic Effects in High Fat Diet/streptozotocin-Induced Diabetes in Rats. *J. Food Biochem.* 44, e13239. doi:10.1111/jfbc.13239

Mbiantcha, M., Khalid, R., Dawe, A., Mehreen, A., Atsamo, D. A., Ateufack, G., et al. (2019). Antihypernociceptive and Neuroprotective Effects of Combretin A and Combretin B on Streptozotocin-Induced Diabetic Neuropathy in Mice. *Naunyn Schmiedebergs Arch. Pharmacol.* 392, 697–713. doi:10.1007/s00210-019-01626-1

McCall, A. L. (2004). Cerebral Glucose Metabolism in Diabetes Mellitus. *Eur. J. Pharmacol.* 490, 147–158. doi:10.1016/j.ejphar.2004.02.052

Md. Shalam, D., Shantakumar, S., and Narasu, M. (2007). Pharmacological and Biochemical Evidence for the Antidepressant Effect of the Herbal Preparation Trans-01. *Indian J. Pharmacol.* 39, 231–234. doi:10.4103/0253-7613.37273

Mu, D. Z., Xue, M., Xu, J. J., Hu, Y., Chen, Y., Ren, P., et al. (2020). Antidepression and Prokinetic Effects of Paeoniflorin on Rats in the Forced Swimming Test via Polypharmacology. *Evid. Based Complement. Alternat. Med.* 2020, 2153571. doi:10.1155/2020/2153571

Mushtaq, N., Schmatz, R., Pereira, L. B., Ahmad, M., Stefanello, N., Vieira, J. M., et al. (2014). Rosmarinic Acid Prevents Lipid Peroxidation and Increase in Acetylcholinesterase Activity in Brain of Streptozotocin-Induced Diabetic Rats. *Cell Biochem. Funct.* 32, 287–293. doi:10.1002/cbf.3014

Ola, M. S., Aleisa, A. M., Al-Rejaie, S. S., Abuohashish, H. M., Parmar, M. Y., Alhomida, A. S., et al. (2014). Flavonoid, Morin Inhibits Oxidative Stress, Inflammation and Enhances Neurotrophic Support in the Brain of Streptozotocin-Induced Diabetic Rats. *Neurol. Sci.* 35, 1003–1008. doi:10.1007/s10072-014-1628-5

Olasehinde, T. A., Oyeleye, S. I., Ibeji, C. U., and Oboh, G. (2020). Beetroot Supplemented Diet Exhibit Anti-amnesic Effect via Modulation of Cholinesterases, Purinergic Enzymes, Monoamine Oxidase and Attenuation of Redox Imbalance in the Brain of Scopolamine Treated Male Rats. *Nutr. Neurosci.*, 1–15. doi:10.1080/1028415X.2020.1831260

Olatunji, O. J., Chen, H., and Zhou, Y. (2017). Effect of the Polyphenol Rich Ethyl Acetate Fraction from the Leaves of Lycium chinenseMill. On Oxidative Stress, Dyslipidemia, and Diabetes Mellitus in Streptozotocin-Nicotinamide Induced Diabetic Rats. *Chem. Biodivers.* 14, e1700277. doi:10.1002/cbdv.201700277

Olatunji, O. J., Chen, H., and Zhou, Y. (2018). *Lycium Chinense* Leaves Extract Ameliorates Diabetic Nephropathy by Suppressing Hyperglycemia Mediated Renal Oxidative Stress and Inflammation. *Biomed. Pharmacother.* 102, 1145–1151. doi:10.1016/j.biopha.2018.03.037

Olatunji, O. J., Zuo, J., and Olatunde, O. O. (2021). *Securidaca Inappendiculata* Stem Extract Confers Robust Antioxidant and Antidiabetic Effects against High Fructose/streptozotocin Induced Type 2 Diabetes in Rats. Exploration of Bioactive Compounds Using UHPLC-ESI-QTOF-MS. *Arch. Physiol. Biochem.*, 1–13. doi:10.1080/13813455.2021.1921811

Rossetti, L., Giaccari, A., and DeFronzo, R. A. (1990). Glucose Toxicity. *Diabetes Care* 13, 610–630. doi:10.2337/diacare.13.6.610

Saha, S., Buttari, B., Panieri, E., Profumo, E., and Saso, L. (2020). An Overview of Nrf2 Signaling Pathway and its Role in Inflammation. *Molecules* 25, 5474. doi:10.3390/molecules25225474

Santiago, R. M., Barbieiro, J., Lima, M. M., Dombrowski, P. A., Andreatini, R., and Vital, M. A. (2010). Depressive-like Behaviors Alterations Induced by Intranigral MPTP, 6-OHDA, LPS and Rotenone Models of Parkinson's Disease Are Predominantly Associated with Serotonin and Dopamine. *Prog. Neuropsychopharmacol. Biol. Psychiatry* 34, 1104–1114. doi:10.1016/j.pnpbp.2010.06.004

Saraswat, N., Sachan, N., and Chandra, P. (2020). Anti-diabetic, Diabetic Neuropathy Protective Action and Mechanism of Action Involving Oxidative Pathway of Chlorogenic Acid Isolated from Selinum Vaginatum Roots in Rats. *Heliyon* 6, e05137. doi:10.1016/j.heliyon.2020.e05137

Schmatz, R., Mazzanti, C. M., Spanevello, R., Stefanello, N., Gutierres, J., Corrêa, M., et al. (2009). Resveratrol Prevents Memory Deficits and the Increase in Acetylcholinesterase Activity in Streptozotocin-Induced Diabetic Rats. *Eur. J. Pharmacol.* 610, 42–48. doi:10.1016/j.ejphar.2009.03.032

Shin, E. J., Kim, J. M., Kang, J. Y., Park, S. K., Han, H. J., Kim, H. J., et al. (2021). Ameliorative Effect of Persimmon (*Diospyros Kaki*) in Cognitively Impaired Diabetic Mice. *J. Food Biochem.* 45, e13581. doi:10.1111/jfbc.13581

Shoaib, A., Badruddeen, Dixit, R. K., Dixit, M., Barreto, G., Ashraf, G. M., and Siddiqui, H. H. (2019). Beneficial Effects of N-Hexane Bark Extract of *Onosma Echioides* L. On Diabetic Peripheral Neuropathy. *J. Cel. Biochem.* 120, 16524–16532. doi:10.1002/jcb.28912

Silva, R. F. M., and Pogačnik, L. (2020). Polyphenols from Food and Natural Products: Neuroprotection and Safety. *Antioxidants (Basel)* 9, 61. doi:10.3390/antiox9010061

Smith, C. D., Carney, J. M., Starke-Reed, P. E., Oliver, C. N., Stadtman, E. R., Floyd, R. A., et al. (1991). Excess Brain Protein Oxidation and Enzyme Dysfunction in normal Aging and in Alzheimer Disease. *Proc. Natl. Acad. Sci. U S A.* 88, 10540–10543. doi:10.1073/pnas.88.23.10540

Soares, Nunes, S., Reis, F., and Pereira, F. (2012). Diabetic Encephalopathy: the Role of Oxidative Stress and Inflammation in Type 2 Diabetes. *Int. J. Interferon. Cytokine Mediat. Res.* 4, 75–85.

Su, B., Wang, X., Nunomura, A., Moreira, P. I., Lee, H. G., Perry, G., et al. (2004). Oxidative Stress Signaling in Alzheimer's Disease. *Curr. Alzheimer Res.* 5, 525–532. doi:10.2174/156720508786898451

Syed, A. A., Reza, M. I., Shafiq, M., Kumariya, S., Singh, P., Husain, A., et al. (2020). Naringin Ameliorates Type 2 Diabetes Mellitus-Induced Steatohepatitis by Inhibiting RAGE/NF-κB Mediated Mitochondrial Apoptosis. *Life Sci.* 257, 118118. doi:10.1016/j.lfs.2020.118118

Tang, C. C., Lin, W. L., Lee, Y. J., Tang, Y. C., and Wang, C. J. (2014). Polyphenol-rich Extract of *Nelumbo nucifera* Leaves Inhibits Alcohol-Induced Steatohepatitis via Reducing Hepatic Lipid Accumulation and Anti-inflammation in C57BL/6J Mice. *Food Funct.* 5, 678–687. doi:10.1039/c3fo60478k

Thakur, A. K., Rai, G., Chatterjee, S. S., and Kumar, V. (2016). Beneficial Effects of an *Andrographis Paniculata* Extract and Andrographolide on Cognitive Functions in Streptozotocin-Induced Diabetic Rats. *Pharm. Biol.* 54, 1528–1538. doi:10.3109/13880209.2015.1107107

Tian, X., Liu, Y., Ren, G., Yin, L., Liang, X., Geng, T., et al. (2016). Resveratrol Limits Diabetes-Associated Cognitive Decline in Rats by Preventing Oxidative Stress and Inflammation and Modulating Hippocampal Structural Synaptic Plasticity. *Brain Res.* 1650, 1–9. doi:10.1016/j.brainres.2016.08.032

Tian, Z., Wang, J., Xu, M., Wang, Y., Zhang, M., and Zhou, Y. (2016). Resveratrol Improves Cognitive Impairment by Regulating Apoptosis and Synaptic Plasticity in Streptozotocin-Induced Diabetic Rats. *Cell. Physiol. Biochem.* 40, 1670–1677. doi:10.1159/000453216

Tsafack, E. G., Mbiantcha, M., Ateufack, G., Djuichou Nguemnang, S. F., Nana Yousseu, W., Atsamo, A. D., et al. (2021). Antihypernociceptive and Neuroprotective Effects of the Aqueous and Methanol Stem-Bark Extracts of *Nauclea Pobeguinii* (Rubiaceae) on STZ-Induced Diabetic Neuropathic Pain. *Evid. Based Complement. Alternat. Med.* 2021, 6637584. doi:10.1155/2021/6637584

Wang, D.-D., Li, Y., Wu, Y.-J., Wu, Y.-L., Han, J., Olatunji, O. J., et al. (2021). Xanthones from *Securidaca Inappendiculata* Antagonized the Antirheumatic Effects of Methotrexate *In Vivo* by Promoting its Secretion into Urine. *Expert Opin. Drug Metab. Toxicol.* 17, 241–250. doi:10.1080/17425255.2021.1843634

Wang, F., Li, R., Zhao, L., Ma, S., and Qin, G. (2020). Resveratrol Ameliorates Renal Damage by Inhibiting Oxidative Stress-Mediated Apoptosis of Podocytes in Diabetic Nephropathy. *Eur. J. Pharmacol.* 885, 173387. doi:10.1016/j.ejphar.2020.173387

Wen, W., Lin, Y., and Ti, Z. (2019). Antidiabetic, Antihyperlipidemic, Antioxidant, Anti-inflammatory Activities of Ethanolic Seed Extract of *Annona Reticulata* L. In Streptozotocin Induced Diabetic Rats. *Front. Endocrinol. (Lausanne)* 10, 716. doi:10.3389/fendo.2019.00716

Xianchu, L., Kang, L., Beiwan, D., Huan, P., and Ming, L. (2021). Apocynin Ameliorates Cognitive Deficits in Streptozotocin-Induced Diabetic Rats. *Bratisl. Lek. Listy.* 122, 78–84. doi:10.4149/BLL_2021_010

Xu, J., Fu, C., Li, T., Xia, X., Zhang, H., Wang, X., et al. (2021). Protective Effect of Acorn (*Quercus Liaotungensis* Koidz) on Streptozotocin-Damaged MIN6 Cells and Type 2 Diabetic Rats via P38 MAPK/Nrf2/HO-1 Pathway. *J. Ethnopharmacol.* 266, 113444. doi:10.1016/j.jep.2020.113444

Ye, T., Meng, X., Zhai, Y., Xie, W., Wang, R., Sun, G., et al. (2018). Gastrodin Ameliorates Cognitive Dysfunction in Diabetes Rat Model via the Suppression of Endoplasmic Reticulum Stress and NLRP3 Inflammasome Activation. *Front. Pharmacol.* 9, 1346. doi:10.3389/fphar.2018.01346

Zarrinkalam, E., Ranjbar, K., Salehi, I., Kheiripour, N., and Komaki, A. (2018). Resistance Training and Hawthorn Extract Ameliorate Cognitive Deficits in Streptozotocin-Induced Diabetic Rats. *Biomed. Pharmacother.* 97, 503–510. doi:10.1016/j.biopha.2017.10.138

Zeliha, S., and Canan, A. E. (2018). General Approaches to the Stem Cell Therapy in Diabetes Mellitus as Innovative Researches. *J. Genet. Mutat.* 1, 4–5.

Zha, H., Wang, Z., Yang, X., Jin, D., Hu, L., Zheng, W., et al. (2015). New Acylated Triterpene Saponins from the Roots of *Securidaca Inappendiculata* Hassk. *Phytochemistry Lett.* 13, 108–113. doi:10.1016/j.phytol.2015.05.022

Zhang, L., Ma, Q., and Zhou, Y. (2020). Strawberry Leaf Extract Treatment Alleviates Cognitive Impairment by Activating Nrf2/HO-1 Signaling in Rats with Streptozotocin-Induced Diabetes. *Front. Aging Neurosci.* 12, 201. doi:10.3389/fnagi.2020.00201

Zhao, L. L., Makinde, E. A., and Olatunji, O. J. (2021). Protective Effects of Ethyl Acetate Extract from *Shorea Roxburghii* against Diabetes Induced Testicular Damage in Rats. *Environ. Toxicol.* 36, 374–385. doi:10.1002/tox.23043

Zuo, J., Ji, C. L., Olatunji, O. J., Yang, Z., Xu, H. F., Han, J., et al. (2020). Bioactive Fractions from *Securidaca Inappendiculata* Alleviated Collagen-Induced Arthritis in Rats by Regulating Metabolism-Related Signaling. *Kaohsiung J. Med. Sci.* 36, 523–534. doi:10.1002/kjm2.12205

Zuo, J., Ji, C. L., Xia, Y., Li, X., and Chen, J. W. (2014a). Xanthones as α-glucosidase Inhibitors from the Antihyperglycemic Extract of Securidaca Inappendiculata. *Pharm. Biol.* 52, 898–903. doi:10.3109/13880209.2013.872673

Zuo, J., Xia, Y., Mao, K. J., Li, X., and Chen, J. W. (2014c). Xanthone-rich Dichloromethane Fraction of *Securidaca Inappendiculata*, the Possible Antirheumatic Material Base with Anti-inflammatory, Analgesic, and Immunodepressive Effects. *Pharm. Biol.* 52, 1367–1373. doi:10.3109/13880209.2014.892143

Zuo, J., Mao, K.-j., Yuan, F., Li, X., and Chen, J.-w. (2014b). Xanthones with Anti-tumor Activity Isolated from *Securidaca Inappendiculata*. *Med. Chem. Res.* 23, 4865–4871. doi:10.1007/s00044-014-1051-8

Conflict of Interest: The authors declare that the research was conducted in the absence of any commercial or financial relationships that could be construed as a potential conflict of interest.

Publisher's Note: All claims expressed in this article are solely those of the authors and do not necessarily represent those of their affiliated organizations, or those of the publisher, the editors and the reviewers. Any product that may be evaluated in this article, or claim that may be made by its manufacturer, is not guaranteed or endorsed by the publisher.

frontiers in Pharmacology

REVIEW
published: 23 November 2021
doi: 10.3389/fphar.2021.715359

Tripterygium hypoglaucum (Lévl.) Hutch and Its Main Bioactive Components: Recent Advances in Pharmacological Activity, Pharmacokinetics and Potential Toxicity

Junqi Zhao[1†], Fangling Zhang[1†], Xiaolin Xiao[2], Zhao Wu[1], Qichao Hu[1], Yinxiao Jiang[1], Wenwen Zhang[1], Shizhang Wei[1], Xiao Ma[1] and Xiaomei Zhang[3]**

[1]State Key Laboratory of Southwestern Chinese Medicine Resources, School of Pharmacy, Chengdu University of Traditional Chinese Medicine, Chengdu, China, [2]Hospital of Chengdu University of Traditional Chinese Medicine, School of Clinical Medicine, Chengdu University of Traditional Chinese Medicine, Chengdu, China, [3]Institute of Medicinal Chemistry of Chinese Medicine, Chongqing Academy of Chinese Materia Medica, Chongqing, China

OPEN ACCESS

Edited by:
Lucia Recinella,
University of Studies G. d'Annunzio Chieti and Pescara, Italy

Reviewed by:
Zhenzhou Jiang,
China Pharmaceutical University, China
Stefania Tacconelli,
University of Studies G. d'Annunzio Chieti and Pescara, Italy

***Correspondence:**
Xiao Ma
tobymaxiao@163.com
Xiaomei Zhang
ZXM761@163.com

[†]These authors have contributed equally to this work and share first authorship

Specialty section:
This article was submitted to Ethnopharmacology, a section of the journal Frontiers in Pharmacology

Received: 26 May 2021
Accepted: 04 November 2021
Published: 23 November 2021

Citation:
Zhao J, Zhang F, Xiao X, Wu Z, Hu Q, Jiang Y, Zhang W, Wei S, Ma X and Zhang X (2021) Tripterygium hypoglaucum (Lévl.) Hutch and Its Main Bioactive Components: Recent Advances in Pharmacological Activity, Pharmacokinetics and Potential Toxicity. Front. Pharmacol. 12:715359. doi: 10.3389/fphar.2021.715359

Tripterygium hypoglaucum (Lévl.) Hutch (THH) is believed to play an important role in health care and disease treatment according to traditional Chinese medicine. Moreover, it is also the representative of medicine with both significant efficacy and potential toxicity. This characteristic causes THH hard for embracing and fearing. In order to verify its prospect for clinic, a wide variety of studies were carried out in the most recent years. However, there has not been any review about THH yet. Therefore, this review summarized its characteristic of components, pharmacological effect, pharmacokinetics and toxicity to comprehensively shed light on the potential clinical application. More than 120 secondary metabolites including terpenoids, alkaloids, glycosides, sugars, organic acids, oleanolic acid, polysaccharides and other components were found in THH based on phytochemical research. All these components might be the pharmacological bases for immunosuppression, anti-inflammatory and anti-tumour effect. In addition, recent studies found that THH and its bioactive compounds also demonstrated remarkable effect on obesity, insulin resistance, fertility and infection of virus. The main mechanism seemed to be closely related to regulation the balance of immune, inflammation, apoptosis and so on in various disease. Furthermore, the study of pharmacokinetics revealed quick elimination of the main component triptolide. The feature of celastrol was also investigated by several models. Finally, the side effect of THH was thought to be the key for its limitation in clinical application. A series of reports indicated that multiple organs or systems including liver, kidney and genital system were involved in the toxicity. Its potential serious problem in liver was paid specific attention in recent years. In summary, considering the significant effect and potential toxicity of THH as well as its components, the combined medication to inhibit the toxicity, maintain effect might be a promising method for clinical conversion. Modern advanced technology such as structure optimization might be another way to

reach the efficacy and safety. Thus, THH is still a crucial plant which remains for further investigation.

Keywords: *Tripterygium hypoglaucum* (Lévl.) Hutch., phytochemistry, pharmacology, pharmacokinetics, toxicity

INTRODUCTION

Effect and toxicity are two important aspects of drugs. Among the compounds obtained from plants or natural sources, agents with remarkable efficacy and potential toxicity have attracted much attention in recent years. It is well-known that some traditional Chinese medicine is highly toxic such as arsenic, *Aconitum carmichaelii* Debx. and *Tripterygium wilfordii* Hook F. (TwHF). Indeed, long-term consumption of arsenic can lead to arsenic accumulation in vital organs with diabetes, atherosclerosis, hypertension, ischemic heart disease, and hepatotoxicity (Khairul et al., 2017). However, arsenic trioxide (As_2O_3) has recently shown significant efficacy in patients with acute promyelocytic leukemia (APL) and many other malignancies, such as adult T-cell leukemia/lymphoma (ATL) and NPM1 mutant acute myeloid leukemia (AML) (Kchour et al., 2009; Mathews et al., 2011; El Hajj et al., 2015). In addition, fatal ventricular tachycardia and asystole may occur if aconite poisoning is severe (Chan, 2012). The processed *Aconitum carmichaelii* Debx. plays an important role as cardiotonic, analgesic and anti-inflammatory in traditional medicine (Chan, 2011). Moreover, TwHF is frequently reported exhibiting multiple toxicity, including reproductive toxicity, renal cytotoxicity, and hepatotoxicity (Li X.-J. et al., 2014). However, due to its significant anti-inflammatory and immunosuppressive effects, TwHF preparations have been widely used for the treatment of autoimmune disorders and inflammatory diseases, such as rheumatoid arthritis (RA) (Luo et al., 2019; Xu et al., 2019). It is worth noting that multiple organ toxicity in TwHF can be resolved after dose adjustment (Zhang et al., 2021a). Therefore, the agents with both remarkable effect and potential toxicity should be paid specific focus.

Tripterygium hypoglaucum (Lévl.) Hutch. (THH), a plant distributed in southwest regions of China and along the south bank of the Yangtze River, has similar pharmacological effects with fewer side effects and lower toxicity than TwHF in the clinic (Li, 2006; Brinker et al., 2007; Ma et al., 2008) (**Figure 1**). Its main chemical components include alkaloids, diterpenoids and triterpenoids. Its root bark demonstrates excellent medicinal properties and has been widely used in folk medicine in China (Li, 2006). Numerous studies have found that terpenoids isolated from THH possess various pharmacological activities including anti-tumour, immunosuppressive and anti-inflammatory effects (Liu, 2011; Lü et al., 2015). Studies have shown that celastrol, a triterpenoid discovered from THH, relieves insulin resistance, reduces body weight, and suppresses polycystic kidney disease (Booij et al., 2020). Despite significant efficacy, the clinical application of THH has a narrow therapeutic window due to severe toxicity, thereby limiting its widespread application (Dudics et al., 2018; Yuan et al., 2019a; Wang et al., 2019).

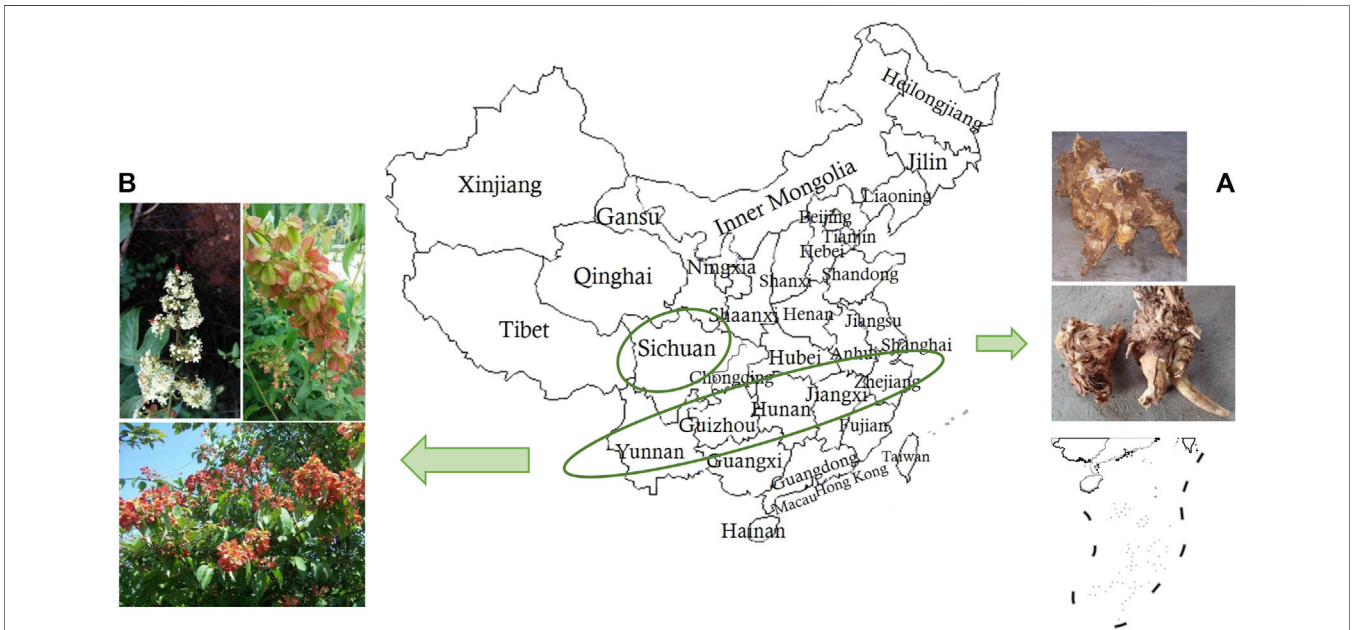

FIGURE 1 | Climatic and ecological adaptability distribution of THH in China. **(A)** Dried root bark of THH, **(B)** Aerial view of THH.

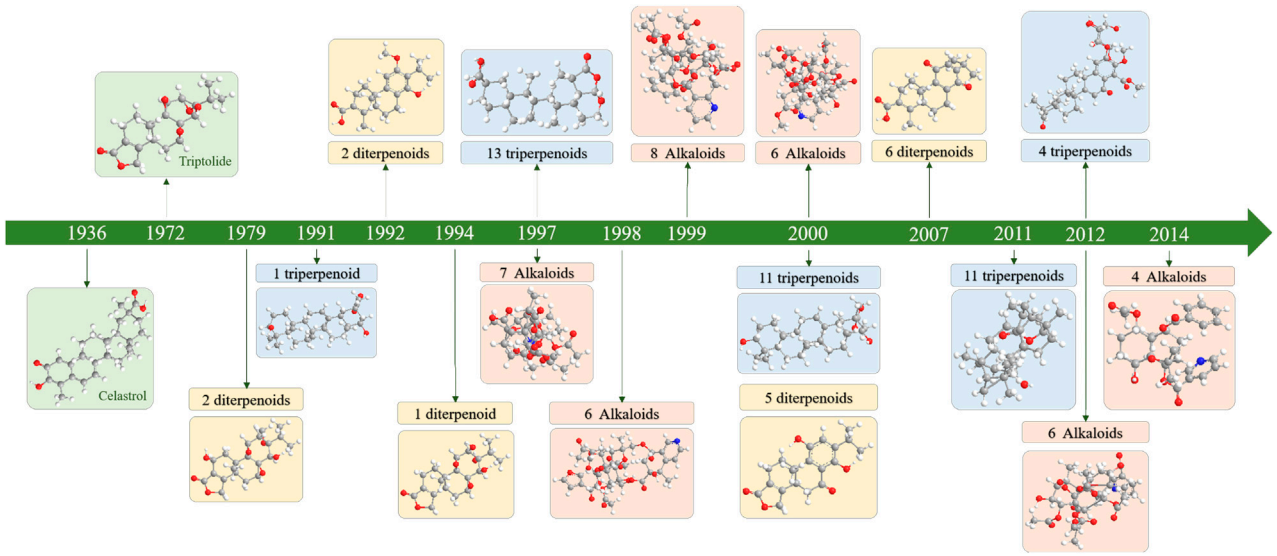

FIGURE 2 | Timeline of the isolation and identification of main chemical components from the genus *Tripterygium*.

Identification of the active chemical ingredients and pharmacological effects of THH is the primary goal of most THH studies, and this information is useful for the development of efficient and low-toxicity modern traditional Chinese medicines. The current research review on THH is limited, and sufficient attention has not been given to the relationship between compounds, pharmacological activities and toxicity. The chemical compositions and pharmacological mechanisms and potential toxicity of THH were studied to provide a scientific basis for the development of a safe medication with better clinical utility. To further clarify the chemical composition, mechanism of action, pharmacological effects and toxicity characteristics of THH, we conducted the following review. We also summarized the pharmacokinetics study of THH in animals.

METHODOLOGY

Database searches using PubMed, China National Knowledge Internet (CNKI) and Wanfang database were conducted until December 2020. *Tripterygium hypoglaucum* (Lévl.) Hutch., *Tripterygium*, triptolide, celastrol and kunmingshanhaitang were searched as key words in the databases mentioned above. All of databases were retrieved twice. Experimental articles related to THH and its active components were included, and some irrelevant literature was excluded through reading abstracts or the full text. In almost all cases, the original articles were obtained and the relevant data was extracted.

Phytochemical Constituents

Since the 1960s, scholars have conducted in-depth research on TwHF through nearly half a century of chemical composition research on the genus *Tripterygium* (**Figure 2**). This plant genus contains more than 100 chemical components such as terpenoids (diterpenes, triterpenes, sesquiterpenes), alkaloids, glycosides, sugars, organic acids, euonymol, euonymus alkaloids, polysaccharides, β-sitosterol and other chemical components. Its characteristic active ingredients include diterpenoids such as triptolide, triptophenolide, triptriolide, triptoquinone A, and triterpenoids, such as celastrol and wilforlide A (Xie et al., 2015) (**Figure 3**).

In the earliest study (1972) of the chemical composition of THH, triptolide, triptolide diol, and triptolide ketone were isolated and identified from the ethanol-ethyl acetate extract of TwHF, a congeneric plant produced in China (Kupchan et al., 1972). In 1979, domestic studies in China first isolated trace amounts of two diterpene lactone chemical constituents, hypolide and tripterolide, from the root bark of TwHF. As a common chemical component of the three species of this genus, hypolides were isolated not only from THH but also from other species of the same genus, and it was hypothesized that hypolides might represent one of the precursors of biosynthesis in this genus (Wu and Sun, 1979).

A study reported that three rosin diterpenes, namely hypoglic acid, triptonoterpene methyl ether and triptonoterpenol could be separated from the ethyl acetate soluble portion of the root ethanol extract by silica gel column chromatography (Wang et al., 2012). An additional three ursolane triterpenes, namely hypoglaulide, triptotriterpenic acid C and regelin were obtained, and 3-acetoxy oleanolic acid was also obtained during the same separation process in 1992 (Zhang et al., 1992a). Ten crystals were obtained from the ethanol extract of the coarse powder of THH root: 3-oxofriedelan-29-oic acid methyl ester; β-sitosterol; 3-epik atonic acid methyl ester; 3β, 22α-dihydroxy-Δ12-oleanen-29-oic acid methyl ester; and 3β, 22α-dihydroxy-Δ12-ursen-30-oic acid methyl ester (Yi and Yang, 1993). In other studies, the chloroform extracts of THH roots were separated by column chromatography, and a total of 12 crystals were obtained. Of

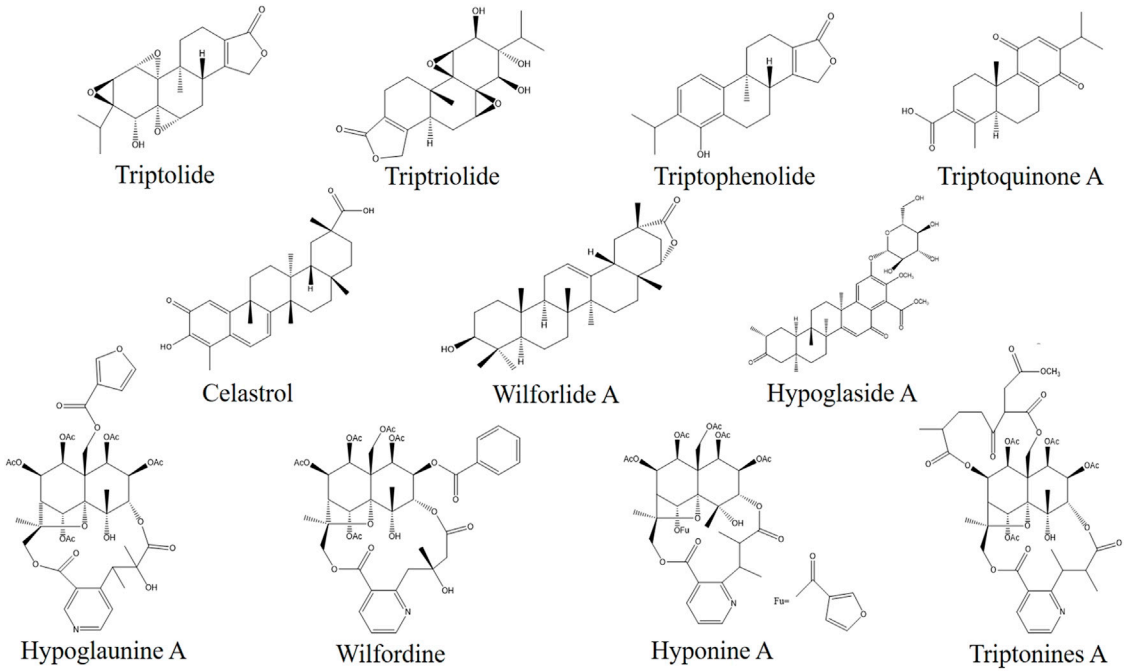

FIGURE 3 | Chemical structures of the existing potential quality control markers in THH.

these, 8 compounds were identified in 1992, including tripteroquinone, triptolide A, triptolide B, tripterygidine, triptolide, 1-epicatechin and β-sitosterol (Zhang and Zhang, 1992). They also reported that three diterpenoid compounds, namely, triptoditerpenic acid, tritoditerpenic acid B and hypodiolide A, were obtained from the chloroform extracts of THH in the same year. In addition, other components, such as wilforgine and daucosterol, have been isolated from THH (Ding, 1991).

Sesquiterpenoids

Sesquiterpenes be isolated from THH mostly combine with pyridine to form alkaloids. At present, only two sesquiterpenoid monomeric compounds have been isolated from THH. In 2000, a sesquiterpene compound was isolated from the methanol extract of the root bark of THH. The molecular formula was $C_{31}H_{36}O_7$, and the structural formula was 1β-benzoyl-8α-cinnamoyl-4α, 5α-dihydroxy dihydroagarofuran (Fujita et al., 2000). In 2014, a sesquiterpene compound was isolated from the 95% ethanol extract of the root bark of THH. The molecular formula was $C_{31}H_{36}O_8$ and the structural formula was: 1α-acetoxy-6β, 9β-dibenzoyloxy-4β-hydroxy-dihydroagarofuran. These compounds exhibited weak cytotoxicity against HeLa cells with an IC_{50} value of 30.2 μM (Liu Z.-Z. et al., 2014). Dihydro-β-agarofuran sesquiterpenes from THH are substrates of P-gp and potential modulators of MDR. These compounds exhibit no cytotoxicity in HepG2 and HepG2/Adr cells. Moreover, these compounds restored the sensitivity of HepG2/Adr cells to Dox and increased the accumulation of intracellular Dox (Yang et al., 2019).

Diterpenoids

Diterpenoids are the most important components in THH, and triptolide exhibits the most remarkable activity. Regarding the structural types of diterpenoids, epoxy-type diterpenoids, randolactone-type diterpenoids, fulfolterpenoid diterpenoids, kaurane-type diterpenoids and abietane-type diterpenoids are primarily observed in THH.

One ranolactone-type diterpenoid, triptonolide, and two ranolterpene-type diterpenoids triptobenzene A and triptobenzene J were isolated from the methanol extract of THH (Duan et al., 1997). In addition, the following diterpenoids were isolated from the methanol extract of THH rhizomes in 2000: two ranolactone-type diterpenoids, triptobenzene K and triptophenolide; two fulfolterpenoid diterpenoids, triptobenzene D and triptobenzene L; and one abietane-type diterpenoid, quinone 21 (Fujita et al., 2000). In 2007, three fulfolterpenoid diterpenoids (triptobenzene H, triptonediol, and triptonoterpene) and three abietane-type diterpenoids (triptoquinone A, triptoquinone B, and triptoquinone H) were isolated from 95% ethanol extracts of THH (Zhang et al., 2007). In 2011, a new fulfolterpenoid diterpenoid named triptonoterpene methyl ether was isolated from a 95% ethanol extract of the root bark of THH (Liu et al., 2011). A randolactone-type diterpenoid, 11-O-β-D-glucopyranosyl neotriptophenolide was isolated from a 95% ethanol extract of THH (Li X, 2006). Four new diterpenoids, 2α, 16α-hydroxy-ent-kauran-19,20-olide, isopimara-8 (14), 15-diene-11β, 19-diol, isopimara-8 (14),15-diene-12α, 19-diol, and 3-oxo-14,15-dihydroxyabieta-8,11,13-trien-19-ol were isolated from THH. Three new terpenoid compounds, epoxyionone A,

TABLE 1 | Diterpenoids isolated from *Tripterygium hypoglaucum*.

Serial number	Compound	Molecular formula	Plant part	References
1	Hypolide	$C_{20}H_{24}O_3$	Root	Wu and Sun (1979)
2	Triptonoterpenol	$C_{21}H_{30}O_4$	Root	Zhang et al. (1992b)
3	Hypoglic acid	$C_{20}H_{26}O_4$	Root	Zhang et al. (1992b)
4	Triptonoterpene methyl ether	$C_{21}H_{30}O_3$	Root	Zhang et al. (1992b)
5	Hypodiolide A	$C_{24}H_{36}O_3$	Root	Zhang and Zhang (1992)
6	Triptoditerpenic acid B	$C_{21}H_{28}O_3$	Root	Zhang and Zhang (1992)
7	Triptonoditerpenic acid	$C_{21}H_{28}O_4$	Root	Zhang and Zhang (1992)
8	Triptoquinone H	$C_{20}H_{26}O_3$	Root	Ding (1991)
9	Triptobenzene L	$C_{22}H_{34}O_3$	Root	Ding (1991)
10	Triptolide	$C_{20}H_{24}O_6$	Root	Duan et al. (1997)
11	Triptonolide	$C_{20}H_{22}O_4$	Root	Duan et al. (1997)
12	Triptobenzene A	$C_{20}H_{28}O_3$	Root	Duan et al. (1997)
13	Triptobenzene J	$C_{20}H_{30}O_3$	Root	Duan et al. (1997)
14	Triptobenzene K	$C_{20}H_{22}O_5$	Root	Duan et al. (1997)
15	Neotriptophenolide	$C_{21}H_{26}O_4$	Root	Duan et al. (1997)
16	2α,16α-Hydroxy-ent-kauran-19,20-olide	$C_{20}H_{30}O_4$	Stem	Li et al. (2015b)
17	Isopimara-8 (14), 15-diene-11β,19-diol	$C_{20}H_{32}O_2$	Stem	Li et al. (2015b)
18	Isopimara-8 (14),15-diene-12α,19-diol	$C_{20}H_{32}O_2$	Stem	Li et al. (2015b)
19	3-Oxo-14,15-dihydroxyabieta-8,11,13-trien-19-ol	$C_{20}H_{28}O_4$	Stem	Li et al. (2015b)
20	Triptobenzene W	$C_{21}H_{30}O_3$	Root	Zheng et al. (2020)
21	Epoxyionone A	$C_{19}H_{28}O_6$	Root	Zheng et al. (2020)
22	Loliolide A	$C_{17}H_{24}O_6$	Root	Zheng et al. (2020)
23	Hypoglicin A	$C_{20}H_{30}O_4$	Stem	Chen et al. (2018b)
24	Hypoglicin B	$C_{20}H_{24}O_3$	Stem	Chen et al. (2018b)
25	Hypoglicin C	$C_{19}H_{20}O_3$	Stem	Chen et al. (2018b)
26	Hypoglicin D	$C_{20}H_{26}O_5$	Stem	Chen et al. (2018b)
27	Hypoglicin E	$C_{20}H_{28}O_2$	Stem	Chen et al. (2018b)
28	Hypoglicin F	$C_{20}H_{28}O_2$	Stem	Chen et al. (2018b)
29	Hypoglicin G	$C_{20}H_{28}O_2$	Stem	Chen et al. (2018b)
30	Hypoglicin H	$C_{20}H_{26}O_3$	Stem	Chen et al. (2018b)
31	Hypoglicin I	$C_{20}H_{26}O_3$	Stem	Chen et al. (2018b)
32	Hypoglicin J	$C_{20}H_{26}O_3$	Stem	Chen et al. (2018b)
33	Hypoglicin K	$C_{20}H_{22}O_6$	Stem	Chen et al. (2018b)
34	Hypoglicin L	$C_{20}H_{22}O_6$	Stem	Chen et al. (2018b)
35	Hypoglicin M	$C_{19}H_{20}O_4$	Stem	Chen et al. (2018b)
36	19-*O*-β-D-Glucopyranosyl-labda-8 (17),14-dien-13-ol	$C_{26}H_{44}O_7$	Aerial parts	Zhao et al. (2018)

triptobenzene W and loliolide A, were isolated from the 95% EtOH extract of the twigs of THH (Zheng et al., 2020). A new diterpenoid, 19-O-β-D-glucopyranosyl-labda-8 (17), 14-dien-13-ol was isolated from the aerial parts of THH (Zhao et al., 2018) (**Table 1**).

The majority of diterpenoids exhibit strong immunosuppressive and anti-inflammatory activities. The inhibitory activity towards LPS-induced NO production of these terpenoids was evaluated in microglial BV-2 cells, and all of the compounds showed inhibitory effects (Zhao et al., 2014). Triptolide is a typical representative abietane terpenoid in THH, that has been reported to have diverse pharmacological effects such as anti-inflammatory, antiproliferative, proapoptotic, immunosuppression, and tumour inhibition effects, and this compound exhibits great efficacy in the treatment of rheumatoid arthritis, asthma, and Shin disease (Shamon et al., 1997; Li J. et al., 2012; Chen S.-R. et al., 2018).

Triterpenoids

Triterpenoids are also one of the main components of THH. The triterpenoids found in THH are mainly pentacyclic triterpenoids, and three types are predominantly noted, including oleanane-type, ursane-type and friedelane-type. Such pentacyclic triterpenoids are active ingredients in the treatment of autoimmune diseases.

One new triterpenoid named 6α-hydroxy triptoline, was isolated from the 95% ethanol extract of THH roots (Song et al., 2021). One friedelane-type triterpenoid (2,3-dihydroxy-6-oxo-D:A-froedo-24 nor-1,3,5 (10), 7-oleanatetraen-29-oic acid) and other types of triterpenoids, including 23-nor-oxopristimerol and hypoglaside A, were isolated from the 95% ethanol extract of THH roots (Li X, 2006). Two oleanane-type triterpenoids, wilforlide A and 3-oxo-oleanoic acid were isolated from the chloroform emulsification layer of THH roots (Wang et al., 2011). One oleanane-type triterpenoid, triptotriterpenic acid A was isolated from 95% ethanol extract of the rhizomes of THH (Ding, 1991). The following triterpenoids were isolated from the methanol extract of THH rhizomes: four oleanane-type triterpenoids, including triptocallic acid D, triptocallic acid C, 3-epikatonic acid, oleanoic acid 3-*O*-acetate; two friedelane-type triterpenoids, 29-hydroxyfriedelan-3-one and polpunonic acid; one ursane-type triterpenoid, 3β-acetoxy-urs-12-ene-28-oic acid; and other types of triterpenoids, such as triptohypol D,

TABLE 2 | Triterpenoids isolated from *Tripterygium hypoglaucum.*

Serial number	Compound	Molecular formula	Plant part	References
37	Celastrol	$C_{29}H_{38}O_5$	Root	Duan et al. (1997)
38	Wilforic acid A	$C_{29}H_{42}O_4$	Root	Duan et al. (1997)
39	Wilforol B	$C_{29}H_{42}O_4$	Root	Duan et al. (1997)
40	Wilforic acid C	$C_{30}H_{48}O_4$	Root	Duan et al. (1997)
41	Celastolide	$C_{30}H_{46}O_5$	Root	Duan et al. (1997)
42	Hypodiol	$C_{30}H_{50}O_2$	Root	Duan et al. (1997)
43	Salaspermic acid	$C_{32}H_{52}O_4$	Root	Duan et al. (1997)
44	Cangoronine	$C_{30}H_{44}O_5$	Root	Duan et al. (1997)
45	Popanonic acid	$C_{30}H_{48}O_3$	Root	Duan et al. (1997)
46	Demthylzeylasteral	$C_{30}H_{38}O_6$	Root	Duan et al. (1997)
47	Mesembryanthemoidigenic acid	$C_{32}H_{52}O_3$	Root	Duan et al. (1997)
48	3-Hydroxy-D: A friedoolean-3-en-2-on-29-oic-acid	$C_{30}H_{46}O_4$	Root	Duan et al. (1997)
49	Triptohypol A	$C_{30}H_{40}O_6$	Root	Duan et al. (1997)
50	Triptohypol B	$C_{30}H_{40}O_5$	Root	Duan et al. (1997)
51	Triptohypol C	$C_{29}H_{39}O_4$	Root	Duan et al. (1997)
52	Triptohypol D	$C_{32}H_{54}O_2$	Root	Fujita et al. (2000)
53	Triptohypol E	$C_{31}H_{52}O_2$	Root	Fujita et al. (2000)
54	Triptohypol F	$C_{31}H_{52}O_2$	Root	Fujita et al. (2000)
55	Regelin	$C_{31}H_{48}O_4$	Root	Zhang et al. (1992a)
56	hypoglaulide	$C_{30}H_{44}O_3$	Root	Zhang et al., (1992a)
57	3-Oxofriedelan-29-oic acid methyl ester	$C_{32}H_{52}O_3$	Root	Yi and Yang (1993)
58	3β,22α-Dihydroxy-Δ^{12}-ursen-30-oic acid methyl ester	$C_{30}H_{48}O_4$	Root	Yi and Yang (1993)
59	3β,22α-Dihydroxy-Δ^{12}-oleanen-29-oic acid methyl ester	$C_{30}H_{50}O$	Root	Yi and Yang (1993)
60	Friedelin	$C_{30}H_{50}O$	Root bark	Liu et al. (2011)
61	3-Oxo-olean-9 (11),12-diene	$C_{30}H_{46}O$	Root bark	Liu et al. (2011)
62	Canophyllal	$C_{30}H_{48}O_2$	Root bark	Liu et al. (2011)
63	6α-Hydroxy triptocslline	$C_{28}H_{42}O_5$	Root	Song et al. (2021)

triptohypol E, triptohypol F, and hypodiol (Fujita et al., 2000). The following triterpenoids were isolated from the methanol extract of THH roots: one oleanane-type triterpenoid, mesembryanthemoidigenic acid; ten friedelane-type triterpenoids, celastolide, triptoethylol A, wilforic acid A, triptohypol B, triptohypol C, wilforol A, wilforol B, demethylzeylasteral, wilforic acid C, and cangoronine; and other types of triterpenoids, including salaspermic acid and 23-nor-6-oxo-demethyl pristimerol (Duan et al., 1997). Three oleanane-type triterpenoids, including 3-acetoxy oleanolic acid, glut-5-en-3β, 28-diol, and 3-oxo-olean-Δ9(11), 12-diene and two friedelane-type triterpenoids, canophyllal and friedelin were isolated from 95% ethanol extracts of the root bark of THH (Liu et al., 2011) (**Table 2**). Celastrol, the first triterpenoid ingredient isolated from the genus *Tripterygium*, is classified as a friedelane-type triterpenoid. Its toxicity is much lower than that of triptolide. Celastrol has significant anticancer effects and relieves insulin resistance. Thus, celastrol has attracted considerable attention in recent years (Petronelli et al., 2009; Yang et al., 2014).

Alkaloids

Alkaloids are one of the strongest bioactive ingredients found in the THH extract. The alkaloids obtained from THH exhibit pyridine alkaloid structures formed by condensation of dihydroagarofuran-type sesquiterpenes with different pyridinic acids. Studies have shown that alkaloids found in THH from traditional Chinese medicine exhibit antitumour activity in animals.

In 1997, seven alkaloids were isolated from the methanol extract of THH roots: euonine, hyponine A, hyponine B, hyponine C, cangorinine E-I, regelidine, and 3-pyridinecarboxylic acid (Duan et al., 1997). Then, six alkaloids were isolated from the methanol extract of THH roots in 1998: hypoglaunine A, hypoglaunine B, hypoglaunine C, hypoglaunine D, euonymine, and wilforine (Duan and Takaishi, 1998). Two new alkaloids, wilfordine and wilformine were isolated from the ethanol extract of THH roots in 1999 (Li et al., 1999). Moreover, hyponines D, hyponines E, hyponines F, neoeunoymine and forestine were isolated from the methanol extract of THH roots (Duan and Takaishi, 1999). In 2000, six alkaloids were isolated from the methanol extract of THH roots: triptonines A, triptonines B, wilfordinines A, wilfordinines B, wilfordinines C and peritassine A (Duan et al., 2000). In 2012, two sesquiterpene pyridine alkaloids, hypoglaunine E and hypoglaunine F were isolated from 95% ethanol extracts of THH roots (Li X, 2006). Then, four alkaloids, 2-*O*-deacetyleuonine, wilfortrine, triptolide (wilforgine) and tripfordine C were isolated from a 95% ethanol extract of the root bark of THH (Xie et al., 2012). In 2014, four new alkaloid compounds were isolated from the methanol extract of the rhizome of THH: 9α-cinnamoyloxy-1β-furoyloxy-4-hydroxy-6α-nicotinoyloxy-β-dihydroagarofuran, 1β,9α-dibenzoyloxy-4-hydroxy-6α-nicotinoyloxy-β-dihydroagarofuran, 1β-benzoyloxy-9α-cinnamoyloxy-4-hydroxy-6α-nicotinoyloxy-β-dihydroagarofuran and 1β-acetoxy-9α-benzoyloxy-4-hydroxy-6α-nicotinoyloxy-β-dihydroagarofuran (Chen X.-L. et al., 2018) (**Table 3**). The alkaloid fraction in THH is characterized by high

TABLE 3 | Alkaloids isolated from *Tripterygium hypoglaucum*.

Serial number	Compound	Molecular formula	Plant part	References
64	Hypoglaunine A	$C_{41}H_{47}O_{20}N$	Root	Duan and Takaishi (1998)
65	Hypoglaunine B	$C_{41}H_{47}O_{20}N$	Root	Duan and Takaishi (1998)
66	Hypoglaunine C	$C_{43}H_{49}O_{19}N$	Root	Duan and Takaishi (1998)
67	Hypoglaunine D	$C_{41}H_{47}O_{19}N$	Root	Duan and Takaishi (1998)
68	Wilforine	$C_{43}H_{49}O_{18}N$	Root	Duan and Takaishi (1998)
69	Wilforgine	$C_{41}H_{47}O_{19}N$	Root	Duan and Takaishi (1998)
70	Wilfordine	$C_{43}H_{49}O_{19}N$	Root	Duan and Takaishi (1998)
71	Wilfortrine	$C_{41}H_{47}O_{20}N$	Root	Duan and Takaishi (1998)
72	Euonymine	$C_{38}H_{47}O_{18}N$	Root	Duan and Takaishi (1998)
73	Wilformine	$C_{41}H_{48}O_{18}N_2$	Root	Duan and Takaishi (1998)
74	Wilfornine	$C_{41}H_{47}O_{19}N$	Root	Duan and Takaishi (1998)
75	Hyponine A	$C_{41}H_{47}O_{19}N$	Root	Duan et al. (1997)
76	Hyponine B	$C_{41}H_{47}O_{19}N$	Root	Duan et al. (1997)
77	Hyponine C	$C_{43}H_{49}O_{18}N$	Root	Duan et al. (1997)
78	Cangorinine E-I	$C_{43}H_{49}O_{18}N$	Root	Duan et al. (1997)
79	Evonine	$C_{36}H_{43}O_{17}N$	Root	Duan et al. (1997)
80	3-Pyridinecarboxylic acid	$C_{29}H_{34}O_7N$	Root	Duan et al. (1997)
81	Hyponine D	$C_{47}H_{50}O_{18}N_2$	Root	Duan and Takaishi, (1999)
82	Hyponine E	$C_{45}H_{48}O_{19}N_2$	Root	Duan and Takaishi (1999)
83	Hyponine F	$C_{41}H_{47}O_{19}N$	Root	Duan and Takaishi (1999)
84	Neoeunoymine	$C_{36}H_{45}O_{17}N$	Root	Duan and Takaishi (1999)
85	Forrestine	$C_{43}H_{49}O_{18}N$	Root	Duan and Takaishi (1999)
86	Peritassine A	$C_{39}H_{49}O_{18}N$	Root	Duan et al. (2000)
87	Regelidine	$C_{35}H_{37}O_8N$	Root	Duan et al. (2000)
88	Triptonine A	$C_{45}H_{55}O_{21}N$	Root	Duan et al. (2000)
89	Triptonine B	$C_{45}H_{55}O_{22}N$	Root	Duan et al. (2000)
90	Wilfordinine A	$C_{36}H_{55}O_{12}N$	Root	Duan et al. (2000)
91	Wilfordinine B	$C_{38}H_{60}O_{13}N$	Root	Duan et al. (2000)
92	Wilfordinine C	$C_{43}H_{60}O_{14}N$	Root	Duan et al. (2000)
93	2-*O*-Deacetyleuonine	$C_{36}H_{45}O_{17}N$	Root bark	Xie et al. (2012)
94	Tripfordine C	$C_{36}H_{45}O_{17}N$	Root bark	Xie et al. (2012)
95	1-α-Benzoyloxy-6*β*-nicotinoyloxy-9*β*-acetoxy-4*β*-hydroxy-dihydro-*β*-agarofuran	$C_{30}H_{35}O_8N$	Root	Duan et al. (2000)

activity and low toxicity; thus, these compounds exhibit potential value in new drug development research.

Flavonoids

In 1998, two flavonoids were isolated from industrial alcohol extracts of THH stems: (+) -catechin and *L*-epicatechin (Zhang and Zhang, 1998). In 2012, two flavonoids were isolated from a 95% ethanol extract of the root bark of THH: 4′-O-(−)methyl-epigallocatechin and (2R, 3R)-3,5,7,3′,5′-pentahydroxyflavan (Xie et al., 2012).

Lignans

Three new lignans, 9′-O-benzoyl-lariciresinol, 9′-O-benzoyl-5′-methoxylariciresinol, and 9′-O-cinnamoyl-lariciresinol, were isolated from the 95% EtOH extract of the twigs of THH. Moreover, only 9′-O-benzoyl-lariciresinol showed weak cytotoxicity against HepG2/Adr cells, with an IC50 value of 30.1 μM *in vitro* (Liu et al., 2011). Recently, syringaresinol, a common bisepoxylignan, was isolated from the 95% EtOH extract of THH (Song et al., 2021).

Other Compounds

In addition to diterpenes, triterpenes and alkaloids, other compounds, such as steroids, fatty acids, tannins and glycosides, have been identified in THH. Although terpenoids are the main pharmacodynamic components of THH, other components also play synergistic roles.

In 1991, two steroidal compounds, β-sitosterol and daucosterol, and one other compound, fumaric acid, were isolated from the 95% ethanol extract of the rhizome of THH (Ding L, 1991). Two steroidal compounds, ergosta-4,6,8 (14), 22-tetraen-3-one and stigmast-4-en-3-one and three other compounds, *p*-hydroxyl benzoic acid, 3,4-dihydroxy-benzoic acid, and 3-meth-oxy-4-hydroxy-benzoic acid were isolated from the ether extract of THH stems (Zhang and Zhang, 1998). In 2011, three fatty acid compounds, palmitic acid, stearic acid and tricosanoic acid were isolated from the 95% ethanol extract of the root bark of THH (Liu et al., 2011). Two tannins were isolated from industrial alcohol extracts of THH stems: procyanidin B-3 and procyanidin B-4 (Zhang and Zhang, 1998). In 2011, a tannin compound, procyanidin B-2, was isolated from the chloroform emulsified layer of THH roots (Petronelli et al., 2009). Two glycosides, 3,4-dimethoxyphenyl-β-D-glucopyranoside and 3,4,5-trimethoxyphenyl-β-D-glucopyranoside were isolated from the 95% ethanol extract of the root bark of THH (Xie et al., 2012).

Pharmacological Activity

THH is a traditional medicine that exhibits various pharmacological activities, including anti-inflammation,

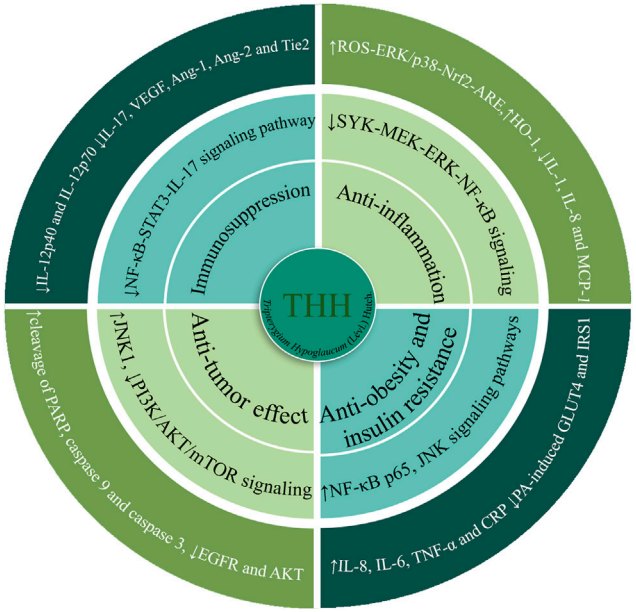

FIGURE 4 | The main signalling pathways and molecular targets of the pharmacologically active components in THH.

immunosuppression, antitumour, obesity and insulin resistance, antifertility, and antiviral effects. These pharmacological effects are mainly related to the alkaloids and terpenoids of THH. These components are expected to exhibit therapeutic significance in various human immunological diseases, such as rheumatoid arthritis, systemic lupus erythematosus, acute infectious hepatitis, chronic nephritis, leukemia, neurodermatitis, and chronic urticaria (Guo et al., 2018; Tang et al., 2020). Here, we summarized several classical pharmacological activities of THH (**Figure 4**, **Tables 4** and **5**).

Anti-Inflammatory Effects

Corticosteroids are widely used as anti-inflammatory drugs, but some serious side effects often occur after long-term use. THH has been shown to be effective in a variety of inflammatory diseases. Under the condition of reasonable control of THH toxicity, THH is expected to play a huge potential as an alternative drug. The therapeutic mechanisms of THH include the inhibition of inflammation and capillary permeability as well as the reduction of infiltrates. Moreover, Hypoglicins B-G and J-M, which are isolated from the stem of THH, inhibited NO production with IC_{50} values ranging from 0.72 to 36.91 μM. Moreover, hypoglicin D and hypoglicin L significantly inhibit the mRNA expression of iNOS at doses of 12.5 and 3.13 μM, respectively (Chen X.-L. et al., 2018). Importantly, the compounds found in THH do not act through the pituitary-adrenal cortex system, so there will be no "rebound" phenomenon after stopping the drug, and even long-term use will not damage the immune system (Zhong et al., 2011), but the toxic accumulation of long-term use must be considered carefully.

The mechanism by which triptolide attenuates the inflammatory pathology of Crohn's disease (CD) involves increasing IL-10 levels and Foxp3+ Tregs in the mucosa and decreasing TNF-α levels in the mucosa (Li G. et al., 2014). The pathogenesis of CD is mainly mediated by the TLR/NF-κB signalling pathway. Triptolide upregulates TLR2 and TLR4 in a CD model in IL-10-null (IL-10 −/−) mice by inhibiting TLR/NF-κB signalling pathways *in vivo*. TLR activation also promotes angiogenesis mediated by exogenous and endogenous ligands in different inflammatory settings (Harmey et al., 2002; Oda and Kitano, 2006; Yu et al., 2010). A key regulator of the signal transduction cascade activated by NF-κB and activator protein-1 is TAK1. However, for TAK1 to be fully activated, it must be induced by a protein activator, TAK1 binding protein (TAB1). Triptolide interferes with the formation of the TAK1TAB1 complex and thus inhibits the activity of TAK1 kinase. The interaction region between triptolide and TAB1 involves the amino acid residues between TAB1373 and 502. Triptolide inhibits MAPK pathway activation in macrophages upon binding to TAB1 (Lu et al., 2014). In addition, triptolide inhibited the activation of microglia and the secretion of inflammatory factors in BV2 cells by upregulating miR96 (Huang et al., 2019). Moreover, the γ-butyrolactone and C-14 β-hydroxyl portions of the triptolide molecules are important components responsible for the compound's anti-inflammatory characteristics and cytotoxicity (Wong et al., 2008). Triptolide suppresses the production of IL-6, IL-8, TNF-α, and IL-1β in human bronchial epithelial cells, and inhibits staphylococcal exotoxin-stimulated T-cell proliferation. Triptolide induces the expression of monocyte chemotactic protein (MCP)-1, IFN-g, TNF, IL-6, IL-1β, macrophage inflammatory protein (MIP)-1β and MIP-1α in peripheral blood mononuclear cells (PBMCs) (Krakauer et al., 2005).

Angiogenesis is a fundamental event in inflammation. Infection leads to inflammation and growth factors released by leukocytes promote angiogenesis. Many chronic inflammatory diseases, such as retinopathy, rheumatoid arthritis, Crohn's disease, atherosclerosis, diabetes and cancer are closely associated with angiogenesis (McDonald, 2001; Rodríguez-Martínez et al., 2006; Costa et al., 2007). Celastrol achieves its effect mainly by regulating various inflammatory mediators (Li et al., 2008; Li G. et al., 2013), inhibiting the production of proinflammatory cytokines (IL-6, IL-2, IFN-γ, TNF, IL-1β, IL-8, etc.,) and proinflammatory enzymes (COX-1, prostaglandin E2, NOS, COX-2 and iNOS, etc.,) through inhibition of NF-κB (Lee et al., 2006; Jung et al., 2007; Kim et al., 2009; Seo et al., 2010, 2011; Cascão et al., 2012; Joshi et al., 2016). In addition, celastrol interferes with the migration, proliferation, and activation of inflammatory cells (Yu et al., 2015). Celastrol suppresses the LPS-induced IκB kinase (IKK)/NF-κB pathway, significantly downregulates TLR4 expression and inhibits VEGF secretion in LP-1 cells. These results suggest that celastrol inhibits LPS-induced angiogenesis by inhibiting TLR4-triggered NF-κB activation (Zhang R. et al., 2019).

Immunosuppression

THH was used to treat various autoimmune diseases based on its action against metabolic pathways, and three metabolites, urocanate, L-glutamate and alanine played very important roles (Guo et al., 2018). The key molecular mechanism of

THH against RA is related to inhibition of the inflammatory response through inactivation of the TNF and NF-κB signalling pathways (Jiang et al., 2020b). THH reduces the expression of related inflammatory cytokines in joint tissue and serum, and the mechanism of THH in the treatment of collagen II-induced arthritis (CIA) mice involves inhibition of the NF-κB-STAT3-IL-17 pathway (Zhou et al., 2020). The formation and function of osteoclasts in CIA mice are directly inhibited by celastrol. Celastrol significantly reduced joint bone damage, and inhibited arthritis, and this activity is associated with the expression of the osteoclast marker serum tartrate-resistant acid phosphatase (TRAP) 5b and osteoclastic genes (Ctr, Mmp-9, Ctsk and Trap) and transcription factors (NFATc1 c-Jun and c-Fos). Moreover, celastrol suppressed bone resorption activity and the formation of TRAP + multinucleate cells in a dose-dependent manner (Gan et al., 2015).

Triptolide and celastrol are the most important active ingredients of THH against RA, and their molecular mechanisms involve many targets, such as inhibition of inflammation, inhibition of angiogenesis, immunosuppression, protection of cartilage, and induction of apoptosis (Kong et al., 2013; Fan et al., 2016, 2018; Wang S. et al., 2018). The expression of chemokines and inflammatory cytokines in RA synovioblasts is inhibited by celastrol through modulation of the OPG/RANKL axis, thereby inhibiting RA inflammation and bone erosion (Feng et al., 2013). Celastrol also decreases the expression of NF-κB, nitrite levels, and TLR2 expression and $CD3^+$ Tlymphocyte counts as assessed by immunohistochemistry; and the cytokine phenotype changes significantly from Th1 to Th2, with increased IL-10 and decreased TNF-α levels. (Abdin and Hasby, 2014). In addition, the binding of LPS to the TLR4/MD2 complex and TLR4 activation were also inhibited by celastrol in a thiol-dependent manner (Lee et al., 2015). Celastrol suppresses the expression of phosph-stat3, c-Myc, Glut1, mTOR, HK2, HIF-1a and Akt in Th17 cells; upregulates the expression of phosph-stat5 in iTreg cells, and upregulates the expression of CPT1A and AMPKα in iTreg cells to promote fatty acid-oxidation (Zhang et al., 2018).

Triptolide inhibits the production of proMMP-1 and -3 induced by IL-1α in human synovial fibroblasts and reduces the messenger RNA levels of IL-1α. In contrast, the IL-1alpha-induced gene expression and production of TIMP-1 and-2 were further augmented by triptolide in synovial cells. Triptolide also inhibited the IL-1alpha-induced production of PGE2 by selectively suppressing the gene expression and production of COX-2, but not COX-1 (Lin et al., 2001) (Hu et al., 2004). Triptolide inhibits the production of IL-2, IL-4, and IFN-γ and the activation of $CD4^+$ and $CD8^+$ T cells in peripheral blood in RA patients, thus exerting an immunosuppressive effect (Ren et al., 2010) (Nong et al., 2019). Professional antigen presenting cells (APCs), such as dendritic cells (DCs), are another target for the immunosuppressive activity of triptolide (Chen et al., 2005). DCs are induced by high concentrations (20 ng/ml) of triptolide via caspase3 activation and sequential p38 MAP kinase phosphorylation (Liu et al., 2004; Liu et al., 2006). Triptolide also inhibits T cells and DC-mediated chemoattraction of neutrophils by reducing NF-κB activation and STAT3 phosphorylation (Zhu et al., 2005). Triptolide prevents the differentiation of immature monocyte-derived DCs (MoDCs), mainly by reducing the ability of MoDCs to stimulate lymphocyte proliferation in allogeneic mixed lymphocyte reactions (MLRs) and downregulating CD86, CD40, CD1a, CD80, and HLA-DR expression. Triptolide reduces IFN-γ-induced expression of CD80 and CD86 in DCs and THP-1 cells (Liu et al., 2005). Recently, it was found that triptolide inhibited IL-12/IL-23 expression in APCs *via* CCAAT/enhancer-binding protein α (Liu et al., 2008).

Antitumour Effects

The alkaloid fraction of THH induced apoptosis at lower concentrations and significantly inhibited tumour growth *in vitro* and *in vivo*. In addition, the apoptotic effect of total alkaloids in tumour cells is potentially mediated through both the extrinsic death receptor pathway and the intrinsic mitochondrial pathway. The total alkaloids fraction of THH induced apoptosis by inhibiting Bcl-xL, Bcl-2, and XIAP and activating PARP and caspase-3, thereby inhibiting the growth of colon cancer cells in a dose-dependent manner *in vitro* (Jiang et al., 2014). Triptonide potently inhibited vasculogenic mimicry mediated by pancreatic cancer cells (Han et al., 2018). In addition, triptonide inhibited the epithelial-mesenchymal transition of gastric cancer-associated fibroblasts (GCAFs) by correcting abnormalities in microRNA expression and subsequently eliminating the epithelial-mesenchymal transition in gastric cancer cells (Wang et al., 2017). Moreover, a cytotoxicity of triptolide and 2-epilactone was observed, particularly in A549, DU145, KB, KBvin, and MDA-MB-231 human tumour cell lines, with IC_{50} values of 0.0012–0.1306 μM *in vitro* (Li X.-L. et al., 2015). The mRNA and protein levels of CD147 and MMPs were reduced, and triptonide also inhibited the expression of caveolin-1, thereby inhibiting the invasion and migration of prostate cancer cells (Yuan et al., 2020).

Pancreatic cancer (PC) cell lines SNU-213, Capan-1 and Capan-2 exhibit different sensitivities to triptolide with IC_{50} values of 0.01, 0.02, and 0.0096 μM, respectively. Phosphorylation of Chk2 was more significant in SNU-213 sensitive to triptolide but, not in SNU-410 insensitive to triptolide, suggesting that the effect of triptolide on different PC cell lines may be related to gene expression (Liu L. et al., 2014; Kim et al., 2018). In addition, triptolide inhibited CRC growth through induction of cleavage and perinuclear translocation of 14-3-3e protein (Liu et al., 2012). Furthermore, triptolide dose-dependently inhibited the proliferation of human scale-cell carcinoma SAS, human cervical carcinoma SKG-II, and human fibrosarcoma HT-1080 cells, an important target molecule in the antitumour effect of triptolide is phosphatidylinositol 3-kinase (PI3K). The reduction of PI3K activity leads to inhibition of tumour cell proliferation, which subsequently leads to enhanced JNK1 phosphorylation through Akt and/or PKC-independent pathways (Miyata et al., 2005).

As an important compound of THH, celastrol exhibits tumour-inhibiting effects in a variety of tumour models, and its antitumour mechanisms have been demonstrated in various

cancers *in vitro* (Li Z. et al., 2012; Lee et al., 2012). There are two main pathways by which celastrol induces apoptosis in cancer cell lines, namely, through the activation of intrinsic pathways (mitochondrial pathways) and extrinsic apoptotic pathways (death receptor pathways) (Mou et al., 2011). Apoptosis, paraptosis, and necrosis are modes of cell death induced by celastrol (Chen et al., 2011); the expression of ERα target genes was suppressed, celastrol also decreased the expression of ERα at the protein and mRNA levels in MCF7 and T47D human breast cancer cells, leading to cell cycle arrest and inhibition of breast cancer cell growth (Jang et al., 2011). Moreover, celastrol induced apoptosis by cleaving the PARP proteins, caspase-3, caspase-9, and caspase-8; increasing FasL and Fas expression; decreasing mitochondrial membrane potential; upregulating proapoptotic Bax expression; and downregulating antiapoptotic Bcl-2 (Mou et al., 2011). In addition, the activation of caspase-3 also involved in the induces myeloma cell apoptosis, and celastrol inhibited NF-κB migration into the nucleus, and treatment of the human myeloma cell line U266 with celastrol induces cell cycle at the G1 phase followed by apoptosis (Tozawa et al., 2011). Moreover, celastrol suppressed the migration of AGS and YCC-2 cells in gastric tumour induced G1 arrest in cell-cycle populations, and increased phosphorylated AMPK levels after reducing the levels of AKT, mTOR, and S6K phosphorylation (Lee et al., 2014). In addition, celastrol can significantly reduce tumour nodules in the liver by decreasing DEN-induced MDM2 levels and activating the p53 pathway, thereby improving DEN-induced liver pathology (Chang et al., 2016). It also induces apoptosis in Bel-7402 cells by the mitochondrial apoptosis pathway (Li P.-P. et al., 2015). Moreover, it upregulates both the mRNA and protein levels of DR4 and DR5, which induce TRAIL/Apo-2 L-mediated apoptosis in cancer cells (Zhu et al., 2010; Lin et al., 2017).

In the last 10 years, given the increased accessibility of oncometabolites, the idea that cancer is a metabolic disorder has gradually emerged (Collins et al., 2017). In reports on colon cancer, many oncometabolites such as histidine, isoleucine, phenylalanine, tyrosine, threonine, glutamate, and pyruvate have been found to be closely related to cancer-associated metabolic pathways (Mishra and Ambs, 2015; Wishart et al., 2016). Treatment with triptolide may help to restore normal metabolite levels in these pathways. Triptolide increases isoleucine, plasma proline, methionine, 2-hydroxyisovalerate (2-HIV), low-density lipoprotein/very low-density lipoprotein (LDL/VLDL) and 2-hydroxyisobutyrate (2-HIB) levels, and reduces plasma pyruvate, 3-hydroxybutyric acid, and glutamine levels. Because 2-HIV, LDL/VLDL and 2-HIB are related to branched-chain amino acid metabolism, lactate and pyruvate metabolism, and cholesterol metabolism, respectively, the antitumour mechanism of triptolide may rely on correcting alterations in serine/glycine/methionine biosynthesis, branched-chain amino acid metabolism, and ketone body metabolism (Li et al., 2019).

Anti-Obesity and Insulin Resistance Effects

Celastrol targets mitochondria, inhibits the inflammatory response and prevents obesity induced by specific diets in mice. Celastrol-administered mice at 100 μg/kg decrease food consumption and body weight *via* a leptin-dependent mechanism (Kyriakou et al., 2018). In 2015, the Umut Ozcan team at Harvard Medical School screened more than 1,000 compounds that reduce ER stress (insulin resistance is a major risk factor for obesity, and ER stress is an important cause of resistance) and found that celastrol can be used as a weight-loss drug. Obese mice treated with celastrol lost 45% of their body weight, and improved insulin sensitivity was observed. Thus, celastrol may exhibit potential therapeutic effects in various diseases, such as type 2 diabetes and fatty liver (Liu et al., 2015). The weight-loss mechanism of celastrol is mediated through interleukin 1 receptor 1 (IL1R1) (Feng X. et al., 2019), it has no effects on weight loss, diabetes or fatty liver in mice if IL1R1 is absent.

Mitochondrial dysfunction and inflammation tend to occur at high levels of fatty acid saturation in insulin-sensitive tissues (Hernández-Aguilera et al., 2013). Celastrol reduces the body weight of obese mice induced by a high leptin diet by up to 45%, increases insulin sensitivity and energy expenditure, and inhibits food intake. Celastrol is a leptin sensitizer, but it has shown effects in leptin-deficient (ob/ob) and leptin receptor-deficient (db/db) mouse models (Liu et al., 2015). Palmitate-mediated insulin resistance could be blocked by celastrol by improving metabolic activity associated with mitochondrial function (Bakar et al., 2014). In addition, celastrol significantly reduced mitochondrial superoxide production; enhanced the cellular fatty acid oxidation rate, intracellular ATP content and mitochondrial membrane potential citrate synthase activity; increased levels of tricarboxylic acid cycle intermediates; improved mitochondrial function; increased mitochondrial DNA content, and inhibited oxidative DNA damage, and glucose uptake activity and enhances the expression of AMPK and GLUT4 proteins were also improved by decreasing the activation of NF-κB and PKCθ (Abu Bakar et al., 2015; Abu Bakar and Tan, 2017).

Importantly, Celastrol showed an anti-IR activity, it was achieved by reducing miR-223, and celastrol re-upregulated the downregulation of miR-150 and miR-223 in HepG2 cells (human hepatocellular carcinoma cell lines) through the GLUT4 pathway, reversing palmitate-induced insulin resistance (Zhang X. et al., 2019). Celastrol treatment significantly enhanced tyrosine-612 phosphorylation of IRS-1 protein and decreased serine-307 in C3A hepatocytes, protecting cells from mitochondrial dysfunction and insulin resistance (Abu Bakar et al., 2017). Meanwhile, it also reduces serum malondialdehyde (MDA) and reactive oxygen species levels, increases antioxidant enzyme activities, reduces oxidative stress and improves lipid metabolism in a dose-dependent manner by alleviating oxidative damage, and inhibiting NADPH oxidase activity by improving ABCA1 expression. These actions inhibit increases in body weight and alleviate cardiovascular damage (Abu Bakar and Tan, 2017). The inhibition of negative regulators protein tyrosine phosphatase (PTP) 1B (PTP1B) and T cell PTP (TCPTP) in the hypothalamic arcuate nucleus (ARC) were also invovled in body weight reduction. The reversible non-competitive binding of celastrol to these proteins is mediated by an allosteric pocket close to the active site (Kyriakou et al., 2018).

Antifertility Effect

In 1986, reversible anti-fertility effects of TwHF extract in male rats were discovered, sparking global interest. The researchers performed bioassay-guided subfractionation of material extracted from plants and isolated a series of six male antifertility diterpene epoxides: triptolide, tripdiolide, triptolidenol, tripchlorolide, 16 hydroxytriptolide and T7/19 (Zhen et al., 1995). At the ED95 dosage levels, metamorphic spermatids as well as testicular and epididymal sperm excoriation and late spermatid basic nuclear protein turnover were inhibited. In addition, treatment with these compounds delayed spermatogenesis and sperm head-to-tail separation as well as microtubule, microfilament, and membrane damage (Zhen et al., 1995). Triptolide inhibited GATA4-mediated glycolysis by suppressing Sp1-dependent PFKP expression in SCs and induced testicular toxicity (Zhang et al., 2021b).

Oral THH reversibly induces infertility in men without significant side effects and does not affect libido or potency (Qian et al., 1988). Triptolide induced complete infertility in adult rats with minimal adverse effect on the testis, and it mainly targets epididymal sperm. No effects on testicular and accessory organ weights, tubular lumen volume and total number of Leydig cells, spermatogonia, tubule diameter, and number of Sertoli cells, pachytene (P) spermatocytes, and preleptotene (PL) were observed. Triptolide significantly reduced tubule volume and the number of round spermatids, making it an attractive lead agent as a post-testicular male contraceptive (Lue et al., 1998). We look forward to more reliable data to verify this possibility.

Antiviral Effects

Many natural products have been found to effectively inhibit unique enzymes and proteins that are essential for the viral life cycle (Vlietinck and Vanden Berghe, 1991; Baker et al., 1995). Hypoglaunine A, hypoglaunine B, triptonine A, and hyponine E have represented compounds extracted and purified from THH roots with anti-HIV viral effects (Cheng et al., 2002). The total alkaloid extracts of THH showed potent anti-HSV-1 activity and low cytotoxicity in Vero cells (Tao et al., 2007). Triptobenzene J and quinone 21 have anti-A/PR/8/34 (H1N1) influenza virus (oseltamivir-resistance) activity with EC_{50} values of 38.6 ± 10.7 μM, and 22.9 ± 6.4 μM, respectively. Quinone 21 exhibited anti-A/Hong Kong/8/68 (H3N2) influenza virus (sensitivity) activity with an EC_{50} value of 21.6 ± 0.6 Mm (Wang et al., 2020).

Moreover, triptolide treatment inhibited macrophage infiltration; inhibited the overproduction of malondialdehyde (MDA), IL-6, TNF-α and IL-1β in reperfusion myocardial tissue; and upregulated the activities of glutathione peroxidase (GPx), antioxidant superoxide dismutase (SOD), and glutathione (GSH), and the nuclear accumulation of Nrf2 and the activity of its downstream target haem oxygenase-1 (HO-1) were enhanced in ischaemic myocardial tissues (Yu et al., 2016). Additionally, triptolide significantly inhibited Epstein-Barr virus (EBV)-positive cell-induced tumour proliferation *in vivo*, and low-dose triptolide significantly decreased the half-life of EBV nuclear antigen 1, obviously reduced the expression of EBV nuclear antigen 1, and enhanced triptolide-induced apoptosis by activating the proteasome-ubiquitin pathway (Zhou et al., 2018). However, mitochondrial dysfunction, apoptotic damage, oxidative stress, and histopathological changes in the heart were noted in normal BALB/C mice treated with 1.2 mg/kg triptolide (Zhou et al., 2014). Therefore, the determination of safe dose is the key to the clinical application of triptolide.

Celastrol also showed effective activities in antivirals, it upregulated ERK1/2 phosphorylation, inhibited reactive oxygen species (ROS) generation, and improved endothelial cell activity and Ang II-mediated HUVEC injury by activating Nrf2 (Li M. et al., 2017); and the nuclear levels of Nrf2, nuclear levels of HSF-1 and cardiac GSH levels are also increased (Wang et al., 2015). Moreover, celastrol also inhibited hepatitis C virus (HCV) replication in both the HCV subgenomic and HCVcc infection systems with EC_{50} values of 0.37 ± 0.022 mM and 0.43 ± 0.019 mM, respectively, the NS3/4A protease activity is inhibited, and further enhancing anti-HCV activity, thereby blocking HCV replication. Interestingly, celastrol showed synergistic effects in combination with the NS5B inhibitors sofosbuvir and interferon-α and the NS5A inhibitor daclatasvir targeting the JNK/Nrf2/HO-1 axis with celastrol presents a promising strategy against HCV infection that could serve as a potential supplement to block HCV replication (Tseng et al., 2017). This result suggests that synergistic use could be a topic in future research.

Other Effects

THH promoted the expression of Foxp3, increased the level of CD4+/CD25 + T cells, decreased the occurrence of aGVHD, and prolonged survival time in mice by regulating cytokine secretion (Li Z. Y. et al., 2013). Syringaresinol has significant protective activity against excitatory damage induced by sodium glutamate in SH-SY5Y neurons, and the mechanism potentially involves antioxidative stress and repair of mitochondrial function and DNA damage to significantly reduce sodium glutamate-induced neuronal apoptosis (Yan et al., 2019).

In recent years, researchers have gradually started to pay attention to the effect of triptolide in AD. Regarding the neuroinflammatory pathology of the AD brain, triptolides potentially exert neuroprotective effects on synapses by partially inhibiting the mechanism of the Aβ-induced immunoinflammatory response, which may effectively slow the neurodegenerative process of AD (Nie et al., 2012). Triptolide inhibits Aβ-induced elevation of IL-1β and TNF-α levels in cultured rat microglia (Jiao et al., 2008). Triptolide promotes synaptophysin expression in hippocampal neurons in an AD cell model (Nie et al., 2012). Tripchlorolide, a novel analogue of triptolide, protected neuronal cells by blocking microglial inflammatory responses to oligomeric Abeta (1–42), inhibited nuclear translocation of nuclear NF-κB without affecting I-κBα phosphorylation and inhibited Aβ-induced JNK phosphorylation, but not ERK or p38 MAPK (Pan et al., 2009). Triptolide also inhibits the upregulated expression of prostaglandin E2 and IL-1β in lymphocytes and AD cell models (Tao et al., 1998; Li et al., 2011).

TABLE 4 | Pharmacological effects of different compounds isolated from *Tripterygium hypoglaucum in vitro* studies.

Pharmacological activity	Compound	Experimental design	Molecular targets/mode of action	References
Anti-inflammatory	THH alkaloids	10 μg of total RNA isolated from THH-treated (40 μg/ml, 8 h) and untreated HL-60 cells	↑genes related to the NF-κB signalling pathway and cell apoptosis (such as NFKBIB, PRG1 and B2M),↓c-myc binding protein and apoptosis-related cysteine proteases caspase-3 and caspase-8	Zhuang et al. (2004)
—	Triptolide	Corneal fibroblasts absence or presence of IL-1 (10 ng/ml), with or without triptolide (30 nM) or dexamethasone (100 nM)	↓IL-1, IL-8 and MCP-1	Lu et al. (2005)
—	Triptolide	Raw 264.7 cells stimulated with LPS (50 ng/ml) in the presence or absence of triptolide (30 μM) for 24 h	↓DNA binding activity of NF-κB, ↓NO production, ↓phosphorylation of c-Jun NH(2)-terminal kinase (JNK)	Kim et al. (2004)
—	Triptolide	Microglia were pre-treated with PBS, triptolide (10, 30, or 50 μM), with or without Bay11-7,082 for 30 min before LPS treatment (10 ng/ml, 24 h)	↓p38-NF-kappaB-COX-2-PGE(2) and JNK-PGE(2)	Gong et al. (2008)
—	Triptolide	TP-mmc (15 μM) with or without TP (1.2, 12, 15, 30 μM) was added to RAW 264.7 cells (middle panel: bar, 50 μM) for 2 h	↓TAK1-TAB1 complex kinase activity	Lu et al. (2014)
—	Celastrol	fibroblast-like synoviocytes (FLSs) were treated with celastrol (0.05, 0.1, 0.2, 0.4 and 0.8 mM) for 24 h	↓MMP-9 promoter activity, ↓TLR4/MyD88/NF-κB pathway, ↓ FLS migration and invasion	Li et al. (2013a)
—	Celastrol	HaCaT cells were incubated with celastrol (0, 0.1, 0.5, 1 μg/ml) for 1h, and stimulated with IFN-c (100 U/ml) for 4 h (for RNA) or 12 h (for protein)	↓IFN-γ-induced ICAM-1 mRNA and protein expression	Seo et al. (2010)
—	Celastrol	HaCaT cells were pretreated with DPI (10 μM), NAC (20 mM) or EUK 134 (50 μM) for 1 h, and then incubated with celastrol (1 μg/ml) for 6 h (for RNA) or 12 h (for protein)	↑ROS-ERK/p38-Nrf2-ARE, ↑HO-1	Seo et al. (2011)
—	Celastrol	RAW264.7 cells were treated with 0–1 μM of celastrol for 24 h	↓ nitric oxide synthase and cyclooxygenase-2, ↓ MPO activity, ↓IL-6 and TNF-α	Kim et al. (2009)
—	Celastrol	BV-2 cells were pre-treated with various concentrations of celastrol (1, 10 and 100 nM) for 30 min prior to stimulation with LPS (10 ng/ml) for 6 h (for TNF-α) and 24 h (for IL-1β)	↓expression of mRNAs of iNOS and cytokines; ↓NO, IL-1β and TNF-α; ↓ERK1/2 phosphorylation and NF-κB activation	Jung et al. (2007)
—	Celastrol	Jurkat T cells were preincubated for 30 min with celastrol (0, 0.3, 1 μg/ml) and followed by the stimulation with of TNF-a (20 ng/ml) or PMA (50 ng/ml) for 90 min	↓IKK activity and IKKβ activity, ↓Bfl-1/A1 expression	Lee et al. (2006)
—	Celastrol	Neutrophils were pre-incubated with different doses of celastrol (0.5–20 μM) or vehicle only at RT for 45 min	↓neutrophil oxidative burst and NET formation, ↓SYK-MEK-ERK-NF-κB signalling cascade	Yu et al. (2015)
Immuno-suppression	Triptolide	Monocytes were cultured for 5 days in the presence of various concentrations (1–20 ng/ml) of triptolide and Dex (10–8–10–6 M)	↓CD1a, CD40, CD80, CD86 and HLA-DR expression; ↑CD14 expression	Zhu et al. (2005)
—	Triptolide	LPS (100 ng/ml)-stimulated U937 cells were treated with or without triptolide (12.5 nM)	↓TREM-1 and DNAX-associated protein (DAP)12, ↓activation of JAK2 and STAT3, ↓TNF-α, IL-1β and IL-6	Fan et al. (2016)
—	Celastrol	Bone marrow-derived macrophages were pre-treated with celastrol (0.1, 0.5 and 1 μM) for 1 h and treated with Alexa Fluor 594 conjugated with LPS (1.5 μg/sample) for 30 min	↓TNF-α, IL-6, IL-12, and IL-1β, ↓LPS binding to the TLR4/MD2 complex	Lee et al. (2015)
—	Celastrol	Purified CD4+CD25− T cells were treated in the presence or absence (control) of Celastrol (200 nM)	↓mTOR, HIF-1α, c-Myc and Akt expression in Th17 cells, ↑FAO of lipids by upregulating CPT1A and AMPKα expression in iTreg cells	Zhang et al. (2018)
—	Triptolide	Confluent synovial cells were treated with recombinant human interleukin-1α (IL-1α; 1 ng/ml), dexamethasone (Dex), and/or triptolide (2.8–140 nM) at the indicated concentrations	↓IL-1α-induced production of proMMP- 1 and -3, ↑IL-1alpha-induced gene expression and production of TIMP-1 and -2	Lin et al. (2001)
—	Triptolide	Human monocytes were cultured for 7 days with G4 medium in the presence of TPT (D2-7, 0.5–10 nM) or medium alone	↓production of IL-12 p70	Chen et al. (2005)
—	Triptolide	C57BL/6 mouse bone marrow cells were cultured with mGM-CSF and mIL-4, and triptolide (0, 1, 5, 10, 20, 50, and 100 ng/ml) added on day 3 of culture (Trip-DC)	↑activation of p38, ↓activation of caspase 3	Liu et al. (2004)
	Triptolide			Liu et al. (2008)

(Continued on following page)

TABLE 4 | (*Continued*) Pharmacological effects of different compounds isolated from *Tripterygium hypoglaucum in vitro* studies.

Pharmacological activity	Compound	Experimental design	Molecular targets/mode of action	References
		THP-1 cells were differentiated into macrophage-like cells upon exposure to Me_2SO, and then cultured with IFN-gamma (500 kU/L) and lipopolysaccharide (LPS) (1 mg/L) with or without triptolide (2.5–0.625 μg/L)	↓CD80 and CD86 expression on IFN-gamma- (500 kU/L) and LPS- (1 mg/L) activated THP-1 cells, ↓IL-12p40 and IL-12p70	
Antitumour effect	Total alkaloids	JB6 Cl41 cells were suspended containing 10% FBS, 10 μM TPA with or without THHta (1.25–10 μg/ml)	↑activation of caspase-3 and PARP, ↓Bcl-2, Bcl-xL and XIAP	Jiang et al. (2014)
—	Triptonide	treatment of the pancreatic cancer cell lines Patu8988 and Panc1 with triptonide at the doses of 0–20 nM	↓VE-cadherin and CXCL2 genes	Han et al. (2018)
—	Triptolide	PC-3 and DU145 cells were incubated with triptolide (0, 25, 50 nM) for 24 h	↓RNA polymerase activity, ↓CDC25A, and MYC and Src oncogenes	Yuan et al. (2020)
—	Triptolide	Malignant (BxPc-3, MIA-PaCa2 and AsPC-1) and nonmalignant (pancreatic ductal cells and MSC) cells grown under normoxia or hypoxia in the presence or absence of triptolide (20 nM)	↓epithelial-mesenchymal transition (EMT) and CSC features	Liu et al. (2014a)
—	Triptolide	Urothelial cancer cells were treated with CDDP at the concentration corresponding to IC25 (30 mM) with or without 1 h pretreatment of 30 nM triptolide for 12 h	↓CDDP-induced p53 transcriptional activity	Matsui et al. (2008)
—	Triptolide	The JNK1 knockdown cells were treated with triptolide (14–56 nM) for 15 h	↓phosphatidylinositol 3-kinase (PI3K) activity, ↑c-Jun NH(2)-terminal kinase 1 (JNK1)	Miyata et al. (2005)
—	Celastrol	SO-Rb 50 cells were treated with celastrol nanoparticles (0–54.4 μg/ml) and the same dosage of PEG-b-PCL micelles without celastrol for 48 h	↓elevated levels of ALT, AST, ALP and AFP; ↓anti-apoptotic Bcl-2 and Bcl-xl; induced the expression of pro-apoptotic Bax, cytochrome C, PARP and caspases	Li et al. (2012b)
—	Celastrol	A549 cells were treated with celastrol (0–8 μM) at the indicated concentration for 24, 48, and 72 h	↑expression of pro-apoptotic Bax, ↓anti-apoptotic Bcl-2 and Akt phosphorylation	Mou et al. (2011)
—	Celastrol	H1650 cells were collected for apoptosis analysis at 24 h after the treatment of celastrol (0.5, 1, 2, 4 μM)	↓EGFR and AKT	Fan et al. (2014)
—	Celastrol	H1299 cells were treated with or without 4 μM celastrol in the absence or presence of 50 μM Z-VAD for 24 h	↑cleavage of PARP, caspase 9 and caspase 3	Chen et al. (2011)
—	Celastrol	Human myeloma cell line U266 cells were treated with celastrol (0.25 and 0.5 μM) for the indicated times (0–48 h)	↑caspase-3 and NF-κB pathways	Tozawa et al. (2011)
Anti-obesity and insulin resistance	Celastrol	Fully differentiated 3T3-L1 adipocytes were incubated with different doses of oligomycin (5, 10, 20 and 30 μg/ml) and celastrol (5, 10, 20 and 30 μM) in DMSO for 48 h	↓oxidative DNA damage, protein carbonylation and lipid peroxidation	Bakar et al. (2014)
—	Celastrol	C3A human hepatocytes were exposed to various concentration (10–50 nM) of celastrol in the serum-free media for 48 h	↓PA-induced GLUT4 and IRS1	Abu Bakar et al. (2017)
—	Celastrol	Myoblasts were treated with different concentrations (10, 20, 30, 40, 50 and 60 nM) of celastrol were prepared and mixed with 0.1% (v/v) DMSO. The vehicle consisted of an equal amount of DMSO was used as a control	↑NF-κB p65, c-Jun NH(2)-terminal kinase (JNK) signalling pathways,↑IL-8, IL-6, TNF-α and CRP	Abu Bakar and Tan (2017)
Antiviral effect	Triptolide	HONE1/Akata, HK1/Akata, C666–1, and CNE1 cells were placed in 35 mm culture dishes (500 cells/dish) and cultured in standard medium with DMSO control (0.01%) or triptolide (1, 2, or 5 nM) for 2 weeks	↓ratio of Bax/Bcl-2, ↑activated caspase-3 and Nrf2	Zhou et al. (2018)
—	Triptolide	Human umbilical vascular endothelial cells (HUVEC) were trested with or without brusatol (40 nmol/L)/celastrol (50 nmol/L)/AngII(400 nmol/L) for 24 h	↑caspase-9-dependent apoptosis	Li et al. (2017a)
—	Celastrol	The transfected ava5 cells were treated with celastrol (0, 0.2,0.3,0.4,0.5 μM) for 3 days	↓iNOS, TNF-α, and NF-κB phospho-p65 expression, ↑nuclear levels of Nrf2 and HSF-1	Tseng et al. (2017)
Other effects	Triptolide	The model microglial group was treated with Aβ1–40 (20 μg/ml). The low-dose triptolide microglial group was treated with Aβ1–40 (20 μg/ml) and triptolide (5 μg/ml). The high-dose triptolide microglial group	↑IL-10, ↓IL-4	Nie et al. (2012)

(Continued on following page)

TABLE 4 | (*Continued*) Pharmacological effects of different compounds isolated from *Tripterygium hypoglaucum in vitro* studies.

Pharmacological activity	Compound	Experimental design	Molecular targets/mode of action	References
		was treated with Aβ1–40 (20 μg/ml) and triptolide (25 μg/ml)		
—	Triptolide	RASF, HM, HFF, or U937 cells were incubated overnight with or without LPS (2 μg/ml) in the presence or absence of the indicated concentrations of T2 (1,2,4 μg/ml), triptolide (1,2,4 ng/ml), DEX (0.1,1,10 μM), or Indo (0.01,0.1 μg/ml)	↓protein levels of inducible nitric oxide synthase (iNOS) and cyclooxygenase-2 (COX-2)	Tao et al. (1998)

Pharmacokinetics

Over the years, scholars have conducted numerous studies on the pharmacodynamics of THH, but studies on the pharmacokinetics of THH compounds in animals, especially those administered intravenously, are limited. Antitumour pharmacodynamics and toxicological studies of triptolide are closely related to the pharmacokinetics and tissue distribution of triptolide, which are important components of new drug evaluation studies. Oral triptolide is rapidly and highly absorbed and distributed in the liver, heart, spleen, lung and kidney. Biotransformation of triptolide in rats includes hydroxylation, sulfate, glucuronide, N-acetylcysteine (NAC) and glutathione (GSH) conjugation and combinations of these pathways. Less than 4% of triptolide was recovered from the faces, bile and urine within 24 h. After repeating the dosage, triptolide was eliminated quickly without accumulation *in vivo*. As a substrate for P-glycoprotein (P-gp) and CYP3A4, triptolide could have clinically significant pharmacokinetic interactions with protein substrates/inhibitors (Song et al., 2019). After injection of three doses (100 μg/kg, 200 μg/kg, 300 μg/kg) of triptolide into the veins of rats, the corresponding $t_{1/2\alpha}$ of each subsequent dose group was: 0.033, 0.021, and 0.026 h, respectively, and the t1/2β values were 0.753, 0.630, and 0.574 h. The AUC was related to the dose, and the compartmental model was a two-compartment model. After intravenous injection of an effective dose (200 μg/kg) of triptolide in rats, rapid and extensive tissue distribution was observed. After 5 min of administration, the highest triptolide levels were noted in lung tissue followed by liver, kidney, heart, brain, spleen, small intestine, gonads, skeletal muscle, and stomach. Fifteen min after administration, the drug concentrations in all tissues decreased with higher concentrations in the lung, kidney, heart and liver. The distribution order is similar to that noted 5 min after administration. One hour after administration, the drug concentration in each tissue decreased significantly, and high drug concentration was still maintained in the liver and small intestine (Shao et al., 2007).

Celastrol exhibited linearity in the concentration range of 0.05–5 μg/ml with R^2 of 0.999. Rats were intravenously (IV) administered 1 mg/kg of pure CL in PEG 300 solution, which resulted in a maximum concentration (C_{max}) value of 0.17 μg/ml at 5 min following administration (Onyeabor et al., 2019). After oral administration of *Tripterygium* wilfordii tablets (1 tablet/kg) to beagle dogs, the changes in plasma celastrol levels followed a one-compartment model (w = 1/cc), and the main pharmacokinetic parameters were C_{max} (35.64 ± 9.540) μg·L^{-1}, Tmax (2.62 ± 0.69) h, T1/2 (2.93 ± 0.29) h, CL (0.308 ± 0.056) Lkg −1·h−1, AUC0–12 (131.16 ± 31.94) μg·L·h−1, and AUC0–∞ (142.83 ± 37.57) μg·L·h−1 (Zhang et al., 2016). Glycyrrhizin significantly decreased the plasma concentration (from 64.36 ng/ml to 38.42 ng/ml) and AUC0-t (from 705.39 to 403.43 μg h/L) of celastrol in rats, and increased the efflux ratio of celastrol (4.02 vs. 6.51). Moreover, glycyrrhizin significantly increased the intrinsic clearance rate of celastrol from 20.3 ± 3.37 to 38.8 ± 4.18 μL/min/mg proteins (Yan et al., 2017).

Toxicity

The targets of toxicity were closely associated with the p53 signalling pathway, PI3K-Akt signalling pathway and other pathways. Although THH has multiple phytochemical activities and pharmacological effects, it is also limited in clinical application given its toxicities associated with multiple targets (Xu et al., 2004). Although triptolide has attracted remarkable efficacy against diseases, the safety margin of the triptolide medication dose is very narrow, and the accumulation of triptolide in the body can lead to severe hepatotoxicity, renal toxicity, and reproductive toxicity (Sun et al., 2013; Kong et al., 2015; Ma et al., 2015). Therefore, dose control is particularly important in clinical treatment (**Figure 5**).

Triptolide mainly causes abnormal purine and pyrimidine metabolites in the body through the metabolism of hypoxanthine, allantoic acid, ADA and other proteins. The mechanism of triptolide-induced liver injury exhibits an important relationship with oxidative stress, and excessive ROS and anionic peroxide production, depletion, autophagy, hepatocyte apoptosis, and suppression of antioxidant enzyme activities are the main causes of oxidative stress (Fu et al., 2011; Xi et al., 2017; Wei et al., 2019). Thus, hepatocyte injury is mainly caused by high levels of ROS and reactive nitrogen species (RNS) inhibiting sodium, ATPase, and calcium pump activities in the cell membrane, resulting in decreased mitochondrial membrane potential (MMP) and release of the apoptosis factor caspase-3 (Li J. et al., 2014; Wang Y. et al., 2018; Tabeshpour et al., 2018; Feng Z. et al., 2019; Yuan et al., 2019b; Hasnat et al., 2019). Moreover, triptolide significantly increased serum ALP, AST, and ALT levels; increased hepatic MDA, IL-6, TNF-α, IFN-γ, and IL-1β levels, induced nuclear translocation of NF-κB; and decreased

TABLE 5 | Pharmacological effects of different compounds isolated from *Tripterygium hypoglaucum in vivo* studies.

Pharmacological activity	Compound	Experimental design	Molecular targets/mode of action	Duration of treatment	Route of administration	References
Anti-inflammation	Triptolide	Triptolide (8, 16 and 32 mg/(kg day); n = 16, respectively), dexamethasone (1 mg/(kg every 2 days); *n* = 16) or vehicle (*n* = 20)	↓metalloproteinases-13 and -3,↓COX-2 and PGE(2),↓IL-1β, TNF-α and IL-6,↑metalloproteinases-1 and -2	Daily for a period of 21 days	Oral administration	Lin et al. (2007)
—	Triptolide	Triptolide (0.1 mg/kg/d) dissolved in 5% dimethyl sulfoxide was intraperitoneally injected into the SCI rats	↑miR-96, ↓Iba-1 and IKKβ/NF-κB-related proteins, ↓IL-1β and TNF-α	Continued for successive 10 days	Intraperitoneal injection	Huang et al. (2019)
—	Tripterine	tripterine (5, 10 and 20 mg kg−1 day−1), or prednisone (10 mg kg−1 day−1); 0.5% CMC solution as vehicle-treated group	↓ IgG and delayed-type hypersensitivity (DTH), ↓IL-1β and TNF-α	5 days	Intragastrical administration	Li et al. (2008)
—	Celastrol	1 μg/g Celastrol or 2 μg/g digoxin were administrated at adjuvant-induced arthritis (AIA) rats	↓IL-1β and TNF	After 4 days (early treatment group) and after 11 days (late treatment group) of disease induction	Intraperitoneal injection	Cascão et al. (2012)
—	Celastrol	Saline (20 μL) containing 4 μg of sPLA2IIA with celastrol (1, 10, 30 μM and 100 μM)/vehicle was injected into the intra-plantar surface of the right hind footpad of mice	↓sPLA2IIA, 5-LOX and COX-2 enzymes	After 45 min, mice were anaesthetized with pentobarbitone (30 mg/kg, i.p.) and euthanized	Injected into the intra-plantar surface of the right hind footpad of mice	Joshi et al. (2016)
—	Celastrol	Hepa1-6 single-cell suspension cells (2 × 107/ml) were injected subcutaneously at a volume of 0.1 ml in the right flank of each mouse	↓AKT pathway and VEGF autocrine system	21 days of administration	Intraperitoneal injection	Zhang et al. (2019a)
Immuno-suppression	THH	C57BL/6 mice were used to model CIA mice received THH 420 mg/kg/day or the same amount of normal saline (NS)	↓TNF-α, IFN-γ, and IL-17A mRNA and protein levels; ↓NF-κB-STAT3-IL-17 pathway	20 days	Intragastrical administration	Zhou et al. (2020)
—	Celastrol	CIA mice were treated intraperitoneally (IP) with celastrol in phosphate buffered saline (PBS; 3 mg/kg) or PBS alone	↓osteoclastic genes (Trap, Ctsk, Ctr, Mmp-9) and transcription factors (c-Fos, c-Jun and NFATc1), ↓NF-κB and MAPK phosphorylation	15 days	Intraperitoneal injection	Gan et al. (2015)
—	Triptolide	CIA rats were treated with triptolide (11–45 μg/kg/day) starting on the day 1 after first immunization	↓Matrigel-induced cell adhesion of HFLS-RA and HUVEC, ↓TNF-α, IL-17, VEGF, VEGFR, Ang-1, Ang-2 and Tie2, ↓IL1-β-induced ERK phosphorylation and p38 and JNK protein levels	Daily for a period of 28 days from day 1 to day 28 of first immunization	Oral administration intragastrically using syringe feeding	Kong et al. (2013)
—	Celastrol	Female Sprague Dawley rats were treated by celastrol (1 mg/kg/day, i.p.)	↑IL-10, ↓TNF-α, ↓immunohistochemical expression of TLR2 and CD3+ T-lymphocytic count	32 days	Intraperitoneal injection	Abdin and Hasby, (2014)
Antitumour effect	Celastrol	C57BL/6N mice were treated with 1 mg/kg of celastrol, 3 mg/kg of celastrol, or a vehicle control. Celastrol was dissolved in vehicle (10% DMSO, 70% Cremophor/ethanol (3:1), and 20% PBS)	↑ROS-mediated caspase-dependent apoptosis; ↓PI3K/AKT/mTOR signalling	20 days	Oral gavage every 2 days	Lee et al. (2012)

(Continued on following page)

TABLE 5 | (*Continued*) Pharmacological effects of different compounds isolated from *Tripterygium hypoglaucum in vivo* studies.

Pharmacological activity	Compound	Experimental design	Molecular targets/mode of action	Duration of treatment	Route of administration	References
Anti-obesity and insulin resistance	Celastrol	C57BL/6 mice were allowed to recover for 2 weeks postsurgery before receiving intraperitoneal vehicle or celastrol (100 μg/kg) at 6 pm each day	↓TC, TG, LDL-c and Apo B in plasma,↓NADPH oxidase activity	10 consecutive days	Intraperitoneal injection	Kyriakou et al. (2018)
—	Celastrol	Sprague–Dawley rats were treated with celastrol (1.0 ml/100 g) or simvastatin (1.0 ml/100 g)	↑protein phosphorylation of insulin signalling cascades with amplified expression of AMPK protein, ↓attenuated NF-κB and PKC θ activation	6 weeks	Intragastrical administration	Wang et al. (2014)
Antiviral effect	Triptolide	Male BALB/C mice were intravenously (i.v.) treated with a single dose of TP (1.2 mg/kg)	↓TNF-α, IL-1β, IL-6 malondialdehyde (MDA) and antioxidative superoxide dismutase (SOD), ↑glutathione (GSH) and glutathione peroxidase (GPx)	24 h	Intravenous injection	Zhou et al. (2014)
Other effects	Celastrol	Celastrol (0.5 and 1.0 mg/kg, i.v.) was administered to anaesthetized rats 2 h before and 30 min after LPS challenge (10 mg/kg, i.v.)	↑Nrf2 activation, ↓Nox2/AT1 receptor expression, ↑phosphorylation of ERK1/2	8 h	Intravenous injection	Wang et al. (2015)

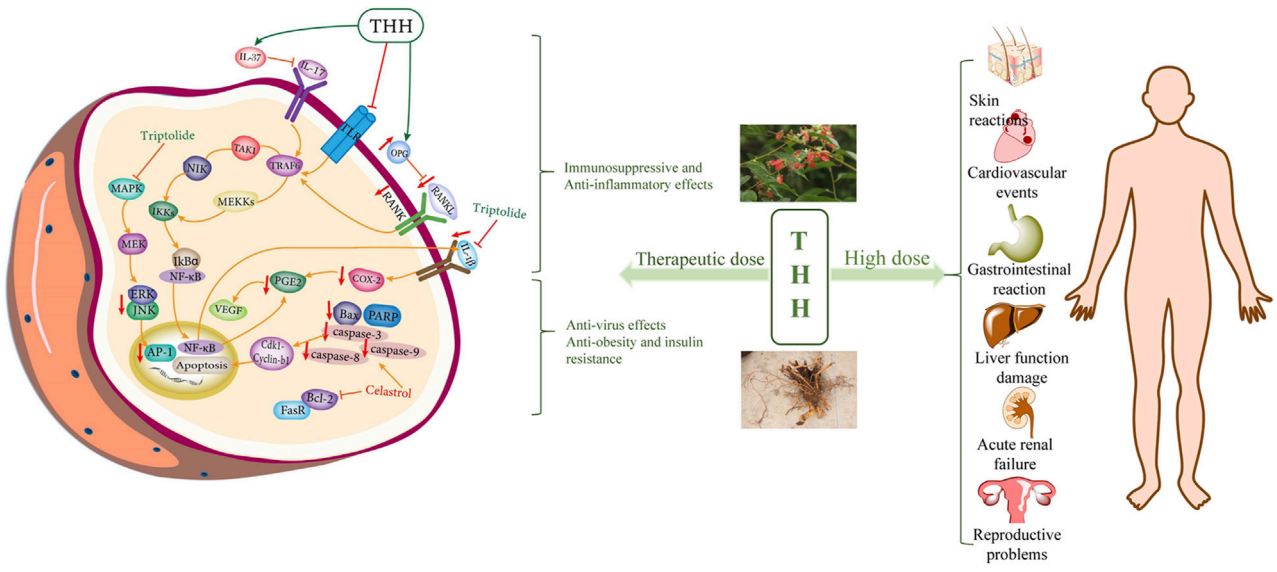

FIGURE 5 | Illustration of the main signalling pathways involved in THH-based therapy and organ toxicities observed at high doses.

hepatic GSH-Px, CAT, and SOD activities (Yang et al., 2017). It also regulates the metabolism of sphingolipids and glycerophospholipids by affecting metabolites and key proteins such as sphingosine, PC, PKC, PAH, LPC, and PLC, which cause disturbances in Ca^{2+} channels and stimulate oxidative stress levels, leading to kidney damage (Xie et al., 2020). Therefore, reducing liver toxicity and nephrotoxicity through chemical modification is an important topic for triptolide to be applied.

Triptolide induced cytotoxicity in L02 cells, caused mitochondrial dysfunction and altered mitochondrial dynamics, mainly characterized by an imbalance in mitochondrial fusion and fission protein mitochondrial

fragmentation. Mitochondrial fragmentation can lead to increasing autophagic flux by triptolide. Changes in mitochondrial dynamics were associated with increasing expression of the Drp1 fission protein. Despite no significant effect on L02 cells, triptolide doses of 12.5, 25 and 50 nM were significantly toxic. Mdivi-1 is a potent mitochondrial fission inhibitor that reverses mitophagy by inhibiting mitochondrial fission and increasing mitophagy *in vitro* and *in vivo* (Hasnat et al., 2019). Treatment of mice with the PPARα agonist fenofibrate alleviated triptolide-induced liver injury, whereas the PPARα antagonist GW6471 increased hepatotoxicity and increased long-chain acylcarnitine through activation of the NOTCH-NRF2 pathway to protect against triptolide-induced liver damage (Hu et al., 2019). The hepatotoxicity of triptolide is closely related to its dose, indicating that the liver is more sensitive to other drugs (CYP450 inhibitors) and their accumulation. Thus, celastrol, which is also a hepatotoxic component of THH and an inhibitor of CYP450, could aggravate triptolide-induced hepatotoxicity, which may explain why the combination of celastrol and triptolide causes more severe liver injury. In summary, celastrol and triptolide damaged primary rat hepatocytes by decreasing cell viability, enhancing cellular stress, decreasing MMP, increasing LDH and ROS levels, and inevitably damaging the cell membrane (Jin C. et al., 2015; Jin et al., 2019).

However, Arctiin exerts antioxidant effects mediated by the Nrf2/ARE pathway and alleviates triptolide-induced hepatotoxicity, and its molecular mechanism may be related to its antioxidative stress ability (Jin J. et al., 2015; Wei et al., 2019). A novel mechanism of triptolide-induced hepatotoxicity is mitochondrial fission associated mitophagy, and triptolide-induced hepatotoxicity can be targeted by mitochondrial fission and mitochondrial autophagy signalling pathways (Hasnat et al., 2019). Specifically, 18β glycyrrhetinic acid (GA) is the main bioactive component of liquorice (*Glycyrrhiza glabra* L.), and low-dose GA (50 mg/kg) effectively reduces triptolide-induced hepatotoxicity in rats through its inflammatory, antioxidative, and antiapoptotic effects (Yang et al., 2017). GA reduced the accumulation of triptolide in HK-2 cells, which were related to P-gp (Li Z. et al., 2017). Pretreatment with GL significantly accelerates the metabolic elimination of triptolide from the body mainly through induction of hepatic CYP3A activity (Tai et al., 2014). Thus, the combination of triptolide with other natural compounds may be an effective measure to control its toxicity and ensure its safety, there still need more further research to investigate its mechanism of combination.

DISCUSSION AND CONCLUSION

Traditional Chinese medicine (TCM) has unique therapeutic advantages in the treatment of a variety of complex diseases and major diseases, such as cholestasis, nonalcoholic fatty liver disease, liver fibrosis, and ischaemic stroke (Jiang et al., 2020a; Hu et al., 2020). The genus *Tripterygium* contains only 3 species, *i.e. Tripterygium wilfordii* Hook. f., *Tripterygium hypoglaucum* (H. Lév.) Hutch. and *Tripterygium regelii* Sprague and Takeda. In the last 10 years, many studies have discussed the plants related to the genus *Tripterygium*. Among them, *Tripterygium wilfordii* Hook. f., as one of the widely reported plants, has occupied almost all the focus of the review of the genus *Tripterygium*. Individual scholars have included the chemical constituents and pharmacological activities of THH in their studies on the genus *Tripterygium* (Lv et al., 2019). In contrast, our study separately investigated the related active components and pharmacological effects of THH, providing more selectivity for the extraction of components from the genus *Tripterygium*. In addition, we updated the recently published experimental studies and supplemented the pharmacokinetic studies of compounds in THH, so as to provide some ideas for the development of new drugs.

In this review, we summarized the various bioactive components of THH, such as sesquiterpenes, diterpenes, triterpenoids, flavonoids, and lignans. In this review, we introduced the structural grouping of 120 secondary metabolites of THH and described the activity data obtained from THH research in the past 2 decades. The compounds isolated from TwHF, including triptolide and tripdiolide, induce male infertility (Wang et al., 2014). Although the prospects of male antifertility drugs have been explored, further safety evaluation results of this drug are needed. Therefore, THH is likely to be a genotoxic agent. Chinese investigators are cautious and suggest that patients should avoid reproduction for 6 months after THH therapy (Liang et al., 2006). In addition, we emphasized the pharmacological effects of triptolide, celastrol and other important bioactive components, and great progress has been made in the identification of the mechanisms associated with these components, such as anti-inflammatory, immunosuppressive, and anti-tumour effects. At 50 nM, triptolide could completely block the LPS-induced PGE2 release. Further, triptolide at 50 or 100 nM in primary microglial cells was not toxic (Jiao et al., 2008). In addition, the animals pretreated with triptolide (100 mg/kg) show significant attenuation of LPS-induced proinflammatory cytokine release in serum, including TNF-a, IL-6, and IL-12, but not IL-1β (Huang et al., 2019). Triptolide could suppress CD80 and CD86 expressions on IFN-γ (500 kU/L) and LPS (1 mg/L)-activated THP-1 cells at 2.5–0.625 μg/L (Liu et al., 2005). Celastrol caused a dose- and time-dependent growth inhibition of A549 cells with an IC_{50} of 2.12 μM at 48 h treatment (Mou et al., 2011). Celastrol at the optimum concentration of 30 nM was able to protect the cells from mitochondrial dysfunction and insulin resistance (Abu Bakar et al., 2017).

At present, the studies *in vitro* and *in vivo* are relatively separate from each other. There is a lack of relevance between experiments *in vitro* and *in vivo* especially in the aspect of dosage. In future studies, more attention should be paid to research to understand whether the concentration used *in vitro* can achieve the same efficacy *in vivo*. In conclusion, some data suggest that triptolide may possess anti-angiogenic effect in RA both *in vivo* and *in vitro* assay systems by downregulating the angiogenic activators and inhibiting the activation of mitogen-activated protein kinase downstream signal pathway (Kong et al., 2013). Triptonide effectively inhibited pancreatic cancer cell-formed capillary-like structures *in vitro* and blood vessels *in vivo*

through suppressing pancreatic cancer cell migration, invasion, and VM via inhibiting expression of tumour VM master gene VE-cadherin and pro-migratory gene chemokine C-X-C motif ligand 2 (CXCL2), mainly via reduction of gene promoter activity (Han et al., 2018). This is particularly crucial for the exploration of anti-tumour effect. However, this promising effect seems less to be displayed *in vivo*. It is to be due to the complex system of the body. Therefore, from the perspective of animals or even humans, we should construct a systematic experiment synchronously carried out the experiment *in vitro* and *in vivo*. Furthermore, the dosage for these studies should confirm the stability of the effect. In addition, researchers have discovered new pharmacological effects of these compounds, including alleviation of AD and insulin resistance as well as anti-obesity, and cardioprotective effects. However, these herbs also have potential multiorgan toxicity that has not been addressed for many years (Wang L. et al., 2018). Pharmacodynamic and toxicological studies of THH are closely related to pharmacokinetics and tissue distribution. Due to the lack of studies on human pharmacokinetics, it is unclear whether the pharmacological effects obtained at the concentrations of compounds used *in vitro* can achieve the same efficacy in humans. Therefore, various toxic reactions might occur in clinical application. Many studies have reported the metabolic processing of toxic active compounds *in vitro* and *in vivo*, aiming to reduce drug toxicity and improve the safety of these agents from a metabolic point of view or using different methods.

Alternatively, many low toxicity active analogues have been developed by drug synthesis researchers from natural active products of the genus *Tripterygium* (Shan et al., 2017; Ning et al., 2018). The Chinese pharmacopoeia indicates that THH patent medicine (Kunming Shanhaitang tablet) is made from extracts of THH dried roots, and this is a legally licenced drug in China. Kunming Shanhaitang tablet is commonly used to treat RA. Inhibition of IL-2 production by human peripheral blood lymphocytes through nuclear inhibition of transcriptional activation of NF-κB, prevention of T cell proliferation, induction of apoptotic death of T lymphocytes, reduction of PGE2 production in human monocytes and rheumatoid arthritis synovial fibroblasts, suppression of complement C3 and the expression of CD40 and B7 in activated human proximal tubular epithelial cells by triptolide indicates a wide range therapeutic target cells of this Chinese herb. Dex is a well-known classical glucocorticoid with potent anti-inflammatory and immunosuppressive effects when gave in pharmacological doses. Though the effect of triptolide is not so strong as Dex in the clinical managements, it shares the properties of Dex such as anti-inflammation and immunosuppression. Here, we demonstrated that DC is a target of triptolide. Due to DC has the unique property to activate native T cells and is required for the induction of a primary response, the suppression of DC function may very efficiently control the specific immune response. One of the mechanisms by which triptolide can suppress the immune response in humans is by inhibiting differentiation, terminal maturation and function of DC. In addition, triptolide abrogates the capacity of mature DCs to secrete IL-12 and also promotes DC apoptosis. These effects result in inhibition of alloreactive T cell activation. Suppression of DC may contribute to the actions of triptolide in the treatment of immune-related diseases and for the prevention of allograft rejection. Adjuvant treatment of facial corticosteroid addiction dermatitis with Kunming Shanhaitang tablet effectively improved symptoms and manifestations within 2 months and was more beneficial than topical drugs alone in significantly improving symptoms in the first 2 weeks. In addition, the effect was comparable to that of antihistamine combined with topical drugs or topical drugs alone (Xue and Wu, 2008). The injection of THH demonstrates a significant inhibitory effect on the production of haemolysin antibodies in mice, and the effect is more obvious with a long period of dosing (Li X, 2006). Tripterygium agents (TAs) extracted from TwHF are a complementary therapy used to treat eczema based on previous experience. However, TA has significant side effects in the treatment of specific eczema, but seems to be effective only in combination with some therapies. Thus, researchers believe that TA cannot be used clinically for eczema in general (Liu et al., 2019). Less toxic preparation of THH could potentially be used as an alternative. In previous separation and extraction experiments, most of the chemical active ingredients of THH were extracted with 95% ethanol, but it was found that column chromatography was replaced by sodium carbonate extraction for removing the acidic compounds and enriching epoxyditerpenoids and alkaloids in the extract. The therapeutic index (IC_{50}/EC_{50}) on murine macrophage Raw 264.7 cells and rat mesangial HBZY-1 cells of the extract prepared by sodium carbonate extraction was significantly higher than that of Tripterygium glycosides (0.8 and 5.2 vs. 0.3 and 2.6), while its cytotoxicity on human liver HL7702 cells was significantly lower (14.5 ± 1.4 vs. 6.8 ± 0.9,). Therefore, *Tripterygium* extract prepared by sodium carbonate extraction may represent a potentially optimal source of medicine with good therapeutic index (Fang et al., 2012). Therefore, many studies have shown that THH is a potential source of various drugs. Here, we consulted the literature and summarized the useful information and evidence. From the current research, it can be seen that a variety of active components of THH show significant efficacy and great potential in many major diseases. Toxicity is the main factor limiting THH in drug development. To date, the research on the mechanism of toxicity caused by THH is not sufficient. A full understanding of the mechanism of toxicity induced by THH is the premise to effectively reduce the toxicity of THH, and it is also the key to the development of THH efficacy. So do other plants of the genus *Tripterygium*. Through continuous in-depth studies of THH and TwHF, our understanding of their structure, pharmacology, toxicology and other aspects will be further advanced, which will provide a solid theoretical basis for their clinical application. In the future, if we focus on preserving the active ingredients and minimizing the toxic components of the preparations, these agents will certainly have broader prospects in various fields.

In conclusion, THH has abundant chemically active components, and some representative components (triptolide, celastrol, etc.,) have been demonstrated to have significant anti-inflammatory, immunosuppressive and anti-tumour effects.

Meanwhile, the toxicity of THH cannot be underestimated. How to effectively control the toxicity of THH and obtain the maximum therapeutic effect is still a problem to be solved. The combination of traditional theory and modern advanced technology will be an important goal for the efficacy and safety of traditional Chinese medicine.

AUTHOR CONTRIBUTIONS

JZ is the major contributor to this manuscript. JZ conducted the analytical part, wrote the first version of the manuscript, FZ, XX, and ZW finalized the manuscript. XX, YJ, and WZ, downloaded the reference and processed the graph and the table in the manuscript. SW, QH, collected the data. XM and XZ (corresponding author) conceived and coordinated the study, and critically evaluated the data. All authors read and approved the final manuscript.

FUNDING

This work was supported by National Natural Science Foundation of China (81874365, 81703725), Sichuan Science and Technology Program (2019YJ0492), Beijing Medical and Health Foundation (YWJKJJHKYJJ-B20645FN), Chengdu University of TCM Found Grant (QNXZ2018025), National Major New Drug Creation Major Science and Technology Projects (2017ZX09101002-002-004), Natural Science Foundation of Chongqing (cstc2017jcyjAX0001, cstc2018jcyjAX0142).

ACKNOWLEDGMENTS

The authors would like to thank the reviewers and also the authors of all references. The reviewer's advice really makes the great improvement of this paper.

REFERENCES

Abdin, A. A., and Hasby, E. A. (2014). Modulatory Effect of Celastrol on Th1/Th2 Cytokines Profile, TLR2 and CD3+ T-Lymphocyte Expression in a Relapsing-Remitting Model of Multiple Sclerosis in Rats. *Eur. J. Pharmacol.* 742, 102–112. doi:10.1016/j.ejphar.2014.09.001

Abu Bakar, M. H., Cheng, K.-K., Sarmidi, M. R., Yaakob, H., and Huri, H. Z. (2015). Celastrol Protects against Antimycin A-Induced Insulin Resistance in Human Skeletal Muscle Cells. *Molecules* 20, 8242–8269. doi:10.3390/molecules20058242

Abu Bakar, M. H., Sarmidi, M. R., Tan, J. S., and Mohamad Rosdi, M. N. (2017). Celastrol Attenuates Mitochondrial Dysfunction and Inflammation in Palmitate-Mediated Insulin Resistance in C3A Hepatocytes. *Eur. J. Pharmacol.* 799, 73–83. doi:10.1016/j.ejphar.2017.01.043

Abu Bakar, M. H., and Tan, J. S. (2017). Improvement of Mitochondrial Function by Celastrol in Palmitate-Treated C2C12 Myotubes via Activation of PI3K-Akt Signalling Pathway. *Biomed. Pharmacother.* 93, 903–912. doi:10.1016/j.biopha.2017.07.021

Bakar, M. H. A., Sarmidi, M. R., Kai, C. K., Huri, H. Z., and Yaakob, H. (2014). Amelioration of Mitochondrial Dysfunction-Induced Insulin Resistance in Differentiated 3T3-L1 Adipocytes via Inhibition of NF-Kb Pathways. *Int. J. Mol. Sci.* 15, 22227–22257. doi:10.3390/ijms151222227

Baker, J. T., Borris, R. P., Carté, B., Cordell, G. A., Soejarto, D. D., Cragg, G. M., et al. (1995). Natural Product Drug Discovery and Development: New Perspectives on International Collaboration. *J. Nat. Prod.* 58, 1325–1357. doi:10.1021/np50123a003

Booij, T. H., Leonhard, W. N., Bange, H., Yan, K., Fokkelman, M., Plugge, A. J., et al. (2020). *In Vitro* 3D Phenotypic Drug Screen Identifies Celastrol as an Effective *In Vivo* Inhibitor of Polycystic Kidney Disease. *J. Mol. Cel Biol.* 12, 644–653. doi:10.1093/jmcb/mjz029

Brinker, A. M., Ma, J., Lipsky, P. E., and Raskin, I. (2007). Medicinal Chemistry and Pharmacology of Genus Tripterygium (Celastraceae). *Phytochemistry* 68, 732–766. doi:10.1016/j.phytochem.2006.11.029

Cascão, R., Vidal, B., Raquel, H., Neves-Costa, A., Figueiredo, N., Gupta, V., et al. (2012). Effective Treatment of Rat Adjuvant-Induced Arthritis by Celastrol. *Autoimmun. Rev.* 11, 856–862. doi:10.1016/j.autrev.2012.02.022

Chan, T. Y. K. (2012). Aconitum Alkaloid Content and the High Toxicity of Aconite Tincture. *Forensic Sci. Int.* 222, 1–3. doi:10.1016/j.forsciint.2012.02.026

Chan, T. Y. K. (2011). Causes and Prevention of Herb-Induced Aconite Poisonings in Asia. *Hum. Exp. Toxicol.* 30, 2023–2026. doi:10.1177/0960327111407224

Chang, W., He, W., Li, P.-P., Song, S.-S., Yuan, P.-F., Lu, J.-T., et al. (2016). Protective Effects of Celastrol on Diethylnitrosamine-Induced Hepatocellular Carcinoma in Rats and its Mechanisms. *Eur. J. Pharmacol.* 784, 173–180. doi:10.1016/j.ejphar.2016.04.045

Chen, G., Zhang, X., Zhao, M., Wang, Y., Cheng, X., Wang, D., et al. (2011). Celastrol Targets Mitochondrial Respiratory Chain Complex I to Induce Reactive Oxygen Species-dependent Cytotoxicity in Tumour Cells. *BMC Cancer* 11, 170. doi:10.1186/1471-2407-11-170

Chen, S.-R., Dai, Y., Zhao, J., Lin, L., Wang, Y., and Wang, Y. (2018a). A Mechanistic Overview of Triptolide and Celastrol, Natural Products from Tripterygium Wilfordii Hook F. *Front. Pharmacol.* 9, 104. doi:10.3389/fphar.2018.00104

Chen, X.-L., Liu, F., Xiao, X.-R., Yang, X.-W., and Li, F. (2018b). Anti-inflammatory Abietanes Diterpenoids Isolated from Tripterygium Hypoglaucum. *Phytochemistry* 156, 167–175. doi:10.1016/j.phytochem.2018.10.001

Chen, X., Murakami, T., Oppenheim, J. J., and Howard, O. M. Z. (2005). Triptolide, a Constituent of Immunosuppressive Chinese Herbal Medicine, Is a Potent Suppressor of Dendritic-Cell Maturation and Trafficking. *Blood* 106, 2409–2416. doi:10.1182/blood-2005-03-0854

Cheng, H.-Y., Lin, C.-C., and Lin, T.-C. (2002). Antiherpes Simplex Virus Type 2 Activity of Casuarinin from the Bark of Terminalia Arjuna Linn. *Antivir. Res* 55, 447–455. doi:10.1016/s0166-3542(02)00077-3

Collins, R. R. J., Patel, K., Putnam, W. C., Kapur, P., and Rakheja, D. (2017). Oncometabolites: A New Paradigm for Oncology, Metabolism, and the Clinical Laboratory. *Clin. Chem.* 63, 1812–1820. doi:10.1373/clinchem.2016.267666

Costa, C., Incio, J., and Soares, R. (2007). Angiogenesis and Chronic Inflammation: Cause or Consequence? *Angiogenesis* 10, 149–166. doi:10.1007/s10456-007-9074-0

Ding, L., and Zhang, Z. (1991). Studies on Chemical Constituents of Tripterygium Hypoglaucum Stems II. *Nanjing J. China Pharm. Univ.*, 25–26.

Duan, H., Kawazoe, K., Bando, M., Kido, M., and Takaishi, Y. (1997). Di- and Triterpenoids from Tripterygium Hypoglaucum. *Phytochemistry* 46, 103–110. doi:10.1016/s0031-9422(97)00288-4

Duan, H., Takaishi, Y., Imakura, Y., Jia, Y., Li, D., Cosentino, L. M., et al. (2000). Sesquiterpene Alkaloids from Tripterygium Hypoglaucum and Tripterygium Wilfordii: a New Class of Potent Anti-HIV Agents. *J. Nat. Prod.* 63, 357–361. doi:10.1021/np990281s

Duan, H., and Takaishi, Y. (1999). Sesquiterpene Evoninate Alkaloids from Tripterygium Hypoglaucum. *Phytochemistry* 52, 1735–1738. doi:10.1016/s0031-9422(99)00179-x

Duan, H., and Takaishi, Y. (1998). Structures of Sesquiterpene Polyol Alkaloids from Tripterygium Hypoglaucum. *Phytochemistry* 49, 357. doi:10.1016/s0031-9422(98)00439-7

Dudics, S., Langan, D., Meka, R. R., Venkatesha, S. H., Berman, B. M., Che, C.-T., et al. (2018). Natural Products for the Treatment of Autoimmune Arthritis: Their Mechanisms of Action, Targeted Delivery, and Interplay with the Host Microbiome. *Int. J. Mol. Sci.* 19, 2508. doi:10.3390/ijms19092508

El Hajj, H., Dassouki, Z., Berthier, C., Raffoux, E., Ades, L., Legrand, O., et al. (2015). Retinoic Acid and Arsenic Trioxide Trigger Degradation of Mutated NPM1, Resulting in Apoptosis of AML Cells. *Blood* 125, 3447–3454. doi:10.1182/blood-2014-11-612416

Fan, D., Guo, Q., Shen, J., Zheng, K., Lu, C., Zhang, G., et al. (2018). The Effect of Triptolide in Rheumatoid Arthritis: From Basic Research towards Clinical Translation. *Int. J. Mol. Sci.* 19, 376. doi:10.3390/ijms19020376

Fan, D., He, X., Bian, Y., Guo, Q., Zheng, K., Zhao, Y., et al. (2016). Triptolide Modulates TREM-1 Signal Pathway to Inhibit the Inflammatory Response in Rheumatoid Arthritis. *Int. J. Mol. Sci.* 17, 498. doi:10.3390/ijms17040498

Fan, X.-X., Li, N., Wu, J.-L., Zhou, Y.-L., He, J.-X., Liu, L., et al. (2014). Celastrol Induces Apoptosis in Gefitinib-Resistant Non-small Cell Lung Cancer Cells via Caspases-dependent Pathways and Hsp90 Client Protein Degradation. *Molecules* 19, 3508–3522. doi:10.3390/molecules19033508

Fang, W., Peng, F., Yi, T., Zhang, C., Wan, C., Xu, H., et al. (2012). Biological Activity and Safety of Tripterygium Extract Prepared by Sodium Carbonate Extraction. *Molecules* 17, 11113–11123. doi:10.3390/molecules170911113

Feng, X., Guan, D., Auen, T., Choi, J. W., Salazar Hernández, M. A., Lee, J., et al. (2019a). IL1R1 Is Required for Celastrol's Leptin-Sensitization and Antiobesity Effects. *Nat. Med.* 25, 575–582. doi:10.1038/s41591-019-0358-x

Feng, X., Lv, C., Wang, F., Gan, K., Zhang, M., and Tan, W. (2013). Modulatory Effect of 1,25-dihydroxyvitamin D 3 on IL1 β -induced RANKL, OPG, TNF α , and IL-6 Expression in Human Rheumatoid Synoviocyte MH7A. *Clin. Dev. Immunol.* 2013, 160123. doi:10.1155/2013/160123

Feng, Z., Zhou, C., Dong, S., Liu, Z., Liu, T., Zhou, L., et al. (2019b). Catalpol and Panax Notoginseng Saponins Synergistically Alleviate Triptolide-Induced Hepatotoxicity through Nrf2/ARE Pathway. *Toxicol. Vitro* 56, 141–149. doi:10.1016/j.tiv.2019.01.016

Fu, Q., Huang, X., Shu, B., Xue, M., Zhang, P., Wang, T., et al. (2011). Inhibition of Mitochondrial Respiratory Chain Is Involved in Triptolide-Induced Liver Injury. *Fitoterapia* 82, 1241–1248. doi:10.1016/j.fitote.2011.08.019

Fujita, R., Duan, H., and Takaishi, Y. (2000). Terpenoids from Triptergyum Hypoglaucum. *Phytochemistry* 53, 715–722. doi:10.1016/s0031-9422(99)00557-9

Gan, K., Xu, L., Feng, X., Zhang, Q., Wang, F., Zhang, M., et al. (2015). Celastrol Attenuates Bone Erosion in Collagen-Induced Arthritis Mice and Inhibits Osteoclast Differentiation and Function in RANKL-Induced RAW264.7. *Int. Immunopharmacol.* 24, 239–246. doi:10.1016/j.intimp.2014.12.012

Gong, Y., Xue, B., Jiao, J., Jing, L., and Wang, X. (2008). Triptolide Inhibits COX-2 Expression and PGE2 Release by Suppressing the Activity of NF-kappaB and JNK in LPS-Treated Microglia. *J. Neurochem.* 107, 779–788. doi:10.1111/j.1471-4159.2008.05653.x

Guo, Y., Wang, Y., Shi, X., Qin, W., Zhang, X., Xu, J., et al. (2018). A Metabolomics Study on the Immunosuppressive Effect of Tripterygium Hypoglaucum (Levl.) Hutch in Mice: The Discovery of Pathway Differences in Serum Metabolites. *Clin. Chim. Acta* 483, 94–103. doi:10.1016/j.cca.2018.04.004

Han, H., Du, L., Cao, Z., Zhang, B., and Zhou, Q. (2018). Triptonide Potently Suppresses Pancreatic Cancer Cell-Mediated Vasculogenic Mimicry by Inhibiting Expression of VE-Cadherin and Chemokine Ligand 2 Genes. *Eur. J. Pharmacol.* 818, 593–603. doi:10.1016/j.ejphar.2017.11.019

Harmey, J. H., Bucana, C. D., Lu, W., Byrne, A. M., McDonnell, S., Lynch, C., et al. (2002). Lipopolysaccharide-induced Metastatic Growth Is Associated with Increased Angiogenesis, Vascular Permeability and Tumour Cell Invasion. *Int. J. Cancer* 101, 415–422. doi:10.1002/ijc.10632

Hasnat, M., Yuan, Z., Naveed, M., Khan, A., Raza, F., Xu, D., et al. (2019). Drp1-associated Mitochondrial Dysfunction and Mitochondrial Autophagy: a Novel Mechanism in Triptolide-Induced Hepatotoxicity. *Cell Biol. Toxicol.* 35, 267–280. doi:10.1007/s10565-018-9447-8

Hernández-Aguilera, A., Rull, A., Rodríguez-Gallego, E., Riera-Borrull, M., Luciano-Mateo, F., Camps, J., et al. (2013). Mitochondrial Dysfunction: a Basic Mechanism in Inflammation-Related Non-communicable Diseases and Therapeutic Opportunities. *Mediators Inflamm.* 2013, 135698. doi:10.1155/2013/135698

Hu, D.-D., Zhao, Q., Cheng, Y., Xiao, X.-R., Huang, J.-F., Qu, Y., et al. (2019). The Protective Roles of PPARα Activation in Triptolide-Induced Liver Injury. *Toxicol. Sci.* 171, 1–12. doi:10.1093/toxsci/kfz146

Hu, Q., Wei, S., Wen, J., Zhang, W., Jiang, Y., Qu, C., et al. (2020). Network Pharmacology Reveals the Multiple Mechanisms of Xiaochaihu Decoction in the Treatment of Non-alcoholic Fatty Liver Disease. *BioData Min* 13, 11. doi:10.1186/s13040-020-00224-9

Huang, Y., Zhu, N., Chen, T., Chen, W., Kong, J., Zheng, W., et al. (2019). Triptolide Suppressed the Microglia Activation to Improve Spinal Cord Injury through miR-96/ikkβ/nf-Kb Pathway. *Spine (Phila. Pa. 1976)* 44, E707–E714. doi:10.1097/BRS.0000000000002989

Jang, S. Y., Jang, S.-W., and Ko, J. (2011). Celastrol Inhibits the Growth of Estrogen Positive Human Breast Cancer Cells through Modulation of Estrogen Receptor α. *Cancer Lett.* 300, 57–65. doi:10.1016/j.canlet.2010.09.006

Jiang, X., Huang, X., Ao, L., Liu, W., Han, F., Cao, J., et al. (2014). Total Alkaloids of Tripterygium Hypoglaucum (levl.) Hutch Inhibits Tumour Growth Both *In Vitro* and *In Vivo*. *J. Ethnopharmacol.* 151, 292–298. doi:10.1016/j.jep.2013.10.045

Jiang, Y., Wen, J., Zhang, W., Ma, Z., Zhang, C., Wang, J., et al. (2020a). Metabolomics Coupled with Integrative Pharmacology Reveals the Therapeutic Effect of L-Borneolum against Cerebral Ischaemia in Rats. *J. Pharm. Pharmacol.* 72, 1256–1268. doi:10.1111/jphp.13294

Jiang, Y., Zhong, M., Long, F., and Yang, R. (2020b). Deciphering the Active Ingredients and Molecular Mechanisms of Tripterygium Hypoglaucum (Levl.) Hutch against Rheumatoid Arthritis Based on Network Pharmacology. *Evid. Based. Complement. Alternat. Med.* 2020, 2361865. doi:10.1155/2020/2361865

Jiao, J., Xue, B., Zhang, L., Gong, Y., Li, K., Wang, H., et al. (2008). Triptolide Inhibits Amyloid-Beta1-42-Induced TNF-Alpha and IL-1beta Production in Cultured Rat Microglia. *J. Neuroimmunol.* 205, 32–36. doi:10.1016/j.jneuroim.2008.08.006

Jin, C., He, X., Zhang, F., He, L., Chen, J., Wang, L., et al. (2015a). Inhibitory Mechanisms of Celastrol on Human Liver Cytochrome P450 1A2, 2C19, 2D6, 2E1 and 3A4. *Xenobiotica* 45, 571–577. doi:10.3109/00498254.2014.1003113

Jin, C., Wu, Z., Wang, L., Kanai, Y., and He, X. (2019). CYP450s-Activity Relations of Celastrol to Interact with Triptolide Reveal the Reasons of Hepatotoxicity of Tripterygium Wilfordii. *Molecules* 24, 2162. doi:10.3390/molecules24112162

Jin, J., Sun, X., Zhao, Z., Wang, W., Qiu, Y., Fu, X., et al. (2015b). Activation of the Farnesoid X Receptor Attenuates Triptolide-Induced Liver Toxicity. *Phytomedicine* 22, 894–901. doi:10.1016/j.phymed.2015.06.007

Joshi, V., Venkatesha, S. H., Ramakrishnan, C., Nanjaraj Urs, A. N., Hiremath, V., Moudgil, K. D., et al. (2016). Celastrol Modulates Inflammation through Inhibition of the Catalytic Activity of Mediators of Arachidonic Acid Pathway: Secretory Phospholipase A(2) Group IIA, 5-lipoxygenase and Cyclooxygenase-2. *Pharmacol. Res.* 113, 265–275. doi:10.1016/j.phrs.2016.08.035

Jung, H. W., Chung, Y. S., Kim, Y. S., and Park, Y.-K. (2007). Celastrol Inhibits Production of Nitric Oxide and Proinflammatory Cytokines through MAPK Signal Transduction and NF-kappaB in LPS-Stimulated BV-2 Microglial Cells. *Exp. Mol. Med.* 39, 715–721. doi:10.1038/emm.2007.78

Kchour, G., Tarhini, M., Kooshyar, M.-M., El Hajj, H., Wattel, E., Mahmoudi, M., et al. (2009). Phase 2 Study of the Efficacy and Safety of the Combination of Arsenic Trioxide, Interferon Alpha, and Zidovudine in Newly Diagnosed Chronic Adult T-Cell Leukemia/lymphoma (ATL). *Blood* 113, 6528–6532. doi:10.1182/blood-2009-03-211821

Khairul, I., Wang, Q. Q., Jiang, Y. H., Wang, C., and Naranmandura, H. (2017). Metabolism, Toxicity and Anticancer Activities of Arsenic Compounds. *Oncotarget* 8, 23905–23926. doi:10.18632/oncotarget.14733

Kim, D. H., Shin, E. K., Kim, Y. H., Lee, B. W., Jun, J.-G., Park, J. H. Y., et al. (2009). Suppression of Inflammatory Responses by Celastrol, a Quinone Methide Triterpenoid Isolated from Celastrus Regelii. *Eur. J. Clin. Invest.* 39, 819–827. doi:10.1111/j.1365-2362.2009.02186.x

Kim, S. T., Kim, S. Y., Lee, J., Kim, K., Park, S. H., Park, Y. S., et al. (2018). Triptolide as a Novel Agent in Pancreatic Cancer: the Validation Using Patient Derived Pancreatic Tumour Cell Line. *BMC Cancer* 18, 1103. doi:10.1186/s12885-018-4995-0

Kim, Y.-H., Lee, S.-H., Lee, J.-Y., Choi, S.-W., Park, J.-W., and Kwon, T. K. (2004). Triptolide Inhibits Murine-Inducible Nitric Oxide Synthase Expression by Down-Regulating Lipopolysaccharide-Induced Activity of Nuclear Factor-Kappa B and C-Jun NH2-terminal Kinase. *Eur. J. Pharmacol.* 494, 1–9. doi:10.1016/j.ejphar.2004.04.040

Kong, L.-L., Zhuang, X.-M., Yang, H.-Y., Yuan, M., Xu, L., and Li, H. (2015). Inhibition of P-Glycoprotein Gene Expression and Function Enhances

Triptolide-Induced Hepatotoxicity in Mice. *Sci. Rep.* 5, 11747. doi:10.1038/srep11747

Kong, X., Zhang, Y., Liu, C., Guo, W., Li, X., Su, X., et al. (2013). Anti-angiogenic Effect of Triptolide in Rheumatoid Arthritis by Targeting Angiogenic cascade. *PLoS One* 8, e77513. doi:10.1371/journal.pone.0077513

Krakauer, T., Chen, X., Howard, O. M. Z., and Young, H. A. (2005). Triptolide Attenuates Endotoxin- and Staphylococcal Exotoxin-Induced T-Cell Proliferation and Production of Cytokines and Chemokines. *Immunopharmacol. Immunotoxicol.* 27, 53–66. doi:10.1081/iph-51294

Kupchan, S. M., Court, W. A., Dailey, R. G. J., Gilmore, C. J., and Bryan, R. F. (1972). Triptolide and Tripdiolide, Novel Antileukemic Diterpenoid Triepoxides from Tripterygium Wilfordii. *J. Am. Chem. Soc.* 94, 7194–7195. doi:10.1021/ja00775a078

Kyriakou, E., Schmidt, S., Dodd, G. T., Pfuhlmann, K., Simonds, S. E., Lenhart, D., et al. (2018). Celastrol Promotes Weight Loss in Diet-Induced Obesity by Inhibiting the Protein Tyrosine Phosphatases PTP1B and TCPTP in the Hypothalamus. *J. Med. Chem.* 61, 11144–11157. doi:10.1021/acs.jmedchem.8b01224

Lee, H.-W., Jang, K. S. Bin., Choi, H. J., Jo, A., Cheong, J.-H., and Chun, K.-H. (2014). Celastrol Inhibits Gastric Cancer Growth by Induction of Apoptosis and Autophagy. *BMB Rep.* 47, 697–702. doi:10.5483/bmbrep.2014.47.12.069

Lee, J.-H., Koo, T. H., Yoon, H., Jung, H. S., Jin, H. Z., Lee, K., et al. (2006). Inhibition of NF-Kappa B Activation through Targeting I Kappa B Kinase by Celastrol, a Quinone Methide Triterpenoid. *Biochem. Pharmacol.* 72, 1311–1321. doi:10.1016/j.bcp.2006.08.014

Lee, J.-H., Won, Y.-S., Park, K.-H., Lee, M.-K., Tachibana, H., Yamada, K., et al. (2012). Celastrol Inhibits Growth and Induces Apoptotic Cell Death in Melanoma Cells via the Activation ROS-dependent Mitochondrial Pathway and the Suppression of PI3K/AKT Signalling. *Apoptosis* 17, 1275–1286. doi:10.1007/s10495-012-0767-5

Lee, J. Y., Lee, B. H., Kim, N. D., and Lee, J. Y. (2015). Celastrol Blocks Binding of Lipopolysaccharides to a Toll-like Receptor4/myeloid Differentiation Factor2 Complex in a Thiol-dependent Manner. *J. Ethnopharmacol.* 172, 254–260. doi:10.1016/j.jep.2015.06.028

Li, C., Li, Z., Zhang, T., Wei, P., Li, N., Zhang, W., et al. (2019). (1)H NMR-Based Metabolomics Reveals the Antitumour Mechanisms of Triptolide in BALB/c Mice Bearing CT26 Tumours. *Front. Pharmacol.* 10, 1175. doi:10.3389/fphar.2019.01175

Li, G., Liu, D., Zhang, Y., Qian, Y., Zhang, H., Guo, S., et al. (2013a). Celastrol Inhibits Lipopolysaccharide-Stimulated Rheumatoid Fibroblast-like Synoviocyte Invasion through Suppression of TLR4/NF-Kb-Mediated Matrix Metalloproteinase-9 Expression. *PLoS One* 8, e68905. doi:10.1371/journal.pone.0068905

Li, G., Ren, J., Wang, G., Gu, G., Hu, D., Ren, H., et al. (2014a). T2 Enhances *In Situ* Level of Foxp3+ Regulatory Cells and Modulates Inflammatory Cytokines in Crohn's Disease. *Int. Immunopharmacol.* 18, 244–248. doi:10.1016/j.intimp.2013.12.014

Li, H., Zhang, Y.-Y., Tan, H.-W., Jia, Y.-F., and Li, D. (2008). Therapeutic Effect of Tripterine on Adjuvant Arthritis in Rats. *J. Ethnopharmacol.* 118, 479–484. doi:10.1016/j.jep.2008.05.028

Li, J., Jin, J., Li, M., Guan, C., Wang, W., Zhu, S., et al. (2012a). Role of Nrf2 in protection against Triptolide-Induced Toxicity in Rat Kidney Cells. *Toxicol. Lett.* 213, 194–202. doi:10.1016/j.toxlet.2012.07.008

Li, J., Shen, F., Guan, C., Wang, W., Sun, X., Fu, X., et al. (2014b). Activation of Nrf2 Protects against Triptolide-Induced Hepatotoxicity. *PLoS One* 9, e100685. doi:10.1371/journal.pone.0100685

Li, M., Liu, X., He, Y., Zheng, Q., Wang, M., Wu, Y., et al. (2017a). Celastrol Attenuates Angiotensin II Mediated Human Umbilical Vein Endothelial Cells Damage through Activation of Nrf2/ERK1/2/Nox2 Signal Pathway. *Eur. J. Pharmacol.* 797, 124–133. doi:10.1016/j.ejphar.2017.01.027

Li, P.-P., He, W., Yuan, P.-F., Song, S.-S., Lu, J.-T., and Wei, W. (2015a). Celastrol Induces Mitochondria-Mediated Apoptosis in Hepatocellular Carcinoma Bel-7402 Cells. *Am. J. Chin. Med.* 43, 137–148. doi:10.1142/S0192415X15500093

Li, X.-J., Jiang, Z.-Z., and Zhang, L. (2014c). Triptolide: Progress on Research in Pharmacodynamics and Toxicology. *J. Ethnopharmacol.* 155, 67–79. doi:10.1016/j.jep.2014.06.006

Li, X.-L., Gao, L.-H., Li, H.-M., Wang, L.-T., Lee, K.-H., and Li, R.-T. (2015b). Diterpenoids from the Stems of Tripterygium Hypoglaucum (Celastraceae) and Cytotoxic Evaluation. *Phytochem. Lett.* 12. doi:10.1016/j.phytol.2015.02.018

Li, X. G., and He, L. (2006). Pharmacological Control Study between Tripterygium Hypoglaucum Hutch and Tripterygium Wilfordii Hook F. *J. Kunming Med. Coll.* 12, 527723. doi:10.3969/j.issn.1005-9202.2011.18.040

Li, Y. B., Nie, J., Lü, C., Hu, X. L., and Xue Gy, L. C. (2011). Influence of Triptolide on the Expression of Interleukin-1β and Prostaglandin E2 in Rat Microglia Induced by Beta-Amyloid Protein. *Chin. J. Gerontol.* 31, 3521–3523.

Li, Z., Wu, X., Li, J., Yao, L., Sun, L., Shi, Y., et al. (2012b). Antitumour Activity of Celastrol Nanoparticles in a Xenograft Retinoblastoma Tumour Model. *Int. J. Nanomedicine* 7, 2389–2398. doi:10.2147/IJN.S29945

Li, Z., Yan, M., Cao, L., Fang, P., Guo, Z., Hou, Z., et al. (2017b). Glycyrrhetinic Acid Accelerates the Clearance of Triptolide through P-Gp *In Vitro*. *Phytother. Res.* 31, 1090–1096. doi:10.1002/ptr.5831

Li, Z. Y., Wu, Q., Yan, Z., Li, D., Pan, X., Qiu, T., et al. (2013b). Prevention of Acute GVHD in Mice by Treatment with Tripterygium Hypoglaucum Hutch Combined with Cyclosporin A. *Hematology* 18, 352–359. doi:10.1179/1607845413Y.0000000076

Liang, Z.-Q., Cao, N., Song, Z.-K., and Wang, X. (2006). *In Vitro* porcine Brain Tubulin Assembly Inhibition by Water Extract from a Chinese Medicinal Herb, Tripterygium Hypoglaucum Hutch. *World J. Gastroenterol.* 12, 1133–1135. doi:10.3748/wjg.v12.i7.1133

Lin, H.-F., Hsieh, M.-J., Hsi, Y.-T., Lo, Y.-S., Chuang, Y.-C., Chen, M.-K., et al. (2017). Celastrol-induced Apoptosis in Human Nasopharyngeal Carcinoma Is Associated with the Activation of the Death Receptor and the Mitochondrial Pathway. *Oncol. Lett.* 14, 1683–1690. doi:10.3892/ol.2017.6346

Lin, N., Liu, C., Xiao, C., Jia, H., Imada, K., Wu, H., et al. (2007). Triptolide, a Diterpenoid Triepoxide, Suppresses Inflammation and Cartilage Destruction in Collagen-Induced Arthritis Mice. *Biochem. Pharmacol.* 73, 136–146. doi:10.1016/j.bcp.2006.08.027

Lin, N., Sato, T., and Ito, A. (2001). Triptolide, a Novel Diterpenoid Triepoxide from Tripterygium Wilfordii Hook. f., Suppresses the Production and Gene Expression of Pro-matrix Metalloproteinases 1 and 3 and Augments Those of Tissue Inhibitors of Metalloproteinases 1 and 2 in Human Synovia. *Arthritis Rheum.* 44, 2193–2200. doi:10.1002/1529-0131(200109)44:9<2193::aid-art373>3.0.co;2-5

Liu, H.-K., Perrier, S., Lipina, C., Finlay, D., McLauchlan, H., Hastie, C. J., et al. (2006). Functional Characterisation of the Regulation of CAAT Enhancer Binding Protein Alpha by GSK-3 Phosphorylation of Threonines 222/226. *BMC Mol. Biol.* 7, 14. doi:10.1186/1471-2199-7-14

Liu, J., Lee, J., Salazar Hernandez, M. A., Mazitschek, R., and Ozcan, U. (2015). Treatment of Obesity with Celastrol. *Cell* 161, 999–1011. doi:10.1016/j.cell.2015.05.011

Liu, J., Wu, Q.-L., Feng, Y.-H., Wang, Y.-F., Li, X.-Y., and Zuo, J.-P. (2005). Triptolide Suppresses CD80 and CD86 Expressions and IL-12 Production in THP-1 Cells. *Acta Pharmacol. Sin.* 26, 223–227. doi:10.1111/j.1745-7254.2005.00035.x

Liu, L., Luo, Y., Zhou, M., Lu, Y., Xing, M., Ru, Y., et al. (2019). Tripterygium Agents for the Treatment of Atopic Eczema: A Bayesian Analysis of Randomized Controlled Trials. *Phytomedicine* 59, 152914. doi:10.1016/j.phymed.2019.152914

Liu, L., Salnikov, A. V., Bauer, N., Aleksandrowicz, E., Labsch, S., Nwaeburu, C., et al. (2014a). Triptolide Reverses Hypoxia-Induced Epithelial-Mesenchymal Transition and Stem-like Features in Pancreatic Cancer by NF-Kb Downregulation. *Int. J. Cancer* 134, 2489–2503. doi:10.1002/ijc.28583

Liu, Q., Chen, T., Chen, H., Zhang, M., Li, N., Lu, Z., et al. (2004). Triptolide (PG-490) Induces Apoptosis of Dendritic Cells through Sequential P38 MAP Kinase Phosphorylation and Caspase 3 Activation. *Biochem. Biophys. Res. Commun.* 319, 980–986. doi:10.1016/j.bbrc.2004.04.201

Liu, Q. (2011). Triptolide and its Expanding Multiple Pharmacological Functions. *Int. Immunopharmacol.* 11, 377–383. doi:10.1016/j.intimp.2011.01.012

Liu, Y., Chen, Y., Liu, F. Q., Lamb, J. R., and Tam, P. K. H. (2008). Combined Treatment with Triptolide and Rapamycin Prolongs Graft Survival in a Mouse Model of Cardiac Transplantation. *Transpl. Int. Off. J. Eur. Soc. Organ. Transpl.* 21, 483–494. doi:10.1111/j.1432-2277.2007.00630.x

Liu, Y., Song, F., Wu, W. K. K., He, M., Zhao, L., Sun, X., et al. (2012). Triptolide Inhibits colon Cancer Cell Proliferation and Induces Cleavage and Translocation of 14-3-3 Epsilon. *Cell Biochem. Funct.* 30, 271–278. doi:10.1002/cbf.2793

Liu, Z.-Z., Zhao, R.-H., Liu, Y.-T., Zhang, H.-W., Ding, G., Ma, Z., et al. (2014b). A New Dihydroagarofuranoid Sesquiterpene from the Roots of Tripterygium Hypoglaucum. *J. Asian Nat. Prod. Res.* 16, 327–331. doi:10.1080/10286020.2013.873410

Liu, Z., Zhao, R., and Zou, Z. (2011). Chemical Constituents from Root Bark of Tripterygium Hypoglaucum. *Zhongguo Zhong Yao Za Zhi* 36, 2503–2506.

Lü, S., Wang, Q., Li, G., Sun, S., Guo, Y., and Kuang, H. (2015). The Treatment of Rheumatoid Arthritis Using Chinese Medicinal Plants: From Pharmacology to Potential Molecular Mechanisms. *J. Ethnopharmacol.* 176, 177–206. doi:10.1016/j.jep.2015.10.010

Lu, Y., Fukuda, K., Nakamura, Y., Kimura, K., Kumagai, N., and Nishida, T. (2005). Inhibitory Effect of Triptolide on Chemokine Expression Induced by Proinflammatory Cytokines in Human Corneal Fibroblasts. *Invest. Ophthalmol. Vis. Sci.* 46, 2346–2352. doi:10.1167/iovs.05-0010

Lu, Y., Zhang, Y., Li, L., Feng, X., Ding, S., Zheng, W., et al. (2014). TAB1: a Target of Triptolide in Macrophages. *Chem. Biol.* 21, 246–256. doi:10.1016/j.chembiol.2013.12.009

Lue, Y., Sinha Hikim, A. P., Wang, C., Leung, A., Baravarian, S., Reutrakul, V., et al. (1998). Triptolide: a Potential Male Contraceptive. *J. Androl.* 19, 479–486.

Luo, D., Zuo, Z., Zhao, H., Tan, Y., and Xiao, C. (2019). Immunoregulatory Effects of Tripterygium Wilfordii Hook F and its Extracts in Clinical Practice. *Front. Med.* 13, 556–563. doi:10.1007/s11684-018-0649-5

Lv, H., Jiang, L., Zhu, M., Li, Y., Luo, M., Jiang, P., et al. (2019). The Genus Tripterygium: A Phytochemistry and Pharmacological Review. *Fitoterapia* 137, 104190. doi:10.1016/j.fitote.2019.104190

Ma, B., Qi, H., Li, J., Xu, H., Chi, B., Zhu, J., et al. (2015). Triptolide Disrupts Fatty Acids and Peroxisome Proliferator-Activated Receptor (PPAR) Levels in Male Mice Testes Followed by Testicular Injury: A GC-MS Based Metabolomics Study. *Toxicology* 336, 84–95. doi:10.1016/j.tox.2015.07.008

Ma, J., Schmidt, B. M., Poulev, A., and Raskin, I. (2008). Determination of Tripdiolide in Root Extracts of Tripterygium Wilfordii by Solid-phase Extraction and Reversed-phase High-Performance Liquid Chromatography. *Phytochem. Anal.* 19, 348–352. doi:10.1002/pca.1059

Mathews, V., Chendamarai, E., George, B., Viswabandya, A., and Srivastava, A. (2011). Treatment of Acute Promyelocytic Leukemia with Single-Agent Arsenic Trioxide. *Mediterr. J. Hematol. Infect. Dis.* 3, e2011056. doi:10.4084/MJHID.2011.056

Matsui, Y., Watanabe, J., Ikegawa, M., Kamoto, T., Ogawa, O., and Nishiyama, H. (2008). Cancer-specific Enhancement of Cisplatin-Induced Cytotoxicity with Triptolide through an Interaction of Inactivated Glycogen Synthase Kinase-3beta with P53. *Oncogene* 27, 4603–4614. doi:10.1038/onc.2008.89

McDonald, D. M. (2001). Angiogenesis and Remodeling of Airway Vasculature in Chronic Inflammation. *Am. J. Respir. Crit. Care Med.* 164, S39–S45. doi:10.1164/ajrccm.164.supplement_2.2106065

Mishra, P., and Ambs, S. (2015). Metabolic Signatures of Human Breast Cancer. *Mol. Cel. Oncol.* 2, e992217. doi:10.4161/23723556.2014.992217

Miyata, Y., Sato, T., and Ito, A. (2005). Triptolide, a Diterpenoid Triepoxide, Induces Antitumour Proliferation via Activation of C-Jun NH2-terminal Kinase 1 by Decreasing Phosphatidylinositol 3-kinase Activity in Human Tumour Cells. *Biochem. Biophys. Res. Commun.* 336, 1081–1086. doi:10.1016/j.bbrc.2005.08.247

Mou, H., Zheng, Y., Zhao, P., Bao, H., Fang, W., and Xu, N. (2011). Celastrol Induces Apoptosis in Non-small-cell Lung Cancer A549 Cells through Activation of Mitochondria- and Fas/FasL-Mediated Pathways. *Toxicol. Vitro* 25, 1027–1032. doi:10.1016/j.tiv.2011.03.023

Nie, J., Zhou, M., Lü, C., Hu, X., Wan, B., Yang, B., et al. (2012). Effects of Triptolide on the Synaptophysin Expression of Hippocampal Neurons in the AD Cellular Model. *Int. Immunopharmacol.* 13, 175–180. doi:10.1016/j.intimp.2012.03.021

Ning, C., Mo, L., Chen, X., Tu, W., Wu, J., Hou, S., et al. (2018). Triptolide Derivatives as Potential Multifunctional Anti-alzheimer Agents: Synthesis and Structure-Activity Relationship Studies. *Bioorg. Med. Chem. Lett.* 28, 689–693. doi:10.1016/j.bmcl.2018.01.019

Nong, C., Wang, X.-Z., Jiang, Z.-Z., and Zhang, L.-Y. (2019). [Progress of Effect and Mechanisms of Tripterygium Wilfordii on Immune System]. *Zhongguo Zhong Yao Za Zhi = Zhongguo Zhongyao Zazhi = China J. Chin. Mater. Med.* 44, 3374–3383. doi:10.19540/j.cnki.cjcmm.20190419.401

Oda, K., and Kitano, H. (2006). A Comprehensive Map of the Toll-like Receptor Signalling Network. *Mol. Syst. Biol.* 2, 0015. doi:10.1038/msb4100057

Onyeabor, F., Paik, A., Kovvasu, S., Ding, B., Lin, J., Wahid, M. A., et al. (2019). Optimization of Preparation and Preclinical Pharmacokinetics of Celastrol-Encapsulated Silk Fibroin Nanoparticles in the Rat. *Molecules* 24, 3271. doi:10.3390/molecules24183271

Pan, X.-D., Chen, X.-C., Zhu, Y.-G., Chen, L.-M., Zhang, J., Huang, T.-W., et al. (2009). Tripchlorolide Protects Neuronal Cells from Microglia-Mediated Beta-Amyloid Neurotoxicity through Inhibiting NF-kappaB and JNK Signalling. *Glia* 57, 1227–1238. doi:10.1002/glia.20844

Petronelli, A., Pannitteri, G., and Testa, U. (2009). Triterpenoids as New Promising Anticancer Drugs. *Anticancer. Drugs* 20, 880–892. doi:10.1097/CAD.0b013e328330fd90

Qian, S. Z., Hu, Y. Z., Wang, S. M., Luo, Y., Tang, A. S., Shu, S. Y., et al. (1988). Effects of Tripterygium Hypoglaucum (Lévl.) Hutch on Male Fertility. *Adv. Contracept. Off. J. Soc. Adv. Contracept.* 4, 307–310. doi:10.1007/BF01849272

Ren, Z., Zhang, C., Wang, L., Cui, Y., Qi, R., Yang, C., et al. (2010). *In Vitro* anti-viral Activity of the Total Alkaloids from Tripterygium Hypoglaucum against Herpes Simplex Virus Type 1. *Virol. Sin.* 25, 107–114. doi:10.1007/s12250-010-3092-6

Rodríguez-Martínez, S., Cancino-Diaz, M. E., Miguel, P.-S., and Cancino-Diaz, J. C. (2006). Lipopolysaccharide from *Escherichia coli* Induces the Expression of Vascular Endothelial Growth Factor via Toll-like Receptor 4 in Human Limbal Fibroblasts. *Exp. Eye Res.* 83, 1373–1377. doi:10.1016/j.exer.2006.07.015

Seo, W. Y., Goh, A. R., Ju, S. M., Song, H. Y., Kwon, D.-J., Jun, J.-G., et al. (2011). Celastrol Induces Expression of Heme Oxygenase-1 through ROS/Nrf2/ARE Signalling in the HaCaT Cells. *Biochem. Biophys. Res. Commun.* 407, 535–540. doi:10.1016/j.bbrc.2011.03.053

Seo, W. Y., Ju, S. M., Song, H. Y., Goh, A. R., Jun, J.-G., Kang, Y.-H., et al. (2010). Celastrol Suppresses IFN-Gamma-Induced ICAM-1 Expression and Subsequent Monocyte Adhesiveness via the Induction of Heme Oxygenase-1 in the HaCaT Cells. *Biochem. Biophys. Res. Commun.* 398, 140–145. doi:10.1016/j.bbrc.2010.06.053

Shamon, L. A., Pezzuto, J. M., Graves, J. M., Mehta, R. R., Wangcharoentrakul, S., Sangsuwan, R., et al. (1997). Evaluation of the Mutagenic, Cytotoxic, and Antitumour Potential of Triptolide, a Highly Oxygenated Diterpene Isolated from Tripterygium Wilfordii. *Cancer Lett.* 112, 113–117. doi:10.1016/S0304-3835(96)04554-5

Shan, W.-G., Wang, H.-G., Chen, Y., Wu, R., Wen, Y.-T., Zhang, L.-W., et al. (2017). Synthesis of 3- and 29-substituted Celastrol Derivatives and Structure-Activity Relationship Studies of Their Cytotoxic Activities. *Bioorg. Med. Chem. Lett.* 27, 3450–3453. doi:10.1016/j.bmcl.2017.05.083

Shao, F., Wang, G., Xie, H., Zhu, X., Sun, J., and Jiye, A. (2007). Pharmacokinetic Study of Triptolide, a Constituent of Immunosuppressive Chinese Herb Medicine, in Rats. *Biol. Pharm. Bull.* 30, 702–707. doi:10.1248/bpb.30.702

Song, Q., Xiang, Y., Gu, J., Chen, J., and Li, X. (2021). Chemical Constituents from the Rhizomes of Tripterygium Hypoglaucum. *J. Chinese Med. Mater.*, 355–358. doi:10.13863/j.issn1001-4454.2021.02.018

Song, W., Liu, M., Wu, J., Zhai, H., Chen, Y., and Peng, Z. (2019). Preclinical Pharmacokinetics of Triptolide: A Potential Antitumour. *Drug. Curr. Drug Metab.* 20, 147–154. doi:10.2174/1389200219666180816141506

Sun, L., Li, H., Huang, X., Wang, T., Zhang, S., Yang, J., et al. (2013). Triptolide Alters Barrier Function in Renal Proximal Tubular Cells in Rats. *Toxicol. Lett.* 223, 96–102. doi:10.1016/j.toxlet.2013.08.014

Tabeshpour, J., Mehri, S., Shaebani Behbahani, F., and Hosseinzadeh, H. (2018). Protective Effects of Vitis vinifera (Grapes) and One of its Biologically Active Constituents, Resveratrol, against Natural and Chemical Toxicities: A Comprehensive Review. *Phytother. Res.* 32, 2164–2190. doi:10.1002/ptr.6168

Tai, T., Huang, X., Su, Y., Ji, J., Su, Y., Jiang, Z., et al. (2014). Glycyrrhizin Accelerates the Metabolism of Triptolide through Induction of CYP3A in Rats. *J. Ethnopharmacol.* 152, 358–363. doi:10.1016/j.jep.2014.01.026

Tang, Y., Zhang, Y., Li, L., Xie, Z., Wen, C., and Huang, L. (2020). Kunxian Capsule for Rheumatoid Arthritis: Inhibition of Inflammatory Network and Reducing Adverse Reactions through Drug Matching. *Front. Pharmacol.* 11, 485. doi:10.3389/fphar.2020.00485

Tao, J., Hu, Q., Yang, J., Li, R., Li, X., Lu, C., et al. (2007). *In Vitro* anti-HIV and -HSV Activity and Safety of Sodium Rutin Sulfate as a Microbicide Candidate. *Antivir. Res* 75, 227–233. doi:10.1016/j.antiviral.2007.03.008

Tao, X., Schulze-Koops, H., Ma, L., Cai, J., Mao, Y., and Lipsky, P. E. (1998). Effects of Tripterygium Wilfordii Hook F Extracts on Induction of Cyclooxygenase 2 Activity and Prostaglandin E2 Production. *Arthritis Rheum.* 41, 130–138. doi:10.1002/1529-0131(199801)41:1<130::AID-ART16>3.0.CO;2-4

Tozawa, K., Sagawa, M., and Kizaki, M. (2011). Quinone Methide Tripterine, Celastrol, Induces Apoptosis in Human Myeloma Cells via NF-Kb Pathway. *Int. J. Oncol.* 39, 1117–1122. doi:10.3892/ijo.2011.1161

Tseng, C.-K., Hsu, S.-P., Lin, C.-K., Wu, Y.-H., Lee, J.-C., and Young, K.-C. (2017). Celastrol Inhibits Hepatitis C Virus Replication by Upregulating Heme Oxygenase-1 via the JNK MAPK/Nrf2 Pathway in Human Hepatoma Cells. *Antivir. Res* 146, 191–200. doi:10.1016/j.antiviral.2017.09.010

Hu, Y. H., Zeng, K. Q., Zhang, M. M., Tu, S. H., Lai, X. Y., Zhang, W. C., et al. (2004). Effects of Triptolide on the Expression and Activity of Nuclear Factor κB in Synovium of Collagen-Induced Arthritis Rats. *Chin. J. Rheumatol.* 25 (5), 543–545. doi:10.1007/BF02896012

Vlietinck, A. J., and Vanden Berghe, D. A. (1991). Can Ethnopharmacology Contribute to the Development of Antiviral Drugs? *J. Ethnopharmacol.* 32, 141–153. doi:10.1016/0378-8741(91)90112-q

Wang, C., Shi, C., Yang, X., Yang, M., Sun, H., and Wang, C. (2014). Celastrol Suppresses Obesity Process via Increasing Antioxidant Capacity and Improving Lipid Metabolism. *Eur. J. Pharmacol.* 744, 52–58. doi:10.1016/j.ejphar.2014.09.043

Wang, F., Zhang, Y., and Zhao, Y. Q., (2011). Study on Chemical Constituents of Tripterygium Hypoglaucum. *Chin. Herb. Med.* 42, 46–49.

Wang, J.-M., Li, J.-Y., Cai, H., Chen, R.-X., Zhang, Y.-Y., Zhang, L.-L., et al. (2019). Nrf2 Participates in Mechanisms for Reducing the Toxicity and Enhancing the Antitumour Effect of Radix Tripterygium Wilfordii to S180-Bearing Mice by Herbal-Processing Technology. *Pharm. Biol.* 57, 437–448. doi:10.1080/13880209.2019.1634106

Wang, L., Xu, D., Li, L., Xing, X., Liu, L., Ismail Abdelmotalab, M., et al. (2018a). Possible Role of Hepatic Macrophage Recruitment and Activation in Triptolide-Induced Hepatotoxicity. *Toxicol. Lett.* 299, 32–39. doi:10.1016/j.toxlet.2018.08.017

Wang, S., Wang, L., and Chen, X., (2020). Diterpenoids of the Stem and Leaf of Tripterygium Hypoglaucum and Their Biological Activities. *J. Kunming Univ. Sci. Technol. Sci. Ed.* 45, 108–114. doi:10.16112/j.cnki.53-1223/n.2020.02.014

Wang, S., Zuo, S., Liu, Z., Ji, X., Yao, Z., and Wang, X. (2018b). Study on the Efficacy and Mechanism of Triptolide on Treating TNF Transgenic Mice with Rheumatoid Arthritis. *Biomed. Pharmacother.* 106, 813–820. doi:10.1016/j.biopha.2018.07.021

Wang, W.-B., Feng, L.-X., Yue, Q.-X., Wu, W.-Y., Guan, S.-H., Jiang, B.-H., et al. (2012). Paraptosis Accompanied by Autophagy and Apoptosis Was Induced by Celastrol, a Natural Compound with Influence on Proteasome, ER Stress and Hsp90. *J. Cel. Physiol.* 227, 2196–2206. doi:10.1002/jcp.22956

Wang, Y.-L., Lam, K.-K., Cheng, P.-Y., and Lee, Y.-M. (2015). Celastrol Prevents Circulatory Failure via Induction of Heme Oxygenase-1 and Heat Shock Protein 70 in Endotoxemic Rats. *J. Ethnopharmacol.* 162, 168–175. doi:10.1016/j.jep.2014.12.062

Wang, Y., Guo, S.-H., Shang, X.-J., Yu, L.-S., Zhu, J.-W., Zhao, A., et al. (2018c). Triptolide Induces Sertoli Cell Apoptosis in Mice via ROS/JNK-dependent Activation of the Mitochondrial Pathway and Inhibition of Nrf2-Mediated Antioxidant Response. *Acta Pharmacol. Sin.* 39, 311–327. doi:10.1038/aps.2017.95

Wang, Z., Ma, D., Wang, C., Zhu, Z., Yang, Y., Zeng, F., et al. (2017). Triptonide Inhibits the Pathological Functions of Gastric Cancer-Associated Fibroblasts. *Biomed. Pharmacother.* 96, 757–767. doi:10.1016/j.biopha.2017.10.046

Wei, Y. M., Luan, Z. H., Liu, B. W., Wang, Y. H., Chang, Y. X., Xue, H. Q., et al. (2019). Autophagy in Triptolide-Mediated Cytotoxicity in Hepatic Cells. *Int. J. Toxicol.* 38, 436–444. doi:10.1177/1091581819864518

Li, W. W., Li, B. G., and Chen, Y. Z. (1999). *Sesquiterpene Alkaloids from Tripterygium Hypoglaucum*. *Phytochemistry* 40. doi:10.1016/S0031-9422(98)00618-9

Wishart, D. S., Mandal, R., Stanislaus, A., and Ramirez-Gaona, M. (2016). Cancer Metabolomics and the Human Metabolome Database. *Metabolites* 6, 10. doi:10.3390/metabo6010010

Wong, K.-F., Chan, J. K., Chan, K.-L., Tam, P., Yang, D., Fan, S.-T., et al. (2008). Immunochemical Characterization of the Functional Constituents of Tripterygium Wilfordii Contributing to its Anti-inflammatory Property. *Clin. Exp. Pharmacol. Physiol.* 35, 55–59. doi:10.1111/j.1440-1681.2007.04740.x

Wu, D. G., Sun, X. C., and Li, F. (1979). *New Diterpene Lactones of Tripterygium Wilfordii - Hypoglaucine and Triptolide CKunming Acta Bot. Yunnanica*. 29–36.

Xi, C., Peng, S., Wu, Z., Zhou, Q., and Zhou, J. (2017). Toxicity of Triptolide and the Molecular Mechanisms Involved. *Biomed. Pharmacother.* 90, 531–541. doi:10.1016/j.etap.2017.09.013

Xie, C. Q., Zhou, P., and Li, X. (2015). Research Progress on Chemical Constituents, Pharmacological Effects, and Clinical Application of Tripterygium Hypoglaucum. *Chin. Tradit. Herbal Drugs.* 46. 1996-2010. doi:10.7501/j.issn.0253-2670.2015.13.024

Xie, F. G., Li, C. J., Yang, J. Z., Luo, Y. M., and Zhang, D. M. (2012). Study on Chemical Constituents from the Root Bark of Tripterygium Hypoglaucum. *J. Chin. Med. Mater.* 35, 1083–1087. doi:10.13863/j.issn1001-4454.2012.07.023

Xie, L., Zhao, Y., Duan, J., Fan, S., Shu, L., Liu, H., et al. (2020). Integrated Proteomics and Metabolomics Reveal the Mechanism of Nephrotoxicity Induced by Triptolide. *Chem. Res. Toxicol.* 33, 1897–1906. doi:10.1021/acs.chemrestox.0c00091

Xu, H.-Y., Zhang, Y.-Q., Liu, Z.-M., Chen, T., Lv, C.-Y., Tang, S.-H., et al. (2019). ETCM: an Encyclopaedia of Traditional Chinese Medicine. *Nucleic Acids Res.* 47, D976–D982. doi:10.1093/nar/gky987

Xu, W., Ziqing, L., Yinrun, D., Xiaoyan, W., and Jinglun, X. (2004). Tripterygium Hypoglaucum (Level) Hutch Induces Aneuploidy of Chromosome 8 in Mouse Bone Marrow Cells and Sperm. *Mutagenesis* 19, 379–382. doi:10.1093/mutage/geh044

Xue, S., and Wu, T. (2008). Chinese Herbal Medicine Tripterygium Hypoglaucum Hutch Tablet for Facial Corticosteroid Addiction Dermatitis. *J. Altern. Complement. Med.* 14, 619. doi:10.1089/acm.2008.0142

Yan, G., Zhang, H., Wang, W., Li, Y., Mao, C., Fang, M., et al. (2017). Investigation of the Influence of Glycyrrhizin on the Pharmacokinetics of Celastrol in Rats Using LC-MS and its Potential Mechanism. *Xenobiotica* 47, 607–613. doi:10.1080/00498254.2016.1211773

Yan, Q., Li, Y., Fan, Y., Zhang, M., Yang, L., Yao, Y., et al. (2019). Protective Effect of Syringaresinol on Excitatory Damage Induced by Sodium Glutamate in SH-Sy5y Cells. *Chin. J. Exp. Tradit. Med. Formulae* 25, 76–82. doi:10.13422/j.cnki.syfjx.20191839

Yang, G., Wang, L., Yu, X., Huang, Y., Qu, C., Zhang, Z., et al. (2017). Protective Effect of 18β-Glycyrrhetinic Acid against Triptolide-Induced Hepatotoxicity in Rats. *Evid. Based. Complement. Alternat. Med.* 2017, 3470320. doi:10.1155/2017/3470320

Yang, L., Li, Y., Ren, J., Zhu, C., Fu, J., Lin, D., et al. (2014). Celastrol Attenuates Inflammatory and Neuropathic Pain Mediated by Cannabinoid Receptor Type 2. *Int. J. Mol. Sci.* 15, 13637–13648. doi:10.3390/ijms150813637

Yang, T., Wang, S., Zheng, H., Wang, L., Liu, D., Chen, X., et al. (2019). Understanding Dihydro-β-Agarofuran Sesquiterpenes from Tripterygium Hypoglaucum as the Modulators of Multi-Drug Resistance in HepG2/Adr Cells. *Biochem. Biophys. Res. Commun.* 508, 742–748. doi:10.1016/j.bbrc.2018.11.188

Yi, J. H., Yang, H., Zhang, Q. L., Pei, T. R., Chen, Z. Z., and Hu, Y. B., (1993). Studies on Chemical Constituents of Tripterygium Hypoglaucum. *Chin. Tradit. Herb. Drugs* 24, 398–400+446.

Yu, H., Shi, L., Zhao, S., Sun, Y., Gao, Y., Sun, Y., et al. (2016). Triptolide Attenuates Myocardial Ischemia/Reperfusion Injuries in Rats by Inducing the Activation of Nrf2/HO-1 Defense Pathway. *Cardiovasc. Toxicol.* 16, 325–335. doi:10.1007/s12012-015-9342-y

Yu, L., Wang, L., and Chen, S. (2010). Endogenous Toll-like Receptor Ligands and Their Biological Significance. *J. Cel. Mol. Med.* 14, 2592–2603. doi:10.1111/j.1582-4934.2010.01127.x

Yu, Y., Koehn, C. D., Yue, Y., Li, S., Thiele, G. M., Hearth-Holmes, M. P., et al. (2015). Celastrol Inhibits Inflammatory Stimuli-Induced Neutrophil Extracellular Trap Formation. *Curr. Mol. Med.* 15, 401–410. doi:10.2174/1566524015666150505160743

Yuan, S., Wang, L., Chen, X., Fan, B., Yuan, Q., Zhang, H., et al. (20202016). Corrigendum to "Triptolide Inhibits the Migration and Invasion of Human Prostate Cancer Cells via Caveolin-1/CD147/MMPs Pathway". *Biomed. Pharmacother.* 84, 1776–1782. doi:10.1016/j.biopha.2019.109782

Yuan, Z., Hasnat, M., Liang, P., Yuan, Z., Zhang, H., Sun, L., et al. (2019a). The Role of Inflammasome Activation in Triptolide-Induced Acute Liver Toxicity. *Int. Immunopharmacol.* 75, 105754. doi:10.1016/j.intimp.2019.105754

Yuan, Z., Zhang, H., Hasnat, M., Ding, J., Chen, X., Liang, P., et al. (2019b). A New Perspective of Triptolide-Associated Hepatotoxicity: Liver Hypersensitivity upon LPS Stimulation. *Toxicology* 414, 45–56. doi:10.1016/j.tox.2019.01.005

Zhang, J., Liu, S.-J., Hu, J.-H., Xu, M.-J., Liu, Z.-X., Zhou, L., et al. (2016). [LC-MS/MS Method for Determination of Tripterine in Plasma Pharmacokinetic Study in Beagles]. *Zhongguo Zhong Yao Za Zhi = Zhongguo Zhongyao Zazhi = China J. Chin. Mater. Med.* 41, 2727–2731. doi:10.4268/cjcmm20161426

Zhang, J., Shan, J., Chen, X., Li, S., Long, D., and Li, Y. (2018). Celastrol Mediates Th17 and Treg Cell Generation via Metabolic Signalling. *Biochem. Biophys. Res. Commun.* 497, 883–889. doi:10.1016/j.bbrc.2018.02.163

Zhang, L., and Zhang, Z. X., (1992). Studies on Chemical Constituents of Tripterygium Hypoglaucum. *Chinese Tradit. Herb. Drugs*. 23, 339–340+360+390.

Zhang, L., Zhang, Z. X., and An, D. K., (1998). Study on Ether Soluble Chemical Constituents of Tripterygium Hypoglaucum. *Chinese Tradit. Herb. Drugs* 35, 441–442. doi:10.3321/j.issn:0253-2670.2007.04.004

Zhang, R., Chen, Z., Wu, S.-S., Xu, J., Kong, L.-C., and Wei, P. (2019a). Celastrol Enhances the Anti-liver Cancer Activity of Sorafenib. *Med. Sci. Monit. Int. Med. J. Exp. Clin. Res.* 25, 4068–4075. doi:10.12659/MSM.914060

Zhang, X. M., Wang, C. F., and Wu, D. G. (1992a). *Aconitine Triterpenes from the Roots of Tripterygium Hypoglaucum*. Kunming Acta Bot. Yunnanica., 211–214.

Zhang, X. M., Wang, C. F., and Wu, D. G. (1992b). *Rosin Alkane Diterpenoids from the Roots of Tripterygium Hypoglaucum*. Kunming Acta Bot. Yunnanica. 319–322.

Zhang, X., Xue, X.-C., Wang, Y., Cao, F.-F., You, J., Uzan, G., et al. (2019b). Celastrol Reverses Palmitic Acid-Induced Insulin Resistance in HepG2 Cells via Restoring the miR-223 and GLUT4 Pathway. *Can. J. Diabetes* 43, 165–172. doi:10.1016/j.jcjd.2018.07.002

Zhang, Y., Mao, X., Li, W., Chen, W., Wang, X., Ma, Z., et al. (2021a). Tripterygium Wilfordii: An Inspiring Resource for Rheumatoid Arthritis Treatment. *Med. Res. Rev.* 41, 1337–1374. doi:10.1002/med.21762

Zhang, Y., Tang, Y., Luo, Y., Luo, L., Shen, F., and Huang, Z. (2021b). Triptolide Impairs Glycolysis by Suppressing GATA4/Sp1/PFKP Signalling axis in Mouse Sertoli Cells. *Toxicol. Appl. Pharmacol.* 425, 115606. doi:10.1016/j.taap.2021.115606

Zhang, Y. W., Fan, Y. S., Wang, X. D., Gao, W. Y., and Duan, H. Q. (2007). Diterpenoids with Immunosuppressive Activity from Tripterygium Hypoglaucum. *Chinese Tradit. Herb. Drugs* 38, 493–496. doi:10.3321/j.issn:0253-2670.2007.04.004

Zhao, P., Wang, H., Jin, D.-Q., Ohizumi, Y., Xu, J., and Guo, Y. (2014). Terpenoids from Tripterygium Hypoglaucum and Their Inhibition of LPS-Induced NO Production. *Biosci. Biotechnol. Biochem.* 78, 370–373. doi:10.1080/09168451.2014.890035

Zhao, Q., Li, H.-M., Chen, X.-Q., Li, R.-T., and Liu, D. (2018). Terpenoids from Tripterygium Hypoglaucum and Their Anti-inflammatory Activity. *Chem. Nat. Compd.* 54. doi:10.1007/s10600-018-2381-4

Zhen, Q. S., Ye, X., and Wei, Z. J. (1995). Recent Progress in Research on Tripterygium: a Male Antifertility Plant. *Contraception* 51, 121–129. doi:10.1016/0010-7824(94)00018-r

Zheng, H., Wang, L., Yang, T., Liu, D., Li, H.-M., Chen, X.-Q., et al. (2020). New Terpenoids and Lignans from the Twigs of Tripterygium Hypoglaucum. *Nat. Prod. Res.* 34, 1853–1861. doi:10.1080/14786419.2018.1564297

Zhong, J., Xian, D., Xu, Y., and Liu, J. (2011). Efficacy of Tripterygium Hypoglaucum Hutch in Adults with Chronic Urticaria. *J. Altern. Complement. Med.* 17, 459–464. doi:10.1089/acm.2009.0648

Zhou, H., Liu, Y., Wang, C., Liu, L., Wang, H., Zhang, Y., et al. (2018). Triptolide Inhibits Epstein-Barr Nuclear Antigen 1 Expression by Increasing Sensitivity of Mitochondria Apoptosis of Nasopharyngeal Carcinoma Cells. *J. Exp. Clin. Cancer Res.* 37, 192. doi:10.1186/s13046-018-0865-5

Zhou, J., Xi, C., Wang, W., Fu, X., Jinqiang, L., Qiu, Y., et al. (2014). Triptolide-induced Oxidative Stress Involved with Nrf2 Contribute to Cardiomyocyte Apoptosis through Mitochondrial Dependent Pathways. *Toxicol. Lett.* 230, 454–466. doi:10.1016/j.toxlet.2014.08.017

Zhou, X., Liu, Q., Zhou, X., Zhang, J., Liu, W., Zhao, X., et al. (2020). THH Relieves CIA Inflammation by Reducing Inflammatory-Related Cytokines. *Cell Biochem. Biophys.* 78, 367–374. doi:10.1007/s12013-020-00911-8

Zhu, H., Liu, X.-W., Ding, W.-J., Xu, D.-Q., Zhao, Y.-C., Lu, W., et al. (2010). Up-regulation of Death Receptor 4 and 5 by Celastrol Enhances the Anti-cancer Activity of TRAIL/Apo-2L. *Cancer Lett.* 297, 155–164. doi:10.1016/j.canlet.2010.04.030

Zhu, K.-J., Shen, Q.-Y., Cheng, H., Mao, X.-H., Lao, L.-M., and Hao, G.-L. (2005). Triptolide Affects the Differentiation, Maturation and Function of Human Dendritic Cells. *Int. Immunopharmacol.* 5, 1415–1426. doi:10.1016/j.intimp.2005.03.020

Zhuang, W. J., Fong, C. C., Cao, J., Ao, L., Leung, C. H., Cheung, H. Y., et al. (2004). Involvement of NF-kappaB and C-Myc Signalling Pathways in the Apoptosis of HL-60 Cells Induced by Alkaloids of Tripterygium Hypoglaucum (levl.) Hutch. *Phytomedicine* 11, 295–302. doi:10.1078/0944711041495128

Conflict of Interest: The authors declare that the research was conducted in the absence of any commercial or financial relationships that could be construed as a potential conflict of interest.

Publisher's Note: All claims expressed in this article are solely those of the authors and do not necessarily represent those of their affiliated organizations, or those of the publisher, the editors and the reviewers. Any product that may be evaluated in this article, or claim that may be made by its manufacturer, is not guaranteed or endorsed by the publisher.

GLOSSARY

17β-HSD 17β-hydroxysteroid dehydrogenase
2-HIB 2-hydroxyisobutyrate
2-HIV 2-hydroxyisovalerate
3β-HSD 3β-hydroxysteroid dehydrogenase
ABCA1 ATP-binding cassette transporter A1
AD Alzheimer's disease
aGVHD acute graft versus host disease
ALP alkaline phosphatase
ALT alanine aminotransfease
AML acute myeloid leukaemia
AMPKα Adenosine 5′-monophosphate (AMP)-activated protein kinase
APCs antigen presenting cells
APL acute promyelocytic leukemia
ARC hypothalamic arcuate nucleus
As_2O_3 arsenic trioxide
AST aspartate aminotransferase
ATL adult T-cell leukaemia/lymphoma
AUC Area Under Curve
Bcl-xL B-cell lymphoma-2
CD Crohn's disease
c-Fos Cellular oncogene fos
CIA collagen II-induced arthritis
c-Jun Cellular Jun
c-Myc cancer-Myc
COX cyclo-oxygen-ase
CPT1A Carnitine Palmitoyl transferase 1A
CRC colorectal carcinoma
Ctr calcitonin receptor
Ctsk cathepsin K
CXCL2 C-X-C motif ligand 2
DCs dendritic cells
Drp1 dynamin-related protein 1
EBV Epstein-Barr virus
ERK extracellular regulated protein kinases
Foxp3 Forkhead box P3
GA glycyrrhetinic acid
GCAFs gastric cancer-associated fibroblasts
GLUT1 glucose transporter 1
GLUT4 glucose transporter 4
GPx glutathione peroxidase;
GSH glutathione
HCV hepatitis C virus
HIF-1α hypoxia-inducible factor 1-α
HK2 hexokinase 2
HLA-DR human leukocyte antigen DR
HO-1 haem oxygenase-1
HSF1 heatshocktranscription factor 1
HSP70 Heat shock 70 kDa protein
HUVEC human umbilical vein endothelial cells
IFN-g interferon gamma
IKK IκB kinase
IL1R1 interleukin 1 receptor 1
IL-1β interleukin-1β
IL-6 interleukin-6
iNOS inducible Nitric Oxide Synthase (enzyme)
JNK1 c-Jun N-terminal kinase 1
LDH Lactic Dehydrogenase
LDL/VLDL low-density lipoprotein/very low-density lipoprotein
LPS lipopolysaccharide
MAPK mitogen-activated protein kinase
MCP monocyte chemotactic protein
MDA malondialdehyde
MDM2 murine double minute2
MDR multidrug resistance
MIP macrophage inflammatory protein
miR-96 microRNA-96
MLRs mixed lymphocyte reactions
Mmp-9 matrix metalloprotein 9
MMPs matrix metalloproteinases
MoDCs monocyte-derived DCs
mTOR mammalian target of Rapamycin
NAC N-acetylcysteine
NADPH nicotinamide adenine dinucleotide phosphate
NFATc nuclear factor activated T-cells
NF-κB nuclear factor kappa-B
NO nitric oxide
OPG osteoprotegerin
P450c17 cytochrome P450 17-hydroxylase
P450scc P450 side-chain cleavage enzyme
PARP poly ADP-ribose polymerase
PBMCs peripheral blood mononuclear cells
PC Pancreatic cancer
PFKP Phosphofructokinase Platelet
PGE2 prostaglandin E2
P-gp P-glycoprotein
PI3K phosphatidylinositol 3-kinase

PKC protein kinase C
PKCθ Protein Kinase C θ
PLC phospholipase C
proMMP-1 pro-matrix metalloproteinase-1
PTP protein tyrosine phosphatase
RA rheumatoid arthritis
RANKL receptor activator of NF-κB ligand
RNS reactive nitrogen species
ROS reactive oxygen species
SOD superoxide dismutase
StAR steroidogenic acute regulatory protein
STAT signal transducers and activators of transcription
TAB1 TAK1 binding protein
TAK1 transforming growth factor β-activated kinase 1
TAs Tripterygium agents
TCM Traditional Chinese medicine
TCPTP T cell PTP
THH Tripterygium hypoglaucum (Lévl.) Hutch.
TLR Toll-like receptors
TNF-α tumour necrosis factor-α
TRAIL TNF-related apoptosis-inducing ligand
TRAP tartrate-resistant acid phosphatase
Tregs T regulatory cells
TwHF Tripterygium wilfordii Hook F.
VEGF vascular endothelial growth factor
XIAP X-linked inhibitor of apoptosis protein

frontiers in Pharmacology

ORIGINAL RESEARCH
published: 11 January 2022
doi: 10.3389/fphar.2021.801910

Anti-Gout Effects of the Medicinal Fungus *Phellinus igniarius* in Hyperuricaemia and Acute Gouty Arthritis Rat Models

Hongxing Li[1,2], *Xinyue Zhang*[1,2], *Lili Gu*[1,2], *Qín Li*[1,2], *Yue Ju*[1,2], *Xuebin Zhou*[1,2], *Min Hu*[1,2] *and Qīn Li*[1,2]*

[1]School of Pharmacy, Hangzhou Medical College, Hangzhou, China, [2]Key Laboratory of Neuropsychiatric Drug Research of Zhejiang Province, Hangzhou Medical College, Hangzhou, China

Background: *Phellinus igniarius* (*P. igniarius*) is an important medicinal and edible fungus in China and other Southeast Asian countries and has diverse biological activities. This study was performed to comparatively investigate the therapeutic effects of wild and cultivated *P. igniarius* on hyperuricaemia and gouty arthritis in rat models.

Methods: UPLC-ESI-qTOF-MS was used to identify the chemical constituents of polyphenols from wild *P. igniarius* (WPP) and cultivated *P. igniarius* (CPP). Furthermore, WPP and CPP were evaluated in an improved hyperuricaemia rat model induced by yeast extract, adenine and potassium oxonate, which was used to examine xanthine oxidase (XO) activity inhibition and anti-hyperuricemia activity. WPP and CPP therapies for acute gouty arthritis were also investigated in a monosodium urate (MSU)-induced ankle swelling model. UHPLC-QE-MS was used to explore the underlying metabolic mechanisms of *P. igniarius* in the treatment of gout.

Results: The main active components of WPP and CPP included protocatechuic aldehyde, hispidin, davallialactone, phelligridimer A, hypholomine B and inoscavin A as identified by UPLC-ESI-qTOF-MS. Wild *P. igniarius* and cultivated *P. igniarius* showed similar activities in reducing uric acid levels through inhibiting XO activity and down-regulating the levels of UA, Cr and UN, and they had anti-inflammatory activities through down-regulating the secretions of ICAM-1, IL-1β and IL-6 in the hyperuricaemia rat model. The pathological progression of kidney damage was also reversed. The polyphenols from wild and cultivated *P. igniarius* also showed significant anti-inflammatory activity by suppressing the expression of ICAM-1, IL-1β and IL-6 and by reducing the ankle joint swelling degree in an MSU-induced acute gouty arthritis rat model. The results of metabolic pathway enrichment indicated that the anti-hyperuricemia effect of WPP was mainly related to the metabolic pathways of valine, leucine and isoleucine biosynthesis and

OPEN ACCESS

Edited by:
Lucia Recinella,
University of Studies G. d'Annunzio Chieti and Pescara, Italy

Reviewed by:
Xianju Huang,
South-Central University for Nationalities, China
Claudio Ferrante,
University of Studies G. d'Annunzio Chieti and Pescara, Italy

***Correspondence:**
Qīn Li
2020000301@hmc.edu.cn

Specialty section:
This article was submitted to Ethnopharmacology, a section of the journal Frontiers in Pharmacology

Received: *26 October 2021*
Accepted: *16 December 2021*
Published: *11 January 2022*

Citation:
Li H, Zhang X, Gu L, Li Q, Ju Y, Zhou X, Hu M and Li Q (2022) Anti-Gout Effects of the Medicinal Fungus Phellinus igniarius *in Hyperuricaemia and Acute Gouty Arthritis Rat Models. Front. Pharmacol. 12:801910. doi: 10.3389/fphar.2021.801910*

Abbreviations: *P. igniarius*, *Phellinus igniarius*; WPP, polyphenols from wild *P. igniarius*; CPP, polyphenols from cultivated *P. igniarius*; XO, xanthine oxidase; MSU, monosodium urate; UA, uric acid; Cr, creatinine; UN, urea nitrogen; QC, quality control; ESI^+, positive ion mode; ESI^-, negative ion mode; PCA, principal component analysis; OPLS-DA, orthogonal projections to latent structures-discriminate analysis; VIP, value of variable importance in the projection.

histidine metabolism. Additionally, the anti-hyperuricemia effect of CPP was mainly related to nicotinate and nicotinamide metabolism and beta-alanine metabolism.

Conclusions: Wild *P. igniarius* and cultivated *P. igniarius* both significantly affected the treatment of hyperuricaemia and acute gouty arthritis models *in vivo* and therefore may be used as potential active agents for the treatment of hyperuricaemia and acute gouty arthritis.

Keywords: *Phellinus igniarius*, hyperuricaemia, monosodium urate, gouty arthritis, metabolomics

INTRODUCTION

Gout is a long-term and recurrent metabolic disease characterized by purine metabolism disorders and/or uric acid metabolism imbalances, and it can be caused by genetic factors that make individuals more susceptible (genetics-environment interactions) or by unhealthy diets (Pascual et al., 2015; Robinson 2018; Punzi et al., 2019; Zhu et al., 2021). The pathogenesis of hyperuricaemia is further promoted by the excessive consumption of purines and increased synthesis or decreased excretion of uric acids. Under increased blood uric acid levels in hyperuricaemia, monosodium urate (MSU) crystal/tophi deposits within intra- and/or peri-articular areas further induce excruciating pain and chronic inflammatory responses that may lead to joint structure damage, named gouty arthritis or gout (Perez-Ruiz et al., 2015; Dhanasekar and Rasool 2016). Gout occurs in approximately 1–4% of the general population, and the prevalence may even be up to 10% in a few countries (Ragab et al., 2017; Elfishawi et al., 2018; Pascart and Lioté 2019). Furthermore, the global incidences of gout are increasing due to poor dietary habits, insufficient exercises and metabolic syndrome, which will likely lead to increasing medical treatment costs (Singh 2013; Dehlin et al., 2020).

Some effective gout therapy treatments based on the pathogenesis of gout include inflammation reduction, pain relief, and improved joint function achieved by reducing the levels of UA in serum/urine and dissolving MSU crystals (Martinon 2010; Kapoor et al., 2011; Sokolove and Lepus 2013; Hainer et al., 2014). Commonly prescribed hyperuricaemia medications, such as allopurinol, febuxostat, probenecid and benzbromarone, aim at reducing uric acid production or increasing uric acid excretion, and prescribed gouty arthritis medications, such as colchicine, nonsteroidal anti-inflammatory drugs (NSAIDs), corticosteroids and analgesic drugs, aim at suppressing joint inflammation progression and relieving pain (Fam 2001; Niel and Scherrmann 2006; Aran et al., 2011; Neogi 2011; Becker et al., 2015). However, some adverse effects of the agents above have been reported, such as skin rash, hypersensitivity, gastrointestinal bleeding, gastrointestinal toxicity (nausea, vomiting, diarrhea), renal/hepatic toxicity, anemia, coma and even death (Ben-Chetrit and Levy 1998; Rostom et al., 2002; Terkeltaub 2009; Le Graverand-Gastineau 2010; Crofford 2013). Therefore, it is thus necessary to focus our research on the discovery of new alternative agents, such as natural herbal medicinal sources, with fewer or reduced side effects and greater efficacy and safety for the prevention and treatment of gout.

Phellinus igniarius (DC. Ex Fr.) Quel (*P. igniarius*), which belongs to the Polyporaceae family, is a perennial medicinal and edible fungus (Wu et al., 2019) that prefers to hosts the stems of aspen, robur, and birch in the wild (Mo et al., 2004; Wu et al., 2010). *P. igniarius*, which is referred to as "Sanghuang" in China, is widely consumed as a health care product for adjunct therapies or as preventive measures (Zhen-ting and Hai-ying 2016). *P. igniarius* has been used for the treatment of bellyache, fester and bloody gonorrhea in traditional Chinese medicine for thousands of years (Wang et al., 2005b). In several folk herbal medicine formulas or recipes, *P. igniarius* is used to treat stomach aches and arthritis (Zheng et al., 2018). Bioactive components from *P. igniarius*, such as flavones, polyphenols, polysaccharides or different extracts, have been reported to possess antiviral (Lee et al., 2013), anti-inflammatory (Sun et al., 2018), antioxidative (Wang et al., 2005b; Zhang et al., 2014), antitumor (Hsin et al., 2017), and immunomodulatory activities (Gao et al., 2017).

Considering the protective effects of *P. igniarius* and its anti-inflammatory and antioxidative activities, this study was designed to investigate the anti-hyperuricaemia and anti-gouty arthritis effects of *P. igniarius* in a rat model. In addition, the development and utilization of *P. igniarius* as a medicinal fungal resource has been restricted because its high medicinal value and the insufficient supply of wild-sourced *P. igniarius* result in it being very expensive. Fortunately, artificial cultivation is a practical way to efficiently obtain *P. igniarius* fruit. However, comparative studies of wild and cultivated *P. igniarius* have not been reported. One of the other goals of this study was to comparatively evaluate the efficacy of wild *P. igniarius* and cultivated *P. igniarius* in the treatment of hyperuricaemia and gouty arthritis.

In this study, we systematically characterized the chemical components of polyphenols from wild and cultivated *P. igniarius* and examined the uric acid-lowering effects in a hyperuricaemia rat model and the anti-inflammatory effects in an acute gouty arthritis rat model. The underlying metabolic mechanism of *P. igniarius* on gout was further investigated by UHPLC-QE-MS for urine metabolomics analysis.

MATERIALS AND METHODS

Plant Material

Wild *P. igniarius* samples were purchased from Zhejiang Qiandao Lake Sangdu Edible Fungus Professional Cooperative (Hangzhou, China). The cultivated *P. igniarius* was an artificially cultivated strain from wild *P. igniarius* named "*Zhehuang No. 1*", which was also provided by Zhejiang Qiandao Lake Sangdu Edible Fungus Professional Cooperative (Hangzhou, China) and was identified as *Phellinus igniarius* by the Horticulture Institute of Zhejiang Academy of Agricultural Sciences and Institute of Edible Fungi of Shanghai Academy of Agricultural Sciences. All samples were stored in a dark environment with a consistent temperature and humidity.

Preparation of Polyphenols From *P. igniarius*

By referencing the polyphenol contents and following scientific principles and environmental protection protocols, response surface methodology was used to determine the optimal parameters for the extraction and purification of polyphenols from *P. igniarius*. Specifically, the dried fruit body of *P. igniarius* was crushed and passed through a 40-mesh screen. The powder was soaked in 70% ethanol for 30 min, extracted with 16-fold 70% ethanol for 2 h at 80°C in the dark and was filtered. The residue was re-extracted under the same conditions. These two filtrates were combined, and the solvent was removed under negative pressure at 60°C without light to yield the ethanol extract of wild *P. igniarius* and cultivated *P. igniarius*. Afterwards, the crude extract solution was adsorbed by the HP20 macroporous resin, impurities were removed with 10% ethanol at 5 times the solution volume and then eluted with 40% ethanol at 5 times the solution volume. The eluates were collected and pooled and then freeze-dried into a powder. The polyphenols from wild *P. igniarius* (WPP) and cultivated *P. igniarius* (CPP) were prepared sequentially, kept in the light and stored at −20°C. The Folin-Ciocalteu method is used to determine the concentration of total polyphenols.

UPLC-ESI-qTOF-MS Analysis of the Constituents From Wild *P. igniarius* and Cultivated *P. igniarius*

WPP (10 mg) and CPP (10 mg) were dissolved in methanol (10 ml) under an ultrasound. The supernatant was separated by centrifugation at 10,000 rpm for 10 min and transferred into a sample bottle for testing.

UPLC-ESI-qTOF-MS analyses were performed using UPLC system (Waters) with an ACQUITY UPLC BEH C18 column (100 × 2.1 mm, 1.7 μm). The column temperature was 40°C, injection volume was 5 μL and flow rate was 0.35 ml/min. A 0.1% formic acid-water (v: v) solution was used as mobile phase A, and 0.1% formic acid-acetonitrile (v: v) was used as mobile phase B. The gradient elution conditions were set as follows: 0–2 min: 10% B; 2–26 min, 10%–90% B; 26–28 min, 90% B; 28–29 min, 90%–10% B; 29–30 min, 10% B.

A Waters Synapt G2 Q-TOF system (Waters Manchester, United Kingdom) equipped with an ESI ion source that operated in both the positive ion mode (ESI^+) and negative ion mode (ESI^-). The ESI source parameters were set as follows: a source temperature of 120°C, desolvation temperature of 350°C, and electrospray capillary voltage of 3.0 kV for the positive ionization mode and −2.5 kV for negative ionization mode. The cone voltage was set at 30 V. Argon and nitrogen were used as collision and cone gases, respectively. The cone and desolvation gas flows were 80 L/h and 800 L/h, respectively. A scan time of 0.2 s with an intrascan time of 0.1 s was utilized. The collision energy was set at 15–30 V, and the collision gas flow was set at 0.4. A lock-mass of leucine enkephalin was used for the positive ion mode ($[M + H]^+$ = 556.2771) and the negative ion mode ($[M-H]^-$ = 554.2615) employed at a flow rate of 5 μL/min through a lockspray interface. The mass spectrometric data were collected from *m/z* 100 to 1,000 in the positive and negative ion modes under the centroid mode.

MassLynx V4.1 software (Waters Corporation) was used to process the data. Manual identification was performed to characterize the chemical constituents from WPP and CPP by comparing the exact mass and fragmentation pattern of the compounds that were previously reported in articles.

Animals

Male SD rats (8 weeks, 180–220 g) were obtained from Zhejiang Laboratory Animal Center (licence No. SYXK 2016–0022). All rats were housed in clean plastic cages and maintained at 23 ± 1°C with 55% relative humidity, a 12-h light/dark cycle (7:00–19:00) and *ad libitum* access to pure water and standard rat pellets. The protocol of the study was reviewed and approved by the Animal Ethics Committees of Hangzhou Medical College. All experiments, including animal breeding, experimental operations, and animal euthanasia, were performed in accordance with the guidelines established by the committee.

Establishment of a Rat Hyperuricaemia Model and Drug Administration

The experimental design was performed as described in previous studies with some modifications (Li et al., 2017). Fifty male SD rats were randomly divided into five groups (n = 10) and orally administered an equal 10 ml/kg dose of a normal saline solution (the control group and model group), 10 mg/kg allopurinol (Macklin Biochemical Technology Co., Ltd., China) (the positive control group), 150 mg/kg polyphenols from wild *P. igniarius* (the WPP-treated group) and 150 mg/kg polyphenols from cultivated *P. igniarius* (the CPP-treated group) for 7 days. Yeast extract (Beyotime Biochemical Technology Co., Ltd., China) (10 g/kg) and adenine (Macklin Biochemical Technology Co., Ltd., China) (100 mg/kg) were gavaged 12 h prior to allopurinol, WPP, and CPP administration every day except for the control group. The model group, positive control group, WPP-treated group and CPP-treated group were intraperitoneally injected with potassium oxonate (Yuanye Biochemical Technology Co., Ltd., China) (300 mg/kg) on days 1, 3, and 7, while the control group was injected with an equal volume of vehicle (0.5% CMC-Na).

Establishment of a Rat Acute Gouty Arthritis Model and Drug Administration

Fifty male SD rats were randomly divided into five groups (n = 10): the control group, model group, positive control group, WPP-treated group and CPP-treated group. The animals in the WPP-treated group, CPP-treated group and positive control group were treated orally with WPP (150 mg/kg), CPP (150 mg/kg) or colchicine (Shanghai Aladdin Biochemical Technology Co., Ltd., China) (0.3 mg/kg) for 7 days. The animals in the control group and model group were treated orally with vehicle (a normal saline solution; 10 ml/kg). On the 8th day, an acute gouty arthritis model was induced by performing intra-articular injections of a MSU (Sigma-Aldrich, United States) suspension (25 mg/ml; 50 μL) into the right ankle of rats in the model group, positive control group, WPP-treated group and CPP-treated group under anesthesia. The contralateral bulge of the joint capsule was regarded as the criterion for successful injection. The MSU suspension in the control group was replaced by the vehicle (95% normal saline solution + 5% Tween 80; 50 μL) suspension. Establishment of the acute gouty arthritis model was roughly considered successful if there was obvious swelling 2 h after MSU injection.

Biochemical Samples Collection and Analysis

Blood samples were collected from the femoral artery of anaesthetized rats by intraperitoneal injection of 10% chloral hydrate (0.3 ml/100 g) on the morning of the 8th day. All blood samples were placed at room temperature for 30 min, and the serum was separated by centrifugation at 3,000 rpm for 10 min at 4°C. All serum samples were stored at −80°C until analysis.

Urine samples were collected during a 12 h period from the evening of the 7th day using metabolic cages. The samples were then centrifuged (4°C, 1,000 rpm, 5 min) to remove particulate contaminants. The supernatants were transferred and stored at −80°C until analysis. The hair around the right ankle joint of the rat was shaved, and the ankle joint capsule was incised along the center of the ankle joint with a scalpel. A normal saline solution was used to repeatedly flush the joint cavity to collect ankle joint synovial fluid. The samples were centrifuged at 1,000 rpm for 20 min at 4°C. The supernatants were transferred and stored at −80°C until analysis.

Evaluations of the ICAM-1, IL-1β and IL-6 levels in the serum and synovial fluid were performed using commercial enzyme-linked immunosorbent assay kits (Enzyme-linked Biotechnology Co., Ltd., Shanghai, China). The levels of uric acid (UA), creatinine (Cr) and urea nitrogen (UN) in the serum and urine were determined by the colorimetric method using different commercial assay kits (Jiancheng Biotechnology Institute, Nanjing, China) according to the manufacturer's instructions.

Swelling Degree Measurement

Ankle oedema was evaluated as an increase in the injected ankle thickness in millimeters (mm) and measured using a digital caliper at the same position, which was marked with a black pen. Right ankle joint oedema was calculated as the difference between the basal value and the test value observed at different time points after the MSU suspension was injected (0, 2, 6, 12, 24, 36, 48 h). The whole measurement process was conducted by only one experimenter to ensure the measurements were accurate.

Swelling degree (%) = [thickness test value (mm)- thickness basal value (mm)]/thickness basal value (mm) × 100%.

Evaluation of Xanthine Oxidase Activity *in vivo*

The liver tissue (100 mg) of each rat was mixed with cold normal saline solution (900 μL) to prepare a 10% liver tissue homogenate. The homogenate samples were centrifuged at 3,500 rpm for 10 min at 4°C. The supernatants were transferred and stored at −80°C until analysis. Part of the supernatant was mixed with 9 times the amount of normal saline solution to prepare a 1% liver tissue homogenate. The absorbance value of 10% liver tissue homogenate and the total protein content of 1% liver tissue homogenate were determined using commercial assay kits (Jiancheng Biotechnology Institute, Nanjing, China) according to the manufacturer's instructions to calculate XO activity.

Histopathological Studies

In the hyperuricaemia models, the kidneys were quickly removed from anaesthetized rats by chloral hydrate, fixed in a buffered 4% paraformaldehyde solution for 24 h, and embedded in paraffin. Finally, paraffin sections (5 μm) were cut and stained with hematoxylin and eosin (H&E).

UHPLC-QE-MS for Urine Metabolomics Analysis

Metabolite Extraction

Each urine sample (1 ml) was added to 10 μL of NaN_3 solution (0.5 mg/L) and quenched in liquid nitrogen for 10 s. Two hundred microliters of extract solution (acetonitrile: methanol = 1:1) containing an isotopically labelled internal standard mixture was added to 50 μL of sample. After vortexing for 30 s, the samples were sonicated for 10 min in an ice-water bath and incubated at −40°C for 1 h to precipitate the proteins. Then, the samples were centrifuged at 12,000 rpm for 15 min at 4°C. The supernatant was transferred to a fresh glass vial for analysis. The quality control (QC) samples were prepared by mixing all the samples in equal aliquots.

UHPLC-QE-MS Analysis

The instrument settings for the UHPLC-QE-MS system were the same as previously described (He et al., 2020). The UHPLC separation process was performed using UHPLC system (Vanquish, Thermo Fisher Scientific) equipped with a UPLC BEH Amide column (2.1 × 100 mm, 1.7 μm) coupled to a Q Exactive HFX mass spectrometer (Orbitrap MS, Thermo). Ammonium acetate (25 mmol/L) and ammonia hydroxide (25 mmol/L) in water (pH = 9.75) were used for mobile phase A, and acetonitrile was used for mobile phase B. The injection volume was 3 μL, and the autosampler temperature was 4°C.

The QE HFX mass spectrometer was chosen for its ability to acquire MS/MS spectra in the information-dependent acquisition mode utilizing the acquisition software controls (Xcalibur, Thermo). In this mode, the acquisition software continuously evaluates the full scan MS spectrum. The electrospray ionization (ESI) source was set to the positive mode (ESI^+) and negative mode (ESI^-). The sheath gas flow rate and Aux gas flow rate were 30 Arb and 25 Arb, respectively. The capillary temperature was 350°C. The full MS resolution and MS/MS resolution were set to 60,000 and 7,500, respectively. The collision energy was set as 10/30/60 in the NCE mode. The spray voltage was set to 3.6 kV (positive) or −3.2 kV (negative).

Data Annotation, Multivariate Statistical Analysis and Metabolic Pathway Analysis

The raw data, including information such as peak detection, extraction, alignment, and integration, were programmatically converted to the mzXML format and then ordered to perform metabolic annotations. The final datasets were imported into the SIMCA V15.0.2 software package (Sartorius Stedim Data Analytics AB, Umea, Sweden) for logarithmic conversion and centralized formatting processing. To visualize group separation and find significantly changed metabolites, principal component analysis (PCA) and orthogonal projections to latent structures-discriminate analysis (OPLS-DA) were carried out sequentially. The value of variable importance in the projection (VIP) was calculated in the OPLS-DA analysis.

Metabolites between the two groups with $p < 0.05$ (Student's t-test) and VIP >1 were considered differential metabolites for subsequent analysis. The up- and down-regulation of differential metabolites were visualized by volcano plots. The differential metabolites obtained were subjected to pathway enrichment analysis in the KEGG database (http://www.genome.jp/kegg/) and MetaboAnalyst (http://www.metaboanalyst.ca/) to find the key metabolic pathways with the highest correlation, which further revealed the related metabolic mechanism of wild and cultivated *Phellinus igniarius* in the treatment of hyperuricaemia.

Statistical Analysis

GraphPad Prism V8.3.0 software was used for the statistical analysis and data visualization. Multiple comparisons of data between groups were performed by one-way ANOVA or two-way ANOVA. The data are expressed as the mean ± standard deviation (SD), and $p < 0.05$ was considered statistically significant.

RESULTS

Chemical Composition of Wild *P. igniarius* and Cultivated *P. igniarius*

The concentration of total polyphenols in WPP is 498.21 ± 22.07 μg/mg (n = 3) and the concentration of total polyphenols in CPP is 346.36 ± 26.23 μg/mg (n = 3). The response values of different chemical compositions differ in the negative ion mode and positive ion mode. Based on the UPLC-ESI-qTOF-MS chromatogram of WPP and CPP, good separations were achieved within 30 min. By comparing the retention time (t_R), exact mass and fragmentation patterns that were reported in the literature, 12 compounds were identified from WPP (**Figures 1A, C**), 13 compounds were identified from CPP (**Figures 1B, D**), and their results are shown in **Tables 1–4**. Among them, the compounds confirmed by comparison with the chemical reference

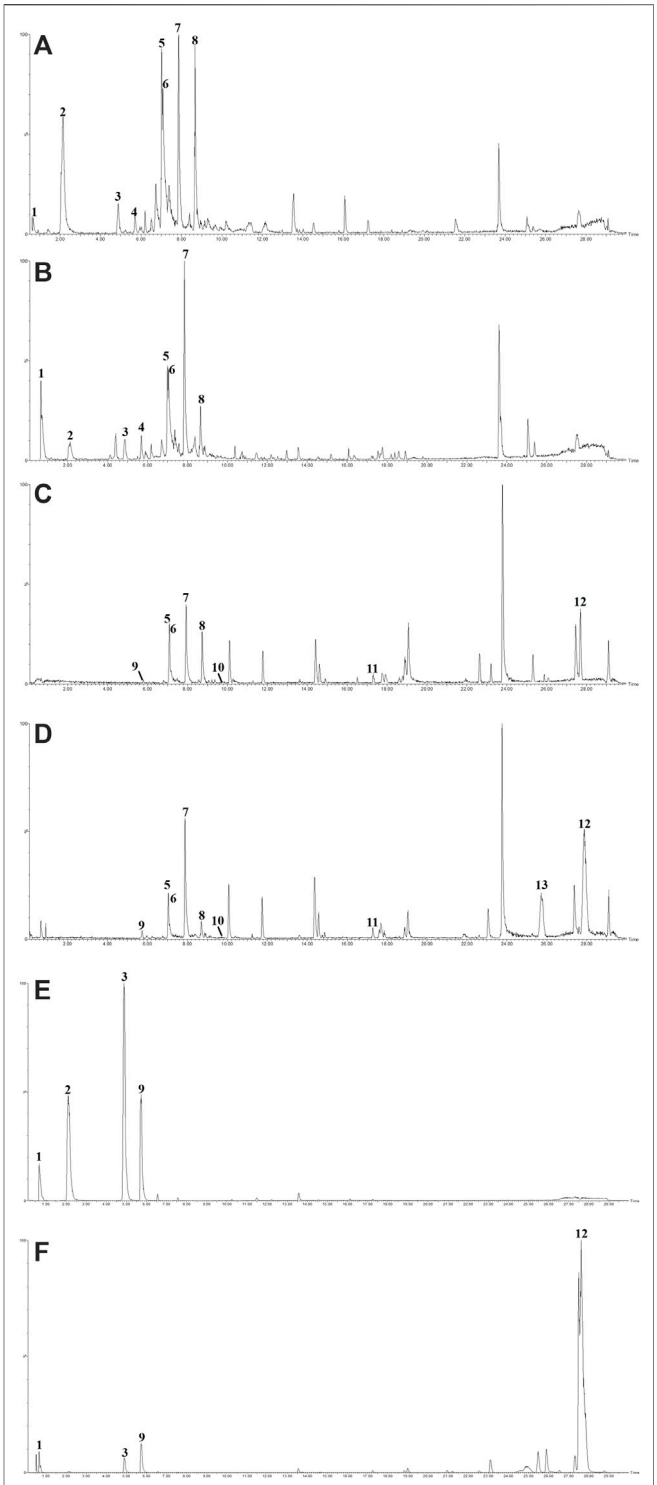

FIGURE 1 | The BPIs of WPP by UPLC-ESI-qTOF-MS analysis in ESI^- **(A)** and ESI^+ **(C)**, the BPIs of CPP by UPLC-ESI-qTOF-MS analysis in ESI^- **(B)** and ESI^+ **(D)** and the BPIs of five mixed standards by UPLC-ESI-qTOF-MS analysis in ESI^- **(E)** and ESI^+ **(F)**.

TABLE 1 | Characterization of the chemical constituents in WPP by UPLC-ESI-qTOF-MS (NEG).

No	t_R (min)	$[M-H]^-$ Formula	$[M-H]^-$ *m/z*	ppm	Identity	References
1▲	0.670	$C_{12}H_{21}O_{11}$	341.1084	1.5	Sucrose	Zhao et al. (2018)
2▲	2.146	$C_7H_5O_3$	137.0239	0	Protocatechuic aldehyde	Dong et al. (2015); Wang et al. (2021)
3▲	4.980	$C_{10}H_9O_3$	177.0552	0.6	Osmundacetone	Dong et al. (2015); Wang et al. (2021)
4	5.908	$C_{12}H_9O_4$	217.0501	2.8	Inotilone	Dong et al. (2015)
5	7.042	$C_{25}H_{19}O_9$	463.1029	0.6	Davallialactone	Dong et al. (2015)
6	7.053	$C_{52}H_{31}O_{20}$	975.1409	0.2	Phelligridimer A	Dong et al. (2015); Wang et al. (2005b)
7	7.875	$C_{26}H_{17}O_{10}$	489.0822	–3.1	Hypholomine B	Dong et al. (2015); Wang et al. (2021)
8	8.741	$C_{25}H_{17}O_9$	461.0873	–1.5	Inoscavin A	Dong et al. (2015); Wang et al. (2021); Zhao et al. (2018)

TABLE 2 | Characterization of the chemical constituents in CPP by UPLC-ESI-qTOF-MS (NEG).

No	t_R (min)	$[M-H]^-$ Formula	$[M-H]^-$ *m/z*	ppm	Identity	References
1▲	0.757	$C_{12}H_{21}O_{11}$	341.1084	0.6	Sucrose	Zhao et al. (2018)
2▲	2.146	$C_7H_5O_3$	137.0239	–1.5	Protocatechuic aldehyde	Dong et al. (2015); Zhao et al. (2018)
3▲	4.859	$C_{10}H_9O_3$	177.0552	–3.4	Osmundacetone	Dong et al. (2015); Wang et al. (2021)
4	5.928	$C_{12}H_9O_4$	217.0501	–3.7	Inotilone	Dong et al. (2015)
5	7.008	$C_{25}H_{19}O_9$	463.1029	4.5	Davallialactone	Dong et al. (2015)
6	7.136	$C_{52}H_{31}O_{20}$	975.1409	1.3	Phelligridimer A	Wang et al. (2005b); Dong et al. (2015)
7	7.863	$C_{26}H_{17}O_{10}$	489.0822	–1.6	Hypholomine B	Dong et al. (2015); Wang et al. (2021)
8	8.644	$C_{25}H_{17}O_9$	461.0873	–1.3	Inoscavin A	Dong et al. (2015); Wang et al. (2021); Zhao et al. (2018)

TABLE 3 | Characterization of the chemical constituents in WPP by UPLC-ESI-qTOF-MS (POS).

No	t_R (min)	$[M + H]^+$ Formula	$[M + H]^+$ *m/z*	ppm	Identity	References
9▲	5.787	$C_{13}H_{11}O_5$	247.0606	–1.2	Hispidin	Dong et al. (2015)
5	7.096	$C_{25}H_{21}O_9$	465.1186	1.3	Davallialactone	Dong et al. (2015)
6	7.172	$C_{52}H_{33}O_{20}$	977.1565	0.5	Phelligridimer A	Dong et al. (2015); Wang et al. (2005b)
7	7.936	$C_{26}H_{19}O_{10}$	491.0978	–0.2	Hypholomine B	Dong et al. (2015); Wang et al. (2021)
8	8.733	$C_{25}H_{19}O_9$	463.1029	–4.1	Inoscavin A	Dong et al. (2015); Wang et al. (2021); Zhao et al. (2018)
10	9.777	$C_{33}H_{21}O_{13}$	625.0982	–3.2	Phelligridin I	Wang et al. (2007)
11	17.312	$C_{15}H_{23}O_2$	235.1698	–4.3	Phellinone	Zhao et al. (2018)
12	27.697	$C_{22}H_{44}NO$	338.3423	–0.6	Erucic amide	Zhao et al. (2018)

standards are marked with the symbol "▲" in **Tables 1–4**, and the results are shown in **Figures 1E, F**. 12 compounds, including sucrose, protocatechuic aldehyde, osmundacetone, inotilone, davallialactone, phelligridimer A, hypholomine B, inoscavin A, hispidin, phelligridin I, phellinone, and erucic amide, were identified from both WPP and CPP, which showed that WPP and CPP have similar compound spectra. In addition, area normalization analysis at 280 nm was performed, and the peak area ratio of the main compounds identified in WPP (75.03%) and CPP (72.11%) unanimously exceeded 70%, indicating that the compounds identified were the main active ingredients of WPP and CPP.

Effects of Wild *P. igniarius* and Cultivated *P. igniarius* on Hyperuricaemia

Uric acid, the culprit of hyperuricaemia, is used clinically to evaluate the quality of kidney function coupled with Cr and UN. As shown in **Figure 2A**, marked increase with significant difference ($p < 0.05$) in the levels of UA, Cr and UN was observed in the serum and urine of hyperuricaemia rats compared with that observed in the control group, indicating that the synthesis of uric acid was increased and the kidney damage was aggravated. Conversely, compared with the model group, the drug group treated orally with WPP (150 mg/kg) and CPP (150 mg/kg) showed significant decreases in the levels of UA, Cr and UN in the serum and urine ($p < 0.05$).

The ICAM-1, IL-1β and IL-6 levels were measured to evaluate the anti-inflammatory effects of WPP and CPP on the treatment of hyperuricaemia. **Figure 3** clearly shows that the combination of yeast extract, adenine and potassium oxonate in the model group significantly elevated the levels of ICAM-1 ($p < 0.001$), IL-1β and IL-6 ($p < 0.01$) in serum. Treatment with colchicine (0.3 mg/kg) significantly decreased ($p < 0.001$) the levels of ICAM-1, IL-1β and IL-6

TABLE 4 | Characterization of the chemical constituents in CPP by UPLC-ESI-qTOF-MS (POS).

No	t_R (min)	[M + H]$^+$ Formula	[M + H]$^+$ *m/z*	ppm	Identity	References
9▲	5.777	$C_{13}H_{11}O_5$	247.0606	2.4	Hispidin	Dong et al. (2015)
5	7.074	$C_{25}H_{21}O_9$	465.1186	0	Davallialactone	Dong et al. (2015)
6	7.117	$C_{52}H_{33}O_{20}$	977.1565	−2.1	Phelligridimer A	Dong et al. (2015); Wang et al. (2005b)
7	7.883	$C_{26}H_{19}O_{10}$	491.0978	−1	Hypholomine B	Dong et al. (2015); Wang et al. (2021)
8	8.702	$C_{25}H_{19}O_9$	463.1029	−2.8	Inoscavin A	Dong et al. (2015); Wang et al. (2021); Zhao et al. (2018)
10	9.671	$C_{33}H_{21}O_{13}$	625.0982	1.4	Phelligridin I	Wang et al. (2007)
11	17.275	$C_{15}H_{23}O_2$	235.1698	−2.6	Phellinone	Zhao et al. (2018)
13	25.760	$C_{28}H_{41}O$	393.3157	−1.5	Ergosta-4,6,8,22-Tetraen-3-One	Zhao et al. (2018)
12▲	27.601	$C_{22}H_{44}NO$	338.3423	0.3	Erucic amide	Zhao et al. (2018)

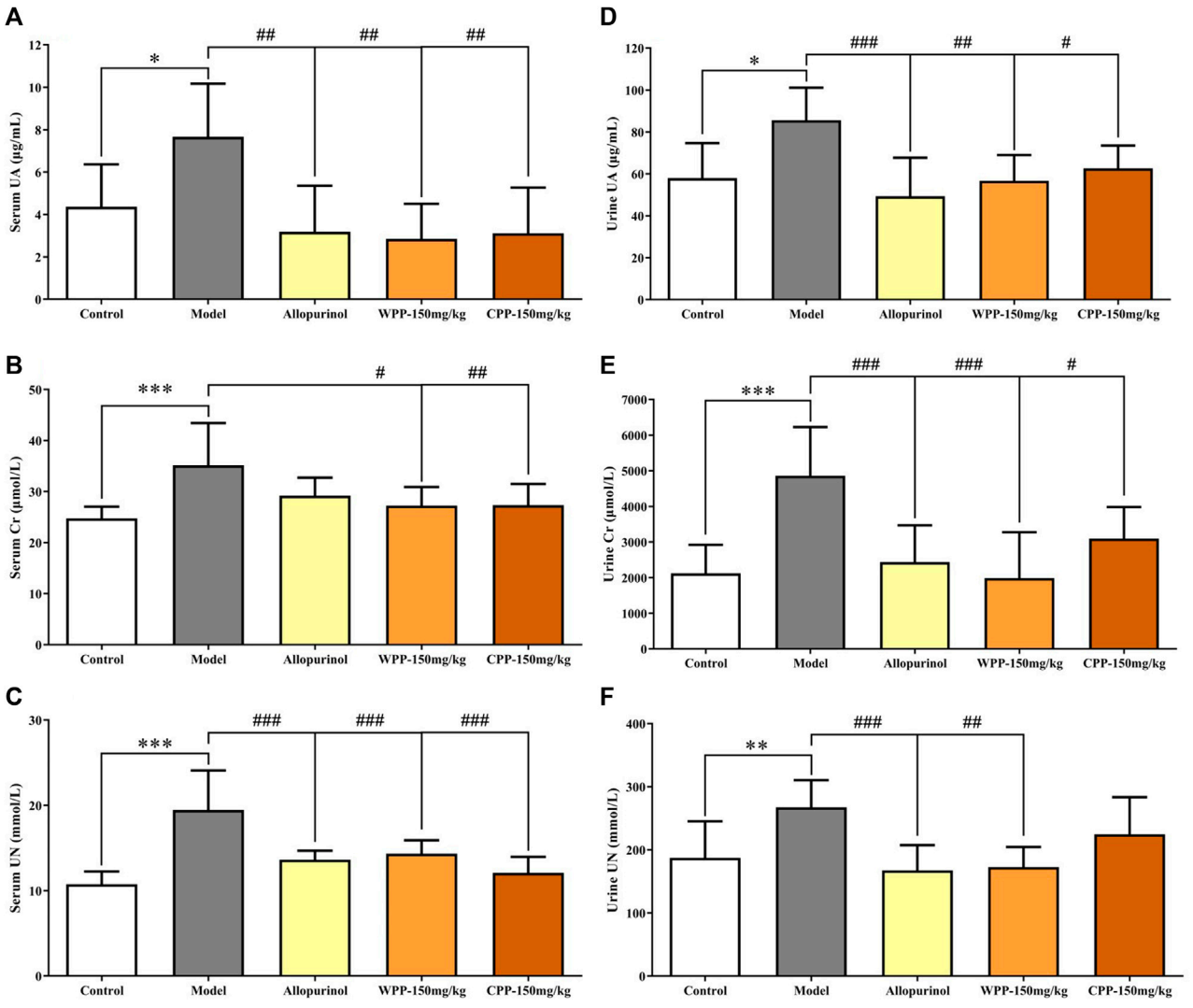

FIGURE 2 | The effects of WPP and CPP on the index levels of renal functions in the serum and urine of hyperuricaemia rats. The levels of UA **(A)**, Cr **(B)** and UN **(C)** in serum and the levels of UA **(D)**, Cr **(E)** and UN **(F)** in urine are shown. Differences were analyzed by one-way ANOVA summary: $p = 0.0032$ **(A)**; $p = 0.0015$ **(B)**; $p < 0.0001$ **(C)**; $p = 0.0023$ **(D)**; $p < 0.0001$ **(E)**; $p = 0.0012$ **(F)**. Data are presented as the mean ± SD. $^*p < 0.05$, $^{**}p < 0.01$, $^{***}p < 0.001$ vs. control group; $^{\#}p < 0.05$, $^{\#\#}p < 0.01$, $^{\#\#\#}p < 0.001$ vs. model group; $n = 10$.

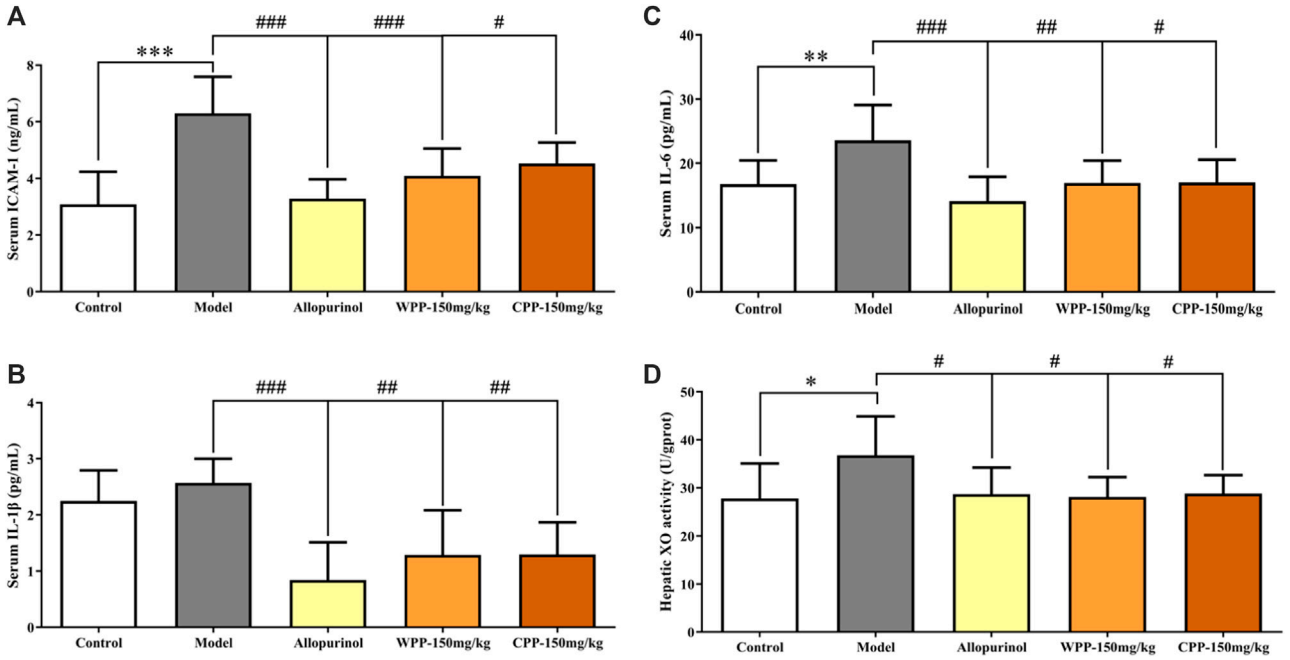

FIGURE 3 | The effects of WPP and CPP on the expression levels of chemokines and pro-inflammatory cytokines in serum and hepatic XO activity of hyperuricaemia rats. The levels of ICAM-1 **(A)**, IL-1β **(B)** and IL-6 **(C)** in serum and hepatic XO activity **(D)** are shown, respectively. Differences were analyzed by one-way ANOVA summary: $p < 0.0001$ **(A)**; $p = 0.0004$ **(B)**; $p = 0.0011$ **(C)**; $p = 0.0313$ **(D)**. Data are presented as the mean ± SD. $^{*}p < 0.05$, $^{**}p < 0.01$, $^{***}p < 0.001$ vs. control group; $^{\#}p < 0.05$, $^{\#\#}p < 0.01$, $^{\#\#\#}p < 0.001$ vs. model group; $n = 10$.

simultaneously. WPP (150 mg/kg) and CPP (150 mg/kg) also significantly down-regulated the secretion of ICAM-1, IL-1β and IL-6 in serum with significant differences ($p < 0.05$) compared with that of the model group.

The activity of XO, one of the key enzymes that catalyse the production of uric acid from xanthine, was examined to evaluate the inhibition of uric acid production. Compared with the control group, the hepatic XO activity of hyperuricaemia rats was significantly increased ($p < 0.05$), indicating that the process of uric acid production was accelerated *in vivo*. After being treated with allopurinol (10 mg/kg), the hepatic XO activity in the positive control group was significantly down-regulated ($p < 0.05$), indicating that allopurinol can inhibit XO activity, which is consistent with its mechanism of action. Similarly, hepatic XO activity in the WPP-treated group and CPP-treated group was significantly down-regulated ($p < 0.05$) after oral administration of WPP (150 mg/kg) and CPP (150 mg/kg).

Compared to the control group kidneys with normal renal structures (**Figure 4A**), the kidneys in model rats showed significant pathological changes including swelling, vacuolar degeneration of renal tubular epithelial cells, renal tubule atrophy, expansion of the lumen in the renal cortex, and atrophy and degeneration of the glomerulus (**Figure 4B**). After being treated with allopurinol (10 mg/kg), WPP (150 mg/kg) and CPP (150 mg/kg), the pathological damage was ameliorated to varying degrees (**Figures 4C–E**). The histological analysis data supported the UA level change observations and were consistent with the levels of Cr and UN observed above.

UHPLC-QE-MS for Urine Metabolomics Analysis

Metabolite spectrum changes in gout treated with WPP (150 mg/kg) and CPP (150 mg/kg) were analyzed by PCA and compared with the control group and model group. The PCA score plot (**Figure 5**) showed that the metabolite spectra between the four groups were somewhat changed in both the ESI^+ and ESI^-. Furthermore, the OPLS-DA plot (**Figures 6A–C**) showed that the control group, model group, WPP-treated group and CPP-treated group could be clearly distinguished from each other. Differential metabolites between the two groups were screened out with $p < 0.05$ (Student's t-test) and VIP >1 in ESI^+ because the database records more information about substances in ESI^+ than in ESI^-. Specifically, there were 65 up-regulated metabolites and 8 down-regulated metabolites between the control and model groups (**Figure 6D**), 71 down-regulated metabolites between the model and WPP-treated groups (**Figure 6E**) and 50 up-regulated metabolites between the model and CPP-treated groups (**Figure 6F**).

Finally, based on the pathway impact value calculated from the pathway topological analysis and the -ln *p*-value obtained from pathway enrichment analysis, the top metabolic pathways were identified and are shown in the bubble plot above. The results (**Figure 7**) suggested that arginine and proline metabolism and

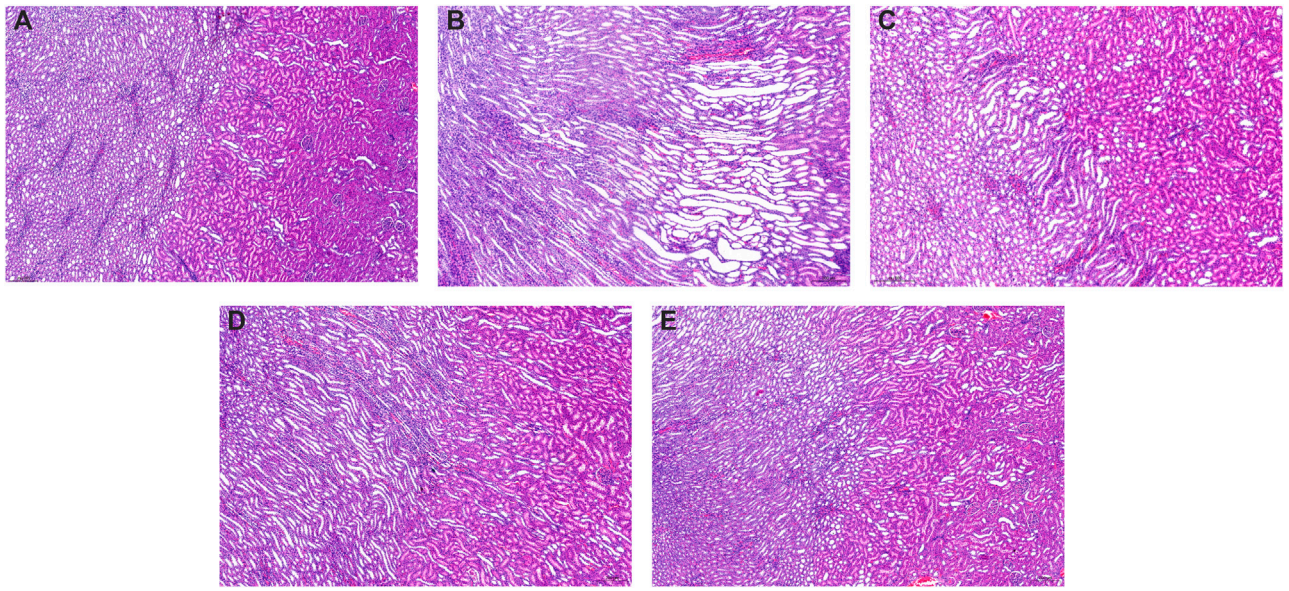

FIGURE 4 | Representative kidney H&E images of the control group **(A)** and model group **(B)**, positive control group **(C)**, WPP-treated group **(D)** and CPP-treated group **(E)** are shown above. Scale bar = 200 μm.

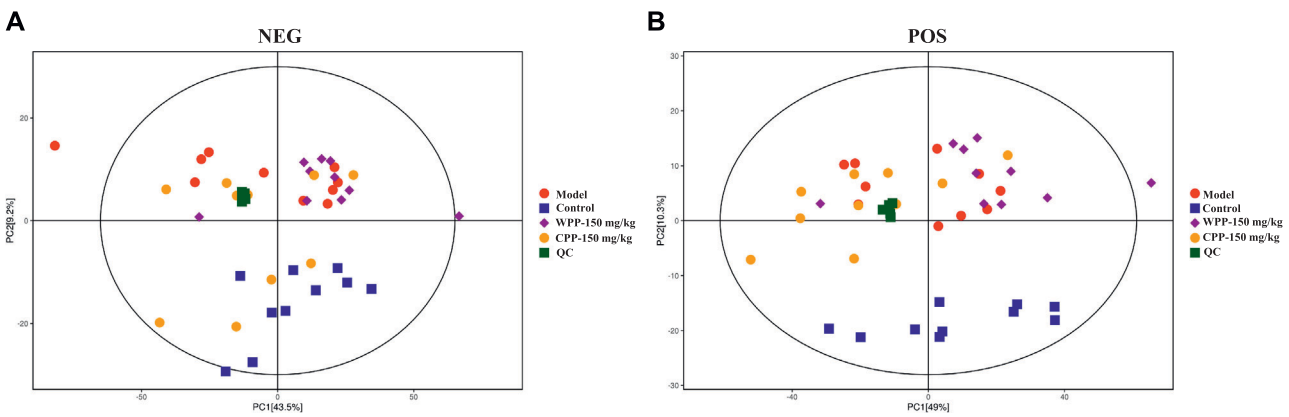

FIGURE 5 | Principal component analysis (PCA) score plot of the control group, model group, WPP-treated group (150 mg/kg) and CPP-treated groups (150 mg/kg) in the negative ion mode (NEG) **(A)** and positive ion mode (POS) **(B)** (n = 10).

taurine and hypotaurine metabolism may mediate the pathogenesis and development of hyperuricaemia. These changed metabolites were found to be primarily involved in valine, leucine and isoleucine biosynthesis metabolism and histidine metabolism of WPP and nicotinate and nicotinamide metabolism and beta-alanine metabolism of CPP for treatment effects on gout.

Effects of Wild *P. igniarius* and Cultivated *P. igniarius* on Acute Gouty Arthritis

As shown in **Figure 8A**, after an equal volume of normal saline solution was injected, there was no obvious joint swelling in the control group rats at any time point, which indicated that the intra-articular injection had no effect on the degree of swelling. Compared with the control group, MSU significantly enhanced the swelling degree of the right ankle in the model group rats only 2 h after injection ($p < 0.001$). The joint swelling in the model group rats increased with time and reached a peak at 12 h (**Figure 8B**). After that, although the swelling degree of rats in the model group gradually decreased with increasing time, it was still significantly greater than that of the control group ($p < 0.001$) at different time points, which indicated that the acute gouty arthritis model was established successfully.

Colchicine (0.3 mg/kg) clearly interferes with MSU-induced joint swelling 2 h after injection. Specifically, the joint swelling in the

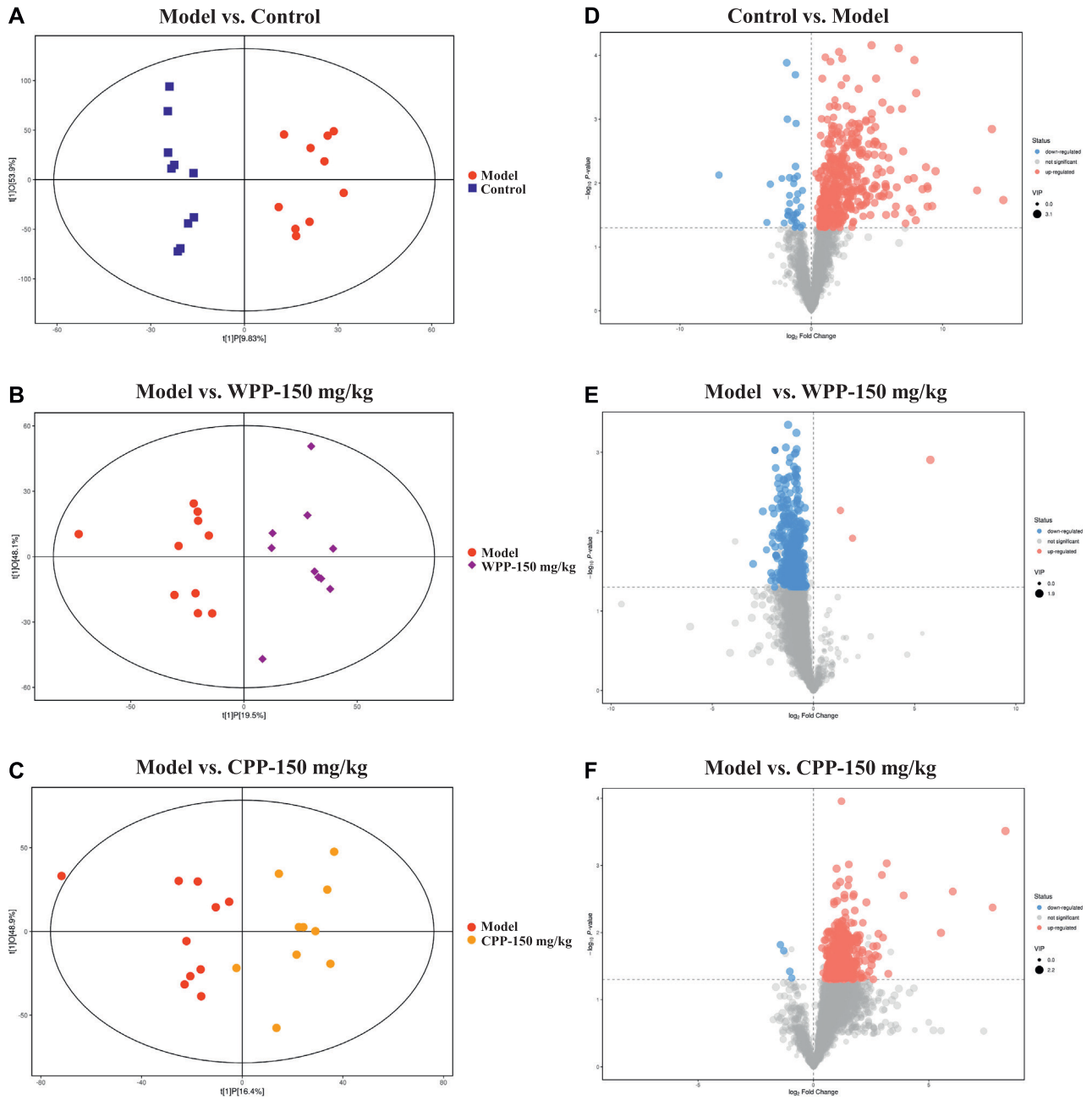

FIGURE 6 | Orthogonal projections for the latent structures-discriminate analysis (OPLS-DA) score plot and volcano plot between the control group, model group, WPP-treated group (150 mg/kg) or CPP-treated groups (150 mg/kg) in the positive ion mode (POS) (n = 10). OPLS-DA score plots between the control group and model group **(A)**, model group and WPP-treated group (150 mg/kg) **(B)** and model group and CPP-treated group (150 mg/kg) **(C)**. The volcano plots between the control group and model group **(D)**, model group and WPP-treated group (150 mg/kg) **(E)** and model group and CPP-treated group (150 mg/kg) **(F)** are also shown above. The X axis and Y axis represent the $\log_2$-fold change and $-\log_{10}$ p-value, respectively.

positive group rats was significantly lower than that of the model control group at 6, 12, 24, 36, and 48 h ($p < 0.01$). Surprisingly, WPP (150 mg/kg) and CPP (150 mg/kg) showed good effects of suppressing the ankle swelling induced by MSU. Obviously, the joint swelling degree in the rats of the WPP-treated group and CPP-treated group at each time point was not observably changed compared with that of the control group, and the joint swelling degree was significantly lower than that of the model control group at the same time point with a significant difference ($p < 0.01$).

The levels of three cytokines were examined to investigate the anti-inflammatory effects of WPP and CPP. The results (**Figure 9**) showed that MSU-induced acute gouty arthritis rats had significantly elevated levels of ICAM-1, IL-1β and IL-6 in serum ($p < 0.05$) and synovial fluid ($p < 0.05$). Treatment with WPP

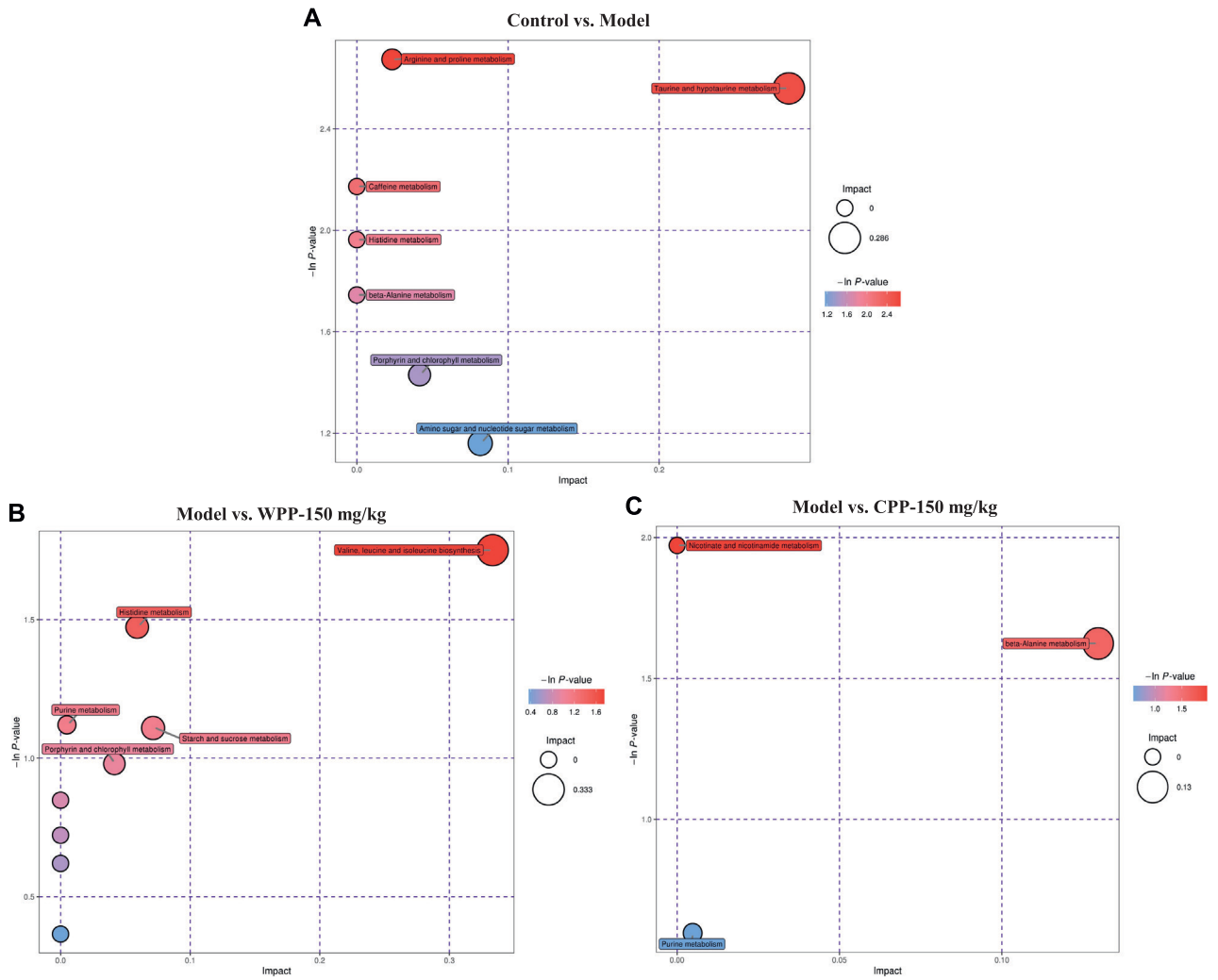

FIGURE 7 | Metabolic pathway bubble plots of the control group and model group **(A)**, the model group and WPP-treated group (150 mg/kg) **(B)** and the model group and CPP-treated group (150 mg/kg) **(C)**. The *X* axis and *Y* axis represent the impact and –ln *p*-values, respectively.

(150 mg/kg) and CPP (150 mg/kg) significantly down-regulated the production of ICAM-1, IL-1β and IL-6 in serum and synovial fluid compared with that in the model group. Colchicine (0.3 mg/kg) also decreased the levels of chemokines and pro-inflammatory cytokines.

DISCUSSION

Naturally sourced products have gradually become an indispensable source of novel pharmaceuticals, which rely on the presence of complex bioactive compounds (Shinkafi et al., 2015). In consideration of the precious medicinal and edible value and diverse biological activities of *P. igniarius*, a large number of studies on its anti-inflammatory, antioxidative, and immunomodulatory activities have been carried out, confirming its activities. Previous research has shown that *P. igniarius* extracts from liquid fermentation can affect the expression of xanthine oxidase (XO) and hypoxanthine-guanine phosphoribosyl transferase (HGPRT), two key enzymes in the uric acid metabolism pathway, to lower uric acid (Shuai-yang et al., 2019). One study also found that the ethanol extract of *P. igniarius* can inhibit XO activity and relieve acute gout inflammation by down-regulating the expression of IL-1β and ICAM-1 *in vitro* (Wang et al., 2021). Therefore, we focused our research on uncovering the active ingredients with anti-gout activity from *P. igniarius*.

In our prior research, a 70% ethanol extract of *P. igniarius* was screened out and was confirmed to possess significant anti-gout activity, which was determined by subjecting 13 extracts of *P. igniarius* to an enzymatic reaction and an *in vitro* cell model. *P. igniarius* is a rich source of secondary metabolites such as polyphenols, which are strong antioxidants (Wang et al., 2005a; Wang et al., 2005b; Lung et al., 2010; Lee and Yun 2011). Therefore, polyphenols from a 70% ethanol extract of wild *P. igniarius* (WPP) were prepared with HP20 macroporous resin to remove impurities and enrich the effective ingredients. In

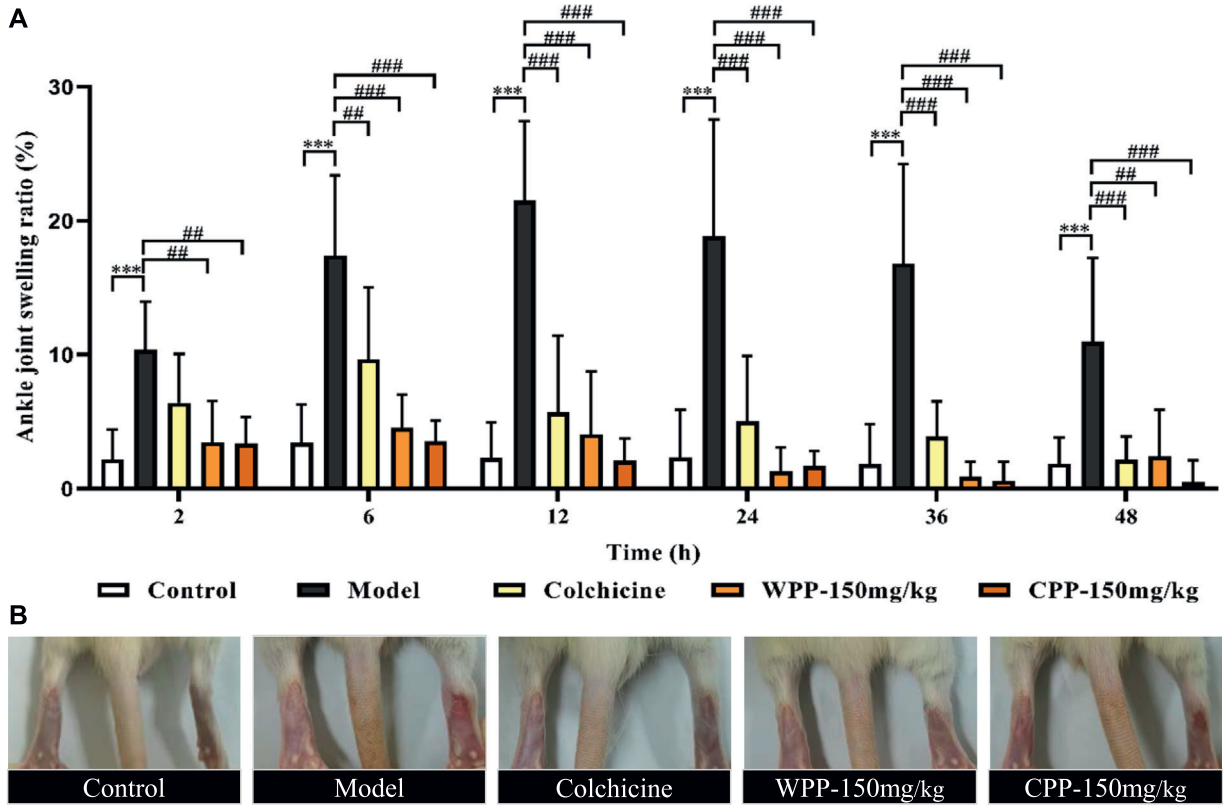

FIGURE 8 | The effects of WPP and CPP on the degree of joint swelling in rats with MSU-induced acute gouty arthritis. **(A)** Measurement of the swelling degree of the right ankle joint of rats at different time points after MSU suspension injection (2, 6, 12, 24, 36, 48 h); **(B)** Representative images of the right ankle joint from each group at 12 h are shown. Differences were analyzed by two-way ANOVA interaction: $p = 0.0027$. Data are presented as the mean ± SD. $^{*}p < 0.05$, $^{**}p < 0.01$, $^{***}p < 0.001$ vs. control group at the corresponding hour; $^{\#}p < 0.05$, $^{\#\#}p < 0.01$, $^{\#\#\#}p < 0.001$ vs. model group at the corresponding hour; $n = 10$.

addition, few studies have focused on comparing the pharmacological activities of wild *P. igniarius* and cultivated *P. igniarius*. The polyphenols of cultivated *P. igniarius* (CPP) were prepared in the same way as above. Furthermore, to elucidate the main active components in WPP and CPP better, UPLC-ESI-qTOF-MS, which is characterized by fast separation, high sensitivity, and accurate relative molecular mass calculation (Ye et al., 2021), was used for identification. Surprisingly, similar active ingredients, such as protocatechuic aldehyde, hispidin, davallialactone, phelligridimer A, hypholomine B and inoscavin A, were identified in both WPP and CPP by UPLC-ESI-qTOF-MS. As members of the polyphenol family, the antioxidant and anti-inflammatory activities of protocatechuic aldehyde (Chang et al., 2011), hispidin (Jin et al., 2021), davallialactone (Lee et al., 2008; Lee et al., 2011), phelligridimer A (Wang et al., 2005b), hypholomine B (Shou et al., 2016) and inoscavin A (Lee et al., 2006; Shou et al., 2016) have been widely reported. A derivative of protocatechuic aldehyde effectively inhibited XO activity and reduced serum uric acid levels in hyperuricaemia mice (Lü et al., 2013). Hispidin also shows good inhibitory activity against bovine milk xanthine oxidase (BXO) *in vitro* and *in silico* (Linani et al., 2021). These active ingredients may provide an explanation for the various biological activities of *P. igniarius*.

Given that UA can be degraded to allantoin by the hepatic enzyme uricase in most mammals but not in humans (Shao et al., 2016), the hyperuricaemia rat model was established by using a uricase inhibitor (potassium oxonate) and large amounts of purine (yeast extract and adenine). In this study, we evaluated the therapeutic potential of WPP and CPP in the treatment of hyperuricaemia by measuring XO activity inhibition, the levels of UA, Cr and UN in serum and urine and the expression of ICAM-1, IL-1β and IL-6, and by observing kidney histological damage. XO, an important enzyme involved in the development of gout, can not only catalyse the hypoxanthine to xanthine and xanthine to uric acid reactions but can also directly catalyse the xanthine to uric acid reaction (Liu et al., 2012). We showed that hepatic XO activity in the drug group was significantly down-regulated after oral administration of WPP and CPP, which suggests that it is possible to screen potential XO inhibitors from *P. igniarius*. UA, the terminal product of purine metabolism, Cr and UN were confirmed to be correlated with the glomerular filtration rate and renal function (Kuroda et al., 2012). Compared with the model group, the expression levels of UA, Cr and UN in hyperuricaemia rats were significantly reduced after administering WPP and CPP, which can also be observed pathologically in the alleviation of

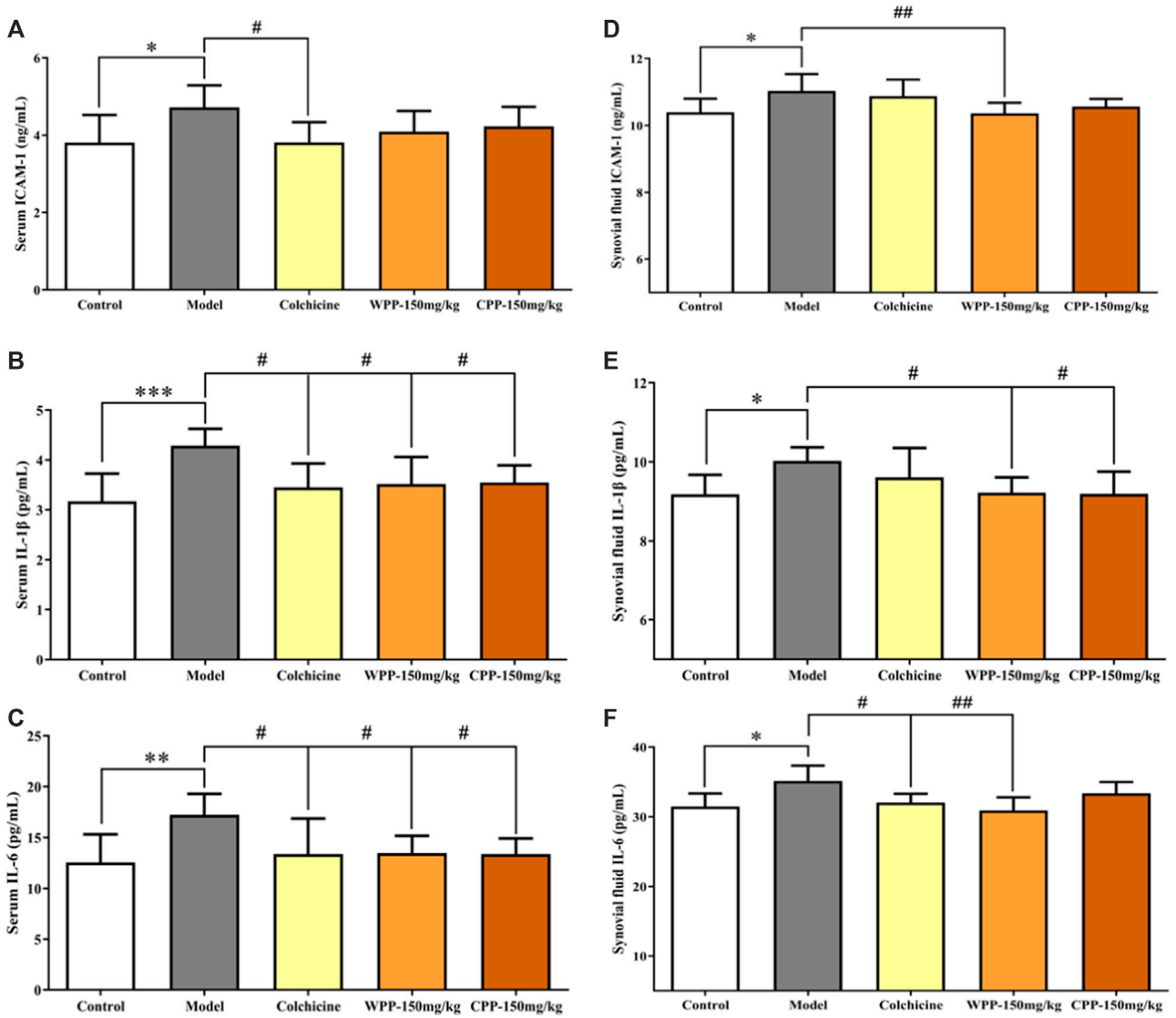

FIGURE 9 | The effects of WPP and CPP on the expression levels of chemokines and pro-inflammatory cytokines in the serum and synovial fluid of MSU-induced acute gouty arthritis rats. The levels of ICAM-1 **(A)**, IL-1β **(B)** and IL-6 **(C)** in serum and the levels of ICAM-1 **(D)**, IL-1β **(E)** and IL-6 **(F)** in synovial fluid are shown. Differences were analyzed by one-way ANOVA summary: $p = 0.0258$ **(A)**; $p = 0.0021$ **(B)**; $p = 0.0075$ **(C)**; $p = 0.0090$ **(D)**; $p = 0.0350$ **(E)**; $p = 0.0143$ **(F)**. Data are presented as the mean ± SD. $^{*}p < 0.05$, $^{**}p < 0.01$, $^{***}p < 0.001$ vs. control group; $^{\#}p < 0.05$, $^{\#\#}p < 0.01$, $^{\#\#\#}p < 0.001$ vs. model group; $n = 10$.

kidney damage. The production of IL-1β, IL-6 and ICAM-1 was also decreased in the WPP-treated group and CPP-treated group to inhibit the inflammatory process in hyperuricaemia.

MSU deposition that is induced by increased blood uric acid levels in the joint cavity activates inflammatory cytokines, inducing the accumulation of monocytes-macrophages and neutrophils, which leads to gouty arthritis (Martinon et al., 2006; Li et al., 2019). During gouty arthritis attacks, MSU stimulates neutrophils and monocytes-macrophages to produce different proinflammatory cytokines, such as interleukin (IL)-1β and IL-6; this results in membranolysis and inflammasome activation, which further induce the expression of chemokines, such as intercellular adhesion molecule-1 (ICAM-1), that play a key role in transporting leukocytes across epithelial and endothelial barriers (Margalit et al., 1997; Neeson et al., 2003; Cianchetti et al., 2008; Shi et al., 2013). We further examined the anti-inflammatory effect of WPP and CPP on the production of proinflammatory cytokines in MSU-induced rats. These results clearly showed that WPP and CPP treatment both relieved joint swelling and inhibited the expression of IL-1β, IL-6 and ICAM-1, which are essential in the initiation and progression of acute gouty arthritis.

Metabolomics is an emerging field of research that has been used to evaluate metabolic perturbations associated with different stages of diseases, identify disease biomarkers, explore potential targets and predict drug safety and efficacy (Shan et al., 2020; Zhao et al., 2020; Song et al., 2021). Non-targeted metabolomics has been conducted extensively to explore biomarkers related to effective hyperuricaemia treatments (Qin et al., 2021; Zhang et al., 2021). Therefore,

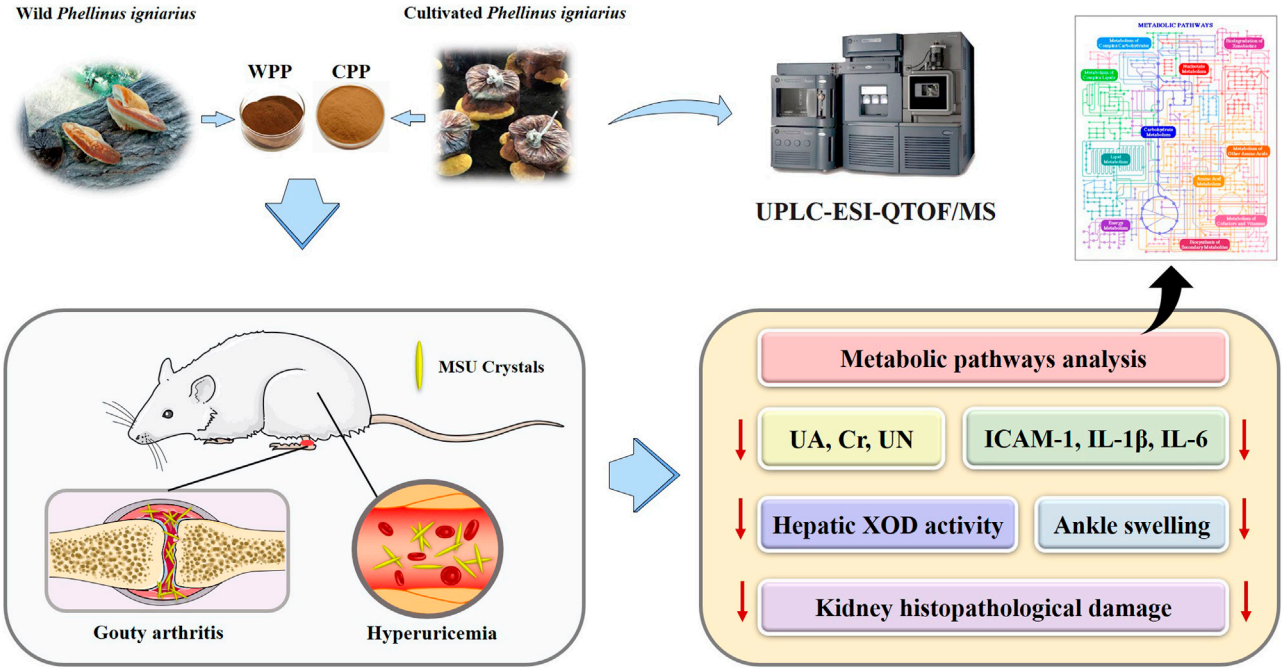

FIGURE 10 | Overview of the anti-gout effects of wild *P. igniarius* and cultivated *P. igniarius*.

metabolomics based on UHPLC-QE-MS, which is suitable for simultaneous and systemic analysis of multiple metabolite fingerprinting, was employed to generate metabolite profiles of urine to characterize the metabolic changes related to hyperuricaemia and uncover the underlying metabolic mechanism of the therapeutic effects of WPP and CPP on gout. The results indicated that the progression of hyperuricaemia induced by potassium oxonate, yeast extract and adenine was mainly related to the metabolic pathways of arginine and proline metabolism and taurine and hypotaurine metabolism. The level of Cr in hyperuricaemia model rats was higher than that in normal rats, suggesting that arginine and proline metabolism was implicated in hyperuricaemia (Jiang et al., 2017; Shan et al., 2021). Up-regulated Cr in hyperuricaemia rats suggests that rats with hyperuricaemia have renal damage, which was consistent with previous studies (Liu et al., 2016). Higher plasma taurine levels have been observed in patients with uric acid stones (Atanassova et al., 2010). Taurine and hypotaurine metabolism has been confirmed to participate in several renal physiological processes and mediate renal uric acid excretion by regulating urate transporters (Feng et al., 2017). The potential therapeutic effect of WPP on gout was found to be primarily involved in leucine and isoleucine biosynthesis metabolism and histidine metabolism. The findings suggest that BCAA supplements (composed of leucine, isoleucine and valine) reduced the purine nucleotide cycle activity of the athletes, subsequently decreased uric acid production and the concentrations of hypoxanthine, and reduced the incidence of gout in individuals that engage in endurance exercises (Tang and Chan, 2017). The treatment effect of CPP on gout was primarily involved in nicotinate and nicotinamide metabolism and beta-alanine metabolism. Research has shown that quinolinic acid is involved in the metabolism of nicotinate and nicotinamide and is eventually metabolized to uric acid, resulting in increased uric acid (Zhao et al., 2020). Collectively, these findings suggest that WPP and CPP can exhibit an anti-gout protective effect by mediating different stages of uric acid metabolism.

CONCLUSION

In summary, we provided evidence supporting that wild *P. igniarius* and cultivated *P. igniarius* have similar active ingredient spectrums and have anti-hyperuricaemia and anti-gout arthritis effects (**Figure 10**). The shared active compounds and analogous pharmacological activities are expected to promote the development and application of cultivated *P. igniarius* to fill the shortage of wild *P. igniarius*. In the future, we focused our research on uncovering the targets and pathways of *P. igniarius* in the treatment of gout.

DATA AVAILABILITY STATEMENT

The original contributions presented in the study are included in the article/supplementary material, further inquiries can be directed to the corresponding author.

ETHICS STATEMENT

The animal study was reviewed and approved by the Animal Ethics Committees of Hangzhou Medical College.

AUTHOR CONTRIBUTIONS

QīnL and XZ designed the study and guided the experiment. HL conducted experiments and wrote manuscript. The data was analyzed by HL, LG, and QínL. YJ, XueZ, and MH revised the paper. All authors read and approved it for publication.

FUNDING

This study was financially supported by the Key Laboratory of Neuropsychiatric Drug Research of Zhejiang Province (2019E10021), the Project of Zhejiang Administration of Traditional Chinese Medicine (2020ZB038), the Zhejiang Provincial Department of Science and Technology of Institution Special Funds (C12002Y-04), Public Wel-fare Technology Application Projects of Zhejiang Province (LGC19H280008), and 2021 High-Level Health Talents Training Object.

ACKNOWLEDGMENTS

We are thankful to all the authors of the study. We would like to thank Shanghai Biotree Biotechnology for the UHPLC-QE-MS/MS and data analyses.

REFERENCES

Aran, S., Malekzadeh, S., and Seifirad, S. (2011). A Double-Blind Randomized Controlled Trial Appraising the Symptom-Modifying Effects of Colchicine on Osteoarthritis of the Knee. *Clin. Exp. Rheumatol.* 29 (3), 513–518.

Atanassova, S. S., Panchev, P., and Ivanova, M. (2010). Plasma Levels and Urinary Excretion of Amino Acids by Subjects with Renal Calculi. *Amino Acids* 38 (5), 1277–1282. doi:10.1007/s00726-009-0359-z

Becker, M. A., Fitz-Patrick, D., Choi, H. K., Dalbeth, N., Storgard, C., Cravets, M., et al. (2015). An Open-Label, 6-month Study of Allopurinol Safety in Gout: The LASSO Study. *Semin. Arthritis Rheum.* 45 (2), 174–183. doi:10.1016/j.semarthrit.2015.05.005

Ben-Chetrit, E., and Levy, M. (1998). Colchicine: 1998 Update. *Semin. Arthritis Rheum.* 28 (1), 48–59. doi:10.1016/s0049-0172(98)80028-0

Chang, Z. Q., Gebru, E., Lee, S. P., Rhee, M. H., Kim, J. C., Cheng, H., et al. (2011). *In Vitro* antioxidant and Anti-inflammatory Activities of Protocatechualdehyde Isolated from Phellinus Gilvus. *J. Nutr. Sci. Vitaminol. (Tokyo)* 57 (1), 118–122. doi:10.3177/jnsv.57.118

Cianchetti, S., Del Fiorentino, A., Colognato, R., Di Stefano, R., Franzoni, F., and Pedrinelli, R. (2008). Anti-inflammatory and Anti-oxidant Properties of Telmisartan in Cultured Human Umbilical Vein Endothelial Cells. *Atherosclerosis* 198 (1), 22–28. doi:10.1016/j.atherosclerosis.2007.09.013

Crofford, L. J. (2013). Use of NSAIDs in Treating Patients with Arthritis. *Arthritis Res. Ther.* 15, S2. doi:10.1186/ar4174

Dehlin, M., Jacobsson, L., and Roddy, E. (2020). Global Epidemiology of Gout: Prevalence, Incidence, Treatment Patterns and Risk Factors. *Nat. Rev. Rheumatol.* 16 (7), 380–390. doi:10.1038/s41584-020-0441-1

Dhanasekar, C., and Rasool, M. (2016). Morin, a Dietary Bioflavonol Suppresses Monosodium Urate crystal-induced Inflammation in an Animal Model of Acute Gouty Arthritis with Reference to NLRP3 Inflammasome, Hypo-Xanthine Phospho-Ribosyl Transferase, and Inflammatory Mediators. *Eur. J. Pharmacol.* 786, 116–127. doi:10.1016/j.ejphar.2016.06.005

Dong, Y., Wang, H., Zhang, Y., An, N., Zhang, Y., and Shou, D. (2015). Ultra High Performance Liquid Chromatography with Synapt High-Definition Mass Spectrometry and a Pattern Recognition Approach to Characterize Chemical Constituents and Rat Metabolites after the Oral Administration of *Phellinus Igniarius*. *J. Sep. Sci.* 38 (7), 1137–1148. doi:10.1002/jssc.201401293

Elfishawi, M. M., Zleik, N., Kvrgic, Z., Michet, C. J., Crowson, C. S., Matteson, E. L., et al. (2018). The Rising Incidence of Gout and the Increasing Burden of Comorbidities: A Population-Based Study over 20 Years. *J. Rheumatol.* 45 (4), 574–579. doi:10.3899/jrheum.170806

Fam, A. G. (2001). Difficult Gout and New Approaches for Control of Hyperuricemia in the Allopurinol-Allergic Patient. *Curr. Rheumatol. Rep.* 3 (1), 29–35. doi:10.1007/s11926-001-0048-8

Feng, Y., Sun, F., Gao, Y., Yang, J., Wu, G., Lin, S., et al. (2017). Taurine Decreased Uric Acid Levels in Hyperuricemic Rats and Alleviated Kidney Injury. *Biochem. Biophys. Res. Commun.* 489 (3), 312–318. doi:10.1016/j.bbrc.2017.05.139

Gao, W., Wang, W., Sun, W., Wang, M., Zhang, N., and Yu, S. (2017). Antitumor and Immunomodulating Activities of Six *Phellinus Igniarius* Polysaccharides of Different Origins. *Exp. Ther. Med.* 14 (5), 4627–4632. doi:10.3892/etm.2017.5191

Hainer, B. L., Matheson, E., and Wilkes, R. T. (2014). Diagnosis, Treatment, and Prevention of Gout. *Am. Fam. Physician* 90 (12), 831–836.

He, T., Liu, J., Wang, X., Duan, C., Li, X., and Zhang, J. (2020). Analysis of Cantharidin-Induced Nephrotoxicity in HK-2 Cells Using Untargeted Metabolomics and an Integrative Network Pharmacology Analysis. *Food Chem. Toxicol.* 146, 111845. doi:10.1016/j.fct.2020.111845

Hsin, M. C., Hsieh, Y. H., Wang, P. H., Ko, J. L., Hsin, I. L., and Yang, S. F. (2017). Hispolon Suppresses Metastasis via Autophagic Degradation of Cathepsin S in Cervical Cancer Cells. *Cell Death Dis.* 8 (10), e3089. doi:10.1038/cddis.2017.459

Jiang, T., Qian, J., Ding, J., Wang, G., Ding, X., Liu, S., et al. (2017). Metabolomic Profiles Delineate the Effect of Sanmiao Wan on Hyperuricemia in Rats. *Biomed. Chromatogr.* 31 (2), e3792. doi:10.1002/bmc.3792

Jin, M. H., Chen, D. Q., Jin, Y. H., Han, Y. H., Sun, H. N., and Kwon, T. (2021). Hispidin Inhibits LPS-Induced Nitric Oxide Production in BV-2 Microglial Cells via ROS-dependent MAPK Signaling. *Exp. Ther. Med.* 22 (3), 970. doi:10.3892/etm.2021.10402

Kapoor, M., Martel-Pelletier, J., Lajeunesse, D., Pelletier, J. P., and Fahmi, H. (2011). Role of Proinflammatory Cytokines in the Pathophysiology of Osteoarthritis. *Nat. Rev. Rheumatol.* 7 (1), 33–42. doi:10.1038/nrrheum.2010.196

Kuroda, T., Tanabe, N., Kobayashi, D., Wada, Y., Murakami, S., Nakano, M., et al. (2012). Significant Association between Renal Function and Area of Amyloid Deposition in Kidney Biopsy Specimens in Reactive Amyloidosis Associated with Rheumatoid Arthritis. *Rheumatol. Int.* 32 (10), 3155–3162. doi:10.1007/s00296-011-2148-8

Le Graverand-Gastineau, M. P. (2010). Disease Modifying Osteoarthritis Drugs: Facing Development Challenges and Choosing Molecular Targets. *Curr. Drug Targets* 11 (5), 528–535. doi:10.2174/138945010791011893

Lee, I. K., Seok, S. J., Kim, W. K., and Yun, B. S. (2006). Hispidin Derivatives from the Mushroom Inonotus Xeranticus and Their Antioxidant Activity. *J. Nat. Prod.* 69 (2), 299–301. doi:10.1021/np050453n

Lee, I. K., and Yun, B. S. (2011). Styrylpyrone-class Compounds from Medicinal Fungi *Phellinus* and *Inonotus Spp.*, and Their Medicinal Importance. *J. Antibiot. (Tokyo)* 64 (5), 349–359. doi:10.1038/ja.2011.2

Lee, N. H., Lee, Y. H., Bhattari, G., Lee, I. K., Yun, B. S., Jeon, J. G., et al. (2011). Reactive Oxygen Species Removal Activity of Davallialactone Reduces Lipopolysaccharide-Induced Pulpal Inflammation through Inhibition of the Extracellular Signal-Regulated Kinase 1/2 and Nuclear Factor Kappa B Pathway. *J. Endod.* 37 (4), 491–495. doi:10.1016/j.joen.2011.01.012

Lee, S., Kim, J. I., Heo, J., Lee, I., Park, S., Hwang, M. W., et al. (2013). The Anti-influenza Virus Effect of *Phellinus Igniarius* Extract. *J. Microbiol.* 51 (5), 676–681. doi:10.1007/s12275-013-3384-2

Lee, Y. G., Lee, W. M., Kim, J. Y., Lee, J. Y., Lee, I. K., Yun, B. S., et al. (2008). Src Kinase-Targeted Anti-inflammatory Activity of Davallialactone from Inonotus Xeranticus in Lipopolysaccharide-Activated RAW264.7 Cells. *Br. J. Pharmacol.* 154 (4), 852–863. doi:10.1038/bjp.2008.136

Li, L., Teng, M., Liu, Y., Qu, Y., Zhang, Y., Lin, F., et al. (20172017). Anti-Gouty Arthritis and Antihyperuricemia Effects of Sunflower (*Helianthus Annuus*) Head Extract in Gouty and Hyperuricemia Animal Models. *Biomed. Res. Int.* 2017, 5852076. doi:10.1155/2017/5852076

Li, S., Li, L., Yan, H., Jiang, X., Hu, W., Han, N., et al. (2019). Anti-gouty A-rthritis and A-nti-hyperuricemia P-roperties of C-elery S-eed E-xtracts in R-odent M-odels. *Mol. Med. Rep.* 20 (5), 4623–4633. doi:10.3892/mmr.2019.10708

Linani, A., Benarous, K., Bou-Salah, L., and Yousfi, M. (2021). Hispidin, Harmaline, and Harmine as Potent Inhibitors of Bovine Xanthine Oxidase: Gout Treatment, *In Vitro*, ADMET Prediction, and SAR Studies. *Bioorg. Chem.* 112, 104937. doi:10.1016/j.bioorg.2021.104937

Liu, G., Wu, X., Jia, G., Chen, X., Zhao, H., Wang, J., et al. (2016). Arginine: New Insights into Growth Performance and Urinary Metabolomic Profiles of Rats. *Molecules* 21 (9), 1142. doi:10.3390/molecules21091142

Liu, S., Xing, J., Zheng, Z., Song, F., Liu, Z., and Liu, S. (2012). Ultrahigh Performance Liquid Chromatography-Triple Quadrupole Mass Spectrometry Inhibitors Fishing Assay: a Novel Method for Simultaneously Screening of Xanthine Oxidase Inhibitor and Superoxide Anion Scavenger in a Single Analysis. *Anal. Chim. Acta* 715, 64–70. doi:10.1016/j.aca.2011.12.003

Lü, J.-M., Yao, Q., and Chen, C. (2013). 3,4-Dihydroxy-5-nitrobenzaldehyde (DHNB) Is a Potent Inhibitor of Xanthine Oxidase: a Potential Therapeutic Agent for Treatment of Hyperuricemia and Gout. *Biochem. Pharmacol.* 86 (9), 1328–1337. doi:10.1016/j.bcp.2013.08.011

Lung, M. Y., Tsai, J. C., and Huang, P. C. (2010). Antioxidant Properties of Edible Basidiomycete *Phellinus Igniarius* in Submerged Cultures. *J. Food Sci.* 75 (1), E18–E24. doi:10.1111/j.1750-3841.2009.01384.x

Margalit, A., Duffin, K. L., Shaffer, A. F., Gregory, S. A., and Isakson, P. C. (1997). Altered Arachidonic Acid Metabolism in Urate crystal Induced Inflammation. *Inflammation* 21 (2), 205–222. doi:10.1023/a:1027322304880

Martinon, F. (2010). Mechanisms of Uric Acid crystal-mediated Autoinflammation. *Immunol. Rev.* 233 (1), 218–232. doi:10.1111/j.0105-2896.2009.00860.x

Martinon, F., Pétrilli, V., Mayor, A., Tardivel, A., and Tschopp, J. (2006). Gout-associated Uric Acid Crystals Activate the NALP3 Inflammasome. *Nature* 440 (7081), 237–241. doi:10.1038/nature04516

Mo, S., Wang, S., Zhou, G., Yang, Y., Li, Y., Chen, X., et al. (2004). Phelligridins C-F: Cytotoxic Pyrano[4,3-C][2]benzopyran-1,6-Dione and Furo[3,2-C]pyran-4-One Derivatives from the Fungus *Phellinus Igniarius*. *J. Nat. Prod.* 67 (5), 823–828. doi:10.1021/np030505d

Neeson, P. J., Thurlow, P. J., Jamieson, G. P., and Bradley, C. (2003). Lymphocyte-facilitated Tumour Cell Adhesion to Endothelial Cells: the Role of High Affinity Leucocyte Integrins. *Pathology* 35 (1), 50–55. doi:10.1080/00313020307517

Neogi, T. (2011). Clinical Practice. Gout. *N. Engl. J. Med.* 364 (5), 443–452. doi:10.1056/NEJMcp1001124

Niel, E., and Scherrmann, J. M. (2006). Colchicine Today. *Jt. Bone Spine* 73 (6), 672–678. doi:10.1016/j.jbspin.2006.03.006

Pascart, T., and Lioté, F. (2019). Gout: State of the Art after a Decade of Developments. *Rheumatology (Oxford)* 58 (1), 27–44. doi:10.1093/rheumatology/key002

Pascual, E., Addadi, L., Andrés, M., and Sivera, F. (2015). Mechanisms of crystal Formation in Gout-A Structural Approach. *Nat. Rev. Rheumatol.* 11 (12), 725–730. doi:10.1038/nrrheum.2015.125

Perez-Ruiz, F., Dalbeth, N., and Bardin, T. (2015). A Review of Uric Acid, crystal Deposition Disease, and Gout. *Adv. Ther.* 32 (1), 31–41. doi:10.1007/s12325-014-0175-z

Punzi, L., Scanu, A., Spinella, P., Galozzi, P., and Oliviero, F. (2019). One Year in Review 2018: Gout. *Clin. Exp. Rheumatol.* 37 (1), 1–11.

Qin, N., Jiang, Y., Shi, W., Wang, L., Kong, L., Wang, C., et al. (2021). High-Throughput Untargeted Serum Metabolomics Analysis of Hyperuricemia Patients by UPLC-Q-TOF/MS. *Evid. Based Complement. Alternat Med.* 2021, 5524772. doi:10.1155/2021/5524772

Ragab, G., Elshahaly, M., and Bardin, T. (2017). Gout: An Old Disease in New Perspective - A Review. *J. Adv. Res.* 8 (5), 495–511. doi:10.1016/j.jare.2017.04.008

Robinson, P. C. (2018). Gout - an Update of Aetiology, Genetics, Co-morbidities and Management. *Maturitas* 118, 67–73. doi:10.1016/j.maturitas.2018.10.012

Rostom, A., Dube, C., Wells, G., Tugwell, P., Welch, V., Jolicoeur, E., et al. (2002). Prevention of NSAID-Induced Gastroduodenal Ulcers. *Cochrane Database Syst. Rev.* (4), CD002296. doi:10.1002/14651858.Cd002296

Shan, B., Ai, Z., Zeng, S., Song, Y., Song, J., Zeng, Q., et al. (2020). Gut Microbiome-Derived Lactate Promotes to Anxiety-like Behaviors through GPR81 Receptor-Mediated Lipid Metabolism Pathway. *Psychoneuroendocrinology* 117, 104699. doi:10.1016/j.psyneuen.2020.104699

Shan, B., Chen, T., Huang, B., Liu, Y., and Chen, J. (2021). Untargeted Metabolomics Reveal the Therapeutic Effects of Ermiao Wan Categorized Formulas on Rats with Hyperuricemia. *J. Ethnopharmacol.* 281, 114545. doi:10.1016/j.jep.2021.114545

Shao, X., Lu, W., Gao, F., Li, D., Hu, J., Li, Y., et al. (2016). Uric Acid Induces Cognitive Dysfunction through Hippocampal Inflammation in Rodents and Humans. *J. Neurosci.* 36 (43), 10990–11005. doi:10.1523/jneurosci.1480-16.2016

Shi, L., Xu, L., Yang, Y., Song, H., Pan, H., and Yin, L. (2013). Suppressive Effect of Modified Simiaowan on Experimental Gouty Arthritis: an *In Vivo* and *In Vitro* Study. *J. Ethnopharmacol.* 150 (3), 1038–1044. doi:10.1016/j.jep.2013.10.023

Shinkafi, T. S., Bello, L., Wara Hassan, S., and Ali, S. (2015). An Ethnobotanical Survey of Antidiabetic Plants Used by Hausa-Fulani Tribes in Sokoto, Northwest Nigeria. *J. Ethnopharmacol.* 172, 91–99. doi:10.1016/j.jep.2015.06.014

Shou, D., Dong, Y., Wang, N., Li, H., Zhang, Y., and Zhu, Y. (2016). Simultaneous Quantification of Antioxidant Compounds in *Phellinus Igniarius* Using Ultra Performance Liquid Chromatography-Photodiode Array Detection-Electrospray Ionization Tandem Mass Spectrometry. *PloS One* 11 (9), e0163797. doi:10.1371/journal.pone.0163797

Shuai-yang, L., Liao, X-Y., Rong-zhen, Y., Yang, Z-Y., Han, L., Guo, Q., et al. (2019). Research on the Inhibition of Uric Acid Synthesis by the Extract of *Phellinus Igniarius*. *Ginseng Res.* 31 (4), 17–20. doi:10.1016/j.msard.2021.103271

Singh, J. A. (2013). Racial and Gender Disparities Among Patients with Gout. *Curr. Rheumatol. Rep.* 15 (2), 307. doi:10.1007/s11926-012-0307-x

Sokolove, J., and Lepus, C. M. (2013). Role of Inflammation in the Pathogenesis of Osteoarthritis: Latest Findings and Interpretations. *Ther. Adv. Musculoskelet. Dis.* 5 (2), 77–94. doi:10.1177/1759720x12467868

Song, Y., Shan, B., Zeng, S., Zhang, J., Jin, C., Liao, Z., et al. (2021). Raw and Wine Processed Schisandra Chinensis Attenuate Anxiety like Behavior via Modulating Gut Microbiota and Lipid Metabolism Pathway. *J. Ethnopharmacol* 266, 113426. doi:10.1016/j.jep.2020.113426

Sun, Y., Zhong, S., Yu, J., Zhu, J., Ji, D., Hu, G., et al. (2018). The Aqueous Extract of *Phellinus Igniarius* (SH) Ameliorates Dextran Sodium Sulfate-Induced Colitis in C57BL/6 Mice. *PloS one* 13 (10), e0205007. doi:10.1371/journal.pone.0205007

Tang, F. C., and Chan, C. C. (2017). Contribution of Branched-Chain Amino Acids to Purine Nucleotide Cycle: a Pilot Study. *Eur. J. Clin. Nutr.* 71 (5), 587–593. doi:10.1038/ejcn.2016.161

Terkeltaub, R. A. (2009). Colchicine Update: 2008. *Semin. Arthritis Rheum.* 38 (6), 411–419. doi:10.1016/j.semarthrit.2008.08.006

Wang, J., Song, J., Zhang, Y., Gou, S., Shi, B., Shi, D., et al. (2021). Screening Anti-gout Compounds from Phellinus Igniarius by Ultrafiltration Liquid Chromatography Mass Spectrometry Based on Evaluation of an *In Vitro* Method Combined with Enzymatic Reaction. *J. Sep. Sci.* 44, 2868–2874. doi:10.1002/jssc.202100109

Wang, Y., Mo, S. Y., Wang, S. J., Li, S., Yang, Y. C., and Shi, J. G. (2005a). A Unique Highly Oxygenated Pyrano[4,3-C][2]benzopyran-1,6-Dione Derivative with Antioxidant and Cytotoxic Activities from the Fungus *Phellinus Igniarius*. *Org. Lett.* 7 (9), 1675–1678. doi:10.1021/ol0475764

Wang, Y., Shang, X. Y., Wang, S. J., Mo, S. Y., Li, S., Yang, Y. C., et al. (2007). Structures, Biogenesis, and Biological Activities of Pyrano[4,3-C]isochromen-4-One Derivatives from the Fungus *Phellinus Igniarius*. *J. Nat. Prod.* 70 (2), 296–299. doi:10.1021/np060476h

Wang, Y., Wang, S. J., Mo, S. Y., Li, S., Yang, Y. C., and Shi, J. G. (2005b). Phelligridimer A, a Highly Oxygenated and Unsaturated 26-membered Macrocyclic Metabolite with Antioxidant Activity from the Fungus *Phellinus Igniarius*. *Org. Lett.* 7 (21), 4733–4736. doi:10.1021/ol0520875

Wu, X., Lin, S., Zhu, C., Yue, Z., Yu, Y., Zhao, F., et al. (2010). Homo- and Heptanor-Sterols and Tremulane Sesquiterpenes from Cultures of *Phellinus Igniarius*. *J. Nat. Prod.* 73 (7), 1294–1300. doi:10.1021/np100216k

Wu, X., Wang, S., Liu, C., Zhang, C., Guo, J., and Shang, X. (2019). A New 2H-Benzindazole Compound from *Alternaria alternata* Shm-1, an Endophytic Fungus Isolated from the Fresh Wild Fruit of *Phellinus Igniarius*. *J. Nat. Med.* 73 (3), 620–626. doi:10.1007/s11418-019-01291-x

Ye, X., Wu, J., Zhang, D., Lan, Z., Yang, S., Zhu, J., et al. (2021). How Aconiti Radix Cocta Can Treat Gouty Arthritis Based on Systematic Pharmacology and UPLC-QTOF-MS/MS. *Front. Pharmacol.* 12, 618844. doi:10.3389/fphar.2021.618844

Zhang, H., Ma, H., Liu, W., Pei, J., Wang, Z., Zhou, H., et al. (2014). Ultrasound Enhanced Production and Antioxidant Activity of Polysaccharides from Mycelial Fermentation of *Phellinus Igniarius*. *Carbohydr. Polym.* 113, 380–387. doi:10.1016/j.carbpol.2014.07.027

Zhang, Y., Zhang, H., Rong, S., Bian, C., Yang, Y., and Pan, H. (2021). NMR Spectroscopy Based Metabolomics Confirms the Aggravation of Metabolic Disorder in Metabolic Syndrome Combined with Hyperuricemia. *Nutr. Metab. Cardiovasc. Dis.* 31 (8), 2449–2457. doi:10.1016/j.numecd.2021.05.015

Zhao, H., Zhang, Y., Liu, B., Zhang, L., Bao, M., Li, L., et al. (2020). A Pilot Study to Identify the Longitudinal Serum Metabolite Profiles to Predict the Development of Hyperuricemia in Essential Hypertension. *Clin. Chim. Acta* 510, 466–474. doi:10.1016/j.cca.2020.08.002

Zhao, T., Wang, Z., Zhang, N., Su, X., Liu, J., Li, P., et al. (2018). Rapid Identification on Chemical Constituents of *Phellinus Igniarius* by UPLC-Q-TOF-MSE Combined with UNIFI Platform. *Spec. Wild Econ. Anim. Plant Res.* 40 (1), 20–25. doi:10.15585/mmwr.mm7040a3

Zhen-ting, S., and Hai-ying, B. (2016). Research Progress on Effective Components and Efficacy of *Phellinus Igniarius*. *Chin. J. Exp. Traditional Med. Formulae* 22 (22), 197–202. doi:10.1016/j.jep.2021.114706

Zheng, S., Deng, S., Huang, Y., Huang, M., Zhao, P., Ma, X., et al. (2018). Anti-diabetic Activity of a Polyphenol-Rich Extract from *Phellinus Igniarius* in KK-Ay Mice with Spontaneous Type 2 Diabetes Mellitus. *Food Funct.* 9 (1), 614–623. doi:10.1039/c7fo01460k

Zhu, C., Sun, B., Zhang, B., and Zhou, Z. (2021). An Update of Genetics, Co-morbidities and Management of Hyperuricaemia. *Clin. Exp. Pharmacol. Physiol.* 48, 1305–1316. doi:10.1111/1440-1681.13539

Conflict of Interest: The authors declare that the research was conducted in the absence of any commercial or financial relationships that could be construed as a potential conflict of interest.

Publisher's Note: All claims expressed in this article are solely those of the authors and do not necessarily represent those of their affiliated organizations, or those of the publisher, the editors and the reviewers. Any product that may be evaluated in this article, or claim that may be made by its manufacturer, is not guaranteed or endorsed by the publisher.

frontiers in Pharmacology

SYSTEMATIC REVIEW
published: 24 January 2022
doi: 10.3389/fphar.2022.808460

Anti-Inflammatory Efficacy of Curcumin as an Adjunct to Non-Surgical Periodontal Treatment: A Systematic Review and Meta-Analysis

Yang Zhang[1,2], *Lei Huang*[3], *Jinmei Zhang*[4], *Alessandra Nara De Souza Rastelli*[5], *Jingmei Yang*[4]* *and Dongmei Deng*[6]

[1]Department of Periodical Press and National Clinical Research Center for Geriatrics, West China Hospital, Sichuan University, Chengdu, China, [2]Chinese Evidence-Based Medicine Center, West China Hospital, Sichuan University, Chengdu, China, [3]West China School of Public Health and West China Fourth Hospital, Sichuan University, Chengdu, China, [4]State Key Laboratory of Oral Disease and National Clinical Research Center for Oral Disease, Department of Periodontics, West China Hospital of Stomatology, Sichuan University, Chengdu, China, [5]Department of Restorative Dentistry, School of Dentistry, São Paulo State University-UNESP, Araraquara, Brazil, [6]Department of Preventive Dentistry, Academic Centre for Dentistry Amsterdam, University of Amsterdam and Vrije Universiteit Amsterdam, Amsterdam, Netherlands

OPEN ACCESS

Edited by:
Lucia Recinella,
University of Studies G. d'Annunzio Chieti and Pescara, Italy

Reviewed by:
Luis A. Salazar,
University of La Frontera, Chile
Andy Wai Kan Yeung,
University of Hong Kong, China

***Correspondence:**
Jingmei Yang
yjm881222@hotmail.com

Specialty section:
This article was submitted to Ethnopharmacology, a section of the journal Frontiers in Pharmacology

Received: *03 November 2021*
Accepted: *06 January 2022*
Published: *24 January 2022*

Citation:
Zhang Y, Huang L, Zhang J, De Souza Rastelli AN, Yang J and Deng D (2022) Anti-Inflammatory Efficacy of Curcumin as an Adjunct to Non-Surgical Periodontal Treatment: A Systematic Review and Meta-Analysis. Front. Pharmacol. 13:808460. doi: 10.3389/fphar.2022.808460

Objective: Curcumin has been used as an adjunct to non-surgical periodontal treatment. However, the efficacy of curcumin in the periodontal therapy remained controversial. This study aimed to evaluate the anti-inflammatory efficacy of curcumin as an adjunct to non-surgical periodontal treatment (NPT) by systematic review.

Methods: Databases including Embase, PubMed, Cochrane Central Register of Controlled Trials (CENTRAL), and ClinicalTrials.gov were searched to identify relevant RCTs on the use of curcumin as an adjunct to NPT for the treatment of periodontal disease from inception to July 21, 2021. Two reviewers independently screened literature, extracted data and assessed the risk of bias of the included studies. Meta-analysis was then performed using Review Manager 5.3 software.

Results: A total of 18 RCTs involving 846 patients/sites were included in this meta-analysis. The results of the meta-analysis revealed that as compared to NPT alone, curcumin as an adjunct to NPT resulted in significant reduction in gingival index (GI) at the 1-week (mean differences (MD) = −0.15, 95% confidence intervals (CI) −0.26 to −0.05, p = 0.005), 2-week (MD = −0.51, 95%CI −0.74 to −0.28, $p < 0.0001$), 3-week (MD = −0.34, 95%CI −0.66 to −0.02, $p = 0.03$), 4-week (MD = −0.25, 95%CI −0.48 to −0.02, $p = 0.04$) or 6-week (MD = −0.33, 95%CI −0.58 to −0.08, $p = 0.01$) follow-ups. Similar significant reductions were also observed for sulcus bleeding index (SBI) at 1, 2, 4, and 12 weeks. However, there were no statistically significant differences in reducing bleeding on probing (BOP) between curcumin as an adjunct and NPT alone at 4, 12, and 24 weeks.

Conclusion: Based on the current evidence, curcumin demonstrates anti-inflammatory efficacies in terms of reducing GI and SBI compared with NPT alone. Moreover, curcumin

is a natural herbal medicine with few side effects, and it is a good candidate as an adjunct treatment for periodontal disease.

Keywords: curcumin, anti-inflammatory, periodontal disease, non-surgical periodontal treatment (NPT), meta-analysis

INTRODUCTION

Periodontal diseases, which include a range of conditions from gingivitis to periodontitis, are the most common chronic oral diseases affecting the majority of populations worldwide. This worldwide health problem has influenced 76% of the population in Europe and the US, ranking as the sixth most prevalent condition globally (Frencken et al., 2017). Dental plaque is the primary etiology attributed to this disease (Sanz et al., 2017), and the main goal of periodontal therapy is addressing the primary etiology. Traditionally, the main treatment modality for eliminating the infection is non-surgical periodontal therapy (NPT), including scaling for gingivitis and scaling and root planing (SRP) for periodontitis. NPT aims to reduce the periodontal pathogen invasion and manage the healing of periodontal tissue. However, the efficacy of NPT could be limited by several factors, such as deep periodontal pockets and complex root anatomy (Tomasi et al., 2007; Heitz-Mayfield and Lang, 2013). Therefore, antibiotics, such as amoxicillin, metronidazole, and tetracycline, have been introduced as adjuncts to mechanical debridement to enhance the efficacy of periodontal therapy (Petersilka et al., 2002; Slots and Ting, 2002). The application of antibiotics is debatable, since antimicrobial resistance has become a threat to global public health (Brinkac et al., 2017), the local application of antibiotics could even lead to oral bacterial resistance (Ahmadi et al., 2021).

Therefore, several alternative adjunctive drugs, especially natural agents, have been suggested as alternative antimicrobial methods. Curcumin, an age-old plant-derived polyphenol extracted from the rhizome of turmeric (Bisht et al., 2010), has become popular in the last 50 years due to its multiple therapeutic functions. Natural curcumin is defined as 1,7-bis-(4-hydroxy-3-methoxyphenyl)-hepta-1,6-diene-3,5-dione with a chemical formula of $C_{21}H_{20}O_6$, according to the International Union of Pure and Applied Chemistry (IUPAC). Extensive research has shown that curcumin possesses anti-inflammatory, antioxidative, antiangiogenic, immunoregulatory, antibacterial, and proapoptotic properties (Pimentel et al., 2020), and curcumin has been proven to be effective in the treatment of rheumatoid arthritis (Conigliaro et al., 2019), inflammatory bowel disease (Sharma et al., 2019) and oral diseases (Tang et al., 2020), such as oral mucosal disease, oral lichen planus, oral squamous cell carcinoma and periodontal disease. Recently, a meta-analysis revealed that local delivery of curcumin showed similar clinical efficacies to chlorhexidine, the gold standard as an adjunct to SRP (Zhang et al., 2021).

However, whether curcumin could strengthen the effectiveness of NPT in periodontal therapy is still controversial. Some studies reported that curcumin, as an adjunctive treatment, could improve gingival inflammation (Gottumukkala et al., 2013; Guru et al., 2020; Mohammad, 2020), whereas other studies did not observe any improvement (Jalaluddin et al., 2019; Kaur et al., 2019; Pérez-Pacheco et al., 2021). Thus, this systematic review aims to perform a meta-analysis to explore whether curcumin as an adjunctive to NPT yields better clinical outcomes in terms of reducing periodontal inflammation than NPT alone.

MATERIALS AND METHODS

This systematic review was registered on the PROSPERO platform (registration number: CRD42021267612) and was conducted following the Preferred Reporting Items for Systematic Reviews and Meta-analyses (PRISMA) guidelines (Page et al., 2021).

Search Strategy

We searched databases including Embase, PubMed, Cochrane Central Register of Controlled Trials (CENTRAL), and ClinicalTrials.gov without language restriction from inception to July 21, 2021, to identify relevant RCTs on the use of curcumin as an adjunct to NPT for the treatment of patients with periodontal disease. We combined MeSH and free text terms to identify the relevant articles. The search strategy is shown in the **Supplementary Material**. An additional search was performed among the references of the included studies to identify potentially eligible studies. We also manually searched the references of published reviews to collect additional relevant studies.

Inclusion Criteria

Studies were included by applying the following population-intervention-comparator-outcomes-study design (PICOS): 1) Participants: Adult patients over 18 years of age diagnosed with periodontal disease. There were no restrictions on ethnicity or disease severity. 2) Interventions and comparisons: patients receiving curcumin (no restriction on dosage and form) as an adjunct to NRP in the intervention group and NPT alone as the control group. 3) Outcomes: The primary outcomes were gingival index (GI), sulcus bleeding index (SBI) and bleeding on probing (BOP). The secondary outcomes included plaque index (PI), microbiological indicators, inflammatory factors and adverse events. Studies reporting at least one primary outcome of interest with reliable and available data were included. 4) Study design: Randomized controlled trials (RCTs) were included in our study. There were no restrictions on the masking method or split-mouth design.

Exclusion Criteria

The exclusion criteria were as follows: 1) Studies on systematic application of curcumin, not topical use in the oral cavity. 2) Studies included patients with systemic diseases. 3) Studies that included only patients who received other adjunct treatments, such as photodynamic therapy, other medications or surgical treatments. 4) Studies included patients who received periodontal treatment or antibiotic therapy prior to NPT. 5) *In vitro* or animal experiments. 6) Studies with incomplete data: targeted outcomes were not reported or could not be obtained after contacting authors. 7) Data were duplicated. 8) Trials were only reported as conference abstracts. 9) Studies were not reported in English.

Data Extraction

Two reviewers independently screened titles, abstracts and full texts for eligible literature and then completed the data extraction. Disagreements were resolved by discussion or consultation with a third reviewer. The following data were extracted from each RCT: 1) Study characteristics: author name, year of publication, country of study, number of patients, and study design. 2) Patient characteristics: sex and age. 3) Interventions and comparisons: details of the curcumin treatment and NPT treatment groups (e.g., drug type, doses used, and duration of treatment). 4) Elements for the risk of bias assessment. 5) Outcomes: primary outcomes (GI, SBI and BOP) and secondary outcomes (PI, microbiological indicators, inflammatory factors and adverse events) at different follow-up time points. If a trial had multiple reports, the data from all sources were carefully examined for consistency.

Risk of Bias Assessment

Two reviewers independently evaluated the risk of bias of the included RCTs according to the Cochrane Collaboration's tool, which is described in the Cochrane Handbook (Higgins et al., 2020). Seven domains were assessed: 1) random sequence generation; 2) allocation concealment; 3) blinding of participants and researchers; 4) blinding of assessors of outcomes; 5) completeness of outcome data; 6) selective reporting bias; and 7) forms of other bias. Finally, the risk of bias was assessed as "high", "low", or "unclear" according to the above seven elements.

Statistical Analysis

Review Manager (RevMan), version 5.3 (Nordic Cochrane Center, Cochrane Collaboration) was used to perform data analysis. Mean differences (MD) were used for continuous outcomes, risk ratios (RR) were used for dichotomous outcomes, and 95% confidence intervals (CI) were calculated for both variables. Heterogeneity among the trials was assessed using the Chi-square test ($p < 0.10$, defined as indicating significant heterogeneity) or I^2 (>50%). If substantial heterogeneity existed, a random effect model was applied; otherwise, a fixed effect model was applied. A narrative summary of the findings is provided for outcomes that could not be pooled. Subgroup analysis was performed for the duration of follow-up. Sensitivity analysis was conducted to evaluate the robustness of the results by excluding individual studies for forest plots. Publication bias was assessed by asymmetry in a funnel plot for GI at 4 weeks.

RESULTS

Search Results and Study Characteristics

Figure 1 shows the study selection process applied to identify the studies involved in this systematic review and meta-analysis. From the 499 potentially relevant reports identified, 37 studies proved potentially eligible after title and abstract screening. Following full text screening, 18 RCTs (Behal et al., 2011; Gottumukkala et al., 2013; Muglikar et al., 2013; Bhatia et al., 2014; Jaswal et al., 2014; Anuradha et al., 2015; Sreedhar et al., 2015; Arunachalam et al., 2017; Chatterjee et al., 2017; Singh et al., 2018; Jalaluddin et al., 2019; Kaur et al., 2019; Raghava et al., 2019; Guru et al., 2020; Mohammad, 2020; Pandey et al., 2021; Pérez-Pacheco et al., 2021; Rahalkar et al., 2021) involving 846 patients/sites were included in this meta-analysis. **Table 1** displays the main characteristics of the 18 included studies. Seventeen studies were from India, and one was from Brazil. The demographic characteristics of the patients varied among the trials. However, the groups of each clinical trial were generally balanced with respect to demographic and clinical characteristics.

Quality Assessment of the Included Studies

The methodological quality results are shown in **Figure 2** and **Figure 3**. Only one (Jalaluddin et al., 2019) study did not mention randomized allocation. Five studies (Gottumukkala et al., 2013; Singh et al., 2018; Guru et al., 2020; Pandey et al., 2021; Pérez-Pacheco et al., 2021) mentioned allocation concealment. Participants and trial staff were not blinded in one study (Jalaluddin et al., 2019), and 13 other studies (Behal et al., 2011; Gottumukkala et al., 2013; Muglikar et al., 2013; Bhatia et al., 2014; Jaswal et al., 2014; Anuradha et al., 2015; Sreedhar et al., 2015; Arunachalam et al., 2017; Singh et al., 2018; Raghava et al., 2019; Mohammad, 2020; Pandey et al., 2021; Rahalkar et al., 2021) failed to mention blinding of participants and personnel. Only four studies (Muglikar et al., 2013; Sreedhar et al., 2015; Kaur et al., 2019; Pérez-Pacheco et al., 2021) that reported outcome assessors were blinded. All studies had complete data and consistent outcomes, as described in the methods section. No study had described the registration of RCTs.

Primary Outcomes

GI

Thirteen RCTs (Behal et al., 2011; Muglikar et al., 2013; Jaswal et al., 2014; Anuradha et al., 2015; Arunachalam et al., 2017; Chatterjee et al., 2017; Singh et al., 2018; Jalaluddin et al., 2019; Raghava et al., 2019; Guru et al., 2020; Mohammad, 2020; Pandey et al., 2021; Rahalkar et al., 2021) reported the GI outcome. Meta-analysis with the random-effects model revealed that there were statistically significant differences in reducing GI between curcumin as an adjunct and NPT alone at 1 week (MD = −0.15, 95%CI −0.26 to −0.05, $p = 0.005$), 2 weeks (MD = −0.51, 95%CI −0.74 to −0.28, $p < 0.000\ 1$), 3 weeks (MD = −0.34, 95%CI −0.66 to −0.02, $p = 0.03$), 4 weeks (MD = −0.25,

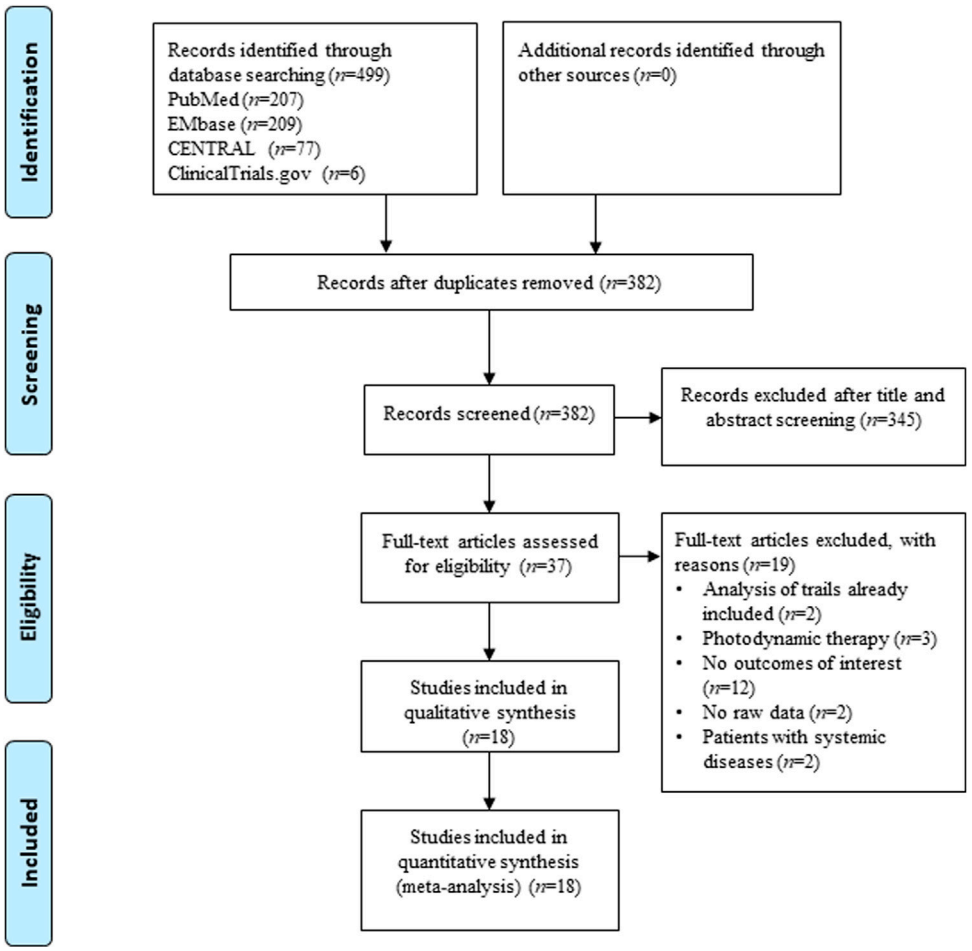

FIGURE 1 | Flow diagram of literature screening.

95%CI −0.48 to −0.02, $p = 0.04$) and 6 weeks (MD = −0.33, 95%CI -0.58 to −0.08, $p = 0.01$) (**Figure 4**). Only one study (Jalaluddin et al., 2019) reported that curcumin as an adjunct had a significantly higher reduction in GI (MD = −0.11, 95%CI −0.19 to −0.04, $p = 0.003$) than NPT alone at the 8-week evaluation. Another study (Singh et al., 2018) showed that there was no significant difference between curcumin as an adjunct to NPT and NPT alone at 12 weeks (MD = −0.04, 95%CI −0.23 to −0.15, $p = 0.68$).

SBI

Seven RCTs (Behal et al., 2011; Bhatia et al., 2014; Sreedhar et al., 2015; Chatterjee et al., 2017; Kaur et al., 2019; Pandey et al., 2021; Rahalkar et al., 2021) involving 360 patients/sites reported the SBI index. Meta-analysis with the random-effects model revealed that there were statistically significant differences in reducing SBI between curcumin as an adjunct and NPT alone at 1 week (MD = −0.20, 95%CI −0.29 to −0.10, $p < 0.0001$), 2 weeks (MD = −0.59, 95%CI −0.68 to −0.50, $p < 0.00001$), 4 weeks (MD = −0.35, 95%CI −0.57 to −0.13, $p = 0.002$) and 12 weeks (MD = −0.12, 95%CI −0.21 to −0.04, $p = 0.006$) (**Figure 5**). There were also statistical differences between curcumin as an adjunct to NPT and NPT alone at 6 weeks (MD = -0.82, 95%CI -0.99 to -0.65, $p < 0.0001$) and 24 weeks (MD = -0.22, 95%CI -0.35 to -0.09, $p = 0.0006$), but there was only one study for each follow-up time.

BOP

Three RCTs (Gottumukkala et al., 2013; Mohammad, 2020; Pérez-Pacheco et al., 2021) reported the BOP outcome. The results of the meta-analysis revealed that there were no statistically significant differences in reducing BOP between curcumin as an adjunct and NPT alone at 4 weeks (MD = 0.82, 95%CI 0.55 to 1.24, $p = 0.35$), 12 weeks (MD = −0.30, 95%CI 0.09 to 1.03, $p = 0.06$), and 24 weeks (MD = 0.64, 95%CI 0.27 to 1.50, $p = 0.30$) (**Figure 6**).

Secondary Outcomes

PI

Seventeen RCTs (Behal et al., 2011; Gottumukkala et al., 2013; Muglikar et al., 2013; Bhatia et al., 2014; Jaswal et al., 2014;

TABLE 1 | Basic characteristics of included studies.

NO.	Study	Country	Study design	Age (years)	Male (%)	Sample size (treatment/ control)	Diagnostic criteria	Study groups	Follow up (weeks)	Outcome indicators	Periodontal outcome evaluated
1	Gottumukkala et al. (2013)	India	SM	30–55	46.2%	23/23	Chronic Periodontitis: At least 3 sites with PPD ≥ 5 mm in three different quadrants and radiographic evidence of horizontal bone loss	1.NPT+1% curcumin subgingival irrigation 2.NPT + saline	4, 12, and 24 weeks	BOP, PI, MI	The 1% curcumin showed a mild to moderate beneficiary effect to NPT
2	Guru et al. (2020)	India	RCT	21–59	80.0%	15/15	Chronic Periodontitis: PPD of 5–7 mm with two or more teeth	1.NPT+2% curcumin nanogel 2.NPT	3 and 6 weeks	GI, PI, MI	The 2% curcumin gel showed an effective improvement of NPT in clinical parameters
3	Jalaluddin et al. (2019)	India	RCT	25–45	NA	20/20	Chronic Periodontitis: PPD ≥ 5 mm in different quadrants of the mouth	1.NPP+1% curcumin irrigation 2.NPT	4 and 8 weeks	GI, PI, MI	The curcumin combined with NPT show similar clinical parameters compared with NPT alone
4	Jaswal et al. (2014)	India	SM	21–55	80.0%	15/15	Chronic Periodontitis	1.NPT+2% gel 2.NPT	4 and 6 weeks	GI, PI	Th curcumin gel help in reduction of PPD.
5	Singh et al. (2018)	India	SM	30–50	55.0%	40/40	Chronic Periodontitis: < 30% of the sites assessed in the mouth demonstrate attachment loss and bone loss; the test sites with PPD 5–8 mm	1.NPT+5% curcumin chip 2.NPT	4 and 12 weeks	GI, PI, AE	Curcumin as an adjunct to NPT proved to be effective in the treatment of periodontitis
6	Behal et al. (2011)	India	SM	NA	NA	30/30	Chronic periodontitis with PD of 5–7 mm in at least 2 nonadjacent sites in different quadrants of the mouth	1.NPT+2% curcumin gel 2.NPT	4 and 6 weeks	GI, SBI, PI, MI, AE	2% curcumin gel can be effectively used as an adjunct to NPT and is more effective than NPT alone
7	Muglikar et al. (2013)	India	RCT	20–40	NA	10/10	Chronic generalized gingivitis manifesting change in the color and bleeding on probing but no signs of periodontitis	1.NPT+20% curcumin mouthwash 2.NPT	1, 2, and 3 weeks	GI, PI	20% curcumin mouthwash have statistically significantly better results compared with NPT alone
8	Bhatia et al. (2014)	India	SM	21–45	60.0%	25/25	Chronic periodontitis	1.NPT+1% curcumin gel 2.NPT	4, 12, 24 weeks	SBI, PI	1% curcumin gel provide significant improvements in

(Continued on following page)

TABLE 1 | (*Continued*) Basic characteristics of included studies.

NO.	Study	Country	Study design	Age (years)	Male (%)	Sample size (treatment/ control)	Diagnostic criteria	Study groups	Follow up (weeks)	Outcome indicators	Periodontal outcome evaluated
											clinical parameters when used as an adjunct to NPT compared with NPT alone
9	Anuradha et al. (2015)	India	SM	25–60	NA	30/30	Chronic periodontitis with pocket depth of 5–7 mm involving various quadrants of the mouth	1.NPT +10 mg/g curcumin gel 2.NPT	4 and 6 weeks	GI, PI	The curcumin gel as an adjunct to NPT with more effect achieved as NPT in periodontitis therapy
10	Chatterjee et al. (2017)	India	RCT	20–30	NA	50/50	Mild to moderate gingivitis with GI less than ≥1, PI ≥ 1	1.NPT+0.1% mouthwash 2.NPT	1, 2, 4 weeks	GI, SBI, PI, AE	0.1% mouthwash combined with NPT reveals statistically significant with NPT alone
11	Sreedhar et al. (2015)	India	SM	35–55	46.7%	15/15	Chronic periodontitis with at least one tooth with PPD > 5 mm in each quadrant	1.NPT+10 mg/g curcumin gel 2.NPT	4 and 12 weeks	SBI, PI, MI	The reduction in SBI scores was reflected in curcumin with NPT compared with NPT alone
12	Arunachalam et al. (2017)	India	RCT	25–60	40.0%	10/10	Chronic gingivitis	1.NPT + curcumin (0.1 curcumin mouthwash) 2.NPT	4w	GI, PI, BM	Curcumin mouthwash show significant reduction in PI and GI compared with NPT alone
13	Kaur et al. (2019)	India	RCT	20–60	NA	15/15	Moderate to severe chronic generalized periodontitis having at least four sites with pocket probing depth of 5 mm or more in one or both of arches	1.NPT+1% curcumin gel 2.NPT	4 and 12 weeks	SBI, PI, BM, AE	Single application of curcumin gel has limited added benefit over NPT in treatment of chronic periodontitis
14	Raghava et al. (2019)	India	SM	25–40	50.0%	10/10	Chronic periodontitis having a PPD ≥ 5 mm	1.NPT + curcumin gel 2.NPT	4 weeks	GI, PI	The local application of curcumin gel when used in conjunction with NPT showed a significant improvement in PI and PPD compared with NPT alone
15	Mohammad (2020)	India	RCT	36.73 ± 6.22	36.7%	30/30	Chronic periodontitis: PPD ≥ 4 mm and CAL ≥	1.NPT+10 mg/g curcumin gel 2.NPT	4 weeks	GI, BOP, PI, BM	Curcumin gel resulted in a more significant reduction in

(Continued on following page)

TABLE 1 | (*Continued*) Basic characteristics of included studies.

NO.	Study	Country	Study design	Age (years)	Male (%)	Sample size (treatment/control)	Diagnostic criteria	Study groups	Follow up (weeks)	Outcome indicators	Periodontal outcome evaluated
							2 mm in at least 40% of the analyzed sites				clinical parameters compared to NPT alone
16	Pérez-Pacheco et al. (2021)	Brazil	SM	37–62	70.0%	40/40	Generalized periodontitis with stage III and Grade A, presenting two non-adjacent sites with PPD ≥ 5 mm and BOP in two different quadrants, and bone loss confirmed by radiographs	1.NPT+0.05 mg/ml curcumin gel 2.NPT	4, 12, 24 weeks	BOP, MI, BM, AE	Local administration of curcumin had no additional benefits to NPT.
17	Pandey et al. (2021)	India	RCT	20–60	NA	30/30	Gingivitis	1.NPT + curcumin gel 2.NPT	1, 2, and 3 weeks	GI, SBI, PI	Curcumin gel has significant effect in the treatment of gingivitis as an adjunct to NPT
18	Rahalkar et al. (2021)	India	SM	37–57	33.3%	15/15	PPD ≥ 5 mm and ≤ 8 mm at three nonadjacent sites in different quadrants of the mouth	1.NPT + curcumin gel 2.NPT	4 weeks	GI, SBI, PI, BM	Curcumin showed significant reduction in PI in curcumin group when compared with NPT

RCT, randomized clinical trial; SM, split-mouth design; PPD, periodontal probing depth; CAL, clinical attachment level; SRP, scaling and root planning; GI, gingival index; SBI, sulcus bleeding index; PI, plaque index; BOP, bleeding on probing; NA, not available; BM, biochemical marker; MI, microbiologic indicator; AE, adverse effect.

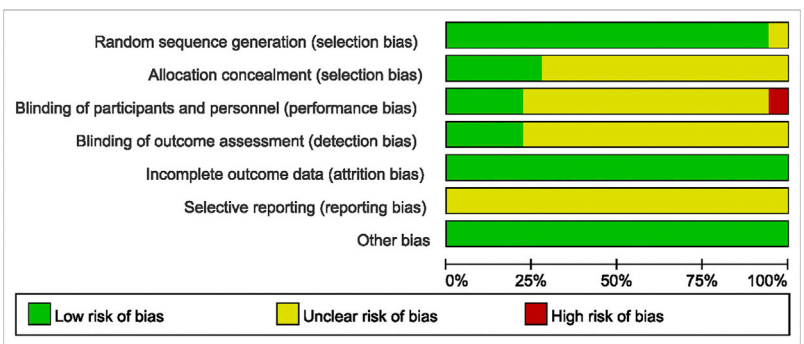

FIGURE 2 | Risk of bias graph.

Anuradha et al., 2015; Sreedhar et al., 2015; Arunachalam et al., 2017; Chatterjee et al., 2017; Singh et al., 2018; Jalaluddin et al., 2019; Kaur et al., 2019; Raghava et al., 2019; Guru et al., 2020; Mohammad, 2020; Pandey et al., 2021; Rahalkar et al., 2021) reported the PI outcome. Meta-analysis with the random-effects model showed that there were statistically significant differences in reducing PI between NPT and curcumin an adjunct to NPT at 2 weeks (MD = −0.46, 95%CI −0.88 to −0.05, $p = 0.03$), 4 weeks (MD = −0.15, 95%CI −0.26 to −0.04, $p = 0.007$), 6 weeks (MD = −0.21, 95%CI −0.38 to −0.03, $p = 0.02$) and 24 weeks (MD = −0.15, 95%CI -0.27 to −0.03, $p = 0.01$). However, there were no significant differences at 1 week (MD = −0.18, 95%CI −0.39 to

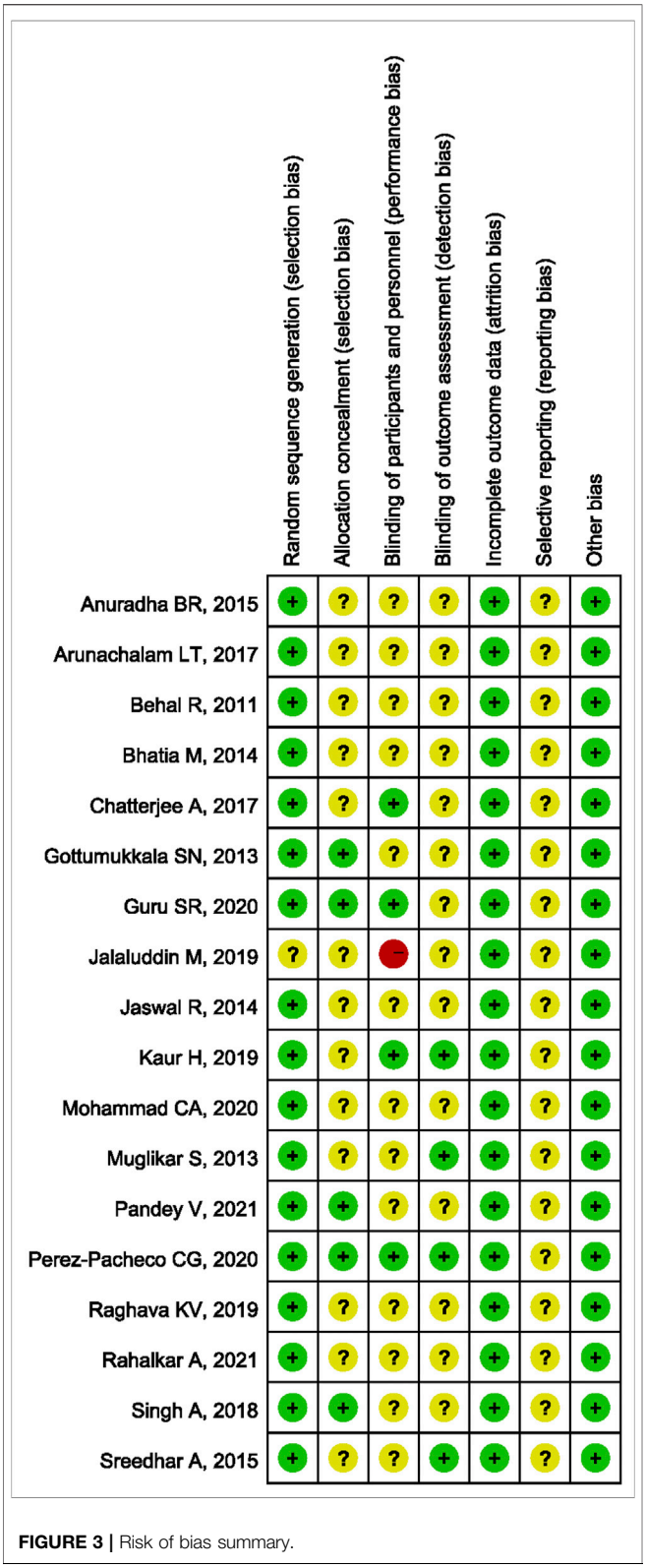

FIGURE 3 | Risk of bias summary.

0.04, $p = 0.10$), 3 weeks (MD = −0.22, 95%CI −0.54 to 0.09, $p = 0.16$), and 12 weeks (MD = −0.09, 95%CI −0.23 to 0.04, $p = 0.18$) (**Figure 7**).

Microbiological Indicators

Seven of the recruited studies compared subgingival microbial levels between NPT and NPT with curcumin (Behal et al., 2011; Gottumukkala et al., 2013; Bhatia et al., 2014; Sreedhar et al., 2015; Guru et al., 2020; Pérez-Pacheco et al., 2021; Rahalkar et al., 2021). Significant reductions in bacterial loads, such as *Porphyromonas gingivalis (P. gingivalis), Treponema denticola (T. denticola), Tannerella forsythia (T. forsythia), Prevetella intermedia (P. intermedia), Fusobacterium nucleatum (F. nucleatum), Actinobacillus actinomycetemcomitans (A. actinomycetemcomitans)* and some other periodontal pathogens (Behal et al., 2011; Gottumukkala et al., 2013; Bhatia et al., 2014; Sreedhar et al., 2015; Guru et al., 2020; Pérez-Pacheco et al., 2021; Rahalkar et al., 2021), were shown once curcumin was used as an adjuvant to NPT, whereas another study reported no benefit in comparison with NPT alone (Rahalkar et al., 2021).

Inflammatory Factors

Data from three articles were demonstrated (Kaur et al., 2019; Mohammad, 2020; Pérez-Pacheco et al., 2021). Clinical studies on NPT combined with curcumin report mixed results: one of the studies indicated that there was no difference in GCF cytokine levels, such as IL-1 and TNF-α, but other studies reported no benefit in comparison with NPT alone (Kaur et al., 2019; Pérez-Pacheco et al., 2021).

Safety

No adverse events were reported during the follow-up in the included studies (Behal et al., 2011; Chatterjee et al., 2017; Singh et al., 2018; Kaur et al., 2019; Pérez-Pacheco et al., 2021). Other studies did not mention adverse events. However, a portion of individuals reported curcumin mouthwash has an unacceptable taste (Chatterjee et al., 2017).

Sensitivity Analysis

All results showed good consistency in both the fixed-effects and random-effects models. The overall effect direction did not change after deleting one study each time for GI and SBI. Sensitivity analysis results indicated that the outcomes were not reversed by removing any study, which had relatively good stability.

Publication Bias

The funnel plot of GI at 4 weeks demonstrated no significant asymmetrical distribution (**Figure 8**).

DISCUSSION

In recent years, curcumin has been used as an adjunct to non-surgical periodontal treatment. However, the efficacy of curcumin in periodontal therapy remains controversial. This study aimed to evaluate the anti-inflammatory efficacy of curcumin as an adjunct to non-surgical periodontal treatment (NPT) by means of a systematic review. The results of the meta-analysis revealed

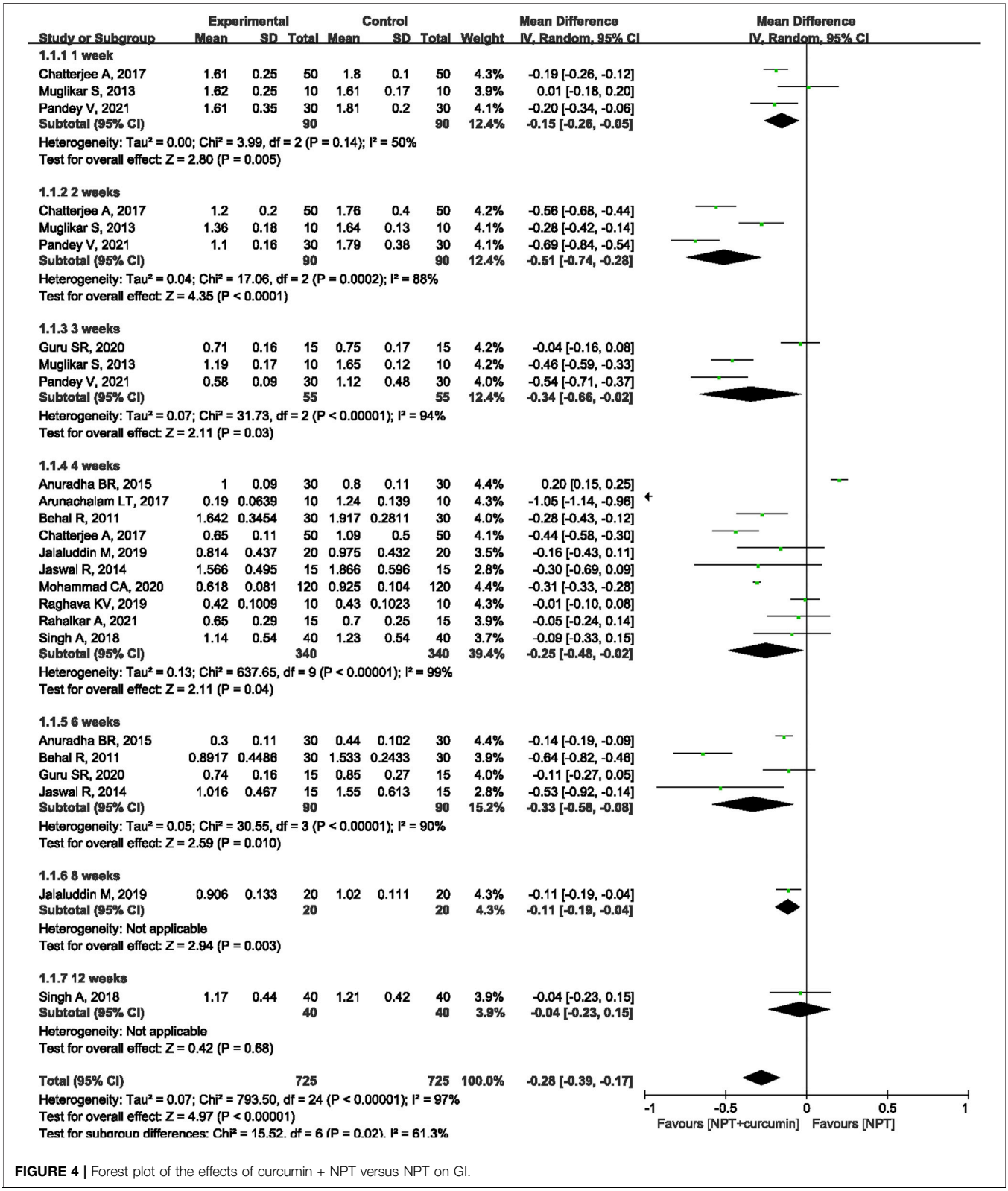

FIGURE 4 | Forest plot of the effects of curcumin + NPT versus NPT on GI.

that there were statistically significant differences in reducing GI between NPT alone and curcumin as an adjunct to NPT at the 1-, 2-, 3-, four- or 6-week follow-ups. Significant differences were also found in reducing SBI between these two groups at weeks 1, 2, 4 and 12. However, there were no statistically significant differences in reducing BOP between curcumin as an adjunct

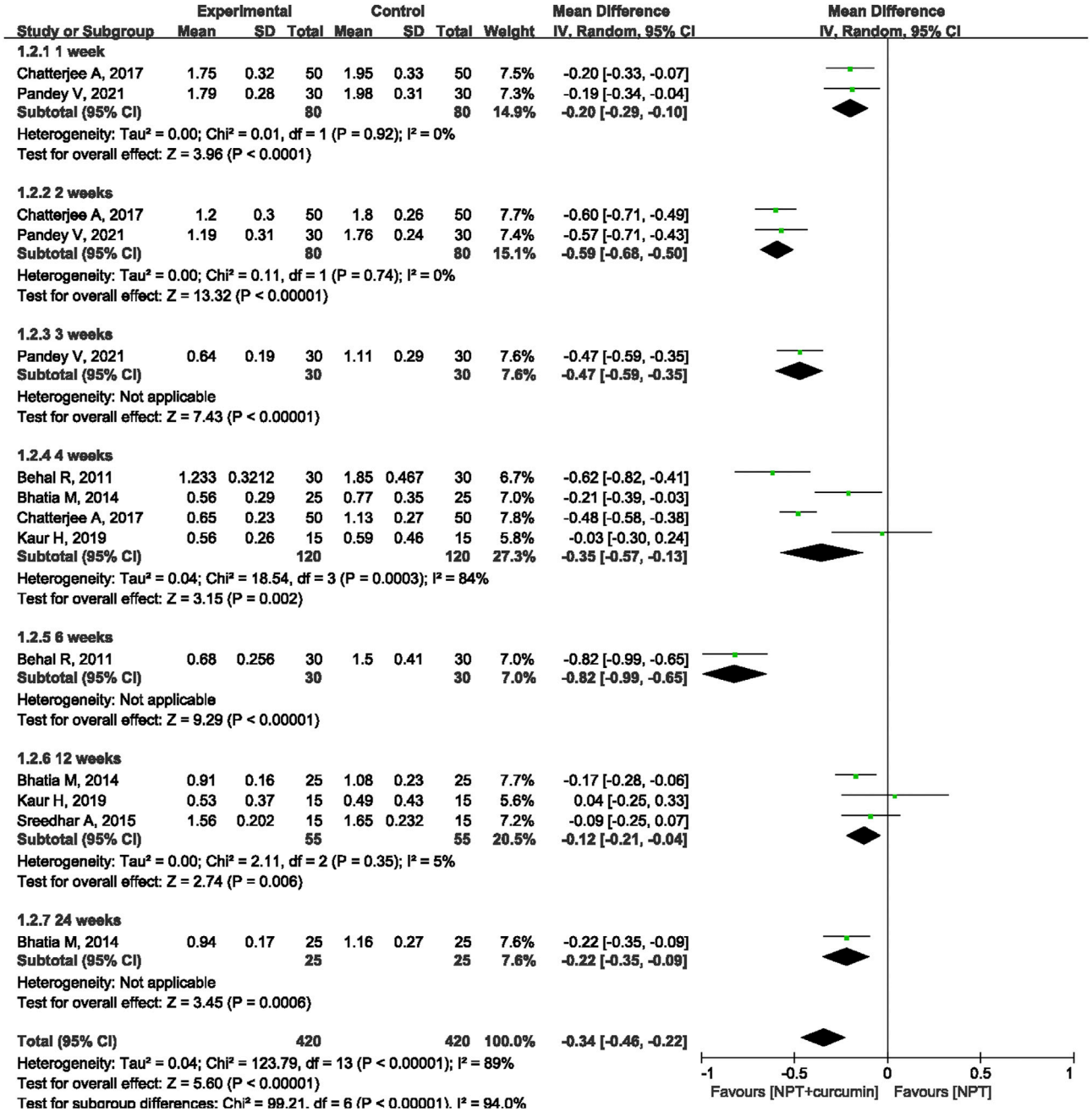

FIGURE 5 | Forest plot of the effects of curcumin + NPT versus NPT on SBI.

and NPT alone at 4, 12, and 24 weeks. Thus, curcumin has a similar effect on reducing GI and SBI compared with NPT alone when applied as an adjunct to NPT for treating periodontal disease.

In the present study, GI, SBI and BOP were used as clinical indications of periodontal inflammation. GI is based on a combination of visual evaluation and mechanical stimulus of marginal periodontal tissues. GI scores demonstrated a significant correlation with histological parameters of inflammation during the development of periodontal disease (da Silva et al., 2021). SBI provides an objective assessment for detecting early inflammatory changes in inflammatory lesions, which are sometimes difficult to visually examine (Newman, 2015). Therefore, the GI and SBI appear to be the most useful and the most easily transferred to clinical practice (Newman, 2015). This systematic review showed that NPT + curcumin could significantly reduce the GI and SBI at the 1-, 2-, 3-, 4-, and 6-week follow-ups compared to the group receiving only mechanical debridement as the treatment modality, demonstrating that using adjunctive curcumin showed better improvement in the

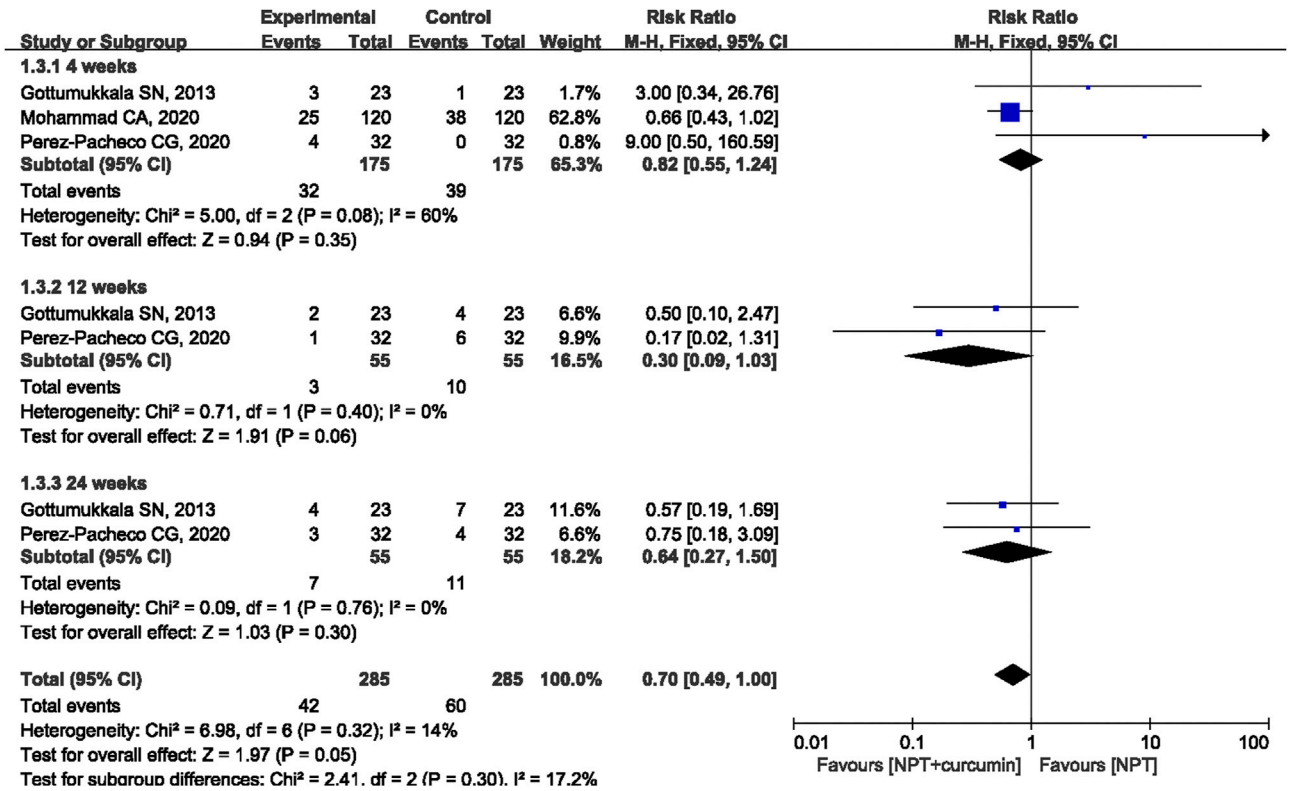

FIGURE 6 | Forest plot of the effects of curcumin + NPT versus NPT on BOP.

reduction of gingival inflammation and bleeding. However, this study revealed that there were no statistically significant differences in reducing BOP between these two groups. The result of SBI varies from that of BOP because color changes may be present without BOP (Greenstein, 1984). Meanwhile, the limited sample sizes may be another factor.

The mechanism of periodontal disease involves the production of several inflammatory mediators. Periodontal pathogens activate NF-κB, Janus kinase (JAK)/signal transducer, activator of transcription (STAT), mitogen-activated protein kinases (MAPK), and other signaling pathways and produce inflammatory cytokines such as IL-6, TNF-α and IL-1β to promote inflammation (Li et al., 2021). Curcumin, the active ingredient in turmeric, has various anti-inflammatory properties and may delay the disease process of periodontal disease in its initial stages. It has been shown to suppress the NF-κB pathway in human gingival fibroblasts in early stages and thus may inhibit *P. gingivalis* LPS-induced COX-2 synthesis (Hu et al., 2013) and the production of TNF-α, IL-8 and IL-6 by inhibiting NF-κB activation in mast cells (Kong et al., 2018). Additionally, curcumin could exert an anti-inflammatory effect by directly inhibiting the JAK/STAT signaling pathway and phosphorylation of p38 MAPK, thereby reducing the expression of iNOS, COX-2, monocyte chemoattractant protein-1 (MCP-1), and intercellular adhesionmolecule-1(ICAM-1) (Guimarães et al., 2013; Boyle et al., 2015) to reduce the inflammatory response.

Previous studies have indicated that curcumin may have an additional antimicrobial effect, although the summaries of the included articles are inconclusive. Dental plaque is an important factor in the pathological process of periodontal disease. *In vitro* studies have proven that curcumin can inhibit the growth of periodontal pathogens (such as *A. actinomycetemcomitans, F. nucleatum, and P. gingivalis*) under planktonic and biofilm conditions (Shahzad et al., 2015). The decrease in periodontal pathogens and LPS in Gram-negative bacterial walls could inhibit innate and adaptive immune responses in periodontal tissues. This effect could also explain why curcumin could suppress the inflammatory process in periodontal tissue.

Curcumin is a polyphenol found in the rhizome of turmeric, which is a spice commonly used in Asian cooking. The utilization of curcumin has proven to be safe for both animals and humans, even at high doses (Shankar et al., 1980; Lao et al., 2006). Therefore, no adverse events were reported during the follow-up in the included studies (Chatterjee et al., 2017; Singh et al., 2018; Kaur et al., 2019; Pérez-Pacheco et al., 2021).

This review has several limitations. First, this study had high statistical heterogeneity, which could not be explained by the duration of follow-up. This seems to be the consequence of both methodological and clinical heterogeneity. The heterogeneity resulted from factors such as variation in disease severity, delivery method and different concentrations of the treatments used. Unfortunately, the included articles did not provide sufficient details for us to analyze the influences of these

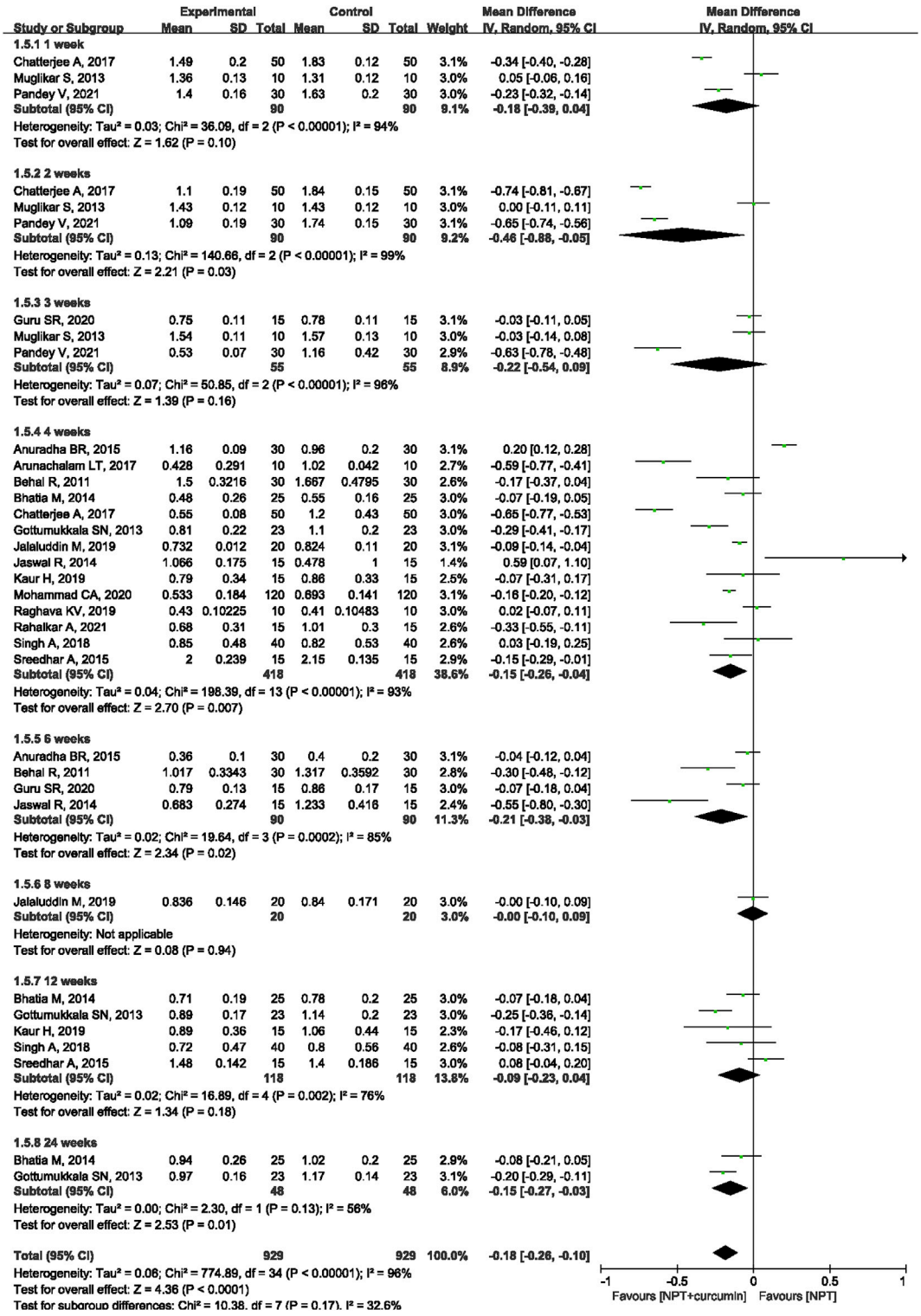

FIGURE 7 | Forest plot of the effects of curcumin + NPT versus NPT on PI.

factors. Second, only the PubMed, Embase, CENTRAL and ClinicalTrials.gov databases were searched in our meta-analysis, which could leave out some literature that may influence the final results. Third, non-English articles were excluded because we cannot understand other languages very accurately. Fourth, almost all included studies are from India.

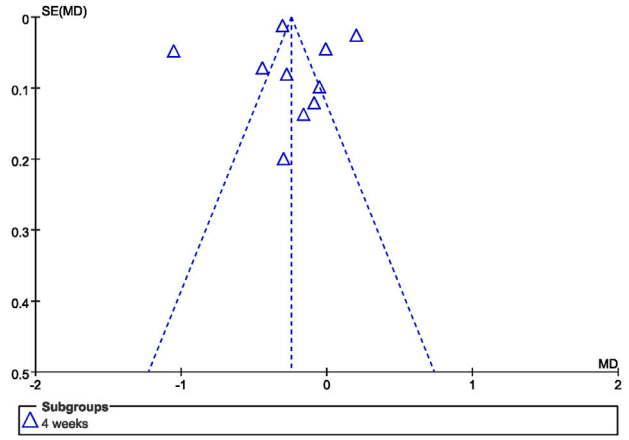

FIGURE 8 | Funnel plot of GI at 4 weeks.

Although studies on curcumin have been conducted in many countries, clinical studies aiming to evaluate the efficacy of curcumin were mainly conducted in India. Multi-center clinical trials will definitely help to verify the clinical application of curcumin. Finally, given the small sample size and limited number of studies on certain outcomes, the results might be insufficient to ensure a significant difference.

Based on the limitations above, more high-quality, registered RCTs with a large-scale sample are needed. In addition, clinical trials regarding the use of curcumin should standardize the severity of periodontal disease and treatment methods to explore the clinical effectiveness of curcumin. Safety evaluations of curcumin also need more attention.

CONCLUSION

In conclusion, based on the current evidence, the results of this systematic review and meta-analysis show that curcumin demonstrates anti-inflammatory efficacies in terms of reducing GI and SBI compared with NPT alone. Moreover, curcumin is a natural herbal medicine with few side effects, and it is a good candidate as an adjunct treatment for periodontal disease. Limited by the quantity and quality of the included studies, further high-quality studies with a large-scale sample are needed to confirm the anti-inflammatory efficacy and safety of curcumin as an adjunct to NPT.

DATA AVAILABILITY STATEMENT

The original contributions presented in the study are included in the article/**Supplementary Material**, further inquiries can be directed to the corresponding author.

AUTHOR CONTRIBUTIONS

JY and YZ had full access to all of the data in the study and took responsibility for the integrity of the data and the accuracy of the data analysis. JY, YZ, and DD designed the study. JY and YZ developed and tested the data collection forms. YZ, JY, and LH acquired the data. YZ, JY, and JZ conducted the analysis and interpreted the data. JY, YZ, and AD drafted the article. All authors critically revised the article. All authors read and approved the final article.

FUNDING

This study was funded by the Science and Technology Department of Sichuan Province (No. 22ZDYF1311), and Research and Development Foundation of West China Hospital of Stomatology, Sichuan University (No. RD-02-201905).

SUPPLEMENTARY MATERIAL

The Supplementary Material for this article can be found online at: https://www.frontiersin.org/articles/10.3389/fphar.2022.808460/full#supplementary-material

REFERENCES

Ahmadi, H., Ebrahimi, A., and Ahmadi, F. (2021). Antibiotic Therapy in Dentistry. *Int. J. Dent* 2021, 6667624. doi:10.1155/2021/6667624

Anuradha, B. R., Bai, Y. D., Sailaja, S., Sudhakar, J., Priyanka, M., and Deepika, V. (2015). Evaluation of Anti-inflammatory Effects of Curcumin Gel as an Adjunct to Scaling and Root Planing: A Clinical Study. *J. Int. Oral Health* 7 (7), 90–93. doi:10.4103/ijabmr.IJABMR_391_19

Arunachalam, L. T., Sudhakar, U., Vasanth, J., Khumukchum, S., and Selvam, V. V. (2017). Comparison of Anti-plaque and Anti-gingivitis Effect of Curcumin and Chlorhexidine Mouth Rinse in the Treatment of Gingivitis: A Clinical and Biochemical Study. *J. Indian Soc. Periodontol.* 21 (6), 478–483. doi:10.4103/jisp.jisp_116_17

Behal, R., Mali, A. M., Gilda, S. S., and Paradkar, A. R. (2011). Evaluation of Local Drug-Delivery System Containing 2% Whole Turmeric Gel Used as an Adjunct to Scaling and Root Planing in Chronic Periodontitis: A Clinical and Microbiological Study. *J. Indian Soc. Periodontol.* 15 (1), 35–38. doi:10.4103/0972-124x.82264

Bhatia, M., Urolagin, S. S., Pentyala, K. B., Urolagin, S. B., K B, M., and Bhoi, S. (2014). Novel Therapeutic Approach for the Treatment of Periodontitis by Curcumin. *J. Clin. Diagn. Res.* 8 (12), Zc65. doi:10.7860/jcdr/2014/8231.5343

Bisht, S., Mizuma, M., Feldmann, G., Ottenhof, N. A., Hong, S. M., Pramanik, D., et al. (2010). Systemic Administration of Polymeric Nanoparticle-Encapsulated Curcumin (NanoCurc) Blocks Tumor Growth and Metastases in Preclinical Models of Pancreatic Cancer. *Mol. Cancer Ther.* 9 (8), 2255–2264. doi:10.1158/1535-7163.Mct-10-0172

Boyle, D. L., Soma, K., Hodge, J., Kavanaugh, A., Mandel, D., Mease, P., et al. (2015). The JAK Inhibitor Tofacitinib Suppresses Synovial JAK1-STAT Signalling in Rheumatoid Arthritis. *Ann. Rheum. Dis.* 74 (6), 1311–1316. doi:10.1136/annrheumdis-2014-206028

Brinkac, L., Voorhies, A., Gomez, A., and Nelson, K. E. (2017). The Threat of Antimicrobial Resistance on the Human Microbiome. *Microb. Ecol.* 74 (4), 1001–1008. doi:10.1007/s00248-017-0985-z

Chatterjee, A., Debnath, K., and Rao, N. K. H. (2017). A Comparative Evaluation of the Efficacy of Curcumin and Chlorhexidine Mouthrinses on Clinical Inflammatory Parameters of Gingivitis: A Double-Blinded Randomized Controlled Clinical Study. *J. Indian Soc. Periodontol.* 21 (2), 132–137. doi:10.4103/jisp.jisp_136_17

Conigliaro, P., Triggianese, P., De Martino, E., Fonti, G. L., Chimenti, M. S., Sunzini, F., et al. (2019). Challenges in the Treatment of Rheumatoid Arthritis. *Autoimmun. Rev.* 18 (7), 706–713. doi:10.1016/j.autrev.2019.05.007

da Silva, F. G., Pola, N. M., Casarin, M., Silva, C. F. E., and Muniz, F. W. M. G. (2021). Association between Clinical Measures of Gingival Inflammation and Obesity in Adults: Systematic Review and Meta-Analyses. *Clin. Oral Investig.* 25 (7), 4281–4298. doi:10.1007/s00784-021-03961-1

Frencken, J. E., Sharma, P., Stenhouse, L., Green, D., Laverty, D., and Dietrich, T. (2017). Global Epidemiology of Dental Caries and Severe Periodontitis - a Comprehensive Review. *J. Clin. Periodontol.* 44 (Suppl. 18), S94–s105. doi:10.1111/jcpe.12677

Gottumukkala, S. N., Koneru, S., Mannem, S., and Mandalapu, N. (2013). Effectiveness of Sub Gingival Irrigation of an Indigenous 1% Curcumin Solution on Clinical and Microbiological Parameters in Chronic Periodontitis Patients: A Pilot Randomized Clinical Trial. *Contemp. Clin. Dent* 4 (2), 186–191. doi:10.4103/0976-237x.114874

Greenstein, G. (1984). The Role of Bleeding upon Probing in the Diagnosis of Periodontal Disease. A Literature Review. *J. Periodontol.* 55 (12), 684–688. doi:10.1902/jop.1984.55.12.684

Guimarães, M. R., Leite, F. R., Spolidorio, L. C., Kirkwood, K. L., and Rossa, C., Jr. (2013). Curcumin Abrogates LPS-Induced Pro-inflammatory Cytokines in RAW 264.7 Macrophages. Evidence for Novel Mechanisms Involving SOCS-1, -3 and P38 MAPK. *Arch. Oral Biol.* 58 (10), 1309–1317. doi:10.1016/j.archoralbio.2013.07.005

Guru, S. R., Reddy, K. A., Rao, R. J., Padmanabhan, S., Guru, R., and Srinivasa, T. S. (2020). Comparative Evaluation of 2% Turmeric Extract with Nanocarrier and 1% Chlorhexidine Gel as an Adjunct to Scaling and Root Planing in Patients with Chronic Periodontitis: A Pilot Randomized Controlled Clinical Trial. *J. Indian Soc. Periodontol.* 24 (3), 244–252. doi:10.4103/jisp.jisp_207_19

Heitz-Mayfield, L. J., and Lang, N. P. (2013). Surgical and Nonsurgical Periodontal Therapy. Learned and Unlearned Concepts. *Periodontol. 2000* 62 (1), 218–231. doi:10.1111/prd.12008

Higgins, J. P. T., Thomas, J., Chandler, J., Cumpston, M., Li, T., Page, M. J., et al. (2020). *Cochrane Handbook for Systematic Reviews of Interventions*. Chichester, UK: John Wiley & Sons. version 6.1. (updated September 2020). Cochrane.

Hu, P., Huang, P., and Chen, M. W. (2013). Curcumin Attenuates Cyclooxygenase-2 Expression via Inhibition of the NF-Kb Pathway in Lipopolysaccharide-Stimulated Human Gingival Fibroblasts. *Cell Biol Int* 37 (5), 443–448. doi:10.1002/cbin.10050

Jalaluddin, M., Jayanti, I., Gowdar, I. M., Roshan, R., Varkey, R. R., and Thirutheri, A. (2019). Antimicrobial Activity of Curcuma Longa L. Extract on Periodontal Pathogens. *J. Pharm. Bioallied Sci.* 11 (Suppl. 2), S203–s207. doi:10.4103/jpbs.Jpbs_295_18

Jaswal, R., Dhawan, S., Grover, V., and Malhotra, R. (2014). Comparative Evaluation of Single Application of 2% Whole Turmeric Gel versus 1% Chlorhexidine Gel in Chronic Periodontitis Patients: A Pilot Study. *J. Indian Soc. Periodontol.* 18 (5), 575–580. doi:10.4103/0972-124x.142445

Kaur, H., Grover, V., Malhotra, R., and Gupta, M. (2019). Evaluation of Curcumin Gel as Adjunct to Scaling & Root Planing in Management of Periodontitis- Randomized Clinical & Biochemical Investigation. *Infect. Disord. Drug Targets* 19 (2), 171–178. doi:10.2174/1871526518666180601073422

Kong, R., Kang, O. H., Seo, Y. S., Zhou, T., Kim, S. A., Shin, D. W., et al. (2018). MAPKs and NF-κB P-athway I-nhibitory E-ffect of B-isdemethoxycurcumin on P-horbol-12-myristate-13-acetate and A23187-induced I-nflammation in H-uman M-ast C-ells. *Mol. Med. Rep.* 17 (1), 630–635. doi:10.3892/mmr.2017.7852

Lao, C. D., Ruffin, M. T., Normolle, D., Heath, D. D., Murray, S. I., Bailey, J. M., et al. (2006). Dose Escalation of a Curcuminoid Formulation. *BMC Complement. Altern. Med.* 6, 10. doi:10.1186/1472-6882-6-10

Li, Y., Jiao, J., Qi, Y., Yu, W., Yang, S., Zhang, J., et al. (2021). Curcumin: A Review of Experimental Studies and Mechanisms Related to Periodontitis Treatment. *J. Periodontal Res.* 56 (5), 837–847. doi:10.1111/jre.12914

Mohammad, C. A. (2020). Efficacy of Curcumin Gel on Zinc, Magnesium, Copper, IL-1β, and TNF-α in Chronic Periodontitis Patients. *Biomed. Res. Int.* 2020, 8850926. doi:10.1155/2020/8850926

Muglikar, S., Patil, K. C., Shivswami, S., and Hegde, R. (2013). Efficacy of Curcumin in the Treatment of Chronic Gingivitis: a Pilot Study. *Oral Health Prev. Dent* 11 (1), 81–86. doi:10.3290/j.ohpd.a29379

Newman, M. (2015). *Carranza`s Clinical Periodontology E-Dition*. Philadelphia: Saunders.

Page, M. J., McKenzie, J. E., Bossuyt, P. M., Boutron, I., Hoffmann, T. C., Mulrow, C. D., et al. (2021). The PRISMA 2020 Statement: an Updated Guideline for Reporting Systematic Reviews. *Bmj* 372, n71. doi:10.1136/bmj.n71

Pandey, V., Kumar, D., Nisha, S., Gupta, A. K., Verma, T., and Kumari, A. (2021). Evaluation of Anti-plaque and Anti-inflammatory Effects of Oral Curcumin Gel as Adjunct to Scaling and Root Planing: A Clinical Study. *Int. J. Appl. Basic Med. Res.* 11 (2), 90–94. doi:10.4103/ijabmr.IJABMR_391_19

Pérez-Pacheco, C. G., Fernandes, N. A. R., Primo, F. L., Tedesco, A. C., Bellile, E., Retamal-Valdes, B., et al. (2021). Local Application of Curcumin-Loaded Nanoparticles as an Adjunct to Scaling and Root Planing in Periodontitis: Randomized, Placebo-Controlled, Double-Blind Split-Mouth Clinical Trial. *Clin. Oral Investig.* 25 (5), 3217–3227. doi:10.1007/s00784-020-03652-3

Petersilka, G. J., Ehmke, B., and Flemmig, T. F. (2002). Antimicrobial Effects of Mechanical Debridement. *Periodontol. 2000* 28, 56–71. doi:10.1034/j.1600-0757.2002.280103.x

Pimentel, S. P., Casati, M. Z., Ribeiro, F. V., Corrêa, M. G., Franck, F. C., Benatti, B. B., et al. (2020). Impact of Natural Curcumin on the Progression of Experimental Periodontitis in Diabetic Rats. *J. Periodontal Res.* 55 (1), 41–50. doi:10.1111/jre.12683

Raghava, K. V., Sistla, K. P., Narayan, S. J., Yadalam, U., Bose, A., and Mitra, K. (2019). Efficacy of Curcumin as an Adjunct to Scaling and Root Planing in Chronic Periodontitis Patients: A Randomized Controlled Clinical Trial. *J. Contemp. Dent Pract.* 20 (7), 842–846. doi:10.5005/jp-journals-10024-2608

Rahalkar, A., Kumathalli, K., and Kumar, R. (2021). Determination of Efficacy of Curcumin and Tulsi Extracts as Local Drugs in Periodontal Pocket Reduction: A Clinical and Microbiological Study. *J. Indian Soc. Periodontol.* 25 (3), 197–202. doi:10.4103/jisp.jisp_158_20

Sanz, M., Beighton, D., Curtis, M. A., Cury, J. A., Dige, I., Dommisch, H., et al. (2017). Role of Microbial Biofilms in the Maintenance of Oral Health and in the Development of Dental Caries and Periodontal Diseases. Consensus Report of Group 1 of the Joint EFP/ORCA Workshop on the Boundaries between Caries and Periodontal Disease. *J. Clin. Periodontol.* 44 (Suppl. 18), S5–s11. doi:10.1111/jcpe.12682

Shahzad, M., Millhouse, E., Culshaw, S., Edwards, C. A., Ramage, G., and Combet, E. (2015). Selected Dietary (Poly)phenols Inhibit Periodontal Pathogen Growth and Biofilm Formation. *Food Funct.* 6 (3), 719–729. doi:10.1039/c4fo01087f

Shankar, T. N., Shantha, N. V., Ramesh, H. P., Murthy, I. A., and Murthy, V. S. (1980). Toxicity Studies on Turmeric (Curcuma Longa): Acute Toxicity Studies in Rats, Guineapigs & Monkeys. *Indian J. Exp. Biol.* 18 (1), 73–75.

Sharma, M., Sharma, S., and Wadhwa, J. (2019). Improved Uptake and Therapeutic Intervention of Curcumin via Designing Binary Lipid Nanoparticulate Formulation for Oral Delivery in Inflammatory Bowel Disorder. *Artif. Cell Nanomed Biotechnol* 47 (1), 45–55. doi:10.1080/21691401.2018.1543191

Singh, A., Sridhar, R., Shrihatti, R., and Mandloy, A. (2018). Evaluation of Turmeric Chip Compared with Chlorhexidine Chip as a Local Drug Delivery Agent in the Treatment of Chronic Periodontitis: A Split Mouth Randomized Controlled Clinical Trial. *J. Altern. Complement. Med.* 24 (1), 76–84. doi:10.1089/acm.2017.0059

Slots, J., and Ting, M. (2002). Systemic Antibiotics in the Treatment of Periodontal Disease. *Periodontol. 2000* 28, 106–176. doi:10.1034/j.1600-0757.2002.280106.x

Sreedhar, A., Sarkar, I., Rajan, P., Pai, J., Malagi, S., Kamath, V., et al. (2015). Comparative Evaluation of the Efficacy of Curcumin Gel with and without Photo Activation as an Adjunct to Scaling and Root Planing in the Treatment of Chronic Periodontitis: A Split Mouth Clinical and Microbiological Study. *J. Nat. Sci. Biol. Med.* 6 (Suppl. 1), S102–S109. doi:10.4103/0976-9668.166100

Tang, W., Du, M., Zhang, S., and Jiang, H. (2020). Therapeutic Effect of Curcumin on Oral Diseases: A Literature Review. *Phytotherapy Res.* 35, 2287–2295. doi:10.1002/ptr.6943

Tomasi, C., Leyland, A. H., and Wennström, J. L. (2007). Factors Influencing the Outcome of Non-surgical Periodontal Treatment: a Multilevel Approach. *J. Clin. Periodontol.* 34 (8), 682–690. doi:10.1111/j.1600-051X.2007.01111.x

Zhang, Y., Huang, L., Mazurel, D., Zheng, H., Yang, J., and Deng, D. (2021). Clinical Efficacy of Curcumin versus Chlorhexidine as an Adjunct to Scaling and Root Planing for the Treatment of Periodontitis: A Systematic Review and Meta-analysis. *Phytotherapy Res.* 35, 5980–5991. doi:10.1002/ptr.7208

Conflict of Interest: The authors declare that the research was conducted in the absence of any commercial or financial relationships that could be construed as a potential conflict of interest.

Publisher's Note: All claims expressed in this article are solely those of the authors and do not necessarily represent those of their affiliated organizations, or those of the publisher, the editors and the reviewers. Any product that may be evaluated in this article, or claim that may be made by its manufacturer, is not guaranteed or endorsed by the publisher.

frontiers in Pharmacology

ORIGINAL RESEARCH
published: 03 February 2022
doi: 10.3389/fphar.2021.748995

Berberine Facilitates Extinction and Prevents the Return of Fear

Shihao Huang[1], *Yu Zhou*[2], *Feilong Wu*[1], *Cuijie Shi*[1], *He Yan*[3], *Liangpei Chen*[3], *Chang Yang*[1,4]* *and Yixiao Luo*[1,4]*

[1]Key Laboratory of Molecular Epidemiology of Hunan Province, School of Medicine, Hunan Normal University, Changsha, China, [2]Yiyang Medical College, Yiyang, China, [3]Department of Forensic Science, School of Basic Medical Science, Central South University, Changsha, China, [4]China Hunan Province People's Hospital, The First-affiliated Hospital of Hunan Normal University, Changsh, China

Exposure to a catastrophic event or intense stimulation can trigger fear memories, and the threatening memories persist even over a lifetime. Exposure therapy is based on extinction learning and is widely used to treat fear-related disorders, but its effect on remote fear memory is modest. Berberine, an isoquinoline alkaloid derived from *Coptis chinensis* or *Berberis* spp., has been recently reported to exert a diversity of pharmacological effects on the central nervous system, such as facilitating extinction of drug memory. Here, we explored the effect of berberine on extinction of fear memory using a classical contextual fear conditioning (CFC) paradigm, which is Pavlovian conditioning, can rapidly create fear memories related to contexts. Twenty-four hours or 30 days after CFC training, mice were subjected to context extinction (10 days) to extinguish their behaviors and treated with 12.5 or 25 mg/kg berberine intragastrically 1 or 6 h after each extinction session, followed by reinstatement and spontaneous recovery tests. The results showed that intragastric administration of 25 mg/kg berberine 1 h after extinction significantly promoted the extinction of recent and remote fear memories and prevented reinstatement and spontaneous recovery of extinguished fear in mice. These findings indicate that berberine combined with extinction training could serve as a promising novel avenue for the treatment of fear-related disorders.

Keywords: berberine, extinction, fear memory, contextual fear conditioning, PTSD

OPEN ACCESS

Edited by:
Annalisa Chiavaroli, University of Studies G. d'Annunzio Chieti and Pescara, Italy

Reviewed by:
Rongji Hui, Hebei Medical University, China
Claudio Ferrante, University of Studies G. d'Annunzio Chieti and Pescara, Italy

***Correspondence:**
Chang Yang
yangchang2370@126.com
Yixiao Luo
luoyx@hunnu.edu.cn

Specialty section:
This article was submitted to Ethnopharmacology, a section of the journal Frontiers in Pharmacology

Received: *28 July 2021*
Accepted: *30 December 2021*
Published: *03 February 2022*

Citation:
Huang S, Zhou Y, Wu F, Shi C, Yan H, Chen L, Yang C and Luo Y (2022) Berberine Facilitates Extinction and Prevents the Return of Fear. Front. Pharmacol. 12:748995. doi: 10.3389/fphar.2021.748995

1 INTRODUCTION

Fear response is an emotional experience necessary to adapt to the new environment. However, an exceedingly strong, persistent, and uncontrollable state of fear can lead to the development of anxiety and fear-related disorders, such as posttraumatic stress disorder (PTSD). PTSD is a mental disorder that has a high incidence and difficult to be completely cured, with a lifetime prevalence of 6.8% (Markowitz et al., 2015). The patients exert repeated and long-term fear responses, and this disorder brings great pain to people's lives and causes a huge social–economic burden.

In the laboratory, fear learning is usually studied by classical (Pavlovian) association between a neutral conditioned stimulus (CS) and a fearsome stimulus (usually one or more footshocks; unconditioned stimulus [US]). After being conditioned to a US, a CS can elicit a fear response (Gutberlet et al., 1902; Mcgaugh, 2000). However, extinction of conditioned fear occurred when repeatedly exposed to a CS without US presentation, which has been proposed to be a new CS–no US memory termed as "extinction memory" (Pavlov, 1927; Morgan and Ledoux, 1999; Berman and Dudai, 2001; Maren et al., 2013; Singewald and Holmes, 2019). Extinction is not the erasure of the

original fear memory, but the formation of a new extinction memory to inhibit the expression of fear (Orsini and Maren, 2012; Izquierdo et al., 2016; Likhtik and Johansen, 2019; Bouton et al., 2021). The new extinction memory also involved acquisition, consolidation, and storage processes (Millan et al., 2011; Orsini and Maren, 2012; Maren et al., 2013; Careaga et al., 2016; Knox, 2016). Studies demonstrate that PTSD subjects lead to extinguished fear relapses due to impaired recall of extinction memory (Vervliet et al., 2013; Goode and Maren, 2014; Qin et al., 2021). Therefore, enhancing consolidation of extinction memory has been considered as a strategy for attenuating the original fear memory. Nevertheless, it is easy to relapse because of the persistence of fear memories in humans and rodents, the response of previously extinguished fear will reemerge when the original US is given unexpectedly, called "reinstatement" (Haaker et al., 2014; Goode and Maren, 2019). Similarly, such responses will reoccur when a substantial amount of time has passed, called "spontaneous recovery" (Rescorla, 2004; Lacagnina et al., 2019). Fear memory was subdivided into recent and remote fear memory after training 1 or 30 days in animal studies, respectively (Anagnostaras et al., 1999; Pan et al., 2020; Vetere et al., 2021). Exposure therapy based on extinction theory described above has less effect on remote fear memory and seldom suppresses the reinstatement and spontaneous recovery of extinguished fear (Costanzi et al., 2011; Graff et al., 2014; An et al., 2017). Also, Dudai's remarkable discovery demonstrated that memories become impervious to interferences that disrupt synaptic consolidation within 6 h after the training, which provides a precise time window to interfere with consolidation memory (Dudai, 2004). Together, there is an urgent need to enhance the efficacy of exposure therapy and develop potential and effective strategies for fear-related disorders treatment.

Berberine is a biologically active isoquinoline alkaloid extracted from the roots or stems of the Chinese traditional medicine *Coptis chinensis* and *Berberis* spp. (Neag et al., 2018; Belwal et al., 2020). It was used as a traditional medicine for centuries and has been clinically widely used as an over-the-counter (OTC) drug for gastrointestinal infections (Domitrovic et al., 2011; Habtemariam, 2020). Recently, growing evidence demonstrates that berberine has therapeutic potential in many central nervous system pathological conditions. Berberine exerted antidepressant-like effect by modulating brain biogenic amines including norepinephrine, serotonin, and dopamine (DA) (Kulkarni and Dhir, 2008; Habtemariam, 2020) and showed neuroprotective effect via modulation of Sirt 1/p38 MAPK expression in traumatic brain injury (Wang et al., 2018). In addition, berberine improves brain DOPA/DA levels to ameliorate Parkinson disease by regulating gut microbiota (Wang et al., 2021). Moreover, berberine modulates oxytocin receptors to attenuate methamphetamine consumption and anxiety-like behaviors (Alavijeh et al., 2019). Furthermore, berberine has been reported to alleviate anxiety-like behavior in rats with posttraumatic stress disorder and facilitate extinction of drug memories (Lee et al., 2018; Shen et al., 2020). In Shen and colleagues' study, they found that brain-derived neurotropic factor (BDNF) and AMPA receptors (GluA1 and GluA2) were associated with enhanced extinction memory consolidation (Shen et al., 2020). AMPA receptor GluR1 signaling is also involved in consolidation of remote fear memories (Andero and Ressler, 2012). Although fear memory and drug memory are different types of memory, they have similar memory processes, underlying neurobiological mechanisms, and both are driven by emotional or traumatic experiences, and thus both of them are considered as pathological emotional memories (Torregrossa et al., 2011; Taylor and Torregrossa, 2015). Besides that, much evidence shows the levels of BDNF, GluA1, and GluA2 deemed for critical roles in both drug extinction memory and fear extinction memory (Yu et al., 2009; Andero and Ressler, 2012; Rakofsky et al., 2012). For the reasons mentioned previously, it is reasonable to speculate that berberine may have effect on fear extinction memory. However, the effects of berberine treatment on the extinction of fear memory and its therapeutic potential for fear-related disorders have not been reported yet.

Taken together, the data to date suggest a hypothesis that berberine plays a critical role in fear extinction memory. Here, we first aimed to evaluate the optimum dose of berberine and then tested the hypothesis that berberine combined with extinction training enhances extinction memory and prevents the return of fear. In the present study, we used a classical contextual fear-conditioning (CFC) model to test the effect of berberine treatment on extinction of both recent and remote fear memory and investigated whether berberine combined with extinction training could persistently attenuate and prevent the return of fear in mice.

2 MATERIALS AND METHODS

2.1 Subjects

Male C57BL/6 mice (initially weighing 20–22 g on arrival) were purchased from the Tianqin Laboratory Animal Technology Co., Ltd., China. A total of 134 mice were used for experiments. Mice were housed in groups of four per cage, maintained on a 12-h light–dark cycle (lights off at 7:00 AM, lights on at 7:00 PM) at a room temperature of 20°C–25°C with *ad libitum* access to food and water. All mice were handled 3-min daily for 3 days before behavioral procedures. The current study and its experiments were conducted according to the Guide of Hunan Province for the Care and Use of Laboratory Animals, and experimental protocols were approved by the Local Committee on Animal Care and Use and Protection of the Hunan Normal University (protocol 2021320).

2.2 Drugs

The doses of berberine were chosen based on our previous study (Shen et al., 2020). Berberine was resuspended with corn oil to concentrations of 12.5 and 25 mg/ml immediately before use. In the control group, mice were administrated with corn oil (1 ml/kg) intragastrically. Berberine was purchased from J&K Chemical Ltd., Shanghai, China.

2.3 Behavioral Procedures

2.3.1 Contextual Fear Conditioning

The CFC procedure was based on our previous study with minor modification (Liu et al., 2015). All mice were handled for 1–2 min per day for 3 days before conditioning. On the training day, they were placed in the conditioning chamber (Shanghai XinRuan Information Technology Co., Ltd.), and three 2-s 0.75-mA foot shocks were delivered on 180, 240, and 300 s, and the mice were allowed to explore the conditioning chamber for an additional 30 s and then removed to their home cages. After removing the mice from the chamber, the chamber was cleaned and scented with 75% alcohol. All training sessions were during the dark cycle (7:00 AM–19:00 PM). Freezing behavior was defined as lack of all movement except respiration. The percentage of freezing time was calculated by dividing the freezing time by the total time.

2.3.2 Extinction and Extinction Test

During 5-min daily extinction sessions for 10 days, the conditions were the same as CFC training except that foot shock was no longer delivered. Mice were administrated with berberine (12.5 and 25 mg/kg) or coin oil (1 ml/kg) orally 1 or 6 h after each extinction session.

Extinction tests were performed 2 days after last extinction session; the conditions were the same as the extinction session.

2.3.3 Reinstatement and Spontaneous Recovery

For reinstatement test, a 0.75-mA foot shock was given after the extinction test to reinstate extinguished fear, followed by a 5-min reinstatement test 24 h later in the training chamber.

The spontaneous recovery test was conducted 30 days after the extinction test in the training chamber. The definition of freezing behaviors was the absence of all movement except of respiration.

2.4 Statistical Analysis

Data were analyzed using repeated-measures analysis of variance (ANOVA) with appropriate between-subjects factor and within-subjects factor followed by Bonferroni *post hoc* test for each experiment (see Results section). Power analysis was used to calculate appropriately the number of animals at 8) with a statistical power of >85%. The results are presented as the mean ± SEM. $p < 0.05$ was considered statistically significant.

2.5 Experimental Design

2.5.1 Experiments 1, 2: The Effect of Berberine Administration After Each Extinction Session on Extinction Training and Subsequent Reinstatement of Recent Fear Memory

In experiment 1, mice were habituated for 3 days. On day 3, the mice received CFC training, and then were divided into three groups: (1) oral gavage administration of corn oil (1 ml/kg) 1 h after each extinction session (control, $n = 8$); (2) oral gavage administration of berberine (12.5 mg/kg) 1 h after each extinction session (12.5 mg/kg berberine, $n = 8$); (3) oral gavage administration of berberine (25 mg/kg) 1 h after each extinction session (25 mg/kg berberine, $n = 8$). Twenty-four hours after CFC training, the mice underwent 5-min daily extinction training with different treatments for 10 consecutive days (Lacagnina et al., 2019). Two days after the last extinction session, the mice were examined for extinction test. After the extinction test, one single shock was given to reinstate extinguished fear. Twenty-four hours later, mice were conducted for reinstatement test (**Figure 1A**).

To test whether berberine specifically facilitates consolidation of extinction memory, in experiment 2, mice were divided into two groups after CFC training: (1) oral gavage administration of corn oil (1 ml/kg) 6 h after each extinction session (6 h + control, $n = 8$); (2) oral gavage administration of berberine (25 mg/kg) 6 h after each extinction session (6 h + berberine, $n = 7$). All mice then underwent the same experimental procedures with **Figure 1A,E**).

2.5.2 Experiments 3, 4: The Effect of Berberine Administration After Each Extinction Session on Extinction Training and Subsequent Spontaneous Recovery of Recent Fear Memory

In experiment 3, mice were habituated for 3 days. On day 3, mice received CFC training and then were divided into two groups: (1) oral gavage administration of corn oil (1 ml/kg) 1 h after each extinction session (1 h + control, $n = 7$); (2) oral gavage administration of berberine (25 mg/kg) 1 h after each extinction session (1 h + berberine, $n = 8$). Twenty-four hours after CFC training, mice underwent 5-min daily extinction training with corn oil or berberine administration for 10 consecutive days. Two days after the last extinction session, the mice were examined for extinction test. One month later, the mice were conducted for spontaneous recovery test (**Figure 2A**).

To examine the effect of delayed administration of berberine on fear extinction and subsequent spontaneous recovery, in experiment 4, mice were divided into two groups after CFC training: (1) oral gavage administration of corn oil (1 ml/kg) 6 h after each extinction session (6 h + control, $n = 8$); (2) oral gavage administration of berberine (25 mg/kg) 6 h after each extinction session (6 h + berberine, $n = 8$). All mice then underwent the same experimental procedures with **Figures 2A,E**).

2.5.3 Experiments 5, 6: Effect of Berberine Administration After Each Extinction Session on Extinction Training and Subsequent Reinstatement of Remote Fear Memory

In experiments 5 and 6, the experimental procedure was the same as that in experiments 1 and 2, except that extinction training sessions were performed 30 days rather than 24 h after the CFC training, $n = 8$ in both groups (**Figures 3A,E**).

2.5.4 Experiments 7, 8: Effect of Berberine Administration After Each Extinction Session on Extinction Training and Subsequent Spontaneous Recovery of Remote Fear Memory

In experiments 7 and 8, the experimental procedure was the same as that in experiments 3 and 4, except that extinction training sessions were performed 30 days rather than 24 h after the CFC training, $n = 8$ in both groups (**Figures 4A,E**).

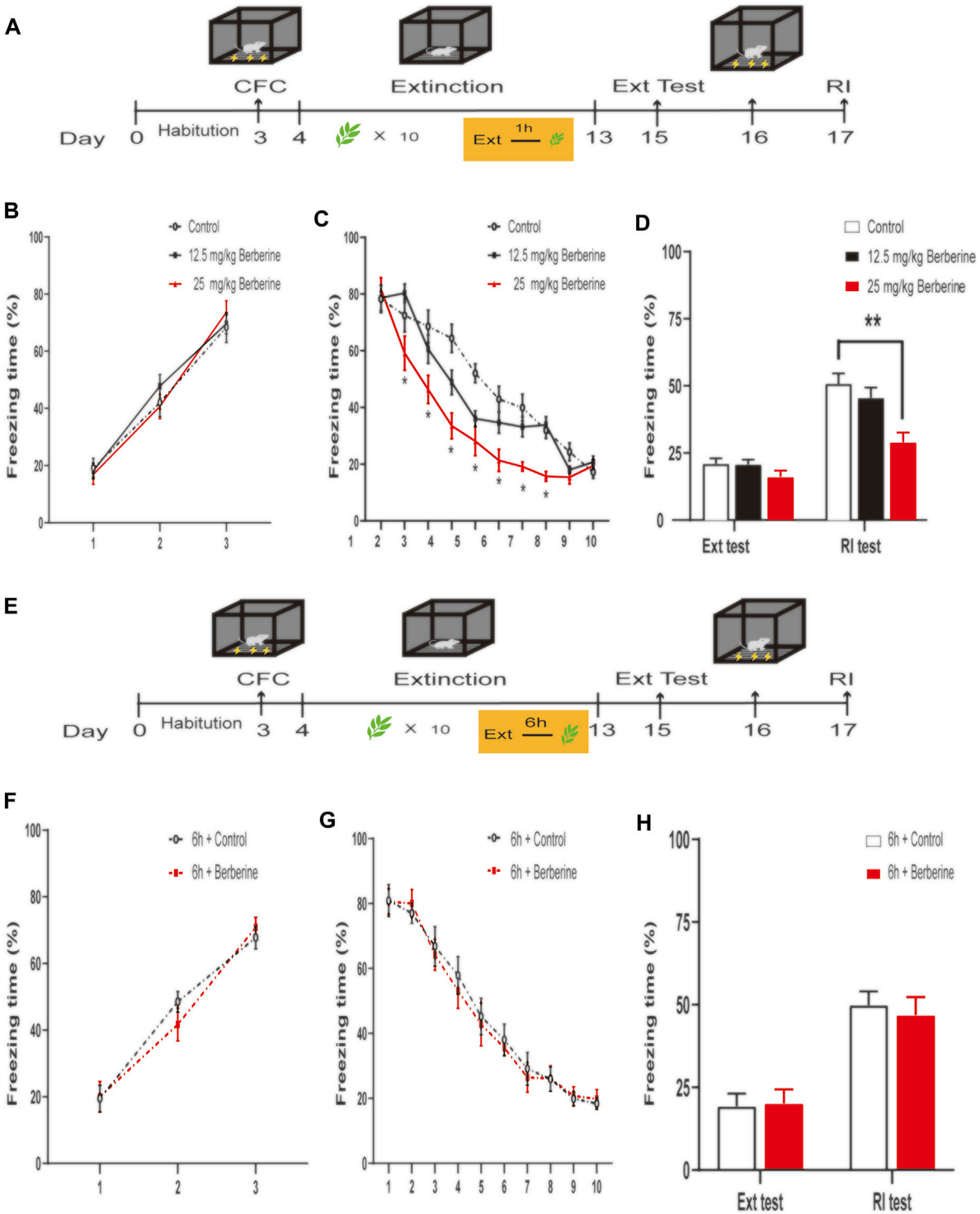

FIGURE 1 | Berberine administration 1 h after extinction enhanced extinction and reduced reinstatement of recent fear. **(A, E)** Timeline of contextual fear conditioning, drug treatment, extinction training, extinction test, and reinstatement test. **(A)** One hour after each extinction training session, corn oil (1 ml/kg, intragastrically [i.g.]) or berberine (12.5 and 25 mg/kg, i.g.) was administered to mice, respectively. **(E)** Six hours after each extinction training session, 1 ml/kg corn oil (i.g.) or 25 mg/kg berberine (i.g.) was administered to mice. **(B, F)** Freezing levels during fear conditioning were similar between different groups. **(C, G)** Freezing behaviors declined during extinction training sessions. **(C)** Repeated-measures ANOVA, effect of the training day, $F_{(9,189)} = 164.1$, $p0.001$; Bonferroni *post hoc* test, $p < 0.05$, during the extinction training days 2–8. **(D, H)** Percentage of freezing time during extinction test (left) and reinstatement test (right). **(D)** Significant freezing time was observed in RI test, $p < 0.01$. $n = 7$–8 mice per group. Data are means ± SEM, $^{*}p < 0.05$, $^{**}p < 0.01$, compared with the control group. CFC, contextual fear conditioning; Ext, extinction; RI, reinstatement.

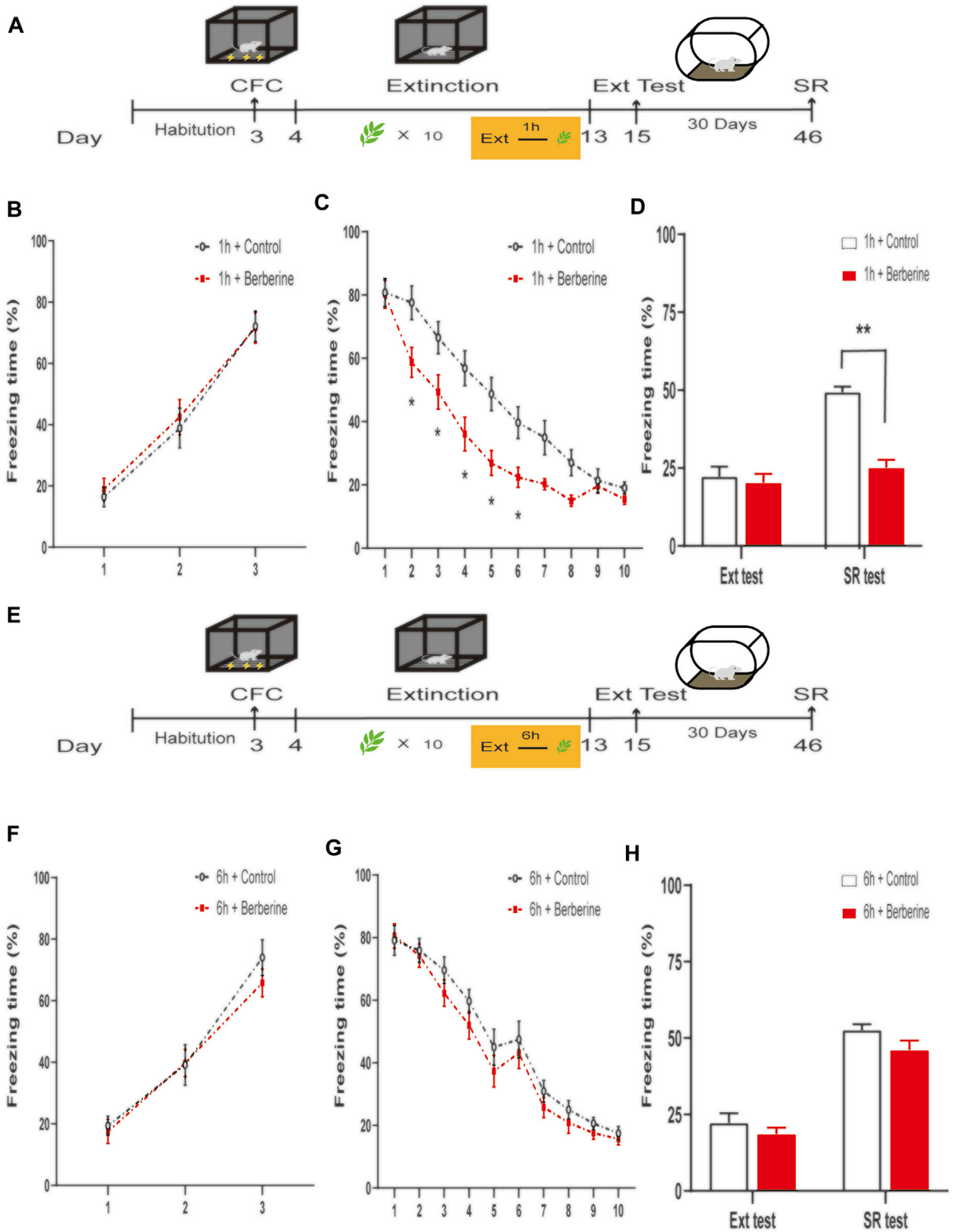

FIGURE 2 | Berberine administration 1 h after extinction enhanced extinction and reduced spontaneous recovery of recent fear. **(A, E)** Timeline of contextual fear conditioning, drug treatment, extinction training, extinction test, and spontaneous recovery test. **(A)** One hour or **(E)** 6 h after each extinction training session, corn oil (1 ml/kg, i.g.) or berberine (25 mg/kg, i.g.) was administered to mice, respectively. **(B, F)** Freezing levels during fear conditioning were similar between different groups. **(C, G)** Freezing behaviors declined during extinction training sessions. **(C)** Repeated-measures ANOVA, effect of the training day, $F_{(9,117)} = 169.3$, $p < 0.001$; Bonferroni *post hoc* test, $p < 0.05$, during the extinction training days 2–6. **(D, H)** Percentage of freezing time during extinction test (left) and spontaneous recovery test (right). **(D)** Significant freezing time was observed in SR test, $p < 0.01$. $n = 7$–8 mice per group. Data are means ± SEM, $^{*}p < 0.05$, $^{**}p < 0.01$, compared with 1 h + control group. CFC, contextual fear conditioning; Ext, extinction; SR, spontaneous recovery.

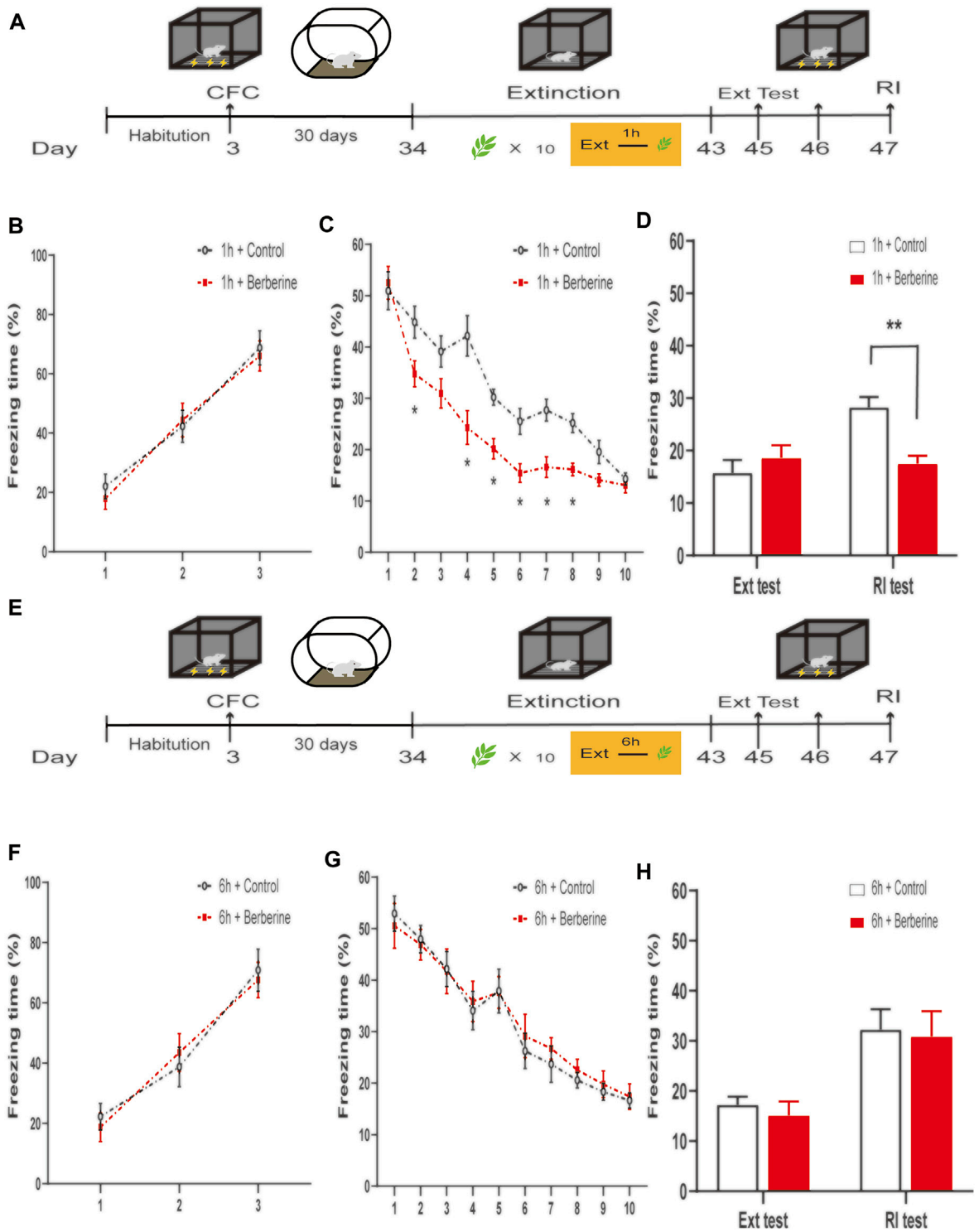

FIGURE 3 | Berberine treatment 1 h after extinction enhanced extinction and reduced reinstatement of remote fear. **(A, E)** Timeline of contextual fear conditioning, drug treatment, extinction training, extinction test, and reinstatement test. **(A)** One hour or **(E)** 6 h after each extinction training session, corn oil (1 ml/kg, i.g.) or berberine (25 mg/kg, i.g.) was administered to mice, respectively. **(B, F)** Freezing levels during fear conditioning were similar between different groups. **(C, G)** Thirty days after CFC, freezing behaviors declined during extinction training sessions. **(C)** Repeated-measures ANOVA, effect of the training day, $F_{(9,126)} = 233.4$, $p < 0.001$; Bonferroni *post hoc* test, $p < 0.05$, during extinction training days 2, 4–8. **(D, H)** Percentage of freezing time during extinction test (left) and reinstatement test (right). **(D)** Significant freezing time was observed in RI test, $p = 0.0027$. $n = 8$ mice per group. Data are means ± SEM, $^{*}p < 0.05$, $^{**}p < 0.01$, and compared with 1 h + control group. CFC, contextual fear conditioning; Ext, extinction; RI, reinstatement.

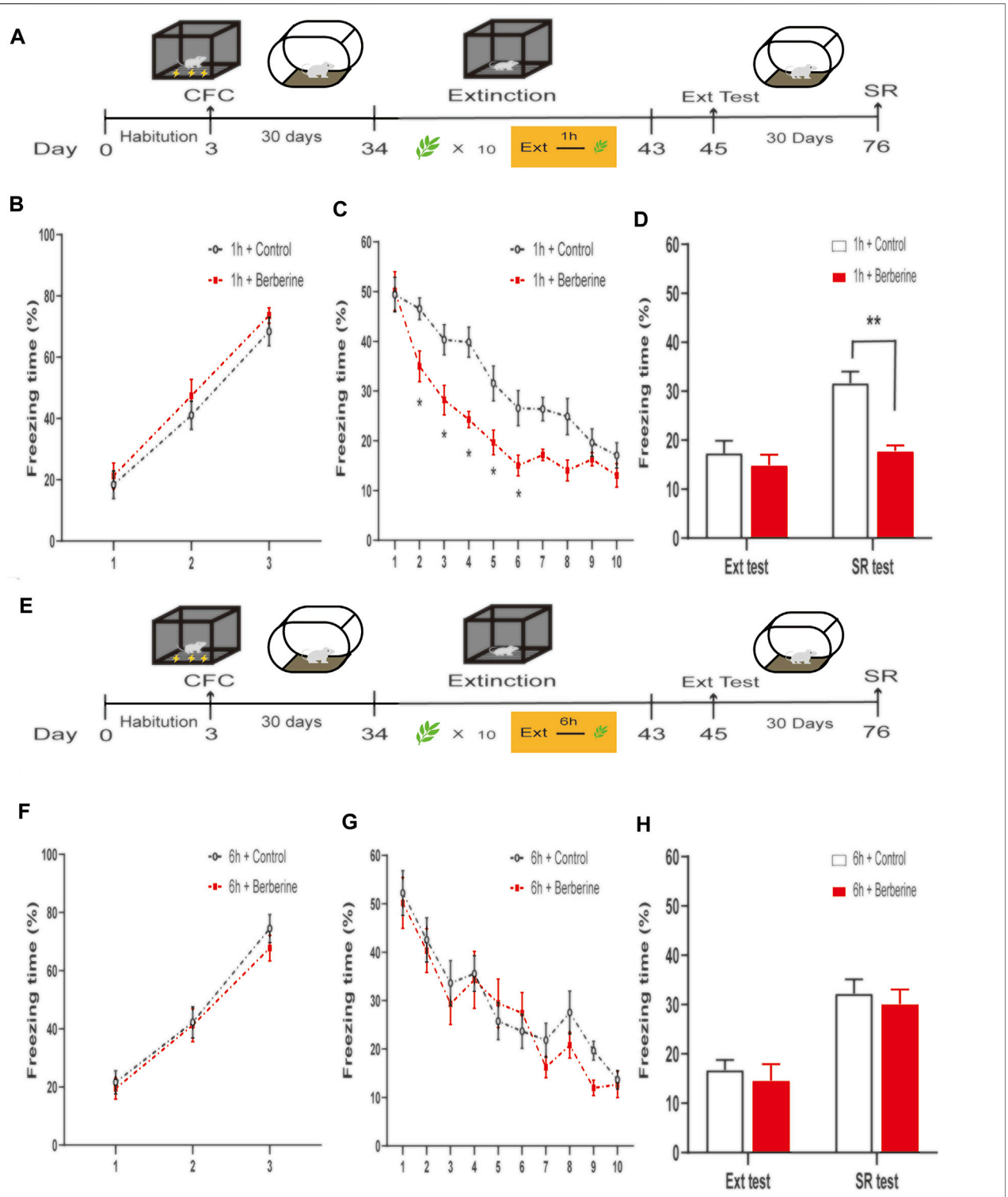

FIGURE 4 | | Berberine treatment 1 h after extinction enhanced extinction and reduced spontaneous recovery of remote fear. **(A, E)** Timeline of contextual fear conditioning, drug treatment, extinction training, extinction test, and spontaneous recovery test. **(A)** One hour or **(E)** 6 h after each extinction training session, corn oil (1 mL/kg, i.g.) or berberine (25 mg/kg, i.g.) was administered to mice, respectively. **(B, F)** Freezing levels during fear conditioning were similar between different groups. **(C, G)** Thirty days after CFC, freezing behaviors declined during extinction training sessions. **(C)** Repeated-measures ANOVA, effect of the training day, $F_{(9,126)}$ = 133.8, $p < 0.001$; Bonferroni *post hoc* test, $p < 0.05$, during the extinction training days 2–6. **(D, H)** Percentage of freezing time during extinction test (left) and spontaneous recovery test (right). **(D)** Significant freezing time was observed in SR test, $p < 0.01$. $n = 8$ mice per group. Data are means ± SEM, $^{*}p < 0.05$, $^{**}p < 0.01$, and compared with 1 h + control group. CFC, contextual fear conditioning; Ext, extinction; SR, spontaneous recovery.

3 RESULTS

3.1 Berberine Administration 1 h After Extinction Enhanced Extinction and Prevented Subsequent Reinstatement of Recent Fear Memory

In experiment 1, we first investigated the optimal doses and time window of berberine treatment on extinction and subsequent reinstatement of recent fear memory (**Figure 1**). On the training day, Percent freezing time was significantly different between the first trial and the last trial during fear conditioning ($p < 0.05$; **Figure 1B**). Extinction training data were analyzed by repeated-measures ANOVA, with the treatment condition (control, 12.5 mg/kg berberine or 25 mg/kg berberine) as a between-subjects factor and different training days as a within-subjects factor. There were significant differences among three groups in the percentage of freezing time during extinction training (main effect of the training day: $F_{(9,189)} = 164.1$, $p < 0.001$; main effect of the treatment condition: $F_{(2,21)} = 7.328$, $p < 0.01$; interaction of training day × treatment condition: $F_{(18,189)} = 5.167$, $p < 0.001$). The Bonferroni *post hoc* test revealed differences between the control and 25 mg/kg berberine groups during the extinction training days 2–8 ($p < 0.05$), suggesting that berberine administration 1 h after extinction promoted extinction of recent fear memory (**Figure 1C**). There was a significant difference in the percentage of freezing time in reinstatement test between control and 25 mg/kg berberine groups (main effect of the different test day: $F_{(1.21)} = 275.3$, $p < 0.001$; main effect of the different treatment condition: $F_{(2,21)} = 6.476$, $p < 0.01$; interaction of test day× treatment condition: $F_{(2,21)} = 13.62$, $p < 0.001$). *Post hoc* test showed that 25 mg/kg berberine significantly reduced the freezing time compared with the control group in the reinstatement test ($p < 0.01$; **Figure 1D**). In experiment 2, percent freezing time was significantly different between the first trial and the last trial during fear conditioning ($p < 0.05$; **Figure 1F**). However, for the freezing time with delayed administration of berberine, there were no significant differences in both extinction training (main effect of the extinction training day: $F_{(9,117)} = 221.5$, $p < 0.001$; main effect of the different treatment condition: $F_{(1,13)} = 0.029$, $p = 0.8659$; interaction of extinction training day × different treatment condition: $F_{(9,117)} = 0.5734$, $p = 0.8166$; **Figure 1G**) and reinstatement test (main effect of the different test day: $F_{(1.13)} = 55.38$, $p < 0.001$; main effect of the different treatment condition: $F_{(1,13)} = 0.0467$, $p = 0.8322$; interaction of test day × treatment condition: $F_{(1,13)} = 0.2576$, $p = 0.6203$; **Figure 1H**) between 6 h + control and 6 h + berberine groups.

In summary, these results suggest that berberine administration 1 h after extinction promoted fear extinction and reduced reinstatement of recent fear memory.

3.2 Berberine Administration 1 h After Extinction Enhanced Extinction and Prevented Subsequent Spontaneous Recovery of Recent Fear Memory

In experiment 3, we further confirmed the time window of berberine treatment on fear memory extinction and spontaneous recovery of recent fear memory (**Figure 2**). On the training day, Percent freezing time was significantly different between the first trial and the last trial during fear conditioning ($p < 0.05$; **Figure 2B**). Extinction training data were analyzed by repeated-measures ANOVA, with the treatment condition (1 h + control or 1 h + berberine) as a between-subjects factor and different training days as a within-subjects factor. There were significant differences between groups in the percentage of freezing time during extinction training (main effect of the training day: $F_{(9,117)} = 169.3$, $p < 0.001$; main effect of the treatment condition: $F_{(1,13)} = 6.617$, $p < 0.05$; interaction of training day × treatment condition: $F_{(9,117)} = 5.732$, $p < 0.001$). The Bonferroni *post hoc* test revealed differences between groups during the extinction training days 2–6 ($p < 0.05$), suggesting that berberine administration 1 h after extinction enhanced extinction of recent fear memory (**Figure 2C**). There was a significant difference in the percentage of freezing time in spontaneous recovery test between groups (main effect of the different test day: $F_{(1.13)} = 29.31$, $p < 0.001$; main effect of the different treatment condition: $F_{(1,13)} = 31.7$, $p < 0.01$; interaction of test day × treatment condition: $F_{(1,13)} = 14.14$, $p < 0.01$). *Post hoc* test showed that berberine administration 1 h after extinction significantly reduced the freezing time compared with the 1 h + control group in the spontaneous recovery test ($p < 0.01$; **Figure 2D**). In experiment 4, percent freezing time was significantly different between the first trial and the last trial during fear conditioning ($p < 0.05$; **Figure 2F**). However, for freezing time with delayed administration of berberine, there were no significant differences in both extinction training (main effect of the extinction training day: $F_{(9,126)} = 217.1$, $p < 0.001$; main effect of the different treatment condition: $F_{(1,14)} = 0.7743$, $p = 0.3937$; interaction of extinction training day × different treatment condition: $F_{(9,126)} = 0.8957$, $p = 0.5313$; **Figure 2G**) and spontaneous recovery test (main effect of the different test day: $F_{(1.14)} = 101.6$, $p < 0.001$; main effect of the different treatment condition: $F_{(1,14)} = 4.4883$, $p = 0.0443$; interaction of test day × treatment condition: $F_{(1,14)} = 0.2508$, $p = 0.6243$; **Figure 2H**) between 6 h + control and 6 h + berberine groups.

These results indicate that berberine administration 1 h after extinction enhanced extinction rates and reduced spontaneous recovery of recent fear memory. Experiments 1, 2, 3, and 4 data verify the hypothesis that berberine combined with extinction training enhance extinction memory and prevent the return of fear.

3.3 Berberine Treatment 1 h After Extinction Enhanced Extinction and Prevented Subsequent Reinstatement of Remote Fear Memory

In experiment 5, we examined whether the facilitating effect of berberine on extinction was also applied to remote fear memory. One month after the CFC training, the mice were administered control or berberine 1 h after each extinction session and then tested for extinction and reinstatement of extinguished fear (**Figure 3**). On the training day, Percent freezing time was significantly different between the first trial and the last trial

during fear conditioning ($p < 0.05$; **Figure 3B**). Extinction training data were analyzed by repeated-measures ANOVA, with the treatment condition as a between-subjects factor and different training days as a within-subjects factor. There was significant difference between 1 h + control and 1 h + berberine groups in the percentage of freezing time during extinction training (main effect of the training day: $F_{(9,126)} = 233.4$, $p < 0.001$; main effect of the treatment condition: $F_{(1,14)} = 6.814$, $p < 0.05$; interaction of training day × treatment condition: $F_{(9,126)} = 12.23$, $p < 0.001$). The Bonferroni *post hoc* test revealed differences between 1 h + control and 1 h + berberine groups during extinction training days 2, 4–8 ($p < 0.05$), suggesting that berberine administration 1 h after extinction enhanced extinction of remote fear memory (**Figure 3C**). Also, there was a significant difference in the percentage of freezing time in reinstatement test between 1 h + control and 1 h + berberine groups (main effect of the different test day: $F_{(1.14)} = 5.842$, $p < 0.05$; main effect of the different treatment condition: $F_{(1,14)} = 4.369$, $p = 0.05$; interaction of test day × treatment condition: $F_{(1,14)} = 8.382$, $p < 0.05$). *Post hoc* test showed that berberine administration 1 h after extinction significantly reduced the freezing time compared with the 1 h + control group in the reinstatement test ($p < 0.01$; **Figure 3D**). In experiment 6, percent freezing time was significantly different between the first trial and the last trial during fear conditioning ($p < 0.05$; **Figure 3F**). However, for freezing time with delayed administration of berberine, there were no significant differences in both extinction training (main effect of the extinction training day: $F_{(9,126)} = 102.9$, $p < 0.001$; main effect of the different treatment condition: $F_{(1,14)} = 0.0389$, $p = 0.8469$; interaction of extinction training day × different treatment condition: $F_{(9,126)} = 0.5504$, $p = 0.5504$; **Figure 3G**) and reinstatement test (main effect of the different test day: $F_{(1.14)} = 17.49$, $p < 0.001$; main effect of the different treatment condition: $F_{(1,14)} = 0.2414$, $p = 0.6308$; interaction of test day × treatment condition: $F_{(1,14)} = 0.01$, $p = 0.9202$; **Figure 3H**) between 6 h + control and 6 h + berberine groups.

These results indicate that berberine administration 1 h after extinction enhanced extinction learning and prevented reinstatement of remote fear memory.

3.4 Berberine Treatment 1 h After Extinction Enhanced Extinction and Prevented Subsequent Spontaneous Recovery of Remote Fear Memory

In experiment 7, we further investigated the effects of berberine treatment on extinction and spontaneous recovery of remote fear memory (**Figure 4**). On the training day, percent freezing time was significantly different between the first trial and the last trial during fear conditioning ($p < 0.05$; **Figure 4B**). Extinction training data were analyzed by repeated-measures ANOVA, with the treatment condition (1 h + control or 1 h + berberine) as a between-subjects factor and different training days as a within-subjects factor. There was significant difference between groups in the percentage of freezing time during extinction training (main effect of the training day: $F_{(9,126)} = 133.8$, $p < 0.001$; main effect of the treatment condition: $F_{(1,14)} = 6.711$, $p = 0.0214$; interaction of training day × treatment condition: $F_{(9,126)} = 6.762$, $p < 0.001$). The Bonferroni *post hoc* test revealed differences between groups during the extinction training days 2–6 ($p < 0.05$), suggesting that berberine administration 1 h after extinction enhanced extinction of remote fear memory (**Figure 4C**). There was a significant difference in the percentage of freezing time in spontaneous recovery test between groups (main effect of the different test day: $F_{(1.14)} = 31.76$, $p < 0.001$; main effect of the different treatment condition: $F_{(1,14)} = 10.29$, $p < 0.01$; interaction of test day × treatment condition: $F_{(1,14)} = 14.05$, $p < 0.01$). *Post hoc* test showed that berberine administration 1 h after extinction significantly reduced the freezing time compared with the 1 h + control group in the spontaneous recovery test ($p < 0.01$; **Figure 4D**). In experiment 8, percent freezing time was significantly different between the first trial and the last trial during fear conditioning ($p < 0.05$; **Figure 4F**). However, for freezing time with delayed administration of berberine, there were no significant differences in both extinction training (main effect of the extinction training day: $F_{(9,126)} = 38.39$, $p < 0.001$; main effect of the different treatment condition: $F_{(1,14)} = 0.3073$, $p = 0.5881$; interaction of extinction training day × different treatment condition: $F_{(9,126)} = 1.069$, $p = 0.3899$; **Figure 4G**) and spontaneous recovery test (main effect of the different test day: $F_{(1.14)} = 43.97$, $p < 0.001$; main effect of the different treatment condition: $F_{(1,14)} = 0.4316$, $p = 0.5218$; interaction of test day × treatment condition: $F_{(1,14)} < 0.01$, $p > 0.99$; **Figure 4H**) between 6 h + control and 6 h + berberine groups.

These findings indicate that berberine administration 1 h after extinction enhanced extinction rates and reduced spontaneous recovery of remote fear memory. All experiments data support the hypothesis that berberine-induced enhancement of extinction memory persistently attenuate fear memory in both recent and remote fear memory.

DISCUSSION

This study provides evidence for the facilitating effects of berberine on fear extinction using the classical CFC paradigm. The main findings of this study are as follows: (1) oral administration of berberine 1 h after each extinction session enhanced extinction rates and reduced the reinstatement of freezing behavior in both recent and remote fear memories; (2) the positive effects of berberine enhancing the extinction memory persisted for at least 30 days; (3) delayed administration of berberine 6 h after each extinction session had no effects on extinction training, reinstatement, and spontaneous recovery of fear-associated behaviors. Altogether, these results indicate that berberine treatment combined with extinction training during the critical time window of extinction memory consolidation leads to persistent attenuation of fear memories and provide evidence for the development of berberine-based postextinction pharmacological interventions for PTSD.

The modulation of pharmacological or behavioral interventions on extinction may have two consequences: extinction or the original fear memory traces (Richardson et al., 2004; Quirk et al., 2010; Kida, 2019; Bouton et al., 2021). We found that

extinguished fear can reemerge in reinstatement and spontaneous recovery test, indicating that the berberine-induced enhancement of extinction did not erase but compete the original fear memory. The formation of extinction memory resulted in suppression of original memory, and extinction memory also involved acquisition, consolidation, and storage processes (Millan et al., 2011; Orsini and Maren, 2012; Maren et al., 2013; Careaga et al., 2016; Knox, 2016). After acquisition, the memory undergoes a consolidation process that typically lasts for 6 h to be completely stored (Bourtchouladze et al., 1998; Schafe et al., 1999; Mcgaugh, 2000; Dudai, 2004; Lalumiere et al., 2017). Berberine treatment 1 h but not 6 h after extinction enhanced extinction memory, indicating that berberine promoted the consolidation of extinction memory. Moreover, berberine treatment 1 h but not 6 h after extinction inhibited subsequent tests of fear freezing behavior, demonstrating that berberine enhanced the consolidation of extinction memory rather than influenced the storage of extinction memory trace. Many studies have shown that cognitive enhancers administered before or after extinction facilitated extinction learning (Walker et al., 2002; Parnas et al., 2005; Lee et al., 2006; Makkar et al., 2010). Nevertheless, most of them do not apply to the clinical population because of their health-related side effects (Steckler and Risbrough, 2012; Singewald et al., 2015). Berberine, an OTC medication in China, has been verified well for safety in clinical trials (Gupte, 1975). Besides, previous studies have shown that berberine affected the DA and *N*-methyl-D-aspartate (NMDA) systems, which is the molecular mechanism of cognitive enhancers (Yoo et al., 2006; Kaplan and Moore, 2011; Kawano et al., 2015; Lee et al., 2018). Shen et al. (2020) demonstrated that extinction training combined with berberine treatment facilitated the extinction of drug memory. However, at least to our knowledge, the effect of berberine treatment on fear memory has not been reported.

In this study, we found that berberine facilitated extinction of fear-related behaviors, as well as reduced reinstatement, and spontaneous recovery of extinguished fear. But what might account for this phenomenon? For the accelerated extinction rates, we speculate that berberine acts as a cognitive enhancer to facilitate the consolidation of fear extinction memory. Growing evidence supports the modulatory effects of berberine on NMDA and DA systems (Kulkarni and Dhir, 2008; Vahdati Hassani et al., 2016). In fact, it has been widely accepted that NMDA and DA receptor agonists facilitated extinction of conditioned fear (Quirk et al., 2006; Peters et al., 2009; Davis, 2011), which provides an underlying pharmacological mechanism of the berberine's enhancement effect in our findings. Previous studies showed that berberine is an antagonist of both DA D1- and D2-like receptors (Kawano et al., 2015); however, only the D2 receptor antagonist has such a reinforcement effect of extinction but the opposite function of D1 (Ponnusamy et al., 2005). This led to the question of the exact receptor that may be affected by berberine, and further study should focus on the relevance between D1 and D2 receptors to elucidate the potential mechanisms underlying the berberine-induced fear extinction enhancement. For the suppression of reinstatement and spontaneous recovery of fear, the most likely explanation is that berberine-induced enhancement of extinction memory takes advantage in competing with the original fear memory. Extinction memory learning can compete with the original fear memory, which results in transitory but not persistent suppression of fear-related behaviors (Furini et al., 2014; Izquierdo et al., 2016). Surprisingly, berberine treatment combined with extinction training significantly suppressed the remote fear memory, indicating that berberine not only enhanced the extinction rates but also possibly gradually altered the plasticity-related proteins to produce such a long-term effect. Shen et al. also observed the alterations of plasticity-related proteins with berberine treatment, and future studies are needed to identify specific proteins to investigate the underlying molecular mechanisms of persistent suppression in remote fear of postextinction berberine treatment.

Notably, in the present data, the difference during extinction between the control and berberine groups that received the substance 1 h after extinction training disappeared in the last two to four trials in all experiments. Two potential explanations account for the interesting phenomenon. One is that berberine produces a transient effect of the substance during extinction training, and the other is the floor effect; the freezing behavior of the mice in the berberine groups has reached the standards of extinction in the last two to four trials so that it blurs the difference between groups. We prefer the second explanation but not the transient effect because such manipulation persistently suppresses the reinstatement and spontaneous recovery of original fear memories.

Although we demonstrated that berberine promoted extinction of fear-related behaviors and persistently attenuated fear memory by enhancing the extinction memory, further research is needed to explore the potential direct targets of berberine's effects. More recently, there is renewed attention to berberine because of its beneficial effects on various neurodegenerative and neuropsychiatric disorders, including anticonvulsant, antidepressant, and anti-Parkinson (Bhutada et al., 2010; Fan et al., 2017; Wang et al., 2021). All these effects of berberine may be attributed to its ability to regulate several neurotransmitter systems, like NMDA and serotonin (Kong et al., 2001; Castillo et al., 2005; Yoo et al., 2006). Moreover, NMDA receptors are important in learning and memory and in experience-dependent forms of plasticity such as LTP, and play a role in the extinction of the fear startle response and CFC (Ledgerwood et al., 2003; Davis et al., 2006). Also, a study examined serotonin reuptake genes in fear conditioning and extinction paradigms in mice, and they found that fear conditioning and extinction were normal but a deficit in extinction recall, indicating that serotonin reuptake may be a mechanism for fear extinction (Wellman et al., 2007). Therefore, we speculate that the suppression of berberine on fear-related behaviors may be related to NMDA and serotonin receptors. Undeniably, we first found the potential therapeutic potential of berberine in fear-related disorders, but more research is needed to reveal the underlying neurochemical and molecular mechanisms of the beneficial effects of postextinction berberine treatment.

Exposure therapy greatly impacts the prognosis of patients with anxiety-related disorders (Singewald et al., 2015; Foa and Mclean, 2016). In our study, considering that berberine promoted extinction of fear-related behaviors, it indicates that berberine may be potentially therapeutic in all anxiety-related disorders based on exposure therapy. Further studies should identify

berberine's enhancement of extinction in pathological fear and anxiety psychiatric conditions, such as social phobia, agoraphobia, obsessive–compulsive disorder, and generalized anxiety (World Health Organization, 2009; Edition, 2013), to investigate whether berberine has such extinction enhancement effect in various types of anxiety-related disorders.

In conclusion, we found that berberine administration orally 1 h after extinction facilitated extinction and led to persistent attenuation of both recent and remote fear memories. Postextinction berberine treatment might be a potential and promising pharmacological intervention for anxiety-related disorders. Further research is needed to elucidate the mechanisms underlying the beneficial effects of berberine on fear-related behaviors, and it is necessary to determine whether the therapeutic effects of berberine are applicable to the clinical population.

DATA AVAILABILITY STATEMENT

The original contributions presented in the study are included in the article/Supplementary Material, further inquiries can be directed to the corresponding authors.

ETHICS STATEMENT

The animal study was reviewed and approved by the Local Committee on Animal Care and Use and Protection of the Hunan Normal University.

AUTHOR CONTRIBUTIONS

Conceptualization, CY, SH, and YL; formal analysis and investigation, CY and YZ; data curation, SH, FW, and CS; writing—original draft preparation, SH, HY, and LC; writing—review and editing, SH, FW, and CS; supervision, CY and YL; funding acquisition, YL. All authors have read and agreed to the published version of the manuscript.

FUNDING

The present research received support from Natural Science Foundation of China (No. 81771434) and Outstanding Innovative Youth Training Program of Changsha (kq2106032).

REFERENCES

Alavijeh, M. M., Vaezi, G., Khaksari, M., and Hojati, V. (2019). Berberine Hydrochloride Attenuates Voluntary Methamphetamine Consumption and Anxiety-like Behaviors via Modulation of Oxytocin Receptors in Methamphetamine Addicted Rats. *Physiol. Behav.* 206, 157–165. doi:10.1016/j.physbeh.2019.03.024

An, X., Yang, P., Chen, S., Zhang, F., and Yu, D. (2017). An Additional Prior Retrieval Alters the Effects of a Retrieval-Extinction Procedure on Recent and Remote Fear Memory. *Front. Behav. Neurosci.* 11, 259. doi:10.3389/fnbeh.2017.00259

Anagnostaras, S. G., Maren, S., and Fanselow, M. S. (1999). Temporally Graded Retrograde Amnesia of Contextual Fear after Hippocampal Damage in Rats: Within-Subjects Examination. *J. Neurosci.* 19, 1106–1114. doi:10.1523/jneurosci.19-03-01106.1999

Andero, R., and Ressler, K. J. (2012). Fear Extinction and BDNF: Translating Animal Models of PTSD to the Clinic. *Genes Brain Behav.* 11, 503–512. doi:10.1111/j.1601-183X.2012.00801.x

Belwal, T., Bisht, A., Devkota, H. P., Ullah, H., Khan, H., Pandey, A., et al. (2020). Phytopharmacology and Clinical Updates of Berberis Species against Diabetes and Other Metabolic Diseases. *Front. Pharmacol.* 11, 41. doi:10.3389/fphar.2020.00041

Berman, D. E., and Dudai, Y. (2001). Memory Extinction, Learning Anew, and Learning the New: Dissociations in the Molecular Machinery of Learning in Cortex. *Science* 291, 2417–2419. doi:10.1126/science.1058165

Bhutada, P., Mundhada, Y., Bansod, K., Dixit, P., Umathe, S., and Mundhada, D. (2010). Anticonvulsant Activity of Berberine, an Isoquinoline Alkaloid in Mice. *Epilepsy Behav.* 18, 207–210. doi:10.1016/j.yebeh.2010.03.007

Bourtchouladze, R., Abel, T., Berman, N., Gordon, R., Lapidus, K., and Kandel, E. R. (1998). Different Training Procedures Recruit Either One or Two Critical Periods for Contextual Memory Consolidation, Each of Which Requires Protein Synthesis and PKA. *Learn. Mem.* 5, 365–374. doi:10.1101/lm.5.4.365

Bouton, M. E., Maren, S., and Mcnally, G. P. (2021). Behavioral and Neurobiological Mechanisms of Pavlovian and Instrumental Extinction Learning. *Physiol. Rev.* 101, 611–681. doi:10.1152/physrev.00016.2020

Careaga, M. B. L., Girardi, C. E. N., and Suchecki, D. (2016). Understanding Posttraumatic Stress Disorder through Fear Conditioning, Extinction and Reconsolidation. *Neurosci. Biobehav Rev.* 71, 48–57. doi:10.1016/j.neubiorev.2016.08.023

Castillo, J., Hung, J., Rodriguez, M., Bastidas, E., Laboren, I., and Jaimes, A. (2005). LED Fluorescence Spectroscopy for Direct Determination of Monoamine Oxidase B Inactivation. *Anal. Biochem.* 343, 293–298. doi:10.1016/j.ab.2005.05.027

Costanzi, M., Cannas, S., Saraulli, D., Rossi-Arnaud, C., and Cestari, V. (2011). Extinction after Retrieval: Effects on the Associative and Nonassociative Components of Remote Contextual Fear Memory. *Learn. Mem.* 18, 508–518. doi:10.1101/lm.2175811

Davis, M., Myers, K. M., Chhatwal, J., and Ressler, K. J. (2006). Pharmacological Treatments that Facilitate Extinction of Fear: Relevance to Psychotherapy. *NeuroRx* 3, 82–96. doi:10.1016/j.nurx.2005.12.008

Davis, M. (2011). NMDA Receptors and Fear Extinction: Implications for Cognitive Behavioral Therapy. *Dialogues Clin. Neurosci.* 13, 463–474. doi:10.31887/DCNS.2011.13.4/mdavis

Domitrovic, R., Jakovac, H., and Blagojevic, G. (2011). Hepatoprotective Activity of Berberine Is Mediated by Inhibition of TNF-Alpha, COX-2, and iNOS Expression in CCl(4)-Intoxicated Mice. *Toxicology* 280, 33–43. doi:10.1016/j.tox.2010.11.005

Dudai, Y. (2004). The Neurobiology of Consolidations, or, How Stable Is the Engram. *Annu. Rev. Psychol.* 55, 51–86. doi:10.1146/annurev.psych.55.090902.142050

Edition, F. (2013). *Diagnostic and Statistical Manual of Mental Disorders*. Washington, D.C.: Am Psychiatric Assoc, 21.

Fan, J., Li, B., Ge, T., Zhang, Z., Lv, J., Zhao, J., et al. (2017). Berberine Produces Antidepressant-like Effects in Ovariectomized Mice. *Sci. Rep.* 7, 1310. doi:10.1038/s41598-017-01035-5

Foa, E. B., and Mclean, C. P. (2016). The Efficacy of Exposure Therapy for Anxiety-Related Disorders and its Underlying Mechanisms: The Case of OCD and PTSD. *Annu. Rev. Clin. Psychol.* 12, 1–28. doi:10.1146/annurev-clinpsy-021815-093533

Furini, C., Myskiw, J., and Izquierdo, I. (2014). The Learning of Fear Extinction. *Neurosci. Biobehav Rev.* 47, 670–683. doi:10.1016/j.neubiorev.2014.10.016

Goode, T. D., and Maren, S. (2014). Animal Models of Fear Relapse. *ILAR J.* 55, 246–258. doi:10.1093/ilar/ilu008

Goode, T. D., and Maren, S. (2019). Common Neurocircuitry Mediating Drug and Fear Relapse in Preclinical Models. *Psychopharmacology (Berl)* 236, 415–437. doi:10.1007/s00213-018-5024-3

Gräff, J., Joseph, N. F., Horn, M. E., Samiei, A., Meng, J., Seo, J., et al. (2014). Epigenetic Priming of Memory Updating during Reconsolidation to Attenuate Remote Fear Memories. *Cell* 156, 261–276. doi:10.1016/j.cell.2013.12.020

Gupte, S. (1975). Use of Berberine in Treatment of Giardiasis. *Am. J. Dis. Child.* 129, 866. doi:10.1001/archpedi.1975.02120440082020

Gutberlet, C., Müller, G. E., and und Pilzecker, A. (1902). Experimentelle Beiträge zur Lehre vom Gedächtniss. *Philosophisches Jahrbuch* 15, 198–200.

Haaker, J., Golkar, A., Hermans, D., and Lonsdorf, T. B. (2014). A Review on Human Reinstatement Studies: an Overview and Methodological Challenges. *Learn. Mem.* 21, 424–440. doi:10.1101/lm.036053.114

Habtemariam, S. (2020). Berberine Pharmacology and the Gut Microbiota: A Hidden Therapeutic Link. *Pharmacol. Res.* 155, 104722. doi:10.1016/j.phrs.2020.104722

Izquierdo, I., Furini, C. R., and Myskiw, J. C. (2016). Fear Memory. *Physiol. Rev.* 96, 695–750. doi:10.1152/physrev.00018.2015

Kaplan, G. B., and Moore, K. A. (2011). The Use of Cognitive Enhancers in Animal Models of Fear Extinction. *Pharmacol. Biochem. Behav.* 99, 217–228. doi:10.1016/j.pbb.2011.01.009

Kawano, M., Takagi, R., Kaneko, A., and Matsushita, S. (2015). Berberine Is a Dopamine D1- and D2-like Receptor Antagonist and Ameliorates Experimentally Induced Colitis by Suppressing Innate and Adaptive Immune Responses. *J. Neuroimmunol* 289, 43–55. doi:10.1016/j.jneuroim.2015.10.001

Kida, S. (2019). Reconsolidation/destabilization, Extinction and Forgetting of Fear Memory as Therapeutic Targets for PTSD. *Psychopharmacology (Berl)* 236, 49–57. doi:10.1007/s00213-018-5086-2

Knox, D. (2016). The Role of Basal Forebrain Cholinergic Neurons in Fear and Extinction Memory. *Neurobiol. Learn. Mem.* 133, 39–52. doi:10.1016/j.nlm.2016.06.001

Kong, L. D., Cheng, C. H., and Tan, R. X. (2001). Monoamine Oxidase Inhibitors from Rhizoma of Coptis Chinensis. *Planta Med.* 67, 74–76. doi:10.1055/s-2001-10874

Kulkarni, S. K., and Dhir, A. (2008). On the Mechanism of Antidepressant-like Action of Berberine Chloride. *Eur. J. Pharmacol.* 589, 163–172. doi:10.1016/j.ejphar.2008.05.043

Lacagnina, A. F., Brockway, E. T., Crovetti, C. R., Shue, F., Mccarty, M. J., Sattler, K. P., et al. (2019). Distinct Hippocampal Engrams Control Extinction and Relapse of Fear Memory. *Nat. Neurosci.* 22, 753–761. doi:10.1038/s41593-019-0361-z

Lalumiere, R. T., Mcgaugh, J. L., and Mcintyre, C. K. (2017). Emotional Modulation of Learning and Memory: Pharmacological Implications. *Pharmacol. Rev.* 69, 236–255. doi:10.1124/pr.116.013474

Ledgerwood, L., Richardson, R., and Cranney, J. (2003). Effects of D-Cycloserine on Extinction of Conditioned Freezing. *Behav. Neurosci.* 117, 341–349. doi:10.1037/0735-7044.117.2.341

Lee, B., Shim, I., Lee, H., and Hahm, D. H. (2018). Berberine Alleviates Symptoms of Anxiety by Enhancing Dopamine Expression in Rats with post-traumatic Stress Disorder. *Korean J. Physiol. Pharmacol.* 22, 183–192. doi:10.4196/kjpp.2018.22.2.183

Lee, J. L., Milton, A. L., and Everitt, B. J. (2006). Reconsolidation and Extinction of Conditioned Fear: Inhibition and Potentiation. *J. Neurosci.* 26, 10051–10056. doi:10.1523/JNEUROSCI.2466-06.2006

Likhtik, E., and Johansen, J. P. (2019). Neuromodulation in Circuits of Aversive Emotional Learning. *Nat. Neurosci.* 22, 1586–1597. doi:10.1038/s41593-019-0503-3

Liu, J. F., Yang, C., Deng, J. H., Yan, W., Wang, H. M., Luo, Y. X., et al. (2015). Role of Hippocampal β-adrenergic and Glucocorticoid Receptors in the novelty-induced Enhancement of Fear Extinction. *J. Neurosci.* 35, 8308–8321. doi:10.1523/JNEUROSCI.0005-15.2015

Makkar, S. R., Zhang, S. Q., and Cranney, J. (2010). Behavioral and Neural Analysis of GABA in the Acquisition, Consolidation, Reconsolidation, and Extinction of Fear Memory. *Neuropsychopharmacology* 35, 1625–1652. doi:10.1038/npp.2010.53

Maren, S., Phan, K. L., and Liberzon, I. (2013). The Contextual Brain: Implications for Fear Conditioning, Extinction and Psychopathology. *Nat. Rev. Neurosci.* 14, 417–428. doi:10.1038/nrn3492

Markowitz, J. C., Petkova, E., Neria, Y., Van Meter, P. E., Zhao, Y., Hembree, E., et al. (2015). Is Exposure Necessary? A Randomized Clinical Trial of Interpersonal Psychotherapy for PTSD. *Am. J. Psychiatry* 172, 430–440. doi:10.1176/appi.ajp.2014.14070908

Mcgaugh, J. L. (2000). Memory--a century of Consolidation. *Science* 287, 248–251. doi:10.1126/science.287.5451.248

Millan, E. Z., Marchant, N. J., and Mcnally, G. P. (2011). Extinction of Drug Seeking. *Behav. Brain Res.* 217, 454–462. doi:10.1016/j.bbr.2010.10.037

Morgan, M. A., and Ledoux, J. E. (1999). Contribution of Ventrolateral Prefrontal Cortex to the Acquisition and Extinction of Conditioned Fear in Rats. *Neurobiol. Learn. Mem.* 72, 244–251. doi:10.1006/nlme.1999.3907

Neag, M. A., Mocan, A., Echeverría, J., Pop, R. M., Bocsan, C. I., Crişan, G., et al. (2018). Berberine: Botanical Occurrence, Traditional Uses, Extraction Methods, and Relevance in Cardiovascular, Metabolic, Hepatic, and Renal Disorders. *Front. Pharmacol.* 9, 557. doi:10.3389/fphar.2018.00557

Orsini, C. A., and Maren, S. (2012). Neural and Cellular Mechanisms of Fear and Extinction Memory Formation. *Neurosci. Biobehav Rev.* 36, 1773–1802. doi:10.1016/j.neubiorev.2011.12.014

Pan, S., Mayoral, S. R., Choi, H. S., Chan, J. R., and Kheirbek, M. A. (2020). Preservation of a Remote Fear Memory Requires New Myelin Formation. *Nat. Neurosci.* 23, 487–499. doi:10.1038/s41593-019-0582-1

Parnas, A. S., Weber, M., and Richardson, R. (2005). Effects of Multiple Exposures to D-Cycloserine on Extinction of Conditioned Fear in Rats. *Neurobiol. Learn. Mem.* 83, 224–231. doi:10.1016/j.nlm.2005.01.001

Pavlov, I. P. (1927). *Conditioned Reflexes: An Investigation of the Physiological Activity of the Cerebral Cortex*. Oxford, England: Oxford Univ. Press.

Peters, J., Kalivas, P. W., and Quirk, G. J. (2009). Extinction Circuits for Fear and Addiction Overlap in Prefrontal Cortex. *Learn. Mem.* 16, 279–288. doi:10.1101/lm.1041309

Ponnusamy, R., Nissim, H. A., and Barad, M. (2005). Systemic Blockade of D2-like Dopamine Receptors Facilitates Extinction of Conditioned Fear in Mice. *Learn. Mem.* 12, 399–406. doi:10.1101/lm.96605

Qin, C., Bian, X. L., Wu, H. Y., Xian, J. Y., Cai, C. Y., Lin, Y. H., et al. (2021). Dorsal Hippocampus to Infralimbic Cortex Circuit Is Essential for the Recall of Extinction Memory. *Cereb. Cortex* 31, 1707–1718. doi:10.1093/cercor/bhaa320

Quirk, G. J., Garcia, R., and González-Lima, F. (2006). Prefrontal Mechanisms in Extinction of Conditioned Fear. *Biol. Psychiatry* 60, 337–343. doi:10.1016/j.biopsych.2006.03.010

Quirk, G. J., Paré, D., Richardson, R., Herry, C., Monfils, M. H., Schiller, D., et al. (2010). Erasing Fear Memories with Extinction Training. *J. Neurosci.* 30, 14993–14997. doi:10.1523/JNEUROSCI.4268-10.2010

Rakofsky, J. J., Ressler, K. J., and Dunlop, B. W. (2012). BDNF Function as a Potential Mediator of Bipolar Disorder and post-traumatic Stress Disorder Comorbidity. *Mol. Psychiatry* 17, 22–35. doi:10.1038/mp.2011.121

Rescorla, R. A. (2004). Spontaneous Recovery. *Learn. Mem.* 11, 501–509. doi:10.1101/lm.77504

Richardson, R., Ledgerwood, L., and Cranney, J. (2004). Facilitation of Fear Extinction by D-Cycloserine: Theoretical and Clinical Implications. *Learn. Mem.* 11, 510–516. doi:10.1101/lm.78204

Schafe, G. E., Nadel, N. V., Sullivan, G. M., Harris, A., and Ledoux, J. E. (1999). Memory Consolidation for Contextual and Auditory Fear Conditioning Is Dependent on Protein Synthesis, PKA, and MAP Kinase. *Learn. Mem.* 6, 97–110. doi:10.1101/lm.6.2.97

Shen, X., Hui, R., Luo, Y., Yu, H., Feng, S., Xie, B., et al. (2020). Berberine Facilitates Extinction of Drug-Associated Behavior and Inhibits Reinstatement of Drug Seeking. *Front. Pharmacol.* 11, 476. doi:10.3389/fphar.2020.00476

Singewald, N., and Holmes, A. (2019). Rodent Models of Impaired Fear Extinction. *Psychopharmacology (Berl)* 236, 21–32. doi:10.1007/s00213-018-5054-x

Singewald, N., Schmuckermair, C., Whittle, N., Holmes, A., and Ressler, K. J. (2015). Pharmacology of Cognitive Enhancers for Exposure-Based Therapy of Fear, Anxiety and Trauma-Related Disorders. *Pharmacol. Ther.* 149, 150–190. doi:10.1016/j.pharmthera.2014.12.004

Steckler, T., and Risbrough, V. (2012). Pharmacological Treatment of PTSD - Established and New Approaches. *Neuropharmacology* 62, 617–627. doi:10.1016/j.neuropharm.2011.06.012

Taylor, J. R., and Torregrossa, M. M. (2015). Pharmacological Disruption of Maladaptive Memory. *Handb Exp. Pharmacol.* 228, 381–415. doi:10.1007/978-3-319-16522-6_13

Torregrossa, M. M., Corlett, P. R., and Taylor, J. R. (2011). Aberrant Learning and Memory in Addiction. *Neurobiol. Learn. Mem.* 96, 609–623. doi:10.1016/j.nlm.2011.02.014

Vahdati Hassani, F., Hashemzaei, M., Akbari, E., Imenshahidi, M., and Hosseinzadeh, H. (2016). Effects of Berberine on Acquisition and

Reinstatement of Morphine-Induced Conditioned Place Preference in Mice. *Avicenna J. Phytomed* 6, 198–204.

Vervliet, B., Craske, M. G., and Hermans, D. (2013). Fear Extinction and Relapse: State of the Art. *Annu. Rev. Clin. Psychol.* 9, 215–248. doi:10.1146/annurev-clinpsy-050212-185542

Vetere, G., Xia, F., Ramsaran, A. I., Tran, L. M., Josselyn, S. A., and Frankland, P. W. (2021). An Inhibitory Hippocampal-Thalamic Pathway Modulates Remote Memory Retrieval. *Nat. Neurosci.* 24, 685–693. doi:10.1038/s41593-021-00819-3

Walker, D. L., Ressler, K. J., Lu, K. T., and Davis, M. (2002). Facilitation of Conditioned Fear Extinction by Systemic Administration or Intra-amygdala Infusions of D-Cycloserine as Assessed with Fear-Potentiated Startle in Rats. *J. Neurosci.* 22, 2343–2351. doi:10.1523/jneurosci.22-06-02343.2002

Wang, H. C., Wang, B. D., Chen, M. S., Chen, H., Sun, C. F., Shen, G., et al. (2018). Neuroprotective Effect of Berberine against Learning and Memory Deficits in Diffuse Axonal Injury. *Exp. Ther. Med.* 15, 1129–1135. doi:10.3892/etm.2017.5496

Wang, Y., Tong, Q., Ma, S. R., Zhao, Z. X., Pan, L. B., Cong, L., et al. (2021). Oral Berberine Improves Brain Dopa/dopamine Levels to Ameliorate Parkinson's Disease by Regulating Gut Microbiota. *Signal. Transduct Target. Ther.* 6, 77. doi:10.1038/s41392-020-00456-5

Wellman, C. L., Izquierdo, A., Garrett, J. E., Martin, K. P., Carroll, J., Millstein, R., et al. (2007). Impaired Stress-Coping and Fear Extinction and Abnormal Corticolimbic Morphology in Serotonin Transporter Knock-Out Mice. *J. Neurosci.* 27, 684–691. doi:10.1523/JNEUROSCI.4595-06.2007

World Health Organization (2009). *International Classification of Diseases-ICD*. Geneva, Switzerland: WHO.

Yoo, J. H., Yang, E. M., Cho, J. H., Lee, J. H., Jeong, S. M., Nah, S. Y., et al. (2006). Inhibitory Effects of Berberine against Morphine-Induced Locomotor Sensitization and Analgesic Tolerance in Mice. *Neuroscience* 142, 953–961. doi:10.1016/j.neuroscience.2006.07.008

Yu, H., Wang, Y., Pattwell, S., Jing, D., Liu, T., Zhang, Y., et al. (2009). Variant BDNF Val66Met Polymorphism Affects Extinction of Conditioned Aversive Memory. *J. Neurosci.* 29, 4056–4064. doi:10.1523/JNEUROSCI.5539-08.2009

Conflict of Interest: The author declares that the research was conducted in the absence of any commercial or financial relationships that could be construed as a potential conflict of interest.

The reviewer RH declared a past co-authorship with one of the authors YL to the handling editor.

Publisher's Note: All claims expressed in this article are solely those of the authors and do not necessarily represent those of their affiliated organizations, or those of the publisher, the editors and the reviewers. Any product that may be evaluated in this article, or claim that may be made by its manufacturer, is not guaranteed or endorsed by the publisher.

frontiers in Pharmacology

REVIEW
published: 24 March 2022
doi: 10.3389/fphar.2022.809324

Anti-Inflammatory Medicinal Plants of Bangladesh—A Pharmacological Evaluation

*Most. Afia Akhtar**

Department of Pharmacy, Faculty of Science, University of Rajshahi, Rajshahi, Bangladesh

Inflammatory diseases are considered major threats to human health worldwide. In Bangladesh, a number of medicinal plants have been used in traditional medicine from time immemorial in the treatment of diverse diseases, including inflammatory disorders. This assignment aims at providing the status of the medicinal plants of Bangladesh which are traditionally used in the management of inflammatory disorders and are investigated for their anti-inflammatory prospects using different preclinical studies and future research directions. The information of medicinal plants assembled in this review was obtained from a literature search of electronic databases such as Google Scholar, PubMed, Scopus, Web of Science and ScienceDirect up to December, 2020 from publications on plants investigated for their anti-inflammatory activities, in which the place of plant sample collection was identified as Bangladesh. Keywords for primary searches were "anti-inflammatory," "Bangladeshi," and "medicinal plants." Criteria followed to include plant species were plants that showed significant anti-inflammatory activities in 1) two or more sets of experiments in a single report, 2) same or different sets of experiments in two or more reports, and, 3) plants which are traditionally used in the treatment of inflammation and inflammatory disorders. In this study, 48 species of medicinal plants have been reviewed which have been used in traditional healing practices to manage inflammatory disorders in Bangladesh. The mechanistic pathways of the *in vivo* and *in vitro* study models used for the evaluation of anti-inflammatory properties of plant samples have been discussed. Selected plants were described in further detail for their habitat, anti-inflammatory studies conducted in countries other than Bangladesh, and anti-inflammatory active constituents isolated from these plants if any. Medicinal plants of Bangladesh have immense significance for anti-inflammatory activity and have potential to contribute toward the discovery and development of novel therapeutic approaches to combat diseases associated with inflammation. However, the plants reviewed in this article had chiefly undergone preliminary screening and require substantial investigations including identification of active molecules, understanding the mechanism of action, and evaluation for safety and efficacy to be followed by the formulation of safe and effective drug products.

Keywords: Bangladeshi, traditional, inflammation, medicinal plants, preclinical study

OPEN ACCESS

Edited by:
Lucia Recinella,
University of Studies G. d'Annunzio Chieti and Pescara, Italy

Reviewed by:
Armando Caceres,
Universidad de San Carlos de Guatemala, Guatemala
Oscar Herrera-Calderon,
Universidad Nacional Mayor de San Marcos, Peru

***Correspondence:**
Most. Afia Akhtar
afia.akhtar@ru.ac.bd
orcid.org/0000-0002-6205-9484

Specialty section:
This article was submitted to Ethnopharmacology, a section of the journal Frontiers in Pharmacology

Received: *04 November 2021*
Accepted: *01 February 2022*
Published: *24 March 2022*

Citation:
Akhtar MA (2022) Anti-Inflammatory Medicinal Plants of Bangladesh—A Pharmacological Evaluation. Front. Pharmacol. 13:809324. doi: 10.3389/fphar.2022.809324

INTRODUCTION

Plants are the most abundant suppliers of safe and successful remedies from time immemorial to present either to humans or to other animals. It is estimated that more than 90% of traditional medicine recipes comprise medicinal plants (Sofowora et al., 2013) which are used to treat a wide array of acute and chronic diseases ranging from common cold to complex cancerous phases throughout the world (Issa et al., 2006). According to the World Health Organization, the use of traditional and complementary medicine is increasing rapidly in most of the countries (World Health Organization, 2013). Medicinal plants constitute 25% of all modern medicines (Birhanu, 2013), and the annual market value of these plants has surpassed $100 billion globally (Sofowora et al., 2013).

Plants are the reservoir of important bioactive molecules classified as phenolics, alkaloids, carotenoids, organosulfur compounds, etc. on the basis of their chemical nature, and these molecules are reclassified as antioxidants, analgesics, cardioactive, anticancerous, immunity potentiating, detoxifying, neuropharmacological agents, etc. on the basis of their pharmacological action (Ugboko et al., 2020). Thus, plants with values in traditional medicine integrated with scientific evidences have provided the opportunity to discover thousands of therapeutically potential drugs (Harvey, 2000).

Traditional Background of Bangladeshi Medicinal Plants

Bangladesh is a small country regarding her land area, but the fertile soil and favorable climate have enriched the country with highly biodiverse plants. The traditional healing practices of Bangladesh have been exercised from time immemorial and are profoundly embedded within the local communities (Ocvirk et al., 2013; Haque et al., 2018). A myriad of medicinal plants grows all over Bangladesh out of which about 1,000 are conservatively considered to have therapeutic usefulness by traditional healers (Mollik et al., 2010). The formulations of Ayurvedic, Unani, and Homeopathic systems of this country have been developed by exploring these natural resources (Rahman et al., 2001; Ghani, 2003). Even at present, traditional medicine is an integral part of the country's overall healthcare system (Haque et al., 2014; Jahan et al., 2019). The usage of medicinal plants in the form of extract, decoction, juice, powder, paste, etc. in such traditional practices possesses the same long history to manage or cure diverse diseases (Akber et al., 2011; Rahmatullah et al., 2011a). The major reasons people of Bangladesh rely on these medicinal plants are 1) little or no access to modern medical assistance, 2) availability and cost-effectiveness of medicinal plants, and, 3) trust in the healing power of these natural gifts that has been built up with time, observations, and experiences. In addition, more than 30 tribes constitute 2% of the total population of Bangladesh, and the tribal healers are their principal health care providers who again rely on medicinal plants for treatment of different diseases (Rahmatullah et al., 2011b; 2012).

The increase in prescription rate and popularity of herbal medicine indicates the shift of the global trend from synthetic drugs toward the medicines of natural origin which has also been considered a promising future medicine (Ahmad Khan and Ahmad, 2019). Similarly, in Bangladesh, the manufacturing of herbal medicines has been increased, and the demand for medicinal plants is also increasing (Dulla and Jahan, 2017). But these plants are yet to undergo detailed scientific investigations for chemical constituents and bioactivities to evaluate their pharmacological properties (Rahman et al., 2001), for instance, anti-inflammatory potential.

Inflammation, Inflammatory Disorders, and Available Anti-Inflammatory Medication

The term "inflammation" is described as a prompt and strictly controlled physiological process (Barton, 2008) triggered by harmful foreign stimuli as well as infected and injured host tissue (Medzhitov, 2008; 2010). The foreign stimuli include pathogenic microbes, toxic chemicals, allergens, mechanical and thermal factors, etc. (Ambriz-Pérez et al., 2016; Arulselvan et al., 2016; Attiq et al., 2018). If not properly coordinated, this natural beneficial physiologic action persists instead of being resolved and evolves pathological consequences, leading to the development and progression of numerous human diseases which encompass asthma, rheumatoid arthritis, inflammatory bowel disease, cancer, atherosclerosis, type 2 diabetes, obesity, and neurodegenerative disorders, for example, Alzheimer's disease, Parkinson's disease, and multiple sclerosis (Nathan, 2002; Glass et al., 2010; Medzhitov, 2010; Fürst and Zündorf, 2014). These inflammatory diseases are the major health issues around the globe, causing an increase in the rate of morbidity and mortality every year (Gou et al., 2017).

Developing an efficacious anti-inflammatory drug product with a higher margin of safety has always been a challenge. The currently prescribed common anti-inflammatory drugs can be divided into three classes 1) nonselective non-steroidal anti-inflammatory drugs (NSAIDs), 2) cyclooxygenase 2 (COX-2) selective NSAIDs, and, 3) steroidal anti-inflammatory drugs (SAIDs) (Recio et al., 2012). NSAIDs act by retarding the biosynthesis of prostanoids from arachidonic acid (AA) by inhibiting cyclooxygenase (COX) enzymes. These COX enzymes can exist as the constitutive COX-1 and the inducible COX-2 isoforms. Though responsible to mediate inflammation, the ubiquitous COX-1 isoform mainly performs physiologic functions associated with homeostasis as well as protection of cells and tissues accompanying the endothelium, monocytes, gastrointestinal epithelial cells, and platelets. On the other hand, COX-2 is mostly induced by cytokines expressed in the vascular endothelium, rheumatoid synovial endothelial cells, monocytes, and macrophages and plays the key role in inducing pain and inflammation (Vane and Botting, 1998; Smyth et al., 2009; Brune and Patrignani, 2015). The nonselective NSAIDs inhibit both COX-1 and -2, and thus besides providing therapeutic actions, their use can result in a number of undesired side effects (**Table 1**) (Davies, 1995). The selective COX-2 inhibitors were considered to be therapeutically

TABLE 1 | Cellular action mechanism of anti-inflammatory medications and their undesired effects.

Types of anti-inflammatory drugs	Cellular action mechanism in brief	Example	Undesired effects
Nonselective nonsteroidal anti-inflammatory drugs (NSAIDs)	Inhibit both COX-1 and -2 isozymes	Aspirin, acetaminophen, ibuprofen, naproxen etc.	Colonic bleeding, iron deficiency anemia, strictures, ulcerations, perforations, inflammatory bowel disease (IBD), diarrhea, hepatotoxicity, cardiovascular diseases, and death
COX-2 selective NSAIDs	Selectively inhibit COX-2 isozyme	Celecoxib, etoricoxib, and rofecoxib (rofecoxib has been withdrawn from the market due to its adverse effects)	Increased risk of heart attack, stroke, and GI events such as perforation, ulceration, and bleeding
Steroidal anti-inflammatory drugs (SAIDs)	Act *via* inhibiting PLA_2 enzymes	Tablet form such as cortisol, prednisolone, prednisone, and methylprednisolone	Bruising of the skin, weight gain, osteoporosis, diabetes, cataracts, swelling of the ankles or feet, joint destruction, impaired wound healing, excessive hair growth, fat redistribution, atherosclerosis, and hypertension
		Inhaled form such as beclomethasone, budesonide, flunisolide, fluticasone propionate, and triamcinolone	Sore mouth, hoarse voice, and infections in the throat and mouth

Sources: (Salvo et al., 2011; Recio et al., 2012; Akhtar, 2018).

superior to the conventional nonselective NSAIDs since they have little or no effect on COX-1 isozymes (Everts et al., 2000; Jackson and Hawkey, 2000), but in later studies, these drugs have also been found to cause cardiovascular events such as myocardial infarction, stroke, and heart failure as well as gastrointestinal (GI) complications (**Table 1**) (Salvo et al., 2011). The other class, that is the steroids, is potent anti-inflammatory agents which can inhibit phospholipase A_2 (PLA_2) enzymes required to release AA from phospholipids. AA liberates eicosanoids, for instance, prostaglandins, thromboxanes, leukotriene, etc. and platelet-activating factor (PAF) which are the principal inflammatory mediators (Balsinde et al., 2002; Ericson-Neilsen and Kaye, 2014). Adverse reactions associated with high dose or long-term use of small dose of steroid tablets and with inhaled steroids are summarized in **Table 1** along with the adverse reactions of NSAIDs and COX-2 selective NSAIDs.

Anti-Inflammatory Compounds of Plant Origin

In recent years, research interest on screening of medicinal plants to discover potential anti-inflammatory agents has been intensified (Bellik et al., 2012; 2013). A variety of plant-derived natural products have been shown to exhibit significant anti-inflammatory activity by inhibiting important proinflammatory mediators (**Figure 1**) and have made way from preclinical studies to clinical trial (Kim et al., 2009; Fürst and Zündorf, 2014). For example, quercetin and kaempferol inhibit inducible nitric oxide synthase (iNOS) expression and signal transducer and activator of transcription-1 (STAT-1) and nuclear factor-κB (NF-κB) activation (Hämäläinen et al., 2007); resveratrol inhibits COX-2 expression followed by modulation of NF-κB and activator protein-1 (AP-1) pathways (Kundu et al., 2006); curcumin, the principal curcuminoid of turmeric (*Curcuma longa* L., Zingiberaceae), acts *via* inhibiting COX-1 and -2, lipoxygenase (LOX), NF-κB, and mitogen-activated protein kinase (MAPK) and also downregulates tumor necrosis factor-α (TNF-α) and interleukin-1β and 6 (IL-1β, and -6) secretion (Hong et al., 2004; Kim et al., 2005; Shah et al., 2010). **Table 2** summarizes some of the known anti-inflammatory molecules of plant origin.

Apu et al. (2012) published a brief review on anti-inflammatory medicinal plants of Bangladesh in 2012, where they enlisted 36 plants. Another report briefly reviewed 15 analgesic and anti-inflammatory medicinal plants of Bangladesh in addition to cognitive enhancer plants (Uddin and Islam, 2020). In the present study, 48 plants have been chosen on the basis of some inclusion and exclusion criteria. These plants are reviewed for their traditional uses and anti-inflammatory activity in various *in vivo* and *in vitro* experimental models, and toxicity test results have also been summarized in **Supplementary Table S1** if conducted in the cited research(s). More insights have been given into selected plants, highlighting their identified anti-inflammatory molecules. The compelling motive behind the current study is to represent the scope and possibilities of medicinal plants of Bangladesh with traditional values supported by scientific evidences in the treatment of inflammation and inflammatory disorders.

METHODS

The plant species included in this review (**Supplementary Table S1**) were based on the reports available from January, 2001 to December, 2020 by searching electronic databases such as Google Scholar, PubMed, Scopus, Web of Science, and ScienceDirect. Keywords used were primarily "anti-inflammatory," "Bangladeshi," and "medicinal plants." A secondary search was conducted similarly with keywords "membrane stabilizing activity," "Bangladeshi," and "medicinal plants" since membrane stabilization is a well-documented mechanism of

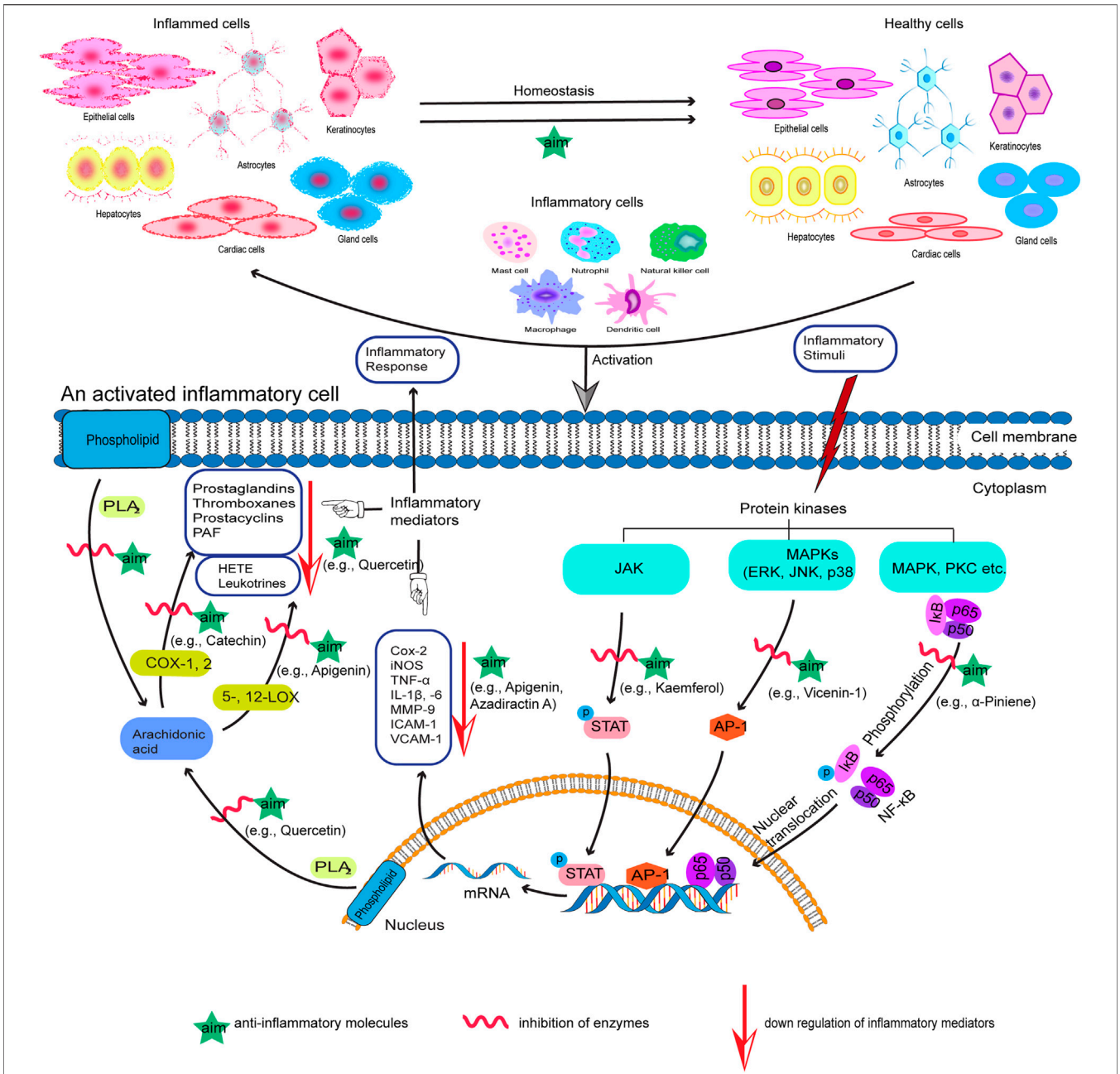

FIGURE 1 | Proposed action mechanism of anti-inflammatory molecules (aim) of plant origin with examples. The specific pathways shown represent only a few of the plenty of diverse pathways involved in the inflammatory process.

anti-inflammatory action, and the *in vitro* membrane stabilizing assay is established as a valid model to study the anti-inflammatory activity of extracts or molecules (Shinde et al., 1999; Thangaraj, 2016). In these published reports, the plants or their parts were collected from different areas of Bangladesh, and the experimental works were conducted in laboratories of Bangladesh and also in abroad as found in few studies.

The common name, local name, and traditional uses of plants included in **Supplementary Table S1** were extracted mainly from the books of Professor Abdul Ghani and Sarder Nasir Uddin and from few other references. The database http://www.worldfloraonline.org/ (previously www.theplantlist.org) was followed for the accepted Latin name of each plant. Criteria followed to include plant species were plants that showed significant anti-inflammatory activities in 1) two or more sets of experiments in a single report, 2) same or different sets of experiments in two or more reports, and 3) plants which are traditionally used in the treatment of inflammation and inflammatory disorders. On the other hand, exclusion criteria include 1) reports not meeting the inclusion criteria, 2) plants

TABLE 2 | Major chemical classes of plant-derived anti-inflammatory molecules.

Secondary metabolite class	Examples	References
Alkaloids	Aconitine, berberine, colchicine, cepharanthine, capsaicin, ephedrine, and pseudo-ephedrine	Ivanovska and Philipov (1996); Barbosa-Filho et al. (2006); Souto et al. (2011)
Essential oils	β-myrcene, limonene, cinnamaldehyde, eugenol, anethole, caryophyllene, 1,8-cineole, and α-pinene	Santos and Rao (2000); Souza et al. (2003); Tung et al. (2008); Miguel (2010); de Cássia da Silveira et al. (2014); Kim et al. (2015b); Özbek and Yılmaz (2017)
Flavonoids	Apigenin, epigallocatechin gallate, genistein, hesperidin, kaempferol, luteolin, myricetin, quercetin, and rutin	Guardia et al. (2001); Kim et al. (2004); González-Gallego et al. (2007); Gomes et al. (2008); Tunon et al. (2009)
Glycosides	Digitoxin, digoxin, ouabain, codonolaside, and oleuropein	Miles et al. (2005); Xu et al. (2008); Fürst et al. (2017)
Phenolics	Lapachol, ellagic acid, caffeic acid, catechol, oleocanthal, bergenin, cannabichromene, tremetone, and vanillic acid	de Almeida et al. (1990); Perez (2001); Miles et al. (2005); Kassim et al. (2010); Kazłowska et al. (2010); Beg et al. (2011); Lucas et al. (2011)
Saponins	Fruticesaponin A-C, ruscogenin, capillarisin, kalopanaxsaponin-A, monodesmosides, ginsenosides, prosapogenin D methyl-ester, and buddlejasaponin I	Just et al. (1998); Huang et al. (2008); Attiq et al. (2018)
Stilbenes	Resveratrol, oxyresveratrol, desoxyrhapontigenin, aiphanol, and isorhapontigenin	Wadsworth and Koop (1999); Guardia et al. (2001); Fang et al. (2008); Choi et al. (2014)
Terpenoids	Artemisin, artemisinin, artemisolide, curcumin, zingiberene, helenalin, andrographolide, hispanolone, acanthoic acid, carnosol, carnosic acid, triptolide, kamebanin, oridonin, ursolic acid, oleanolic acid, betulinic acid, glycyrrhizin, β-carotene, lycopene, and lupeol	Fernández et al. (2001); Salminen et al. (2008); de las Heras and Hortelano (2009); Beg et al. (2011); Kashyap et al. (2016)

reported with insufficient data or no data of doses of the sample or extract and/or positive control, and 3) plants showing anti-inflammatory activity in a single set of experiments in a single report. This review is, therefore, not exhaustive for all the medicinal plants of Bangladesh reported to have anti-inflammatory activity. The toxicity test results summarized in **Supplementary Table S1** have been extracted from the same report reviewed for anti-inflammatory activity of plants if toxicity had been tested in the study.

RESULT AND DISCUSSION

This study represents 48 medicinal plants of Bangladesh from 47 genera belonging to 29 families which have traditional values in the treatment of inflammatory disorders along with other medicinal uses. Inflammatory diseases such as arthritis, asthma, tumor, etc. have been managed conservatively using different parts or products of these plants (**Supplementary Table S1**). *Acanthus ilicifolius* L., *Acmella paniculata* (Wall. ex DC.) R.K.Jansen, *Aegiceras corniculatum* (L.) Blanco, *Ageratum conyzoides* (L.) L., *Alangium salviifolium* (L.f.) Wangerin, *Alocasia macrorrhizos* (L.) G.Don, *Argyreia argentea* (Roxb.) Sweet, *Azadirachta indica* A. Juss., *Cyanthillium cinereum* (L.) H.Rob., *C. patulum* (Dryand. ex Dryand.) H.Rob., *Glycosmis pentaphylla* (Retz.) DC., *Heliotropium indicum* L., *Lantana camara* L., *Mangifera indica* L., *Manilkara zapota* (L.) P.Royen, *Mussaenda roxburghii* Hook.f., *Oroxylum indicum* (L.) Kurz, *Phrynium imbricatum* Roxb., *Phyllodium pulchellum* (L.) Desv., *Piper retrofractum* Vahl, *Steudnera colocasiifolia* K.Koch, *Swietenia mahagoni* (L.) Jacq., *Thunbergia grandiflora* (Roxb. ex Rottl.) Roxb., *Toona ciliata* M.Roem., *Vigna unguiculata* (L.) Walp., *Vitex negundo* L., and *Withania somnifera* (L.) Dunal have values in the treatment of arthritis. *Clerodendrum infortunatum* L., *Coccinia grandis* (L.) Voigt, *Eclipta prostrata* (L.) L., *Euphorbia hirta* L., *Flemingia stricta* Roxb., *P. retrofractum*, and *Terminalia arjuna* (Roxb. ex DC.) Wight & Arn. have been used as a traditional remedy for asthma. Examples of plants credited for antitumor properties include *Butea monosperma* (Lam.) Taub., *Gynura nepalensis* DC., *Leea macrophylla* Roxb. ex Hornem., *Mallotus repandus* (Willd.) Müll.Arg., *Microcos paniculata* L., *Premna esculenta* Roxb., and *Typhonium trilobatum* (L.) Schott. Furthermore, *Aglaia cucullata* (Roxb.) Pellegr., *M. zapota*, and *Urena sinuata* L. are known to be efficacious against inflammation besides other traditional uses. These plants were reported to possess significant anti-inflammatory activities which were evaluated using various *in vivo* and *in vitro* experimental models. The mechanistic pathways of these models have been taken into consideration for discussion, which provides better understanding of the action mechanism of plants reviewed in this study.

Common Experimental Methods to Evaluate Anti-Inflammatory Activity of Natural Products

Numerous biochemical mediators work jointly to commence and continue the inflammatory cascade. Crude extracts and/or pure compounds derived from plants target these mediators and have paved the way for the development of new therapeutic approaches. *In vitro* methods are mainly based on the

inhibition of such activated mediators. The potent biochemical mediators include, enzymes (PLA_2, COX-1, COX-2, 5-LOX, 12-LOX, 15-LOX, MMP-2, MMP-9, inosine monophosphate dehydrogenase, and β-hexosaminidase); free radicals (ROS, RNS, and SOD); prostaglandins (PGE_2, TXA_2; hydroxyleicosatetraenoic acid [HETE]); leukotrienes (LTB_4, LTC_4); cluster of differentiation molecules (CD-2, CD-11a, CD-11b, CD-18, and CD-49d), etc. (Venkatesha et al., 2011; Asante-Kwatia et al., 2020). Other important biochemical targets include proinflammatory cytokines (TNF-α, INF-γ, IL-1, IL-6, and IL-1β) and chemokines (IL-8, ICAM-1, and VCAM-1). In addition to these, a number of transcription factors including nuclear factor (NF)-κB, mitogen-activated protein kinases (MAPKs), extracellular signal–regulated kinase (ERK), c-Jun-N-terminal kinase (JNK), signal transducer and activator of transcription-1 (STAT-1), p38 kinases, and AP-1 have been used as molecular targets of inflammation (Luster et al., 2005; Venkatesha et al., 2011). Red blood cell (RBC) membrane stabilization and protein denaturation assays have also been reported in a vast number of studies.

On the other hand, commonly used *in vivo* methods are carrageenan-induced paw edema, croton oil or TPA (12-*O*-tetradecanoylphorbol-13-acetate)-induced acute inflammation, xylene-induced ear edema, cotton pellet–induced granuloma, Freunds' complete adjuvant (FCA)–induced arthritis, *in vivo* xanthine oxidase assay, LPS-induced peritonitis mouse model, acetic acid–induced vascular permeability assay or measuring writhing reflexes, UV erythema, pleurisy test, etc. (Ferrari et al., 2016; Asante-Kwatia et al., 2020).

Preclinical Models Used to Investigate Plants Included in this Review

In Vivo Studies

In this report, carrageenan-induced paw edema is found to be an extensively used *in vivo* model used in 28 investigations. In other studies, paw edema is induced using formalin, egg albumin, and also by exogenous administration of histamine and serotonin. Ear edema models are induced using xylene and croton oil. Cotton pellet–implanted granuloma has been exercised in 12 studies. Other *in vivo* studies include acetic acid–induced writhing test.

Paw Edema Model

Carrageenan-induced paw edema is found to be the most extensively used *in vivo* test procedure to screen medicinal plants for their anti-inflammatory activities by Bangladeshi researchers (**Supplementary Table S1**). This seaweed-derived sulfated polysaccharide is injected to experimental animals such as mouse or rat to induce acute and local inflammation. Paw edema induced by carrageenan is considered to be a highly sensitive, reproducible, and well-established model to investigate anti-inflammatory drugs. This model is characterized by biphasic response. Paw inflammation develops resulting in the synthesis of histamine, serotonin, and bradykinin in the first phase (0–1 h) followed by production of COX-2–mediated prostaglandins and cytokines such as IL-1β, IL-6, IL-10, and TNF-α in the second phase (2–3 h). These mediators can be generated *in situ* either by cellular infiltration or at the site of the local inflammatory insult. The second phase is sensitive to both steroidal and nonsteroidal anti-inflammatory drugs (Posadas et al., 2004; Dzoyem et al., 2017).

Histamine, serotonin, formalin, and egg albumin are injected to obtain paw inflammation in other sets of studies included in this review.

Histamine is a potent inflammatory mediator and is injected to rat or mice paw to induce acute inflammation. This vasoactive amine elicits the release of neuropeptides and prostaglandins from endothelial cells, contributes to neutrophil recruitments, and causes vasodilatation and increased vascular permeability leading to pain and inflammation (Yong et al., 2013b).

Serotonin is another vasoactive amine and inflammatory mediator which increases vascular permeability and can produce acute paw edema *via* direct injection (Yong et al., 2013a).

Formalin-induced paw edema is also a common method to screen medicinal plants for anti-inflammatory activity and is described as a biphasic response in studies. Neurogenic pain develops in the initial phase, and the second phase involves development of inflammatory responses generated by the release of mediators such as histamine, serotonin, bradykinin, prostaglandin, cytokines (IL-1β, IL-6, TNF-α, etc.), and nitric oxide (NO). Formalin-induced paw edema can be modeled for both acute and chronic type of inflammatory assays (John and Shobana, 2012; Arzi et al., 2015).

Paw edema induced by egg albumin is an acute and triphasic phenomenon as described by Dzoyem et al. (2017), where the first phase is mediated by histamine and serotonin and then the bradykinin-mediated second phase is followed by a third phase mediated by cyclooxygenase to produce bradykinin proteases and prostanoids (Dzoyem et al., 2017).

Usually the changes in thickness, volume, weight, and histology of edematous paw induced by any of the abovementioned methods are examined, and by comparison among the control and treated groups, the anti-inflammatory activities of the plant samples are determined (Kim et al., 2006).

Ear Edema Model

Xylene-induced ear edema is another *in vivo* model exercised to determine anti-inflammatory activity of plants. Topical administration of xylene causes cutaneous ear inflammation which is acute in nature and is characterized by vasodilatation, cellular infiltration, and edema formation (Lu et al., 2006). Ear edema can be induced by applying croton oil to the ear of rats or mice. This acute inflammatory action is also marked by synthesis of prostaglandins, migration of neutrophils, increased vascular permeability, and development of edema (Luo et al., 2014). In such models, the rats or mice are killed, and circular sections of ears are collected to examine the changes in weight, thickness, and histology profile, which are then compared among the control and treated groups to evaluate the anti-inflammatory activities of the plant samples.

Cotton Pellet–Induced Granuloma Model

Cotton pellet–inserted granuloma in rodents is described as a chronic model which is the proliferative phase of inflammation.

This pharmacological procedure consists of three phases, namely, 1) transudative, 2) exudative, and, 3) proliferative (Swingle and Shideman, 1972). The granuloma is actually a highly vascularized tissue which is formed at the site of the subcutaneously implanted cotton pellet due to migration of monocytes, proliferation of fibroblasts, increased vascular permeability, and accumulation of fluid and proteinaceous components (Dzoyem et al., 2017). Anti-inflammatory substances can inhibit the growth of granuloma tissue *via* interfering with the phases of granuloma formation.

Acetic Acid–Induced Writhing Test

Acetic acid induced writhing is explained as a model of visceral inflammatory pain, generated by releasing endogenous mediators which can trigger nociceptors and are sensitive to nonsteroidal anti-inflammatory drugs and drugs that act on the central nervous system (Bighetti et al., 1999; Jones et al., 2005). Acetic acid is injected into the peritoneal cavity of the experimental animal which causes release of proinflammatory cytokines such as TNF-α, IL-1β, and IL-8 by peritoneal macrophages and mast cells (Ribeiro et al., 2000). As a result, acute inflammatory response arises in the peritoneal area of the experimental animals, and then the animals react with characteristic writhing (Dzoyem et al., 2017). Substances with anti-inflammatory property can inhibit the number of writhes over a time course.

In Vitro Studies

In vitro assays minimize the ethical issues associated with the use of animals in the early phases of drug discovery (Williams et al., 2008). They are mostly cell-based and protein-based and are usually rapid, easy to conduct, and cost-effective, and most importantly, they help understand the molecular mechanism of bioactive compounds to render anti-inflammatory activity (Dzoyem et al., 2017).

RBC membrane stabilization assay is the most extensively used screening tool which has been found to be exercised in 36 studies in this report. Other *in vitro* experiments include protein denaturation, protease inhibition, and direct estimation of lipoxygenase (LOX) inhibition by the plant samples using the LOX inhibition assay.

RBC Membrane Stabilization Method

In RBC membrane stabilization assay, the red blood cells (erythrocytes) are exposed to various injurious stimuli which can be thermal (heat), mechanical (hypotonic solution), or chemical (methyl salicylate, phenyl hydrazine, etc.) to induce hemolysis. The RBC membrane has a structure similar to that of the lysosome which is a membrane-bound cellular organelle and can release enzymes (PLA_2, protease, etc.) capable of inducing inflammatory process. Stabilization of the lysosomal membrane prevents the release of those inflammatory mediators. Therefore, plant extracts or compounds effective in protecting the rupture of the erythrocyte membrane are expected to inhibit the release of inflammatory mediators from the lysosome by stabilizing the lysosomal membrane and hence considered to possess anti-inflammatory activity (Umapathy et al., 2010; Anosike et al., 2012).

Protein Anti-Denaturation Assay

Denaturation of protein has also served as an *in vitro* pharmacological method to screen anti-inflammatory activity of plant extracts. Bovine serum albumin (BSA) and egg albumin are commonly used proteins for this purpose. The protein loses its secondary and tertiary structures when exposed to heat or substances such as strong acid or base, concentrated salt solution, or organic solvent. Biologically active proteins usually lose their biological activity upon denaturation (Nirmal and Panichayupakaranant, 2015). As explained by Williams et al. (2008), the extracts or molecules which exhibit anti-denaturation property at a very low concentration (ng/ml) should be selected for further drug development processes.

Protease Inhibition Assay

Proteases (also called proteinase) are enzymes that catalyze proteolysis, that is, the hydrolysis of peptide bonds, leading to breakdown of proteins (López-Otín and Overall, 2002). Activation of these enzymes can cause tissue damage associated with inflammatory disorders and can be prevented with drugs having protease inhibitory activity (Kumar et al., 2013). Examples of proteases involved in inflammatory reactions include human neutrophil elastase, MMPs (MMP-2 and -9), trypsin etc. (Benedek et al., 2007; Aziz et al., 2015) and are utilized by the researchers to study the *in vitro* anti-inflammatory potential of plants.

Toxicological Aspect

Toxicology is defined as a branch of science that deals with poisons (Hodgson, 2004), and as stated by Macht (1938), "every drug that is worth anything as a medicinal agent is also a poison." Toxicity arises due to the interaction between cellular macromolecules and poisons or toxicants (Jothy et al., 2011). Evaluation of toxicity of such agents is, therefore, also crucial besides evaluating their pharmacological properties. To assure the safe medicinal use of plants or plant products, estimation of toxicity is a must. Numerous laboratory procedures have been developed for this purpose.

It can be noticed in the present study that toxicity studies have not been conducted with almost half of the plants (**Supplementary Table S1**) at the same time when the anti-inflammatory activities are being evaluated. Out of 48 plants, 25 have undergone preliminary assessment of toxicity by at least one of the cited works. The acute toxicity text and brine shrimp (*Artemia salina*) lethality test were found to be the primarily used assay methods to assess the toxicity of plant extracts.

The acute toxicity test is an initial screening step to assess and evaluate toxic properties of substances. LD_{50} which is the dose of the test sample that leads to 50% lethality in the tested group of animals can be determined using this assay (Akhila et al., 2007). Multiple graded doses or a considerably higher single dose than that of the plant extract under investigation were commonly administered to rats or mice to make an estimation of the margin of safety using the acute toxicity test (**Supplementary Table S1**). Another assay, brine shrimp lethality test, is appraised to be the

FIGURE 2 | Plants with anti-inflammatory activity, namely, *A. indica*, *C. infortunatum*, *C. asiaticum*, *G. pentaphylla*, *H. indicum*, *M. paniculata, P. retrofractum*, *S. villosa*, *and T. trilobatum* were obtained from Wikimedia Commons under GNU free documentation license (http://en.wikipedia.org/wiki/GNU_Free_Documentation_License), whereas *P. reticulatus* was obtained from the web page "Flora of Bangladesh," from the Survey of Vascular Flora of Chittagong and the Chittagong Hill Tracts Project, Bangladesh National Herbarium (http://bnh-flora.gov.bd), Ministry of Environment & Forest, People's Republic of Bangladesh.

most convenient method to monitor toxicity of the medicinal plants. This is a rapid and simple predictive tool for toxic potential of plant extracts in humans (Hamidi et al., 2014). Brine shrimp is commonly used as the test organism. LC_{50} which is the concentration of the test sample that leads to 50% lethality in the nauplii is determined usually by using the graph of mean percentage mortality vs. the log of concentration (Syahmi et al., 2010). The *Allium cepa* toxicity test is also a common test used by researchers to investigate the toxicity of various substances. This is a sensitive *in vivo* test method and is used to determine cytotoxic and genotoxic effect of different substances. This test can serve as an indicator of toxicity of the tested samples since it shows good correlation with tests in other living systems. An inhibition of root growth or mitotic index values in the treated onion roots indicates cytotoxic effects, and the chromosomal aberration in the treated onion root tip meristems indicates genotoxic effects of the materials or plant extracts under investigation (Adegbite and Sanyaolu, 2009).

Overview on Selected Anti-Inflammatory Plants

Each of the plant included in the present work is useful in traditional medicine to manage inflammation or inflammatory diseases since that was one of the inclusion criteria. However, for ease of discussion, the following nine plants have been selected (**Figure 2**), which have demonstrated remarkable anti-inflammatory activity in three or more individual reports (**Supplementary Table S1**). The habitat, similar studies conducted with the species other than the Bangladeshi one, and anti-inflammatory molecules reported from these plants have been overviewed.

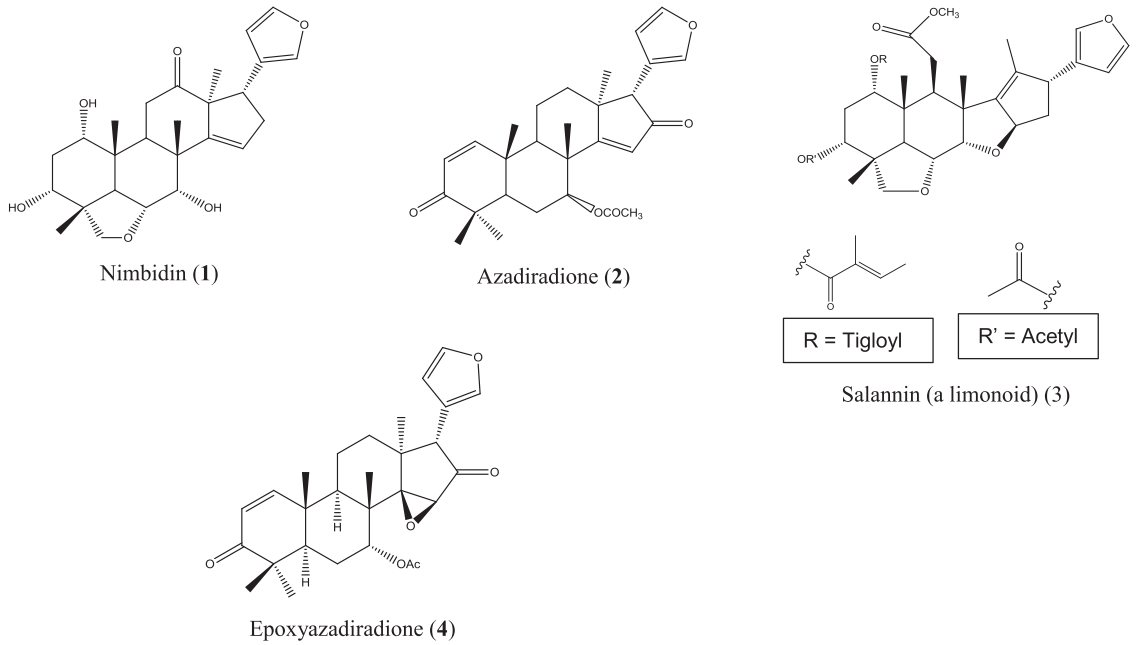

FIGURE 3 | Anti-inflammatory compounds isolated from *A. indica*.

Azadirachta indica A. Juss.

A. indica is locally known as neem and is commonly found all over Bangladesh and in India, Pakistan, and Nepal. This herb is used in traditional healing practices, including Ayurvedic, Unani, and Homeopathic systems, to a great extent (Alzohairy, 2016). Though originated from Asia, neem is now cultivated worldwide. Medicinal values, most importantly the anti-inflammatory action of neem extracts and neem compounds, have been reported in a number of studies. Indian neem leaf extract and neem seed oil have inhibited cotton pellet–induced granuloma and carrageenan-induced paw edema, respectively, in rats (Chattopadhyay, 1998; Naik et al., 2014). The Nigerian variety of neem showed pronounced anti-inflammatory activity by reducing carrageenan-induced rat paw edema (Okpanyi and Ezeukwu, 1981). Polysaccharide fractions from the neem seed tegument of Brazil exhibited potent anti-inflammatory activity in acute inflammatory test models (Pereira et al., 2012). However, in another Brazilian study, the ethanolic neem fruit extract did not reduce abdominal edema in the carrageenan-induced inflammatory model of zebrafish and was found to be nontoxic in zebra fish as well as the *A. salina* lethality test (Batista et al., 2018). The neem fruit extract azadirachtin A, purchased in China, markedly reduced the levels of TNF-α, IL-6, IL-1b, TLR4, and NF-κB followed by inhibition of tissue inflammation (He et al., 2020). In a study, conducted in Luxembourg, a strong effect of the neem extract has been observed on proinflammatory cell signaling *via* modulation of the NF-κB pathway (Schumacher et al., 2011). The neem compounds which have significantly attenuated inflammation and related diseases are nimbidin (**1**) (Pillai and Santhakumari, 1981; Kaur et al., 2004), azadiradione (**2**) (Ilango et al., 2013), salannin (**3**), epoxyazadiradione (**4**) (Alam et al., 2012) (**Figure 3**), and a series of other limonoids (Akihisa et al., 2011; Islas et al., 2020).

Clerodendrum infortunatum L.

C. infortunatum is a shrub and is widely distributed throughout Bangladesh, India, Sri Lanka, Thailand, and Malaysia, and is used in the indigenous systems of medicine, including Ayurveda, Unani, and Homeopathy (Ahmed et al., 2007; Kekuda et al., 2019). Ethanol extract of leaf and aqueous acetone extract of the root bark prepared from the Indian species of this plant have shown anti-inflammatory activity by inhibiting paw edema in rats (Chandrashekar and Rao, 2013; Helen et al., 2018), whereas hydroethanolic extract of the leaf, stem, and root of *C. infortunatum* dose-dependently inhibited NO production in LPS-stimulated macrophage and showed no sign of mortality in the acute toxicity study (Dutta et al., 2018). In another study, both leaf and root extracts were found safe in the *in vivo* experimental model (Nandi et al., 2017). Several compounds have been identified from *C. infortunatum* with important medicinal values (Nandi and Mawkhlieng Lyndem, 2016), the major being 3-deoxy-d-mannoic lactone, glycerin, and xylitol as analyzed using the gas chromatography coupled with mass spectroscopy (GC-MS) technique (Ghosh et al., 2015) along with viscosene and several flavonoid glycosides (Uddin et al., 2020). Anti-inflammatory moieties reported from this plant include apigenin (**5**) (Sinha et al., 1981), quercetin (**6**) (Gupta and Gupta, 2012), oleanolic acid (**7**) (Sannigrahi et al., 2012), β-sitosterol (**8**) (Gupta and Singh, 2012; Paniagua-Pérez et al., 2017), and squalene (**9**) (**Figure 4**) (Choudhury et al., 2009).

Crinum asiaticum L.

C. asiaticum is an evergreen herb found in Bangladesh, India, Sri Lanka, Myanmar, Thailand, Malaysia, China, and Japan. This

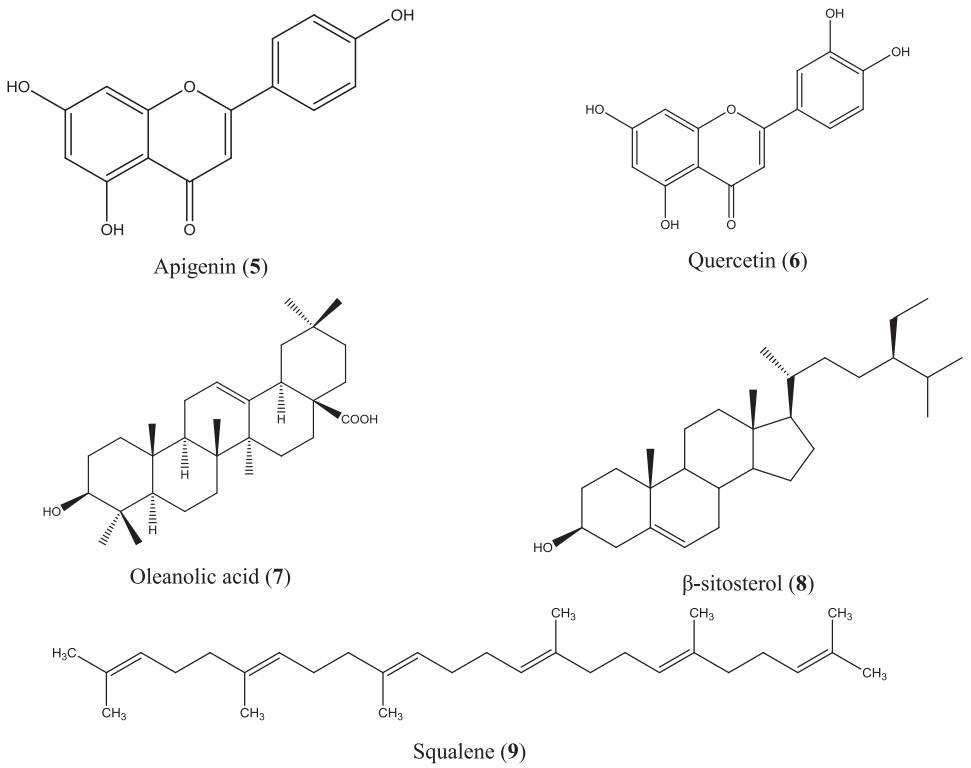

FIGURE 4 | Anti-inflammatory compounds isolated from *C. infortunatum*.

herb is randomly inhabited in the hilly areas of Bangladesh, especially the Chittagong Hill Tracts, and has widely been used in traditional and Ayurvedic systems of medicines (Rahman et al., 2013; Sharma et al., 2020). The Malaysian species of this plant caused significant reduction of mice paw edema (Samud et al., 1999) and prevented new blood vessel formation from the aortic ring explants, exhibiting potential anticancer activity known to be influenced by inflammation (Yusoff et al., 2017). The list of compounds isolated from this plant is also long and includes lycorine, crinamin, stigmasterol, cycloartenol, etc. (World Health Organization, 1998), among which stigmasterol (**10**) (Al-Attas et al., 2015) and lycorine (**11**) (**Figure 5**) (Çitoğlu et al., 1998; Saltan Çitoğlu et al., 2012) are reported to be anti-inflammatory molecules. Crinamin, a protein isolated from the latex of *C. asiaticum* leaf exhibited anti-inflammatory activity by reducing carrageenan-induced paw edema and cotton pellet–induced granuloma in rats and also showed protein anti-denaturation and RBC membrane stabilization activity (Rai et al., 2018).

Glycosmis pentaphylla (Retz.) DC.

G. pentaphylla is a shrub or small tree that grows at low altitudes of Bangladesh, India, Malaysia, southern China, and the Philippine Islands (Hossain S. M. et al., 2012). Root extract from the same Indian plant inhibited carrageenan- and egg

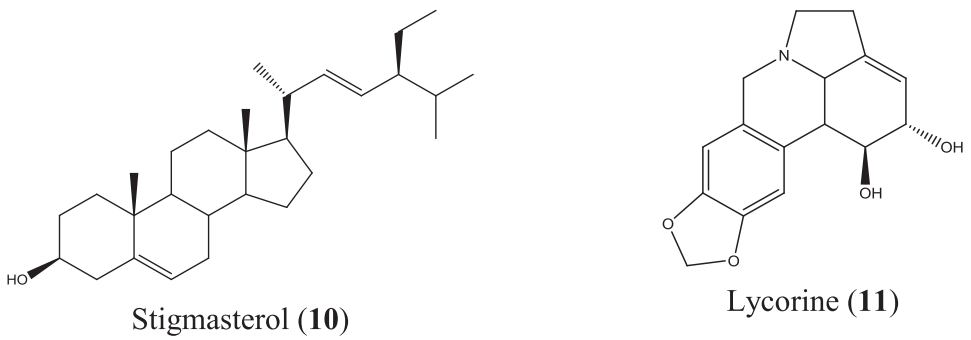

FIGURE 5 | Anti-inflammatory compounds isolated from *C. asiaticum*.

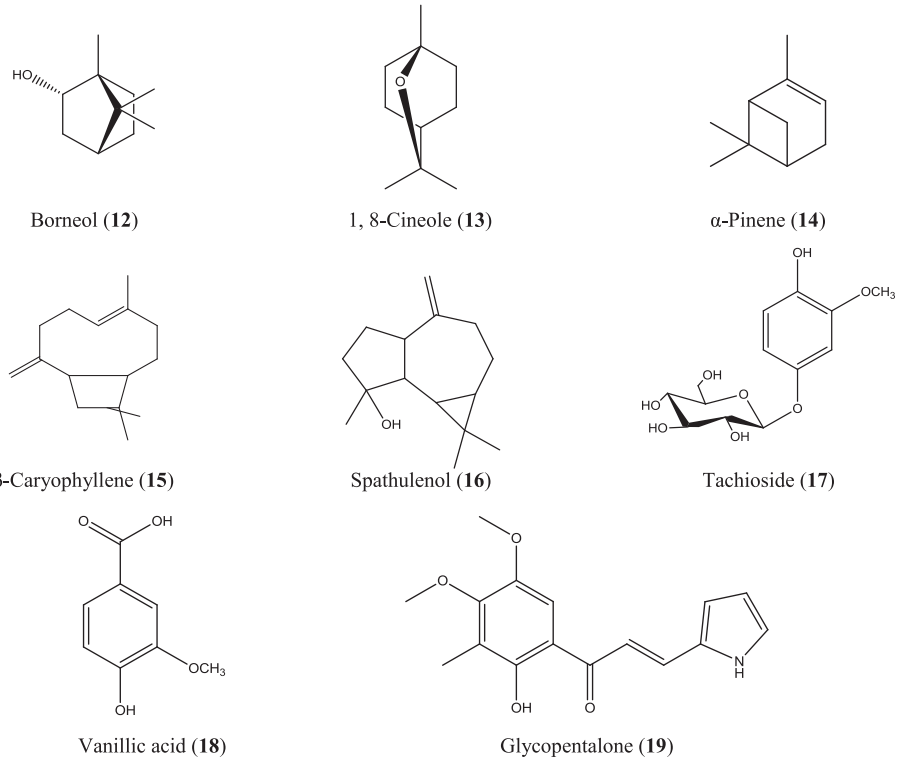

FIGURE 6 | Anti-inflammatory compounds isolated from *G. pentaphylla*.

albumin–induced paw edema, xylene-induced ear edema, and formalin-induced arthritic inflammation in rats (Rao and Raju, 2009; Arora and Arora, 2016). The essential oils obtained from the bark, leaf, and seed of *G. pentaphylla* are enriched with numerous bioactive constituents (Ahmed et al., 2000), and some of them have well-documented anti-inflammatory activity such as borneol (**12**) (Zou et al., 2017), 1, 8-cineole (**13**) (Santos and Rao, 2000), α-pinene (**14**) (Kim DS. et al., 2015; Özbek and Yılmaz, 2017), caryophyllene (**15**), caryophyllene oxide (Tung et al., 2008), and spathulenol (**16**) (**Figure 6**) (do Nascimento et al., 2018). In studies in China, a number of prenylated sulfur-containing amides and a phenolic glycoside (tachioside) (**17**) (**Figure 6**) isolated from this plant also exhibited anti-inflammatory activity *via* downregulation of nitric oxide (NO) production in LPS-stimulated RAW 264.7 macrophages (Tian et al., 2014; Nian et al., 2020). Numerous other compounds have been isolated from this plant, including anti-inflammatory stigmasterol (**10**) (**Figure 5**), vanillic acid (**18**) (Siddiqui et al., 2019; Soma et al., 2019; Chokchaisiri et al., 2020; Ziadlou et al., 2020), and glycopentalone (**19**) (**Figure 6**) (Sreejith and Asha, 2015; Sasidharan and Vasumathi, 2017).

Heliotropium indicum L.

H. indicum is a perennial herb indigenous to Bangladesh, India, Sri Lanka, Nepal, and Thailand and also grows in some parts of Africa (Samira et al., 2016). The Indian *H. indicum* has been found to attenuate carrageenan-, egg white–, and formalin-induced paw edema and cotton pellet–inserted granuloma in rats (Srinivas et al., 2000; Betanabhatla et al., 2007; Ramamurthy et al., 2009; Shalini and Shaik, 2010), whereas the Thai and Ghanaian species have been reported to inhibit proinflammatory mediators in LPS-stimulated RAW 264.7 macrophages (Chunthorng-Orn et al., 2016; Kyei et al., 2016). Analyses on volatile oil composition of this plant have been carried out where phenylacetaldehyde and phytol were found to be the major constituents, and a number of pyrrolizidine alkaloids have also been reported from *H. indicum* (Birecka et al., 1984; Machan et al., 2006; Ogunbinu et al., 2009). In another GC-MS analysis of essential oil, it was revealed that this plant is rich in phenyl derivatives, where methyl salicylate is the major constituent (Joshi, 2020), and interestingly, a small concentration of methyl salicylate is used in topical preparations for the treatment of mild aches and pains of arthritis (Martin et al., 2004).

Microcos paniculata L.

M. paniculata is a shrub native to southern China, Southeast Asia, and South Asia. In Bangladesh, this plant is common at the Sylhet and Chittagong divisions (Al-Amin Sarker et al., 2016; Jiang and Liu, 2019). Besides numerous traditional uses, a diverse range of compounds have been identified from different parts of the plant which include some well-documented anti-inflammatory molecules such as apigenin (**5**), quercetin (**6**)

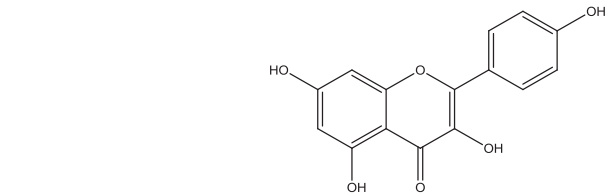

Kaempferol (**20**)

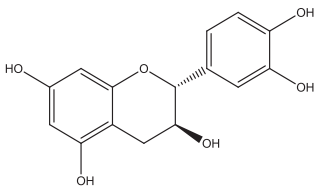

Catechin (**21**)

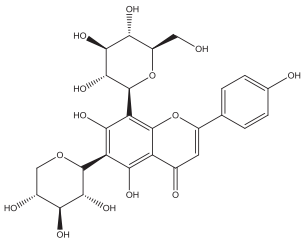

Vicenin-1 (an apigenin C-glycoside) (**22**)

FIGURE 7 | Anti-inflammatory compounds isolated from *M. paniculata*.

(**Figure 4**), kaempferol (**20**), catechin (**21**), epicatechin (Perez, 2001; García-Mediavilla et al., 2007; Hämäläinen et al., 2007; Kim SH. et al., 2015; Lesjak et al., 2018), and apigenin C-glycosides (e.g., vicenin-1) (**22**) (Li et al., 2018) (**Figure 7**). A total flavonoid glycoside fraction obtained from Chinese *M. paniculata* demonstrated potential anti-inflammatory activity by reducing xylene-induced mice ear edema and suppressing proinflammatory cytokines (IL-6, IL-1β, and TNF-α) in LPS-stimulated RAW 264.7 macrophages. In the same study, ten flavone glycosides have been characterized from the total flavonoid glycoside fraction (Yuan et al., 2019).

Piper retrofractum Vahl

P. retrofractum is a flowering vine native to South and Southeast Asia including Bangladesh, India, Malaysia, Indonesia, Singapore, and Sri Lanka. This plant is used as a culinary herb in some regions of Bangladesh and is commonly known as Choi or Chui jhal (Islam MT. et al., 2020). Methanolic leaf extract of the same Indian species has been investigated using chronic anti-inflammatory study models, including carrageenan- and dextran-induced paw edema and an acute model of cotton pellet–induced granuloma (Vaghasiya et al., 2007). *P. retrofractum* fruit extract is an ingredient of a Thai traditional medicine "Benjakul" which has demonstrated strong anti-inflammatory activity in *in vitro* and *in vivo* test systems (Kuropakornpong et al., 2020). In another Thai study, the ethanolic fruit extract of *P. retrofractum* inhibited ethyl phenylpropiolate–induced ear edema and carrageenan-induced paw edema in rats (Sireeratawong et al., 2012). Chabamides, piperine, piplartine, etc. have been reported from this plant (Islam MT. et al., 2020). Essential oil composition of the fruit oils of *P. retrofractum* has also been analyzed, which contains 5.2% of β-caryophyllene (**15**) (**Figure 6**) (Tewtrakul et al., 2000).

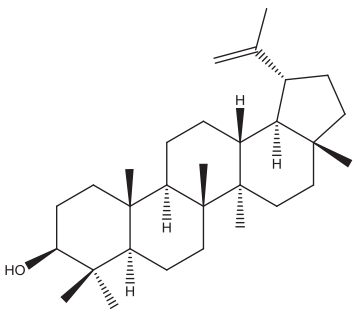

Lupeol (**23**)

FIGURE 8 | Anti-inflammatory compounds isolated from *S. villosa*.

Sterculia villosa Roxb.

S. villosa is a deciduous small to large tree found in tropical and subtropical countries, including Bangladesh, India, Sri Lanka, and southern China (Hossain M. K. et al., 2012; Hossain et al., 2016). This plant has received special importance for its anti-inflammatory ethnomedicinal value besides many other traditional uses (Namsa et al., 2009; Thabet et al., 2018). Along with different bioactive molecules such as chrysoeriol, chrysoeriol 7-O-β-D-glucoside, diosmetin, etc., anti-inflammatory lupeol (**23**) (**Figure 8**) has also been reported from *S. villosa* (Seetharaman, 1990; Das et al., 2017).

Typhonium trilobatum (L.) Schott

T. trilobatum or Bengal arum is a perennial herb native to Asia, including Bangladesh, India, and to South Pacific. This is a soft plant that grows in the damp and moist places in Chittagong, Sylhet, and other areas of Bangladesh (Ghani, 2003; Haldar et al.,

2011). This plant has plenty of traditional uses and has been evaluated in several studies for its anti-inflammatory action (**Supplementary Table S1**), but individual phytoconstituents from this plant have not been documented properly yet (Manna et al., 2016).

In addition to the abovementioned nine species, the following species have been found to be studied tremendously in recent years for anti-inflammatory activities and been reviewed here in brief.

Ageratum conyzoides (L.) L.

A. conyzoides is an annual herb with a long history of uses in traditional medicine in the tropical and subtropical countries (Kotta et al., 2020). This plant is very common in West Africa, South America, and some parts of Asia, including Bangladesh (Okunade, 2002; Hassan et al., 2012). Crude extract, organic fractions, and isolated compounds (5′- ethoxynobiletin, 1,2-benzopyrone and eupalestin) from the Brazilian variety of this plant inhibited carrageenan-induced pleurisy in mice by reducing the concentration of myeloperoxidase (MPO), adenosine deaminase (ADA), and NO, and by inhibiting several proinflammatory mediators (e.g., IL-17A, IL-6, TNF-α, and IFN-γ). The isolated compounds also reduced phosphorylation of NF-κB and MAPK (Vigil de Mello et al., 2016). In another study conducted in Brazil, the ethanol extract of the standardized polymethoxyflavone extract of this plant exhibited anti-inflammatory activity in mice (Faqueti et al., 2016), whereas Indonesian *A. conyzoides* leaf extract decreased TNF-α and MMP-9 levels in monosodium iodoacetate–induced osteoarthritis in rats, and anti-inflammatory quercetin (**6**) was detected in the extract (Bahtiar et al., 2017).

Eclipta prostrata (L.) L.

E. prostrata is an annual herb and a common weed native of Asia but is now widely distributed in tropical and sub-tropical areas over the world (Chung et al., 2017; Feng et al., 2019; Yu et al., 2020). In Asia, this plant grows in Bangladesh, India, Indonesia, Cambodia, Malaysia, Nepal, Pakistan, the Philippines, Sri Lanka, Thailand, Vietnam, China, Japan, and Korea (Uddin et al., 2015). The Korean variety of *E. prostrata* ethanolic extract prepared conventionally and using ultrasound as well as wedenolactone (a compound isolated from this plant) exhibited anti-inflammatory activity by reducing IL-6, TNF-α, and PGE_2 levels (Lee, 2017). In another investigation, a series of flavonoid, flavonoid derivative, triterpenoid, and triterpenoid glycosides were isolated from this plant which reduced the NO level in LPS-stimulated RAW 264.7 cells in varying degrees, where 7-*O*-methylorobol-4′-*O*-*β*-D-glucopyranoside was found to be the most potent compound and reported as an inhibitor of IκB phosphorylation (Le et al., 2020). The aqueous seed extract of the Sri Lankan variety of this plant dose-dependently inhibited denaturation of egg albumin (Kannadas et al., 2020).

Lawsonia inermis L.

L. inermis commonly known as henna has plenty of traditional uses (**Supplementary Table S1**). This evergreen shrub is mainly cultivated for cosmetic purposes and also for its use in traditional medicine all over the world, but the plant is native to tropical and subtropical countries such as Bangladesh, India, Sri Lanka, and the Middle East (Ghani, 2003; Sharma et al., 2016). Flavonoids isolated from the Indian species of this plant inhibited carrageenan-induced rat paw edema (Manivannan et al., 2015), whereas the flower extract from the Tunisian species inhibited 5-LOX (Chaibi et al., 2015). The ethanol extract from the leaves of this plant reduced formalin-induced (Humaish, 2017) and carrageenan-induced (Vijayaraj and Kumaran, 2018) rat paw edema in studies conducted in Iraq and India. respectively. The Nigerian *L. inermis* leaf extract prepared with n-butanol and ethylacetate reduced carrageenan-induced foot edema in chicks (Chuku et al., 2020). Additionally, a topical formulation prepared from Iranian henna leaves improved contact dermatitis in patients using lower limb prosthetics (Niazi et al., 2020).

Manilkara zapota (L.) P.Royen

M. zapota is an evergreen tree thought to originate from Mexico, Central America, and West Indies and is cultivated throughout Bangladesh and India (Ganguly et al., 2013; Yong and Abdul Shukkoor, 2020). The leaf extract of Indian *M. zapota* inhibited hemolysis of the RBC membrane (Sravani et al., 2015) and inhibited PLA_2 and 5-LOX, and carrageenan-induced rat paw edema in *in vitro* and *in vivo* experimental models, respectively (Konuku et al., 2017). Apigenin-7-O-β-D-glucuronide methyl ester isolated from Ethiopian *M. zapota* leaves downregulated COX-2 mRNA expression in MCF-7 breast cancer cells (Kamalakararao et al., 2018b) and also inhibited NO and PGE_2 production in LPS-induced RAW 264.7 macrophages (Kamalakararao et al., 2018a). The fruit extract prepared from the Thai variety exhibited anti-inflammatory potential by inhibiting the TNF-α level in LPS-activated human PMBC cells (Leelarungrayub et al., 2019). Again, several prenylated coumarins identified from Chinese *M. zapota* fruit suppressed NO production in LPS-activated RAW 264.7 cells (Liu et al., 2019).

Withania somnifera (L.) Dunal

W. somnifera is an evergreen woody shrub commonly known as winter cherry or Indian ginseng distributed in tropical and subtropical regions of the world which include Bangladesh, India, Pakistan, Afghanistan, Sri Lanka, China, Egypt, Morocco, Jordan, Congo, and South Africa. This plant is extensively used in Unani and Ayurvedic systems of medicine (Shahriar et al., 2014; Dar et al., 2015; Dar and Ahmad, 2020). Several studies conducted with the Indian species of this plant exhibited significant anti-inflammatory activities. For example, root extract of *W. somnifera* exhibited acute and chronic anti-inflammatory activity in carrageenan-induced rat paw edema and Freund's adjuvant–induced arthritis models, respectively (Giri, 2016), as well as in collagen-induced arthritic rats (Khan et al., 2019). Leaf extract demonstrated anti-neuroinflammatory activity by attenuating TNF-α, IL-1β, IL-6, RNS, and ROS production *via* the inhibition of NF-κB, AP-1, JNK, and MAPK pathways (Gupta and Kaur, 2016; 2018). Fatty acids from seeds inhibited the release of proinflammatory cytokines (IL-6 and TNF-α) and reduced NF-κB expression and were found to reduce edema besides repairing psoriatic lesions in the TPA-induced psoriatic mouse model. In the same study, the fatty acid components

were identified as linoleic acid, oleic acid, palmitic acid, stearic acid, 11,14,17-eicosatrienoic acid, and nervonic acid along with other unidentified components (Balkrishna et al., 2020).

The brief analyses of the abovementioned plants again signify the values of Bangladeshi medicinal plants to be explored for novel anti-inflammatory molecules. However, the reported anti-inflammatory activities of the plants investigated in Bangladesh are primarily based on the anti-inflammatory activity of their crude organic extracts or partitionates. Therefore, a great detail is yet to be unveiled of these plants regarding the purification and characterization of their chemical constituents, which requires different separation techniques and spectroscopic analyses to pinpoint the anti-inflammatory molecules.

According to literature, a huge number of Bangladeshi medicinal plants are used in traditional medicines to combat inflammation and inflammatory disorders. However, due to the set criteria of plant selection, a limited number of plants have been summarized in the present study. The plants reviewed here are useful in traditional medicine to manage inflammation or inflammatory diseases such as arthritis, asthma, hepatitis, psoriasis, bronchitis, and tumor. The anti-inflammatory activities of these plants have been evaluated scientifically using different assay models. The plant samples were administered usually in graded doses of the extract or as a single dose of each of different organic fractions. Thus, in case of graded doses, plant extracts were found to inhibit inflammation in a dose-dependent manner, and in case of different organic fractions, a single dose of different samples demonstrated varying degrees of activity. The significance of activity was assessed in comparison with positive controls. Acetyl salicylic acid, diclofenac sodium, indomethacin, ibuprofen, phenylbutazone, hydrocortisone, etc. were commonly used as positive control drugs for these experiments.

Selected plants, namely, *A. indica*, *C. infortunatum*, *C. asiaticum*, *G. pentaphylla*, *H. indicum*, *M. paniculata*, *P. retrofractum*, *S. villosa*, and *T. trilobatum* were focused in further detail. In addition, *A. conyzoides*, *E. prostrata*, *L. inermis*, *M. zapota*, and *W. somnifera* have been reviewed briefly. Most of these plants have been found to be studied for the same purpose in other Asian countries, including India, Sri Lanka, Thailand, Malaysia, China, Korea, and Indonesia along with countries such as Brazil, Nigeria, Ghana, Ethiopia, Iraq, Iran, and Luxembourg where these plants have been proved again to have potential for anti-inflammatory activities. A number of well-documented anti-inflammatory molecules, for example, apigenin (**5**), quercetin (**6**), 1,8-cineole (**13**), α-pinene (**14**), β-caryophyllene (**15**), kaempferol (**20**), catechin (**21**), and apigenin C-glycosides (e.g., vicenin-1) (**22**) have been characterized from these plants.

Although attributed for diverse beneficial effects with a rich source of therapeutic agents' plants have toxicological properties as well. The acute toxicity test has been conducted by many of the researchers to determine dose ranges for subsequent pharmacological assays and to observe changes in behavior that is signs such as restlessness, respiratory distress, general irritation, coma, convulsion, locomotor ataxia, diarrhea, and weight loss elicited by the plant samples under investigation. The brine shrimp lethality test is also used by the investigators to estimate toxicity of plant extracts. LC_{50} values of the extracts have been determined using this assay. Higher LC_{50} values indicate higher margin of safety, whereas samples with lower LC_{50} values are considered to be toxic and often recommended to be evaluated for anticancer properties. However, crude extract from plants usually is a combination of few or many biologically active constituents. Thus, the compound(s) demonstrating useful pharmacological activity may or may not be responsible for the elicited toxicity. Therefore, identifying the active constituent and evaluation of toxicity of that active constituent is highly crucial for these traditionally important anti-inflammatory plants of Bangladesh.

CONCLUDING REMARKS

This review indicates that the medicinal plants of Bangladesh have immense significance for anti-inflammatory activity and have the potential to contribute toward the discovery and development of novel therapeutic approaches to combat inflammatory disorders which are the leading cause of innumerable human diseases all over the globe. Though possessing traditional significance to manage inflammatory diseases, these plants chiefly underwent preliminary screening for anti-inflammatory effects and require intensive research studies, including identification of active constituents, understanding the mechanism of action precisely, evaluation for safety and efficacy, and formulation of safe and effective drug products.

These early-stage screenings of Bangladeshi medicinal plants were mostly carried out for academic purposes, and there was hardly any industrial support behind these projects. Proper industrial collaboration can forge the aforementioned stages of exploration and can thereby contribute to extend the anti-inflammatory therapeutic armory.

AUTHOR CONTRIBUTIONS

The author confirms being the sole contributor of this study and has approved it for publication.

ACKNOWLEDGMENTS

I sincerely acknowledge Professor Gerald Muench, Western Sydney University, Australia who is the inspiration for my research in the field of inflammation. I also thank Md. Rafiqur Rahman for helping me with the facilities of Central Library, Rajshahi University, Bangladesh.

SUPPLEMENTARY MATERIAL

The Supplementary Material for this article can be found online at: https://www.frontiersin.org/articles/10.3389/fphar.2022.809324/full#supplementary-material

REFERENCES

Adegbite, A. E., and Sanyaolu, E. B. (2009). Cytotoxicity Testing of Aqueous Extract of Bitter Leaf (*Vernonia Amygdalina* Del.) Using the *Allium cepa* Chromosome Aberration Assay. *Scientific Res. Essays* 4 (11), 311–1314. doi:10.5897/SRE.9000315

Ahmad Khan, M. S., and Ahmad, I. (2019). "Herbal Medicine," in *New Look to Phytomedicine*. Editors M. S. Ahmad Khan, I. Ahmad, and D. Chattopadhyay (Academic Press), 3–13. doi:10.1016/b978-0-12-814619-4.00001-x

Ahmed, F., Shahid, I. Z., Biswas, U. K., Roy, B. A., Das, A. K., and Choudhuri, M. S. K. (2007). Anti-inflammatory, Antinociceptive, and Neuropharmacological Activities ofClerodendron Viscosum. *Pharm. Biol.* 45 (7), 587–593. doi:10.1080/13880200701501342

Ahmed, R., Choudhury, S., Vajczikova, I., and Leclercq, P. A. (2000). Essential Oils ofGlycosmis pentaphylla(Cor.). A New Report from Assam, India. *J. Essent. Oil Res.* 12 (4), 471–474. doi:10.1080/10412905.2000.9699568

Akber, M., Seraj, S., Nahar, N., Islam, F., Ahsan, S., Ferdausi, D., et al. (2011). A Survey of Medicinal Plants Used by the Traditional Medicinal Practitioners of Khulna City, Bangladesh. *American-Eurasian J. Sustainable Agric.* 5 (2), 177–195.

Akhila, J. S., Shyamjith, D., and Alwar, M. C. (2007). Acute Toxicity Studies and Determination of Median Lethal Dose. *Curr. Sci.* 93 (7), 917–920. Availableat: http://www.jstor.org/stable/24099255.

Akhtar, M. A. (2018). Australian Native Plants - A Source of Novel Anti-inflammatoty Compounds *[Online]*. Sydney, NSW, Australia: Western Sydney University. Availableat: https://core.ac.uk/download/pdf/226479947.pdf (Accessed January 12, 2021).

Akihisa, T., Takahashi, A., Kikuchi, T., Takagi, M., Watanabe, K., Fukatsu, M., et al. (2011). The Melanogenesis-Inhibitory, Anti-inflammatory, and Chemopreventive Effects of Limonoids in *N*-Hexane Extract of *Azadirachta indica* A. Juss. (Neem) Seeds. *J. Oleo Sci.* 60 (2), 53–59. doi:10.5650/jos.60.53

Aktar, A., Hassan, S. M. H., Parvin, T., Akhlas, M. B., Khatun, F., Islam, M. T., et al. (2019). Further Phytochemical Screening; Non-clinical Evaluation of Toxic and Anti- Inflammatory Effects of Crude Aqueous Extract of *Gynura Nepalensis*. *Pharmacologyonline* 1, 136–153.

Aktar, F., Kuddus, M. R., Kabir, S., Rashid, M. A., and Chakma, K. (2013). Membrane Stabilizing and Cytotoxic Activities of Different Kupchan Partitionates of *Oroxylum Indicum* (L.) Vent. Leaf and Bark Extracts. *Dhaka Univ. J. Pharm. Sci.* 12 (2), 181–183. doi:10.3329/dujps.v12i2.17625

Akter, M., Hira, T. E., Mian, M. Y., Ahmed, I., Rahman, M. M., and Rahman, S. M. A. (2014). Cytotoxic, Thrombolytic and Membrane Stabilizing Activities of *Swietenia Mahagoni* (L.) Jacq. Bark Extract. *J. SUB* 5 (1), 32–38.

Al Mahmud, Z., Emran, T. B., Qais, N., Bachar, S. C., Sarker, M., and Uddin, M. M. (2015). Evaluation of Analgesic, Anti-inflammatory, Thrombolytic and Hepatoprotective Activities of Roots of *Premna Esculenta* (Roxb). *J. Basic Clin. Physiol. Pharmacol.* 27, 63–70. doi:10.1515/jbcpp-2015-0056

Al-Amin Sarker, M., Banik, S., Saddam Hussain, M., Ghosh, A., and S. Hossain, M. M. (2016). *In-vitro* and *In-Vivo* Pharmacological Activities with Phytochemical Evaluation of Methanolic Extract of *Microcos Paniculata* Stem Barks. *Cdth* 11 (2), 142–149. doi:10.2174/1574885511666160520154529

Al-Attas, A. A., El-Shaer, N. S., Mohamed, G. A., Ibrahim, S. R., and Esmat, A. (2015). Anti-inflammatory Sesquiterpenes from *Costus Speciosus* Rhizomes. *J. Ethnopharmacol* 176, 365–374. doi:10.1016/j.jep.2015.11.026

Alam, A., Haldar, S., Thulasiram, H. V., Kumar, R., Goyal, M., Iqbal, M. S., et al. (2012). Novel Anti-inflammatory Activity of Epoxyazadiradione against Macrophage Migration Inhibitory Factor: Inhibition of Tautomerase and Proinflammatory Activities of Macrophage Migration Inhibitory Factor. *J. Biol. Chem.* 287 (29), 24844–24861. doi:10.1074/jbc.M112.341321

Alam, M. A., Rahman, M. M., Subhan, N., Majumder, M. M., Hasan, S. M. R., Akter, R., et al. (2009a). Antioxidant Potential of the Ethanol Extract of the Leaves of *Vitex Negundo* L. *Turkish J. Pharm. Sci.* 6 (1), 11–20.

Alam, M. A., Subhan, N., Awal, M. A., Alam, M. S., Sarder, M., Nahar, L., et al. (2009b). Antinociceptive and Anti-inflammatory Properties ofRuellia Tuberosa. *Pharm. Biol.* 47 (3), 209–214. doi:10.1080/13880200802434575

Alam, M. N., Biozid, M. S., Islam, M. R., Rahman, M. M., Chowdhury, A. I., and Mazumdar, M. M. U. (2015). *In-vitro* Comparative Study of Anti-inflammatory and Anti-arthritic Effects of the Methanol Extract of *Cissus Pentagona* Roxb. And *Thunbergia Grandiflora* Roxb. Leaf. *Pharma Innovation J.* 4 (4), 39–42.

Ali, K., Ashraf, A., and Nath Biswas, N. (2012). Analgesic, Anti-inflammatory and Anti-diarrheal Activities of Ethanolic Leaf Extract of *Typhonium Trilobatum* L. Schott. *Asian Pac. J. Trop. Biomed.* 2 (9), 722–726. doi:10.1016/S2221-1691(12)60217-2

Alzohairy, M. A. (2016). Therapeutics Role of *Azadirachta indica* (Neem) and Their Active Constituents in Diseases Prevention and Treatment. *Evid. Based Complement. Alternat Med.* 2016, 7382506. doi:10.1155/2016/7382506

Ambriz-Perez, D. L., Leyva-Lepez, N., Gutierrez-Grijalva, E. P., and Heredia, J. B. (2016). Phenolic Compounds: Natural Alternative in Inflammation Treatment. A Review. *Cogent Food Agric.* 2 (1), 1131412. doi:10.1080/23311932.2015.1131412

Anosike, C. A., Obidoa, O., and Ezeanyika, L. U. (2012). Membrane Stabilization as a Mechanism of the Anti-inflammatory Activity of Methanol Extract of Garden Egg (*Solanum Aethiopicum*). *Daru* 20 (1), 76. doi:10.1186/2008-2231-20-76

Ansari, P., Azam, S., Reyad-ul-ferdous, M., Hossain, A., Azad, T., Goswami, S., et al. (2015). Potential Investigation of Anti-inflammatory Activity and Phytochemical Investigations of Ethanolic Extract of *Glycosmis Pentaphylla* Leaves. *Am. J. Biomed. Res.* 3 (1), 6–8. doi:10.12691/ajbr-3-1-2

Anwar, R., Sultana, S. R., Hossen, S., and Chowdhury, M. R. H. (2018). Ethnopharmacological Investigation in *Sterculia Villosa* to Determine Anti-diabetic, Anti-inflammatory, Antioxidant, Thrombolytic, and Cytotoxic Effect. *J. Pharmacognosy Phytochemistry* 7 (2), 3203–3211.

Apu, A. S., Bhuyan, S. H., Prova, S. S., and Muhit, M. A. (2012). Anti-Inflammatory Activity of Medicinal Plants Native to Bangladesh: A Review. *J. Appl. Pharm. Sci.* 2 (2), 7–10.

Arefin, S. M. A., Islam, M. A., Rashid, S. T. B., Rayhan, M. A., Hossen, M. M., Alam, M. J., et al. (2015). Analgesic, Anti-inflammatory, Anticonvulsant and CNS Effect of the Ethanolic Extract of *Butea Monosperma* Roots. *Jahangirnagar Univ. J. Biol. Sci.* 4 (1), 9–18. doi:10.3329/jujbs.v4i1.27781

Arora, N., and Arora, P. (2016). Anti-inflammatory Activity of Methanolic Extract of Roots of *Glycosmis Pentaphylla*. *Asian J. Pharm. Res. Development* 4 (2), 1–4. doi:10.18203/2349-2902.isj20164471

Arulselvan, P., Fard, M. T., Tan, W. S., Gothai, S., Fakurazi, S., Norhaizan, M. E., et al. (2016). Role of Antioxidants and Natural Products in Inflammation. *Oxid Med. Cel Longev* 2016, 5276130. doi:10.1155/2016/5276130

Arzi, A., Olapour, S., Yaghooti, H., and Sistani Karampour, N. (2015). Effect of Royal Jelly on Formalin Induced-Inflammation in Rat Hind Paw. *Jundishapur J. Nat. Pharm. Prod.* 10 (1), e22466. doi:10.17795/jjnpp-22466

Asante-Kwatia, Evelyn., Abraham Yeboah, Mensah., and Baidoo, M. F. (2020). "Analgesic and Anti-inflammatory Effect of Ghanaian Medicinal Plants," in *Medicinal Plants - Use in Prevention and Treatment of Diseases*. Editor B. A. R. Hassan (IntechOpen, 1–22. doi:10.5772/intechopen.90154

Attiq, A., Jalil, J., Husain, K., and Ahmad, W. (2018). Raging the War against Inflammation with Natural Products. *Front. Pharmacol.* 9, 976. doi:10.3389/fphar.2018.00976

Aziz, M. A. (2015). Qualitative Phytochemical Screening and Evaluation of Anti-inflammatory, Analgesic and Antipyretic Activities of *Microcos Paniculata* Barks and Fruits. *J. Integr. Med.* 13 (3), 173–184. doi:10.1016/S2095-4964(15)60179-0

Aziz, M. A., Akter, M. I., Sajon, S. R., Rahman, S. M. M., and Rana, M. S. (2018). Anti-inflammatory and Anti-pyretic Activities of the Hydro-Methanol and Petroleum-Benzene Extracts of *Microcos Paniculata* Barks. *Pharmacologyonline* 2, 23–30.

Aziz, M. A., Rahman, S., Islam, T., Islam, T., Alam, A. S., Uddin, N., et al. (2015). Anti-inflammatory, Anthelmintic & Antidiabetic Activity of Aqueous Extract of *Microcos Paniculata* Fruits. *Pharmacologyonline* 1, 121–125.

Bahtiar, A., Nurazizah, M., Roselina, T., Tambunan, A. P., and Arsianti, A. (2017). Ethanolic Extracts of Babandotan Leaves (Ageratum Conyzoides L.) Prevents Inflammation and Proteoglycan Degradation by Inhibiting TNF-α and MMP-9 on Osteoarthritis Rats Induced by Monosodium Iodoacetate. *Asian Pac. J. Trop. Med.* 10 (3), 270–277. doi:10.1016/j.apjtm.2017.03.006

Balkrishna, A., Nain, P., Chauhan, A., Sharma, N., Gupta, A., Ranjan, R., et al. (2020). Super Critical Fluid Extracted Fatty Acids from Withania Somnifera Seeds Repair Psoriasis-like Skin Lesions and Attenuate Pro-inflammatory Cytokines (TNF-α and IL-6) Release. *Biomolecules* 10(2), 185. doi: doi:10.3390/biom10020185

Balsinde, J., Winstead, M. V., and Dennis, E. A. (2002). Phospholipase A(2) Regulation of Arachidonic Acid Mobilization. *FEBS Lett.* 531 (1), 2–6. doi:10.1016/S0014-5793(02)03413-0

Barbosa-Filho, J. M., Piuvezam, M. R., Moura, M. D., Silva, M. S., Lima, K. V. B., da-Cunha, E. V. L., et al. (2006). Anti-inflammatory Activity of Alkaloids: a Twenty-century Review. *Rev. Bras. Farmacogn.* 16 (1), 109–139. doi:10.1590/S0102-695X2006000100020

Barton, G. M. (2008). A Calculated Response: Control of Inflammation by the Innate Immune System. *J. Clin. Invest.* 118 (2), 413–420. doi:10.1172/JCI34431

Bashar, M., Ibrahim, M., Sultana, I., Hossain, M. I., Tasneem, Z., Kuddus, M. R., et al. (2014). Preliminary Phytochemical Screenings and Antipyretic, Analgesic and Anti-inflammatory Activities of Methanol Extract of *Vernonia Cinerea* Less. (Fam: Asteraceae). *Ejmp* 4 (10), 1178–1185. doi:10.9734/EJMP/2014/10050

Batista, F. L. A., Lima, L. M. G., Abrante, I. A., de Araújo, J. I. F., Batista, F. L. A., Abrante, I. A., et al. (2018). Antinociceptive Activity of Ethanolic Extract of *Azadirachta indica* A. Juss (Neem, Meliaceae) Fruit through Opioid, Glutamatergic and Acid-Sensitive Ion Pathways in Adult Zebrafish (*Danio rerio*). *Biomed. Pharmacother.* 108, 408–416. doi:10.1016/j.biopha.2018.08.160

Beg, S., Swain, S., Hasan, H., Barkat, M. A., and Hussain, M. S. (2011). Systematic Review of Herbals as Potential Anti-inflammatory Agents: Recent Advances, Current Clinical Status and Future Perspectives. *Pharmacogn Rev.* 5 (10), 120–137. doi:10.4103/0973-7847.91102

Begum, F., Begum, Z., Uddin, M., Haider, A., and Barman, R. (2012). Effects of Methanol Extract of *Piper Chaba* Stem Bark on Acute Inflammation in Rats. *Faridpur Med. Coll. J.* 7 (1), 26–28. doi:10.3329/fmcj.v7i1.10294

Begum, F., Uddin, K., Sultana, S., Ferdous, A. H., and Begum, Z. A. (2008). Effects of Methanol Extract of Piper Chaba Stem Bark on Chronic Inflamation in Rats. *Ibrahim Med. Coll. J.* 2 (2), 37–39. doi:10.3329/imcj.v2i2.2934

Begum, M. M., Islam, A., Begum, R., Uddin, M. S., Rahman, M. S., Alam, S., et al. (2019). Ethnopharmacological Inspections of Organic Extract of *Oroxylum Indicum* in Rat Models: A Promising Natural Gift. *Evid. Based Complement. Alternat Med.* 2019, 1562038. doi:10.1155/2019/1562038

Bellik, Y., Boukraâ, L., Alzahrani, H. A., Bakhotmah, B. A., Abdellah, F., Hammoudi, S. M., et al. (2013). Molecular Mechanism Underlying Anti-inflammatory and Anti-allergic Activities of Phytochemicals: An Update. *Molecules* 18 (1), 322–353. doi:10.3390/molecules18010322

Bellik, Y., Hammoudi, S. M., Abdellah, F., Iguer-Ouada, M., and Boukraâ, L. (2012). Phytochemicals to Prevent Inflammation and Allergy. *Recent Pat Inflamm. Allergy Drug Discov.* 6 (2), 147–158. doi:10.2174/187221312800166886

Benedek, B., Kopp, B., and Melzig, M. F. (2007). *Achillea millefolium* L. s.L. -- Is the Anti-inflammatory Activity Mediated by Protease Inhibition? *J. Ethnopharmacol* 113 (2), 312–317. doi:10.1016/j.jep.2007.06.014

Betanabhatla, K. S., Sajni, R., Karthik, R., Raamamurthy, J., Christina, A. J. M., and Sasikumar, S. (2007). Anti-inflammatory and Anti-nociceptive Activities of *Heliotropium Indicum* Linn. In Experimental Animal Models. *Pharmacologyonline* 3, 438–445.

Bighetti, E. J., Hiruma-Lima, C. A., Gracioso, J. S., and Brito, A. R. (1999). Anti-inflammatory and Antinociceptive Effects in Rodents of the Essential Oil of *Croton Cajucara* Benth. *J. Pharm. Pharmacol.* 51 (12), 1447–1453. doi:10.1211/0022357991777100

Bin Emran, T., Uddin, M. M. N., Rahman, M. A., Uddin, M., and Islam, M. (2015). Phytochemical, Antimicrobial, Cytotoxic, Analgesic and Anti-inflammatory Properties of *Azadirachta ind*ica: A Therapeutic Study. *J. Bioanal. Biomed.* 01007, 1–7. doi:10.4172/1948-593X.S12-007

Biozid, M. S., Rahman, M. M., Alam, M. N., Sayeed, M. A., Chowdhury, A. I., Faruk, M., et al. (2015). *In-vitro* Comparative Study of Anti-inflammatory and Anti-arthritic Effects of *Flemingia Stricta* Roxb. And *Nymphaea Nouchali* Leaf. *Int. J. Pharm. Pharm. Sci.* 7 (8), 49–52. Availableat: https://innovareacademics.in/journals/index.php/ijpps/article/view/6552.

Birecka, H., DiNolfo, T. E., Martin, W. B., and Frohlich, M. W. (1984). Polyamines and Leaf Senescence in Pyrrolizidine Alkaloid-Bearing *Heliotropium* Plants. *Phytochemistry* 23 (5), 991–997. doi:10.1016/S0031-9422(00)82598-4

Birhanu, Z. (2013). Traditional Use of Medicinal Plants by the Ethnic Groups of Gondar Zuria District, north-western Ethiopia. *J. Nat. Remedies* 8. doi:10.18311/jnr/2013/117

Biswas, R., Rahman, S. M. M., Didarul Islam, K. M., Billah, M. M., Aunjum, A., Nurunnabi, T. R., et al. (2019). Antioxidant, Anti-inflammatory, and Anticoagulation Properties of *Aegiceras corniculatum* and *Acanthus ilicifolius*. *Pbr* 5 (3), 35–44. doi:10.18502/pbr.v5i3.2117

Brune, K., and Patrignani, P. (2015). New Insights into the Use of Currently Available Non-steroidal Anti-inflammatory Drugs. *J. Pain Res.* 8, 105–118. doi:10.2147/JPR.S75160

Chaibi, R., Romdhane, M., Ferchichi, A., and Bouajila, J. (2015). Assessment of Antioxidant, Anti-inflammatory, Anti-cholinesterase and Cytotoxic Activities of Henna (*Lawsonia Inermis*) Flowers. *J. Nat. Prod.* 8, 85–92.

Chattopadhyay, R. R. (1998). Possible Biochemical Mode of Anti-inflammatory Action of *Azadirachta indica* A. Juss. In Rats. *Indian J. Exp. Biol.* 36 (4), 418–420. Availableat: http://europepmc.org/abstract/MED/9717455.

Chaudhuri, T., Dutta, S., Chakraborty, A., Kar, P., Dey, P., and Sen, A. (2018). Stimulation of Murine Immune Response by *Clerodendrum Infortunatum*. *Phcog Mag.* 14 (57), 417–429. doi:10.4103/pm.pm_549_17

Choi, R. J., Chun, J., Khan, S., and Kim, Y. S. (2014). Desoxyrhapontigenin, a Potent Anti-inflammatory Phytochemical, Inhibits LPS-Induced Inflammatory Responses via Suppressing NF-Kb and MAPK Pathways in RAW 264.7 Cells. *Int. Immunopharmacol* 18 (1), 182–190. doi:10.1016/j.intimp.2013.11.022

Chokchaisiri, S., Apiratikul, N., and Rukachaisirikul, T. (2020). A New Ent-Abietane Lactone from *Glycosmis Pentaphylla*. *Nat. Prod. Res.* 34 (21), 3019–3026. doi:10.1080/14786419.2018.1540477

Choudhury, M. D., Paul, S. B., Choudhury, S., Choudhury, S., and Choudhury, P. P. N. (2009). Isolation, Characterization and Bio-Activity Screening of Compound from *Clerodendrum Viscosum* Vent. *Assam Univ. J. Sci. Technol. Biol. Sci.* 4 (1), 29–34.

Chowdhury, M., Sultana, M. I., Tasneem, M. Z., and Jubair, A. A. b. (2015). Phytochemical and Pharmacological Screening of *Glycosmis Pentaphylla* (Retz) A.DC. (Fam. Rutaceae). *Int. J. Scientific Eng. Res.* 6 (10), 928–934.

Chowdury, M., Alam, M., Chowdhury, S., Biozid, M., Faruk, M., Mazumdar, M., et al. (2015). Evaluation of *Ex-Vivo* Anti-arthritic, Anti-inflammatory, Anti-cancerous and Thrombolytic Activities of *Mussaenda Roxburghii* Leaf. *Ejmp* 10 (4), 1–7. doi:10.9734/EJMP/2015/20483

Chuku, L. C., Chinaka, N. C., and Damilola, D. (2020). Phytochemical Screening and Anti-inflammatory Properties of Henna Leaves (*Lawsonia Inermis*). *Ejmp* 31 (18), 23–28. doi:10.9734/EJMP/2020/v31i1830340

Chung, I. M., Rajakumar, G., Lee, J. H., Kim, S. H., and Thiruvengadam, M. (2017). Ethnopharmacological Uses, Phytochemistry, Biological Activities, and Biotechnological Applications of *Eclipta Prostrata*. *Appl. Microbiol. Biotechnol.* 101 (13), 5247–5257. doi:10.1007/s00253-017-8363-9

Chunthorng-Orn, J., Dechayont, B., Phuaklee, P., Prajuabjinda, O., Juckmeta, T., and Itharat, A. (2016). Cytotoxic, Anti-inflammatory and Antioxidant Activities of *Heliotropium Indicum* Extracts. *J. Med. Assoc. Thai* 99, S102–S109.

Çitoğlu, G., Tanker, M., and Gümüşel, B. (1998). Anti-inflammatory Effects of Lycorine and Haemanthidine. *Phytotherapy Res.* 12, 205–206. doi:10.1002/(sici)1099-1573(199805)12:3<205::Aid-ptr203>3.0.Co;2-7

Dar, N. J., Hamid, A., and Ahmad, M. (2015). Pharmacologic Overview of *Withania Somnifera*, the Indian Ginseng. *Cell Mol Life Sci* 72 (23), 4445–4460. doi:10.1007/s00018-015-2012-1

Dar, N. J., and MuzamilAhmad, M. (2020). Neurodegenerative Diseases and *Withania Somnifera* (L.): An Update. *J. Ethnopharmacol* 256, 112769. doi:10.1016/j.jep.2020.112769

Das, A., Jawed, J. J., Das, M. C., Sandhu, P., De, U. C., Dinda, B., et al. (2017). Antileishmanial and Immunomodulatory Activities of Lupeol, a Triterpene Compound Isolated from *Sterculia Villosa*. *Int. J. Antimicrob. Agents* 50 (4), 512–522. doi:10.1016/j.ijantimicag.2017.04.022

Das, A. K., Shahid, I. Z., Choudhuri, M. S. K., Shilpi, J., and Ahmed, F. (2005). Anti-inflammatory, Antinociceptive and Diuretic Activities of *Amoora Cucullata* Roxb. *Oriental Pharm. Exp. Med.* 5 (1), 37–42. doi:10.3742/opem.2005.5.1.037

Das, N., Goshwami, D., Hasan, M. S., Mahmud, Z. A., Raihan, S. Z., and Sultan, M. Z. (2015). Evaluation of Antinociceptive, Anti-inflammatory and Anxiolytic Activities of Methanolic Extract of *Terminalia Citrina* Leaves. *Asian Pac. J. Trop. Dis.* 5, S137–S141. doi:10.1016/S2222-1808(15)60875-1

Das, N., Hasan, M. S., Raihan, S. Z., and Sultan, M. Z. (2016). Antinociceptive, Anti-inflammatory and Hypoglycemic Activities of *Terminalia Citrina* Leaves. *Bangla Pharma J.* 19 (1), 25–31. doi:10.3329/bpj.v19i1.29232

Davies, N. M. (1995). Toxicity of Nonsteroidal Anti-inflammatory Drugs in the Large Intestine. *Dis. Colon Rectum* 38 (12), 1311–1321. doi:10.1007/BF02049158

de Almeida, E. R., da Silva Filho, A. A., Dos Santos, E. R., and Correia Lopes, C. A. (1990). Antiinflammatory Action of Lapachol. *J. Ethnopharmacology* 29 (2), 239–241. doi:10.1016/0378-8741(90)90061-w

de Cássia da Silveira E Sá, R., Andrade, L. N., dos Reis Barreto de Oliveira, R., and de Sousa, D. P. (2014). A Review on Anti-inflammatory Activity of Phenylpropanoids Found in Essential Oils. *Molecules* 19 (2), 1459–1480. doi:10.3390/molecules19021459

de las Heras, B., and Hortelano, S. (2009). Molecular Basis of the Anti-inflammatory Effects of Terpenoids. *Inflamm. Allergy Drug Targets* 8 (1), 28–39. doi:10.2174/187152809787582534

Dina, T. A., Taslima, M. A., Ahmed, N. U., and Uddin, M. N. (2010). Analgesic and Anti-inflammatory Properties of *Argyreia Argentea* Methanol Extract in Animal Model. *J. Taibah Univ. Sci.* 3, 1–7. doi:10.1016/S1658-3655(12)60014-4

do Nascimento, K. F., Moreira, F. M. F., Alencar Santos, J., Kassuya, C. A. L., Croda, J. H. R., Cardoso, C. A. L., et al. (2018). Antioxidant, Anti-inflammatory, Antiproliferative and Antimycobacterial Activities of the Essential Oil of *Psidium Guineense* Sw. And Spathulenol. *J. Ethnopharmacol* 210, 351–358. doi:10.1016/j.jep.2017.08.030

Dulla, O., and Jahan, F. I. (2017). Ethnopharmacological Survey on Traditional Medicinal Plants at Kalaroa Upazila, Satkhira District, Khulna Division, Bangladesh. *J. Intercult Ethnopharmacol* 6 (3), 316–325. doi:10.5455/jice.20170719010256

Dzoyem, J. P., McGaw, L. J., Kuete, V., and Bakowsky, U. (2017). "Anti-inflammatory and Anti-nociceptive Activities of African Medicinal Spices and Vegetables," in *Medicinal Spices and Vegetables from Africa*. Editor V. Kuete (Academic Press), 239–270. doi:10.1016/b978-0-12-809286-6.00009-1

Emran, T., E-Mowla, T., Ahmed, S., Zahan, S., Rakib, A., Hasan, M., et al. (2018). Sedative, Anxiolytic, Antinociceptive, Anti-inflammatory and Antipyretic Effects of a Chloroform Extract from the Leaves of *Urena Sinuata* in Rodents. *Jalsi* 16 (3), 1–19. doi:10.9734/JALSI/2018/39073

Ericson-Neilsen, W., and Kaye, A. D. (2014). Steroids: Pharmacology, Complications, and Practice Delivery Issues. *Ochsner J.* 14 (2), 203–207. Availableat: http://www.ochsnerjournal.org/content/ochjnl/14/2/203.full.pdf.

Everts, B., Währborg, P., and Hedner, T. (2000). COX-2-Specific Inhibitors-Tthe Emergence of a New Class of Analgesic and Anti-inflammatory Drugs. *Clin. Rheumatol.* 19 (5), 331–343. doi:10.1007/s100670070024

Fang, S. C., Hsu, C. L., and Yen, G. C. (2008). Anti-inflammatory Effects of Phenolic Compounds Isolated from the Fruits of *Artocarpus Heterophyllus*. *J. Agric. Food Chem.* 56 (12), 4463–4468. doi:10.1021/jf800444g

Faqueti, L. G., Brieudes, V., Halabalaki, M., Skaltsounis, A. L., Nascimento, L. F., Barros, W. M., et al. (2016). Antinociceptive and Anti-inflammatory Activities of Standardized Extract of Polymethoxyflavones from *Ageratum Conyzoides*. *J. Ethnopharmacol* 194, 369–377. doi:10.1016/j.jep.2016.09.025

Faruq, A. A., Ibrahim, M., Mahmood, A., Chowdhury, M. M. U., Rashid, R. B., Kuddus, M. R., et al. (2014). Pharmacological and Phytochemical Screenings of Ethanol Extract of *Leea Macrophylla* Roxb. *Innov. Pharmaceuticals Pharmacother.* 2 (1), 321–327.

Feng, L., Zhai, Y. Y., Xu, J., Yao, W. F., Cao, Y. D., Cheng, F. F., et al. (2019). A Review on Traditional Uses, Phytochemistry and Pharmacology of *Eclipta Prostrata* (L.) L. *J. Ethnopharmacol* 245, 112109. doi:10.1016/j.jep.2019.112109

Fernández, M. A., de las Heras, B., Garcia, M. D., Sáenz, M. T., and Villar, A. (2010). New Insights into the Mechanism of Action of the Anti-inflammatory Triterpene Lupeol. *J. Pharm. Pharmacol.* 53 (11), 1533–1539. doi:10.1211/0022357011777909

Ferrari, F. C., Lemos Lima, Rde. C., Schimith Ferraz Filha, Z., Barros, C. H., de Paula Michel Araújo, M. C., and Antunes Saúde-Guimarães, D. (2016). Effects of *Pimenta Pseudocaryophyllus* Extracts on Gout: Anti-inflammatory Activity and Anti-hyperuricemic Effect through Xantine Oxidase and Uricosuric Action. *J. Ethnopharmacol* 180, 37–42. doi:10.1016/j.jep.2016.01.007

Fürst, R., Zündorf, I., and Dingermann, T. (2017). New Knowledge about Old Drugs: The Anti-inflammatory Properties of Cardiac Glycosides. *Planta Med.* 83 (12-13), 977–984. doi:10.1055/s-0043-105390

Fürst, R., and Zündorf, I. (2014). Plant-derived Anti-inflammatory Compounds: Hopes and Disappointments Regarding the Translation of Preclinical Knowledge into Clinical Progress. *Mediators Inflamm.* 2014, 1–9. doi:10.1155/2014/146832

Ganguly, A., Mahmud, Z. A., Uddin, M. M. N., and Rahman, S. A. (2013). *In-vivo* Anti-inflammatory and Anti-pyretic Activities of *Manilkara Zapota* Leaves in Albino Wistar Rats. *Asian Pac. J. Trop. Dis.* 3 (4), 301–307. doi:10.1016/S2222-1808(13)60073-0

García-Mediavilla, V., Crespo, I., Collado, P. S., Esteller, A., Sánchez-Campos, S., Tuñón, M. J., et al. (2007). The Anti-inflammatory Flavones Quercetin and Kaempferol Cause Inhibition of Inducible Nitric Oxide Synthase, Cyclooxygenase-2 and Reactive C-Protein, and Down-Regulation of the Nuclear Factor kappaB Pathway in Chang Liver Cells. *Eur. J. Pharmacol.* 557 (2), 221–229. doi:10.1016/j.ejphar.2006.11.014

Ghani, A. (2003). *Medicinal Plants of Bangladesh with Chemical Constituents and Uses*. Dhaka, Bangladesh: The Asiatic Society of Bangladesh.

Ghosh, G., Panda, P., Rath, M., Pal, A., Sharma, T., and Das, D. (2015). GC-MS Analysis of Bioactive Compounds in the Methanol Extract of *Clerodendrum Viscosum* Leaves. *Pharmacognosy Res.* 7 (1), 110–113. doi:10.4103/0974-8490.147223

Giri, K. R. (2016). Comparative Study of Anti-inflammatory Activity of *Withania Somnifera* (Ashwagandha) with Hydrocortisone in Experimental Animals (Albino Rats). *J. Med. Plants Stud.* 4 (1), 78–83.

Glass, C. K., Saijo, K., Winner, B., Marchetto, M. C., and Gage, F. H. (2010). Mechanisms Underlying Inflammation in Neurodegeneration. *Cell* 140 (6), 918–934. doi:10.1016/j.cell.2010.02.016

Gomes, A., Fernandes, E., Lima, J. L., Mira, L., and Corvo, M. L. (2008). Molecular Mechanisms of Anti-inflammatory Activity Mediated by Flavonoids. *Curr. Med. Chem.* 15 (16), 1586–1605. doi:10.2174/092986708784911579

González-Gallego, J., Sánchez-Campos, S., and Tuñón, M. J. (2007). Anti-inflammatory Properties of Dietary Flavonoids. *Nutrición Hospitalaria* 22 (3), 287–293.

Gou, K. J., Zeng, R., Dong, Y., Hu, Q. Q., Hu, H. W., Maffucci, K. G., et al. (2017). Anti-inflammatory and Analgesic Effects of *Polygonum Orientale* L. Extracts. *Front. Pharmacol.* 8 (562), 562. doi:10.3389/fphar.2017.00562

Guardia, T., Rotelli, A. E., Juarez, A. O., and Pelzer, L. E. (2001). Anti-inflammatory Properties of Plant Flavonoids. Effects of Rutin, Quercetin and Hesperidin on Adjuvant Arthritis in Rat. *Farmaco* 56 (9), 683–687. doi:10.1016/S0014-827X(01)01111-9

Guha, G., Rajkumar, V., Ashok Kumar, R., and Mathew, L. (2011). Therapeutic Potential of Polar and Non-polar Extracts of *Cyanthillium cinereum In Vitro*. *Evid. Based Complement. Alternat Med.* 2011, 784826. doi:10.1093/ecam/nep155

Gupta, M., and Kaur, G. (2016). Aqueous Extract from the *Withania Somnifera* Leaves as a Potential Anti-neuroinflammatory Agent: a Mechanistic Study. *J. Neuroinflammation* 13 (1), 193. doi:10.1186/s12974-016-0650-3

Gupta, M., and Kaur, G. (2018). *Withania Somnifera* as a Potential Anxiolytic and Anti-inflammatory Candidate against Systemic Lipopolysaccharide-Induced Neuroinflammation. *Neuromolecular Med.* 20 (3), 343–362. doi:10.1007/s12017-018-8497-7

Gupta, R., and Singh, H. (2012). Detection and Quantitation of SS-Sitosterol in Clerodendrum Infortunatum and Alternanthera Sessilis by HPTLC. *Phcog Commn.* 2 (1), 31–36. doi:10.5530/pc.2012.1.6

Gupta, S., and Gupta, R. (2012). Detection and Quantification of Quercetin in Roots, Leaves and Flowers of *Clerodendrum Infortunatum* L. *Asian Pac. J. Trop. Dis.* 2, S940–S943. doi:10.1016/S2222-1808(12)60296-5

Haldar, K. M., Ghosh, P., and Chandra, G. (2011). Evaluation of Target Specific Larvicidal Activity of the Leaf Extract of *Typhonium Trilobatum* against *Culex quinquefasciatus* Say. *Asian Pac. J. Trop. Biomed.* 1 (2Suppl. ment), S199–S203. doi:10.1016/S2221-1691(11)60156-1

Hämäläinen, M., Nieminen, R., Vuorela, P., Heinonen, M., and Moilanen, E. (2007). Anti-inflammatory Effects of Flavonoids: Genistein, Kaempferol, Quercetin, and Daidzein Inhibit STAT-1 and NF-kappaB Activations, whereas Flavone, Isorhamnetin, Naringenin, and Pelargonidin Inhibit Only

NF-kappaB Activation along with Their Inhibitory Effect on iNOS Expression and NO Production in Activated Macrophages. *Mediators Inflamm.* 2007, 45673. doi:10.1155/2007/45673

Hamidi, M. R., Jovanova, B., and Panovska, T. K. (2014). Toxicological Evaluation of the Plant Products Using Brine Shrimp (*Artemia salina* L.) Model. *Macedonian Pharm. Bull.* 60 (1), 9–18. doi:10.33320/maced.pharm.bull.2014.60.01.002

Hamiduzzaman, M., Nur, F., and Bhuiyan, M. I. (2017). Evaluation of Anti-inflammatory Activity through Assaying the Stability of Erythrocytes' Membrane by Different Organic Extracts of *Heliotropium Indicum* (Boraginacea). *J. Nat. Product. Plant Resour.* 7 (2), 74–78.

Haque, M. A., Louis, V. R., Phalkey, R., and Sauerborn, R. (2014). Use of Traditional Medicines to Cope with Climate-Sensitive Diseases in a Resource Poor Setting in Bangladesh. *BMC Public Health* 14 (1), 202. doi:10.1186/1471-2458-14-202

Haque, M. I., Chowdhury, A. B. M. A., Shahjahan, M., and Harun, M. G. D. (2018). Traditional Healing Practices in Rural Bangladesh: a Qualitative Investigation. *BMC Complement. Altern. Med.* 18 (1), 62. doi:10.1186/s12906-018-2129-5

Harvey, A. (2000). Strategies for Discovering Drugs from Previously Unexplored Natural Products. *Drug Discov. Today* 5 (7), 294–300. doi:10.1016/S1359-6446(00)01511-7

Hasan, M. M., Uddin, N., Hasan, M. R., Islam, A. F., Hossain, M. M., Rahman, A. B., et al. (2014). Analgesic and Anti-inflammatory Activities of Leaf Extract of Mallotus Repandus (Willd.) Muell. Arg. *Biomed. Res. Int.* 2014, 539807. doi:10.1155/2014/539807

Hasan, M. R., Uddin, N., Sana, T., Hossain, M. M., Mondal, M., Kanta, I. J., et al. (2018). Analgesic and Anti-inflammatory Activities of Methanolic Extract of *Mallotus Repandus* Stem in Animal Models. *Orient Pharm. Exp. Med.* 18 (2), 139–147. doi:10.1007/s13596-018-0312-3

Hassan, M., Khan, S., Shaikat, A., Hossain, M., Islam, S., Hoque, M., et al. (2013). Analgesic and Anti-inflammatory Effects of Ethanol Extracted Leaves of Selected Medicinal Plants in Animal Model. *Vet. World* 6 (2), 68–71. doi:10.5455/vetworld.2013.68-71

Hassan, M. M., Daula, A. F. M. S., Jahan, I. A., Nimmi, I., Adnan, M., and Hossain, H. (2012). Anti-inflammatory Activity, Total Flavonoids and Tannin Content from the Ethanolic Extract of *Ageratum Conyzoide*s Linn. Leaf. *Int. J. Pharm. Phytopharmacological Res.* 1 (5), 234–241.

He, J. B., Fang, M. J., Ma, X. Y., Li, W. J., and Lin, D. S. (2020). Angiogenic and Anti-inflammatory Properties of Azadirachtin A Improve Random Skin Flap Survival in Rats. *Exp. Biol. Med. (Maywood)* 245 (18), 1672–1682. doi:10.1177/1535370220951896

Helen, L. R., Jayesh, K., Vysakh, A., and Latha, M. (2018). Polyphenolic Content Correlates with Anti-inflammatory Activity of Root Bark Extract from *Clerodendrum Infortunatum* L. And Inhibit Carrageenan Induced Paw Edema. *J. Pharmacognosy Phytochemistry* 7 (2), 2032–2014.

Hira, A., Dey, S. K., Howlader, M. S., Ahmed, A., Hossain, H., and Jahan, I. A. (2013). Anti-inflammatory and Antioxidant Activities of Ethanolic Extract of Aerial Parts of *Vernonia Patula* (Dryand.) Merr. *Asian Pac. J. Trop. Biomed.* 3 (10), 798–805. doi:10.1016/S2221-1691(13)60158-6

Hodgson, E. (2004). *A Textbook of Modern Toxicology*. Hoboken, New Jersey, United States of America: John Wiley & Sons.

Hong, J., Bose, M., Ju, J., Ryu, J. H., Chen, X., Sang, S., et al. (2004). Modulation of Arachidonic Acid Metabolism by Curcumin and Related Beta-Diketone Derivatives: Effects on Cytosolic Phospholipase A(2), Cyclooxygenases and 5-lipoxygenase. *Carcinogenesis* 25 (9), 1671–1679. doi:10.1093/carcin/bgh165

Hoque, T., Sikder, M. A. A., Kaisar, M. A., Chowdhury, A. A., and Rashid, M. A. (2011). Biological Screenings of Two Araceous Plants Growing in Bangladesh. *Dhaka Univ. J. Pharm. Sci.* 10 (2), 131–135. doi:10.3329/dujps.v10i2.11794

Hossain, H., Akbar, P. N., Rahman, S. E., Khan, T. A., Rahman, M. M., and Jahan, I. A. (2014a). *In Vivo* anti-inflammatory and *In Vitro* Antioxidant Activities of *Toona Ciliata* Leaves Native to Bangladesh. *Glob. J. Med. Res. (B)* 14 (7), 17–26.

Hossain, M. F., Talukder, B., Rana, M. N., Tasnim, R., Nipun, T. S., Uddin, S. M., et al. (2016). *In Vivo* sedative Activity of Methanolic Extract of *Stericulia Villosa* Roxb. Leaves. *BMC Complement. Altern. Med.* 16 (1), 398. doi:10.1186/s12906-016-1374-8

Hossain, M. H., Jahan, F., JahanHowlader, M. S. I. H., Dey, S. K., Hira, A. H., Ahmed, A. A., et al. (2012a). Evaluation of Anti-inflammatory Activity and Total Flavonoids Content of *Manilkara Zapota* (Linn.) Bark. *Int. J. Pharm. Phytopharmacological Res.* 2 (1), 35–39. Availableat: https://eijppr.com/uP6NLQj.

Hossain, M. K., Prodhan, M. A., Even, A. S. M. I. H., Morshed, H., and Hossain, M. M. (2012b). Anti-inflammatory and Antidiabetic Activity of Ethanolic Extracts of *Sterculia Villosa* Barks on Albino Wistar Rats. *J. App. Pharm. Sci.* 2 (8), 96–100. doi:10.7324/JAPS.2012.2815

Hossain, M. M., Ahamed, S. K., Dewan, S. M., Hassan, M. M., Istiaq, A., Islam, M. S., et al. (2014b). *In Vivo* antipyretic, Antiemetic, *In Vitro* Membrane Stabilization, Antimicrobial, and Cytotoxic Activities of Different Extracts from *Spilanthes Paniculata* Leaves. *Biol. Res.* 47, 45. doi:10.1186/0717-6287-47-45

Hossain, M. M., Kabir, M. S. H., Hasanat, A., Kabir, M. I., Chowdhury, T. A., and Kibria, A. S. M. G. (2015). Investigation of *In Vitro* Anti-arthritic and Membrane Stabilizing Activity of Ethanol Extracts of Three Bangladeshi Plants. *Pharma Innovation J.* 4 (1), 76–80.

Hossain, M. S., Alam, M. B., Chowdhury, N. S., Asadujjama, M., Zahan, R., Islam, M. M., et al. (2011). Antioxidant, Analgesic and Anti-inflammatory Activities of the Herb *Eclipta Prostrata*. *J. Pharmacol. Toxicol.* 6 (5), 468–480. doi:10.3923/jpt.2011.468.480

Hossain, S. M., Islam, F., Sharmin, T., Sheikh, H., Hasan, A. R., and Rashid, M. A. (2012c). *In Vitro* antioxidant, Membrane Stabilizing and Thrombolytic Activities of *Glycosmis Arborea*. *Bangla Pharma J.* 15 (2), 141–143. doi:10.3329/bpj.v15i2.12579

Huang, Y. L., Kou, J. P., Ma, L., Song, J. X., and Yu, B. Y. (2008). Possible Mechanism of the Anti-inflammatory Activity of Ruscogenin: Role of Intercellular Adhesion Molecule-1 and Nuclear Factor-kappaB. *J. Pharmacol. Sci.* 108 (2), 198–205. doi:10.1254/jphs.08083fp

Humaish, H. H. (2017). Study Comparison Analgesic, Antipyretic and Anti-inflammatory Activity of Aqueous and Alcoholic Leaves Extract of *Lawsonia Inermis* L. (Henna) with Ketoprofen in Male Albino Rats. *Kufa J. Vet. Med. Sci.* 8 (2), 88–100.

Ilango, K., Maharajan, G., and Narasimhan, S. (2013). Anti-nociceptive and Anti-inflammatory Activities of *Azadirachta indica* Fruit Skin Extract and its Isolated Constituent Azadiradione. *Nat. Prod. Res.* 27 (16), 1463–1467. doi:10.1080/14786419.2012.717288

Imam, H., Mahbub, N. U., Khan, M. F., Hana, H. K., and Sarker, M. M. (2013). Alpha Amylase Enzyme Inhibitory and Anti-inflammatory Effect of *Lawsonia Inermis*. *Pak J. Biol. Sci.* 16 (23), 1796–1800. doi:10.3923/pjbs.2013.1796.1800

Islam, M. E., Islam, K. M. D., Billah, M. M., Biswas, R., Sohrab, M. H., and Rahman, S. M. M. (2020a). Antioxidant and Anti-inflammatory Activity of *Heritiera Fomes* (Buch.-Ham), a Mangrove Plant of the Sundarbans. *Adv. Tradit Med. (Adtm)* 20 (2), 189–197. doi:10.1007/s13596-019-00401-0

Islam, M., Mannan, M., Kabir, M., Islam, A., and Olival, K. (2010). Analgesic, Anti-inflammatory and Antimicrobial Effects of Ethanol Extracts of Mango Leaves. *J. Bangladesh Agric. Univ.* 8 (2), 239–244. doi:10.3329/jbau.v8i2.7932

Islam, M. T., Hasan, J., Snigdha, H. M. S. H., Ali, E. S., Sharifi-Rad, J., Martorell, M., et al. (2020b). Chemical Profile, Traditional Uses, and Biological Activities of *Piper Chaba* Hunter: A Review. *J. Ethnopharmacol* 257, 112853. doi:10.1016/j.jep.2020.112853

Islas, J. F., Acosta, E., G-Buentello, Z., Delgado-Gallegos, J. L., Moreno-Treviño, M. G., Escalante, B., et al. (2020). An Overview of Neem (*Azadirachta indica*) and its Potential Impact on Health. *J. Funct. Foods* 74, 104171. doi:10.1016/j.jff.2020.104171

Issa, A. Y., Volate, S. R., and Wargovich, M. J. (2006). The Role of Phytochemicals in Inhibition of Cancer and Inflammation: New Directions and Perspectives. *J. Food Compost. Anal.* 19 (5), 405–419. doi:10.1016/j.jfca.2006.02.009

Ivanovska, N., and Philipov, S. (1996). Study on the Anti-inflammatory Action of *Berberis Vulgaris* Root Extract, Alkaloid Fractions and Pure Alkaloids. *Int. J. Immunopharmacol* 18 (10), 553–561. doi:10.1016/S0192-0561(96)00047-1

Jackson, L. M., and Hawkey, C. J. (2000). COX-2 Selective Nonsteroidal Anti-inflammatory Drugs: Do They Really Offer Any Advantages? *Drugs* 59 (6), 1207–1216. doi:10.2165/00003495-200059060-00001

Jahan, F. I., Sultana, S., Brishti, S. A., and Dulla, O. (2019). Ethnopharmacological Survey on Traditional Medicinal Plants at Keraniganj, Dhaka, Bangladesh. *Orient Pharm. Exp. Med.* 19 (3), 331–339. doi:10.1007/s13596-019-00362-4

Jiang, Y. Q., and Liu, E. H. (2019). *Microcos Paniculata*: A Review on its Botany, Traditional Uses, Phytochemistry and Pharmacology. *Chin. J. Nat. Med.* 17 (8), 561–574. doi:10.1016/S1875-5364(19)30058-5

John, N. A. A., and Shobana, G. (2012). Anti-inflammatory Activity of *Talinum Fruticosum* L. On Formalin Induced Paw Edema in Albino Rats. *J. Appl. Pharm. Sci.* 2 (1), 123–127.

Jones, C. K., Peters, S. C., and Shannon, H. E. (2005). Efficacy of Duloxetine, a Potent and Balanced Serotonergic and Noradrenergic Reuptake Inhibitor, in Inflammatory and Acute Pain Models in Rodents. *J. Pharmacol. Exp. Ther.* 312 (2), 726–732. doi:10.1124/jpet.104.075960

Joshi, R. K. (2020). GC-MS Analysis of Volatile Organic Constituents of Traditionally Used Medicinal Plants from the Western Ghats of India: *Blumea Lanceolaria* (Roxb.) Druce., *Heliotropium Indicum* L. And *Triumfetta Rhomboidea* Jacq. *J. Mex. Chem. Soc.* 64, 74–82. doi:10.29356/jmcs.v64i2.1093

Jothy, S. L., Zakaria, Z., Chen, Y., Lau, Y. L., Latha, L. Y., and Sasidharan, S. (2011). Acute Oral Toxicity of Methanolic Seed Extract of *Cassia Fistula* in Mice. *Molecules* 16 (6), 5268–5282. doi:10.3390/molecules16065268

Just, M. J., Recio, M. C., Giner, R. M., Cuéllar, M. J., Máñez, S., Bilia, A. R., et al. (1998). Anti-inflammatory Activity of Unusual Lupane Saponins from *Bupleurum Fruticescens*. *Planta Med.* 64 (5), 404–407. doi:10.1055/s-2006-957469

Kader, M. A., Parvin, S., Chowduri, M. A. U., and Haque, M. E. (2014). Antibacterial, Antifungal and Insecticidal Activities of *Ruellia Tuberosa* (L.) Root Extract. *J. Bio-sci.* 20 (0), 91–97. doi:10.3329/jbs.v20i0.17720

Kamalakararao, K., Gopalakrishnan, V. K., Hagos, Z., Rao, G. D., Padal, S. B., and Chaithanya, K. K. (2018a). Anti-inflammatory Activity of Bioactive Flavonoid Apigenin-7-O-β-D-Glucuronide Methyl Ester from Ethyl Acetate Leaf Extract of *Manilkara Zapota* on Lipopolysaccharide-Induced Pro-inflammatory Mediators Nitric Oxide (NO), Prostaglandin E_2 (PGE_2) in Raw 264.7 Cells. *Drug Invention Today* 10 (4), 531–535.

Kamalakararao, K., Rao, D., Muthulingam, M., Gopalakrishnan, V. K., Hagos, Z., Palleti, J., et al. (2018b). Effect of Isolated Bioactive Flavonoid Apigenin-7-O-β-D-Glucuronide Methyl Ester on Cyclooxygenase-2 Gene Expression in the Breast Cancer MCF-7 Cell Lines. *Drug Invention Today* 10 (4), 3552–3555.

Kannadas, S., Pathirana, R., and Ratnasooriya, W. (2020). In-vitro Investigation of Anti-inflammatory Activity and Evaluation of Phytochemical Profile of *Eclipta Prostrata* (L.). *J. Pharmacognosy Phytochemistry* 9 (2), 831–835.

Kashyap, D., Sharma, A., Tuli, H. S., Punia, S., and Sharma, A. K. (2016). Ursolic Acid and Oleanolic Acid: Pentacyclic Terpenoids with Promising Anti-inflammatory Activities. *Recent Pat Inflamm. Allergy Drug Discov.* 10 (1), 21–33. doi:10.2174/1872213x10666160711143904

Kassim, M., Achoui, M., Mustafa, M. R., Mohd, M. A., and Yusoff, K. M. (2010). Ellagic Acid, Phenolic Acids, and Flavonoids in Malaysian Honey Extracts Demonstrate *In Vitro* Anti-inflammatory Activity. *Nutr. Res.* 30 (9), 650–659. doi:10.1016/j.nutres.2010.08.008

Kaur, G., Sarwar Alam, M., and Athar, M. (2004). Nimbidin Suppresses Functions of Macrophages and Neutrophils: Relevance to its Antiinflammatory Mechanismsflammatory Mechanisms. *Phytother Res.* 18 (5), 419–424. doi:10.1002/ptr.1474

Kawsar, M. H., Sikder, M. A. A., Rana, M. S., Nimmi, I., and Rashid, M. A. (2011). Studies of Thrombolytic, Antioxidant and Cytotoxic Properties of Two Asteraceous Plants of Bangladesh. *Bangladesh Pharm. J.* 14 (2), 103–106.

Kazłowska, K., Hsu, T., Hou, C. C., Yang, W. C., and Tsai, G. J. (2010). Anti-inflammatory Properties of Phenolic Compounds and Crude Extract from *Porphyra Dentata*. *J. Ethnopharmacol* 128 (1), 123–130. doi:10.1016/j.jep.2009.12.037

Khan, M. A., Ahmed, R. S., Chandra, N., Arora, V. K., and Ali, A. (2019). *In Vivo*, Extract from *Withania Somnifera* Root Ameliorates Arthritis *via* Regulation of Key Immune Mediators of Inflammation in Experimental Model of Arthritis. *Antiinflamm Antiallergy Agents Med. Chem.* 18 (1), 55–70. doi:10.2174/1871523017666181116092934

Khan, M. S. S., Syeed, S. H., Uddin, M. H., Akter, L., Ullah, M. A., Jahan, S., et al. (2013). Screening and Evaluation of Antioxidant, Antimicrobial, Cytotoxic, Thrombolytic and Membrane Stabilizing Properties of the Methanolic Extract and Solvent-Solvent Partitioning Effect of *Vitex Negundo* Bark. *Asian Pac. J. Trop. Dis.* 3 (5), 393–400. doi:10.1016/S2222-1808(13)60090-0

Khatry, N., Kundu, J., Bachar, S. C., Uddin, M. N., and Kundu, J. K. (2005). Studies on Antinociceptive, Antiinflammatory and Diuretic Activities of Methanol Extract of the Aerial Parts of Clerodendron Viscosum Vent. *Dhaka Univ. J. Pharm. Sci.* 5 (1-2), 63–66. doi:10.3329/dujps.v5i1.231

Kim, D. S., Lee, H. J., Jeon, Y. D., Han, Y. H., Kee, J. Y., Kim, H. J., et al. (2015a). Alpha-Pinene Exhibits Anti-inflammatory Activity through the Suppression of MAPKs and the NF-Kb Pathway in Mouse Peritoneal Macrophages. *Am. J. Chin. Med.* 43 (04), 731–742. doi:10.1142/s0192415x15500457

Kim, G. Y., Kim, K. H., Lee, S. H., Yoon, M. S., Lee, H. J., Moon, D. O., et al. (2005). Curcumin Inhibits Immunostimulatory Function of Dendritic Cells: MAPKs and Translocation of NF-Kappa B as Potential Targets. *J. Immunol.* 174 (12), 8116–8124. doi:10.4049/jimmunol.174.12.8116

Kim, H. D., Cho, H. R., Moon, S. B., Shin, H. D., Yang, K. J., Jang, H. J., et al. (2006). Effect of Exopolymers from *Aureobasidium Pullulans* on Formalin-Induced Chronic Paw Inflammation in Mice. *J. Microbiol. Biotechnol.* 12 (16), 1954–1060.

Kim, H. P., Son, K. H., Chang, H. W., and Kang, S. S. (2004). Anti-inflammatory Plant Flavonoids and Cellular Action Mechanisms. *J. Pharmacol. Sci.* 96 (3), 229–245. doi:10.1254/jphs.crj04003x

Kim, S. H., Park, J. G., Lee, J., Yang, W. S., Park, G. W., Kim, H. G., et al. (2015b). The Dietary Flavonoid Kaempferol Mediates Anti-inflammatory Responses via the Src, Syk, IRAK1, and IRAK4 Molecular Targets. *Mediators Inflamm.* 2015, 904142. doi:10.1155/2015/904142

Kim, Y. S., Young, M. R., Bobe, G., Colburn, N. H., and Milner, J. A. (2009). Bioactive Food Components, Inflammatory Targets, and Cancer Prevention. *Cancer Prev. Res. (Phila)* 2 (3), 200–208. doi:10.1158/1940-6207.Capr-08-0141

Konuku, K., Karri, K. C., Gopalakrishnan, V. K., Hagos, Z., Kebede, H., Naidu, T. K., et al. (2017). Anti-inflammatory Activity of *Manilkara Zapota* Leaf Extract. *Int. J. Curr. Pharm. Sci.* 9 (4), 130–134. doi:10.22159/ijcpr.2017v9i4.20977

Kotta, J. C., Lestari, A. B. S., Candrasari, D. S., and Hariono, M. (2020). Medicinal Effect, *In Silico* Bioactivity Prediction, and Pharmaceutical Formulation of *Ageratum Conyzoides* L.: A Review. *Scientifica (Cairo)* 2020, 6420909. doi:10.1155/2020/6420909

Kumar, A. D. N., Bevara, G. B., Laxmikoteswramma, K., and Malla, R. R. (2013). Antioxidant, Cytoprotective and Anti-inflammatory Activities of Stem Bark Extract of *Semecarpus Anacardium*. *Asian J. Pharm. Clin. Res.* 6, 213–219.

Kundu, J. K., Shin, Y. K., and Surh, Y. J. (2006). Resveratrol Modulates Phorbol Ester-Induced Pro-inflammatory Signal Transduction Pathways in Mouse Skin *In Vivo*: NF-kappaB and AP-1 as Prime Targets. *Biochem. Pharmacol.* 72 (11), 1506–1515. doi:10.1016/j.bcp.2006.08.005

Kuropakornpong, P., Itharat, A., Panthong, S., Sireeratawong, S., and Ooraikul, B. (2020). *In Vitro* and *In Vivo* Anti-inflammatory Activities of Benjakul: A Potential Medicinal Product from Thai Traditional Medicine. *Evid. Based Complement. Alternat Med.* 2020, 9760948. doi:10.1155/2020/9760948

Kyei, S., Koffuor, G. A., Ramkissoon, P., Ameyaw, E. O., and Asiamah, E. A. (2016). Anti-inflammatory Effect of *Heliotropium Indicum* Linn on Lipopolysaccharide-Induced Uveitis in New Zealand white Rabbits. *Int. J. Ophthalmol.* 9 (4), 528–535. doi:10.18240/ijo.2016.04.08

Laboni, F. R., Sultana, T., Kamal, S., Karim, S., Das, S., Harun-Or-Rashid, M., et al. (2017). Biological Investigations of the Ethanol Extract of the Aerial Part (Leaf) of *Coccinia Grandis* L. *J. Pharmacognosy Phytochemistry* 6 (2), 134–138.

Le, D. D., Nguyen, D. H., Ma, E. S., Lee, J. H., Min, B. S., Choi, J. S., et al. (2021). PTP1B Inhibitory and Anti-inflammatory Properties of Constituents from *Eclipta Prostrata* L. *Biol. Pharm. Bull.* 44, 298–304. doi:10.1248/bpb.b20-00994

Lee, H. (2017). Enhancement of Skin Anti-inflammatory Activities of *Eclipta Prostrata* L. From the Ultrasonic Extraction Process. *Appl. Sci.* 7 (12), 1227. doi:10.3390/app7121227

Leelarungrayub, J., Sriboonreung, T., Pothasak, Y., Kaju, J., and Puntumetakul, R. (2019). Anti-oxidant and Anti-inflammatory Activities of *Manilkara Zapota* (Sapodilla) *In Vitro* and Efficiency in Healthy Elderly Persons. *Biomed. J. Scientific Tech. Res.* 15 (2), 11294–11308. doi:10.26717/bjstr.2019.15.002684

Lesjak, M., Beara, I., Simin, N., Pintać, D., Majkić, T., Bekvalac, K., et al. (2018). Antioxidant and Anti-inflammatory Activities of Quercetin and its Derivatives. *J. Funct. Foods* 40, 68–75. doi:10.1016/j.jff.2017.10.047

Li, K., He, Z., Wang, X., Pineda, M., Chen, R., Liu, H., et al. (2018). Apigenin C-Glycosides of *Microcos Paniculata* Protects Lipopolysaccharide Induced Apoptosis and Inflammation in Acute Lung Injury through TLR4 Signaling Pathway. *Free Radic. Biol. Med.* 124, 163–175. doi:10.1016/j.freeradbiomed.2018.06.009

Liu, Y. P., Yan, G., Guo, J. M., Liu, Y. Y., Li, Y. J., Zhao, Y. Y., et al. (2019). Prenylated Coumarins from the Fruits of *Manilkara Zapota* with Potential

Anti-inflammatory Effects and Anti-HIV Activities. *J. Agric. Food Chem.* 67 (43), 11942–11947. doi:10.1021/acs.jafc.9b04326

López-Otín, C., and Overall, C. M. (2002). Protease Degradomics: A New challenge for Proteomics. *Nat. Rev. Mol. Cel Biol.* 3 (7), 509–519. doi:10.1038/nrm858

Lu, H. M., Liang, Y. Z., Yi, L. Z., and Wu, X. J. (2006). Anti-inflammatory Effect of *Houttuynia Cordata* Injection. *J. Ethnopharmacol* 104 (1), 245–249. doi:10.1016/j.jep.2005.09.012

Lucas, L., Russell, A., and Keast, R. (2011). Molecular Mechanisms of Inflammation. Anti-inflammatory Benefits of virgin Olive Oil and the Phenolic Compound Oleocanthal. *Curr. Pharm. Des.* 17 (8), 754–768. doi:10.2174/138161211795428911

Luo, H., Lv, X. D., Wang, G. E., Li, Y. F., Kurihara, H., and He, R. R. (2014). Anti-inflammatory Effects of Anthocyanins-Rich Extract from Bilberry (*Vaccinium Myrtillus* L.) on croton Oil-Induced Ear Edema and *Propionibacterium Acnes* Plus LPS-Induced Liver Damage in Mice. *Int. J. Food Sci. Nutr.* 65 (5), 594–601. doi:10.3109/09637486.2014.886184

Luster, A. D., Alon, R., and von Andrian, U. H. (2005). Immune Cell Migration in Inflammation: Present and Future Therapeutic Targets. *Nat. Immunol.* 6 (12), 1182–1190. doi:10.1038/ni1275

Machan, T., Korth, J., Liawruangrath, B., Liawruangrath, S., and Pyne, S. G. (2006). Composition and Antituberculosis Activity of the Volatile Oil ofHeliotropium Indicum Linn. Growing in Phitsanulok, Thailand. *Flavour Fragr. J.* 21 (2), 265–267. doi:10.1002/ffj.1577

Mahabub-Uz-Zaman, M., Ahmed, N. U., Akter, R., Ahmed, K., Aziz, M. S. I., and Ahmed, M. S. (2009). Studies on Anti-inflammatory, Antinociceptive and Antipyretic Activities of Ethanol Extract of *Azadirachta indica* Leaves. *Bangladesh J. Scientific Ind. Res.* 44 (2), 199–206.

Manivannan, R., Aeganathan, R., Aeganathan, R., and Prabakaran, K. (2015). Anti-microbial and Anti-inflammatory Flavonoid Constituents from the Leaves of *Lawsonia Inermis*. *J. Phytopharmacol* 4 (4), 212–216. doi:10.31254/phyto.2015.4404

Manna, K., Debnath, B., Das, M., and Marwein, S. (2016). A Comprehensive Review on Pharmacognostical Investigation and Pharmacology of Typhonium Trilobatum. *Npj* 6 (3), 172–178. doi:10.2174/2210315506666160810145157

Martin, D., Valdez, J., Boren, J., and Mayersohn, M. (2004). Dermal Absorption of Camphor, Menthol, and Methyl Salicylate in Humans. *J. Clin. Pharmacol.* 44 (10), 1151–1157. doi:10.1177/0091270004268409

Md, A. R., S M Azad, H., Nazim, U. A., and Md, S. I. (2013). Analgesic and Anti-inflammatory Effects of *Crinum asiaticum* Leaf Alcoholic Extract in Animal Models. *Afr. J. Biotechnol.* 12 (2), 212–218. doi:10.5897/AJB12.1431

Md. Atiar Rahman, M. A., Akter, N., Rashid, H., Ahmed, N. U., and Islam, M. S. (2012). Analgesic and Anti-inflammatory Effect of Whole *Ageratum Conyzoides* and *Emilia Sonchifolia* Alcoholic Extracts in Animal Models. *Afr. J. Pharm. Pharmacol.* 6 (20), 1469–1476. doi:10.5897/AJPP12.083

Medzhitov, R. (2010). Inflammation 2010: New Adventures of an Old Flame. *Cell* 140 (6), 771–776. doi:10.1016/j.cell.2010.03.006

Medzhitov, R. (2008). Origin and Physiological Roles of Inflammation. *Nature* 454 (7203), 428–435. doi:10.1038/nature07201

Miguel, M. G. (2010). Antioxidant and Anti-inflammatory Activities of Essential Oils: a Short Review. *Molecules* 15 (12), 9252–9287. doi:10.3390/molecules15129252

Miles, E. A., Zoubouli, P., and Calder, P. C. (2005). Differential Anti-inflammatory Effects of Phenolic Compounds from Extra virgin Olive Oil Identified in Human Whole Blood Cultures. *Nutrition* 21 (3), 389–394. doi:10.1016/j.nut.2004.06.031

Mollik, M. A. H., Hossan, M. S., Paul, A. K., Taufiq-Ur-Rahman, M., Jahan, R., and Rahmatullah, M. (2010). A Comparative Analysis of Medicinal Plants Used by Folk Medicinal Healers in Three Districts of Bangladesh and Inquiry as to Mode of Selection of Medicinal Plants. *Ethnobot. Res. App.* 8, 195–218. doi:10.17348/era.8.0.195-218

Morshed, M. A., Uddin, M., Hasan, T., Ahmed, T., Uddin, F., Zakaria, M., et al. (2011). Evaluation of Analgesic and Anti-inflammatory Effect of *Terminalia Arjuna* Ethanol Extract. *Int. J. Pharm. Sci. Res.* 2 (10), 2577–2585.

Mosaddek, A. S. M., and Rashid, M. M. U. (2008). A Comparative Study of the Anti-inflammatory Effect of Aqueous Extract of Neem Leaf and Dexamethasone. *Bangladesh J. Pharmacol.* 3, 44–47. doi:10.3329/bjp.v3i1.836

Mourin, N. A., Sharmin, T., Chowdhury, S. R., Islam, F., Rahman, M. S., and Rashid, M. A. (2013). Evaluation of Bioactivities of *Heliotropium Indicum*, a Medicinal Plant of Bangladesh. *Pharma Innovation* 2 (5), 217–221.

Naik, M., Agrawal, D., Behera, R., Bhattacharya, A., Dehury, S., and Kumar, S. (2014). Study of Anti-inflammatory Effect of Neem Seed Oil (*Azadirachta indica*) on Infected Albino Rats. *J. Health Res. Rev.* 1 (3), 66–69. doi:10.4103/2394-2010.153880

Namsa, N. D., Tag, H., Mandal, M., Kalita, P., and Das, A. K. (2009). An Ethnobotanical Study of Traditional Anti-inflammatory Plants Used by the Lohit Community of Arunachal Pradesh, India. *J. Ethnopharmacol* 125 (2), 234–245. doi:10.1016/j.jep.2009.07.004

Nandi, S., and Lyndem, L. M. (2016). *Clerodendrum Viscosum*: Traditional Uses, Pharmacological Activities and Phytochemical Constituents. *Nat. Prod. Res.* 30 (5), 497–506. doi:10.1080/14786419.2015.1025229

Nandi, S., Ukil, B., and Lyndem, L. M. (2017). Acute and Sub-acute Toxicological Evaluation of the Alcoholic Leaf and Root Extracts of *Clerodendrum Infortunatum* L. *Nat. Prod. Res.* 32 (17), 2062–2066. doi:10.1080/14786419.2017.1360879

Nathan, C. (2002). Points of Control in Inflammation. *Nature* 420 (6917), 846–852. doi:10.1038/nature01320

Nesa, L., Munira, S., Mollika, S., Islam, M., Choin, H., Chouduri, A. U., et al. (2014). Evaluation of Analgesic, Anti-inflammatory and CNS Depressant Activities of Methanolic Extract of *Lawsonia Inermis* Barks in Mice. *Avicenna J. Phytomed* 4 (4), 287–296. doi:10.9734/bjpr/2014/7845

Nian, H., Xiong, H., Zhong, F., Teng, H., Teng, H., Chen, Y., et al. (2020). Anti-inflammatory and Antiproliferative Prenylated sulphur-containing Amides from the Leaves of *Glycosmis Pentaphylla*. *Fitoterapia* 146, 104693. doi:10.1016/j.fitote.2020.104693

Niazi, M., Mehrabani, M., Namazi, M. R., Salmanpour, M., Heydari, M., Karami, M. M., et al. (2020). Efficacy of a Topical Formulation of Henna (*Lawsonia Inermis* L.) in Contact Dermatitis in Patients Using Prosthesis: A Double-Blind Randomized Placebo-Controlled Clinical Trial. *Complement. Ther. Med.* 49, 102316. doi:10.1016/j.ctim.2020.102316

Nirmal, N. P., and Panichayupakaranant, P. (2015). Antioxidant, Antibacterial, and Anti-inflammatory Activities of Standardized Brazilin-Rich *Caesalpinia Sappan* Extract. *Pharm. Biol.* 53 (9), 1339–1343. doi:10.3109/13880209.2014.982295

Noor, S., Rahman, S. M. A., Ahmed, Z., Das, A., and Hossain, M. M. (2013). Evaluation of Anti-inflammatory and Antidiabetic Activity of Ethanolic Extracts of *Desmodium Pulchellum* Benth. (Fabaceae) Barks on Albino Wistar Rats. *J. Appl. Pharm. Sci.* 3 (7), 48–51. doi:10.9734/bjpr/2013/3505

Ocvirk, S., Kistler, M., Khan, S., Talukder, S. H., and Hauner, H. (2013). Traditional Medicinal Plants Used for the Treatment of Diabetes in Rural and Urban Areas of Dhaka, Bangladesh--an Ethnobotanical Survey. *J. Ethnobiol. Ethnomed* 9 (1), 43. doi:10.1186/1746-4269-9-43

Ogunbinu, A. O., Flamini, G., Cioni, P. L., Adebayo, M. A., and Ogunwande, I. A. (2009). Constituents of *Cajanus Cajan* (L.) Millsp., *Moringa Oleifera* Lam., *Heliotropium Indicum* L. And *Bidens Pilosa* L. from Nigeria. *Nat. Prod. Commun.* 4 (4), 573–578. doi:10.1177/1934578x0900400427

Okpanyi, S. N., and Ezeukwu, G. C. (1981). Anti-inflammatory and Antipyretic Activities of *Azadirachta indica*. *Planta Med.* 41 (01), 34–39. doi:10.1055/s-2007-971670

Okunade, A. L. (2002). *Ageratum Conyzoides* L. (Asteraceae). *Fitoterapia* 73 (1), 1–16. doi:10.1016/s0367-326x(01)00364-1

Özbek, H., and Yılmaz, B. S. (2017). Anti-inflammatory and Hypoglycemic Activities of Alpha-Pinene. *actapharm* 55 (4), 7–14. doi:10.23893/1307-2080.APS.05522

Paniagua-Pérez, R., Flores-Mondragón, G., Reyes-Legorreta, C., Herrera-López, B., Cervantes-Hernández, I., Madrigal-Santillán, O., et al. (2016). Evaluation of the Anti-inflammatory Capacity of Beta-Sitosterol in Rodent Assays. *Ajtcam* 14 (1), 123–130. doi:10.21010/ajtcam.v14i1.13

Parvin, T., Akhlas, M. B., Khatun, F., Akter, A., Al Amin, M., Islam, M. T., et al. (2019). Phytochemical Screening and Evaluation of Pharmacological Activities of Aqueous Extract of *Typhonium Trilobatum* (L.) Schott. *Orient Pharm. Exp. Med.* 19 (4), 445–454. doi:10.1007/s13596-019-00382-0

Pereira, L. d. P., Silva, K. E. S. d., Silva, R. O. d., Assreuy, A. M. S., and Pereira, M. G. (2012). Anti-inflammatory Polysaccharides of *Azadirachta indica* Seed

Tegument. *Rev. Bras. Farmacogn.* 22 (3), 617–622. doi:10.1590/S0102-695X2012005000031

Perez, R. M. (2001). Anti-inflammatory Activity of Compounds Isolated from Plants. *ScientificWorldJournal* 1, 713–784. doi:10.1100/tsw.2001.77

Pillai, N. R., and Santhakumari, G. (1981). Anti-arthritic and Anti-inflammatory Actions of Nimbidin. *Planta Med.* 43 (09), 59–63. doi:10.1055/s-2007-971474

Posadas, I., Bucci, M., Roviezzo, F., Rossi, A., Parente, L., Sautebin, L., et al. (2004). Carrageenan-induced Mouse Paw Oedema Is Biphasic, Age-Weight Dependent and Displays Differential Nitric Oxide Cyclooxygenase-2 Expression. *Br. J. Pharmacol.* 142 (2), 331–338. doi:10.1038/sj.bjp.0705650

Prashith Kekuda, T. R., Dhanya Shree, V. S., Saema Noorain, G. K., Sahana, B. K., and Raghavendra, H. L. (2019). Ethnobotanical Uses, Phytochemistry and Pharmacological Activities of *Clerodendrum Infortunatum* L. (Lamiaceae): A Review. *J. Drug Deliv. Ther.* 9 (2), 547–559. doi:10.22270/jddt.v9i2.2433

Qais, N., Mahmud, Z. A., Karim, M. R., and Bachar, S. C. (2011). Anti-nociceptive, Anti-inflammatory and Sedating Activities of Leaf Extracts of *Premna Esculenta* (Roxb). *J. Pharm. Res.* 4 (10), 3463–3465.

R, C., and Rao, S. N. (2013). Chronic Anti-inflammatory Activity of Ethanolic Extract of Leaves of *Clerodendrum Viscosum* by Carrageenin Induced Paw Oedema in Wistar Albino Rats. *Bjpr* 3 (4), 579–586. doi:10.7897/2277-4343.04227

Rahman, M. A., Sharmin, R., Uddin, M. N., Mahbub Uz, Z., Rana, S., and Ahmed, N. U. (2011a). Antinociceptive and Anti-inflammatory Effect of *Crinum asiaticum* Bulb Extract. *Asian J. Pharm. Clin. Res.* 4 (3), 34–37.

Rahman, M. A., Solaiman, M., Haque, M. E., and Das, A. K. (2011b). Analgesic and Anti-inflammatory Activities of *Alocasia Indica* (Roxb.) Schott. *Orient Pharm. Exp. Med.* 11 (3), 143–146. doi:10.1007/s13596-011-0027-1

Rahman, S., Akter, M., Hira, T. E., Sharmin, T., and Nayeen, M. J. (2014). Cytotoxic, Thrombolytic and Membrane Stabilizing Activities of *Swietenia Mahagoni* (L.) Jacq. Flower Extract. *Ejmp* 4 (10), 1232–1239. doi:10.9734/ejmp/2014/11047

Rahman, S., Hasnat, A., Hasan, C. M., Rashid, M. A., and Ilias, M. (2001). Pharmacological Evaluation of Bangladeshi Medicinal Plants - a Review. *Pharm. Biol.* 39 (1), 1–6. doi:10.1076/phbi.39.1.1.5939

Rahmatullah, M., Jahan, R., Azam, F. M., Hossan, S., Mollik, M. A., and Rahman, T. (2011b). Folk Medicinal Uses of Verbenaceae Family Plants in Bangladesh. *Afr. J. Tradit Complement. Altern. Med.* 8, 53–65. doi:10.4314/ajtcam.v8i5S.15

Rahmatullah, M., Khatun, Z., Hasan, A., Parvin, W., Moniruzzaman, M., Khatun, A., et al. (2012). Survey and Scientific Evaluation of Medicinal Plants Used by the Pahan and Teli Tribal Communities of Natore District, Bangladesh. *Afr. J. Tradit Complement. Altern. Med.* 9 (3), 366–373. doi:10.4314/ajtcam.v9i3.10

Rahmatullah, M., Azam, M. N. K., Rahman, M. M., Seraj, S., Mahal, M. J., Mou, S. M., et al. (2011a). A Survey of Medicinal Plants Used by Garo and Non-garo Traditional Medicinal Practitioners in Two Villages of Tangail District, Bangladesh. *American-Eurasian J. Sustainable Agric.* 5 (3), 350–357.

Rai, U., Rawal, A., and Singh, S. (2018). Evaluation of the Anti-inflammatory Effect of an Anti-platelet Agent Crinumin on Carrageenan-Induced Paw Oedema and Granuloma Tissue Formation in Rats. *Inflammopharmacology* 26 (3), 769–778. doi:10.1007/s10787-017-0411-7

Ramamurthy, V., Fathima, M. A., Govindaraju, G., and Raveendran, S. (2009). Anti-inflammatory Activity of *Heliotropium Indicum* Extract on Formaldehyde Induced Inflammation in Rats. *J. Ecobiology* 24 (4), 345–351. Availableat: http://www.palaniparamount.com.

Rao, B. G., and Raju, N. J. (2009). Investigation of Anti-inflammatory Activity of *Glycosmis Pentaphylla* (Rutaceae). *Int. J. Chem. Sci.* 7 (4), 2891–2899.

Razia, S., Kamrun, N., and Sitesh, C. B. (2018). *In-vitro* Membrane Stabilizing, Thrombolytic, Antioxidant and Antimicrobial Activities of Bangladeshi Origin *Coccinia Indica* (Cucurbitaceae). *Afr. J. Pharm. Pharmacol.* 12 (16), 188–192. doi:10.5897/AJPP2018.4913

Recio, M. C., Andujar, I., and Rios, J. L. J. (2012). Anti-inflammatory Agents from Plants: Progress and Potential. *Curr. Med. Chem.* 19 (14), 2088–2103. doi:10.2174/092986712800229069

Ribeiro, R. A., Vale, M. L., Thomazzi, S. M., Paschoalato, A. B., Poole, S., Ferreira, S. H., et al. (2000). Involvement of Resident Macrophages and Mast Cells in the Writhing Nociceptive Response Induced by Zymosan and Acetic Acid in Mice. *Eur. J. Pharmacol.* 387 (1), 111–118. doi:10.1016/S0014-2999(99)00790-6

Ripon, S. S., Mahmood, A., Chowdhury, M. M. U., and Islam, M. T. (2016). A Possible Cytoprotectivity Triggering Anti- Atherothrombosis Activity of *Lantana Camera* L. Methanol Extract. *Asian J. Ethnopharmacology Med. Foods* 2 (6), 1–5.

Sabikunnahar, J., Jalal, U., and Labu, Z. K. (2016). Naturally Growing Medicinal Plant *Clerodendrum Viscosum* in Bangladesh - Thrombolytic, Membrane Stabilizing and Anti-microbial Properties. *Int. J. Pharm.* 7 (1), 2678–2684.

Saddam Hus, M., Mazbah Udd, A. H. M., Azmerin, M., Tohidul Am, M., Hasan, M., Das Aka, T., et al. (2019). An *In Vivo* and *In Vitro* Evaluation of Anti-inflammatory Action of Seeds of *Vigna Unguiculata* Available in Bangladeshi Region. *J. Appl. Sci.* 19 (2), 62–67. doi:10.3923/jas.2019.62.67

Salminen, A., Lehtonen, M., Suuronen, T., Kaarniranta, K., and Huuskonen, J. (2008). Terpenoids: Natural Inhibitors of NF-kappaB Signaling with Anti-inflammatory and Anticancer Potential. *Cel Mol Life Sci* 65 (19), 2979–2999. doi:10.1007/s00018-008-8103-5

Saltan Çitoğlu, G., Bahadır Acıkara, Ö., Sever Yılmaz, B., and Özbek, H. (2012). Evaluation of Analgesic, Anti-inflammatory and Hepatoprotective Effects of Lycorine from *Sternbergia Fisheriana* (Herbert) Rupr. *Fitoterapia* 83 (1), 81–87. doi:10.1016/j.fitote.2011.09.008

Salvo, F., Fourrier-Réglat, A., Bazin, F., Robinson, P., Riera-Guardia, N., Haag, M., et al. (2011). Cardiovascular and Gastrointestinal Safety of NSAIDs: A Systematic Review of Meta-Analyses of Randomized Clinical Trials. *Clin. Pharmacol. Ther.* 89 (6), 855–866. doi:10.1038/clpt.2011.45

Samira, K., Md, K., Laboni, F. R., Julie, A. S., Jalal, U., and Labu, Z. K. (2016). Biological Investigations of Medicinal Plants of *Heliotropium Indicum* Indigenous to Bangladesh. *J. Coast Life Med.* 4 (11), 874–878. doi:10.12980/jclm.4.2016J6-175

Samud, A. M., Asmawi, M. Z., Sharma, J. N., and Yusof, A. P. (1999). Anti-inflammatory Activity of *Crinum asiaticum* Plant and its Effect on Bradykinin-Induced Contractions on Isolated Uterus. *Immunopharmacology* 43 (2), 311–316. doi:10.1016/S0162-3109(99)00132-0

Sannigrahi, S., Mazumder, U. K., Pal, D., and Mishra, S. L. (2012). Terpenoids of Methanol Extract of Clerodendrum Infortunatum Exhibit Anticancer Activity against Ehrlich's Ascites Carcinoma (EAC) in Mice. *Pharm. Biol.* 50 (3), 304–309. doi:10.3109/13880209.2011.604089

Santos, F. A., and Rao, V. S. (2000). Antiinflammatory and Antinociceptive Effects of 1,8-cineole a Terpenoid Oxide Present in many Plant Essential Oils. *Phytother Res.* 14 (4), 240–244. doi:10.1002/1099-1573(200006)14:4<240::aid-ptr573>3.0.co;2-x

Sasidharan, S. P., and Vasumathi, A. V. (2017). *In Vitro* pharmacological, *In Vivo* Toxicological and In Silico Molecular Docking Analysis of Glycopentalone, a Novel Compound from *Glycosmis Pentaphylla* (Retz.) Correa. *Med. Chem. Res.* 26 (8), 1697–1707. doi:10.1007/s00044-017-1880-3

Schumacher, M., Cerella, C., Reuter, S., Dicato, M., and Diederich, M. (2011). Anti-inflammatory, Pro-apoptotic, and Anti-proliferative Effects of a Methanolic Neem (Azadirachta indica) Leaf Extract Are Mediated via Modulation of the Nuclear Factor-Kb Pathway. *Genes Nutr.* 6 (2), 149–160. doi:10.1007/s12263-010-0194-6

Seetharaman, T. R. (1990). Flavonoids of *Firmiana Simplex* and *Sterculia Villosa*. *Fitoterapia* 61 (4), 373–374.

Shafa, F., Shahriar, M., Opo, F. A. D. M., Akhter, R., Hossain, M. M., and Choudhury, N. (2016). Characterization of Phytoconstituents, *In Vitro* Antioxidant Activity and Pharmacological Investigation of the Root Extract of *Typhonium Trilobatum*. *Int. J. Pharm. Sci. Res.* 7 (4), 1694–1704. doi:10.13040/IJPSR.0975-8232.7(4).1694-04

Shah, V. O., Ferguson, J. E., Hunsaker, L. A., Deck, L. M., and Vander Jagt, D. L. (2010). Natural Products Inhibit LPS-Induced Activation of Pro-inflammatory Cytokines in Peripheral Blood Mononuclear Cells. *Nat. Prod. Res.* 24 (12), 1177–1188. doi:10.1080/14786410903112680

Shahriar, M., Alam, F., and Uddin, M. M. N. (2014). Membrane Stabilizing and Thrombolytic Activity of *Withania Somnifera* Root. *Am. J. Phytomedicine Clin. Ther.* 2 (2), 252–256.

Shahriar, M., Sharmin, F. A., Islam, A. S. M., Dewan, I., and Kabir, S. (2012). Membrane Stabilizing and Anti-thrombolytic Activities of Four Medicinal Plants of Bangladesh. *Exp.* 4 (4), 265–270.

Shahriar, M., Tithi, N. A., Akhter, R., Kamal, S., Narjish, S. N., and Bhuiyan, M. A. (2015). Phytochemical and Pharmacological Investigation of the Crude Extract of *Typhonium Trilobatum* (L.) Schott. *World J. Pharm. Res.* 4 (2), 167–188.

Shalini, S., and Shaik, F. (2010). Study on the Anti-inflammatory Activity of *Heliotropium Indicum*. *J. Innovative Trends Pharm. Sci.* 1 (1), 43–46.

Sharma, B., Vasudeva, N., and Sharma, S. (2020). Phytopharmacological Review on *Crinum asiaticum*: A Potential Medicinal Herb. *Npj* 10 (4), 342–354. doi:10.2174/2210315509666190731142333

Sharma, R. K., Goel, A., and Bhatia, A. K. (2016). *Lawsonia Inermis* Linn: A Plant with Cosmetic and Medical Benefits. *Int. J. Appl. Sci. Biotechnol.* 4 (1), 15–20. doi:10.3126/ijasbt.v4i1.14728

Shinde, U. A., Phadke, A. S., Nair, A. M., Mungantiwar, A. A., Dikshit, V. J., and Saraf, M. N. (1999). Membrane Stabilizing Activity - a Possible Mechanism of Action for the Anti-inflammatory Activity of Cedrus Deodara wood Oil. *Fitoterapia* 70, 251–257. doi:10.1016/S0367-326X(99)00030-1

Siddiqui, S., Kamal, A., Khan, F., Jamali, K. S., and Saify, Z. S. (2019). Gallic and Vanillic Acid Suppress Inflammation and Promote Myelination in an *In Vitro* Mouse Model of Neurodegeneration. *Mol. Biol. Rep.* 46 (1), 997–1011. doi:10.1007/s11033-018-4557-1

Sikder, M. A. A., Rahman, M. A., Islam, M. R., Kaisar, M. A., Rahman, M. S., and Rashid, M. A. (2010). *In Vitro* antioxidant , Reducing Power, Free Radical Scavenging and Membrane Stabilizing Activities of *Spilanthes Calva*. *Bangladesh Pharm. J.* 13 (1), 63–67.

Sinha, N. K., Seth, K. K., Pandey, V. B., Dasgupta, B., and Shah, A. H. (1981). Flavonoids from the Flowers of *Clerodendron Infortunatum*. *Planta Med.* 42 (07), 296–298. doi:10.1055/s-2007-971645

Sireeratawong, S., Itharat, A., Lerdvuthisopon, N., Piyabhan, P., Khonsung, P., Boonraeng, S., et al. (2012). Anti-inflammatory, Analgesic, and Antipyretic Activities of the Ethanol Extract of *Piper Interruptum* Opiz. And *Piper Chaba* Linn. *ISRN Pharmacol.* 2012, 480265. doi:10.5402/2012/480265

Sm, M. R., Rana, S., Afm, A. I., Kumer, A., Hashem, A. K., Rahman, H., et al. (2019). Antithrombotic and Anti-inflammatory Activities of Leaf Methanolic Extract of Euphorbia Hirta Lin. *Ijcam* 12 (4), 154–162. doi:10.15406/ijcam.2019.12.00466

Smyth, E. M., Grosser, T., Wang, M., Yu, Y., and FitzGerald, G. A. (2009). Prostanoids in Health and Disease. *J. Lipid Res.* 50, S423–S428. doi:10.1194/jlr.R800094-JLR200

Sofowora, A., Ogunbodede, E., and Onayade, A. (2013). The Role and Place of Medicinal Plants in the Strategies for Disease Prevention. *Afr. J. Tradit Complement. Altern. Med.* 10 (5), 210–229. doi:10.4314/ajtcam.v10i5.2

Soma, M. A., Khan, M. F., Tahia, F., Al-Mansur, M. A., Rahman, M. S., and Rashid, M. A. (2019). Cyclooxygenase-2 Inhibitory Compounds from the Leaves of *Glycosmis Pentaphylla* (Retz.) A. DC.: Chemical and *In Silico* Studies. *Asian J. Chem.* 31, 1260–1264. doi:10.14233/ajchem.2019.21913

Souto, A. L., Tavares, J. F., da Silva, M. S., Diniz, Mde. F., de Athayde-Filho, P. F., and Barbosa Filho, J. M. (2011). Anti-inflammatory Activity of Alkaloids: an Update from 2000 to 2010. *Molecules* 16 (10), 8515–8534. doi:10.3390/molecules16108515

Souza, M. C., Siani, A. C., Ramos, M. F., Menezes-de-Lima, O. J., Henriques, M. G., Jr, and Henriques, M. G. M. O. (2003). Evaluation of Anti-inflammatory Activity of Essential Oils from Two Asteraceae Species. *Pharmazie* 58 (8), 582–586. Availableat: https://www.ingentaconnect.com/content/govi/pharmaz/2003/00000058/00000008/art00014.

Sravani, D., Aarathi, K., Kumar, N. S. S., Krupanidhi, S., Ramu, D. V., and Venkateswarlu, T. C. (2015). In VitroAnti-Inflammatory Activity ofMangifera indicaandManilkara zapotaLeaf Extract. *Rese. Jour. Pharm. Technol.* 8 (11), 1477–1480. doi:10.5958/0974-360x.2015.00264.4

Sreejith, P. S., and Asha, V. V. (2015). Glycopentalone, a Novel Compound from *Glycosmis Pentaphylla* (Retz.) Correa with Potent Anti-hepatocellular Carcinoma Activity. *J. Ethnopharmacol* 172, 38–43. doi:10.1016/j.jep.2015.05.051

Srinivas, K., Rao, M. E. B., and Rao, S. S. (2000). Anti-inflammatory Activity of *Heliotropium Indicum* Linn. And *Leucas Aspera* Spreng. in Albino Rats. *Indian J. Pharmacol.* 32 (1), 37–38.

Sufian, M., Chowdhury, T., Mian, M., Mohiuddin, M., Koly, S., Uddin, M., et al. (2017). *In Vitro* study on Thrombolytic and Membrane Stabilizing Activities of *Alternanthera Paronychioides* and *Vernonia Patula* Leaves and Stems. *Arrb* 15 (3), 1–9. doi:10.9734/ARRB/2017/34776

Sukardimanand Ervina, M. (2020). The Recent Use of *Swietenia Mahagoni* (L.) Jacq. As Antidiabetes Type 2 Phytomedicine: A Systematic Review. *Heliyon* 6 (3), e03536. doi:10.1016/j.heliyon.2020.e03536

Sumi, F., Ansari, P., Sikder, B., AnaytullaZhumur, N. A., Zhumur, N., Mohamed, M., et al. (2015). Investigation of the Different Ethnopharmacological Activity of Fractional Root Extracts of *Mussaenda Roxburghii* in *In Vitro* Model. *Ejmp* 10 (2), 1–9. doi:10.9734/EJMP/2015/19315

Swingle, K. F., and Shideman, F. E. (1972). Phases of the Inflammatory Response to Subcutaneous Implantation of a Cotton Pellet and Their Modification by Certain Anti-inflammatory Agents. *J. Pharmacol. Exp. Ther.* 183 (1), 226–234. Availableat: http://jpet.aspetjournals.org/content/jpet/183/1/226.full.pdf.

Syahmi, A. R., Vijayarathna, S., Sasidharan, S., Latha, L. Y., Kwan, Y. P., Lau, Y. L., et al. (2010). Acute Oral Toxicity and Brine Shrimp Lethality of *Elaeis Guineensis* Jacq., (Oil palm Leaf) Methanol Extract. *Molecules* 15 (11), 8111–8121. doi:10.3390/molecules15118111

Tania, K. N., Islam, M. T., Mahmood, A., Ibrahim, M., Chowdhury, M. M. U., Kuddus, M. R., et al. (2013). Pharmacological and Phytochemical Screenings of Ethanol Extract of *Sterculia Villosa* Roxb. *J. Biomed. Pharm. Res.* 2 (1), 9–14.

Taufiq-Ur-Rahman, M., Shilpi, J. A., Ahmed, M., and Faiz Hossain, C. (2005). Preliminary Pharmacological Studies on *Piper Chaba* Stem Bark. *J. Ethnopharmacol* 99 (2), 203–209. doi:10.1016/j.jep.2005.01.055

Tewtrakul, S., Hase, K., Kadota, S., Namba, T., Komatsu, K., and Tanaka, K. (2000). Fruit Oil Composition of *Piper Chaba* Hunt., *P. Longum* L. And *P. Nigrum* L. *J. Essent. Oil Res.* 12 (5), 603–608. doi:10.1080/10412905.2000.9712168

Thabet, A. A., Youssef, F. S., El-Shazly, M., and Singab, A. N. B. (2018). *Sterculia* and *Brachychiton*: a Comprehensive Overview on Their Ethnopharmacology, Biological Activities, Phytochemistry and the Role of Their Gummy Exudates in Drug Delivery. *J. Pharm. Pharmacol.* 70 (4), 450–474. doi:10.1111/jphp.12876

Thangaraj, P. (2016). "Anti-inflammatory Activity," in *Pharmacological Assays of Plant-Based Natural Products. Progress in Drug Research* (Cham: Springer). doi:10.1007/978-3-319-26811-8_16

Tian, E. L., Cui, Y. Y., Yang, G. Z., Mei, Z. N., and Chen, Y. (2014). Phenolic Glycosides from *Glycosmis Pentaphylla*. *J. Asian Nat. Prod. Res.* 16 (12), 1119–1125. doi:10.1080/10286020.2014.951924

Tung, Y. T., Chua, M. T., Wang, S. Y., and Chang, S. T. (2008). Anti-inflammation Activities of Essential Oil and its Constituents from Indigenous Cinnamon (*Cinnamomum Osmophloeum*) Twigs. *Bioresour. Technol.* 99 (9), 3908–3913. doi:10.1016/j.biortech.2007.07.050

Tuñón, M. J., García-Mediavilla, M. V., Sánchez-Campos, S., and González-Gallego, J. (2009). Potential of Flavonoids as Anti-inflammatory Agents: Modulation of Pro-inflammatory Gene Expression and Signal Transduction Pathways. *Curr. Drug Metab.* 10 (3), 256–271. doi:10.2174/138920009787846369

Uddin, J., Biswas, A. J., and Labu, Z. K. (2018). *In Vitro* assessment of *Butea Monosperma* (Lam.) Leaves: Thrombolytic, Membrane Stabilizing Potentials and Total Phenolic Content. *Npj* 8 (3), 239–246. doi:10.2174/2210315508666180410143634

Uddin, J., Julie, A. S., Ali, M. H., Islam, M. N., Khan, S. A., and Labu, Z. K. (2015). Antimicrobial, Thrombolytic, Membrane Stabilizing Activities and Total Flavonoid Content of Various Partitionates of Aerial Parts of *Eclipta alba* (L.) Hassk. *Dhaka Univ. J. Pharm. Sci.* 14 (2), 207–213. doi:10.3329/dujps.v14i2.28512

Uddin, M., Begum, J., Rahman, M. A., Ahmed, N., Akter, R., and Abdullah, A. M. (2010). Antinociceptive and Anti-inflammatory Properties of the Methanol Leaf Extract of *Argyreia Argentea*. *J. Pharm. Sci. Res.* 2 (8), 465–471.

Uddin, M. J., Çiçek, S. S., Willer, J., Shulha, O., Abdalla, M. A., Sönnichsen, F., et al. (2020). Phenylpropanoid and Flavonoid Glycosides from the Leaves of *Clerodendrum Infortunatum* (Lamiaceae). *Biochem. Syst. Ecol.* 92, 104131. doi:10.1016/j.bse.2020.104131

Uddin, M. S. (2019). *Medicinal Plants of Bangladesh*. Dhaka: MPB. Availableat: https://www.natureinfo.com.bd/mpb/ (Accessed July 25, 2021).

Uddin, M., Uddin, M. Z., Emran, T. B., Nath, A. K., Jenny, A., Duttaa, M., et al. (2012). Anti-inflammatory and Antioxidant Activity of Leaf Extract of *Crinum asiaticum*. *J. Pharm. Res.* 05 (12), 5553–5556.

Uddin, S. N. (2006). *Traditional Uses of Ethnomedicinal Plants of the Chittagong hill Tracts*. Dhaka, Bangladesh: Bangladesh National Herbarium.

Uddin, S. S., and Islam, M. S. (2020). Anti-inflammatory, Analgesic and Cognitive Enhancer Plants Present in Bangladesh: A Study Review. *Univ. J. Pharm. Res.* 5 (5). doi:10.22270/ujpr.v5i5.490

Ugboko, H. U., Nwinyi, O. C., Oranusi, S. U., Fatoki, T. H., and Omonhinmin, C. A. (2020). Antimicrobial Importance of Medicinal Plants in Nigeria. *ScientificWorldJournal* 2020, 7059323. doi:10.1155/2020/7059323

Ullah, H. M. A., Akter, L., Zaman, S., Juhara, F., Tareq, S. M., Bhattacharjee, R., et al. (2015). Anti-inflammatory and Analgesic Activities of Methanolic Seed Extract of *Sterculia Villosa* Roxb. *Asian J. Pharm. Clin. Res.* 8 (5), 285–289.

Umapathy, E. U., Ndebia, E., Meeme, A., Adam, B., Menziwa, P., Nkeh-Chungag, B., et al. (2010). An Experimental Evaluation of *Albuca Setosa* Aqueous Extract on Membrane Stabilization, Protein Denaturation and white Blood Cell Migration during Acute Inflammation. *J. Med. Plants Res.* 4 (9), 789–795.

Vaghasiya, Y., Nair, R., and Chanda, S. (2007). Investigation of Some *Piper* Species for Anti-bacterial and Anti-inflammatory Property. *Int. J. Pharmacol.* 3 (5), 400–405. doi:10.3923/ijp.2007.400.405

Vane, J. R., and Botting, R. M. (1998). Mechanism of Action of Nonsteroidal Anti-inflammatory Drugs. *Am. J. Med.* 104 (3Suppl. 1), 2S–22S. doi:10.1016/S0002-9343(97)00203-9

Venkatesha, S. H., Berman, B. M., and Moudgil, K. D. (2011). Herbal Medicinal Products Target Defined Biochemical and Molecular Mediators of Inflammatory Autoimmune Arthritis. *Bioorg. Med. Chem.* 19 (1), 21–29. doi:10.1016/j.bmc.2010.10.053

Vigil de Mello, S. V., da Rosa, J. S., Facchin, B. M., Luz, A. B., Vicente, G., Faqueti, L. G., et al. (2016). Beneficial Effect of *Ageratum Conyzoides* Linn (Asteraceae) upon Inflammatory Response Induced by Carrageenan into the Mice Pleural Cavity. *J. Ethnopharmacol* 194, 337–347. doi:10.1016/j.jep.2016.09.003

Vijayaraj, R., and Kumaran, N. S. (2018). Protective Effect of *Lawsonia Inermis* Linn. On Chronic Inflammation in Rats. *Int. J. Green Pharm.* 12 (3), S549–S554.

Wadsworth, T. L., and Koop, D. R. (1999). Effects of the Wine Polyphenolics Quercetin and Resveratrol on Pro-inflammatory Cytokine Expression in RAW 264.7 Macrophages. *Biochem. Pharmacol.* 57 (8), 941–949. doi:10.1016/s0006-2952(99)00002-7

Williams, L. A., O'Connar, A., Latore, L., Dennis, O., Ringer, S., Whittaker, J. A., et al. (2008). The *In Vitro* Anti-denaturation Effects Induced by Natural Products and Non-steroidal Compounds in Heat Treated (Immunogenic) Bovine Serum Albumin Is Proposed as a Screening Assay for the Detection of Anti-inflammatory Compounds, without the Use of Animals, in the Early Stages of the Drug Discovery Process. *West. Indian Med. J.* 57 (4), 327–331.

World Health Organization (1998). *Medicinal Plants in the South Pacific : Information on 102 Commonly Used Medicinal Plants in the South Pacific*. Manila: WHO Regional Office for the Western Pacific.

World Health Organization (2013). *WHO Traditional Medicine Strategy: 2014-2023*. Geneva: World Health Organization.

Xu, L. P., Wang, H., and Yuan, Z. (2008). Triterpenoid Saponins with Anti-inflammatory Activity from *Codonopsis Lanceolata*. *Planta Med.* 74 (11), 1412–1415. doi:10.1055/s-2008-1081318

Yesmin, S., Paul, A., Naz, T., Rahman, A. B. M. A., Akhter, S. F., Wahed, M. I. I., et al. (2020). Membrane Stabilization as a Mechanism of the Anti-inflammatory Activity of Ethanolic Root Extract of Choi (*Piper Chaba*). *Clin. Phytosci* 6 (1), 59. doi:10.1186/s40816-020-00207-7

Yong, K. Y., and Abdul Shukkoor, M. S. (2020). *Manilkara Zapota*: A Phytochemical and Pharmacological Review. *Mater. Today Proc.* 29, 30–33. doi:10.1016/j.matpr.2020.05.688

Yong, Y. K., Sulaiman, N., Hakim, M. N., Lian, G. E., Zakaria, Z. A., Othman, F., et al. (2013a). Suppressions of Serotonin-Induced Increased Vascular Permeability and Leukocyte Infiltration by *Bixa Orellana* Leaf Extract. *Biomed. Res. Int.* 2013, 463145. doi:10.1155/2013/463145

Yong, Y. K., Zakaria, Z. A., Kadir, A. A., Somchit, M. N., Ee Cheng Lian, G., and Ahmad, Z. (2013b). Chemical Constituents and Antihistamine Activity of *Bixa Orellana* Leaf Extract. *BMC Complement. Altern. Med.* 13, 32. doi:10.1186/1472-6882-13-32

Yu, S. J., Yu, J. H., Yu, Z. P., Yan, X., Zhang, J. S., Sun, J. Y., et al. (2020). Bioactive Terpenoid Constituents from *Eclipta Prostrata*. *Phytochemistry* 170, 112192. doi:10.1016/j.phytochem.2019.112192

Yuan, M., Zhang, C., He, Z., Liu, C., and Li, K. (2019). Anti-inflammatory Effect and Chemical Constituents of *Microcos Paniculata* Total Flavone Glycosides Fraction. *IOP Conf. Ser. Earth Environ. Sci.* 332, 032018. doi:10.1088/1755-1315/332/3/032018

Yusoff, S. a. M., Asmawi, M. Z., Abdul Majid, S., Asif, M., Basheer, M. K. A., Mohamed, S. K., et al. (2017). Anti-angiogenesis as a Possible Mechanism of Action for Anti-tumor (Potential Anti-cancer) Activity of *Crinum asiaticum* Leaf Methanol Extract. *J. Angiotherapy* 1 (1), E012–E017. doi:10.25163/angiotherapy.11000210419100517

Zahan, R., Nahar, L., and Nesa, M. L. (2013). Antinociceptive and Anti-inflammatory Activities of Flower (*Alangium Salvifolium*) Extract. *Pak J. Biol. Sci.* 16 (19), 1040–1045. doi:10.3923/pjbs.2013.1040.1045

Ziadlou, R., Barbero, A., Martin, I., Wang, X., Qin, L., Alini, M., et al. (2020). Anti-inflammatory and Chondroprotective Effects of Vanillic Acid and Epimedin C in Human Osteoarthritic Chondrocytes. *Biomolecules* 10 (6), 932. doi:10.3390/biom10060932

Zou, L., Zhang, Y., Li, W., Zhang, J., Wang, D., Fu, J., et al. (2017). Comparison of Chemical Profiles, Anti-inflammatory Activity, and UPLC-Q-TOF/MS-based Metabolomics in Endotoxic Fever Rats between Synthetic Borneol and Natural Borneol. *Molecules* 22 (9), 1446. doi:10.3390/molecules22091446

Conflict of Interest: The author declares that the research was conducted in the absence of any commercial or financial relationships that could be construed as a potential conflict of interest.

Publisher's Note: All claims expressed in this article are solely those of the authors and do not necessarily represent those of their affiliated organizations, or those of the publisher, the editors, and the reviewers. Any product that may be evaluated in this article, or claim that may be made by its manufacturer, is not guaranteed or endorsed by the publisher.

GLOSSARY

ADA adenosine deaminase
AA arachidonic acid
AP-1 activator protein-1
BSA bovine serum albumin
CD cluster of differentiation
COX cyclooxygenase
ELISA enzyme-linked immunosorbent assay
ERK extracellular signal–regulated kinase
FCA Freund's' complete adjuvant
GC-MS gas chromatography–mass spectroscopy
GI gastrointestinal
HETE hydroxyleicosatetraenoic acid
IBD inflammatory bowel disease
ICAM-1 intercellular adhesion molecule-1
IκB inhibitory κB
IL interleukin
INF-γ interferon-γ
IP intraperitoneal
JAK Janus kinase
JNK c-Jun-N-terminal kinase
LOX lipoxygenase
LC_{50} lethal concentration
LD_{50} lethal dose
LTB4 leukotriene B4
LTC4 leukotriene C4
LPS lipopolysaccharide
MMP matrix metalloproteinase
MAPKs mitogen-activated protein kinases
MPO myeloperoxidase
NF-κB nuclear factor-κB
ng nanogram
NO nitric oxide
NSAIDs nonsteroidal anti-inflammatory drugs
PAF platelet-activating factor
PKC protein kinase C
PLA2 phospholipase A2
PBMCs peripheral blood mononuclear cells
PGE2 prostaglandin E2
P.O. per oral
RBC red blood cell
RNS reactive nitrogen species
ROS reactive oxygen species
SAIDs steroidal anti-inflammatory drugs
SOD superoxide dismutase
STAT signal transducer and activator of transcription
TNF-α tumor necrosis factor-α
TPA 12-O-tetradecanoylphorbol-13-acetate
TXA2 thromboxane A2
VCAM-1 vascular cell adhesion molecule-1

frontiers | Frontiers in Pharmacology

ORIGINAL RESEARCH
published: 13 May 2022
doi: 10.3389/fphar.2022.819826

Ilex rotunda Thunb Protects Against Dextran Sulfate Sodium-Induced Ulcerative Colitis in Mice by Restoring the Intestinal Mucosal Barrier and Modulating the Oncostatin M/Oncostatin M Receptor Pathway

Yao Li[1], Xu Yang[1], Jia-ni Yuan[2], Rui Lin[3], Yun-yuan Tian[4], Yu-xin Li[1], Yan Zhang[1], Xu-fang Wang[1], Yan-hua Xie[1], Si-wang Wang[1]* and Xiao-hui Zheng[1]**

[1]The College of Life Sciences, Northwest University, Xi'an, China, [2]Air Force Hospital of Western Theater Command, Chengdu, China, [3]Department of Pharmacy, Xijing Hospital, Xi'an, China, [4]Department of Chinese Materia Medica and Natural Medicines, Air Force Medical University, Xi'an, China

Ilex rotunda Thunb (IR) is a traditional Chinese medicine used for the clinical treatment of gastric ulcers and duodenal ulcers; however, the effect of IR on ulcerative colitis (UC) and its underlying mechanism remains unclear. This study investigated the therapeutic effect of IR on UC mice induced by dextran sulfate sodium (DSS) as well as the potential underlying mechanism. The main components of IR were analyzed by ultra-performance liquid chromatography-quadrupole time-of-flight mass spectrometry. Then we established a model of UC mice by administering 2.0% DSS for 7 days followed by 2 weeks of tap water for three cycles and administered IR. On day 56, the disease activity index (DAI), colon length, pathological changes, and inflammatory response of the colon tissue of mice were assessed. The oxidative stress and apoptosis of colon tissue were detected, and the integrity of the intestinal mucosal barrier was evaluated to assess the effect of IR. Furthermore, the relationship between oncostatin M (OSM) and its receptor (OSMR) in addition to the IR treatment of UC were evaluated using a mouse model and Caco2 cell model. The results showed that IR significantly alleviated the symptoms of UC including rescuing the shortened colon length; reducing DAI scores, serum myeloperoxidase and lipopolysaccharide levels, pathological damage, inflammatory cell infiltration and mRNA levels of interleukin one beta, tumor necrosis factor alpha, and interleukin six in colon tissue; alleviating oxidative stress and apoptosis by decreasing kelch-like ECH-associated protein 1 expression and increasing nuclear factor-erythroid factor 2-related factor 2 and heme oxygenase-1 protein expression; and promoting the regeneration of epithelial cells. IR also promoted the restoration of the intestinal mucosal barrier and modulated the OSM/OSMR pathway to alleviate UC. It was found that IR exerted therapeutic effects on UC by restoring the intestinal mucosal barrier and regulating the OSM/OSMR pathway.

Keywords: *Ilex rotunda thunb*, ulcerative colitis, inflammation, intestinal mucosal barrier, OSM/OSMR pathway

OPEN ACCESS

Edited by:
Enkelejda Goci,
Aldent University, Albania

Reviewed by:
Bang xing Han,
West Anhui University, China
Antonella Fazio,
University Medical Center Hamburg-Eppendorf, Germany
Olatunde Farombi,
University of Ibadan, Nigeria

****Correspondence:***
Yan-hua Xie
1987743525@qq.com
Si-wang Wang
wangsiw@nwu.edu.cn
Xiao-hui Zheng
zhengxh318@nwu.edu.cn

Specialty section:
This article was submitted to Ethnopharmacology, a section of the journal Frontiers in Pharmacology

Received: *22 November 2021*
Accepted: *26 April 2022*
Published: *13 May 2022*

Citation:
Li Y, Yang X, Yuan J-n, Lin R, Tian Y-y, Li Y-x, Zhang Y, Wang X-f, Xie Y-h, Wang S-w and Zheng X-h (2022) Ilex rotunda Thunb Protects Against Dextran Sulfate Sodium-Induced Ulcerative Colitis in Mice by Restoring the Intestinal Mucosal Barrier and Modulating the Oncostatin M/Oncostatin M Receptor Pathway. Front. Pharmacol. 13:819826. doi: 10.3389/fphar.2022.819826

INTRODUCTION

Ulcerative colitis (UC) is an inflammatory bowel disease (IBD) with a complex etiology involving the interaction of genetic susceptibility, environmental factors, intestinal microbial disorders, and dysregulated immune responses (Adams and Bornemann, 2013). The occurrence of UC affects the quality of patients' life and health. More than 80% of patients experience fatigue, weakness, and exhaustion during disease episodes; more than half of patients have their work and studies affected by IBD; and even the fertility of some female patients is affected (Kim et al., 2017; Clark-Snustad et al., 2020; Truta, 2021). Epidemiological investigation has suggested that the incidence of IBD is increasing in countries such as Africa, Asia, and South America with the economic development and changing lifestyles (Ng et al., 2017). The annual percentage change of UC in Brazil and Taiwan has increased by 14.9 and 4.8%, respectively (Ng et al., 2017). The average incidence of IBD was 14,000 per 100,000 in Asia in 2011, and the incidence of UC was twice that of Crohn's disease (Du and Ha, 2020). Although the incidence of IBD is stabilizing in Western countries, the burden remains high because the prevalence still exceeds 0.3% (Sairenji et al., 2017). Currently, the medications for UC include 5-aminosalicylic acid (5-ASA), hormones, immunosuppressants, and biologics. 5-ASA drugs are the first-line treatment for mild to moderate UC (de Chambrun et al., 2018). Furthermore, corticosteroids are an option for patients who fail to achieve remission with 5-ASA. Anti-tumor necrosis factor alpha (TNF-α) drugs such as infliximab are considered for patients who do not respond to corticosteroid therapy (Effinger et al., 2020). Despite considerable advances in the recognition and treatment of UC, the use of 5-ASA drugs such as mesalazine is still accompanied by a series of adverse events including inflammatory reactions, pancreatitis, cardiotoxicity, hepatotoxicity, musculoskeletal complaints, respiratory symptoms, nephropathies and sexual dysfunction (Sehgal, et al., 2018). The incidence of adverse reactions of biological agents such as infliximab is 10.5%, and more than 40% of patients do not respond to infliximab treatment in clinical practice (Danese et al., 2015; Danese et al., 2019). Thus, there is a need for research and innovation into preventive and therapeutic drugs for UC.

The dried bark of *Ilex rotunda Thunb* (IR) of the family *Aquifoliaceae* with the name "Jiubiying" has been included in the "Chinese Pharmacopoeia," and has heat-clearing and detoxifying effects, removes dampness, and relieves pain (Wang et al., 2014). It is used for the treatment of damp-heat diarrhea, abdominal pain, and bloating in traditional clinical applications. The chemical components of IR are triterpenes and their glycosides, steroids, and aromatics (Kim et al., 2012). And, triterpenes and their glycosides and aromatic compounds have the highest content in IR (Kim et al., 2012). The "Chinese Pharmacopoeia," of 2020 specifies pedunculoside and syringin as quality-controlled components of IR, and requires their content to be ≥1.0% and ≥4.5%, respectively. Pedunculoside can prevent collagen-induced arthritis and dextran sulfate sodium (DSS)-induced acute UC (Ma et al., 2019; Liu et al., 2020). Syringin can inhibit LPS- or DSS-induced acute UC by inhibiting the activation of nuclear factor kappa B (NF-κB) and nuclear factor-erythroid factor 2-related factor 2 (Nrf2) (Zhang et al., 2020). Furthermore, previous studies have shown that rotundic acid derived from IR can treat non-alcoholic steatohepatitis, lipopolysaccharide (LPS)-induced lung damage, and colitis-related cancer (Han et al., 2019; Li X. X. et al., 2021; Liu et al., 2021). In addition, the triterpenoids in IR have anti-platelet aggregation effects (Yang et al., 2018); however, the preventive and therapeutic effects of IR and its underlying mechanism of action in chronic UC mice remain unclear. Therefore, in this study, we investigated the therapeutic effects of IR in mice with chronic UC, and illustrated the mechanisms of action related to restoration of intestinal mucosal barrier and regulation of the OSM/OSMR pathway.

MATERIALS AND METHODS

Extract of *Ilex rotunda Thunb*

The raw herb of IR was purchased from Xi'an Traditional Chinese Herbal Medicine Co. Ltd. (Batch No: 20200118; Xi'an, China) and was identified by associate chief pharmacist Ling-bian Sun. IR samples (500 g) were extracted twice with water, first with 4 L of water for 2 h and then with 3 L of water for 1 h. Then the two filtrates were combined and concentrated and dried with a high-speed centrifugal spray dryer (HSD-8; Shanghai Universal Pharmaceutical Machinery Co., Ltd., Shanghai, China).

Characterization of *Ilex rotunda Thunb* by Ultra-Performance Liquid Chromatography-Quadrupole Time-of-Flight Mass Spectrometry

The IR samples were separated and analyzed using the Waters I-Class VION IMS QTOF system coupled with the ACQUITY UPLC BEH C_{18} column (1.7 μm, 2.1 × 50 mm; Waters Co., Wilmslow, UK). The column temperature was 35°C, the flow rate was 0.4 ml/min, and the injection volume was 2 μl. Ultrapure water with 0.01% formic acid (A) and methanol (B) served as the mobile phase, and the gradient elution program was as follows: 0–3 min, 5–24% B; 3–5 min, 24–52% B; 5–10 min, 52–66% B; 10–15 min, 66–80% B. The electrospray ionization (ESI) source was combined with a mass spectrometer (ESI-QTOF-MS) to complete the mass spectrometry detection, and both positive and negative ions served as the ion scanning mode. The capillary voltage was 2.0 Kv. Nitrogen was used as the drying gas and atomizing gas, the temperature and flow rate of the drying gas were 500°C and 13 L/min, respectively, the scanning speed was 0.2 s, and the leucine enkephalin solution was used as an external standard to calibrate the relative molecular mass. Argon was used as the collision gas with a flow rate of 0.8 L/min, and the CID was cracked. The mass scanning range was 50–2000 Da. Data collection and processing were carried out with the Waters UNIFI Scientific Information System. The external standard method was used to quantify the quality control components (pedunculoside, syringin) of IR. Linear regression for the calibration curve and the value of the coefficient of

TABLE 1 | DAI scoring standards of UC mice.

Weight loss (%)	Stool morphology	Hematochezia	Score
0	Normal	Normal	0
1–5	Loose stools	Positive occult blood	1
5–10	Loose stools	Visible mild bloody stools	2
10–15	Mucous stools	Visible bloody stools	3

determination were y = 40130x + 5221, y = 10600x + 6805; and R^2 = 0.9948, R^2 = 0.9902. Finally, the IR (0.4 mg) was dissolved in 50% methanol (1 ml), sonicated for 30 min, and passed through a 0.22 μm filter for quantification.

Animal Treatment

Sixty specific pathogen-free C57BL/6 J male mice, weighing 21–24 g, were obtained from the Air Force Medical University Experimental Animal Center (Xi'an, China). All animal experimental procedures were approved by the Laboratory Animal Welfare and Ethics Committee of Air Force Medical University (No. 20191206). Mice were randomly divided into six groups with 10 mice, including control, DSS, IR-0.45 g/kg, IR-0.9 g/kg, and IR-1.8 g/kg, and positive control (balsalazide; Hubei Baikehendi Pharmaceutical Company, Hubei, China) groups. The control group drank tap water and the other five groups drank 2.0% DSS [molecular weight (MW): 36,000–50,000; MP Biomedicals, LLC, Irvine, CA, United States] for 7 days followed by 2 weeks of tap water as one cycle, which was repeated for three cycles. The last cycle of drinking tap water for 2 weeks was adjusted to 1 week (Wirtz et al., 2017). At the beginning of the second modeling cycle, mice in the IR-0.45 g/kg, IR-0.9 g/kg, and IR-1.8 g/kg groups were gavaged with IR at 0.45, 0.9, and 1.8 g/kg, respectively, and the positive control group was given balsalazide at 3.4 g/kg. The dosage of balsalazide was calculated based on the human clinical dosage (mouse dosage = human daily dosage/60 kg body weight × 9.1) (Wei, 2002). During the treatment period, the body weight of mice was measured and recorded daily. The specific experimental steps are shown in **Figure 2A**.

Disease Activity Index Score

The behavioral state and stool morphology of the mice were observed, and the disease activity index (DAI) score was evaluated by comprehensively scoring the degree of weight loss, stool characteristics and morphology, and state of hematochezia. The detailed scoring criteria are shown in **Table 1** (Zhou et al., 2020).

Histopathology Analysis

Hematoxylin and eosin staining (H & E) was used to evaluate the histopathological changes of the colon. The colon tissue was fixed in paraformaldehyde, dehydrated, and embedded in a paraffin block. After the sections were cut into 3–5 μm slices, H & E staining was performed and sections were observed under a microscope at ×40 and ×200 magnifications. Histopathological scoring was previously reported for the degree of inflammatory cell infiltration, crypt destruction, and scope of the lesion (Zhang et al., 2018).

Blood Routine Examination

Blood (50 μl) was collected from the venous plexus of the fundus and placed in a 0.5 ml tube with EDTA anticoagulation. Then it was analyzed with a fully automatic hematology analyzer to detect white blood cells (WBCs), red blood cells (RBCs), and hemoglobin (HGB) in the whole blood.

Quantitative Polymerase Chain Reaction Analysis

Total RNA from colon tissue was extracted using a Total RNA Kit (Omega Bio-Tek, Inc., Guangzhou, China). cDNA was synthesized by QuantiNova SYBR Green PCR Kit (Qiagen, Germany). Then the cDNA was used to determine the mRNA levels of IL-1β, TNF-α, and IL-6 through quantitative polymerase chain reaction (qPCR). β-actin was used as an internal control. The primer sequences used for qPCR were designed by Shanghai Sangon Biotech Co., Ltd. (Shanghai, China) and are shown in **Supplementary Table S1**.

Detection of Serum Lipopolysaccharide

An enzyme-linked immunosorbent assay (ELISA) kit for LPS (Cloud-Clone Co., Houston, TX, United States) was employed to detect the concentration of LPS in the serum of mice. According to the instructions, six concentration standards were diluted and 50 μl of each dilution of standard, blank, and samples was added to the pre-coated 96-well plate. Then 50 μl Detection Reagent A was immediately added to each well and incubated for 1 h at 37°C. Each well was washed with 350 μl of ×1 Wash Solution, followed by the addition of 100 μl Detection Reagent B and incubation for 30 min at 37°C. The wash process was repeated and then 90 μl Substrate Solution was added to each well and incubated for 10–20 min at 37°C, followed by the addition of 50 μl Stop Solution and measurement by a microplate reader at 450 nm.

Detection of Serum Myeloperoxidase

Myeloperoxidase (MPO) content was closely related to the severity of UC. The Mouse MPO ELISA Kit was used to detect the content of MPO in the serum of mice according to the manufacturer's instructions (MultiSciences (Lianke) Biotech Co., Ltd., China).

Detection of Serum Fluorescein Isothiocyanate

At the end of the experiment, mice were gavaged with 0.6 mg/g fluorescein isothiocyanate (FITC)-dextran (MW: 40 kDa; TdB Labs AB, Uppsala, Sweden), and blood was collected from the venous plexus of the fundus of the mouse after 4 h. The serum FITC content was measured by a fluorescence microplate reader.

Alcian Blue Staining

The paraffin slides of the colon tissue were dewaxed and stained with Alcian blue dye solution A for 10–15 min. After washing with tap water, the slides were stained with Alcian blue dye solution B for 3 min. The slides were observed under ×100 magnification.

Terminal Deoxynucleotidyl Transferase dUTP Nick-End Labeling Analysis

Proteinase K working solution was added to the paraffin slides and incubated at 37°C for 25 min, followed by permeabilization and equilibrium at room temperature. Take appropriate amount of terminal deoxynucleotidyl transferase enzyme, dUTP, and buffer in the terminal deoxynucleotidyl transferase dUTP nick-end labeling (TUNEL) kit were mixed at a 1:5:50 ratio and incubated on the tissue at 37°C for 2 h. The nucleus was stained with DAPI. The excitation was measured at 465–495 nm and the emission was measured at 515–555 nm with a fluorescence microscope (Nikon).

Detection of Oxidative Stress Indexes

Colon tissues was fully homogenized with extraction reagent on ice, centrifuged at 8000 g for 10 min to separate the supernatant, and the protein concentration was determined by BCA quantitative kit. Then the glutathione (GSH), oxidized glutathione (GSSG), and malondialdehyde (MDA) levels were measured by micro GSH assay kit, micro GSSG assay kit, and MDA assay kit according to the instructions, respectively (Solarbio Science and Technology, Beijing, China). Then the GSH/GSSG ratio was calculated.

Immunohistochemical Analysis

After antigen retrieval, paraffin sections were blocked in bovine serum albumin for 30 min and incubated overnight at 4°C with primary antibodies against E-cadherin and Ki-67 (Servicebio, Wuhan, China). After washing slides three times with phosphate-buffered saline, slides were incubated with horseradish peroxidase-labeled secondary antibody in the dark for 50 min followed by the addition of DAB for color development and microscopy (Nikon).

Cell Culture

The Caco2 cell line was obtained from Xijing Hospital of Digestive Diseases (Shaanxi, China), cultured in high-glucose Dulbecco's modified Eagle medium (DMEM) (Meilunbio, Beijing, China) medium supplemented with 10% fetal bovine serum and 1% penicillin-streptomycin antibiotics, and maintained at 37°C in 5% CO_2.

Cell Viability Assay

Cell Counting Kit-8 (CCK-8) (Glpbio, Montclair, CA, United States) was used to detect cell viability. Briefly, 100 μl Caco2 cell suspension (5×10^4 cells/ml) was added to each well of a 96-well plate and cultured overnight. Then DMEM was replaced with a medium containing different concentrations of IR or LPS and incubated for 12, 24, and 48 h. Then 10 μl CCK-8 per 100 μl DMEM was added to the wells and incubated at 37°C for 2 h. The absorbance was detected at 450 nm.

Establishment of Colitis Cell Model

Caco2 cells (1×10^6 cells/well) were seeded in 6-well plates and cultured overnight. The culture medium was replaced with a medium containing 1 μg/ml LPS (Sigma-Aldrich, St. Louis, MO, United States). After incubating for 4, 8, 12, and 24 h, total cell protein was extracted, and the protein expression of oncostatin M (OSM), OSM receptor (OSMR), and IL-6 was detected by western blot analysis to determine the best modeling time.

Western Blot Analysis

Proteins from the colon tissues of mice or Caco2 cells were separated by sodium dodecyl sulfate-polyacrylamide gel electrophoresis and electro transferred to PVDF membranes. Then membranes were blocked in 5% non-fat milk and incubated overnight at 4°C with the following primary antibodies: anti-signal transducer and activator of transcription 3 (STAT3) (WL01836; Wanleibio, Shenyang, China), anti-phosphorylated STAT3 (p-STAT3) (#9145; Cell Signaling Technology, Danvers, MA, United States), anti-IL-6 (WL02841; Wanleibio), anti-Keap-1 (WL03285; Wanleibio), anti-Nrf2 (WL02135; Wanleibio), anti-heme oxygenase 1 (HO-1) (WL02400; Wanleibio), anti-zonula occludens-1 (ZO-1) (WL03419; Wanleibio), anti-occludin (WL01996; Wanleibio), anti-claudin-1 (WL03073; Wanleibio), anti-OSM (PA5-81453; Invitrogen, Carlsbad, CA, United States), and anti-OSMR (ab210771; abcam, Cambridge, MA, United States); anti-β-actin (AT0001; Engibody Biotechnology, Inc., Milwaukee, United States) served as the internal control. Then membranes were incubated with the appropriate secondary antibody for 1 h at room temperature. The intensity of each band was scanned by the ChemiDoc™XRS+ Imaging System and analyzed with ImageJ software.

Statistical Analyses

Data were analyzed using SPSS 23.0 software (IBM SPSS Statistics, Armonk, NY, United States). One-way analysis of variance was performed with equal variances; otherwise, nonparametric tests were performed. The data are presented as the mean ± standard deviation, with $p < 0.05$ considered significantly different.

RESULTS

Chemical Analyses of *Ilex rotunda Thunb*

The components of IR were analyzed by ultra-performance liquid chromatography-quadrupole time-of-flight mass spectrometry.

(UPLC-QTOF-MS.). The total ions chromatogram (TIC) in positive ion mode is shown in **Figure 1**. Combining the literature and mass spectrometry MS information including molecular weight and fragment ion peaks, we have confirmed a total of 23 components in IR, and the results were shown in (**Table 2**.). In addition, pedunculoside and syringin as the quality control components of IR were quantified by external standard quantitative analysis, and the contents of pedunculoside and syringin were 18.8 μg/mg and 6.5 μg/mg, respectively.

Ilex rotunda Thunb Significantly Improves the Symptoms of Dextran Sulfate Sodium-Induced Ulcerative Colitis

After drinking 2% DSS combined with tap water for three cycles, compared with the control group, the body weight of the mice in

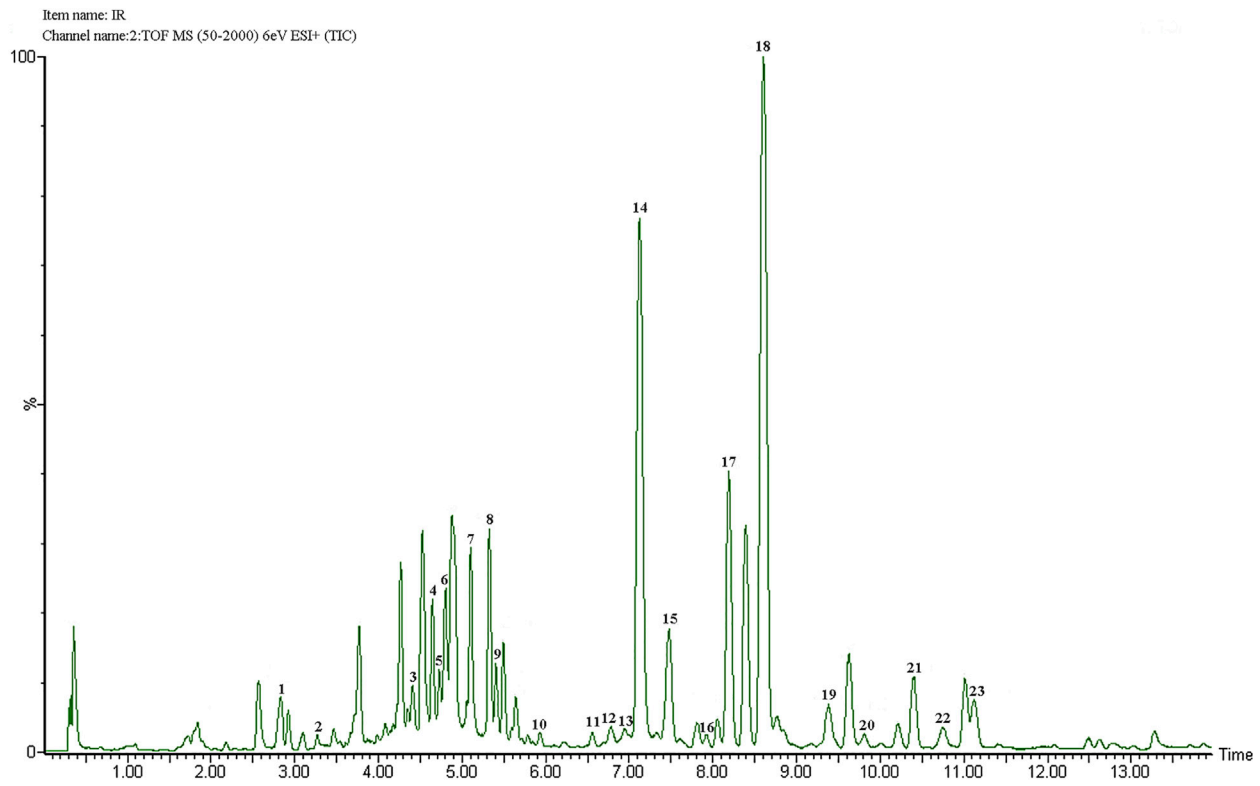

FIGURE 1 | TIC of IR in positive ion mode.

the DSS group was reduced, and the difference was statistically significant since day 29 of modeling ($p < 0.01$; **Figure 2C**). The body weight of mice in the IR-1.8 g/kg group and balsalazide group was higher than that of the DSS group on days 51 and 52 ($p < 0.05$), but IR-0.45 g/kg and IR-0.9 g/kg did not improve the body weight of the UC mice ($p > 0.05$; **Figure 2C**). The DAI score is an important indicator for evaluating the success of the UC model. Compared with the control group, the DAI score of mice in the DSS group was increased ($p < 0.01$). On day 49, the mucopurulent bloody stool was obvious (**Figure 2B**). By day 56, although the weight had rebounded, the bloody stool still existed, indicating that the chronic UC model was successfully established. Compared with the DSS group, IR improved the bloody stool of UC mice and reduced the DAI score, with statistical significance between the IR-0.9 and IR-1.8 g/kg groups ($p < 0.05$ and $p < 0.01$, respectively; **Figure 2B**). We found that the colon length was shortened, and the spleen, lung, and brain coefficients were increased in the DSS group compared to the control group on day 56 (**Figures 2D–H**). Administration of IR reversed all of these effects in a dose-dependent manner (**Figures 2D–H**). In the balsalazide group, the liver coefficient of mice was higher than that of the control group when it exerted therapeutic effects on UC mice, which suggests that it may cause liver damage during long-term use (**Figure 2I**). We also observed the preventive and therapeutic effects of IR on acute UC mice and found that IR improved the weight loss and colon shortening of acute UC mice in a dose-dependent manner; and reduced the DAI score and spleen, lung, and brain coefficients (**Supplementary Figure S1**).

Ilex rotunda Thunb Alleviates the Inflammation of Dextran Sulfate Sodium-Induced Ulcerative Colitis Mice

Histopathological examination showed that the colon cells of the control group were tightly arranged, with no pathological changes. In the DSS group, we observed that the tissue structure was disordered, the inflammatory cells infiltrated into the muscle layer, the goblet cell numbers were reduced, and the crypts disappeared accompanied by submucosa edema (**Figures 3A,B,D**). Compared with the DSS group, the IR-0.45 g/kg group had partial recovery of the colon structure and increased goblet cells and submucosal edema, but it had more areas of inflammatory cell infiltration. The colons of mice in the IR-0.9 g/kg, IR-1.8 g/kg, and balsalazide groups were infiltrated with few inflammatory cells, and the tissue structure was restored (**Figures 3A,B,D**, **Supplementary Figure S2A**). MPO is positively correlated with the inflammatory response of UC. Detection of the MPO in the serum showed that compared with the control group, the MPO content of mice in the DSS group was increased ($p < 0.01$; **Figure 3C**). After treatment with different dosages of IR, the MPO in the serum of UC mice was reduced in a dose-dependent manner ($p < 0.05$ or $p < 0.01$; **Figure 3C**). Routine blood analysis found that the number of

TABLE 2 | Main components of IR identified by UPLC-QTOF-MS.

No	t_R (min)	Measured (m/z)	Error (ppm)	Formula	Fragment ions (m/z)	Identification
1	2.83	372	1.5	$C_{17}H_{24}O_9$	353.1294, 193.1090, 163.0585, 161.0795	Syringin
2	3.27	370	3.6	$C_{17}H_{22}O_9$	209.1069, 177.0772	Sinapaldehyde glucoside
3	4.41	426	2.9	$C_{20}H_{26}O_{10}$	325.1310, 163.0585	Caffeic acid (1-hydroxyl-4-O-β-D-glucopyranosylprenyl)-ester
4	4.65	580	1.2	$C_{28}H_{36}O_{13}$	573.2634, 402.2126, 401.2088, 383.1967, 330.1488	(-)-Syringaresinol-4-O-beta-D-glucopyranoside
5	4.72	640	3.2	$C_{29}H_{36}O_{16}$	581.2554, 559.2475, 479.2119, 443.1870, 277.1040, 263.1234, 163.0601	Kelampayoside B
6	4.81	426	5.1	$C_{20}H_{26}O_{10}$	247.1272	4-caffeoyl-3-methyl-but-2-ene-1,4-diol 1-O-β-D-glucopyranoside
7	5.11	604	–2.6	$C_{35}H_{56}O_8$	340.2998, 279.2770	3β-[(α-L-arabinopyanosyl) oxy]-19α-hydroxyolean-12-en-28-oic acid
8	5.33	604	–1.3	$C_{35}H_{56}O_8$	425.1754, 397.3508, 396.8493, 263.1234, 163.0585	Ziyuglycoside II
9	5.41	678	–4.1	$C_{37}H_{58}O_{11}$	500.1883, 499.1853, 445.2390	19α,23-dihydroxyurs-12-en-28-oic acid
10	5.94	812	5.1	$C_{42}H_{68}O_{15}$	703.4561, 673.4752, 645.0314, 623.0475, 487.3038, 429.2686, 241.1711	Ilexoside XLI
11	6.57	810	2.5	$C_{42}H_{66}O_{15}$	805.5347, 671.4646, 455.4050, 437.3941, 435.3761	Ilexoside XLVIII
12	6.78	664	4.8	$C_{36}H_{56}O_{11}$	503.3972, 485.3865, 439.3741, 279.1262	Ilexasprellanoside D
13	6.90	780	3.2	$C_{42}H_{68}O_{13}$	671.4613, 641.4467, 451.3751, 398.2888, 376.3059, 282.2395	3-O-β-D-glucopyranosyl-oleanolic acid 28-O-β-D-glucopyranoside
14	7.12	650	0.6	$C_{36}H_{58}O_{10}$	471.4030, 453.3918, 435.3788, 407.3809	pedunculoside
15	7.48	928	2.0	$C_{47}H_{76}O_{18}$	789.5362, 657.4775, 560.3391, 487.2982, 455.4077, 437.3941	Ilexoside K
16	7.92	766	3.9	$C_{41}H_{66}O_{13}$	657.4775, 456.4119, 455.4077, 437.3941	Ziyuglycoside I
17	8.19	650	1.5	$C_{36}H_{58}O_{10}$	471.4030, 453.3918, 435.3788	Ilexoside V
18	8.60	664	0.9	$C_{36}H_{56}O_{11}$	503.3972, 485.3865, 467.3714, 457.3873, 439.3741, 421.36	Ilexsaponin A1
19	9.38	488	2.3	$C_{30}H_{48}O_5$	471.4057, 454.3965, 453.3918, 436.3818, 435.3788,288.3236	Rutundic acid
20	9.82	810	1.8	$C_{42}H_{66}O_{15}$	671.4613, 655.4648, 455.4104, 437.3941, 327.1188, 299.1984, 277.2140	Ilekudinoside B
21	10.40	794	1.8	$C_{42}H_{66}O_{14}$	655.4615, 641.4821, 440.4138, 439.4114, 431.2565, 191.2025	Scheffleside L
22	10.75	488	2.5	$C_{30}H_{48}O_5$	471.4057, 453.3918, 436.3818, 435.3788, 407.3809	Rotungenic acid
23	11.12	502	1.7	$C_{30}H_{46}O_6$	485.3865, 467.3741, 439.3741, 421.3627	Ilexgenin A

WBCs in the whole blood of mice of the DSS group was higher than that of the control group, indicating that the mice had an obvious inflammatory response (**Figure 3E**, **Supplementary Figure S2B**). Administering IR and balsalazide reduced the WBCs of chronic and acute UC mice, and the IR-1.8 g/kg and balsalazide groups were statistically significant compared with the DSS group for the treatment of chronic UC mice (**Figure 3E**, **Supplementary Figure S2B**). In addition, routine blood tests also found that the RBCs and HGB of mice in the DSS group were lower than those in the control group, and IR also increased the RBCs and HGB in the whole blood of chronic and acute UC mice compared with the DSS group (**Figures 3F,G**, **Supplementary Figures S2C,D**).

To further identify the inflammatory response of mice, the mRNA levels of inflammatory cytokines including IL-1β, IL-6, and TNF-α were measured and found to be increased in the DSS group compared with the control group; whereas IL-1β, IL-6, and TNF-α levels were decreased after treatment with IR ($p < 0.05$ or $p < 0.01$) (**Figures 3H–J**, **Supplementary Figures S2E–H**). The detection of inflammatory-related proteins in the colon tissue showed that compared with the control group, the expression of p-STAT3/STAT3 and IL-6 proteins in the DSS group was increased, and IR treatment reduced the expression of p-STAT3/STAT3 and IL-6 proteins in the colon tissue of chronic and acute UC mice ($p < 0.05$ and $p < 0.01$, respectively) (**Figures 3K–M**, **Supplementary Figures S2I–K**). Otherwise, balsalazide could reduce the expression of IL-6 protein in the colon, but did not affect the expression of p-STAT3/STAT3 proteins (**Figures 3K–M**, **Supplementary Figures S2I,K**).

Ilex rotunda Thunb Attenuates the Oxidative Stress and Apoptosis of Colon Tissue in Dextran Sulfate Sodium-Induced Mice

TUNEL and Ki67 staining were employed to evaluate the apoptosis and proliferation of colon tissues. The results showed that compared with the control group, there was a large number of apoptotic cells and fewer proliferating cells in the intestinal epithelium of the DSS group, which was consistent with the destruction of the tissue structure and the appearance of a large number of necrotic areas observed in (**Figures 3**, **4A–D–D**). Compared with the DSS group, mucosal layer proliferating cells were less in IR-0.45 g/kg-treated mice, but plenty of apoptotic cells still existed, while IR-0.9 g/kg and IR-1.8 g/kg and balsalazide treatment reduced colon apoptotic

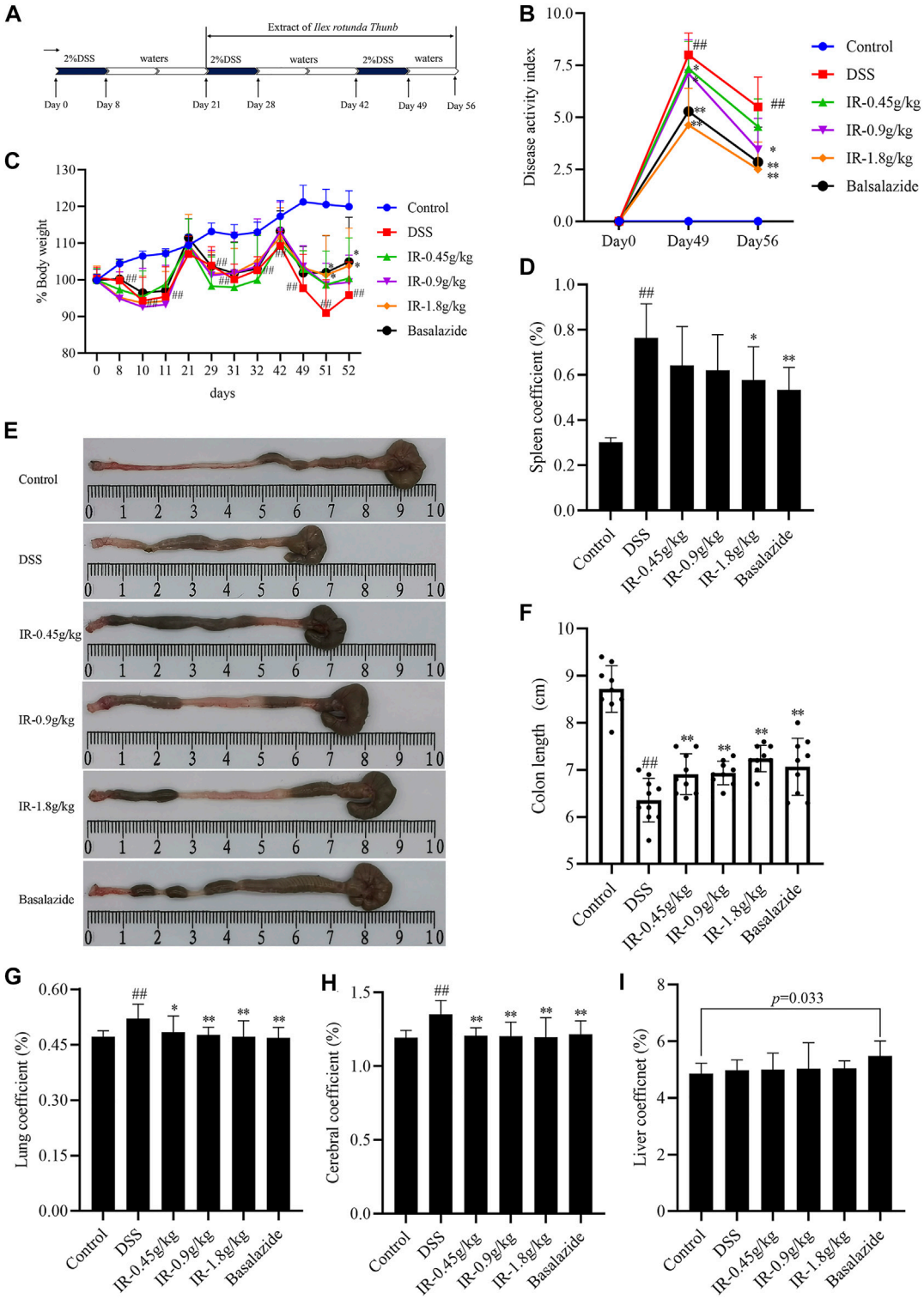

FIGURE 2 | IR alleviates the pathological symptoms of DSS-induced chronic UC mice. **(A)** Experimental design. **(B)** Disease activity index of each group. **(C)** The body weight change of mice in each group during the experiment. **(D)** Spleen coefficient of mice in each group. **(E)** Representative colon images at day 56. **(F)** Statistical graph of colon length. **(G)** Lung coefficient. **(H)** Cerebral coefficient. **(I)** Liver coefficient. All data were compared using one-way ANOVA, and *p*-values reflected differences between experimental groups (n = 9).

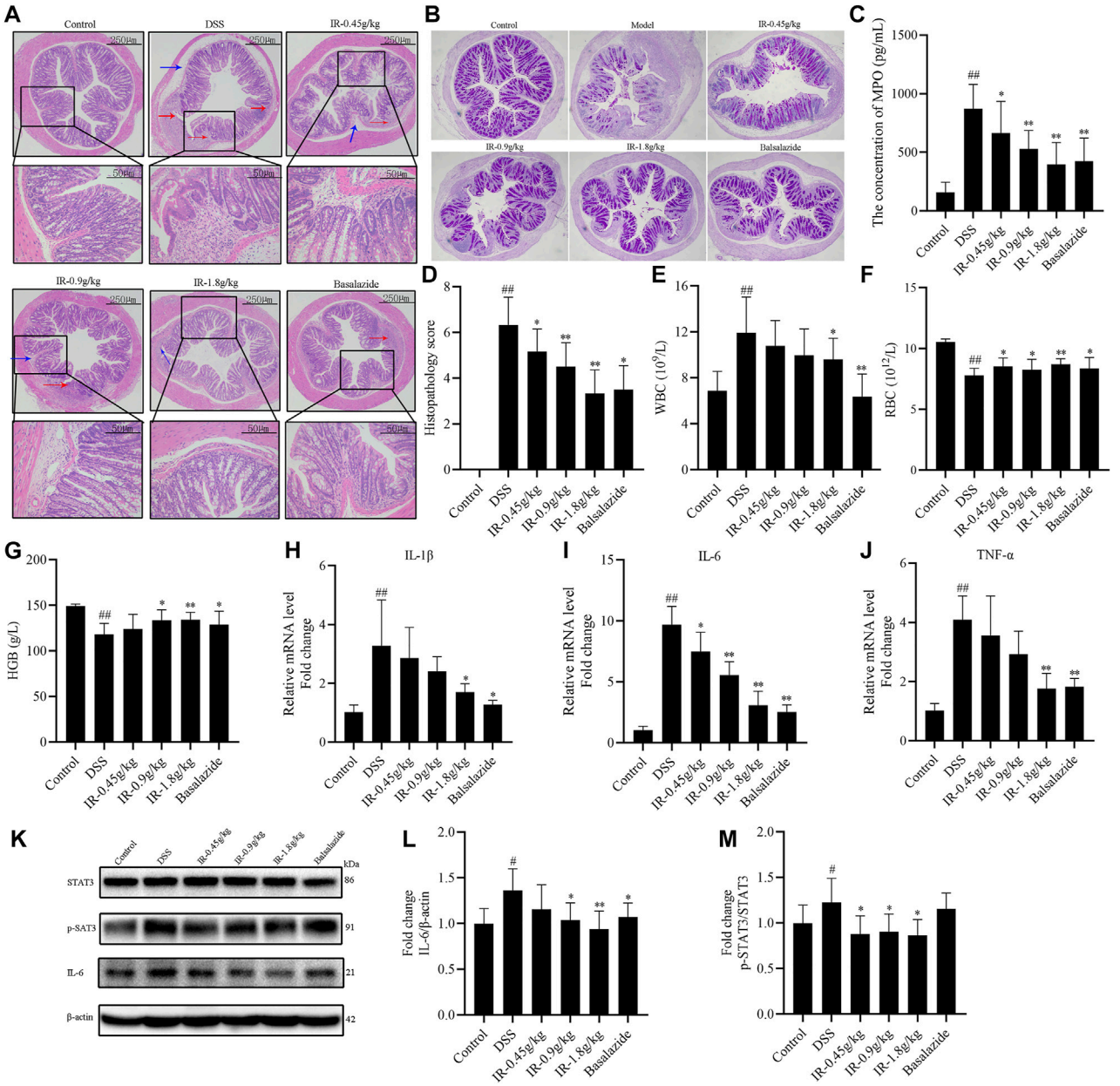

FIGURE 3 | IR suppress inflammation of UC mice. **(A)** Representative H & E staining colon tissue of mice (day 56). **(B)** PAS staining colon tissue of mice (day 56). **(C)** MPO content was measured by ELISA in serum of mice. **(D)** Histopathology scores. **(E)** The number of WBC in each group of mice tested by routine analysis of blood. **(F)** The number of RBC in each group of mice. **(G)** The concentration of HGB in each group of mice tested by routine analysis of blood. **(H–J)** The mRNA levels of IL-1β, IL-6, and TNF-α from the colon of mice. **(K)** The protein levels of STAT3, p-STAT3, and IL-6 in colon detected by western blotting. **(L)** The gray intensity analysis of IL-6. **(M)** The gray intensity analysis of p-STAT3/STAT3. All data were compared using one-way ANOVA, and *p*-values reflected differences between experimental groups.

cells, and promoted the proliferation of mucosal cells (**Figures 4A–D**). The imbalance between oxidation and antioxidation triggers oxidative stress, and excessive oxidative stress can cause inflammatory infiltration of neutrophils and cell necrosis. The intracellular GSH, GSSG, and MDA contents could well reflect the redox state and lipid oxidation level of the organism. The results showed that compared with the control group, the GSH content and GSH/GSSG ratio of colon in mice of DSS group decreased and the MDA content increased significantly, while the GSH content and GSH/GSSG ratio were increased in the colon of mice in IR-0.9 g/kg and IR-1.8 g/kg groups, and the MDA contents decreased, indicating that IR treatment could improve the antioxidant capacity of UC mice and reduce their lipid oxidation levels (**Figures 4E–H**). Furthermore, detecting the expression of oxidative stress-related proteins such as Keap-1, Nrf2, and HO-1

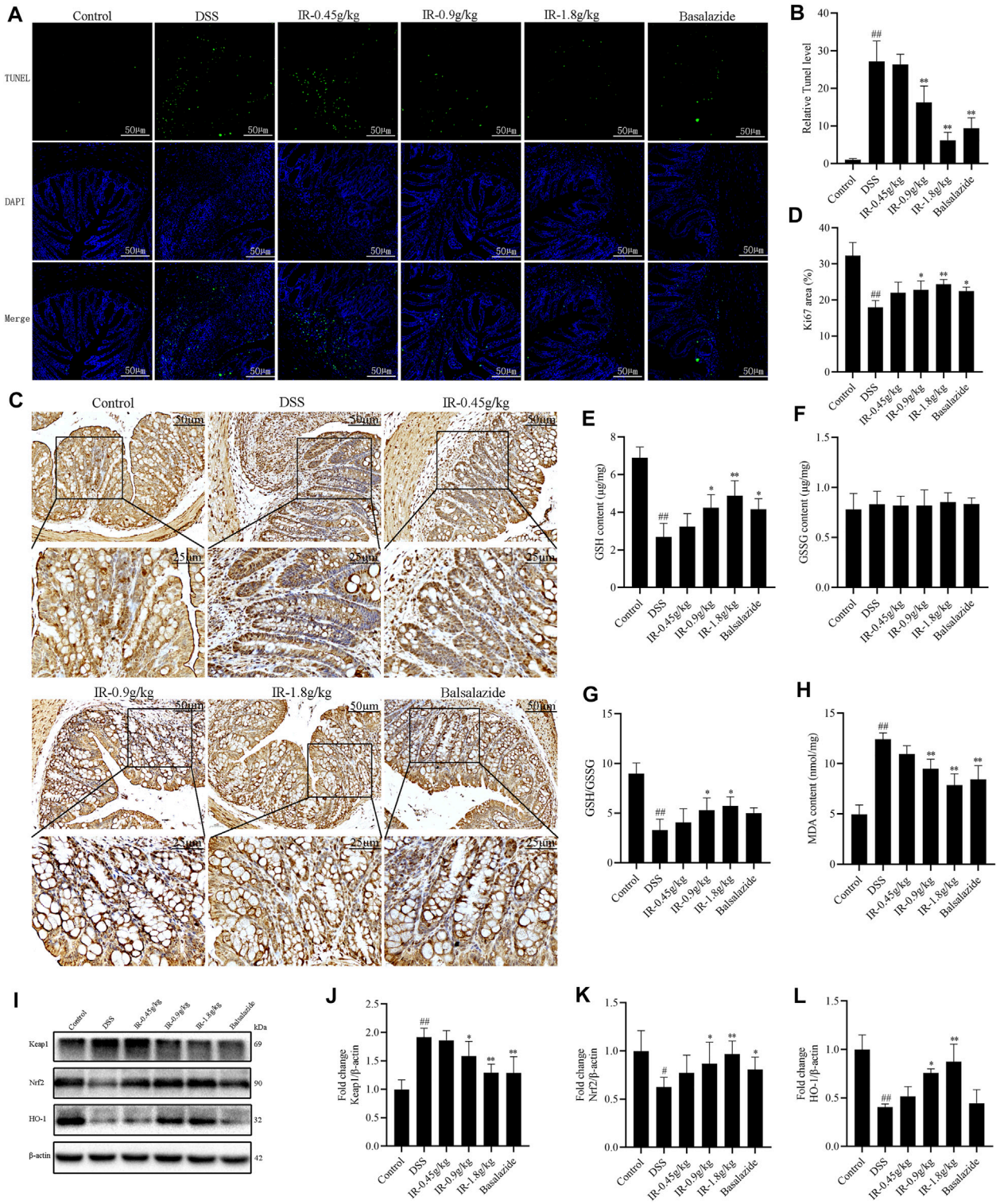

FIGURE 4 | IR alleviates the apoptosis and oxidative stress of colon tissue in UC mice. **(A)** Colon cell apoptosis detected by Tunel staining. **(B)** Positive area statistics of Tunel. **(C)** Colonic epithelial cell proliferation detected by Ki67 staining. **(D)** Histochemical positive area statistics of Ki67. **(E,F)** The content of glutathione (GSH) and oxidized glutathione (GSSG). **(G)** The ratio of GSH/GSSG. **(H)** The content of malondialdehyde (MDA). **(I)** The protein levels of Keap1, Nrf2, and HO-1 in colon detected by western blotting. **(J-L)** The gray intensity analysis of Keap1, Nrf2, and HO-1 proteins, respectively. All data were compared using one-way ANOVA, and *p*-values reflected differences between experimental groups (n = 3).

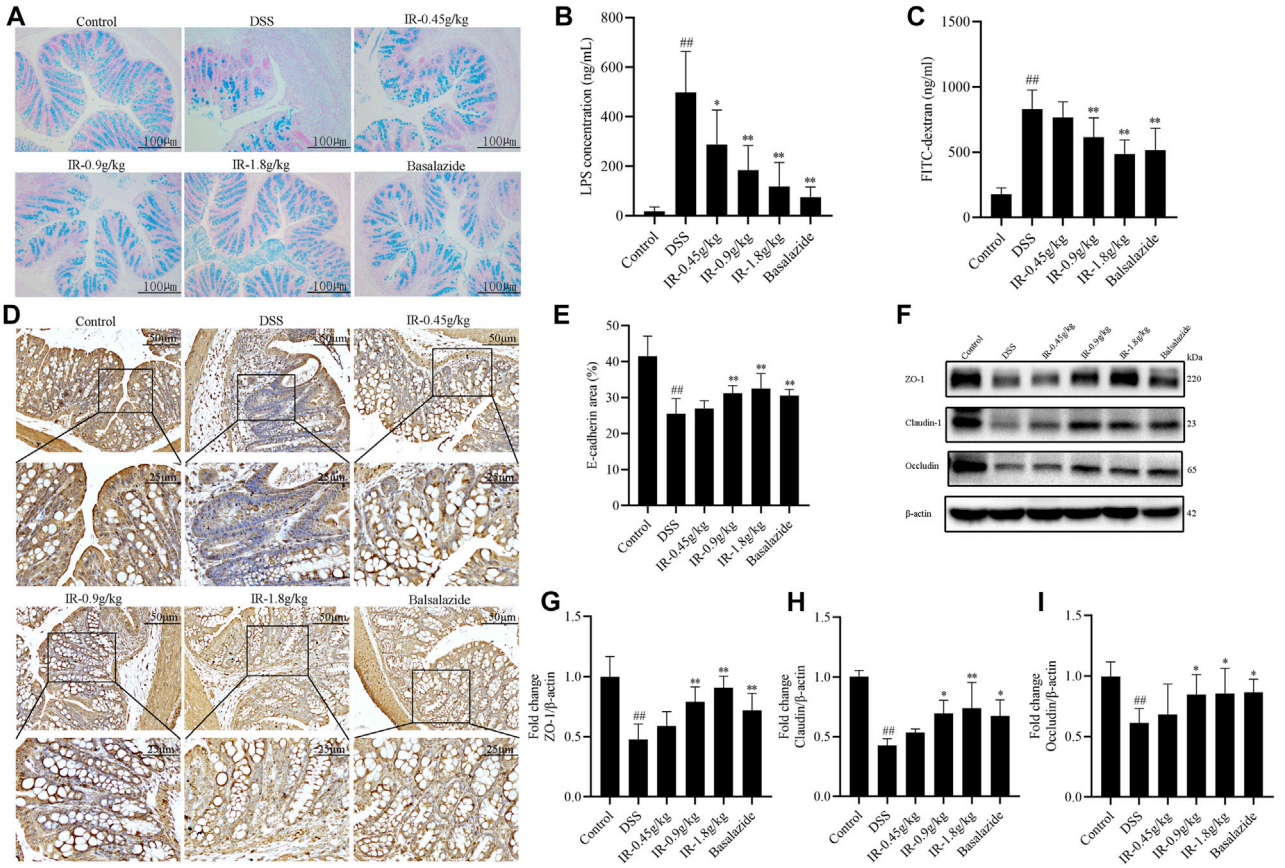

FIGURE 5 | IR alleviates intestinal mucosal barrier damage in UC mice. **(A)** Detection of acidic mucus layer in colon of mice by alcian blue staining ($n = 6$). **(B)** The LPS content in serum of mice ($n = 6$). **(C)** The FITC-dextran content in serum of mice ($n = 6$). **(D)** Immunohistochemical detection of E-cadherin protein expression in colon of mice ($n = 3$). **(E)** Histochemical positive area statistics of E-cadherin ($n = 3$). **(F)** The protein levels of ZO-1, claudin-1, and occludin in colon detected by western blotting. **(G–I)** The gray intensity analysis of ZO-1, claudin-1, and occludin proteins, respectively ($n = 3$). All data were compared using one-way ANOVA, and p-values reflected differences between experimental groups.

showed that, compared with the control group, the expression of Keap-1 protein increased, accompanied by the decreased expression of Nrf2 and HO-1 proteins in mice of the DSS group, indicating that the colon of UC mice had excessive oxidative stress. IR treatment alleviated the oxidative stress of UC mice by reducing Keap-1 protein expression and increasing Nrf2 and HO-1 protein expression (**Figures 4I–L**).

Ilex rotunda Thunb Protects Against Injury to the Intestinal Mucosal Barrier

The intestinal mucus layer and intercellular tight junction are important components of the intestinal mucosal barrier. Alcian blue staining was used to detect the integrity of the colon mucus layer due to its ability to combine with acidic groups to make the acidic mucous on the colon appear blue. The results showed that the colon mucus layer of the control group was intact and distributed neatly on the cell surface, and the colon mucus layer of the DSS group was destroyed and disappeared in some areas of the colon tissue (**Figure 5A**). After IR treatment, the colonic mucous layer of chronic and acute UC mice was restored in a dose-dependent manner (**Figure 5A**, **Supplementary Figure S3A**). After the intestinal mucosal barrier was damaged, the mucosal permeability was increased, and LPS produced by intestinal flora and FITC given by gavage were more likely leaks into the blood from the intestine. Compared with the control group, the LPS and FITC in the serum of mice in the DSS group were significantly increased, and IR reduced the LPS in the serum of acute and chronic UC mice ($p < 0.05$ or $p < 0.01$) (**Figure 5B**, **Supplementary Figure S3B**). Furthermore, IR reduced FITC from the intestine into the serum of chronic UC mice (**Figure 5C**). Adhesion junction proteins such as E-cadherin and tight junction proteins including occludin, claudin-1, and ZO-1 are the main parts of cell-cell junctions. Compared with the control group, the expression of E-cadherin, occludin, claudin-1, and ZO-1 proteins in the colon of the DSS group was significantly reduced, and the intestinal mucosal barrier was damaged (**Figures 5D–I**). IR partially restored the reduced expression of E-cadherin, occludin, claudin-1, and ZO-1 proteins to protect the integrity of the intestinal mucosal barrier (**Figures 5D–I**, **Supplementary Figures S3C–F**).

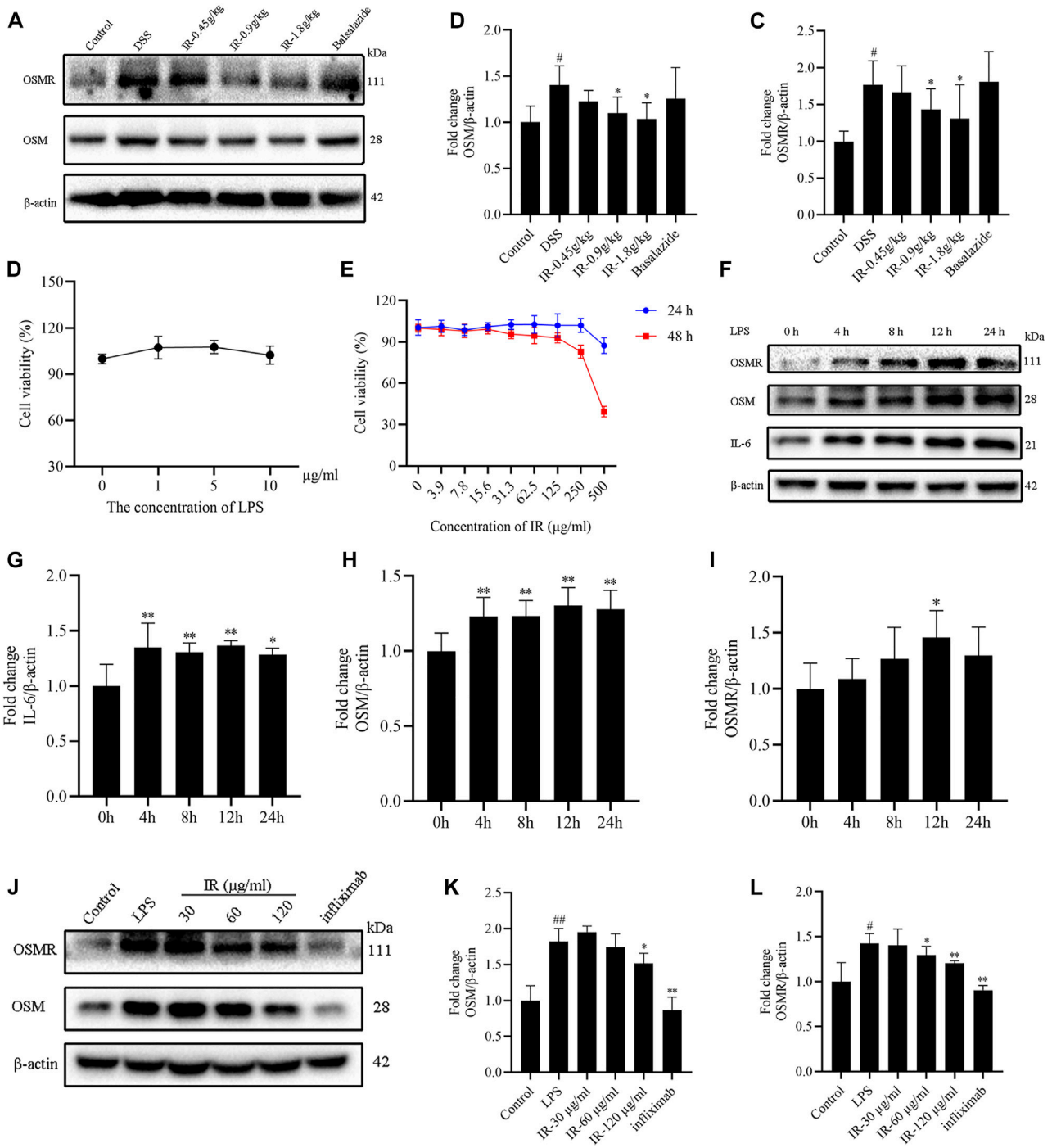

FIGURE 6 | IR ameliorates UC in mice by regulating OSM/OSMR pathway. **(A)** The protein levels of OSM and OSMR in colon of mice detected by western blotting, with gray intensity analysis shown in panel **(B,C)**. **(D)** Cell viability of Caco2 cells treated with different concentrations of LPS for 24 h. **(E)** Cell viability of Caco2 cells treated with different concentrations of IR for 24 and 48 h. **(F)** The expression of OSM, OSMR, and IL-6 proteins of Caco2 cells detected by western blotting after 1 μg/ml LPS stimulated, with gray intensity analysis shown in panel **(G–I)**. **(J)** The effect of IR on the expression of OSM and OSM proteins of Caco2 cells after LPS stimulated, with gray intensity analysis shown in panel **(K,L)**. All data were compared using one-way ANOVA, and *p*-values reflected differences between experimental groups ($n = 3$).

Ilex rotunda Thunb Alleviates Colitis by Modulating the Oncostatin M/Oncostatin M Receptor Pathway

OSM is an important member of the IL-6-related cytokine subfamily and is closely related to the occurrence and development of UC (Rose-John, 2018). The results indicated that compared with the control group, the protein expression of OSM and OSMR was increased in the colon of mice of the DSS group ($p < 0.05$), consistent with our previous study on acute UC mice (Li Y. et al., 2021). Compared with the DSS group, IR treatment reduced the expression of OSM and OSMR proteins (**Figures 6A–C**).

LPS was used to stimulate Caco2 cells to establish a colitis model. We found that 1, 5, 10 μg/ml LPS did not affect the viability of Caco2 cells, whereas 1 μg/ml LPS stimulated Caco2 cells for 0, 4, 8, 12, and 24 h. The expression of IL-6, OSM, and OSMR proteins in the cells increased along with prolonged action time, peaking at 12 h. Therefore, we chose 1 μg/ml LPS to stimulate Caco2 cells for 12 h to establish a cell colitis model (**Figures 6F–I**). The cytotoxicity of IR (0–500 μg/ml) was tested in Caco2 cells for 24 and 48 h, and the results showed that an IR concentration below 250 μg/ml did not affect the viability of Caco2 cells. Hence, 30, 60, and 120 μg/ml IR were selected to pretreat Caco2 cells for 12 h. Then the cells were cultured for an additional 12 h in a fresh medium containing 1 μg/ml LPS, followed by the detection of OSM and OSMR proteins in cells. The different dosages of IR decreased the expression of OSM and OSMR proteins caused by LPS stimulation (**Figures 6J–L**). These results indicate that IR can alleviate UC by regulating the OSM/OSMR pathway.

DISCUSSION

The pathogenesis of UC is complex, involving the interaction of genetic susceptibility, environmental factors, gut microbial disorders, and disturbances in immune homeostasis. With economic development and lifestyle changes in developing countries, the incidence of UC has been increasing in countries in Africa, Asia and South America (Ng et al., 2017). Because of the long and indolent course of UC, the frequent alternation between active and remission phases of the disease, and the high rate of colorectal cancer transformation, the work and life of UC patients are seriously affected (Gajendran et al., 2019; Damas and Abreu, 2020). Despite the great progress has been made in the understanding and treatment of UC, some patients still lose response or intolerance to UC therapeutic drugs in clinical application, about 15% of patients still need to undergo colectomy, and 5-ASA therapeutic drugs such as mesalazine and biological agents such as infliximab are accompanied by adverse effects in the process of use (Magro et al., 2012; Sehgal, et al., 2018). Thus, it is important to develop new drugs that can effectively treat UC from natural products.

In the Jiangxi "Handbook of Herbal Medicine," there is a record that IR can be used to treat gastric and duodenal ulcers. Previous studies have pointed out that Kuijieling, which uses IR as the "Jun drug," can exert therapeutic effects on UC by regulating the differentiation of regulatory T cells and T helper 17 cells and improving the intestinal flora of mice (Long et al., 2018; Pan et al., 2020). Our previous research also demonstrated that FYC, with IR as one of the important prescription drugs, can alleviate UC by regulating OSM/OSMR and improving intestinal flora (Li X. X. et al., 2021). However, it is still unclear whether IR has a therapeutic effect on UC and the underlying mechanism of action is unknown.

In this study, we analyzed the components of IR with UPLC-QTOF-MS, identified 23 main components through literature and standard substance comparison, and determined the contents of syringin and pedunculoside. Most UC patients have recurrent attacks, with alternating periods of active and remission, requiring long-term drug treatment and maintenance in clinical practice. DSS can induce a UC model that is similar to human UC in both immunological and pathological manifestations. The chronic UC model induced by DSS is established by treatment with DSS for 7 days and tap water for 14 days as a cycle, repeated for three cycles. It can better simulate the alternating occurrence of the active phase and remission phase in the clinic (McQueen et al., 2019). However, as the time of drinking tap water was prolonged, symptoms such as bloody stool and weight loss of the mice gradually decreased. To be more conducive to the observation of the experimental results, we chose a modified modeling method that changed the tap water drinking time in the last cycle to 7 days according to the literature and evaluated the therapeutic effect of IR on UC. The results showed that IR ameliorated the general symptoms of UC mice in a dose-dependent manner, including bloody stools, weight loss, colon shortening, and the pathological damage of the colon. Although balsalazide as the positive control drug can also relieve the symptoms of UC, in the treatment of chronic UC, the liver coefficient of mice increased after long-term administration, which suggests that long-term use of balsalazide may lead to side effects on the liver.

Cytokines participate in multiple biological processes of the organism, including immune and inflammatory responses (Feghali and Wright, 1997). Overactivity of pro-inflammatory factors such as IL-1β, IL-6, and TNF-α play important roles in inducing and maintaining colitis intestinal inflammation. The NF-κB pathway is activated in IBD patients, accompanied by the upregulation of inflammatory factors such as IL-1β, TNF-α, and IL-6 (Park and Hong, 2016). As a downstream target of the IL-6 signaling pathway, STAT3 is considered an important pathway leading to UC (Hirano, 2021). The IL-6-mediated STAT3 signaling pathway is the main target for the treatment of colorectal cancer and IBD (Akanda et al., 2018). We detected the mRNA levels of cytokines including IL-1β, IL-6, TNF-α, and IL-6/STAT3 pathway-related protein expression, and found that IR treatment could reduce the inflammatory response in mice by reducing the production of cytokines and inhibiting the IL-6/STAT3 signal pathway. A moderate inflammatory response is conducive to the body's self-protection, but an excessive inflammatory response can lead to cell apoptosis and oxidative stress. Hagiwara et al. (2002) confirmed that apoptosis is the main reason for intestinal epithelial cell loss in UC patients, and

excessive apoptosis will counteract epithelial defense and aggravate the disease in patients with active UC. Pro-inflammatory factors can cause oxidative stress by promoting the production of reactive oxygen species by immune cells. The continuous accumulation of oxidative stress weakens the immune system and further aggravates UC (Jeon et al., 2020). Our study showed that IR can reduce apoptosis and promote the regeneration of colonic epithelial cells, reduce the expression of Keap1 protein, and increase the expression of HO-1 and Nrf2 proteins at the same time, thereby enhancing the body's antioxidant capacity, further preventing damage to the colon of UC mice.

Tight junctions and adherent junctions are important components of the intestinal mucosal barrier. Proteins of the occludin, claudin, and ZO families form a barrier at the top of the adjacent epithelial cell membrane to prevent the paracellular transport of intercellular molecules (Mehandru and Colombel, 2021). Adhesive proteins such as E-cadherin and β-catenin located under the basolateral of tight junctions interact with tight proteins and form adhesions between adjacent epithelial cells to close the intestinal barrier. The homeostasis of the intestinal epithelial barrier depends on the dynamic balance between apoptosis and proliferation, and its damage is considered an important pathogenic factor leading to IBD (Patankar and Becker, 2020). We found that the intestinal mucosal barrier of UC mice was severely damaged, the acidic mucous layer was destroyed, and LPS extravasated into the blood. IR repaired the damaged acidic mucous layer and upregulated the protein expression of occludin, claudin-1, and ZO-1 to promote the recovery of the intestinal epithelial barrier.

OSM is a multifunctional cytokine, belonging to the IL-6 cytokine family, which can be secreted by T cells, macrophages, and neutrophils. OSM mainly activates the corresponding signaling pathway by combining with its receptor OSMR and plays an important role in inflammation, cell growth, and hematopoiesis (Kalla et al., 2021). West et al. (2017) reported that the overexpression of cytokines OSM and OSMR in the intestinal tissues of IBD patients is positively correlated with histopathology disease severity, and can be used to predict the response of IBD patients to anti-TNF-α agents. Verstockt et al., 2021 considered that OSM can be used as a diagnostic and postoperative recovery biomarker in the tissues and serum of IBD patients. In a previous study, through transcriptome sequencing, we found that OSM and OSMR are crucial in the pathogenesis of UC and treatment with FYC (Li Y. et al., 2021). The OSM and OSMR proteins in the colon of UC mice were significantly increased, and FYC could ameliorate UC by reducing the expression of OSM and OSMR (Li X. X. et al., 2021). Because IR is an important prescription drug in FYC and plays an important role in the treatment of UC with FYC, and in the prescription of FYC lacking IR, the curative effect of prescription in the treatment of UC is weakened. Therefore, we studied the modulating effect of IR on OSM/OSMR. We detected the protein expression of OSM and OSMR in the colon of mice and found that OSM and OSMR proteins levels were significantly higher than those in normal mice, which were reduced by IR treatment. The protein expression of OSM and OSMR was increased in Caco2 cells stimulated with LPS, and IR pretreatment inhibited the increase of OSM and OSMR of Caco2 cells caused by LPS, thereby reducing the cellular inflammatory response.

Thus, IR exerts therapeutic effects on UC by regulating the OSM/OSMR signaling pathway to reduce colonic inflammation and colonic epithelial cell apoptosis, thereby improving antioxidant capacity and protecting the intestinal mucosal barrier in mice.

DATA AVAILABILITY STATEMENT

The original contributions presented in the study are included in the article/**Supplementary Material**, further inquiries can be directed to the corresponding authors.

ETHICS STATEMENT

The animal study was reviewed and approved by The Laboratory Animal Welfare and Ethics Committee of Air Force Medical University. Written informed consent was obtained from the owners for the participation of their animals in this study.

AUTHOR CONTRIBUTIONS

YL designed and completed the experiments; XY, J-NY, RL, and Y-YT assisted in the completion of some experiments; Y-XL, YZ, and X-FW analyzed the data and completed the figures; Y-HX revised the manuscript; S-WW and X-HZ checked the experimental design and implementation, and provided research funding. All authors read and approved the final manuscript.

FUNDING

This work was supported by the Key Research and Development Plan of Shaanxi Province, China (Grant Numbers: 2019SF-279 and 2020SF-337); the Project of Shaanxi Provincial Administration of Traditional Chinese Medicine, China (Grant Number: 2019-GJ-JC013); the Science and Technology Innovation Project of Shaanxi Province, China (Grant Number: S2018-ZC-GCZXXY-SF-0005); the Shaanxi Key Laboratory of Biomedicine, China (Grant Number: 2018SZS41); and the Social Development of Shaanxi Province Key Project, China (Grant Number: 2017ZDXM-SF-019).

SUPPLEMENTARY MATERIAL

The Supplementary Material for this article can be found online at: https://www.frontiersin.org/articles/10.3389/fphar.2022.819826/full#supplementary-material

REFERENCES

Adams, S. M., and Bornemann, P. H. (2013). Ulcerative Colitis. *Am. Fam. Physician* 87 (10), 699–705.

Akanda, M. R., Nam, H. H., Tian, W., Islam, A., Choo, B. K., and Park, B. Y. (2018). Regulation of JAK2/STAT3 and NF-κB Signal Transduction Pathways; Veronica Polita Alleviates Dextran Sulfate Sodium-Induced Murine Colitis. *Biomed. Pharmacother.* 100, 296–303. doi:10.1016/j.biopha.2018.01.168

Clark-Snustad, K., Butnariu, M., and Afzali, A. (2020). Women's Health and Ulcerative Colitis. *Gastroenterol. Clin. North Am.* 49 (4), 769–789. doi:10.1016/j.gtc.2020.07.004

Damas, O. M., and Abreu, M. T. (2020). Are Patients with Ulcerative Colitis Still at Increased Risk of Colon Cancer? *Lancet* 395 (10218), 92–94. doi:10.1016/S0140-6736(19)33225-8

Danese, S., Allez, M., van Bodegraven, A. A., Dotan, I., Gisbert, J. P., Hart, A., et al. (2019). Unmet Medical Needs in Ulcerative Colitis: An Expert Group Consensus. *Dig. Dis.* 37 (4), 266–283. doi:10.1159/000496739

Danese, S., Vuitton, L., and Peyrin-Biroulet, L. (2015). Biologic Agents for IBD: Practical Insights. *Nat. Rev. Gastroenterol. Hepatol.* 12 (9), 537–545. doi:10.1038/nrgastro.2015.135

de Chambrun, G. P., Tassy, B., Kollen, L., Dufour, G., Valats, J. C., Bismuth, M., et al. (2018). The Treatment of Refractory Ulcerative Colitis. *Best. Pract. Res. Clin. Gastroenterol.* 32-33, 49–57. doi:10.1016/j.bpg.2018.05.009

Du, L., and Ha, C. (2020). Epidemiology and Pathogenesis of Ulcerative Colitis. *Gastroenterol. Clin. North Am.* 49 (4), 643–654. doi:10.1016/j.gtc.2020.07.005

Effinger, A., M O'Driscoll, C., McAllister, M., and Fotaki, N. (2020). Gastrointestinal Diseases and Their Impact on Drug Solubility: Ulcerative Colitis. *Eur. J. Pharm. Sci.* 152, 105458. doi:10.1016/j.ejps.2020.105458

Feghali, C. A., and Wright, T. M. (1997). Cytokines in Acute and Chronic Inflammation. *Front. Biosci.* 2, d12–26. doi:10.2741/a171

Gajendran, M., Loganathan, P., Jimenez, G., Catinella, A. P., Ng, N., Umapathy, C., et al. (2019). A Comprehensive Review and Update on Ulcerative Colitis. *Dis. Mon.* 65 (12), 100851. doi:10.1016/j.disamonth.2019.02.004

Hagiwara, C., Tanaka, M., and Kudo, H. (2002). Increase in Colorectal Epithelial Apoptotic Cells in Patients with Ulcerative Colitis Ultimately Requiring Surgery. *J. Gastroenterol. Hepatol.* 17 (7), 758–764. doi:10.1046/j.1440-1746.2002.02791.x

Han, Y., Zhang, L., Li, W., Liu, X., Xiao, J., Chen, G., et al. (2019). Natural CAC Chemopreventive Agents from Ilex Rotunda Thunb. *J. Nat. Med.* 73 (3), 456–467. doi:10.1007/s11418-019-01281-z

Hirano, T. (2021). IL-6 in Inflammation, Autoimmunity and Cancer. *Int. Immunol.* 33 (3), 127–148. doi:10.1093/intimm/dxaa078

Jeon, Y. D., Lee, J. H., Lee, Y. M., and Kim, D. K. (2020). Puerarin Inhibits Inflammation and Oxidative Stress in Dextran Sulfate Sodium-Induced Colitis Mice Model. *Biomed. Pharmacother.* 124, 109847. doi:10.1016/j.biopha.2020.109847

Kalla, R., Adams, A. T., Bergemalm, D., Vatn, S., Kennedy, N. A., Ricanek, P., et al. (2021). Serum Proteomic Profiling at Diagnosis Predicts Clinical Course, and Need for Intensification of Treatment in Inflammatory Bowel Disease. *J. Crohns Colitis* 15 (5), 699–708. doi:10.1093/ecco-jcc/jjaa230

Kim, M. H., Park, K. H., Oh, M. H., Kim, H. H., Choe, K. I., Park, S. H., et al. (2012). Two New Hemiterpene Glycosides from the Leaves of Ilex Rotunda. Thunb. *Arch. Pharm. Res.* 35 (10), 1779–1784. doi:10.1007/s12272-012-1010-1

Kim, Y. S., Jung, S. A., Lee, K. M., Park, S. J., Kim, T. O., Choi, C. H., et al. (2017). Impact of Inflammatory Bowel Disease on Daily Life: an Online Survey by the Korean Association for the Study of Intestinal Diseases. *Intest. Res.* 15 (3), 338–344. doi:10.5217/ir.2017.15.3.338

Li, X. X., Yuan, R., Wang, Q. Q., Han, S., Liu, Z., Xu, Q., et al. (2021). Rotundic Acid Reduces LPS-Induced Acute Lung Injury *In Vitro* and *In Vivo* through Regulating TLR4 Dimer. *Phytother. Res.* 35 (8), 4485–4498. doi:10.1002/ptr.7152

Li, Y., Chen, F., Xie, Y., Yang, Q., Luo, H., Jia, P., et al. (2021). Feiyangchangweiyan Capsule Protects against Ulcerative Colitis in Mice by Modulating the OSM/OSMR Pathway and Improving Gut Microbiota. *Phytomedicine* 80, 153372. doi:10.1016/j.phymed.2020.153372

Liu, H. J., Cao, S. T., Wen, B. Y., Han, X., Li, Y., Li, S., et al. (2021). Rotundic Acid Ameliorates Non-alcoholic Steatohepatitis via SREBP-1c/SCD1 Signaling Pathway and Modulating Gut Microbiota. *Int. Immunopharmacol.* 99, 108065. doi:10.1016/j.intimp.2021.108065

Liu, K., Li, G., Guo, W., and Zhang, J. (2020). The Protective Effect and Mechanism of Pedunculoside on DSS (Dextran Sulfate Sodium) Induced Ulcerative Colitis in Mice. *Int. Immunopharmacol.* 88, 107017. doi:10.1016/j.intimp.2020.107017

Long, Y., Li, S., Qin, J., Xie, L., Gan, L., Jie, F., et al. (2018). Kuijieling Regulates the Differentiation of Treg and Th17 Cells to Ameliorate Experimental Colitis in Rats. *Biomed. Pharmacother.* 105, 781–788. doi:10.1016/j.biopha.2018.06.011

Ma, X., Chen, G., Wang, J., Xu, J., Zhao, F., Hu, M., et al. (2019). Pedunculoside Attenuates Pathological Phenotypes of Fibroblast-like Synoviocytes and Protects against Collagen-Induced Arthritis. *Scand. J. Rheumatol.* 48 (5), 383–392. doi:10.1080/03009742.2019.1600716

Magro, F., Rodrigues, A., Vieira, A. I., Portela, F., Cremers, I., Cotter, J., et al. (2012). Review of the Disease Course Among Adult Ulcerative Colitis Population-Based Longitudinal Cohorts. *Inflamm. Bowel Dis.* 18 (3), 573–583. doi:10.1002/ibd.21815

McQueen, P., Busman-Sahay, K., Rieder, F., Noël-Romas, L., McCorrister, S., Westmacott, G., et al. (2019). Intestinal Proteomic Analysis of a Novel Non-human Primate Model of Experimental Colitis Reveals Signatures of Mitochondrial and Metabolic Dysfunction. *Mucosal Immunol.* 12 (6), 1327–1335. doi:10.1038/s41385-019-0200-2

Mehandru, S., and Colombel, J. F. (2021). The Intestinal Barrier, an Arbitrator Turned Provocateur in IBD. *Nat. Rev. Gastroenterol. Hepatol.* 18 (2), 83–84. doi:10.1038/s41575-020-00399-w

Ng, S. C., Shi, H. Y., Hamidi, N., Underwood, F. E., Tang, W., Benchimol, E. I., et al. (2017). Worldwide Incidence and Prevalence of Inflammatory Bowel Disease in the 21st Century: A Systematic Review of Population-Based Studies. *Lancet* 390 (10114), 2769–2778. doi:10.1016/S0140-6736(17)32448-0

Pan, G., Liu, B., Li, S., Han, M., Gao, L., Xu, G., et al. (2020). Kuijieling, a Chinese Medicine Alleviates DSS-Induced Colitis in C57BL/6Jmouse by Improving the Diversity and Function of Gut Microbiota. *FEMS Microbiol. Lett.* 367 (13), fnaa082. doi:10.1093/femsle/fnaa082

Park, M. H., and Hong, J. T. (2016). Roles of NF-κB in Cancer and Inflammatory Diseases and Their Therapeutic Approaches. *Cells* 5 (2), 15. doi:10.3390/cells5020015

Patankar, J. V., and Becker, C. (2020). Cell Death in the Gut Epithelium and Implications for Chronic Inflammation. *Nat. Rev. Gastroenterol. Hepatol.* 17 (9), 543–556. doi:10.1038/s41575-020-0326-4

Rose-John, S. (2018). Interleukin-6 Family Cytokines. *Cold Spring Harb. Perspect. Biol.* 10 (2), a028415. doi:10.1101/cshperspect.a028415

Sairenji, T., Collins, K. L., and Evans, D. V. (2017). An Update on Inflammatory Bowel Disease. *Prim. care* 44 (4), 673–692. doi:10.1016/j.pop.2017.07.010

Sehgal, P., Colombel, J. F., Aboubakr, A., and Narula, N. (2018). Systematic Review: Safety of Mesalazine in Ulcerative Colitis. *Aliment. Pharmacol. Ther.* 47 (12), 1597–1609. doi:10.1111/apt.14688

Truta, B. (2021). The Impact of Inflammatory Bowel Disease on Women's Lives. *Curr. Opin. Gastroenterol.* 37 (4), 306–312. doi:10.1097/MOG.0000000000000736

Verstockt, S., Verstockt, B., Machiels, K., Vancamelbeke, M., Ferrante, M., Cleynen, I., et al. (2021). Oncostatin M Is a Biomarker of Diagnosis, Worse Disease Prognosis, and Therapeutic Nonresponse in Inflammatory Bowel Disease. *Inflamm. Bowel Dis.* 27 (10), 1564–1575. doi:10.1093/ibd/izab032

Wang, C., Chao, Z., Sun, W., Wu, X., and Ito, Y. (2014). Enrichment and Purification of Pedunculoside and Syringin from the Barks of Ilex Rotunda with Macroporous Resins. *J. Liq. Chromatogr. Relat. Technol.* 37 (4), 572–587. doi:10.1080/10826076.2012.749499

Wei, W. (2002). *Pharmacological Experimental Methodology*. Beijing: People's Medical Publishing House, 20–52.

West, N. R., Hegazy, A. N., Owens, B. M. J., Bullers, S. J., Linggi, B., Buonocore, S., et al. (2017). Oncostatin M Drives Intestinal Inflammation and Predicts Response to Tumor Necrosis Factor-Neutralizing Therapy in Patients with Inflammatory Bowel Disease. *Nat. Med.* 23 (5), 579–589. doi:10.1038/nm.4307

Wirtz, S., Popp, V., Kindermann, M., Gerlach, K., Weigmann, B., Fichtner-Feigl, S., et al. (2017). Chemically Induced Mouse Models of Acute and Chronic Intestinal Inflammation. *Nat. Protoc.* 12 (7), 1295–1309. doi:10.1038/nprot.2017.044

Yang, B., Zhu, J. P., Rong, L., Jin, J., Cao, D., Li, H., et al. (2018). Triterpenoids with Antiplatelet Aggregation Activity from Ilex Rotunda. *Phytochemistry* 145, 179–186. doi:10.1016/j.phytochem.2017.11.005

Zhang, H., Gu, H., Jia, Q., Zhao, Y., Li, H., Shen, S., et al. (2020). Syringin Protects against Colitis by Ameliorating Inflammation. *Arch. Biochem. Biophys.* 680, 108242. doi:10.1016/j.abb.2019.108242

Zhang, X. J., Yuan, Z. W., Qu, C., Yu, X. T., Huang, T., Chen, P. V., et al. (2018). Palmatine Ameliorated Murine Colitis by Suppressing Tryptophan Metabolism and Regulating Gut Microbiota. *Pharmacol. Res.* 137, 34–46. doi:10.1016/j.phrs.2018.09.010

Zhou, X. L., Yang, J., Qu, X. J., Meng, J., Miao, R. R., and Cui, S. X. (2020). M10, a Myricetin-3-O-B-D-Lactose Sodium Salt, Prevents Ulcerative Colitis through Inhibiting Necroptosis in Mice. *Front. Pharmacol.* 11, 557312. doi:10.3389/fphar.2020.557312

Conflict of Interest: The authors declare that the research was conducted in the absence of any commercial or financial relationships that could be construed as a potential conflict of interest.

Publisher's Note: All claims expressed in this article are solely those of the authors and do not necessarily represent those of their affiliated organizations, or those of the publisher, the editors and the reviewers. Any product that may be evaluated in this article, or claim that may be made by its manufacturer, is not guaranteed or endorsed by the publisher.

frontiers | Frontiers in Pharmacology

ORIGINAL RESEARCH
published: 12 July 2022
doi: 10.3389/fphar.2022.810344

Assessment of the Potential of *Sarcandra glabra (Thunb.)* Nakai. in Treating Ethanol-Induced Gastric Ulcer in Rats Based on Metabolomics and Network Analysis

Chao Li[1†], *Rou Wen*[2†], *DeWen Liu*[3], *LiPing Yan*[2], *Qianfeng Gong*[2*] *and Huan Yu*[2*]

[1]School of Pharmacy, Tianjin University of Traditional Chinese Medicine, Tianjin, China, [2]School of Pharmacy, Jiangxi University of Chinese Medicine, Nanchang, China, [3]Institute of Chinese Materia Medica, China Academy of Chinese Medical Sciences, Beijing, China

OPEN ACCESS

Edited by:
Enkelejda Goci,
Aldent University, Albania

Reviewed by:
Pouya Hassandarvish,
University of Malaya, Malaysia
Abdel Nasser B. Singab,
Ain Shams University, Egypt

***Correspondence:**
Qianfeng Gong
gongqf2002@163.com
Huan Yu
huanhuanyu2006@163.com

[†]These authors have contributed equally to this work and share first authorship.

Specialty section:
This article was submitted to Ethnopharmacology, a section of the journal Frontiers in Pharmacology

Received: 06 November 2021
Accepted: 22 June 2022
Published: 12 July 2022

Citation:
Li C, Wen R, Liu D, Yan L, Gong Q and Yu H (2022) Assessment of the Potential of Sarcandra glabra (Thunb.) Nakai. in Treating Ethanol-Induced Gastric Ulcer in Rats Based on Metabolomics and Network Analysis. Front. Pharmacol. 13:810344. doi: 10.3389/fphar.2022.810344

Gastric ulcer (GU) is one of the most commonly diagnosed diseases worldwide, threatening human health and seriously affecting quality of life. Reports have shown that the Chinese herbal medicine *Sarcandra glabra* (Thunb.) Nakai (SGN) can treat GU. However, its pharmacological effects deserve further validation; in addition, its mechanism of action is unclear. An acute gastric ulcer (AGU) rat model induced by alcohol was used to evaluate the gastroprotective effect of SGN by analysis of the histopathological changes in stomach tissue and related cytokine levels; the potential mechanisms of action of SGN were investigated via serum metabolomics and network pharmacology. Differential metabolites of rat serum were identified by metabolomics and the metabolic pathways of the identified metabolites were enriched via MetaboAnalyst. Furthermore, the critical ingredients and candidate targets of SGN anti-AGU were elucidated. A compound-reaction-enzyme-gene network was established using Cytoscape version 3.8.2 based on integrated analysis of metabolomics and network pharmacology. Finally, molecular docking was applied to verify the acquired key targets. The results showed that SGN exerted a certain gastroprotective effect via multiple pathways and targets. The effects of SGN were mainly caused by the key active ingredients isofraxidin, rosmarinic, and caffeic acid, which regulate hub targets, such as PTGS2, MAPK1, and KDR, which maintain the homeostasis of related metabolites. Signal pathways involved energy metabolism as well as immune and amino acid metabolism. Overall, the multi-omics techniques were proven to be promising tools in illuminating the mechanism of action of SGN in protecting against

Abbreviations: AGU, acute gastric ulcer; CASP3, Caspase-3; CAT, catalase; ELISA, enzyme-linked immunosorbent assay; GU, gastric ulcer; HE, Hematoxylin-eosin; IL-1β, Interleukin-1β; KDR, Vascular Endothelial Growth Factor Receptor-2; MAPK1, Mitogen-Activated Protein Kinase 1; NFE2L2, Nuclear factor erythroid 2-related factor 2; PPI, Protein-protein interaction; MDA, Malondialdehyde; MMP2, matrix metalloproteinase-2; MMP9, matrix metalloproteinase-9; MPO, myeloperoxidase; OPLS-DA, Orthogonal Partial Least Squares Discriminant Analysis; PCA, principal components analysis; PGE2, Prostaglandin E2; PTGS2, prostaglandin-endoperoxide synthase 2 / cyclooxygenase-2; SGN, Sarcandra glabra (Thunb.) Nakai; TCM, traditional Chinese medicine; TCMSP, Traditional Chinese Medicine Systems Pharmacology; TNF-α, Tumor Necrosis Factor-α; VEGFA, vascular endothelial growth factor A.

diseases. This integrated strategy provides a basis for further research and clinical application of SGN.

Keywords: metabolomics, network pharmacology, *Sarcandra glabra* (thunb.) nakai, gastric ulcer, gastroprotection

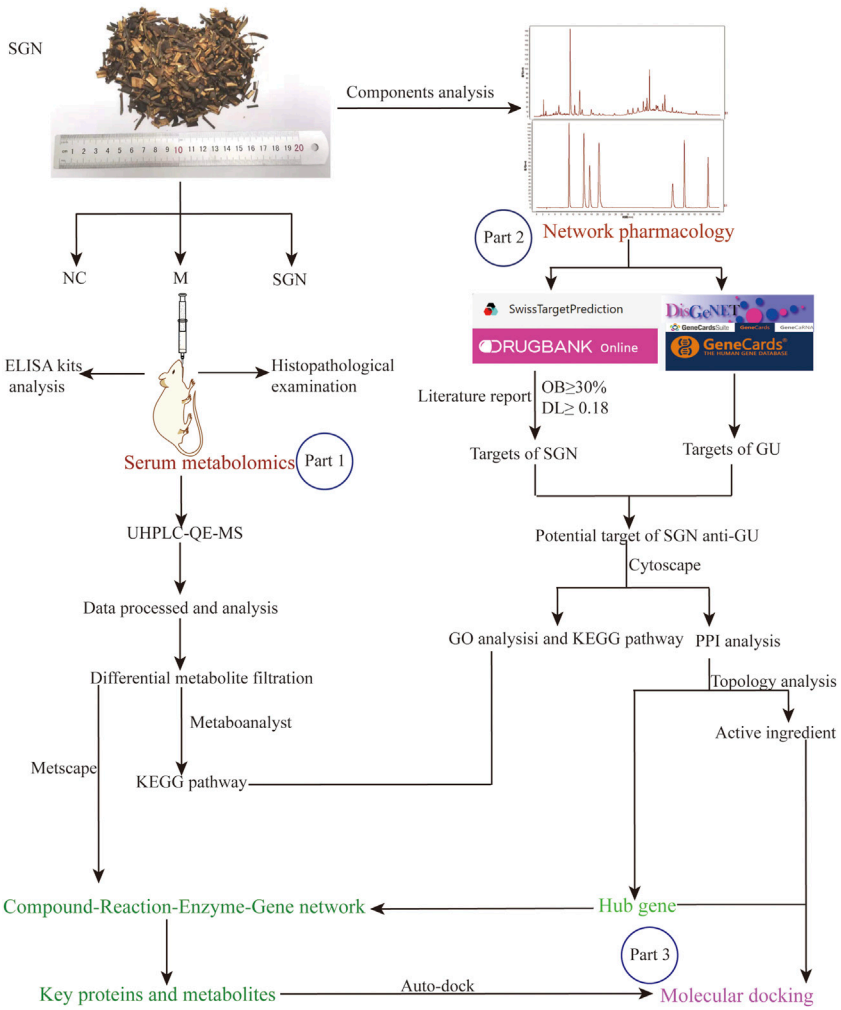

GRAPHICS ABSTRACT | Flowchart of multi-omics integrated analysis. The part 1: The mechanism of action of SGN against AGU was comprehensively clarified based on non-targeted metabolomics. The part 2: The active ingredients anti-AGU in SGN, the potential hub genes and their protective mechanisms were identified by performing network pharmacology. Part 3: The potential connection between biomarkers and hub genes was obtained and molecular docking was applied to verify the acquired key targets with the key ingredient.

1 INTRODUCTION

Gastric ulcer (GU) is a common peptic ulcer caused by the destruction of the gastric mucosa. GU is hard to cure and can easily induce infection; GU relapse is common. Based on epidemiological surveys, the incidence of GU in Western countries about 2.4%. Furthermore, the incidence of GU in some areas of mainland China is up to about 6.07% and approximately 22.5% of patients with gastrointestinal symptoms have GU (Li et al., 2010). Besides impacting human health, GU also has a heavy economic burden on patients and their families. For instance, the average annual medical cost of treating GU patients in the United States is 23,819 United States dollars and 59.6–2,553.10 United States dollars in South Korea (Song et al., 2013). GU has a complex pathogenesis that is unclear and can be caused by a variety of factors, such as alcohol, drugs, and *Helicobacter pylori*; however, it is mainly caused by the imbalance of aggressive factors and defense mechanisms of the gastric mucosa (Valcheva-Kuzmanova et al., 2019). It is reported that alcohol is one of the typical gastric mucosal attack factors.

Alcohol is first digested and absorbed by the digestive system, including the gastrointestinal tract, before entering the blood; therefore, intake of highly concentrated alcohol erodes, destroys the protective layer, and causes irreversible damage to the gastric mucosa through the digestion of gastric mucus and bicarbonate, thus inducing acute gastric ulcers (AGU) (Zheng et al., 2016; Zhang et al., 2019). Additionally, the histological characteristics and healing process of the rat alcoholic GU model are similar to those of human gastric mucosal damage; it can be produced efficiently and can effectively model similar systems. This model has been widely used in research regarding gastroprotective medicine (Bai et al., 2020; Lian et al., 2020). Pathological studies have shown that the onset of acute alcoholic GU is closely associated with neutrophil infiltration, release of pro-inflammatory factors, and oxidative stress (Zheng et al., 2016). In recent decades, various specific treatments for GU have been found, with drug therapy being the primary GU treatment method. Appropriate medication regiments, such as proton pump inhibitors (PPIs), *Helicobacter pylori* eradication, and nonsteroidal anti-inflammatory drugs (NSAIDs), can effectively treat GU patients. However, several reports have shown that these drugs have some safety issues and side effects after long-term chronic treatment. Some of the safety issues are related to the possible long-term effects of chronic hypergastrinemia (Lee et al., 2019), leading to loss of muscle function (Vinke et al., 2020), nephrotic syndrome, and chronic renal failure (Harirforoosh and Jamali, 2009).

Therefore, more effective and less toxic therapies are needed for GU treatment. Both clinical and experimental studies have demonstrated that herbal medicines exert protective effects against GU with fewer side effects and lower medical expenses (Devanesan et al., 2018; Zhang et al., 2018; Sudi et al., 2020). Traditional Chinese Medicine (TCM) has been widely used in China for maintaining health and treating diseases for several years. *Sarcandra glabra* (thunb.) Nakai (SGN) (Chinese name called Zhong jie feng, Jiu jie cha, or cao shan hu) is an essential herb used in TCM with a range of biological applications, including treating cancer, rheumatism, pneumonia, digestive tract inflammations, traumatic injuries, and fractures (Zhou et al., 2013). Furthermore, SGN has been widely used in food, medicine, health care products, cosmetics, etc., It has been demonstrated that SGN has great development potential. In addition, several studies have demonstrated that SGN exhibits anti-inflammatory activity (Liu et al., 2017; Tsai et al., 2017; Feng et al., 2022) and can protect mesenchymal stem cells from OH-induced oxidative stress (Liu et al., 2016). It should be mentioned that mesenchymal stem cells can repair damaged cells, including damaged gastrointestinal mucosal tissue (Xiang et al., 2022). Thus, we speculate that SGN may have potential anti-GU ability. To date, gastroprotective effects of SGN on ethanol-induced GU and its underlying mechanisms have also not been evaluated. More importantly, the mechanism of action of SGN on GU should be elucidated to promote the clinical application of SGN.

TCM is a multi-component, multi-target, and multi-pathway treatment that achieves its particular protective pharmacological activity by modulating the biological network of body systems (Zhao et al., 2010). Therefore, it is difficult to detect the precise mechanisms of TCM via the conventional experimental method alone. Consequently, new and appropriate approaches are needed to systematically and comprehensively assess the mechanisms of Chinese materia medica. Metabolomics and network pharmacology can efficiently and systemically determine the molecular and pharmacological mechanisms due to the rapid advancement of analytical techniques and bioinformatics (Wang et al., 2019; Zhang et al., 2020). Unlike the earlier reductionist "one drug, one target" method, metabolomics and network pharmacology are based on the fact that numerous active ingredients interact with multiple diverse genes or proteins, similar to TCM. Metabolomics and network pharmacology can reflect and illustrate the interactive relationship between multiple drugs, targets, and diseases. Meanwhile, metabolomics combining chemometrics and multivariate statistical analysis methods can comprehensively analyze metabolites *in vivo* and characterize differential biomarkers to explore the correlation between metabolites and the physiological and pathological changes in the organism under drug treatment (Lucarelli et al., 2015). Network pharmacology abstracts the relationship into a network model and illustrates the action of drugs on the human biological network from a systematic perspective (Yang et al., 2020). In the present study, a metabolomics and network pharmacology approach were performed to investigate the impact of SGN on AGU, induced with ethanol, to clarify its medical value. Additionally, a potential novel insight was provided to systematically investigate the mechanism of action of SGN.

2 MATERIALS AND METHODS

2.1 Materials and Reagents

SGN was obtained from the Yanbao Ecological Agricultural Farmers Professional Cooperative of Yong'an City, Fujian Province (voucher specimen NO20190813) and was identified as the dry whole plant of *Sarcandra glabra* (Thunb.) Nakai (Chloranthaceae) by Professor Qianfeng Gong of the Jiangxi University of Chinese Medicine. Chlorogenic acid reference substance (catalog number 110753-201716, purity ≥99.3%), rosmarinic acid reference substance (catalog number 111871-201505, purity ≥98%), and isofraxidin reference substance (catalog number 110837-201608, purity ≥98%) were obtained from the National Institutes for Food and Drug Control (Beijing, China). Neochlorogenic acid (catalog number BCTG-0231, purity ≥98%), cryptochlorogenic acid (catalog number BCTG-0210, purity ≥98%), caffeic acid (catalog number BCTG-0286), purity ≥98%), and astilbin (catalog number BCTG-0233, purity ≥98%) were acquired from the China National Engineering Research Center for Solid Preparation Manufacturing Technology (Jiangxi, China). Rat Tumor Necrosis Factor (TNF-α) ELISA Kit (catalog number: CSB-E11987r), Rat Interleukin 6 (IL-6) ELISA Kit (catalog number: CSB-E04640r), and Rat Prostaglandin E2 (PGE2) ELISA Kit (catalog number: CSB-E07967r) were provided by CUSABIO BIOTECH CO. Ltd. The myeloperoxidase (MPO) assay kit (catalog number: A044-1-1), superoxide Dismutase (SOD)

assay kit (catalog number: A001-3-2), catalase (CAT) assay kit (catalog number: A007-1-1), malondialdehyde (MDA) assay kit (catalog number: A003-1-2), and nitric oxide (NO) assay kit (catalog number: A013-2-1) were purchased from Nanjing Jiancheng Bioengineering Institute. Methanol (CAS number: 67-56-1), acetonitrile (CAS number:75-05-8), ammonium acetate (CAS number: 631-61-8), and ammonium hydroxide (CAS number: 1336-21-6) were LC-MS grade. All other reagents and chemicals were of analytical grade.

2.2 Sample Preparation

2.2.1 Preparation of Serum Samples of Rats

The serum sample (100 μL) was transferred to an EP tube; then, 400 μL of extract solution (acetonitrile: methanol = 1:1, containing isotopically labeled internal standard mixture) was added. The samples were vortexed for 30 s, sonicated in an ice-water bath for 10 min, and incubated at −40°C for 1 h to precipitate proteins. The samples were then centrifuged at 12,000 rpm and 4°C for 15 min to obtain the supernatant. The supernatant was transferred to a fresh glass vial for analysis. The quality control (QC) sample was prepared by mixing an equal aliquot of the supernatants from all the samples.

2.2.2 Preparation of SGN Extract (Liu and Chen, 2016)

Eight times the volume of water was added to SGN herbal pieces (400 g) to soak for 1 h; they were decocted for 1 h, and six and four times the volume of water were added prior to them being decocted for 0.5 h. The solution was filtered with absorbent cotton after cooling. The filtrates were combined and evaporated to obtain a crude drug concentration of 1 gmL^{-1}.

2.2.3 High-Performance Liquid Chromatography for the Determination of Main Components

HPLC was performed using a Waters 2695 HPLC with quaternary solvent manager, column thermostat, diode array (PDA) detector, and Empower 3 chromatographic workstation (Waters Company, United States). A chromatographic Diamonsil C_{18} column (250 × 4.6 mm, 5 μm) with a mobile phase consisting of acetonitrile and 0.1% formic acid aqueous solution was used (flow rate, 0.8 ml/min; column temperature, 35°C, and elution as follows: 0–5 min, 6%–10% acetonitrile; 5–32 min, 10%–12% acetonitrile; 32–45 min, 12%–20% acetonitrile; 45–78 min, 20%–35% acetonitrile; 78–80 min, 35%–6% acetonitrile). The detection wavelength was 330 nm. The standard compounds were used for standard quantitative analysis.

2.3 Establishment of an Ethanol-Induced AGU Model

Male Sprague-Dawley (weight: 180–200 g) rats were obtained from Hunan SJA Laboratory Animal Co., Ltd. (Changsha, China) (License NO. SYXK 2019-0004). The animals were kept in an isolated room at 22°C ± 2°C and 55% ± 10% relative humidity with a 12-h light-dark cycle following the Jiangxi University of Chinese Medicine guidelines. The rats were randomly separated into three groups: SGN group (n = 8), model group (M) (n = 8), and normal control (NC) group (n = 6). Rats in the SGN group were orally administered SGN decoction (10 gkg^{-1}), and those in the NC and M groups were given distilled water (10 ml kg^{-1} d^{-1}) for seven consecutive days.

Rats were fasted but permitted access to water for 24 h before modeling. Rats in the NC group were given distilled water via gavage (5 ml kg^{-1}), and the M group and SGN group were given an equal volume of anhydrous ethanol 1 h after the last administration for modeling. After 1 h, rats in each group were anesthetized and their blood was collected via the abdominal aorta. Their stomachs were photographed and removed immediately (Yoo et al., 2020; Yeo et al., 2021). This experiment was approved by the Experimental Animal Ethics Committee of Jiangxi University of Traditional Chinese Medicine (Animal Ethics Committee No. JZLLSC 2020_0108) and performed following the guidelines of the Chinese Ethics Committee.

2.4 Analysis of Pathology and ELISA of Rat Stomachs

The collected rat stomach tissues were cut symmetrically. Half of the tissues were put in a 4% paraformaldehyde solution for fixation for 24 h, then washed with flowing water to remove the fixative. The tissues were transferred to a 70% ethanol solution for storage. The tissues were successively put in 70%, 85%, 90%, and 100% ethanol for gradient dehydration until the tissue blocks were completely dehydrated and transparent. The tissues were then embedded, sectioned (6 μm), and HE-stained. A 100 × microscope was used to obtain the cytopathological image of gastric mucosal tissue (Lívero et al., 2016). The other half of the tissue was washed with pre-cooled PBS and weighed, and the corresponding volume of PBS (1 g: 9 ml) was added. The tissues were then ground on ice, frozen, and thawed repeatedly. The tissues were centrifuged at 5,000 r/min for 10 min to obtain a gastric tissue homogenate. The supernatants were assessed following the instruction of ELISA kits.

2.5 Metabolomic Analysis of Rat Serum

2.5.1 UHPLC-QE-MS Analysis of the Rat Plasma

UHPLC system (Vanquish, Thermo Fisher Scientific) with a UPLC BEH Amide column (2.1 × 100 mm, 1.7 μm) coupled to a Q Exactive HFX mass spectrometer (Orbitrap MS, Thermo) was used for LC-MS/MS analyses. The mobile phase contained 25 mmol/L ammonium acetate and 25 mmol/L ammonia hydroxide in water (pH = 9.75) (A) and acetonitrile (B). The elution gradient was as follows: 0–0.5 min, 95% B; 0.5–7.0 min, 95%–65% B; 7.0–8.0 min, 65%–40% B; 8.0–9.0 min, 40% B; 9.0–9.1 min, 40%–95% B; and 9.1–12.0 min, 95% B. The column and auto-sampler temperatures were 30°C and 4°C, respectively, and the injection volume was 3 μL.

The QE HFX mass spectrometer can acquire MS/MS spectra on information-dependent acquisition (IDA) mode via the acquisition software (Xcalibur, Thermo), which continuously evaluates the full scan MS spectrum. The ESI source conditions were as follows: sheath gas flow rate; 50 Arb, Aux gas flow rate; 10 Arb, capillary temperature; 320°C, full MS resolution; 60,000, MS/MS resolution; 7,500, collision energy;

10/30/60 in NCE mode, spray Voltage; 3.5 kV (positive) or −3.2 kV (negative).

2.5.2 Data Preprocessing and Biomarker Identification

ProteoWizard was used to convert the raw data to the mzXML format. The data were processed with an in-house program developed using R and XCMS for peak detection, extraction, alignment, and integration. After obtaining the sorted data, several multivariate pattern recognition analyses were conducted. A principal component analysis (PCA) was used to find the projection method that best represents the original data through dimensionality and noise reduction, visually displaying the differences between samples in a multi-dimensional space. Orthogonal partial least squares method-discriminant analysis (orthogonal projections to latent structures-discriminant analysis, OPLS-DA) was used to further analyze the results for better visualization and subsequent analysis. OPLS-DA analysis was used to filter metabolites unrelated to the categorical variables and separately analyze the non-orthogonal and orthogonal variables to obtain more reliable metabolite differences. SIMCA software (V14.1, Sartorius Stedim Data Analytics AB, Umea, Sweden) was used for logarithmic (LOG) conversion and UV formatting processing on the data to obtain relevant group information. First, OPLS-DA modeling was conducted on the first principal component. The quality of the model was determined via the seven-fold validation (7-foldcrossvalidation) test. The R2X (the interpretability of the model to the categorical variable ×) and Q2 (the predictability of the model) were obtained after cross-validation and used to evaluate the validity of the model. The permutation test was conducted to randomly change the arrangement of the categorical variable Y many times to obtain different random Q2 and R2 values and further test the validity of the model. The variable importance in the projection (VIP) value was obtained using the OPLS-DA mode discriminant analysis, and the *p*-value was obtained via the Student's *t*-test analysis of standardized peak area. The different metabolites in each group were screened at $p < 0.05$ and VIP >1. MS1 mass spectrometry data with accurate molecular masses were recognized by searching Metlin, HMDB, and KEGG pathway databases, while identification of secondary spectra was based on the XCMS program package and the laboratory's self-built database. The significantly different metabolites were identified. Finally, the metabolic pathways of the identified metabolites were obtained from MetaboAnalyst 5.0 (https://www.metaboanalyst.ca/) (Pang et al., 2021).

2.6 Network Pharmacology Analysis

2.6.1 The Specific Operation of Network Pharmacology Analysis

Network pharmacology was used to comprehensively and systematically determine the material basis for the treatment of AGU using SGN, the relationship between metabolites and target proteins, and the mechanism of SGN treatment. The main steps were as follows: 1) The source of the active ingredients in SGN: 1) Traditional Chinese Medicine Systems Pharmacology Database and Analysis Platform (TCMSP) was used to obtain active ingredients. Oral bioavailability (OB) >30% and drug similarity (DL) >0.18 were used as the screening criteria. 2) The other chemical components in SGN were obtained via HPLC. 3) Prediction of component targets: The canonical SMILES structural formula of the active ingredients of SGN was obtained from the PubChem (https://pubchem.ncbi.nlm.nih.gov/) database. Swiss Target Prediction (www.swisstargetprediction.ch/) and DrugBank (https://go.drugbank.com/) were used to predict the targets of the active ingredients. 4) Disease target prediction: The targets of GU were obtained from the Genecards (https://www.genecards.org/) and DisGeNET (http://www.disgenet.org/) databases. 5) Establishment of Protein-Protein Interaction (PPI) network: The intersection targets of components and disease were imported to STRING 10.5 (https://string -db.org) to obtain the protein interaction network (PIN). 6) ClueGO (plug-in in Cytoscape software) was used to visually display the Gene Ontology (GO) enrichment and KEGG pathway on potential targets. The key signal pathways for SGN treatment of GU were screened out. This software can be used as a mutual verification of metabolic pathways obtained via metabolomics or complements of each other. 7) Component-reaction-enzyme-gene network was obtained by importing the metabolites obtained from metabolomics analysis into MetScape 3.1.3 [MetScape (http://metscape.ncibi.org/)]. Metscape is a visual Cytoscape software plug-in that can detect the relationship among metabolites, proteins, and corresponding regulatory genes in the human metabolic network. It can also interpret metabolome data. 8) The key metabolites and proteins were identified by integrating the network obtained in step 6 with hub genes and metabolic pathways.

2.7 Integrated Metabolomics and Network Pharmacology Analysis

To comprehensively understand the mechanism of SGN against AGU, the differential metabolites identified by metabolomics were imported into MetScape, and pathway-based analysis was performed to obtain the Compound-Reaction-Enzyme-Gene network. The targets predicted by MetScape were matched with the targets predicted by network pharmacology, and the hub genes were acquired.

2.7.1 Molecular Docking Verification of Key Targets

In order to better illuminate the binding activity between the potential targets of SGN to prevent AGU with the corresponding active ingredients, the critical active ingredients were obtained from the analysis of the "ingredient-target" network, while the key targets were acquired through the joint strategy, and the binding ability of them were tested for molecular docking verification. The crystal structures of the core target protein receptor were downloaded from the RCSB PDB database (https://www.rcsb.org/) and PyMoL software was applied to delete the target irrelevant protein receptor ligands and non-protein molecules (such as water molecules). AutoDock Tools (version 1.5.6) was used to perform routine pretreatment of the target protein receptors and small ligand molecules, the Grid Box with the ligand was used as the center, and the docking active site and binding energy were gained using the Autogrid module and by performing molecular docking, respectively. Generally, lower energy means that the conformation of the compound molecule and the receptor may be more stable and the docking result may

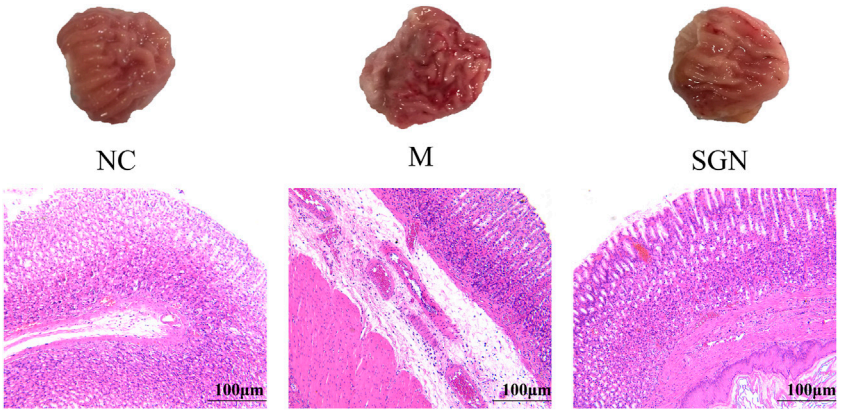

FIGURE 1 | Pathological section of rat stomach tissue in each group (× 100). Black arrow: edema in the submucosal layer, eosinophil infiltration, damage to the glandular mucosal structure. Green arrow: bleeding on the mucosal surface, vasodilation, and congestion in the muscle layer.

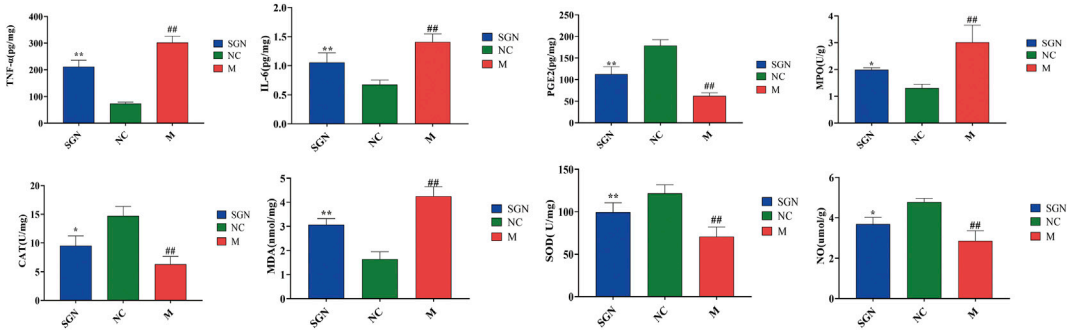

FIGURE 2 | The effect of SGN on TNF-α, IL-6, PGE-2, NO, MPO, MDA, CAT, and SOD in gastric homogenate (mean ± SD, $n = 6$). Note: Compared with NC group, ##$p < 0.01$, compared with model group, *$p < 0.05$, **$p < 0.01$.

be more reliable. The component with the lowest docking binding energy to the target protein was selected to visualize the results by PyMoL.

2.7.2 Western Blot to Validate the Results of the Integrated Analysis

Specific information on grouping and handling of rats can be found in the Supplementary file. RIPA lysis buffer was used to extract protein from rat stomach tissue, and the protein concentration was determined and calculated using the bicinchoninic acid (BCA) method. A Bio-Rad electroporation instrument transfer membrane was used to separate the proteins through SDS-PAGE using the same amount of protein per sample (30 μg/sample). The membranes were blocked for 2 hours at room temperature, treated with 1:500 diluted primary antibody, and kept overnight at 4°C. The membrane was washed three times with TBS-T for 10 min each time, then treated with a 1:5,000 dilution of horseradish peroxidase-labeled secondary antibody, and incubated at room temperature for 2 hours; the membrane was washed three times with TBS-T for 10 min each time. ECL luminescent agent was used for 1 minute in a dark room before being exposed. A gel imaging analysis system was used for quantitative analysis, GAPDH was used as an internal reference, and the ratio of the gray value of the target protein to the gray value of GAPDH was used to reflect the expression of related proteins.

2.8 Statistical Analysis

SPSS version 21.0 (SPSS Inc. Chicago, Illinois) was used for all statistical analyses. The data are expressed as mean ± SD. One-way ANOVA was used for the significance test. The SNK test was used for multiple comparisons when the variance was uniform, while the Tamhane test was used if the variance was uneven. A p-value < 0.05 was considered a statistically significant difference.

3 RESULTS

3.1 HPLC for the Determination of Main Components in SGN

The chromatogram of SGN decoction is shown in **Supplementary Figure S1**. The liquid chromatogram shows that there are mainly 7 chromatographic peaks. A total of 7

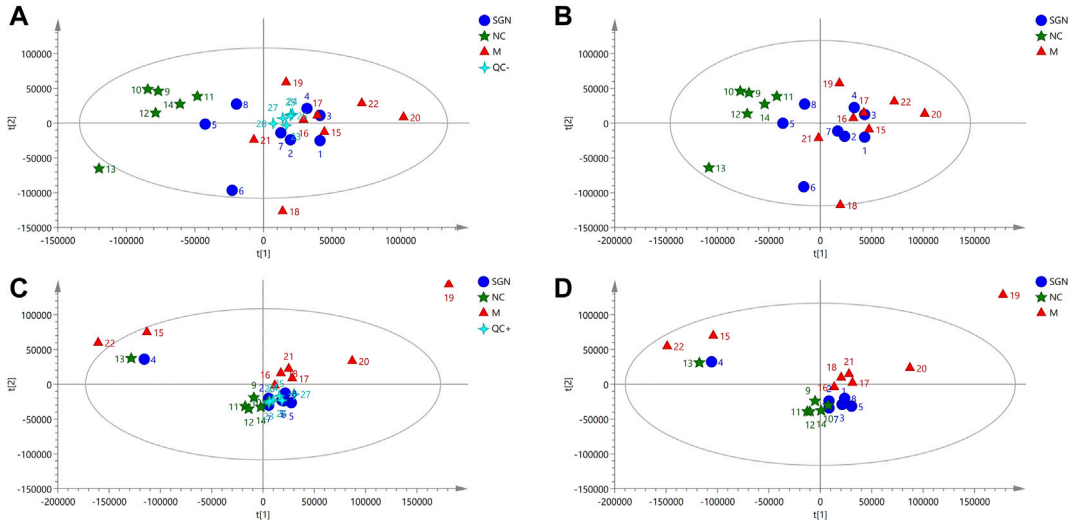

FIGURE 3 | PCA score plots of serum in positive and negative modes.

compounds have been identified by comparing these peaks with the chemical reference, namely neochlorogenic, chlorogenic, cryptochlorogenic, caffeic, and rosmarinic acid, as well as isofraxidin and astilbin.

3.2 Effects of SGN on the Histopathological Morphology of Rat Stomachs

The rats in the M group showed edema in the submucosal layer, bleeding on the mucosal surface, severe damage to the glandular mucosal structure, vasodilation, and significant congestion in the muscle layer compared with those in the normal group. Slight lamellar bleeding was also seen in the SGN group. However, congestion in the gastric mucosa, bleeding, and mucosal damage was significantly reduced in the SGN group compared with those in the M group. SGN decoction reduced GU bleeding and protected the gastric mucosa. The pathological sections results showed that the epithelial cells of the model group were defective and had several inflammatory cell infiltrations compared with those in the NC group. The gastric mucosal layer of rats was completely repaired, and the inflammatory exudate and inflammatory cells were significantly reduced in the SGN group compared to those in the M group (See **Figure 1**).

3.3 Analysis of Related Cytokine Levels by ELISA Kits

The effect of SGN on inflammatory and oxidative stress indexes in rats with ethanol-induced GU is shown in **Figure 2**. The ethanol gavage significantly increased the levels of inflammatory factors TNF-α and IL-6 in the gastric tissue of the rats ($p < 0.01$), while the contents of PGE-2 and NO were significantly decreased compared with those in the NC group ($p < 0.01$). Furthermore, the oxidative stress index, MDA content, and MPO enzyme activity were significantly increased ($p < 0.01$), while the enzyme activity of CAT and SOD was significantly decreased ($p < 0.01$). SGN gavage significantly increased the content of PGE2 and NO in rat gastric tissue compared with that in the M group ($p < 0.05$). SGN gavage also reversed the downward trend of TNF-α and IL-6 ($p < 0.01$). SGN decoction improved the oxidative stress level of the gastric tissue of the rats. The SOD enzyme activity and CAT content increased, while the MPO enzyme activity was significantly inhibited and the MDA content level was significantly decreased ($p < 0.05$).

3.4 Integrated Strategy Based on Metabolomics and Network Pharmacology

3.4.1 PCA of Rat Serum in all Groups

The PCA results of SGN extract on serum metabolites of ethanol-induced AGU model rats showed that all QC samples were similar and that they were well gathered near the origin. These results indicate that the detection platform was stable, the instrument precision was good, and the method was reliable (**Figures 3A,C**). The distance was furthest between the M and NC group, indicating that the serum metabolites of the M group was significantly changed after the model development. The SGN group was between the M group and NC groups, indicating that SGN reversed the cause after administration. The disturbance and deviation of serum metabolites caused by the model are shown in **Figures 3B,D**. The total ion current diagram is shown in **Supplementary Figure S2**.

3.4.2 OPLS-DA Analysis of Rat Serum in Each Group

The OPLS intrinsic structure projection method was used to analyze each experimental group to eliminate the influence of irrelevant noise, such as intra-group differences and cross factors. OPLS-DA analysis was used to filter and classify metabolites. Orthogonal variables with uncorrelated variables and separate

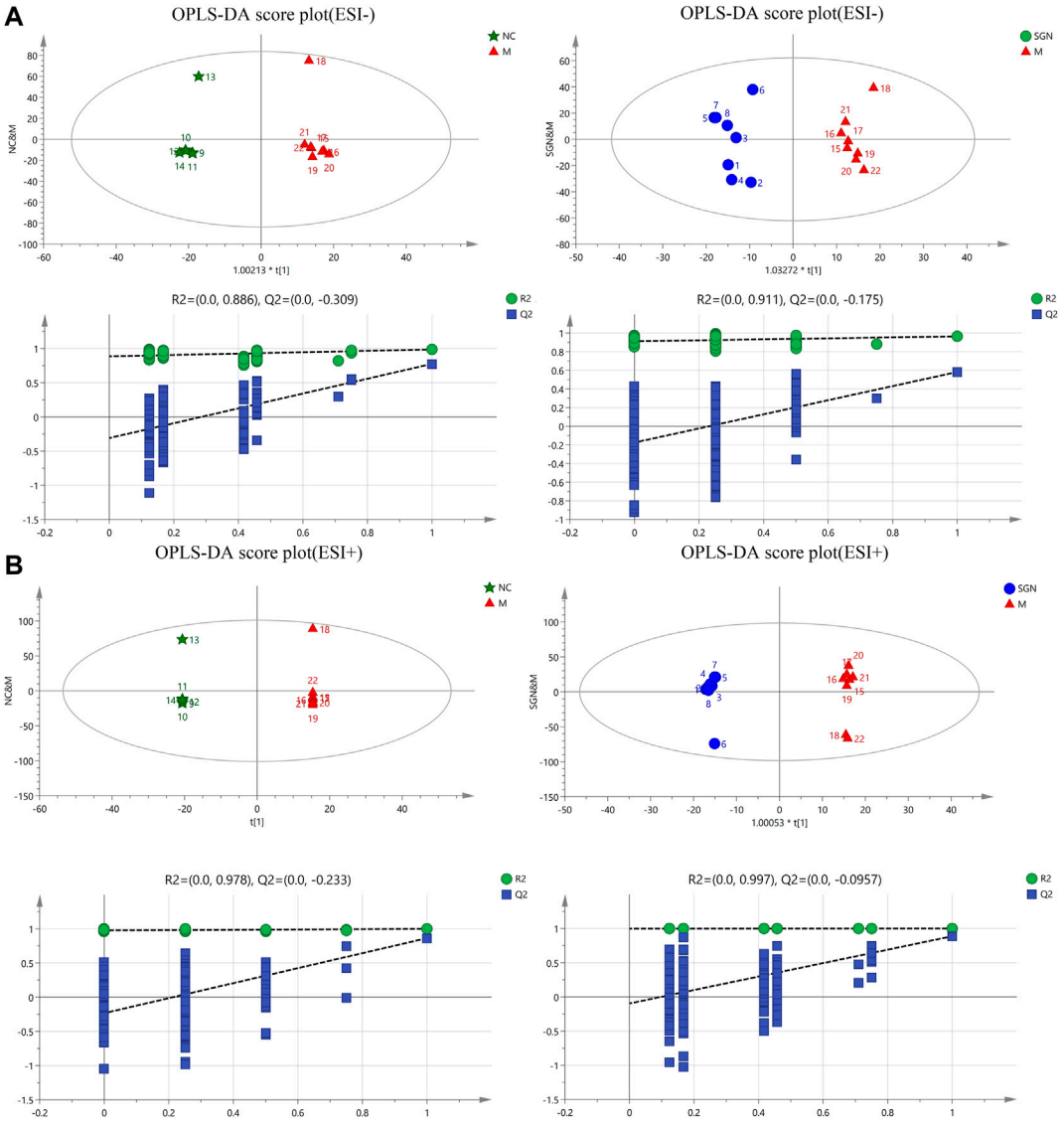

FIGURE 4 | OPLS-DA score plots and corresponding model validation plot of rat serum samples in positive and negative modes.

analyses of non-orthogonal and orthogonal variables were conducted to obtain a more reliable correlation between metabolite differences and experimental groups. The score of OPLS-DA indicated that all samples were within the 95% confidence interval (Hotelling T2 ellipse). The cumulative values of R2Y and Q2 were greater than 0.6, indicating that the OPLS-DA model was suitable for determining the difference between the two groups of samples. The difference further confirmed the significant changes in the relevant metabolic components of the ethanol-induced GU model rats (Figures 4A–1, 2 and B-1, 2). Finally, a 200-permutation test was used to discriminate the OPLS-DA model to verify its stability and reliability. The cross-validation (Q2) analysis revealed that the change in all data (R2) determined that the model did not overfit (Figures 4A–3, 4 and B-3, 4).

3.4.3 Identification of Characteristic Metabolites in Rat Serum and Related Metabolic Pathway Analysis

The metabolites with VIP score >1 and $p < 0.05$ were filtered and collected. The precursor ions and MS/MS fragments obtained via high-resolution UHPLC-QE-MS, and the metabolite information obtained from the HMDB, Metlin, and KEGG databases were used to determine if the error between the extracted mass value and the experimental mass value was less than 10 ppm. The metabolites that met the above conditions were identified as candidate biomarkers. Volcano-plots were used to further imply the changed metabolites ($p < 0.05$) among the different groups (**Figure 5A**). Finally, 23 metabolites (**Table 1**) were identified as candidate biomarkers (**Figure 5B**). The expression levels of the candidate biomarkers were assessed and compared to determine the expression of metabolites in

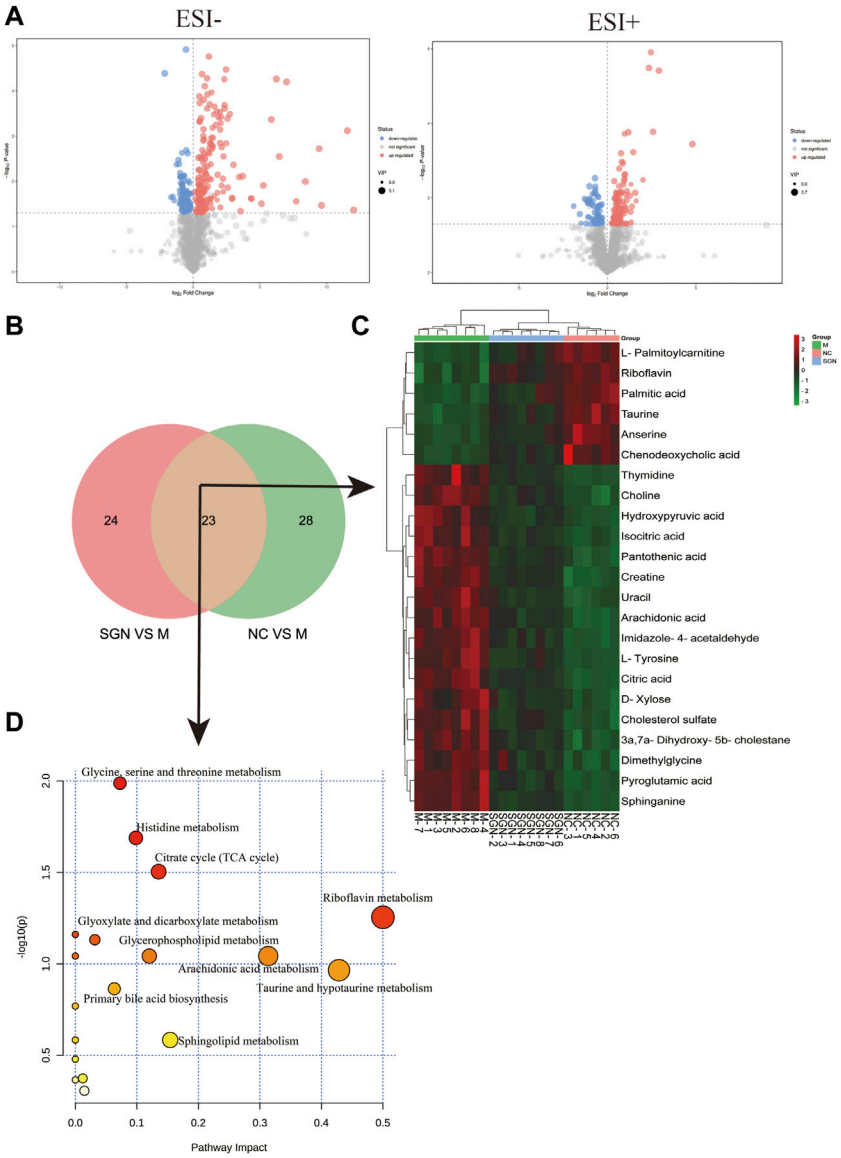

FIGURE 5 | (A) Differential metabolite volcano plot of SGN VS. M in negative and positive ion mode. **(B)** Venn plot of common metabolites in the SGN and NC groups. **(C)** Heatmap of different endogenous metabolites. Rows represent the metabolites, and columns represent the corresponding group. **(D)** Serum metabolism pathway in ethanol-induced GU rats treated with SGN.

the NC, M, and SGN groups (metabolite thermogram, **Figure 5C**). The color change on the heat map indicates the overall change in metabolites among the groups. For instance, the levels of arachidonic acid, sphingosine, and citric acid were higher in the M group than in the NC group. The abundance of arachidonic acid and sphingosine was lower in the SGN group than in the M group. The results indicated that SGN treatment had a reversal effect on most of the metabolites and were regulated to recover to levels similar to the NC group. The VIP value is indicated by the size of the circle, red indicates significant upregulation, and blue represents significant downregulation. Moreover, the related metabolic pathways were established by MetaboAnalyst 5.0 (**Figure 5D**).

3.5 Analysis of the Anti-GU Mechanisms of SGN Based on Network Pharmacology

3.5.1 Network Analysis of Potential Active Ingredients and Candidate Targets of SGN

Active SGN ingredients (17) (**Supplementary Table S1**) were obtained following the procedure outlined in section 2.8. However, one had no target and was removed. A total of 245 potential targets were identified after removing the duplicate values. The targets were used to construct a candidate compound-candidate target network regulatory network in SGN (**Supplementary Figure S4**). The network had 262 nodes and 477 edges. The network graph also showed

TABLE 1 | Differential metabolites identification of serum.

NO	Name	HMDB	VIP	*p*-value	Formula	m/z	FC	Retention time(s)	Adduct
1	Pantothenic acid	HMDB0000210	1.819954	0.004677	$C_9H_{17}NO_5$	218.1027	1.556969	287.41	$[M–H]^-$
2	Citric acid	HMDB0000094	1.777119	0.016476	$C_6H_8O_7$	191.0191	2.478995	132.1855	$[M–H]^-$
3	Isocitric acid	HMDB0000193	1.928636	0.001459	$C_6H_8O_7$	191.0192	2.428676	101.09	$[M–H]^-$
4	L-Tyrosine	HMDB0000158	1.439888	0.032418	$C_9H_{11}NO_3$	180.0657	1.759687	322.721	$[M–H]^-$
5	Dimethylglycine	HMDB0000092	2.052247	2.86E-06	$C_4H_9NO_2$	102.0551	4.051005	343.131	$[M–H]^-$
6	Taurine	HMDB0000251	1.919971	0.003001	$C_2H_7NO_3S$	124.0064	1.460747	313.703	$[M–H]^-$
7	Thymidine	HMDB0000273	1.343658	0.038894	$C_{10}H_{14}N_2O_5$	241.0824	1.523908	91.8446	$[M–H]^-$
8	D-Xylose	HMDB0000098	1.840493	0.00347	$C_5H_{10}O_5$	149.0446	1.507816	166.024	$[M–H]^-$
9	Uracil	HMDB0000300	1.454253	0.004192	$C_4H_4N_2O_2$	111.019	1.416469	79.7947	$[M–H]^-$
10	Pyroglutamic acid	HMDB0000267	1.484675	0.014249	$C_5H_7NO_3$	128.0343	1.366563	317.204	$[M–H]^-$
11	Arachidonic acid	HMDB0001043	1.394256	0.00403	$C_{20}H_{32}O_2$	303.2322	1.307376	38.1969	$[M–H]^-$
12	Cholesterol sulfate	HMDB0000653	1.39984	0.029981	$C_{27}H_{46}O_4S$	465.3045	1.358335	26.0519	$[M–H]^-$
13	Hydroxypyruvic acid	HMDB0001352	1.947684	0.003819	$C_3H_4O_4$	103.0027	2.621461	97.4662	$[M–H]^-$
14	Chenodeoxycholic acid	HMDB0000518	1.954149	0.013724	$C_{24}H_{40}O_4$	391.2847	0.341368	169.658	$[M–H]^-$
15	Anserine	HMDB0000194	1.964544	0.032861	$C_{10}H_{16}N_4O_3$	239.1145	1.892027	432.811	$[M–H]^-$
16	Palmitic acid	HMDB0000220	1.701405	0.022209	$C_{16}H_{32}O_2$	255.2323	1.422017	220.4415	$[M–H]^-$
17	Creatine	HMDB0000064	1.828211	0.020049	$C_4H_9N_3O_2$	130.0612	1.449975	367.008	$[M–H]^-$
18	L-Palmitoylcarnitine	HMDB0000222	1.740218	0.045599	$C_{23}H_{46}NO_4$	401.3404	0.761472	201.0715	$[M + H]^+$
19	3a,7a-Dihydroxy-5b-cholestane	HMDB0006893	1.93586	0.013094	$C_{27}H_{48}O_2$	405.3709	1.601535	177.359	$[M + H]^+$
20	Riboflavin	HMDB0000244	1.325923	0.048874	$C_{17}H_{20}N_4O_6$	377.144	1.435412	234.177	$[M + H]^+$
21	Imidazole-4-acetaldehyde	HMDB0003905	3.003304	0.008703	$C_5H_6N_2O$	111.0553	2.4061	79.35665	$[M + H]^+$
22	Sphinganine	HMDB0000269	1.762494	0.049348	$C_{18}H_{39}NO_2$	302.3038	1.488641	130.652	$[M + H]^+$
23	Choline	HMDB0000097	2.379748	0.033347	$C_5H_{14}NO$	103.0993	1.774886	404.484	$[M + H]^+$

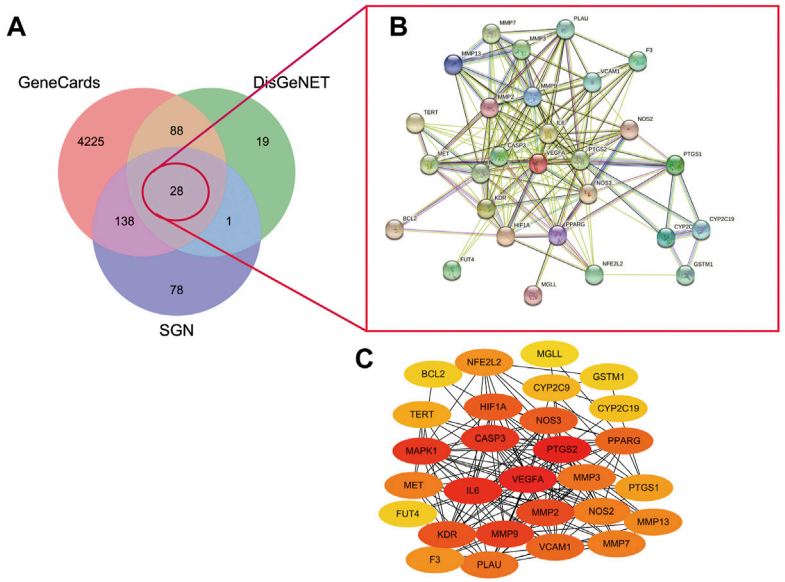

FIGURE 6 | A. Venny diagram of targets of SGN with AGU.B. PPI network of SGN and GU overlap targets C. core targets plot. The redder the color mean more important of the targets.

complex correlations between different components and targets. Analyze Network was used for network analysis to identify more relevant active ingredients. Quercetin, isofraxidin, and rosmarinic acid had the highest degree of connection with the target protein (**Supplementary Table S2**).

3.5.2 Screening Hub Targets of SGN Against GU Based on a PPI Network

A total of 136 and 4479 GU-related targets were obtained from DisGeNET and GeneCards databases, respectively. Out of these, 116 overlapped in the two databases. The 28 main targets were obtained by matching predicted targets of the components in the

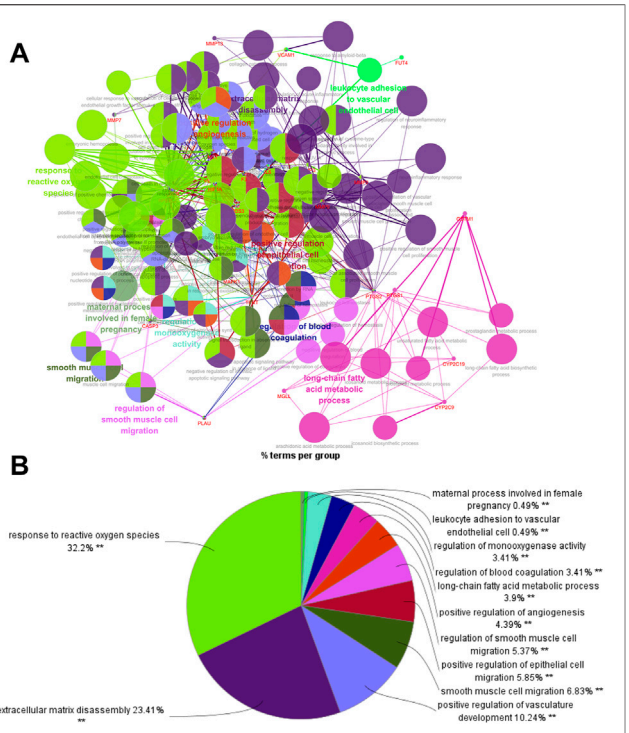

FIGURE 7 | Biological process of GO enrichment analysis (from ClueGO).

SGN with the GU-related targets (as shown in **Figure 6A**). The hub targets in the constructed PPI network (**Figure 6B**) were identified via cytoHubba (**Figure 6C**). The redder the color, the higher the degree value. PTGS2, VEGFA, CASP3, IL6, MMP2, MMP9, MAPK1, and KDR had a high degree value in the PPI network and play indispensable roles in network regulation (See **Supplementary Table S5** for details).

3.5.3 Enrichment Analysis of GO and KEGG Pathway for SGN Against GU

ClueGO was used for GO and KEGG function annotation and enrichment analysis on the 28 key target genes. The biological process network diagram of GO enrichment analysis is shown in **Figure 7A**. Each node represents an enrichment pathway, the line of the node indicates the number of genes shared among the pathways, and the color indicates the enrichment classification of the node. GO enrichment analysis showed that SGN is involved in 108 biological processes, including response to reactive oxygen species, leukocyte homeostasis, the release of cytochrome c from mitochondria, cell migration for sprouting angiogenesis, cytokine production for inflammatory response, regulation of acute inflammatory response, and prostanoid metabolic process. GO analysis also revealed that SGN is mainly involved in oxidative stress, immune system processes, and the regulation of defense responses in anti-GU (**Figure 7B**). Therefore, the etiology of ethanol-induced GU may be related to oxidative stress and immune response. KEGG functional annotation enrichment analysis suggested that SGN is involved in 38 pathways, including arachidonic acid metabolism, the HIF-1 signaling pathway, the TNF signaling pathway, the AGE-RAGE signaling pathway, and the sphingolipid signaling pathway (**Figure 8**). **Figure 8A** shows the enrichment analysis result of ClueGO, and **Figure 8B** shows the DAVID database result, as a supplement to the result of A. Therefore, SGN treats GU by regulating multiple biological processes and through the

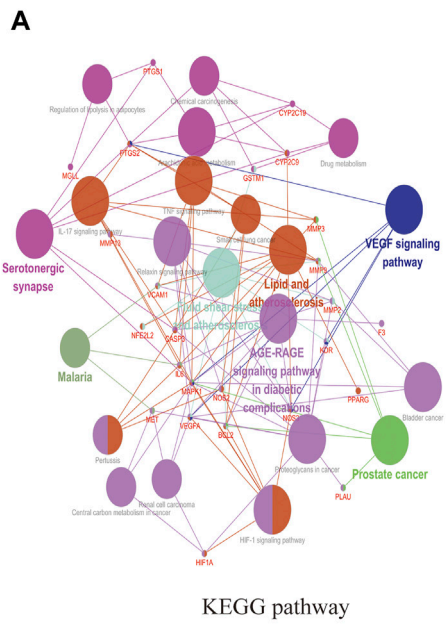

FIGURE 8 | Pathways in KEGG enrichment analysis.

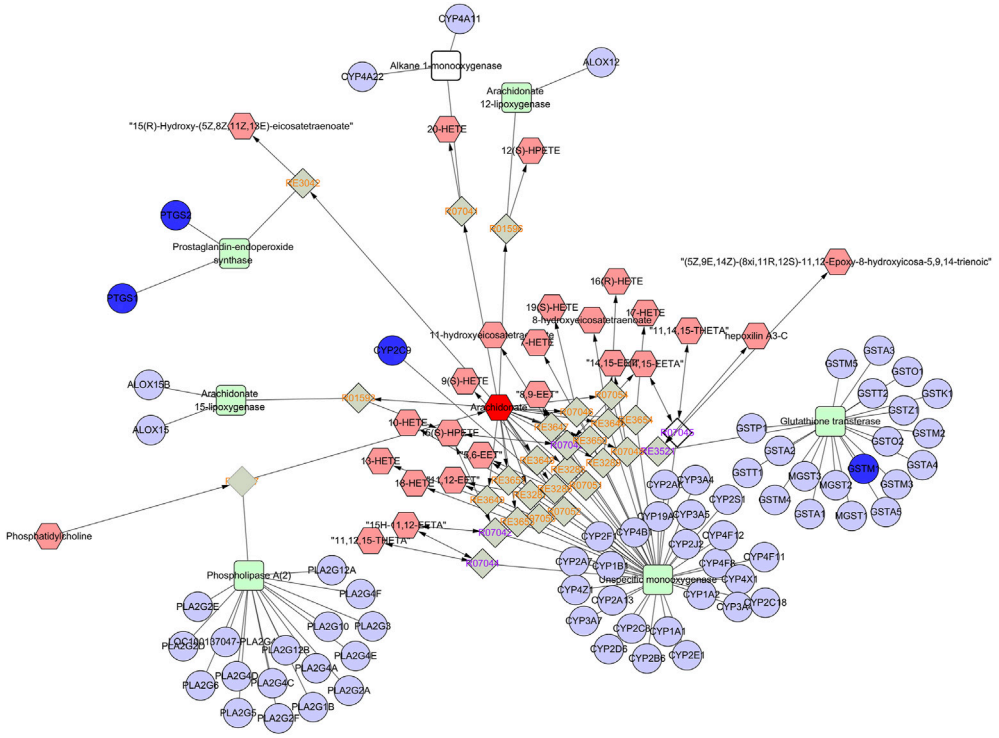

FIGURE 9 | Part of compound-reaction-enzyme-gene network (Arachidonic acid metabolism). Red hexagons, gray diamonds, green rectangles, and purple circles represent active compounds, reactions, proteins and genes, respectively.

coordination of multiple pathways. Moreover, KEGG enrichment indicated that the regulatory mechanisms of the disease were interrelated and influenced each other. Enrichment analysis showed that malaria, pertussis, amoebiasis, hepatitis B, and cancers (prostate cancer, bladder cancer, and small cell lung cancer) were significantly enriched.

3.6 Integration Analysis of Metabolomics and Network Pharmacology

An interaction network was built by combining metabolomics with network pharmacology via MetScape (**Figure 9**) to fully understand the mechanism of SGN against GU. Eleven key targets, including PTGS2, MAPK1, KDR, and PTGS1, were identified. C00219 (arachidonic acid), C00114 (choline), and C00836 (sphinganine) were the major related key metabolites. Arachidonic acid, glycerophospholipid, and sphingolipid metabolism were the main pathways involved in the correlation analysis. These genes play a crucial role in the protective effect of SGN through the above pathways and the metabolites may be potential markers of GU; the overall compound-reaction-enzyme-gene network is shown in **Supplementary Figure S5**.

3.7 The Result of Molecular Docking

Isofraxidin was finally selected for molecular docking based on the results of HPLC liquid phase component identification and the component-target network. The binding ability of isofraxidin was predicted with hub targets such as PTGS2, MAPK1, and KDR. The binding energy, which was less than −4.25 kcal mol^{-1}, indicated that the ligand has a certain binding activity with the receptor; less than −5.0 kcal mol^{-1} implied good binding activity, while less than −7.0 kcal mol^{-1} suggested strong binding activity. The results showed that isofraxidin has good binding ability with PTGS2, MAPK1, and KDR, with binding energies of −6.0, −6.6, and −5.3 kcal mol^{-1}, respectively, and its docking results were visualized, as shown in **Figure 10**.

3.8 Expression of Related Proteins Detected by Western Blotting

Compared with the NC group, MAPK1, cyclooxygenase (COX-2), and VEGFR2 protein expressions were significantly increased in the M group ($p < 0.001$). While compared with the M group, the isofraxidin group could significantly reduce the protein expression of MAPK1, COX-2, and VEGFR2 ($p < 0.01$ or $p < 0.05$), and the SGN group could significantly reduce the expression levels of MAPK1, COX-2, and VEGFR2 ($p < 0.001$ or $p < 0.01$). See **Figure 11**.

4 DISCUSSION

In the present study, an alcohol-induced AGU model was used to investigate the potential protective mechanism of SGN on GU. The pharmacodynamic evaluation was conducted using

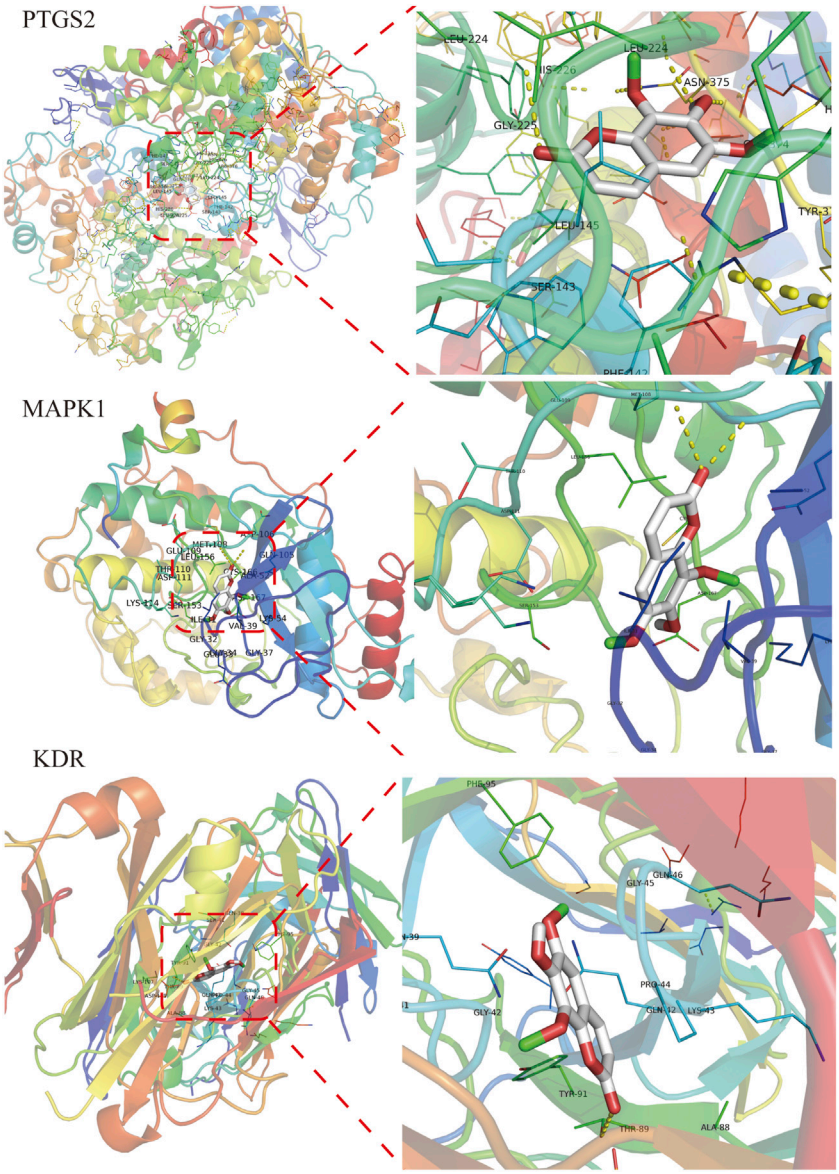

FIGURE 10 | Docking results of isofraxidin with key targets.

traditional pharmacodynamic indicators, such as histopathological examination and related cytokine levels. Meanwhile, conjoint analysis of metabolomics and network pharmacology was also used for further comprehensive analysis of the active ingredients of SGN acting on GU. UHPLC-QE-MS metabolomics technology was used to detect the collected serum samples of rats in each group. Multivariate statistics and other metrology were used for screening differentially expressed metabolites and to analyze related metabolic pathways. Metabonomics identified 23 serum biomarkers related to GU. Additionally, SGN treatment had a significant reverse effect on 8 rat serum pharmacodynamic markers. The protective effect of SGN on GU could be through the regulation of the serum metabolic profile. Network pharmacology showed that SGN acted on multiple targets, such as PTGS2, MAPK1, and KDR, through multiple active ingredients, including quercetin, isofraxidin, and rosmarinic acid. Furthermore, one target had multiple components. SGN was also associated with multiple signaling pathways related to cell inflammation and immunity, signal transduction, metabolism, apoptosis, and differentiation.

4.1 The Mechanism of Action of SGN Against AGU Based on Metabolomics

It has been reported that the occurrence of alcohol-induced GU is mainly related to oxidative stress, inflammation, and lipid peroxidation (Kobayashi et al., 2001; Zhang et al., 2019;

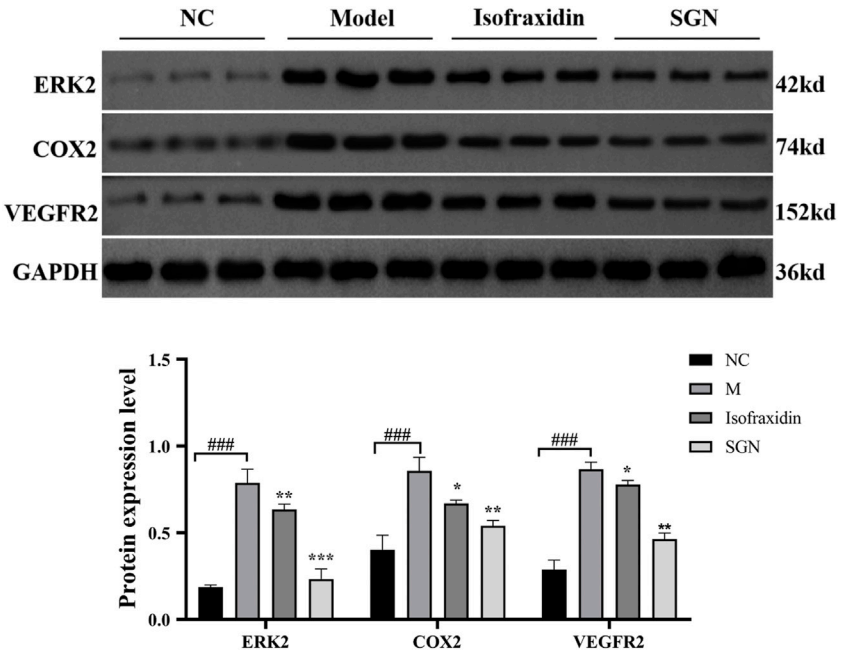

FIGURE 11 | The expression of related proteins in each group of rats. The data presented are means ± SD ($n = 3$). ###$p < 0.01$ relative to the NC group. Compared with the M group, *$p < 0.05$, **$p < 0.01$ and ***$p < 0.01$.

Ahmed et al., 2020). Oxidative stress is the excessive production of free radicals when the body is subjected to various harmful stimuli (radiation, ischemia, hypoxia, etc.,) which the antioxidant system cannot effectively and efficently remove, causing an imbalance between the oxidation and antioxidant system, thus leading to tissue damage (Tan et al., 2018). Oxidative damage can lead to gastric mitochondrial dysfunction and directly induces ATP production. The TCA cycle is essential for carbohydrate, fat, and protein metabolism and crucial for energy metabolism to produce ATP. Succinic, citric, fumaric, and isocitric acid are the main products of the TCA cycle. Excessive alcohol consumption can inhibit the activity of mitochondria in the stomach, which leads to the production of reactive oxygen species (ROS) and an increased oxidative stress response, further mediated by the massive release of inflammatory mediators, causing submucosal microvascular circulation disorders and insufficient blood supply (Cappel et al., 2019). In addition, clinical studies have shown that histidine exhibits anti-inflammatory, antioxidant, and free radical scavenging activities.

Interestingly, SGN can also alleviate the body's oxidative damage by regulating the metabolism of citric, isocitric, and hydroxypyruvic acid. Additionally, ethanol can infiltrate neutrophils in the gastric mucosa and release MPO, oxygen-free radicals, active oxidative metabolites such as superoxide anion (O_2^-), and protease. These can adhere to the vascular endothelium to cause large blood vessel occlusion, thus leading to mucosal damage (Zhao et al., 2016). Additionally, MPO-catalyzed reaction generates excessive oxidants (HOCl, 3-chlorinated tyrosine, tyrosyl, nitrotyrosine, etc.,) which can cause oxidative stress and oxidize when it exceeds the defense reaction of local antioxidants, thus leading to tissue damage (Goud et al., 2021). SOD scavenges free radicals when its level is regarded as an intuitive indicator of aging and death (Schatzman and Culotta, 2018). CAT is an antioxidant enzyme that can prevent the toxic effects of excessive hydrogen peroxide on cells (Rakotoarisoa et al., 2019). These indicators are commonly used to measure oxidative damage in the body. In the present study, SGN alleviated oxidative stress in rats with GU by promoting the antioxidant enzyme activity (SOD), increasing CAT content, and balancing excess oxidation products (MPO) in stomach tissues, similar to the results presented by most TCMs that protect the stomach (Byeon et al., 2018).

Notably, ROS promotes the development of GU (Perez et al., 2017), which may attack the polyunsaturated fatty acids in the phospholipids of biological membranes, further causing lipid peroxidation. The free radicals can damage the gastric mucosa, which can be indicated by the increased content of its metabolite MDA in the tissues (Busch and Binder, 2017). Additionally, we found that arachidonic acid (AA) and sphinganine levels were significantly elevated in the M group; however, SGN suppressed the elevation of the two. According to literature reports, AA is an omega-6 polyunsaturated fatty acid that is most widely distributed in the body and has important biological activities. When the inflammatory substance invades the organism, the phospholipase A2 (PLA2) in the body is activated to catalyze the phospholipid two-position acyl group. Hydrolysis breaks down AA into its free form and releases it into the cell fluid. Free AA is mainly metabolized by three pathways, COX, lipoxygenase (LOX), and cytochrome P450 (CYP450), to produce a series of different substances with strong biological activity (Liu et al.,

2019). Sphingolipids are structural components of cell membranes, associated with a host of metabolic networks in the body, and play signaling roles that regulate a multitude of activities, including mitochondrial function and cell death (Manzanares-Estreder et al., 2017). This evidence suggested that ethanol treatment induces oxidative stress in rat gastric tissue, which further induces inflammation and metabolic disturbance and may eventually lead to apoptosis. Our results revealed that the treatment of SGN may play a preventive role in the development of GU.

Incidentally, the protective mechanism of SGN also involves related amino acid metabolism, and we speculate that these amino acid metabolites act by attenuating the destruction of antioxidant defense systems, glutathione (GSH) and NO production in tissues, and neutrophil infiltration to protect rat gastric tissue from oxidative damage. Previous studies have shown that the antioxidant effect of taurine restores the homeostasis of the redox microenvironment in rats by promoting the content of glutathione, accomplishing gastroprotection against indomethacin-induced gastric injury (Motawi et al., 2007). Flavin mononucleotide (FMN) and flavin adenine dinucleotide (FAD) are the active forms of riboflavin (vitamin B2) in the body (Ashoori and Saedisomeolia, 2014). Glutathione reductase (GR) is a FAD enzyme. The redox cycle of GSH can remove lipid peroxides. Animal experiments have shown that riboflavin deficiency is associated with redox system metabolism disorder, lipid peroxide accumulation, decreased GSH activity, increased oxidized glutathione (GSSG) activity, and decreased GSH-PX and GR activity (Horiuchi et al., 1984). Therefore, riboflavin deficiency can contribute to enhanced lipid peroxidation. Moreover, glycine, glutamic acid, and cysteine are the raw materials for the synthesis of GSH. Glycine is essential for the metabolism of glycine, serine, and threonine. The reduction of glycine level indirectly affects the synthesis of GSH and the body's antioxidant capacity, SGN is capable of restoring the homeostasis of related metabolic pathways in SGU rats, indicating that SGN could treat GU via the inhibition of lipid peroxidation.

4.2 Potential Active Components and Mechanism of Action of SGN Against AGU Based on Network Pharmacology

The chemical composition of TCM is intricate and includes many active ingredients. Moreover, the ingredients have different biological activities, physical and chemical properties, and contents. Therefore, identifying the active ingredients in traditional Chinese medicine is one of the key points to clarify the treatment or defense of traditional Chinese medicine. Based on the network pharmacology analysis, a total of 17 active components of SGN were screened out, and the drug-component-target network model was constructed; the key active components were mainly isofraxidin, astilbin, and rosmarinic, caffeic, neochlorogenic, and chlorogenic acid. Previous studies have demonstrated that rosmarinic acid and astilbin exhibit various pharmacological activities, such as anti-inflammatory (Chu et al., 2012), hepatoprotective (Guo et al., 2020), and anti-oxidative activities (Sharma et al., 2020; Wang et al., 2020). Phenolic compounds, including neochlorogenic, chlorogenic, cryptochlorogenic, and caffeic acid, can treat metabolic syndrome since they exert anti-oxidative, anti-inflammatory, and antilipidemic effects (Banjari et al., 2017; Santana-Galvez et al., 2017; Zhao et al., 2020). More importantly, isofraxidin is used as an index component for evaluating the quality of SGN medicinal materials and their preparations in the Chinese Pharmacopoeia; it mainly exhibits anti-inflammatory activity and is a potential ROS scavenger (Li et al., 2014; Su et al., 2019; Liu et al., 2020).

The 28 anti-AGU targets of SGN were found through target mapping. The PPI network revealed that the hub targets mainly include PTGS2, VEGFA, CASP3, IL6, MMP2, MMP9, MAPK1, and KDR and that these targets are closely related to the pathogenesis of AGU. CASP3 is the most important terminal cleavage enzyme in the process of cell apoptosis, whose high expression is usually closely related to the pathogenesis of peptic ulcers (Xie et al., 2020). MMPs play a critical role in the degradation of gastric extracellular matrix proteins. MMP9 is involved in the repair of GU tissue and can also recruit inflammatory cells and participate in the inflammatory response. MMP2 is a gelatinase involved in the remodeling of the extracellular matrix required for the healing process (Rudra et al., 2022). It is well known that VEGF (including VEGFA) is a powerful stimulator of angiogenesis, and it plays a crucial role in angiogenesis and the promotion of wound healing (Bueno et al., 2021). As an endogenous vasodilator factor, NO can regulate gastric acid, gastric mucus secretion, and bicarbonate production and plays a direct role in maintaining mucosal integrity and mucosal defense (Almasaudi et al., 2016). Our study showed that SGN treatment could significantly improve the aberrant NO regulation in rats and maintain it at a normal level. Besides, inflammation is essential in the formation and development of AGU, and acute inflammation can stimulate the upregulation of the transcriptional expression of pro-inflammatory factors (TNF-α, 1L-6, and 1L-1β) (Lin et al., 2014). TNF-α, 1L-6, and 1L-1β are the most common pro-inflammatory factors in the body, which can regulate the expression of apoptosis-related genes (Yang et al., 2019).

4.3 Integrated Analysis of Metabolomics and Network Pharmacology

Life activities in cells are joined by genes, proteins, and small molecule metabolites, and the functional changes in upstream (nucleic acid, protein, etc.,) macromolecules are ultimately reflected at the metabolic level, with the metabolome being downstream of gene regulatory networks and protein action networks. Therefore, integrating metabolomics and network pharmacology to analyze the correlation of differential metabolites and potential upstream targets, so as to explore the potential mechanism of SGN anti-AGU, is warranted. The results of the integrated analysis indicated that excessive alcohol could stimulate the microcirculation of blood vessels on the gastric mucosa, producing several inflammatory mediators and cytokines, which disturb the normal structure and physiological function of gastric tissue (Zeng et al., 2017). The inflammation can then stimulate the metabolism of AA to release its metabolites, leading to inflammatory reactions, such as fever,

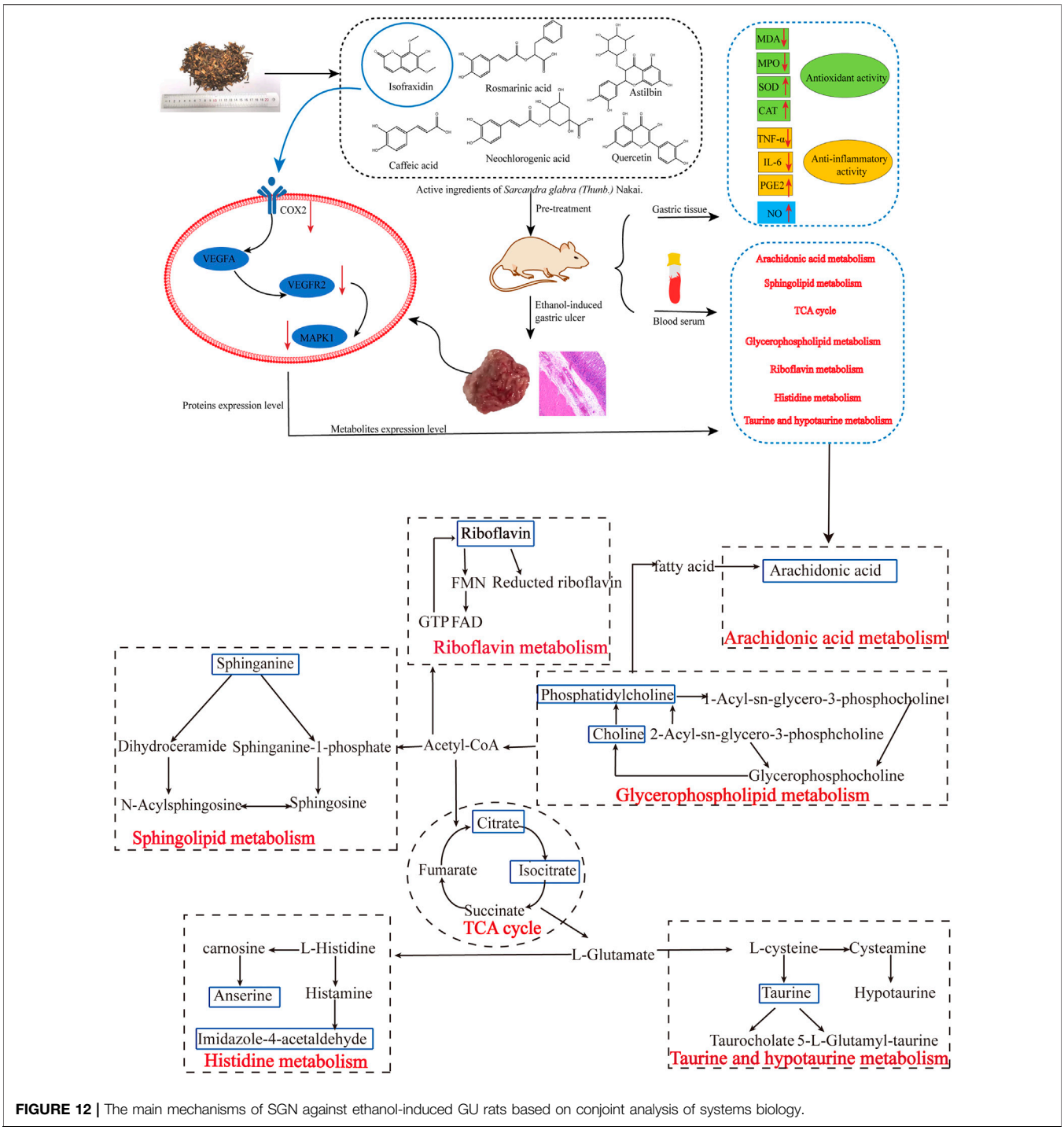

FIGURE 12 | The main mechanisms of SGN against ethanol-induced GU rats based on conjoint analysis of systems biology.

pain, and vasodilation. Prostaglandins (PGs) are the main metabolites of AA. PGE2 has various biological functions and provides local protection for the gastric mucosa. Furthermore, it can increase gastric mucosal blood flow, vascular permeability, and glandular mucus secretion, enhancing the local mucosal barrier function. It can also promote the regeneration of gastric mucosal epithelial cells, induce basal mucosal cells to migrate to the surface, and promote the self-repair of the ulcer surface (Amorim et al., 2016). PGs biosynthesis is regulated by COX-1 and COX-2, also named PTGS2 and PTGS1 (Hirose et al., 2002). PTGS2 is an important enzyme induced in the inflammatory process and traditional anti-GU drugs including NSAIDs are able to exert anti-inflammatory effects by inhibiting COX-2. In addition, previous studies have found that COX-2 is highly expressed in GU tissue. Inhibiting COX-2 can reduce gastric acid secretion in patients with GU, promoting the healing

of GU, and reduce recurrence (Saxena et al., 2008; Hu et al., 2020). Furthermore, it can induce tissues to produce VEGFA-KDR, also called VEGFR2, which plays an important role in regulating endothelial cell proliferation and differentiation. Inhibition of VEGFR2 is also an option for gastric cancer targeted therapy. Moreover, it is the main mediator of VEGF-induced angiogenesis signal transduction. After VEGFA binds to its receptor KDR, it activates MAPK1/8 or c-Jun N-terminal kinase (JNK). The activation of MAPK1 is closely related to the invasion of gastric cancer cells, and knockdown of MAPK1 expression in gastric cancer cell lines can inhibit cell proliferation, migration and invasion, and induce apoptosis (Lim et al., 2018; Sierra et al., 2018). Furthermore, MAPK1 is involved in sphingolipid metabolism, and sphingolipid signaling may also be essential in numerous pathophysiologies, such as inflammation, vascular injury, and cancer (Batheja et al., 2003). Even more importantly, based on the algorithms for network pharmacology and analysis results of HPLC, isofraxidin was finally selected as key active ingredient. Additionally, the proteins with high degree value, that also appeared in the integrated analysis, were selected, as the critical proteins and experimental verification was carried out. The results of the western blot analysis indicated that both SGN and isofraxidin could inhibit the abnormal expression of these hub proteins (See **Figure 12**).

5 CONCLUSION

Taken together, SGN can prevent alcohol-induced AGU most likely by protecting the integrity of the gastric mucosa, improving the tissue oxidative stress state, and inhibiting the expression of inflammatory factors. However, this study has some limitations. 1) The functions of the metabolites identified via metabolomics are unknown in the body and require more in-depth research; 2) Most KEGG pathways were predicted through network pharmacology, and only two metabolic pathways were consistent with the results of metabolomics; 3) The active ingredients in SGN were only identified through HPLC and public databases, which cannot identify components in the blood; and 4) The results acquired from rats may not be directly extrapolated to humans. In the future, a comprehensive analysis of the blood components of SGN will be carried out. Furthermore, the SGN-based anti-GU mechanism is mainly related to oxidative stress. *NFE2L2*, predicted by the network pharmacology, encodes nuclear factor erythroid 2 related factor 2 (Nrf2) protein, and the Kelch-like ECH-associated protein 1 (Keap1)-Nrf2/antioxidant response element (ARE) signaling pathway is the crucial antioxidant pathway in the body. In the future, we will further analyze the deep molecular mechanism of action of SGN against GU in relation to the Keap1-Nrf2/ARE signaling pathway. Ultimately, clinical studies on SGN will be conducted to better understand the gastroprotective efficacy of SGN on the human body.

DATA AVAILABILITY STATEMENT

The original contributions presented in the study are included in the article/**Supplementary Material**, further inquiries can be directed to the corresponding authors.

ETHICS STATEMENT

The animal study was reviewed and approved by Experimental Animal Ethics Committee of Jiangxi University of Traditional Chinese Medicine.

AUTHOR CONTRIBUTIONS

CL designed the experiments. CL and RW conducted the experiments and wrote the manuscript. DL and RW analyzed the data. LY completed the experiments of rats with AGU model. RW and LY collected data from public platforms. HY and QG refined the manuscript for publication. All authors read and approved the final manuscript.

FUNDING

The State Administration of Traditional Chinese Medicine of the People's Republic of China (ZYBZH-Y-JX-27), first-class discipline Chinese Medicine in Jiangxi Province (1050 project) and National Natural Science Foundation of China (82160749) (82104392) supported this study.

ACKNOWLEDGMENTS

We thank Elsevier Language Editing Services (https://webshop.elsevier.com/) for polishing this manuscript (Serial number: LEEX-18149-0A17AC762D1B).

SUPPLEMENTARY MATERIAL

The Supplementary Material for this article can be found online at: https://www.frontiersin.org/articles/10.3389/fphar.2022.810344/full#supplementary-material

REFERENCES

Ahmed, O. A. A., Fahmy, U. A., Bakhaidar, R., El-Moselhy, M. A., Alfaleh, M. A., Ahmed, A. F., et al. (2020). Pumpkin Oil-Based Nanostructured Lipid Carrier System for Antiulcer Effect in NSAID-Induced Gastric Ulcer Model in Rats. *Int. J. Nanomedicine* 15, 2529–2539. doi:10.2147/IJN.S247252

Almasaudi, S. B., El-Shitany, N. A., Abbas, A. T., Abdel-Dayem, U. A., Ali, S. S., Al Jaouni, S. K., et al. (2016). Antioxidant, Anti-Inflammatory, and Antiulcer Potential of Manuka Honey against Gastric Ulcer in Rats. *Oxid. Med. Cell Longev.* 2016, 3643824. doi:10.1155/2016/3643824

Amorim, M. M., Pereira, J. O., Monteiro, K. M., Ruiz, A. L., Carvalho, J. E., Pinheiro, H., et al. (2016). Antiulcer and Antiproliferative Properties of Spent Brewer's Yeast Peptide Extracts for Incorporation into Foods. *Food Funct.* 7, 2331–2337. doi:10.1039/c6fo00030d

Ashoori, M., and Saedisomeolia, A. (2014). Riboflavin (Vitamin B_2) and Oxidative Stress: A Review. *Br. J. Nutr.* 111, 1985–1991. doi:10.1017/S0007114514000178

Bai, K., Hong, B., Tan, R., He, J., and Hong, Z. (2020). Selenium Nanoparticles-Embedded Chitosan Microspheres and Their Effects upon Alcohol-Induced Gastric Mucosal Injury in Rats: Rapid Preparation, Oral Delivery, and Gastroprotective Potential of Selenium Nanoparticles. *Int. J. Nanomedicine* 15, 1187–1203. doi:10.2147/IJN.S237089

Banjari, I., Misir, A., Šavikin, K., Jokić, S., Molnar, M., De Zoysa, H. K. S., et al. (2017). Antidiabetic Effects of Aronia Melanocarpa and its Other Therapeutic Properties. *Front. Nutr.* 4, 53. doi:10.3389/fnut.2017.00053

Batheja, A. D., Uhlinger, D. J., Carton, J. M., Ho, G., and D'andrea, M. R. (2003). Characterization of Serine Palmitoyltransferase in Normal Human Tissues. *J. Histochem. Cytochem.* 51, 687–696. doi:10.1177/002215540305100514

Bueno, G., Chavez Rico, S. L., Périco, L. L., Ohara, R., Rodrigues, V. P., Emílio-Silva, M. T., et al. (2021). The Essential Oil from Baccharis Trimera (Less.) DC Improves Gastric Ulcer Healing in Rats through Modulation of VEGF and MMP-2 Activity. *J. Ethnopharmacol.* 271, 113832. doi:10.1016/j.jep.2021.113832

Busch, C. J., and Binder, C. J. (2017). Malondialdehyde Epitopes as Mediators of Sterile Inflammation. *Biochim. Biophys. Acta Mol. Cell Biol. Lipids* 1862, 398–406. doi:10.1016/j.bbalip.2016.06.016

Byeon, S., Oh, J., Lim, J. S., Lee, J. S., and Kim, J. S. (2018). Protective Effects of Dioscorea Batatas Flesh and Peel Extracts against Ethanol-Induced Gastric Ulcer in Mice. *Nutrients* 10 (11), 1680. doi:10.3390/nu10111680

Cappel, D. A., Deja, S., Duarte, J. A. G., Kucejova, B., Iñigo, M., Fletcher, J. A., et al. (2019). Pyruvate-Carboxylase-Mediated Anaplerosis Promotes Antioxidant Capacity by Sustaining TCA Cycle and Redox Metabolism in Liver. *Cell Metab.* 29, 1291–1305. e1298. doi:10.1016/j.cmet.2019.03.014

Chu, X., Ci, X., He, J., Jiang, L., Wei, M., Cao, Q., et al. (2012). Effects of a Natural Prolyl Oligopeptidase Inhibitor, Rosmarinic Acid, on Lipopolysaccharide-Induced Acute Lung Injury in Mice. *Molecules* 17, 3586–3598. doi:10.3390/molecules17033586

Devanesan, A. A., Zipora, T., G Smilin, B. A., Deviram, G., and Thilagar, S. (2018). Phytochemical and Pharmacological Status of Indigenous Medicinal Plant Pedalium Murex L.-A Review. *Biomed. Pharmacother.* 103, 1456–1463. doi:10.1016/j.biopha.2018.04.177

Feng, Q., Si, Y., Zhu, L., Wang, F., Fang, J., Pan, C., et al. (2022). Anti-Inflammatory Effects of a SERP 30 Polysaccharide from the Residue of Sarcandra Glabra against Lipopolysaccharide-Induced Acute Respiratory Distress Syndrome in Mice. *J. Ethnopharmacol.* 293, 115262. doi:10.1016/j.jep.2022.115262

Goud, P. T., Bai, D., and Abu-Soud, H. M. (2021). A Multiple-Hit Hypothesis Involving Reactive Oxygen Species and Myeloperoxidase Explains Clinical Deterioration and Fatality in COVID-19. *Int. J. Biol. Sci.* 17, 62–72. doi:10.7150/ijbs.51811

Guo, C., Shangguan, Y., Zhang, M., Ruan, Y., Xue, G., Ma, J., et al. (2020). Rosmarinic Acid Alleviates Ethanol-Induced Lipid Accumulation by Repressing Fatty Acid Biosynthesis. *Food Funct.* 11, 2094–2106. doi:10.1039/c9fo02357g

Harirforoosh, S., and Jamali, F. (2009). Renal Adverse Effects of Nonsteroidal Anti-Inflammatory Drugs. *Expert Opin. Drug Saf.* 8, 669–681. doi:10.1517/14740330903311023

Hirose, M., Miwa, H., Kobayashi, O., Oshida, K., Misawa, H., Kurosawa, A., et al. (2002). Inhibition of Proliferation of Gastric Epithelial Cells by a Cyclooxygenase 2 Inhibitor, JTE522, is Also Mediated by a PGE2-independent Pathway. *Aliment. Pharmacol. Ther.* 16 (Suppl. 2), 83–89. doi:10.1046/j.1365-2036.16.s2.28.x

Horiuchi, S., Hirano, H., and Ono, S. (1984). Reduced and Oxidized Glutathione Concentrations in the Lenses of Riboflavin-Deficient Rats. *J. Nutr. Sci. Vitaminol. (Tokyo)* 30, 401–403. doi:10.3177/jnsv.30.401

Hu, Y., Ren, D., Song, Y., Wu, L., He, Y., Peng, Y., et al. (2020). Gastric Protective Activities of Fucoidan from Brown Alga Kjellmaniella Crassifolia through the NF-κB Signaling Pathway. *Int. J. Biol. Macromol.* 149, 893–900. doi:10.1016/j.ijbiomac.2020.01.186

Kobayashi, T., Ohta, Y., Yoshino, J., and Nakazawa, S. (2001). Teprenone Promotes the Healing of Acetic Acid-Induced Chronic Gastric Ulcers in Rats by Inhibiting Neutrophil Infiltration and Lipid Peroxidation in Ulcerated Gastric Tissues. *Pharmacol. Res.* 43, 23–30. doi:10.1006/phrs.2000.0748

Lee, L., Ramos-Alvarez, I., Ito, T., and Jensen, R. T. (2019). Insights into Effects/Risks of Chronic Hypergastrinemia and Lifelong PPI Treatment in Man Based on Studies of Patients with Zollinger-Ellison Syndrome. *Int. J. Mol. Sci.* 20 (20), 5128. doi:10.3390/ijms20205128

Li, P., Zhao, Q. L., Wu, L. H., Jawaid, P., Jiao, Y. F., Kadowaki, M., et al. (2014). Isofraxidin, a Potent Reactive Oxygen Species (ROS) Scavenger, Protects Human Leukemia Cells from Radiation-Induced Apoptosis via ROS/mitochondria Pathway in P53-independent Manner. *Apoptosis* 19, 1043–1053. doi:10.1007/s10495-014-0984-1

Li, Z., Zou, D., Ma, X., Chen, J., Shi, X., Gong, Y., et al. (2010). Epidemiology of Peptic Ulcer Disease: Endoscopic Results of the Systematic Investigation of Gastrointestinal Disease in China. *Am. J. Gastroenterol.* 105, 2570–2577. doi:10.1038/ajg.2010.324

Lian, Y. Z., Lin, I. H., Yang, Y. C., and Chao, J. C. (2020). Gastroprotective Effect of Lycium Barbarum Polysaccharides and C-Phycocyanin in Rats with Ethanol-Induced Gastric Ulcer. *Int. J. Biol. Macromol.* 165, 1519–1528. doi:10.1016/j.ijbiomac.2020.10.037

Lim, H. N., Jang, J. P., Han, J. M., Jang, J. H., Ahn, J. S., and Jung, H. J. (2018). Antiangiogenic Potential of Microbial Metabolite Elaiophylin for Targeting Tumor Angiogenesis. *Molecules* 23 (3), 563. doi:10.3390/molecules23030563

Lin, T. H., Yao, Z., Sato, T., Keeney, M., Li, C., Pajarinen, J., et al. (2014). Suppression of Wear-Particle-Induced Pro-Inflammatory Cytokine and Chemokine Production in Macrophages via NF-κB Decoy Oligodeoxynucleotide: A Preliminary Report. *Acta Biomater.* 10, 3747–3755. doi:10.1016/j.actbio.2014.04.034

Liu, C. P., Liu, J. X., Gu, J., Liu, F., Li, J. H., Bin, Y., et al. (2020). Combination Effect of Three Main Constituents from Sarcandra Glabra Inhibits Oxidative Stress in the Mice Following Acute Lung Injury: A Role of MAPK-NF-κB Pathway. *Front. Pharmacol.* 11, 580064. doi:10.3389/fphar.2020.580064

Liu, J. X., Zhang, Y., Hu, Q. P., Li, J. Q., Liu, Y. T., Wu, Q. G., et al. (2017). Anti-Inflammatory Effects of Rosmarinic Acid-4-O-β-D-Glucoside in Reducing Acute Lung Injury in Mice Infected with Influenza Virus. *Antivir. Res.* 144, 34–43. doi:10.1016/j.antiviral.2017.04.010

Liu, T. Y., and Chen, S. B. (2016). Sarcandra Glabra Combined with Lycopene Protect Rats from Lipopolysaccharide Induced Acute Lung Injury via Reducing Inflammatory Response. *Biomed. Pharmacother.* 84, 34–41. doi:10.1016/j.biopha.2016.09.009

Liu, Y., Tang, H., Liu, X., Chen, H., Feng, N., Zhang, J., et al. (2019). Frontline Science: Reprogramming COX-2, 5-LOX, and CYP4A-Mediated Arachidonic Acid Metabolism in Macrophages by Salidroside Alleviates Gouty Arthritis. *J. Leukoc. Biol.* 105, 11–24. doi:10.1002/JLB.3HI0518-193R

Lívero, F. A., Martins, G. G., Queiroz Telles, J. E., Beltrame, O. C., Petris Biscaia, S. M., Cavicchiolo Franco, C. R., et al. (2016). Hydroethanolic Extract of Baccharis Trimera Ameliorates Alcoholic Fatty Liver Disease in Mice. *Chem. Biol. Interact.* 260, 22–32. doi:10.1016/j.cbi.2016.10.003

Lucarelli, G., Rutigliano, M., Galleggiante, V., Giglio, A., Palazzo, S., Ferro, M., et al. (2015). Metabolomic Profiling for the Identification of Novel Diagnostic Markers in Prostate Cancer. *Expert Rev. Mol. Diagn* 15, 1211–1224. doi:10.1586/14737159.2015.1069711

Liu, J., Li, X., Lin, J., Li, Y., Wang, T., Jiang, Q., et al. (2016). Sarcandra glabra (Caoshanhu) protects mesenchymal stem cells from oxidative stress: a bioevaluation and mechanistic chemistry. *BMC Complement Altern Med* 16, 423.

Manzanares-Estreder, S., Pascual-Ahuir, A., and Proft, M. (2017). Stress-Activated Degradation of Sphingolipids Regulates Mitochondrial Function and Cell Death in Yeast. *Oxid. Med. Cell Longev.* 2017, 2708345. doi:10.1155/2017/2708345

Motawi, T. K., Abd Elgawad, H. M., and Shahin, N. N. (2007). Modulation of Indomethacin-Induced Gastric Injury by Spermine and Taurine in Rats. *J. Biochem. Mol. Toxicol.* 21, 280–288. doi:10.1002/jbt.20194

Pang, Z., Chong, J., Zhou, G., De Lima Morais, D. A., Chang, L., Barrette, M., et al. (2021). MetaboAnalyst 5.0: Narrowing the Gap between Raw Spectra and Functional Insights. *Nucleic Acids Res.* 49, W388–W396. doi:10.1093/nar/gkab382

Pérez, S., Taléns-Visconti, R., Rius-Pérez, S., Finamor, I., and Sastre, J. (2017). Redox Signaling in the Gastrointestinal Tract. *Free Radic. Biol. Med.* 104, 75–103. doi:10.1016/j.freeradbiomed.2016.12.048

Rakotoarisoa, M., Angelov, B., Espinoza, S., Khakurel, K., Bizien, T., and Angelova, A. (2019). Cubic Liquid Crystalline Nanostructures Involving Catalase and Curcumin: BioSAXS Study and Catalase Peroxidatic Function after Cubosomal

Nanoparticle Treatment of Differentiated SH-SY5Y Cells. *Molecules* 24 (17), 3058. doi:10.3390/molecules24173058

Rudra, D. S., Pal, U., Chowdhury, N., Maiti, N. C., Bagchi, A., and Swarnakar, S. (2022). Omeprazole Prevents Stress Induced Gastric Ulcer by Direct Inhibition of MMP-2/TIMP-3 Interactions. *Free Radic. Biol. Med.* 181, 221–234. doi:10.1016/j.freeradbiomed.2022.02.007

Santana-Gálvez, J., Cisneros-Zevallos, L., and Jacobo-Velázquez, D. A. (2017). Chlorogenic Acid: Recent Advances on its Dual Role as a Food Additive and a Nutraceutical against Metabolic Syndrome. *Molecules* 22 (3)–358. doi:10.3390/molecules22030358

Saxena, A., Prasad, K. N., Ghoshal, U. C., Bhagat, M. R., Krishnani, N., and Husain, N. (2008). Polymorphism of -765G > C COX-2 is a Risk Factor for Gastric Adenocarcinoma and Peptic Ulcer Disease in Addition to H Pylori Infection: A Study from Northern India. *World J. Gastroenterol.* 14, 1498–1503. doi:10.3748/wjg.14.1498

Schatzman, S. S., and Culotta, V. C. (2018). Chemical Warfare at the Microorganismal Level: A Closer Look at the Superoxide Dismutase Enzymes of Pathogens. *ACS Infect. Dis.* 4, 893–903. doi:10.1021/acsinfecdis.8b00026

Sharma, A., Gupta, S., Chauhan, S., Nair, A., and Sharma, P. (2020). Astilbin: A Promising Unexplored Compound with Multidimensional Medicinal and Health Benefits. *Pharmacol. Res.* 158, 104894. doi:10.1016/j.phrs.2020.104894

Sierra, J. C., Asim, M., Verriere, T. G., Piazuelo, M. B., Suarez, G., Romero-Gallo, J., et al. (2018). Epidermal Growth Factor Receptor Inhibition Downregulates Helicobacter Pylori-Induced Epithelial Inflammatory Responses, DNA Damage and Gastric Carcinogenesis. *Gut* 67, 1247–1260. doi:10.1136/gutjnl-2016-312888

Song, H. J., Kwon, J. W., Kim, N., and Park, Y. S. (2013). Cost Effectiveness Associated with *Helicobacter P* Screening and Eradication in Patients Taking Nonsteroidal Anti-inflammatory Drugs and/or Aspirin. *Gut Liver* 7, 182–189. doi:10.5009/gnl.2013.7.2.182

Su, X., Liu, B., Gong, F., Yin, J., Sun, Q., Gao, Y., et al. (2019). Isofraxidin Attenuates IL-1β-Induced Inflammatory Response in Human Nucleus Pulposus Cells. *J. Cell Biochem.* 120, 13302–13309. doi:10.1002/jcb.28604

Sudi, I. Y., Ahmed, M. U., and Adzu, B. (2020). Sphaeranthus Senegalensis DC: Evaluation of Chemical Constituents, Oral Safety, Gastroprotective Activity, and Mechanism of Action of its Hydroethanolic Extract. *J. Ethnopharmacol.* 268, 113597. doi:10.1016/j.jep.2020.113597

Tan, B. L., Norhaizan, M. E., and Liew, W. P. (2018). Nutrients and Oxidative Stress: Friend or Foe? *Oxid. Med. Cell Longev.* 2018, 9719584. doi:10.1155/2018/9719584

Tsai, Y. C., Chen, S. H., Lin, L. C., and Fu, S. L. (2017). Anti-Inflammatory Principles from Sarcandra Glabra. *J. Agric. Food Chem.* 65, 6497–6505. doi:10.1021/acs.jafc.6b05125

Valcheva-Kuzmanova, S., Denev, P., Eftimov, M., Georgieva, A., Kuzmanova, V., Kuzmanov, A., et al. (2019). Protective Effects of Aronia Melanocarpa Juices Either Alone or Combined with Extracts from Rosa Canina or Alchemilla Vulgaris in a Rat Model of Indomethacin-Induced Gastric Ulcers. *Food Chem. Toxicol.* 132, 110739. doi:10.1016/j.fct.2019.110739

Vinke, P., Wesselink, E., Van Orten-Luiten, W., and Van Norren, K. (2020). The Use of Proton Pump Inhibitors May Increase Symptoms of Muscle Function Loss in Patients with Chronic Illnesses. *Int. J. Mol. Sci.* 21 (1), 323. doi:10.3390/ijms21010323

Wang, J., Deng, H., Zhang, J., Wu, D., Li, J., Ma, J., et al. (2020). α-Hederin Induces the Apoptosis of Gastric Cancer Cells Accompanied by Glutathione Decrement and Reactive Oxygen Species Generation via Activating Mitochondrial Dependent Pathway. *Phytother. Res.* 34, 601–611. doi:10.1002/ptr.6548

Wang, S. J., Chen, Q., Liu, M. Y., Yu, H. Y., Xu, J. Q., Wu, J. Q., et al. (2019). Regulation Effects of Rosemary (Rosmarinus Officinalis Linn.) on Hepatic Lipid Metabolism in OA Induced NAFLD Rats. *Food Funct.* 10, 7356–7365. doi:10.1039/c9fo01677e

Xiang, Z., Hua, M., Hao, Z., Biao, H., Zhu, C., Zhai, G., et al. (2022). The Roles of Mesenchymal Stem Cells in Gastrointestinal Cancers. *Front Immunol* 13, 844001.

Xie, L., Guo, Y. L., Chen, Y. R., Zhang, L. Y., Wang, Z. C., Zhang, T., et al. (2020). A Potential Drug Combination of Omeprazole and Patchouli Alcohol Significantly Normalizes Oxidative Stress and Inflammatory Responses against Gastric Ulcer in Ethanol-Induced Rat Model. *Int. Immunopharmacol.* 85, 106660. doi:10.1016/j.intimp.2020.106660

Yang, J., Tian, S., Zhao, J., and Zhang, W. (2020). Exploring the Mechanism of TCM Formulae in the Treatment of Different Types of Coronary Heart Disease by Network Pharmacology and Machining Learning. *Pharmacol. Res.* 159, 105034. doi:10.1016/j.phrs.2020.105034

Yang, L., Zhang, S., Duan, H., Dong, M., Hu, X., Zhang, Z., et al. (2019). Different Effects of Pro-Inflammatory Factors and Hyperosmotic Stress on Corneal Epithelial Stem/Progenitor Cells and Wound Healing in Mice. *Stem Cells Transl. Med.* 8, 46–57. doi:10.1002/sctm.18-0005

Yeo, D., Hwang, S. J., Song, Y. S., and Lee, H. J. (2021). Humulene Inhibits Acute Gastric Mucosal Injury by Enhancing Mucosal Integrity. *Antioxidants (Basel)* 10 (5), 761. doi:10.3390/antiox10050761

Yoo, J. H., Park, E. J., Kim, S. H., and Lee, H. J. (2020). Gastroprotective Effects of Fermented Lotus Root against Ethanol/HCl-Induced Gastric Mucosal Acute Toxicity in Rats. *Nutrients* 12 (3), 808. doi:10.3390/nu12030808

Zeng, Q., Ko, C. H., Siu, W. S., Li, L. F., Han, X. Q., Yang, L., et al. (2017). Polysaccharides of Dendrobium Officinale Kimura & Migo Protect Gastric Mucosal Cell against Oxidative Damage-Induced Apoptosis *In Vitro* and *In Vivo*. *J. Ethnopharmacol.* 208, 214–224. doi:10.1016/j.jep.2017.07.006

Zhang, W., Chen, Y., Jiang, H., Yang, J., Wang, Q., Du, Y., et al. (2020). Integrated Strategy for Accurately Screening Biomarkers Based on Metabolomics Coupled with Network Pharmacology. *Talanta* 211, 120710. doi:10.1016/j.talanta.2020.120710

Zhang, X., Wang, Y., Li, X., Dai, Y., Wang, Q., Wang, G., et al. (2019). Treatment Mechanism of Gardeniae Fructus and its Carbonized Product against Ethanol-Induced Gastric Lesions in Rats. *Front. Pharmacol.* 10, 750. doi:10.3389/fphar.2019.00750

Zhang, Y., Wang, H., Mei, N., Ma, C., Lou, Z., Lv, W., et al. (2018). Protective Effects of Polysaccharide from Dendrobium Nobile against Ethanol-Induced Gastric Damage in Rats. *Int. J. Biol. Macromol.* 107, 230–235. doi:10.1016/j.ijbiomac.2017.08.175

Zhao, F., Shi, B., Sun, D., Chen, H., Tong, M., Zhang, P., et al. (2016). Effects of Dietary Supplementation of Artemisia Argyi Aqueous Extract on Antioxidant Indexes of Small Intestine in Broilers. *Anim. Nutr.* 2, 198–203. doi:10.1016/j.aninu.2016.06.006

Zhao, J., Jiang, P., and Zhang, W. (2010). Molecular Networks for the Study of TCM Pharmacology. *Brief. Bioinform* 11, 417–430. doi:10.1093/bib/bbp063

Zhao, X. L., Yu, L., Zhang, S. D., Ping, K., Ni, H. Y., Qin, X. Y., et al. (2020). Cryptochlorogenic Acid Attenuates LPS-Induced Inflammatory Response and Oxidative Stress via Upregulation of the Nrf2/HO-1 Signaling Pathway in RAW 264.7 Macrophages. *Int. Immunopharmacol.* 83, 106436. doi:10.1016/j.intimp.2020.106436

Zheng, H., Chen, Y., Zhang, J., Wang, L., Jin, Z., Huang, H., et al. (2016). Evaluation of Protective Effects of Costunolide and Dehydrocostuslactone on Ethanol-Induced Gastric Ulcer in Mice Based on Multi-Pathway Regulation. *Chem. Biol. Interact.* 250, 68–77. doi:10.1016/j.cbi.2016.03.003

Zhou, H., Liang, J., Lv, D., Hu, Y., Zhu, Y., Si, J., et al. (2013). Characterization of Phenolics of Sarcandra Glabra by Non-Targeted High-Performance Liquid Chromatography Fingerprinting and Following Targeted Electrospray Ionisation Tandem Mass Spectrometry/Time-Of-Flight Mass Spectrometry Analyses. *Food Chem.* 138, 2390–2398. doi:10.1016/j.foodchem.2012.12.027

Conflict of Interest: The authors declare that the research was conducted in the absence of any commercial or financial relationships that could be construed as a potential conflict of interest.

Publisher's Note: All claims expressed in this article are solely those of the authors and do not necessarily represent those of their affiliated organizations, or those of the publisher, the editors and the reviewers. Any product that may be evaluated in this article, or claim that may be made by its manufacturer, is not guaranteed or endorsed by the publisher.

Advantages of publishing in Frontiers

OPEN ACCESS
Articles are free to read for greatest visibility and readership

FAST PUBLICATION
Around 90 days from submission to decision

HIGH QUALITY PEER-REVIEW
Rigorous, collaborative, and constructive peer-review

TRANSPARENT PEER-REVIEW
Editors and reviewers acknowledged by name on published articles

Frontiers
Avenue du Tribunal-Fédéral 34
1005 Lausanne | Switzerland

Visit us: www.frontiersin.org
Contact us: frontiersin.org/about/contact

REPRODUCIBILITY OF RESEARCH
Support open data and methods to enhance research reproducibility

DIGITAL PUBLISHING
Articles designed for optimal readership across devices

FOLLOW US
@frontiersin

IMPACT METRICS
Advanced article metrics track visibility across digital media

EXTENSIVE PROMOTION
Marketing and promotion of impactful research

LOOP RESEARCH NETWORK
Our network increases your article's readership